

1127-2/

112

JOURNAL OF COLLOID SCIENCE

Editor-in-Chief

VICTOR K. LA MER, Columbia University, New York

Advisory Board

C. O. BECKMANN

KATHARINE B. BLODGETT

K. F. BONHOEFFER

J. A. CHRISTIANSEN

M. L. CORRIN

P. J. W. DEBYE

JOHN T. EDSALL

I. FANKUCHEN

JOHN D. FERRY

A. R. GORDON

WILFRIED HELLER

ERIC HUTCHINSON

JOHN G. KIRKWOOD

E. C. LINGAFELTER

L. G. LONGSWORTH

J. TH. G. OVERBEEK

R. RUYSSSEN

E. K. RIDEAL

WILLIAM SEIFRIZ

LEO SHEDLOVSKY

THEODORE SHEDLOVSKY

ROBERT SIMHA

JACINTO STEINHARDT

THE SVEDBERG

HUGH S. TAYLOR

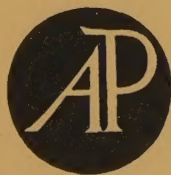
ARNE TISELIUS

ROBERT D. VOLD

BERNARD VONNEGUT

RALPH W. G. WYCKOFF

BRUNO H. ZIMM



VOLUME 8

1953

ACADEMIC PRESS INC.—PUBLISHERS
NEW YORK, N. Y.

JOURNAL OF COLLOID SCIENCE

Editor-in-Chief

VICTOR K. LA MER, Columbia University, New York

Advisory Board

C. O. BECKMANN

J. TH. G. OVERBEEK

KATHARINE B. BLODGETT

R. RUYSEN

K. F. BONHOEFFER

E. K. RIDEAL

M. L. CORRIN

WILLIAM SEIFRIZ

P. J. W. DEBYE

LEO SHEDLOVSKY

JOHN T. EDSALL

THEODORE SHEDLOVSKY

I. FANKUCHEN

ROBERT SIMHA

JOHN D. FERRY

JACINTO STEINHARDT

A. R. GORDON

THE SVEDBERG

WILFRIED HELLER

HUGH S. TAYLOR

ERIC HUTCHINSON

ARNE TISELIUS

JOHN G. KIRKWOOD

ROBERT D. VOLD

E. C. LINGAFELTER

BERNARD VONNEGUT

L. G. LONGSWORTH

RALPH W. G. WYCKOFF

BRUNO H. ZIMM



VOLUME 8

1953

ACADEMIC PRESS INC.—PUBLISHERS
NEW YORK, N. Y.

JOURNAL OF COLLOID SCIENCE

Volume 12, Number 1, January 1953

Published by Academic Press, Inc.

Copyright © 1953, Academic Press, Inc.

Printed in the United States of America

Second-class postage paid at New York, N. Y.

Postmaster: Send address changes in U. S. A. to

JOURNAL OF COLLOID SCIENCE, 1221 Avenue of the

Stars, New York 17, New York

Subscription prices: U. S. and possessions, \$12.00

per annum in advance; Canada, \$14.00; Europe,

Japan, and other foreign countries, \$16.00

per annum. Single copies, \$1.00 each.

Claims for missing issues will only be considered

if made immediately on receipt of following

issue. Payment of subscription price does not

entitle subscriber to return of missing issues.

Second-class postage paid at New York, N. Y.

Postmaster: Send address changes in U. S. A. to

JOURNAL OF COLLOID SCIENCE, 1221 Avenue of the

Stars, New York 17, New York



Copyright 1953, by Academic Press Inc.
Made in United States of America

Contents of Volume 8

NUMBER 1, FEBRUARY, 1953

EDWIN R. FITZGERALD AND JOHN D. FERRY. Method for Determining the Dynamic Mechanical Behavior of Gel and Solids at Audio-frequencies; Comparison of Mechanical and Electrical Properties	1
P. SHERMAN. Studies in Water-in-Oil Emulsions. III. The Properties of Interfacial Films of Sorbitan Sesquioleate.....	35
J. L. VAN DER MINNE AND P. H. J. HERMANIE. Electrophoresis Measurements in Benzene-Correlation with Stability. II. Results of Electrophoresis, Stability, and Adsorption.....	38
R. MATALON. On Monolayer Penetration.....	53
G. J. HARMSSEN, J. VAN SCHOOTEN, AND J. TH. G. OVERBEEK. Viscosity and Electroviscous Effect of the AgI Sol. I. Influence of the Velocity Gradient and of Aging of the Sol.....	64
G. J. HARMSSEN, J. VAN SCHOOTEN AND J. TH. G. OVERBEEK. Viscosity and Electroviscous Effect of the AgI Sol. II. Influence of the Concentration of AgI and of Electrolyte on the Viscosity.....	72
HENRY L. FRIEDMAN AND MILTON KERKER. Ultraviolet Absorption of Aqueous Sulfur Solutions.....	80
MARTIN B. MATHEWS AND ERNESTINE HIRSCHHORN. Solubilization and Micelle Formation in a Hydrocarbon Medium.....	86
E. L. PIPPEN, T. H. SCHULTZ AND H. S. OWENS. Effect of Degree of Esterification on Viscosity and Gelation Behavior of Pectin....	97
B. D. FLOCKHART AND H. GRAHAM. Study of Dilute Aqueous Solutions of Sodium Oleate.....	105
GEORGE W. LOWER, WILLIAM C. WALKER AND ALBERT C. ZETTMAYER. The Rheology of Printing Inks. II. Temperature Control Studies in the Rotational Viscometer.....	116
SAMUEL H. MARON AND BENJAMIN P. MADOW. Rheology of Synthetic Latex. III. Concentration Dependence of Flow in Type III GR-S Latex.....	130
W. H. BANKS AND C. C. MILL. Tacky Adhesion—A Preliminary Study.	137
EDWIN R. FITZGERALD AND ROBERT F. MILLER. Dielectric Properties of the System Polyvinyl Chloride Dimethylthianthrene.....	148
ARTHUR L. MEADER, JR. AND DEAN W. CRIDDLE. Force-Area Curves of Surface Films of Soluble Surface-Active Agents.....	170
LETTER TO THE EDITORS:	
KARL SOLLNER. Some Remarks Concerning the Measurement of Ion Activities in Colloidal Systems and the Suspension Effect.....	179

BOOK REVIEWS:

CHARLES POTTER. <i>Advances in Catalysis</i> . Vols. I, II, and III.....	183
W. MANSFIELD CLARK. <i>Hydrogen Ion Concentration. New Concepts in a Systematic Treatment</i>	184
ERRATA.....	185

NUMBER 2, APRIL, 1953

G. M. POUND, L. A. MADONNA AND S. L. PEAKE. <i>Critical Supercooling of Pure Water Droplets by a New Microscopic Technique</i>	187
H. W. FOX, E. F. HARE AND A. ZISMAN. <i>The Spreading of Liquids on Low-Energy Surfaces. VI. Branched-Chain Monolayers, Aromatic Surfaces, and Thin Liquid Films</i>	194
WARREN W. EWING AND FRED W. J. LIU. <i>Adsorption of Dyes from Aqueous Solutions on Pigments</i>	204
B. ROGER RAY AND F. E. BARTELL. <i>Hysteresis of Contact Angle of Water on Paraffin. Effect of Surface Roughness and of Purity of Paraffin</i>	214
JOHN D. FERRY AND EDWIN R. FITZGERALD. <i>Mechanical and Electrical Relaxation Distribution Functions of Two Compositions of Polyvinyl Chloride and Dimethyl Thianthrene</i>	224
W. R. MOORE AND J. RUSSELL. <i>Viscosity and Initial Phase Separation Studies on Solutions of Cellulose Acetate</i>	243
A. P. BRADY, A. G. BROWN AND HARRIETTE HUFF. <i>The Polymerization of Aqueous Potassium Silicate Solutions</i>	252
BOOK REVIEW:	
J. J. BIKERMAN. <i>Comité International de Thermodynamique et de Cinétique Electrochimiques. Comptes rendus de la IIIe réunion. Berne, 1951</i>	277

NUMBER 3, JUNE, 1953

H. N. DUNNING. <i>The Interfacial Activity of Mesoporphyrin IX and Some Derivatives</i>	279
MANUEL N. FINEMAN AND PHYLLIS J. KLINE. <i>The Role of the Substrate in the Detergency Process</i>	288
SAMUEL H. MARON AND BENJAMIN P. MADOW. <i>Rheology of Synthetic Latex. IV. Effect of Polydispersity on Flow Behavior</i>	300
E. D. GODDARD AND J. H. SCHULMAN. <i>Molecular Interaction in Monolayers. I. Complex Formation</i>	309
E. D. GODDARD AND J. H. SCHULMAN. <i>Molecular Interaction in Monolayers. II. Steric Effects in the Nonpolar Portion of the Molecules</i>	329
TARO TACHIBANA AND KIYOSHI INOKUCHI. <i>Rheological Approach for the Study of Protein Monolayers</i>	341

SADHAN BASU AND PARES CH. DAS GUPTA. Studies on Polyelectrolytes. III. Polyglucosamine.....	355
J. H. BURGOYNE AND L. COHEN. The Production of Monodisperse Aerosols of Large Drop Size.....	364
E. G. RICHARDSON. The Flow of Emulsions. II.....	367
BOOK REVIEWS:	
HANS JENNY. Soil Physical Conditions and Plant Growth.....	374
VICTOR K. LA MER. Kinetics and Mechanism.....	374

NUMBER 4, AUGUST, 1953

Obituary of James W. McBain.....	375
ROBERT B. DEAN, KENNETH E. HAYES AND ROY G. NEVILLE. The Sorption of Vapors by Monolayers. VII. The Effect of Anesthetic Vapors on Some Monolayers of Biological Interest.....	377
SYDNEY ROSS, C. E. KWARTLER, AND JOHN HAYS BAILEY. Colloidal Association and Biological Activity of Some Related Quaternary Ammonium Salts.....	385
E. W. ANACKER. Light Scattering by Solutions of Octyltrimethylammonium Octanesulfonate and Octyltrimethylammonium Decanesulfonate.....	402
HIRA LAL. The Specific and Partial Specific Volumes of Potassium Laurate and Lauryl Sulfonic Acid in Aqueous Solutions.....	414
J. TH. G. OVERBEEK. Thermodynamics of Electrokinetic Phenomena.....	420
B. D. FLOCKHART AND A. R. UBBELOHDE. Electrical Conductance of Some Paraffin-Chain Salts in Propanol-Water and Propionic Acid-Water Mixtures.....	428
E. G. COCKBAIN AND T. S. McROBERTS. The Stability of Elementary Emulsion Drops and Emulsions.....	440
VIRGIL L. KOENIG AND J. D. PERRINGS. Critical Sedimentation and Viscosity Studies on Calf Thymus Sodium Desoxyribonucleate...	452
K. W. SCOTT AND A. V. TOBOLSKY. Statistical Thermodynamics of a One-Dimensional Polymer Chain Incorporating Energy and Entropy Effects.....	474
J. W. MCBAIN AND S. GULVADY DAS GUPTA. Solubilization of Benzene in Certain Detergent Solutions That Appear to Give Two Different Values.....	474

LETTER TO THE EDITORS:

RONALD BULKLEY. Retardation of Flow in Narrow Capillaries.....	485
--	-----

BOOK REVIEWS:

FREDERICK R. EIRICH. Colloid Science. Vol. I. <i>Irreversible Systems</i> ...	487
B. P. DAILEY. General College Chemistry.....	487
Fourth Symposium on Plasticity.....	488
Errata.....	489

NUMBER 5, OCTOBER, 1953

A. G. BROWN, WILLIAM C. THUMAN, AND J. W. MCBAIN. The Surface Viscosity of Detergent Solutions as a Factor in Foam Stability. . .	491
A. G. BROWN, WILLIAM C. THUMAN, AND J. W. MCBAIN. Transfer of Air Through Adsorbed Surface Films as a Factor in Foam Stability	508
EMIL J. BURCIK. Effect of Electrolytes on the Rate of Surface Tension Lowering; The Rate of Surface Equilibrium Attainment as a Factor in Detergency.	520
JOHN D. FERRY, LESTER D. GRANDINE, JR., AND DOYLE C. UDY. Viscosities of Concentrated Polymer Solutions. III. Polystyrene and Styrene-Maleic Acid Copolymer.	529
SAMUEL H. MARON AND SHIU-MING FOK. Effect of Concentration on Flow Behavior of Glass Sphere Suspensions.	540
LETTERS TO THE EDITORS:	
EDMUND N. HARVEY, JR. Effect of Magnetic Fields on the Rheology of Ferromagnetic Dispersions.	543
J. J. KIPLING AND A. D. NORRIS. Molecular Cross Sections in Films of Fatty Acids on Water.	547
RAYMOND L. NEUBAUER AND BERNARD VONNEGUT. Supplement to "Production of Monodisperse Liquid Particles by Electrical Atomization.	551
BOOK REVIEW	
W. A. SELKE. Ion Exchangers in Analytical Chemistry.	553

NUMBER 6, DECEMBER, 1953

FRANK T. GUCKER, JR., AND STANLEY H. COHN. Numerical Evaluation of the Mie Scattering Functions; Table of the Angular Functions π_n and τ_n of Orders 1 to 32, at 2.5° Intervals.	555
A. M. POSNER AND A. E. ALEXANDER. The Kinetics of Adsorption from Solution to the Air/Water Interface. Part I. Normal Aliphatic Alcohols.	575
A. M. POSNER AND A. E. ALEXANDER. The Kinetics of Adsorption from Solution to the Air/Water Interface. Part II. Anionic and Cationic Soaps.	585
J. TH. G. OVERBEEK. Donnan-E.M.F. and Suspension Effect.	593
LETTER TO THE EDITORS	
MATHIAS H. J. WEIDEN AND LELAND B. NORTON. Detergent Solubility as a Limiting Factor in Solubilization by Aqueous Solutions of Two Nonionic Detergents.	606
BOOK REVIEW	
R. H. EWART. Review of Textile Progress.	611
AUTHOR INDEX.	613
SUBJECT INDEX.	616
INDEX OF BOOK REVIEWS.	619

METHOD FOR DETERMINING THE DYNAMIC MECHANICAL BEHAVIOR OF GELS AND SOLIDS AT AUDIO-FREQUENCIES; COMPARISON OF MECHANICAL AND ELECTRICAL PROPERTIES ^{1, 2}

Edwin R. Fitzgerald ³ and John D. Ferry

Departments of Physics and Chemistry, University of Wisconsin, Madison, Wisconsin

Received June 23, 1952

INTRODUCTION

During the past five years increasing interest in dynamic mechanical properties has led to the development of many methods for dynamic measurements on rubberlike solids (1-7), but in general none of these can be used over a very wide frequency or temperature range or for a range of sample consistencies from weak gels or concentrated solutions to stiff solids such as are encountered in plasticized polymer systems. Moreover, the precision in many cases is not very good. Nolle (1), for example, has used a vibrating reed for measurements from -60 to $+50^{\circ}\text{C}$. ($\pm 1^{\circ}\text{C}$.) with a frequency range of 12.5 to 580 cycles/sec., and the propagation of longitudinal waves in thin strips (500 to 17,000 cycles/sec.) to measure a complex Young's modulus; but the estimated uncertainty (8) in these measurements is 15-20%. On the other hand, Fletcher and Gent (5) use a forced resonance method to obtain a complex shear modulus with an experimental error of less than 2% at temperatures of 10 to 50°C . ($\pm 2^{\circ}\text{C}$.) but with a frequency range of only 66 to 68 cycles/sec. Nielsen and Buchdahl (9) use a recording torsional pendulum to measure the decay of free vibration at temperatures from -30 to $+60^{\circ}\text{C}$. ($\pm 0.5^{\circ}\text{C}$.) and at frequencies from 0.1 to 10 cycles/sec. with an experimental error (8) of 5 to 10% (6). It is apparently the results of measurements in this frequency range which have been compared by them with dielectric measurements at 1000 cycles/sec.

Electromagnetic transducers have been used by Smith, Ferry, and Schremp (2) and Marvin, Fitzgerald, and Ferry (3) to measure the complex shear modulus over a continuous frequency range from 200 to 400

¹ Based in part on a thesis submitted by Edwin R. Fitzgerald in partial fulfillment of the requirements for the Ph.D. degree, University of Wisconsin, 1951.

² Presented in part at the 312th Meeting of the American Physical Society, Columbus, Ohio, March 20, 1952.

³ Now at Department of Physics, Pennsylvania State College, State College, Penna.

cycles/sec. and 25 to 250 cycles/sec., respectively, at temperatures from -15 to $+50^{\circ}\text{C}$. with a precision of $\pm 5\%$. The limited frequency and temperature ranges of these instruments, however, are a serious handicap.

The apparatus described here is of the transducer type but has been designed for measurements of the complex shear modulus (or complex compliance) on samples ranging from soft gels to stiff solids at temperatures from -50 to $+150^{\circ}\text{C}$. and over a continuous frequency range of 25 to 5000 cycles/sec. The mechanical impedance (and hence complex shear modulus) is determined by an electrical measuring circuit designed to take advantage of the special features of a double transducer; by a proper choice of sample dimensions a precision of $\pm 2\%$ or better is obtained, although a single sample cannot be measured with this precision at all temperatures and frequencies.

Experimental results are given for a sample of polyisobutylene from the National Bureau of Standards (8), for a polyvinyl chloride-dimethylthianthrene gel (10% polymer by volume), and for polyvinyl chloride plasticized with dimethylthianthrene (40% polymer by volume). Dynamic mechanical measurements on the polyvinyl chloride-dimethylthianthrene compositions are compared with dielectric measurements at the same temperatures and frequencies previously reported for these concentrations by Fitzgerald and Miller (10,11).

GENERAL METHOD

The transducer method measures mechanical impedance in terms of electrical circuit elements, ideally in terms of electrical resistance and capacitance. A rigid tube with coils wound around the ends is suspended by eight fine wires so that it is free to move axially as shown in Fig. 1. If coil 1 is in a radial magnetic field of uniform and constant flux density B_1 whose direction is perpendicular to the wire in the coil, then an alternating current $i_1 = I_m \sin \omega t$ passed through the coil will cause a force $f = F_m \sin \omega t$ to be exerted on the coil given by f (newtons) $= B_1 l_1 i_1$ (webers/m.², meters, amperes) where l_1 is the length of wire in coil 1. The tube will consequently oscillate with an instantaneous velocity, v (meters/sec.) $= V_m \sin (\omega t + \theta) = f/Z_M^0$ where Z_M^0 is the mechanical impedance arising from the mass of the tube and coils and θ is the phase shift due to Z_M^0 . If coil 2 is similarly in a magnetic field of flux density B_2 , then the open circuit voltage generated in coil 2 due to the motion of the tube is e_2 (volts) $= B_2 l_2 v$ (webers/m.², meters, meters/sec.). Combining these relationships we obtain the fundamental expression for a double transducer

$$Z_M^0 = f/v - (B_1 l_1)(B_2 l_2) i_1 / e_2, \quad [1]$$

which gives the mechanical impedance in terms of an electrical transfer admittance $Y_{12} = i_1/e_2$. It is tacitly assumed in Eq. [1] that the coils are

securely fastened to the tube and that the entire unit is rigid⁴ so that it moves with a single velocity, \mathbf{v} . The voltage induced in coil 2 due to mutual inductance between the coils also has been assumed small compared to the motional e.m.f.⁴; this will not be true for stiff samples or high frequencies unless provision is made for eliminating the effective mutual inductance between coils. The manner in which this difficulty is overcome will be discussed in the section on electrical measuring circuits.

The motion of the driving tube can be modified by introducing a sample of viscoelastic material between the tube and a fixed or heavy inner core as shown in Fig. 2. The total mechanical impedance opposing

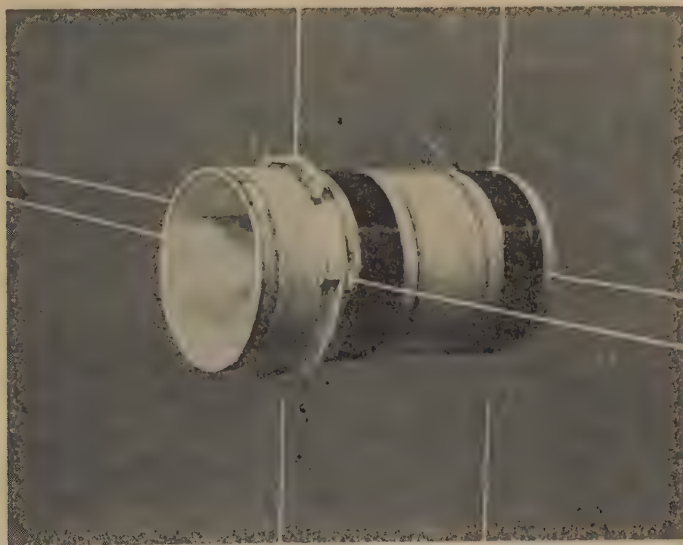


FIG. 1. Typical driving tube: device for transmitting shearing stress to samples in transducer. Driving coils 1A (left) and 2A (right) are placed in radial magnetic fields and alternating currents passed through the coils.

the applied force is then $\mathbf{Z}_M = \mathbf{Z}_M^0 + \mathbf{Z}_M'$ where \mathbf{Z}_M' is the mechanical impedance of the sample, the components of which may be functions of frequency and temperature, and \mathbf{Z}_M^0 is the mechanical impedance presented by the driving tube alone. Thus \mathbf{Z}_M' can be determined by measurements made with and without a sample, \mathbf{Z}_M and \mathbf{Z}_M^0 being derived from the measured complex ratio $\mathbf{i}_1/\mathbf{e}_2$ and a known value of $B_1 l_1 B_2 l_2$. From the value of mechanical impedance \mathbf{Z}_M' and a knowledge of sample dimensions, a complex dynamic viscosity $\eta^* = \eta' - i\eta''$ or a complex dynamic

⁴ The transducer of Marvin, Fitzgerald, and Ferry (3) had no provision for eliminating mutual inductance between coils, and in addition had a mechanical resonance in the driving tube itself at 3000 cycles/sec., making measurements with stiff samples or at high frequencies in error.

rigidity $G^* = G' + iG''$ can be calculated for the material tested. Thus if a thin disk-shaped sample of cross-sectional area A and thickness h is sheared between the tube and inner core (cf. Fig. 2) we have⁵ $\eta^* = Z_M' h/A$; or, since $G^* = i\omega\eta^*$, $G^* = i\omega Z_M' h/A$. The mechanical properties of a viscoelastic material can, of course, be represented equally well by the reciprocals of rigidity and viscosity, i.e., a complex compliance $J^* = J' - iJ''$ or a complex fluidity $\mu^* = \mu' + i\mu''$.

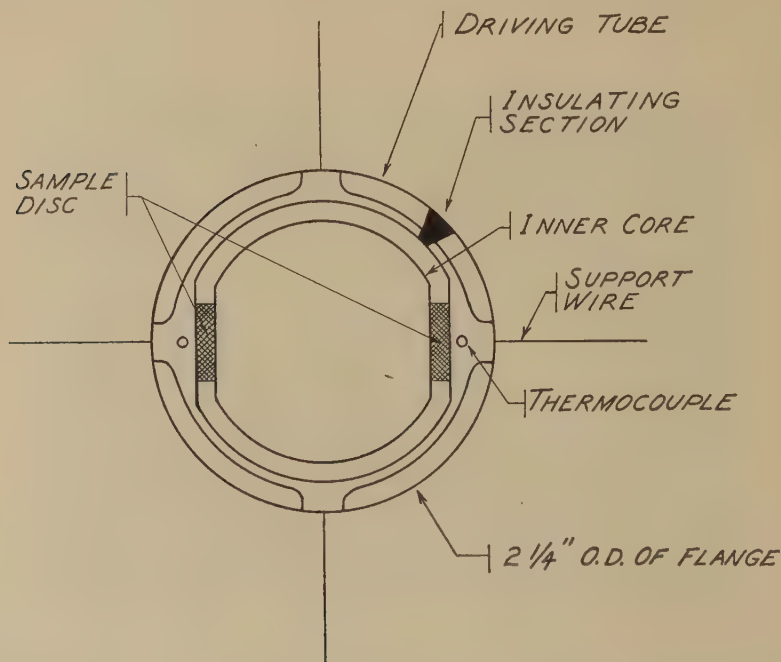


FIG. 2. End view of typical driving tube showing position of samples. The driving tube oscillates perpendicularly to the plane of the page.

ELECTRICAL CIRCUIT FOR TRANSDUCER MEASUREMENTS

Mechanical impedance is measured by the electrical circuit shown in Fig. 3. One of the transducer driving coils (2A) is placed in the arm of a bridge where it acts as an impedance Z_2' , while the other driving coil (1A) in series with a resistance R_A parallels the bridge circuit. For a particular setting of C_4 and R_3 the bridge is balanced by adjusting R_1 and C_1 ; and at balance $Z_2' = Z_3 Z_1 / Z_4$. The dynamic impedance Z_2' will equal the

⁵ This relationship holds if the sample is thin enough so that only simple shear takes place. For thicker samples the effect of constraints on the sample surfaces together with bending effects or bulging due to static compression may alter this expression. A detailed discussion of the effect of sample dimensions is given in a subsequent section.

(vector) sum of the stationary or intrinsic impedance Z_2^0 of coil 2A and an effective impedance E_2/I_2 where E_2 is the back e.m.f. generated as a result of the motion of coil 2A in the magnetic field. Thus, $Z_2' = Z_2^0 - (E_2/I_2)$ and since $E_2 = B_2 l_2 V$ where V is the velocity of the driving tube we have

$$Z_2' = Z_2^0 - (B_2 l_2 V / I_2). \quad [2]$$

Now $V = F/Z_M$ where F is the total applied force and Z_M is the total mechanical impedance presented by the moving system so that $Z_2' = Z_2^0 - (B_2 l_2 F / Z_M I_2)$. In turn, F is the (vector) sum of the forces on coil 1A and coil 2A given by $F = B_1 l_1 I_1 + B_2 l_2 I_2$; or if we let $B_1 l_1 = K_1$, $B_2 l_2 = K_2$, and $K_1/K_2 = a$, the force is $F = K_2 (a I_1 + I_2)$ so that the dynamic electrical impedance (Eq. [2]) becomes

$$Z_2' = Z_2^0 - [K_2^2 (a I_1 / I_2 + 1) / Z_M] \quad [3]$$

and, replacing the complex ratio I_1/I_2 by r , the final form of the expression is

$$Z_2' = Z_2^0 - [K_2^2 (1 + ar) / Z_M]. \quad [4]$$

The impedance Z_2' therefore depends on Z_M and r , since Z_2^0 , a , and K_2^2 are all constants of the apparatus (although Z_2^0 will vary with temperature). The current ratio, r , can be determined from the values of R_A and R_3 , since when the bridge is balanced

$$\begin{aligned} I_1 &= E / (R_A + Z_1'), \\ I_2 &= E / (R_3 + Z_2'), \end{aligned}$$

where Z_2' and Z_1' are the dynamic electrical impedances of coils 2A and 1A, respectively. This gives for r

$$r = I_1/I_2 = (R_3 + Z_2') / (R_A + Z_1').$$

R_3 and R_A are known, and $Z_1' \cong Z_2'$ can be found from the bridge balance. However in practice R_3 and R_A are made very large compared to Z_2' and Z_1' , so that the approximation $r = R_3/R_A$ is valid. From Eq. [4] it is apparent that the mechanical impedance can be found from the expression $Z_M = -K_2^2 (1 + ar) / (Z_2' - Z_2^0)$. However, this method is not satisfactory because of the difficulty of obtaining reliable values for the intrinsic impedance Z_2^0 at all frequencies and temperatures.

This difficulty and the necessity of making a series of separate measurements with the driving tube "clamped"⁶ can be avoided as follows. The electrical impedance Z_2' is measured for two values of the ratio r and the mechanical admittance (and hence impedance) is found from

⁶ From Eqs. [2] and [3] for the clamped case ideally $V = 0$ or $Z_M = \infty$ so $Z_2' = Z_2^0$. In practice, absolute clamping is difficult to achieve, particularly at high frequencies, without introducing extraneous effects due to mechanical coupling with the main body of the apparatus.

the difference between the electrical impedances:

$$\begin{aligned}(\mathbf{Z}_2')_1 &= \mathbf{Z}_2^0 - K_2^2(1 + ar_1)\mathbf{Y}_M, \\ (\mathbf{Z}_2')_2 &= \mathbf{Z}_2^0 - K_2^2(1 + ar_2)\mathbf{Y}_M,\end{aligned}$$

and subtracting

$$\mathbf{Z}_{12} = \mathbf{Y}_M K^2 = [(\mathbf{Z}_2')_1 - (\mathbf{Z}_2')_2]/(r_2 - r_1), \quad [5]$$

where $aK_2^2 = K^2$ and $\mathbf{Y}_M = 1/\mathbf{Z}_M$.

In terms of the bridge components (cf. Fig. 3) this gives

$$\mathbf{Z}_{12} = \frac{(R_3 \mathbf{Z}_1 / \mathbf{Z}_4)_1 - (R_3 \mathbf{Z}_1 / \mathbf{Z}_4)_2}{(R_3 / R_A)_2 - (R_3 / R_A)_1} \quad [6]$$

The current ratio can be varied by changing either R_3 or R_A or both, but keeping them large compared to the dynamic electrical impedances of coils 2A and 1A. For the special case where the current ratio is changed by varying R_A only,

$$\mathbf{Z}_{12} = \frac{(\mathbf{Z}_1 / \mathbf{Z}_4)_1 - (\mathbf{Z}_1 / \mathbf{Z}_4)_2}{(1/R_A)_2 - (1/R_A)_1} \quad [7]$$

giving a determination independent of the value of R_3 . This is essential at high frequencies where the large value of R_3 ($\sim 10^5$ ohms) makes its shunt capacitance, C_3 ($\sim 10 \mu\text{f.}$), of considerable importance giving an impedance, \mathbf{Z}_3 , instead of a simple resistance. Equation [7] determines \mathbf{Z}_{12} independently of any knowledge of \mathbf{Z}_3 .

An alternative is to measure \mathbf{Z}_2' with \mathbf{E}_2 reversed keeping r constant. Reversing \mathbf{E}_2 will change the applied force, since \mathbf{F}_1 will then be opposed instead of aided by \mathbf{F}_2 , i.e., $\mathbf{F} = \mathbf{F}_1 - \mathbf{F}_2$ and Eq. [4] becomes as shown in [4a].

$$(\mathbf{Z}_2')_+ = \mathbf{Z}_2^0 - [K_2^2(ar + 1)/\mathbf{Z}_M], \quad [4]$$

$$(\mathbf{Z}_2')_- = \mathbf{Z}_2^0 + [K_2^2(ar - 1)/\mathbf{Z}_M]. \quad [4a]$$

Subtracting [4] from [4a] we have

$$\mathbf{Z}_{12} - K^2/\mathbf{Z}_M = [(\mathbf{Z}_2')_- - (\mathbf{Z}_2')_+]/2r,$$

and since R_3 is unchanged

$$\mathbf{Z}_{12} = [(\mathbf{Z}_1 / \mathbf{Z}_4)_- - (\mathbf{Z}_1 / \mathbf{Z}_4)_+]R_A/2. \quad [8]$$

The impedance ratio $\mathbf{Z}_1/\mathbf{Z}_4$ appearing in Eqs. [6]–[8] is given by $\mathbf{Z}_1/\mathbf{Z}_4 = P + iQ$ where $P = \alpha R_1 \omega C_4 / (1 + \alpha^2)$ and $Q = R_1 \omega C_4 / (1 + \alpha^2)$; $\alpha = \omega R_1 C_1$ and $\omega = 2\pi \times \text{frequency}$. For maximum precision the differences in dynamic electrical impedance should be as large as possible and this can be accomplished by making the differences in r large (Eq. [5]) or R_A small⁷ (Eq. [8]).

⁷ However, R_A must be large compared to the dynamic electrical impedance \mathbf{Z}_1' of coil 1A or alternatively \mathbf{Z}_1' must be known. In practice R_A is selected to be at least 100 times as large as either the real or imaginary part of \mathbf{Z}_1' , and \mathbf{Z}_1' is neglected.

So far no detailed mention has been made of the effect of mutual inductance between coils 1A and 2A. Since the coils are coaxial, only 1.75 in. apart, and surround a soft iron core, it is clear that considerable coupling will exist, and serious interference can arise from this quarter whenever the motional e.m.f. generated in coil 2A is small compared to the e.m.f. of mutual inductance. To remove this difficulty a third, shielding coil 1B, wound on the inside of a coil form, is placed immediately around coil 1A, but not touching it. This shielding coil is cemented to the pole piece while 1A is, of course, free to oscillate with the suspended driving tube. The shielding coil is matched as nearly as possible to the driving coil 1A, but because of the slight difference in diameter and environment of the two coils, it is impossible to match their inductances exactly at all

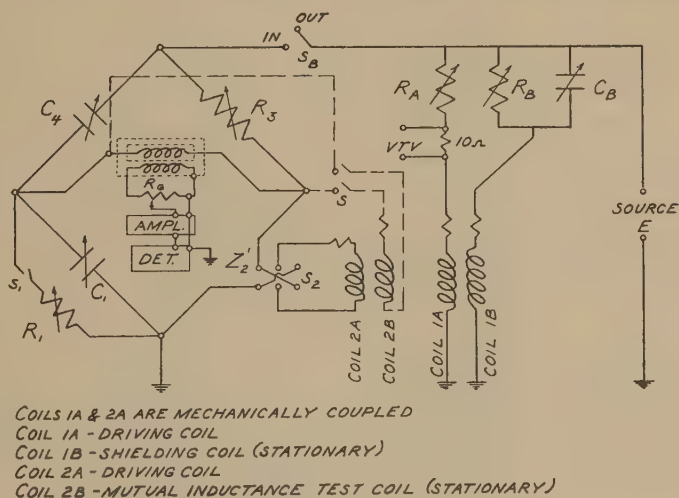


FIG. 3. Electrical circuit for measuring mechanical impedance.

frequencies. Therefore the shielding coil is placed in parallel with driving coil 1A (cf. Fig. 3) and the current through it adjusted in phase and magnitude until $I_A Z_{t^a} = I_B Z_{t^b}$ where Z_{t^a} is the transfer impedance between coils 1A and 2A, and Z_{t^b} is the transfer impedance between coils 1B and 2A. Then the induced e.m.f. in coil 2A is $E_i = I_A Z_{t^a} - I_B Z_{t^b} = 0$. In order to know when I_B has been adjusted to the proper value, a fourth, stationary coil 2B is placed on the inside of a coil form just outside of coil 2A. With the bridge circuit open (S_B out) and coil 2B placed across the detector (S closed) R_B and C_B are adjusted to give zero output in coil 2B. The assumption is made that when there is zero induced voltage in coil 2B there will be likewise no induced voltage in 2A because of their nearly identical locations. This adjustment is made at each frequency before determining Z_2' .

The resistance R_1 is composed of five General Radio⁸ type 510 decade resistors (0.1 to 10,000 ohms); C_1 is made up of three General Radio type 380 decade capacitors and a type 848B 1100- $\mu\text{mf.}$ variable air capacitor; C_4 is a type 848B 1100- $\mu\text{mf.}$ variable air capacitor with a National⁹ 500-division vernier dial to allow exact resetting; while R_3 is made up of three General Radio type 510 decade resistors (10^3 to 10^6 ohms) and R_A consists of four type 510 decade resistors (10 to 10^5 ohms). The bridge components were calibrated by the direct substitution method at 1000 cycles/sec. and did not differ by more than 1% from the rated values.

The source is a McIntosh¹⁰ model 20w 20-w. power amplifier driven by a General Radio type 1304-A beat-frequency oscillator. A current of 10 ma. can be supplied to each of the coils 1A and 1B with less than 1% distortion in the frequency range 20 to 20,000 cycles/sec.

A General Radio type 578 shielded transformer is used to isolate the bridge from the detector, which consists of a Ballantine¹¹ model 220 decade amplifier and a General Radio type 760A sound analyzer. To avoid overloading when the bridge is far off balance, a 200,000-ohm resistor R_G is used as a potential divider across the output of the bridge transformer to allow regulation of the unbalanced voltage supplied to the amplifier. The current through driving coil 1A is read from a Ballantine model 302A vacuum-tube voltmeter placed across a 10-ohm resistor in series with R_A .

DESCRIPTION OF TRANSDUCER

The material tested is subjected to a sinusoidal shearing stress in the electromagnetic transducer shown in cross section in Fig. 4. Two sample disks of nearly identical dimensions are pressed outward from a stainless steel floating (suspended) mass against the inside flat sections of the dural driving tube (cf. Fig. 2). Enough compression is applied to prevent slipping between the sample and the driving tube or the suspended mass. This is done with a stainless steel micrometer head¹² which pushes a tapered extension rod through the floating mass forcing out two $\frac{3}{4}$ -in. diameter cylinders at right angles to the axis of travel. The assembly is calibrated to give the perpendicular travel of the cylinders in terms of the micrometer setting so that sample thicknesses can be measured to within ± 0.001 in., but more accurate values (± 0.01 mm.) are obtained by observations with a traveling telescope.¹³ The cylinders can be locked in

⁸ General Radio Co., Cambridge, Mass.

⁹ National Company, Inc., Malden, Mass.

¹⁰ McIntosh Engineering Laboratory Inc., Binghamton, N. Y.

¹¹ Ballantine Laboratories, Inc., Boonton, New Jersey.

¹² Made to order of nonmagnetic stainless steel by the Brown and Sharpe Co., Providence, R. I.

¹³ Using a Gaertner M-340 micrometer slide, Gaertner Scientific Corp., Chicago, Illinois.

place by stainless steel set screws which force brass pins against them, allowing removal of the micrometer head and tapered rod. Two 3/16-in. diameter phosphor bronze extension springs pull the cylinders in to release pressure on the samples and force the extension rod out as the micrometer is backed off. For tacky samples it is usually necessary to insert a thin pry between the sample and driving tube to allow the springs to collapse the cylinders.

The driving tube has the two coils 1A and 2A cemented to it and transmits the actual shearing stress to the samples. There are four major considerations in its design: (a) The mass of the tube and coils should be

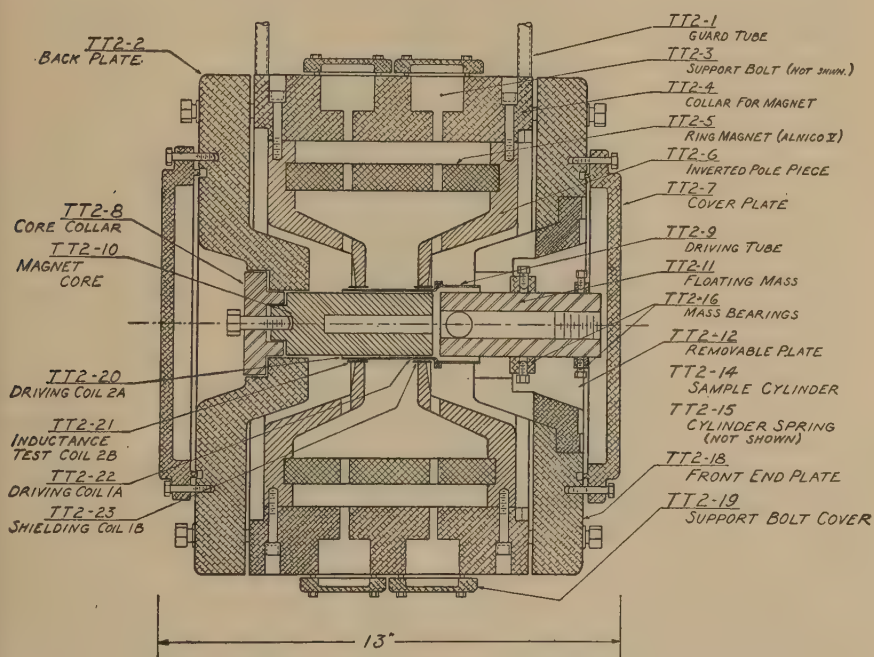


FIG. 4. Cross section (side view) of transducer apparatus.

as small as possible; (b) the entire unit must be rigid; (c) large variations in temperature (-50 to $+150^{\circ}\text{C}.$) must be withstood without distortion or softening; and (d) provision must be made to prevent the presence of any but the motional e.m.f. in coil 2A. The last has already been discussed; the others are met by winding driving coil 1A on a split dural form $2\frac{1}{2}$ in. long with a minimum wall thickness of 0.010 in., and driving coil 2A on a nonconducting section made up of layers of paper and polyvinyl butyral cement¹⁴ extending $1\frac{1}{4}$ in. beyond the metal section. The nonconducting form is essential for coil 2A to prevent interference from

¹⁴ Snyderweld or Plastalock 500, B. F. Goodrich Co., Akron, Ohio.

eddy currents, while the metal section is split to prevent a short circuit in the magnetic field. This tube has a total mass of 33.191 g. and shows no fundamental mechanical resonance below 50,000 cycles/sec. The driving coils 1A and 2A are $\frac{1}{2}$ in. wide and are wound with two layers of No. 36 and No. 34 B. & S. gage enameled copper wire, respectively. The non-conducting section butts up to and overlaps the metallic section by $\frac{1}{2}$ in. and is formed and cured separately and then cemented to the dural section. Finally, the coils are wound and cemented, and the entire unit is cured at 150° for 5 hr. The shielding coil 1B and stationary pickup coil 2B are wound on the inside of coil forms and cemented to the pole pieces. When properly centered by adjusting the eight support wire bolts, the clearance between the magnet core and driving tube is 0.020 in. and that between the stationary and moving coils is 0.020 in.

An Alnico V ring magnet 6 in. long with a wall thickness of $\frac{3}{4}$ in. and outside diameter of 9 in. provides the magnetic fields in which the driving coils are located. This magnet was cast in four sections by the Indiana Steel Products Co.,¹⁵ assembled demagnetized with inverted pole pieces, and the entire unit was fitted into an aluminum collar as indicated in Fig. 4. The pole pieces are machined from Armco¹⁶ magnetic ingot iron and designed inverted, i.e., with the ends drawn in to bring the poles of the magnet close together (thus allowing a short driving tube) and yet provide for a long magnet to give a high flux density in the gaps.

Aluminum end plates are bolted to the magnet collar. The back end plate has a hub which fits inside the pole piece and to which is fastened the magnet core. The core is made of Armco ingot iron and has a diameter of 1.80 in. with $\frac{3}{4}$ -in. wide flats along the sides corresponding to similar flat sections on the floating mass; the pole pieces have an inside diameter of 2.00 in. so that the working gap is 0.10 in. and has a nominal flux density of 10,000 gauss.

Cover plates with a tongue and groove gasket joint are used to seal off the ends of the instrument to allow for immersion in a constant-temperature bath. Teflon (polytetrafluoroethylene) gaskets are used for the cover plate seals, and to seal the support bolt caps to the magnet collar. Coil leads and thermocouple wires are brought out through dural tubes.

The complete apparatus, weighing 200 lb., is suspended on four $1\frac{1}{4}$ -in. sections of B. F. Goodrich¹⁷ No. 10 Vibro insulators to isolate it from building vibrations above 20 cycles/sec. A picture of the transducer sealed and in place above the constant-temperature bath is given in Fig. 5.

The volume of each sample is determined from its density and mass,

¹⁵ Indiana Steel Products Co., Valparaiso, Indiana.

¹⁶ Armco Steel Corporation, Middletown, Ohio.

¹⁷ B. F. Goodrich Co., Akron, Ohio.



FIG. 5. Transducer in position above constant-temperature bath.

and the sample coefficient A/h then found by $A/h = \text{volume}/h^2$ where h is the thickness of the sample measured in the apparatus after compression. The bearings which support the floating mass and the magnet core bearing are slotted so that a traveling telescope can be focused on each sample to measure its thickness to 0.01 mm. The telescope is also used to align the sample cylinders (and sample) parallel to the flat sections of the driving tube and to center the floating mass with respect to the driving tube. Since a sample 1 mm. thick can be measured to within 1%, and the volume can be determined to within 0.2%, A/h is known to within 2% or less for samples 1 mm. or more thick. Samples up to 11/16 in. in diameter and $\frac{1}{4}$ in. thick can be used so that A/h values from 25 to 0.25 cm. are obtained.

TEMPERATURE CONTROL AND MEASUREMENT

The constant temperature bath for model TT2 transducer, which can be seen in Fig. 5, is made of stainless steel with four cold pockets and four

500-w. immersion heaters¹⁸ spaced around the outer edge. An outer tank of stainless steel surrounds the bath and the 3-in. space between is filled with Fiberglas insulation. To cover the temperature range from -50 to $150^{\circ}\text{C}.$, two bath liquids are used: a 50:50 gasoline-kerosene mixture (flash point $40^{\circ}\text{C}.$) for temperatures from -50 to $20^{\circ}\text{C}.$ and mineral oil (flash point $196^{\circ}\text{C}.$) for temperatures from 20 to $150^{\circ}\text{C}.$ One cold pocket is filled with Dry Ice and gasoline for temperatures from -50 to $25^{\circ}\text{C}.$, and the bath is heated to the desired temperature by two of the 500-w. heaters operated on-off by a direct-current relay¹⁹ activated by a Fenwal²⁰ type No. 17100 thermoswitch with a 10-in. temperature-sensitive shell. The bath temperature is controlled to within $\pm 0.1^{\circ}\text{C}.$, but because of the large mass of the instrument (90 kg.) the temperature variation within the apparatus is less than $0.05^{\circ}\text{C}.$ The bath liquid is stirred by a 1/12-h.p. Fasco²¹ induction motor driving two 2-in. propellers at 1500 r.p.m. and the propeller shaft is tilted to provide rotation of the liquid around the bath.

The temperature of the driving tube, measured by a two-junction copper-constantan thermocouple (No. 30 B. & S. gage), is taken as the sample temperature after enough time for thermal equilibrium has elapsed. The thermocouple junctions are located in the flat sections of the driving tube less than 0.050 in. from each sample face so that the sample temperature cannot differ much from that indicated. The couple e.m.f. is determined by a Rubicon potentiometer and spotlight galvanometer²² giving readings to within 0.002 mv. corresponding to about $0.03^{\circ}\text{C}.$ for a two-junction couple. The thermocouple was calibrated²³ against a platinum resistance thermometer at five temperatures between -75 and $100^{\circ}\text{C}.$

About 20 min. is required to change the bath temperature $10^{\circ}\text{C}.$, but about 4 hr. is required for the driving tube to reach equilibrium after such a change. This, however, is an inherent characteristic to be expected of the suspended system which is deliberately isolated mechanically from the body of the apparatus.

DETERMINATION OF THE TRANSDUCER CONSTANT, K^2

The mechanical admittance of the transducer system can be related to the electrical impedance Z_{12} , defined as in Eq. [5], i.e., $Z_{12} = \mathbf{Y}_M K^2$, but to find \mathbf{Y}_M the value of K^2 must be known. Since $K^2 = K_1 K_2 = B_1 l_1$

¹⁸ Type TMO, Edwin L. Wiegand Co., Pittsburgh, Pa.

¹⁹ American Instrument Co., Silver Spring, Md.

²⁰ Fenwal Inc., Ashland, Mass.

²¹ F. A. Smith Mfg. Co., Rochester, N. Y.

²² Rubicon Co., Philadelphia, Pa.

²³ The calibration was done with the help of L. D. Grandine, Jr.

$B_2 l_2$, this constant in theory could be determined from the length of wire on coils 1A and 2A and measured values of B_1 and B_2 if a uniform flux density existed throughout the regions where the coils are located. In practice, however, this is not the case, as the $\frac{1}{2}$ -in. wide coils are located under $\frac{1}{4}$ -in. thick pole pieces, and an experimental value of K^2 must be found.

This is readily accomplished if the driving tube system (without a sample) can be represented by the mechanical circuit of Fig. 6. Then the total mechanical impedance of the moving system is $Z_M^0 = R_M^0 + i(\omega m - S_M^0/\omega)$ where m is the mass of the coils and tube, S_M^0 is a small elastance contributed by the eight support wires, and R_M^0 is a small

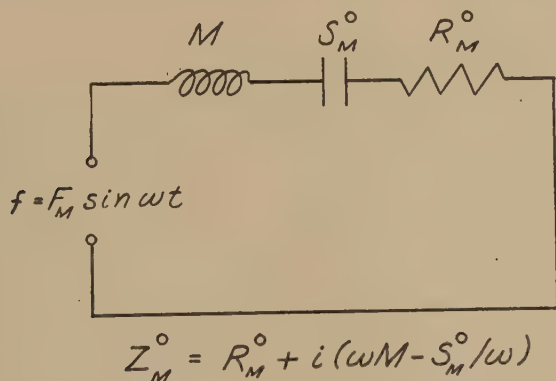


FIG. 6. Mechanical circuit diagram for transducer without sample.

residual mechanical resistance due to stretching of the support wires and air resistance. The mechanical admittance is

$$Y_M = \frac{R_M^0}{(R_M^0)^2 + (\omega m - S_M^0/\omega)^2} - i \frac{\omega m - S_M^0/\omega}{(R_M^0)^2 + (\omega m - S_M^0/\omega)^2}. \quad [9]$$

The real and imaginary parts of this expression can be related to the real and imaginary parts of the complex electrical impedance Z_{12}^0 (which is the experimental quantity directly determined) by Eq. [5] giving

$$R_{12}^0 = K^2 R_M^0 / [(R_M^0)^2 + (\omega m - S_M^0/\omega)^2]$$

and

$$X_{12}^0 = -K^2 (\omega m - S_M^0/\omega) / [(R_M^0)^2 + (\omega m - S_M^0/\omega)^2],$$

where

$$Z_{12}^0 = R_{12}^0 + iX_{12}^0.$$

Examination of Eq. [9] reveals that a resonance will occur when $\omega = (S_M^0/m)^{\frac{1}{2}}$, at which frequency $X_{12} = 0$ and R_{12}^0 passes through a maximum; $(R_{12}^0)_{\max} = K^2/R_M^0$. At frequencies beyond this maximum,

values of R_{12} and X_{12} should asymptotically approach zero owing to the presence of ωm in the denominator. Actual values of Z_{12}^0 for the driving tube ($m = 33.191$ g.) are given in Fig. 7. R_{12}^0 reaches a value of 24 ohms (not shown) at 25 cycles/sec., but there is no indication of a maximum so it can be surmised only that the resonant frequency is less than 25 cycles/sec.

A small unpredicted resonance appears at 10,000 cycles/sec.²⁴ where the value of R_{12}^0 passes through a minimum of -1.26 ohms. The probable

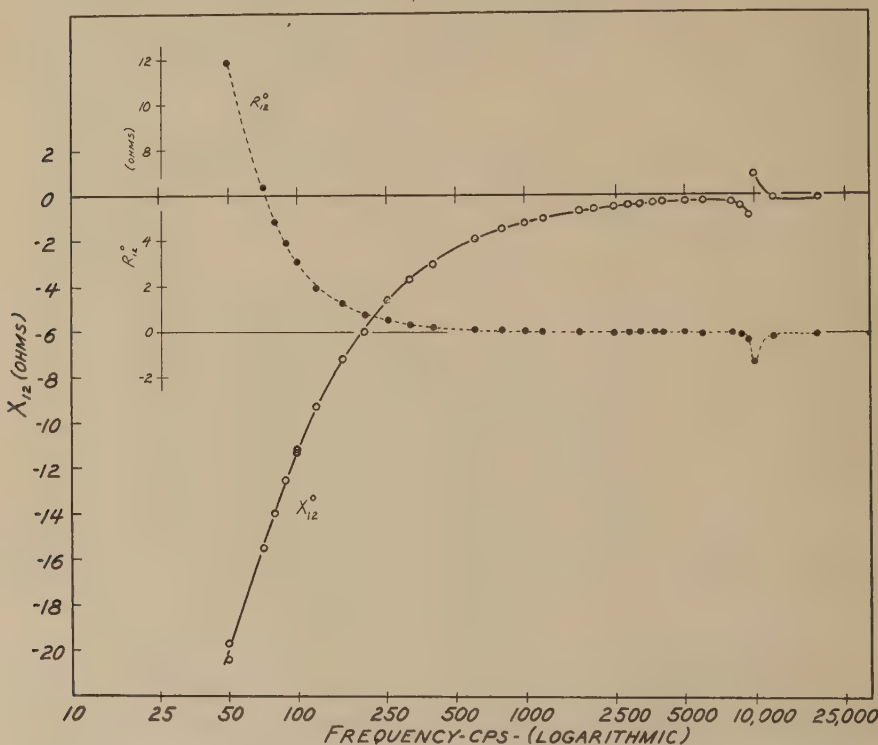


FIG. 7. Variation of Z_{12}^0 (proportional to mechanical admittance) with frequency for driving tube without sample. The curves should asymptotically approach zero at high frequencies.

origin of this extraneous resonance will be discussed later with main attention now directed toward the frequency range from 25 to 5000 cycles/sec.

It is convenient to use the electrical admittance $Y_{12}^0 = 1/Z_{12}^0$ for the actual determination of K^2 , for then $Y_{12}^0 = Z_M^0/K^2$ or $G_{12}^0 = R_M^0/K^2$ and $B_{12}^0 = (\omega m - S_M^0/\omega)/K^2$ where $Y_{12}^0 = G_{12}^0 + iB_{12}^0$. For values of ω

²⁴ For frequencies above 7500 cycles/sec. a vacuum-tube voltmeter is used as detector.

much above the resonant frequency the contribution of S_M^0/ω will rapidly diminish so the expression for B_{12}^0 becomes very nearly

$$B_{12}^0 = \omega m / K^2 \quad [10]$$

and K^2 is determined from the measured values of B_{12}^0 and known values of ω and m . The validity of the approximation of [10] can easily be tested by plotting B_{12}^0 vs. ω which should give a straight line of slope m/K^2 . Such a straight line is obtained from 25 to 2500 cycles/sec. and a constant

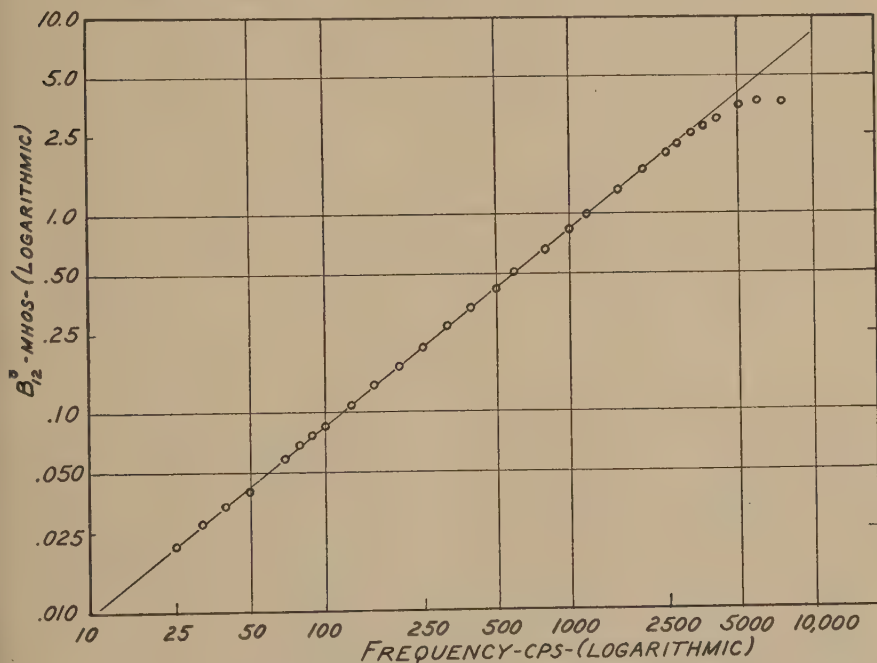


FIG. 8. Variation of B_{12}^0 with frequency. Experimental points should be on the solid line drawn with a slope of 1.

value of $K^2 = 2.50 \times 10^5$ ohms dyne-sec./cm. calculated from the slope.²⁵ Above 2500 cycles/sec. the observed values of B_{12}^0 begin to curve downward as a result of the interference of the 10,000 cycles/sec. resonance. This departure from linearity might be attributed to a variation in K^2 but a plot of $\log B_{12}^0$ vs. $\log \omega$ which should give a slope of 1 independent of the value of K shows this same deviation (see Fig. 8). The mechanical resistance R_M^0 has a constant value of 5.5×10^2 dyne-sec./cm. (corre-

²⁵ Without making any assumptions about the importance of the S_M^0/ω term it is possible to determine K^2 by plotting ωB_{12}^0 vs. ω^2 . Since $\omega B_{12}^0 = (\omega_m^2 - S_M^0)/K^2$ this will give a straight line of slope m/K^2 and intercept S_M^0/K^2 . The same value of 2.50×10^5 is obtained for K^2 using this procedure.

sponding to $G_{12}^0 = 0.022$ mho) up to about 1000 cycles/sec., above which it decreases and becomes negative.

Measurements without a sample were made at 25, 50, 75, 100, and 125°C., revealing no variation of K^2 with temperature.

At the outset the extraneous resonance found at 10,000 cycles/sec. might reasonably be attributed to compliance in the driving tube unit, slipping of the driving coils, or some associated phenomena. However, the identical resonance was observed for seven widely different driving tubes used in evolving the design of the tube now in use, and it seems unlikely, therefore, that it is a driving tube characteristic. A probable explanation is that a resonant frequency of some part of the surrounding apparatus is reached at 10,000 cycles/sec. and the driving tube motion modified through acoustic coupling between the tube and the main body of the

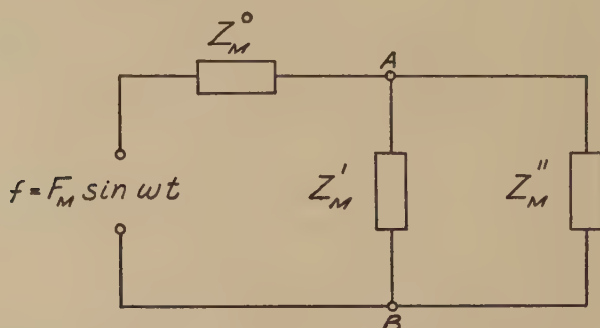


FIG. 9. Mechanical circuit diagram for transducer with sample. Z_M^0 is the mechanical impedance of driving tube and support wires; Z_M' is the mechanical impedance of the sample; Z_M'' is mechanical impedance of the floating mass and its support wires.

apparatus. The result is to introduce a mechanical admittance in parallel with that of the driving tube system and thus modify the apparent mechanical admittance measured as shown in Fig. 7. Since the mechanical impedance of a sample is found by subtracting impedances with and without a sample, this deviation will not affect the results so long as it is relatively small. Because of this spurious resonance, however, measurements cannot be evaluated accurately beyond about 5000 cycles/sec.

DETERMINATION OF SHEAR MODULUS AND COMPLIANCE

In order to avoid mechanical coupling between the driving tube and the body of the transducer, the sample disks are sheared between the tube and a heavy mass as previously noted. The mass is suspended by eight phosphor bronze wires which represent the only connection between it and the bulk of the apparatus. This eliminates the direct introduction of stray resonances but makes it necessary to take into account the effect

of any slight motion of the mass. The mechanical circuit representing the situation is shown in Fig. 9 where, as before, Z_M^0 represents the mechanical impedance of the driving tube and suspension wires, Z_M' is the mechanical impedance of the two sample disks, and Z_M'' signifies the mechanical impedance of the suspended mass (including the bearings) and its support wires. If Z_M is the total measured impedance of the system then the impedance due to the sample and floating mass is

$$Z_{AB} = Z_M - Z_M^0$$

and the mechanical admittance, Y_M' , of the sample is

$$Y_M' = Y_{AB} - Y_M'',$$

where $Y_{AB} = 1/Z_{AB}$ and $Y_M'' = 1/Z_M''$. The admittance of the floating mass, M , is given very nearly by $Y_M'' = -i/\omega M$ and at high frequencies is small. Actual values of Y_M'' to be used at each frequency were determined by cementing the floating mass directly to the driving tube (equivalent to setting $Z_M' = \infty$ in Fig. 9) and measuring the resulting mechanical impedance.

Complex compliance $J^* = J' - iJ''$ is then found from

$$J^* = -iY_M'C/\omega, \quad [11]$$

where C is a coefficient depending on the shape and dimensions of the sample and the complex shear modulus $G^* = G' + iG''$ is determined from $G^* = 1/J^*$. For two samples of constant cross-sectional areas A_1 and A_2 and heights h_1 and h_2 , where the diameter is large compared to the height, this coefficient is simply $C = A_1/h_1 + A_2/h_2$, or, if the samples have identical dimensions, $2A/h$.

CALCULATION OF SAMPLE COEFFICIENT

To prevent slipping between the sample and driving tube or floating mass it is ordinarily necessary to apply a (static) compressive stress which may cause bulging of the sample as shown in Fig. 10. If we assume that this bulge is circular of radius, r , then it can be demonstrated that for samples of thickness h ,

$$\begin{aligned} C &\cong \pi r / \tanh^{-1}(h/2r) \\ &\cong \frac{2\pi r^2}{h} \left/ \left[1 + \frac{1}{3} \left(\frac{h}{2r} \right)^2 + \frac{1}{5} \left(\frac{h}{2r} \right)^4 + \dots \right] \right., \end{aligned} \quad [12]$$

where the bulge is assumed to be such that its center of curvature is located very near the center of the disk-shaped sample, and the two samples are again assumed to have nearly identical dimensions. A more general case can be treated by considering the bulge to be parabolic.

In this case

$$C = \frac{2\pi c^2}{h} \left/ \left[\frac{1}{2(1-h^2/4bc)} + \frac{1}{2} \left\{ 1 + \frac{1}{3} \left(\frac{h}{2\sqrt{bc}} \right)^2 + \frac{1}{5} \left(\frac{h}{2\sqrt{bc}} \right)^4 + \dots \right\} \right] \right], \quad [13]$$

where the vertex of the parabolic bulge is located a distance c from the center of the sample, the latus rectum is b , and h is the thickness of the disk-shaped sample. Whenever $h \ll 2r$ or $h \ll 2\sqrt{bc}$ the coefficient will approach the value of $2A/h$ obtained for a constant cross-sectional area ($A = \pi r^2$ or πc^2).

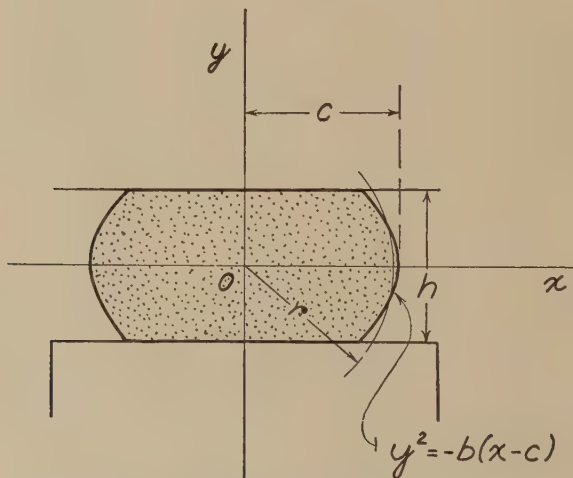


FIG. 10. Cross section of sample showing bulging that may occur due to static compression.

The amount of bulging taking place depends on the adhesion between the sample and the metal parts between which it is compressed and the static rigidity of the sample; the extent to which this will modify the simple value of $C = 2A/h$ is determined by the sample dimensions and the shape of the bulge. In general, for a material which is stiff the compressive stress necessary to prevent slipping of the samples on the parallel metal surfaces between which they are sheared is not enough to produce appreciable bulging. On the other hand a compliant but slippery sample will undergo a uniform increase in cross-sectional area when compressed to compensate for the decrease in thickness, and the coefficient C is given by dividing the volume (assumed constant) by the square of the final thickness. In any case the effect of moderate bulging on the sample

coefficient will be negligible for thin samples of large diameter ($h \ll r$, Eq. [12] or $h \ll c$, Eq. [13]).

The samples used were circular disks varying in (uncompressed) dimensions from 1/32 in. thick and 11/16 in. diameter to 3/16 in. thick and 5/16 in. diameter corresponding to nominal sample coefficients ($C = 2A/h$) of 60.4 cm. and 2.08 cm., respectively. To determine experimentally the extent to which bulging occurs, the sample profile is projected on a large screen and the outline is drawn as the sample is progressively compressed. From this outline suitable parameters for a circular or parabolic bulge are found and the extent to which the sample coefficient deviates from that given by $2A/h$ is estimated.

Values of the sample coefficient at temperatures other than 25°C. were calculated from experimentally determined values of thermal expansion coefficients, assuming that the value of h , fixed by the dimensions of the apparatus, was independent of temperature.

EXPERIMENTAL RESULTS

Dynamic mechanical measurements have been made on samples of polyvinyl chloride (PVC) of weight average molecular weight $63,000 \pm 3000$ combined with dimethylthianthrene (DMT) to give concentrations of 40 and 10% PVC by volume. The sample of 40% PVC by volume²⁶ was formed by mixing PVC powder and DMT on a mill and then molding under pressure for 15 min. at 160°C. This produced a rubbery solid (at room temperature) from which the sample disks for mechanical testing were obtained by punching out samples of the approximate diameter desired and remolding for 10 min. at 130°C. into the exact shape to be used. Measurements were made on three sets of samples whose dimensions were (approximately) 7/16 in. diam. by 1/16 in. thick, 3/8 in. diam. by 1/8 in. thick, and 5/16 in. diam. by 3/16 in. thick, corresponding to nominal sample coefficients when compressed ($C = 2A/h$) of 12.9, 4.52, and 1.68 cm. The 10% PVC concentration was obtained by dissolving PVC powder in DMT at 150°C. This yields a clear gel-like material which is firm enough to maintain a molded shape when cooled to room temperature. The samples used in mechanical testing were poured into molds at 100°C. and then molded under pressure for 10 min. at 140°C. Measurements were made on three sets of samples whose dimensions were (approximately) 11/16 in. diam. by 1/32 in. thick, 3/8 in. diam. by 1/8 in. thick, and 5/16 in. diam. by 3/16 in. thick, corresponding to nominal sample coefficients when compressed of 82.6, 5.08, and 2.42 cm. Effects of thermal history are described subsequently.

²⁶ The polyvinyl chloride powder, liquid dimethylthianthrene, and 40% PVC samples were furnished by the B. F. Goodrich Co. Research Center at Brecksville, Ohio.

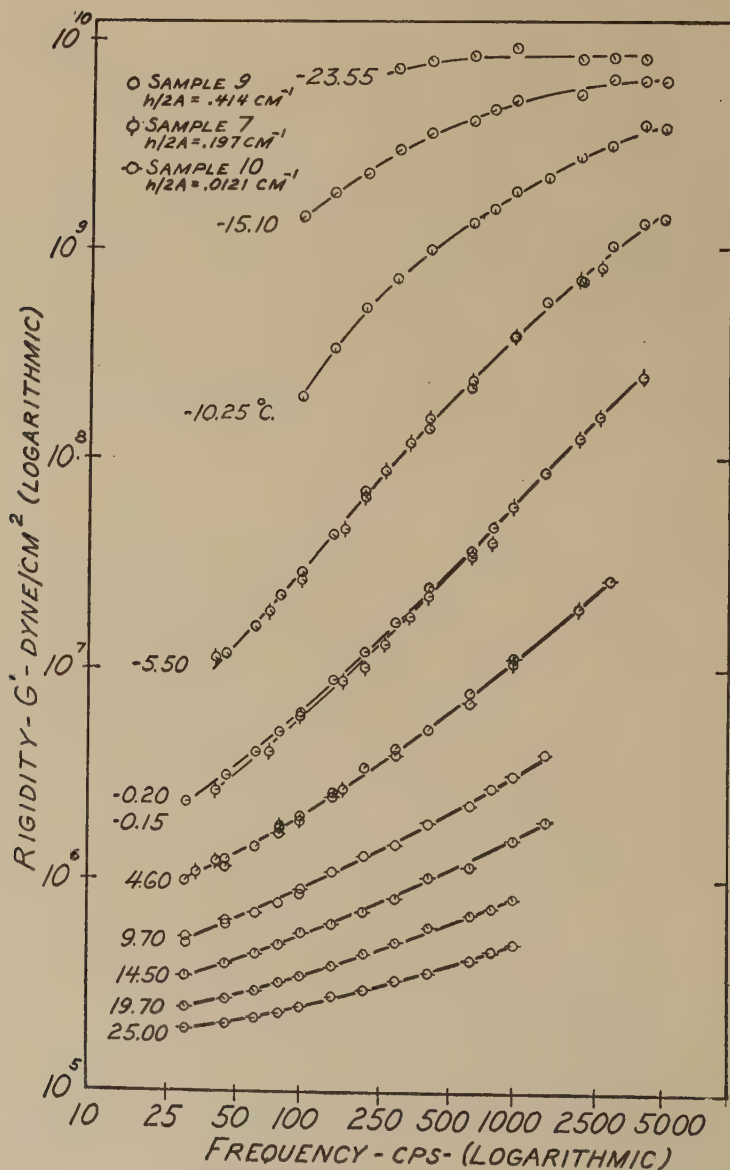


FIG. 11. Variation of the real part of the complex shear modulus, G' , with frequency for a PVC-DMT gel (10% PVC by volume). Results are shown for three sample shapes and at ten temperatures as indicated.

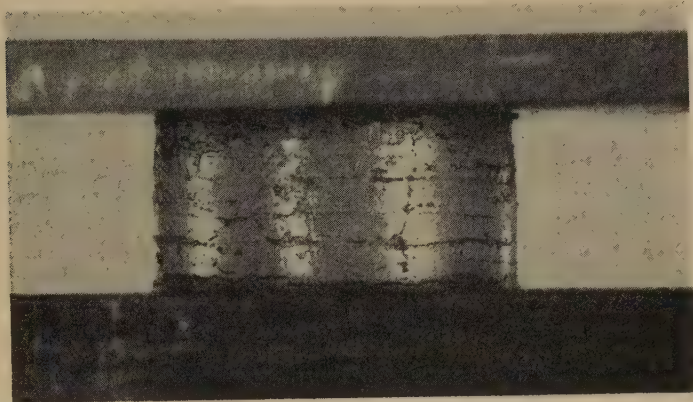


FIG. 12. Photograph of a thick sample of the 10% PVC gel of Fig. 11. Compressed 5%. Note that little bulging takes place.

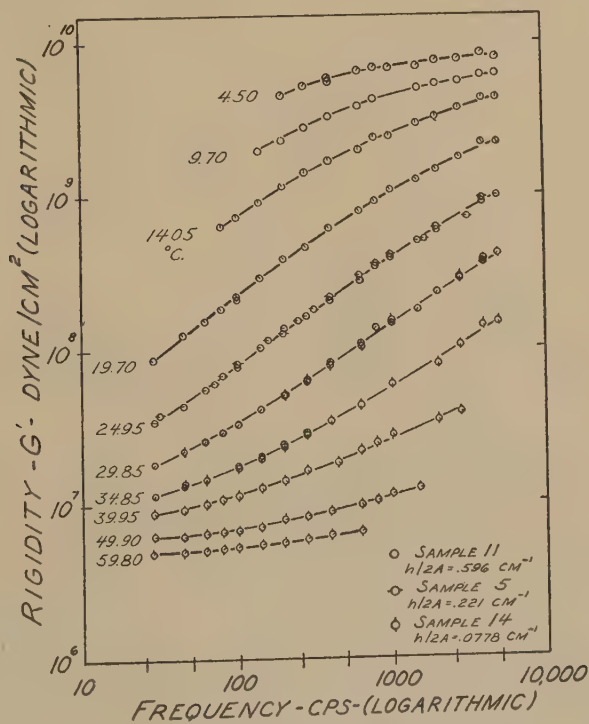


FIG. 13. Variation of the real part of the complex shear modulus, G' , with frequency for a PVC-DMT composition (40% PVC by volume). Results are shown for three sample shapes and at ten temperatures as indicated.

The variation of the real part of the complex shear modulus, G' , with frequency at ten temperatures is given in Fig. 11 for the PVC-DMT gel (10% PVC by volume). Values of G' are seen to be the same for samples of different dimensions, indicating that no bulging occurs (cf. Fig. 12) and that even for the thick sample there is no appreciable error introduced because of bending or constraints on the sample surfaces (which are maintained flat by the metal surfaces between which the sample is sheared). The variation of the real part of the complex shear modulus

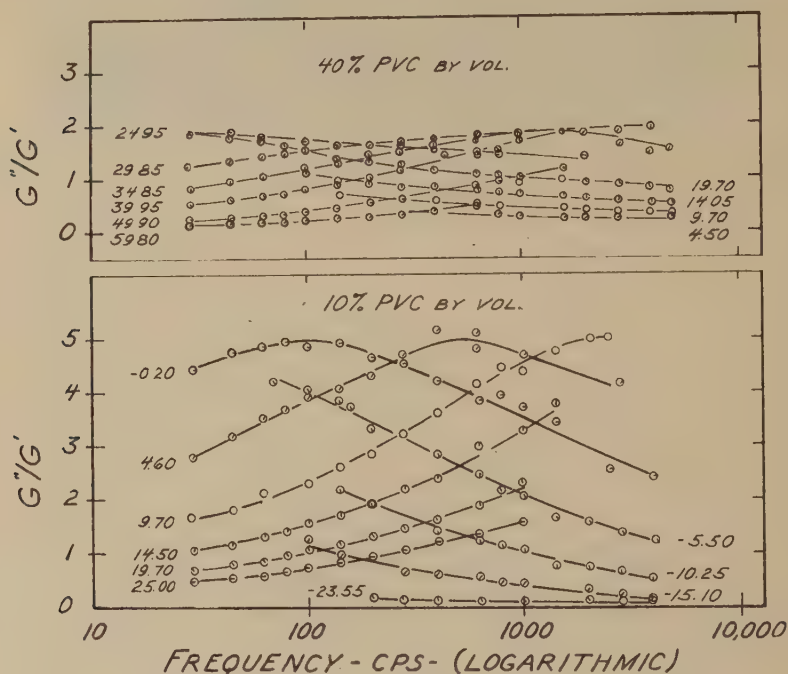


FIG. 14. Variation of mechanical loss tangent ($G''/G' = J''/J'$) with frequency for 10 and 40% (by volume) concentrations of PVC in DMT. Results are shown at ten temperatures for each concentration as indicated.

with frequency at ten temperatures is shown in Fig. 13 for 40% PVC by volume combined with DMT. Values of G' for different sample dimensions are again seen to be the same. The variations of loss tangent G''/G' or J''/J' with frequency are compared for the 10 and 40% PVC concentrations in Fig. 14. The loss tangents pass through maxima which appear to shift regularly with temperature. The response of the material to mechanical stress is indicated by its complex compliance which is analogous to a complex dielectric constant in the electrical case (since the complex dielectric constant is indicative of response to electrical stress);

the variation of the real and imaginary parts of the compliance as a function of frequency and temperature are given in Figs. 15-18 for the 10 and 40% PVC concentrations.

The values of electrical impedance from which the mechanical impedance of the transducer system is found can be determined within 0.5% over the frequency range of 25 to 5000 cycles/sec. This does not mean

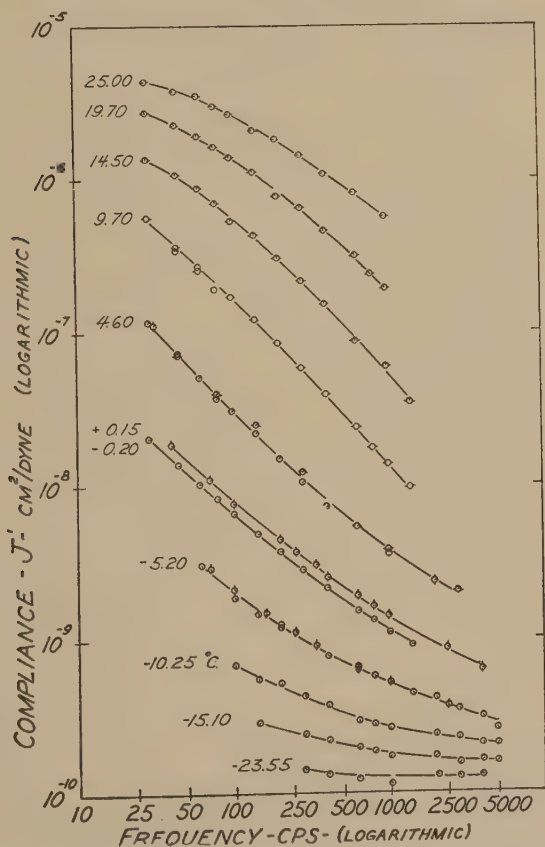


FIG. 15. Variation of the real part of the dynamic shear compliance, J' , with frequency for a PVC-DMT gel (10% PVC by volume). Results are given at ten temperatures as indicated.

that the sample admittance and hence J' and J'' (or G' and G'') are determined with the same precision, however. The sample impedance is found by subtracting the calibration impedance (measured without a sample) from the total mechanical impedance with a sample, and when this difference is small the results are correspondingly uncertain even though each of the quantities involved in the subtraction is known pre-

cisely. Thus at high frequencies, for example, the impedance of the driving tube itself ($\sim \omega m$) may predominate and mask the influence of the sample. This difficulty can be partly overcome by using a stiff sample (thin and of large diameter) although the sample shape is limited by the accuracy with which the thickness can be measured and the size of the driving tube.

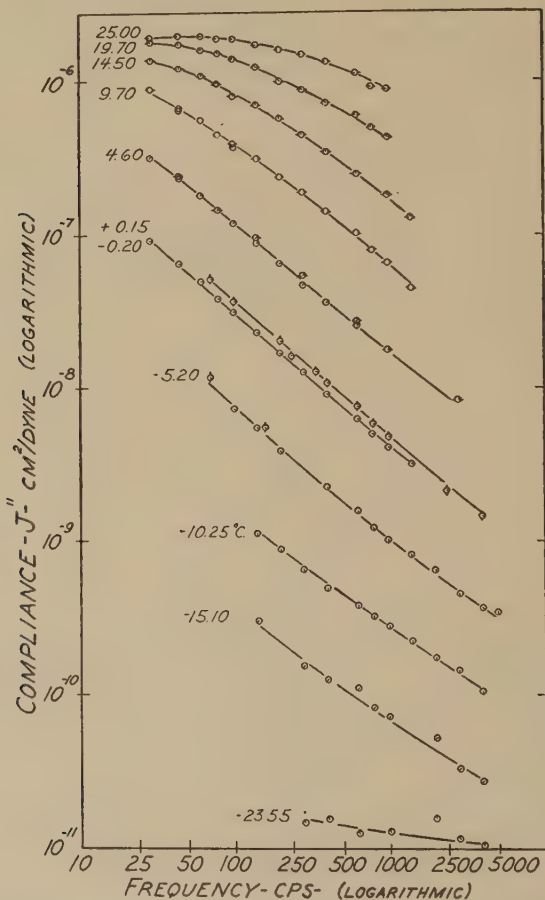


FIG. 16. Variation of the imaginary part of the dynamic shear compliance, J'' , with frequency for the PVC-DMT gel of Fig. 15.

On the other hand, if the sample is too hard or stiff, the floating mass and driving tube will oscillate as a single rigid unit whose motion is independent of the sample properties. This tendency will be partially overcome at high frequencies as the impedance of the floating mass increases ($\sim \omega M$) but can be most effectively taken care of by substituting a softer sample (thick and of small diameter). Therefore, to maintain adequate precision over a range of frequencies and temperatures a series

of sample shapes must be used to provide optimum sample impedances that will be neither too large nor too small. Whenever the differences are so small as to produce an uncertainty of $\pm 2\%$, measurements on a particular sample are discontinued; thus at low temperatures the low frequency values of compliance are not given, while at high temperatures the high frequency compliance values are not shown (cf. Figs. 15-18). In view of the wide range of values of compliance covered ($\sim 10^{-8}$ to 10^{-10} cm.²/dyne), this limitation cannot be considered a serious disadvantage.

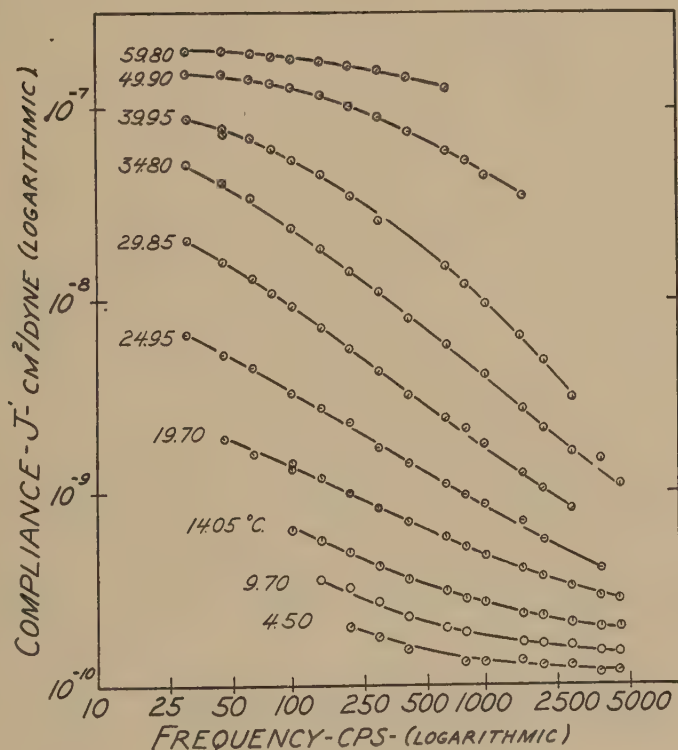


FIG. 17. Variation of the real part of the dynamic shear compliance, J' , with frequency for PVC combined with DMT (40% PVC by volume). Results are given at ten temperatures as indicated.

There is considerable evidence of crystalline structure in polyvinyl chloride (13) and polyvinyl chloride compositions (14) so that there is a possibility of more complex mechanical behavior than that to be expected from a completely amorphous linear polymer. Accordingly, some effort was made to determine the effect of thermal history on the mechanical properties of the two concentrations investigated, although no very thorough study was carried out. Thus after molding for 10 min. at 140°C .

two samples of the 10% PVC-DMT gel were allowed to equilibrate for 20 days at 30°C. before testing, while a third sample (prepared at a different time) was tested within 1 day after molding. The results in both cases were the same (Fig. 11). During the measurements the temperature was lowered in 5-degree steps and in one case was held at 5°C. for three days during which time no change in the mechanical properties was observed.

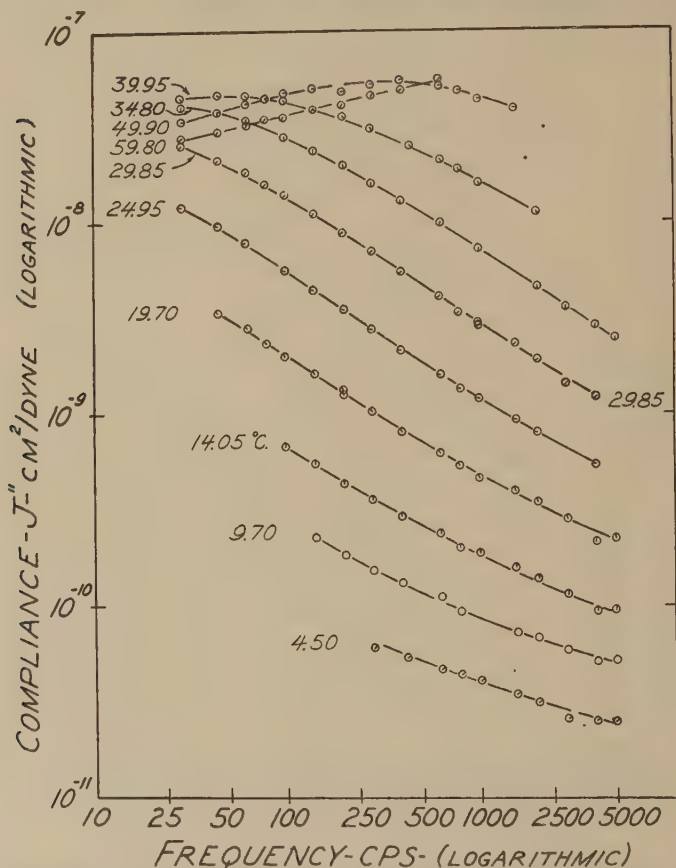


FIG. 18. Variation of the imaginary part of the dynamic shear compliance, J'' , with frequency for the PVC-DMT composition of Fig. 17.

In all cases the values of compliance were redetermined at 25°C. after measurements at lower temperatures were completed (covering a period of 12 days) and found to be the same as those initially determined. From these results it may be inferred that any changes in crystallinity that may occur in this 10% system do not appreciably affect the measured properties, which are probably due only to the amorphous regions.

Samples of the 40% PVC concentration, on the other hand, showed a

change in mechanical properties if kept above about 50°C. for more than a few hours. The three samples for which the results are given were kept at 60°C. for 85 hr. before testing in order to establish a relatively stable proportion of crystalline and amorphous regions. Measurements were then made as the temperature was lowered from 25 to 5°C. After the 5°C. run the measurements at 25°C. were repeated and found to be the same as those initially determined. The temperature was then raised in steps to 60°C. to obtain the data above 25°C; values of compliance subsequently redetermined at 25°C. were found to be about 5–7% higher and the shape of the log J' vs. log frequency curve slightly different. Thus addi-

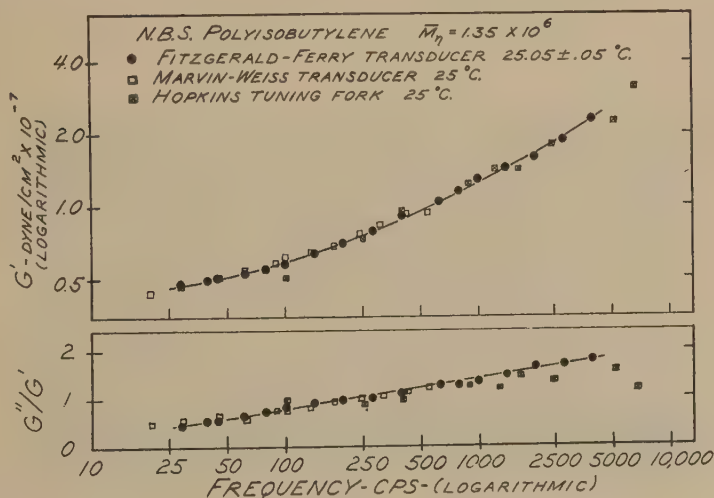


FIG. 19. Variation of the real part of the dynamic rigidity, G' , and the mechanical loss tangent, G''/G' , with frequency for a National Bureau of Standards sample of polyisobutylene at 25°C. $\bar{M}_\eta = 1.35 \times 10^6$. Results are compared with those obtained by Marvin and Weiss, and Hopkins for this same material.

tional changes in the structure must have taken place while at higher temperatures.

There are no mechanical measurements on PVC-DMT systems with which the results shown in Figs. 15–18 can be compared, but there are data on polyisobutylene (PIB) taken in connection with the cooperative program of dynamic testing inaugurated by the National Bureau of Standards (8). The variation of G' and G''/G' with frequency at 25°C. is compared in Fig. 19 with values²⁷ obtained by R. S. Marvin and F. Weiss and by I. L. Hopkins for this PIB (viscosity average molecular weight 1.35×10^6). Experimental values of G' and G''/G' found by the method described here are about the same but show less scatter than

²⁷ These data were kindly furnished by Dr. R. S. Marvin, Rubber Section, National Bureau of Standards, Washington, D. C.

those furnished by the National Bureau of Standards. While nominal sample coefficients gave identical results for samples of PIB 1/32 and 1/16 in. thick, samples 1/8 in. or thicker showed considerable bulging when compressed 10% (cf. Fig. 20), making necessary the calculation of the sample coefficient, C , according to Eq. [13]. The corrected value was about 13% lower than that obtained if bulging is ignored, and with this taken into account, all sample shapes gave the same results, as shown in Fig. 19.

All of the measurements described were made under conditions yielding very small shearing strains. Actually measurements were made with the driving force (determined chiefly by the current through driving coil 1A) essentially constant so that for the different sizes of samples used and the different frequencies at which measurements were made the shear



Fig. 20. Thick sample of polyisobutylene compressed 8%.
Note that considerable bulging occurs.

strain varied between 10^{-3} and 10^{-6} . In this region Hooke's law might be expected to hold; by varying the current over a factor of five or so at each frequency and observing that the bridge balance remains unchanged it can be verified that the mechanical admittance (Eq. [4]) is indeed independent of strain in the region under consideration. This check was made for each measurement. By increasing the driving current the effect of large strains might easily be studied if desired but any such effect has been carefully avoided in the results given here.

COMPARISON OF DYNAMIC ELECTRICAL AND MECHANICAL BEHAVIOR

The variation of complex dielectric constant with frequency and temperature previously reported for PVC-DMT combinations by Fitzgerald and Miller (10,11,12) offers a basis for comparison of dynamic electrical and mechanical properties. The variation of dielectric constant (ϵ') and electrical loss tangent (ϵ''/ϵ') with frequency is shown in Fig. 21 for the

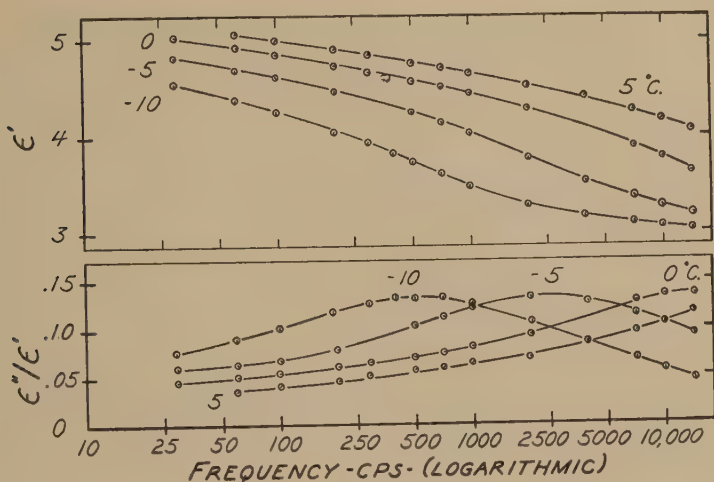


FIG. 21. Variation of the real part of the complex dielectric constant, ϵ' , and the electrical loss tangent, ϵ''/ϵ' , with frequency for a PVC-DMT gel (10% PVC by volume). Results are shown at four temperatures.

PVC-DMT gel (10% PVC by volume), while the variations of compliance (J') and mechanical loss tangent (J''/J') with frequency are given in Figs. 14 and 15. In Fig. 22 the variation of ϵ' and ϵ''/ϵ' with temperature for 40% PVC by volume can be compared with the variation of J' and

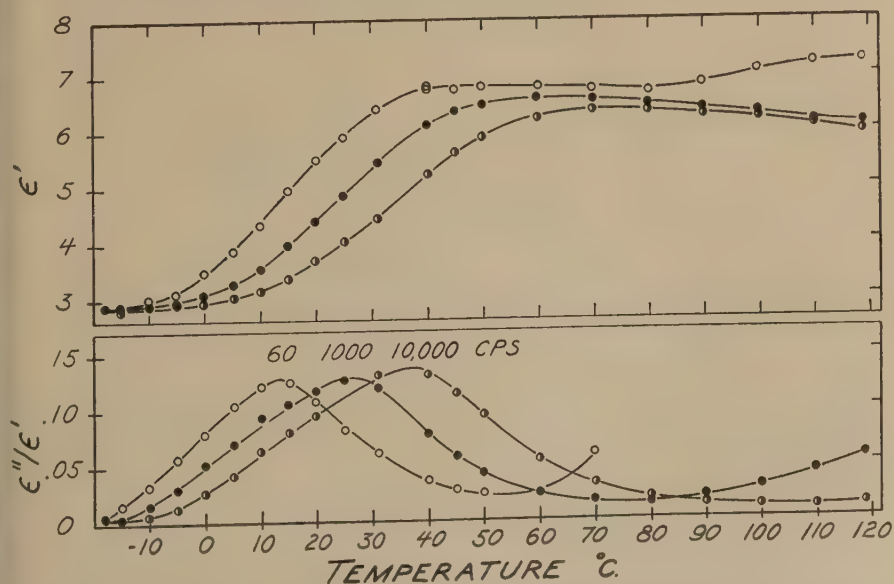


FIG. 22. Variation of the real part of the complex dielectric constant, ϵ' , and the electrical loss tangent, ϵ''/ϵ' , with temperature for PVC combined with DMT (40% PVC by volume). Results are given at 60, 1000, and 10,000 cycles/sec.

J''/J' with temperature given in Fig. 23 for this concentration. From these data it is evident that the dielectric constant and compliance show dispersion in roughly the same temperature-frequency region.

Regardless of the particular model or schematic representation used, there are inherently two similar actions taking place in a material subjected to either an alternating electrical or alternating mechanical stress: (a) energy is dissipated during each cycle, and (b) energy is stored and

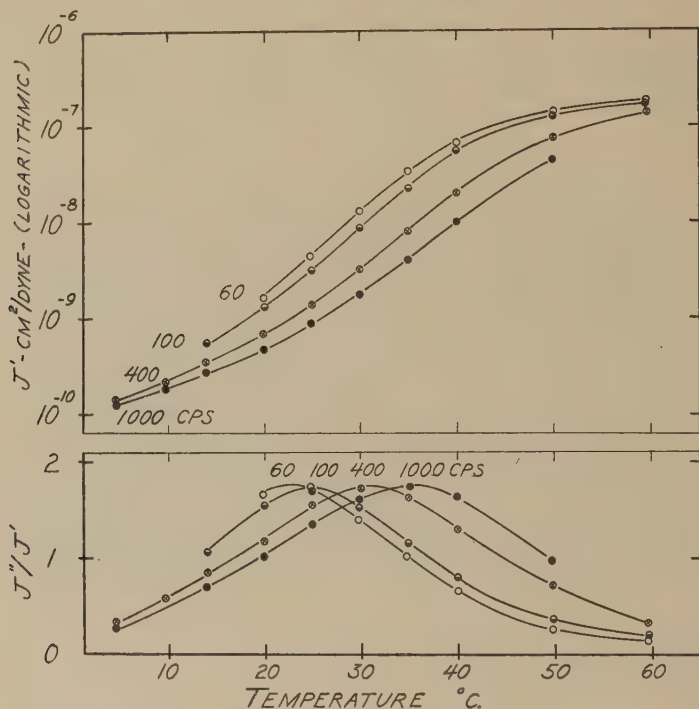


FIG. 23. Variation of the real part of the dynamic shear compliance, J' , and the mechanical loss tangent, J''/J' , with temperature for the PVC-DMT composition of Fig. 22. Results are shown at 60, 100, 400, and 1000 cycles/sec.

subsequently released each $\frac{1}{4}$ cycle. Therefore it seems likely that a fundamental comparison can be made on the basis of the ratio of energy lost per cycle to energy stored per cycle for each case. We recall that for a dielectric

$$\frac{\text{Energy lost/cycle}}{\text{Energy stored/cycle}} = \pi \epsilon''/\epsilon',$$

while for a material undergoing alternating mechanical stress it can be shown that

$$\frac{\text{Energy lost/cycle}}{\text{Energy stored/cycle}} = \pi J''/J'.$$

Thus the loss tangents ϵ''/ϵ' and J''/J' offer a means for comparison as shown, for example, in Fig. 24 for the PVC-DMT gel (10% PVC by volume). Both the mechanical and electrical loss tangents pass through maxima which shift regularly with temperature (cf. Fig. 25). It is clear that the simplest correlation does not hold, i.e., the frequency for maxima loss tangent is not the same at a given temperature for both mechanical and electrical oscillations. For example, at 0°C. the electrical loss tangent has a maximum at about 12,000 cycles/sec., while at -0.2°C. the mechanical loss tangent has a maximum around 100 cycles/sec.

By plotting the frequency of maximum loss tangent vs. the reciprocal of the absolute temperature it is possible to obtain an estimate of the

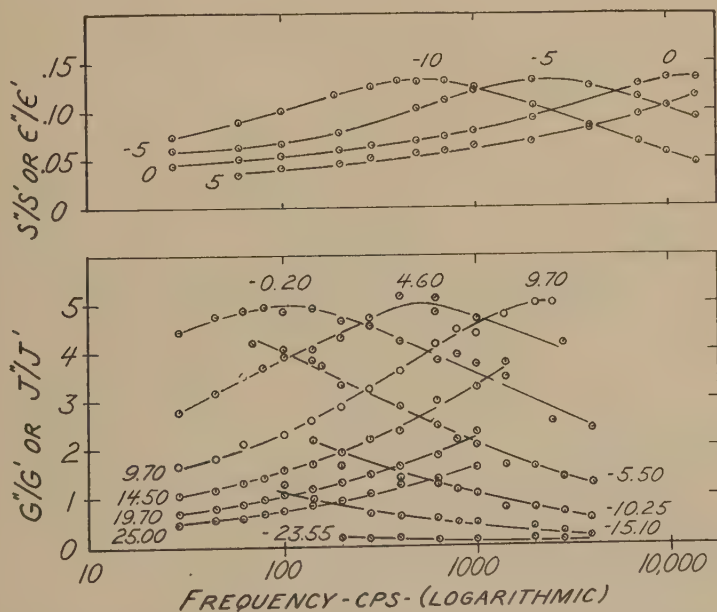


Fig. 24. Variation of electrical and mechanical loss tangents (ϵ''/ϵ' and J''/J') with frequency for a PVC-DMT gel (10% PVC by volume).

activation energies involved in electrical and mechanical orientation. This is done in Figs. 25 and 26 for the 10 and 40% PVC concentrations. For each concentration the slopes of the $\log f_m$ vs. $1/T$ curves are identical for the electrical and mechanical cases, indicating that the activation energy necessary for electrical response (i.e., dipole rotation) is the same as that for mechanical response. From a practical viewpoint this means (if confirmed over a wide temperature range and for other concentrations) that the temperature variation of dynamic compliance might be predicted from that of the dielectric constant or vice versa.

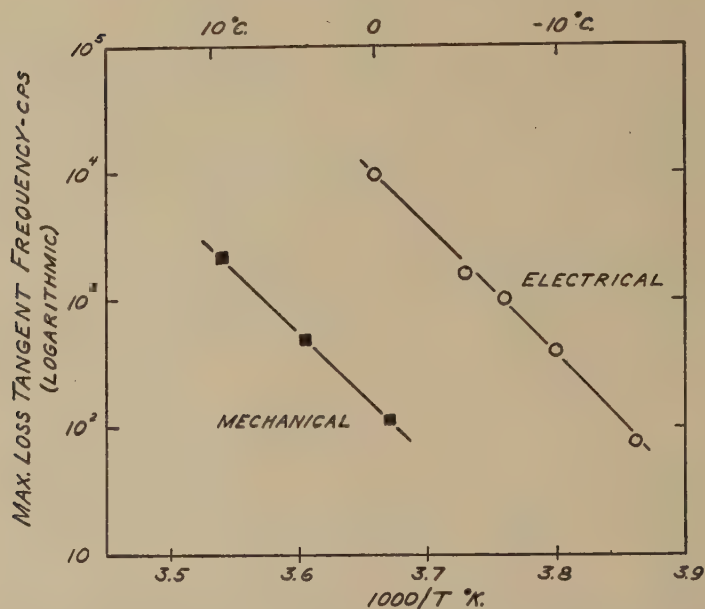


FIG. 25. Frequency of maximum electrical and mechanical loss tangents vs. reciprocal of absolute temperature for the PVC-DMT gel of Fig. 24.

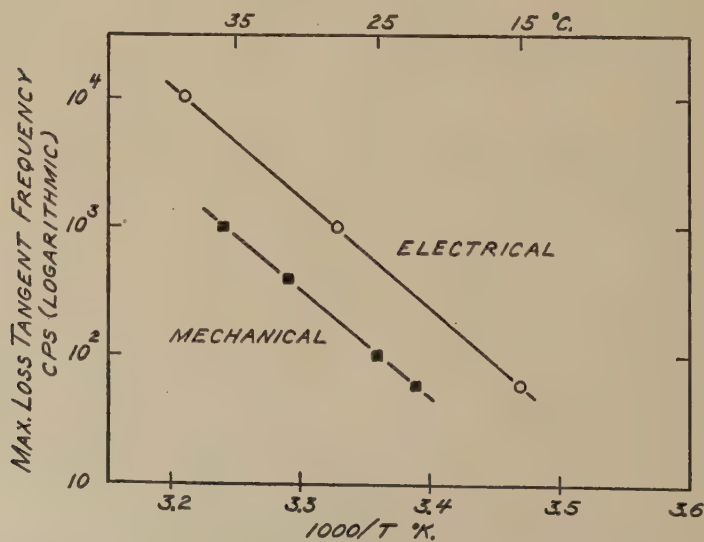


FIG. 26. Frequency of maximum electrical and mechanical loss tangents vs. reciprocal of absolute temperature for the PVC-DMT composition of Fig. 22.

Another striking fact is that the maximum loss tangent for the mechanical case is much larger than the electrical maximum for both the 10 and 40% PVC concentrations. For the 10% PVC gel the mechanical maxima are about 5.0, while electrically the maxima are about 0.14; for the 40% PVC concentration the mechanical loss tangent maxima are 1.9 while the electrical loss tangent maxima are again 0.14. Thus mechanically much more energy is lost than is stored, while electrically the reverse is true and there is always more energy stored than dissipated.²⁸

Additional mechanical data on other concentrations of PVC-DMT as well as other polymer-solvent combinations are needed in order to formulate a comprehensive view of the effect of solvent concentration and the relative influence of polymer and solvent on the mechanical properties of these systems. However, it seems probable that such data when available and considered in conjunction with dielectric properties may lead to a better understanding of the molecular processes contributing to the response to electrical and mechanical stress.

ACKNOWLEDGMENTS

The apparatus was constructed largely by Mr. Thomas Puddester of the University of Wisconsin machine shop, who not only did the machine work with unflinching accuracy but also made numerous suggestions on details for many of the parts which resulted in improvements in the technical aspects of the design. In addition, M. C. Robertson, F. D. Kite, and E. A. Kraft gave advice on construction and did some of the machine work. Mr. Kite's help in checking the mechanical drawings and his advice on materials to be used were of particular benefit and did much to insure the practical nature of the final design.

Samples of materials to be tested as well as some of the parts used in the construction of the mounting were kindly furnished by the B. F. Goodrich Co. Research Center, Brecksville, Ohio. We are particularly indebted to Mr. R. F. Miller for his cooperation in this respect.

This work was supported in part by a grant from Research Corporation and in part by the Research Committee of the Graduate School of the University of Wisconsin from funds supplied by the Wisconsin Alumni Research Foundation. Since March, 1951 it has been part of a program of research on the physical structure and properties of cellulose derivatives and other polymers supported by the Allegheny Ballistics Laboratory, Cumberland, Maryland, an establishment owned by the United States Navy and operated by the Hercules Powder Company under Contract NOrd 10431.

SUMMARY

A method is described for measurements of complex shear modulus or compliance on samples ranging from soft gels to stiff solids at -50 to $+150^{\circ}\text{C.}$ over the frequency range 25 to 5000 cycles/sec. By a proper choice of sample dimensions a precision of $\pm 2\%$ is obtained for values of

²⁸ This applies only to the dipole loss. In regions of high ionic conductivity (low frequencies or high temperatures) the energy loss may be high and ϵ''/ϵ' greater than 1; e.g., for this gel at 60 cycles/sec. and 100°C. , $\epsilon''/\epsilon' = 1.2$.

compliance varying from about 10^{-5} to 10^{-10} cm.²/dyne although a single sample cannot be measured with this precision over the entire frequency-temperature range. Results are given for a sample of polyisobutylene from the National Bureau of Standards at 25.0°C., for a polyvinyl chloride-dimethylthianthrene gel (10% polymer by volume) at ten temperatures between -25 and 25°C., and for polyvinyl chloride plasticized with dimethylthianthrene (40% polymer by volume) at ten temperatures between 5 and 60°C.

Comparison of the dynamic mechanical results with measurements of complex dielectric constant previously reported for the polyvinyl chloride-dimethylthianthrene compositions shows that the dielectric constant and compliance give roughly the same type of temperature-frequency dispersion. While the frequency of maximum electrical loss tangent (ϵ''/ϵ') and that of maximum mechanical loss tangent (J''/J') are not the same at a given temperature, these maxima do appear to shift the same amount with temperature. Thus for each concentration the slopes of curves obtained by plotting the logarithm of the frequency of maximum loss tangent against the reciprocal of the absolute temperature are identical for the electrical and mechanical cases. This indicates that the activation energies for electrical and mechanical responses are the same. The maximum loss tangent for the mechanical case is much larger than the electrical maximum for both the 10 and 40% polyvinyl chloride concentrations.

REFERENCES

1. NOLLE, A. W., *J. Applied Phys.* **19**, 753 (1948).
2. SMITH, T. L., FERRY, J. D., AND SCHREMP, F. W., *J. Applied Phys.* **20**, 144 (1949).
3. MARVIN, R. S., FITZGERALD, E. R., AND FERRY, J. D., *J. Applied Phys.* **21**, 197 (1950).
4. WITTE, R. S., MROWCA, B. A., AND GUTH, E., *J. Applied Phys.* **20**, 486 (1949).
5. FLETCHER, W. P., AND GENT, A. N., *Trans. Inst. Rubber Ind.* **26**, 45 (1950).
6. NIELSEN, L. E., AND BUCHDAHL, R., *ASTM Bull.* No. 165, p. 49 (1950).
7. HOPKINS, I. L., *Trans. Am. Soc. Mech. Engrs.* **73**, 195 (1951).
8. MARVIN, R. S., Interim Report on the Cooperative Program on Dynamic Testing. National Bureau of Standards, 1951.
9. NIELSEN, L. E., BUCHDAHL, R., AND LEVREAU, R., *J. Applied Phys.* **21**, 607 (1950).
10. FITZGERALD, E. R., AND MILLER, R. F., presented at the 305th Meeting of the American Physical Society at Washington, D. C., April 27, 1951.
11. MILLER, R. F., FITZGERALD, E. R., DAVIES, J. M., AND SEARS, W. C., presented at the 312th Meeting of the American Physical Society at Columbus, Ohio, March 20, 1952.
12. FITZGERALD, E. R., AND MILLER, R. F., *J. Colloid Sci.*, in press.
13. NATTA, G., AND RIGAMONTI, R., *Atti reale accad. Lincei* **24**, 381 (1936); FULLER, C. S., *Chem. Revs.* **26**, 143 (1940).
14. ALFREY, T., WIEDERHORN, N., STEIN, R., AND TOBOLSKY, A., *Ind. Eng. Chem.* **41**, 701 (1949).

STUDIES IN WATER-IN-OIL EMULSIONS. III. THE PROPERTIES OF INTERFACIAL FILMS OF SORBITAN SESQUIOLEATE

P. Sherman

Gestetner Ltd., Tottenham, N. 17, England

Received April 24, 1952

INTRODUCTION

The significance of the emulsifying agent in the production of stable emulsions has long been appreciated (1). Bancroft (2) suggested the development between the disperse and continuous phases of a film which formed a distinct entity, and could therefore be considered as a third phase, while more recently stress has been placed on the importance of the physical nature of the interfacial film in emulsion stabilization by Schulman and Cockbain (3). The present work was carried out with the view to investigating the properties of the interfacial films produced by the nonionic emulsifier sorbitan sesquioleate at the mineral oil-water interface, and the effect of time thereon, as a preliminary to parallel work on water-in-oil emulsion systems and the change in their consistency on aging.

EXPERIMENTAL

The interfacial films were developed in accordance with the method of Serrallach and Jones (4), and the viscosity was measured as described by Wilson and Ries (5). Fifty ml. distilled water was placed in a circular glass dish and the glass disk of the pendulum suspension immersed until only the upper surface protruded. Ten ml. mineral oil, in which the appropriate concentration of emulsifier had previously been dissolved, was then carefully pipetted onto the surface of the water. Viscosity measurements were carried out periodically over several days at a temperature of $25 \pm 1^\circ\text{C}$. The influence of increasing concentration of emulsifier on the interfacial viscosity, and the effect of aging, were examined in this manner. (See Fig. 1; the emulsifier concentration is expressed as a w/w percentage of the oil phase.) As the period of oscillation was rather short, even though a 200-g. weight was attached to the pendulum system, it was found more suitable to measure the amplitude of every third swing. Figure 2 illustrates the form of a typical \log_{10} amplitude *vs.* number of oscillations plot.

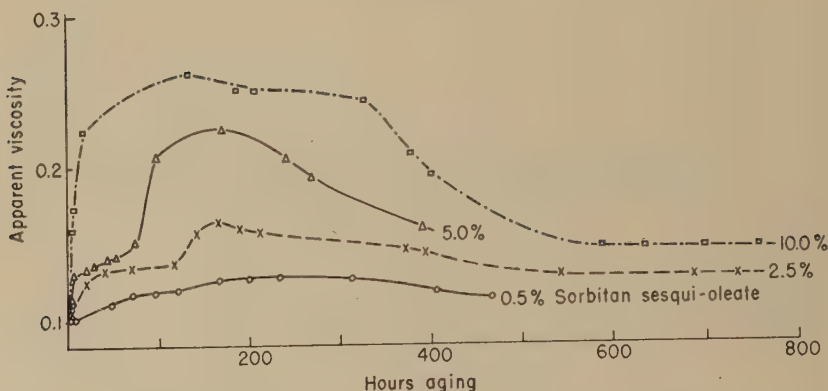


FIG. 1. Sorbitan sesquioleate. Interfacial viscosity: mineral oil and water.

RESULTS AND DISCUSSION

At no concentration of emulsifier was there any pronounced development of plasticity in the interfacial films, although they were found to be solid in appearance.

Adsorption of the emulsifier at the mineral oil-water interface is a relatively slow process, presumably due to the low tension as compared with the air-water interface (6). The interfacial viscosity rises to a maximum, and then falls more gradually to a constant level. The maximum value, the rate at which it is attained, and the subsequent decrease, are higher the greater the concentration of emulsifier employed. It was

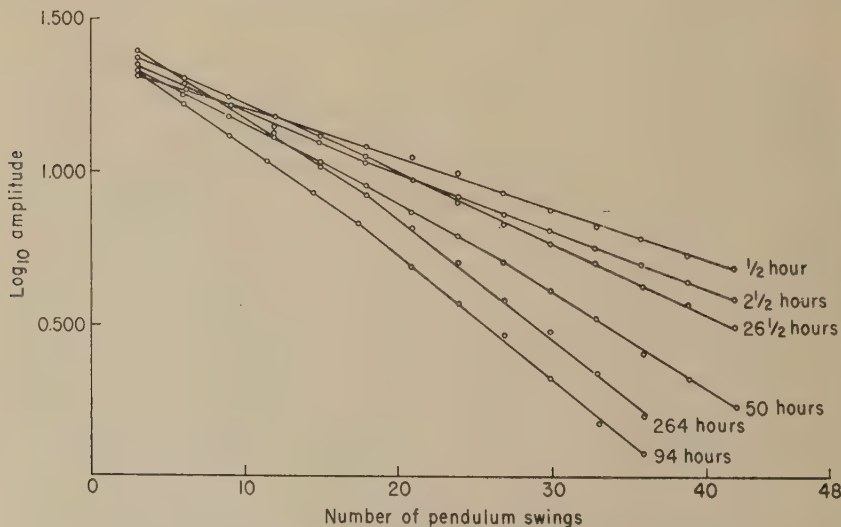


FIG. 2. Plot of \log_{10} amplitude and number of pendulum swings for 5.0% sorbitan sesquioleate, and illustrating the influence of aging.

observed at the higher concentrations that folds appeared in the film surface as the viscosity approached the maximum, and that they disappeared subsequently with a fall in viscosity. This is reminiscent of the behavior of protein molecules which show a tendency to fold up into polymolecular skins. At the three lower concentrations of emulsifier, the adsorption process pursues the characteristic adsorption isotherm form initially, followed by a phase in which the rate increases rapidly. At still higher concentrations, e.g., 10.0%, the second phase is superimposed so rapidly that the two become indistinguishable. Holmes and Cameron (7) working with cellulose nitrate-stabilized emulsions, and Bull and Neurath (8) with protein solutions, suggested that the adsorption process consists of two phases, viz., normal adsorption at the interface, followed by a rapid increase corresponding to the onset of coagulation. The latter process is an irreversible one, however, whereas in this instance the viscosity falls after reaching a maximum, thus suggesting some rearrangement of interfacial structure.

As a result of the slow adsorption of emulsifier at the interface, water-in-oil emulsions prepared with sorbitan sesquioleate as emulsifier, and containing high concentrations (e.g., 70–75%) of disperse phase, would be expected to show a progressive increase in viscosity over several days to a maximum value. Preliminary experiments have confirmed this, and furthermore, they indicate that this is followed by a fall to an approximately constant value.

SUMMARY

The films formed at the mineral oil–water interface by sorbitan sesquioleate are viscous and solid in appearance. Adsorption, which probably occurs in two stages, is a slow process extending over many days, and is characterized by an over-all rise in interfacial viscosity to a maximum, to be followed subsequently by a fall to a constant value. This may be of importance in the aging behavior of water-in-oil emulsions of high disperse phase concentration.

REFERENCES

1. *E.g.*, RAMSDEN, W., *Proc. Roy. Soc. (London)* **72**, 156 (1903); CLOWES, G. H. A., *J. Phys. Chem.* **120**, 407 (1916); CLARK, G. L., AND MANN, W. A., *J. Biol. Chem.* **52**, 182 (1922).
2. BANCROFT, W. D., *J. Phys. Chem.* **17**, 514 (1913).
3. SCHULMAN, G. H., AND COCKBAIN, E. G., *Trans. Faraday Soc.* **36**, 651 (1940); *ibid.* **36**, 661 (1940).
4. SERRALLACH, J. A., JONES, G., AND OWEN, R. J., *Ind. Eng. Chem.* **23**, 1016 (1931).
5. WILSON, R. E., AND RIES, E. D., *Colloid Symposium Monograph*, p. 145 (1923).
6. ALEXANDER, A. E., AND JOHNSON, P., *Colloid Science*, p. 655. Oxford University Press, London, 1949.
7. HOLMES, H. N., AND CAMERON, D. H., *J. Am. Chem. Soc.* **44**, 66 (1922).
8. BULL, H. B., AND NEURATH, H. J., *J. Biol. Chem.* **118**, 163 (1937); *Chem. Revs.* **23**, 291 (1938).

ELECTROPHORESIS MEASUREMENTS IN BENZENE-CORRELATION WITH STABILITY. II. RESULTS OF ELECTROPHORESIS, STABILITY, AND ADSORPTION ¹

J. L. van der Minne and P. H. J. Hermanie

Koninklijke/Shell-Laboratorium, Delft, Holland

Received September 18, 1951; revised May 2, 1952

INTRODUCTION

As reported in earlier work (1), the addition of a calcium soap to a suspension of carbon particles in mineral oil resulted in peptization. So had the addition of the so-called oxidation resins. When both together were added in a certain ratio the result was flocculation. Peptization resulted when one of these additives was present in excess of the other.

It was the intention of the authors to study the correlation of these phenomena with electrophoresis and to that end they developed the apparatus and method described in part I(2).

It was decided to work with better-defined substances and it appeared that benzene made a good substitute for the mineral oil; the calcium soap was well defined: calcium salt of diisopropylsalicylic acid (Ca dips); the other peptizing agent, the oxidation resin, was not. For the latter could be substituted one of the benzene-soluble electrolytes referred to in the works on electrochemistry of Fuoss and Kraus (3), to which Prof. Rutgers (Ghent) had drawn our attention. Tetraisoamylammonium picrate (tiap) proved a good substitute; it had a peptizing effect on the carbon suspension although not such a strong one as that of the oxidation resin, and it also showed antagonism to the calcium soap.

With suspensions made up of these substances the electrophoresis and flocculation tests were carried out.

A. EXPERIMENTAL METHODS

Flocculation tests were best carried out in suspensions containing 0.1% of carbon; for the microscopic observation in the electrophoresis measurements a much lower concentration, viz. 0.003%, was required in order to obtain sharp microscopic pictures. To correlate the two experiments the following procedure was followed.

¹ Parts I and II of this paper were presented at the XIIth International Congress of Pure and Applied Chemistry (Section of Physical and Inorganic Chemistry), New York, Sept. 10-13, 1951.

1. Procedure for Correlating Flocculation Test and Electrophoretic Velocity Determination

A suspension was made containing 0.1% of carbon black and the reagents in the various concentrations. With this suspension the flocculation experiments were carried out. Part of this suspension was centrifuged, and to 30 ml. of the clear upper layer 1 ml. of the 0.1% suspension was added. Thus a second suspension was made, containing about 0.003% of carbon black, which only differed from the first suspension in the amount of carbon present. The equilibrium liquid was exactly the same in both cases.

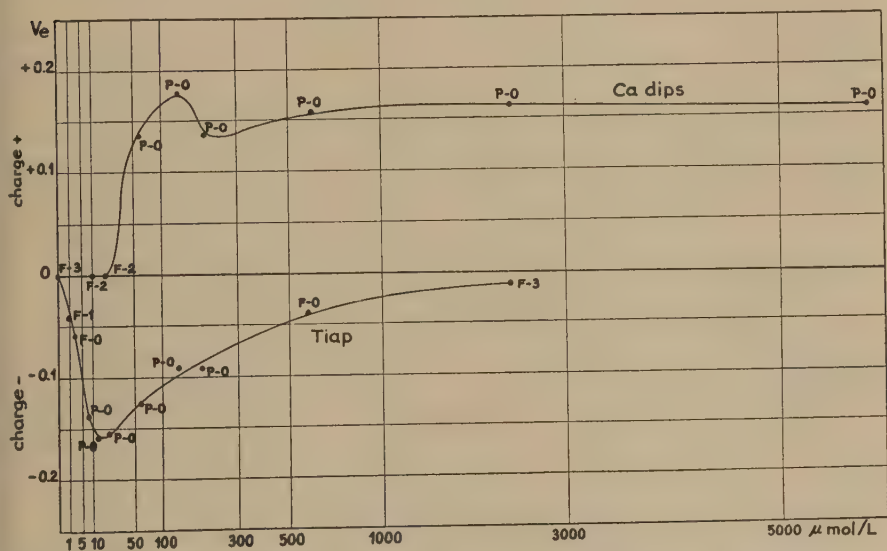


FIG. 1. Electrophoretic velocity v_e as a function of concentration of Ca dips and tiap.

Care was taken to avoid differences in time between the two experiments; suspensions and centrifugate were never stored for more than 1 day.

2. Electrophoresis Measurements

These were carried out as described in Part I (2). The data are reported in Tables I, II, and III and in Figs. 1 and 2.

Concentrations of additives are expressed in micromoles/liter; for conciseness, they are plotted on a square root scale. E is field strength (voltage divided by the distance of 4 cm.). The electrophoretic velocity v_e and the electroosmotic velocity v_0 along the quartz wall are expressed in microns (10^{-4} cm.)/sec./v./cm.

3. Flocculation Measurements

During electrophoresis experiments the tendency of particles to flocculate was observed microscopically. Microscopic flocculation will be indicated by *F* and peptization by *P*; *P:F* means that flocs of adhering particles are observed, *P* that the particles are entirely free.

In addition macroscopic flocculation experiments were carried out. To that end the suspensions with 0.1% of carbon black were poured into equal test tubes with flat bottoms and the time for visible and distinct flocculation at room temperature was noted. The least stable suspension flocculated in between 10 and 20 min., and this degree of flocculation is indicated by the value 3; suspensions with greater stability are indicated

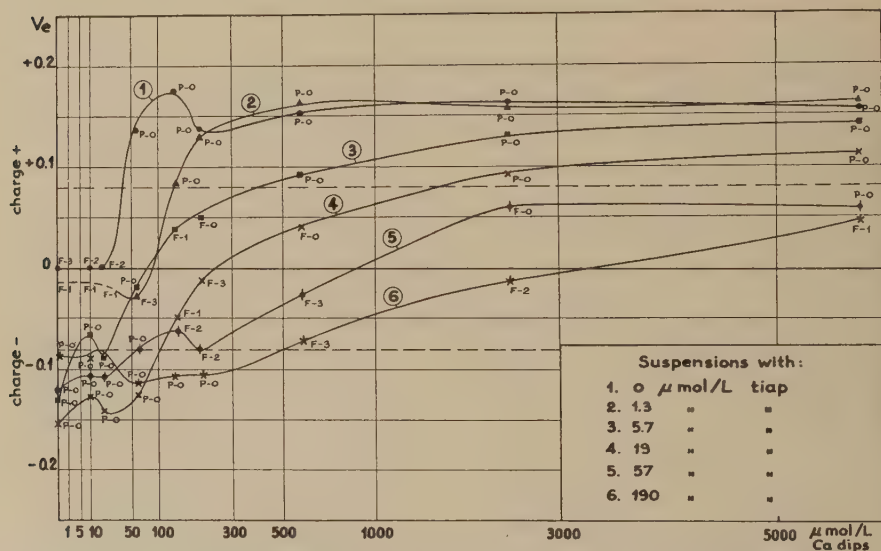


FIG. 2. Electrophoretic velocities v_e as functions of varying concentrations of Ca dips with constant concentrations of tiap.

below by the values 2, 1, and 0. The value 0 indicates that no visible macroscopic flocculation takes place within 90 min. In that case the microscope reveals either that particles do not form flocs, or that flocs are indeed formed.

Thus we have the following degrees of flocculation:

F-3, microscopic: flocculation; macroscopic: flocculation between 10 and 20 min.

F-2, microscopic: flocculation; macroscopic: flocculation between 20 and 30 min.

F-1, microscopic: flocculation; macroscopic: flocculation between 30 and 90 min.

F-0, microscopic: flocculation; macroscopic: no flocculation.

P-0, microscopic: no flocculation; macroscopic: no flocculation.

Contrary to what occurs with other colloids these measurements of flocculation times can be repeated after the suspension has been stirred. The impetus imparted to the large particles (approx. $0.5\ \mu$) by the stirring of the liquid is strong enough to disperse the flocs.

4. Materials Used

Calcium diisopropyl salicylate (Ca dips) was prepared from the acid, m. p. 117°C . (lit. 118.5°C ., *Bull. soc. chim. France* **1948**, 68–70).

It is only slightly soluble in benzene. After recrystallization from acetone containing some water and drying at 120°C . a product was obtained that is soluble in benzene. The calcium content was 7.98% (calcium content calculated on dry product is 8.28%, and with one molecule of crystallization water, 8.00%). Also, if some water is added to the benzene-insoluble product when it is being boiled in benzene it is readily soluble up to 2.5%. Excess water is removed by boiling on a condenser with a water trap.

Benzene (*Analar*) thiophene-free (analytical), dried over CaCl_2 , filtered, and distilled twice. Distillation causes the water to pass over first, and the water content of the later distillate is below 0.01%. M. p.: $5.0\text{--}5.2^{\circ}\text{C}$.; b. p.: $80.1\text{--}80.5^{\circ}\text{C}$.

Tetraisoamylammonium picrate: recrystallized from a mixture of chloroform and diethyl ether. M. p.: 87.7°C .

Carbon black, see p. 605, part I(2).

B. RESULTS OF ELECTROPHORETIC MEASUREMENTS AND OF FLOCCULATION TESTS

1. Positively and Negatively Charging Electrolytes Considered Separately

The following Tables I and II and Fig. 1 show the influence of calcium diisopropyl salicylate and of tetraisoamylammonium picrate.

All measurements were made between 23 and 25°C .

Discussion

The suspension without any additive does not show any electrophoresis. Only in one case after a very long "running-in time" (2) was a slight movement to the positive pole observed.

Ca dips added (Table I): The first low concentrations of Ca dips, up to $20\ \mu\text{moles/l.}$, do not cause any change in the electrophoretic velocity, which is zero or very small. Then at $60\ \mu\text{moles/l.}$ a velocity to the negative pole [charge of particles (+)] sets in which at $140\ \mu\text{moles/l.}$ rises to $0.17\ \mu/\text{sec.}$ and at higher concentrations (up to $200\ \mu\text{moles/l.}$) decreases to

TABLE I

Electrophoretic Velocity (v_e), Electroendosmotic Velocity (v_0) and Flocculation of Carbon Black Suspensions with Calcium Diisopropyl Salicylate

Ca dips $\mu\text{moles/l.}$	E	v_e	v_0	Flocculation
0	225	0	0	F-3
10	225	0	0	F-2
20	225	0	0	F-2
60	154	+0.135	+0.165	P-0
140	102	+0.175	+0.275	P-0
200	102	+0.135	+0.265	P-0
600	102	+0.155	+0.315	P-0
2000	102	+0.165	+0.395	P-0
6000	102	+0.155	+0.42	P-0

0.135 $\mu\text{/sec.}$ This decrease is real and is often reproduced with other kinds of carbon black as well. At much higher concentrations the charge remains positive.

Tiap added (Table II): Very small concentrations of tiap (6 $\mu\text{moles/l.}$) make the particles negative; the highest velocity of 0.16 $\mu\text{/sec.}$ is reached at 13–20 $\mu\text{moles/l.}$ At higher concentrations the velocity is gradually reduced until at 1900 $\mu\text{moles/l.}$ it is practically zero.

As regards the relation between electrophoretic velocity and stability it may be stated that the suspensions showing the higher velocities are stable and that those with low or zero velocity are unstable (see also Fig. 1).

With Ca dips the electroendosmotic velocity along the quartz wall roughly follows the same trend as the electrophoretic velocity of the carbon particles, but reaches a much higher value (0.42 μ).

Unlike the values of v_e , the values of v_0 for tiap (electroendosmotic velocity along quartz wall) were in some cases not too well reproducible. This is

TABLE II

Electrophoretic Velocity (v_e), Electroendosmotic Velocity (v_0) and Flocculation of Carbon Black Suspensions with Tiap

Tiap $\mu\text{moles/l.}$	E	v_e	v_0	Flocculation
0	231	0?	0?	F-3
1.33	234	Neg.?	?	F-1
1.9	154	-0.06?	-0.02?	F-0
5.7	104	-0.135	-0.245	P-0
13.3	102	-0.16	-0.265	P-0
19	104	-0.155	-0.25	P-0
57	154	-0.125	-0.10	P-0
133	102	-0.09	-0.175	P-0
190	104	-0.09	-0.185	P-0
570	154	-0.035	-0.045	F-0
1900	230	-0.015	-0.015	F-3

probably due to the fact that the wall still shows the influence of preceding experiments. In this apparatus the tube must not be cleaned with aqueous chromic acid but only with alcohol and benzene, because it is sealed in with a water glass cement. On the other hand, the fact that with different v_0 values on the wall the same values for v_e are obtained is further evidence of the exactness of this method of electrophoresis determination.

2. Positively and Negatively Charging Electrolyte Added Together

The relation between electrophoretic velocity and stability is studied in more detail in the following experiments, where the influence of mixtures of Ca dips and tiap is investigated. In these mixtures, as already mentioned, each additive counteracts the peptizing effect of the other.

In these series the same flocculation tests (with 0.1% suspension) and electrophoresis measurements as before were carried out with the same suspension. In these series, varying amounts of Ca dips were added to fixed concentrations of tiap.

The results of the electrophoretic velocity (v_e), the electroendosmotic velocity (v_0), and flocculation measurements are given in Table III and in Fig. 2.

Discussion

The curve indicated by zero tiap is the same as that for calcium diisopropyl salicylate in Fig. 1. The addition of very small amounts of tiap (1.3 and 5.7 μ moles/l. tiap) markedly decreases the positive charge given by 100 μ moles of Ca dips and even makes the charge negative if only 60 μ moles or less of Ca dips is present. Even at very high concentrations of Ca dips (6000 μ moles) the influence of 19 and 57 μ moles tiap is considerable.

Also, when relatively high concentrations of tiap are present and the charge is negative the first amounts of Ca dips do not cause much change, and even at higher concentrations of Ca dips the charge only gradually becomes positive. Very small amounts of Ca dips even seem to increase the negative charge; this is more pronounced in the case of the electroendosmotic velocity v_0 (see Table III). The changes in v_0 are generally the same as those in v_e .

C. RELATION BETWEEN PEPTIZATION AND ELECTROPHORETIC VELOCITY (OR ζ -POTENTIAL)

A definite and clear relationship is seen to exist over the whole range of concentrations; this can be expressed as follows:

The suspensions showing an electrophoretic velocity larger than 0.07–0.08 μ /sec./v./cm. are peptized; those showing a smaller value are flocculated.

There are only two points of exception, both lying on the 5.7- μ mole tiap line and both lying on steep parts of the curve where minor varia-

TABLE III

Electrophoretic Velocity (v_e), Electroendosmotic Velocity (v_0) and Flocculation of Carbon Black Suspensions with both Calcium Diisopropyl Salicylate and Tiap

		Tiap, $\mu\text{moles/l.}$							
		0				1.33			
		E	v_e	v_0	Floc.	E	v_e	v_0	Floc.
Ca dips $\mu\text{moles/l.}$	0	225	0	0	F-3	234	Neg. ?	—	F-1
	10	225	0	0	F-2	234	Neg. ?	—	F-1
	20	225	0	0	F-2	234	Neg. ?	—	F-1
	60	154	+0.135	+0.165	P-0	234	-0.03	-0.035	F-3
	140	102.5	+0.175	+0.275	P-0	156	+0.085	+0.18	P-0
	200	102.5	+0.135	+0.265	P-0	104	+0.13	+0.23	P-0
	600	102.5	+0.155	+0.315	P-0	104	+0.165	+0.325	P-0
	2000	102.5	+0.165	+0.395	P-0	104	+0.16	+0.38	P-0
	6000	102.5	+0.155	+0.42	P-0	104	+0.165	+0.425	P-0
		Tiap, $\mu\text{moles/l.}$							
		5.7				19			
		E	v_e	v_0	Floc.	E	v_e	v_0	Floc.
Ca dips $\mu\text{moles/l.}$	0	104	-0.135	-0.245	P-0	104	-0.155	-0.25	P-0
	10	104	-0.065	-0.14	P-0	104	-0.125	-0.20	P-0
	20	104	-0.09	-0.15	P-0	104	-0.14	-0.185	P-0
	60	156	-0.025	-0.025	P-0	104	-0.125	-0.225	P-0
	140	156	+0.04	+0.08	F-1	156	-0.05	-0.11	F-1
	200	104	+0.05	+0.165	F-0	156	-0.01	-0.01	F-3
	600	104	+0.09	+0.27	P-0	156	+0.04	+0.185	F-0
	2000	104	+0.13	+0.36	P-0	104	+0.09	+0.275	P-0
	6000	104	+0.145	+0.455	P-0	104	+0.115	+0.36	P-0
		Tiap, $\mu\text{moles/l.}$							
		57				190			
		E	v_e	v_0	Floc.	E	v_e	v_0	Floc.
Ca dips $\mu\text{moles/l.}$	0	154	-0.125	-0.10	P-0	104	-0.09	-0.185	P-0
	10	154	-0.105	-0.095	P-0	104	-0.09	-0.17	P-0
	20	154	-0.11	-0.07	P-0	104	-0.085	-0.165	P-0
	60	154	-0.085	-0.205	P-0	104	-0.115	-0.28	P-0
	140	154	-0.055	-0.195	F-2	104	-0.105	-0.31	P-0
	200	154	-0.08	-0.19	F-2	104	-0.105	-0.295	P-0
	600	154	-0.025	-0.025	F-3	156	-0.07	-0.175	F-3
	2000	154	+0.06	+0.02	F-0	156	-0.015	0	F-2
	6000	154	+0.06	+0.12	P-0	156	+0.055	+0.105	F-1

tions in concentration due to centrifuging or to time effects might have played a role.

The relation also holds for the data for tiap alone; see Fig. 1 (Table II).

The critical ζ -potential has been calculated from this critical electrophoretic velocity according to Helmholtz's equation, taking for dielectric constant, ϵ , that of benzene (2.28), and for viscosity, η , that of benzene at 25°C. = 0.00605 poise; v_e is expressed in $\mu/\text{sec.}$ (10^{-4} cm.).

$$\zeta \text{ (mv.)} = \frac{4\pi\eta v_e}{10^4 \epsilon} \times 300 \times 300 \times 1000 = 300v_e.$$

The viscosities of the benzene solutions have been found to be the same to within 1% as that of benzene. (The dielectric constant for benzene solutions is only changed in the highest concentrations of the Ca dips mentioned by less than 1% and of tiap by *ca.* 7%).

The value of this critical ζ -potential is then found to be 21–24 mv.

One is struck by the fact that this value is of the same order of magnitude as that for aqueous solutions (30–40 mv.). Moreover, as far as can be judged these benzene suspensions comply better with the rule than aqueous suspensions do (remember the difficulties with many univalent electrolytes).

The antagonism between the peptizing properties of Ca dips and those of tiap could now be explained, as could also the curious antagonism, mentioned at the beginning, between the Ca dips and the so-called oxidation resin. Just like tiap, the oxidation resin appeared to induce a negative ζ -potential on the carbon particles, and the mechanism of mutual flocculation in that case must therefore also be ascribed to the lowering of the electrokinetic potential.

ADSORPTION MEASUREMENTS

In order to understand better the difference in behavior between calcium soap and tiap in respect to the charge on the carbon particles, it was thought necessary to make adsorption measurements.

Method

The concentration of both electrolytes in benzene could be well determined even in very weak solutions.

The tetraisoamylammonium picrate solution in benzene is yellow in color and the concentration may be determined by light absorption to within a few micromoles per liter.

The calcium diisopropyl salicylate is colorless in solution; by adding a benzene solution of Rhodamine B a strong red coloration is obtained even at very low concentrations [see Arkin and Singleterry (4)]. Thus a concentration of 1 $\mu\text{mole/l.}$ may be determined.

A Coleman junior colorimeter was used; first the absorption spectra were determined; see Fig. 3.

It followed that tiap could be determined at 400 $m\mu$ and calcium diisopropyl salicylate-Rhodamine B complex at 550 $m\mu$ (wavelength).

Tiap in benzene follows Lambert-Beer's law up to 20 μ moles only; calcium soap-Rhodamine B up to 10 μ moles only. Therefore calibration curves had to be made.

For those cases where both electrolytes are present it appears that the Ca dips interferes with the light absorption of tiap. The interference of

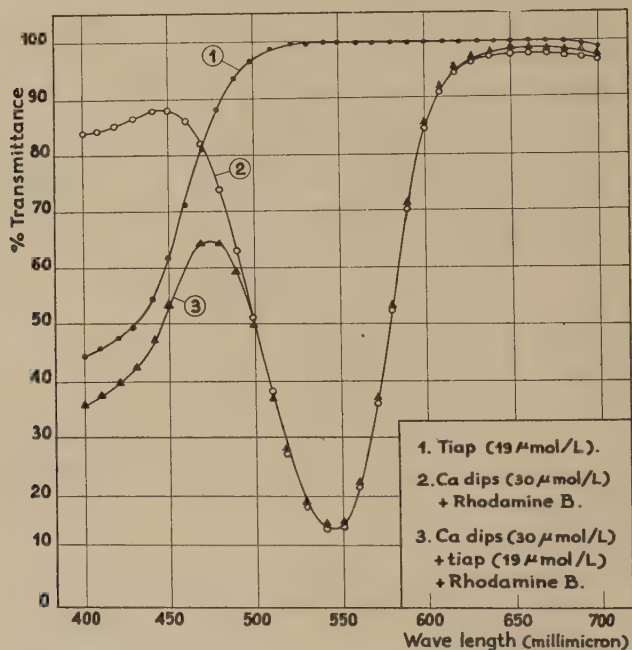


FIG. 3. Light absorption spectra of solutions in benzene (Ca dips and tiap, separately and combined).

tiap with the Ca dips determination is only slight, ceasing at concentrations of Ca dips below 20 μ moles. Therefore for the determination of the concentration of Ca dips present the solution was diluted (if necessary) to below this concentration. Then the concentration of Ca dips was determined and, this concentration being known, the concentration of tiap could be determined from the calibration curve of the mixture.

A single preparation of Rhodamine B stock solution in benzene was used for all of the measurements. A colorless solution was made as follows: 0.5 g. of Rhodamine B was boiled with 1 l. of benzene, filtered, and treated with some decolorizing carbon; this nearly colorless solution gives the

red coloration with Ca dips just as the original colored solution does; accuracy is thus improved. It contained 60 mg. of Rhodamine B/l. ($= 125 \mu\text{moles/l.}$).

In the determinations of Ca dips $40 \mu\text{moles/l.}$ of Rhodamine B was used; Ca dips concentration did not run higher than $20 \mu\text{moles/l.}$; thus enough of the Rhodamine B was always present (higher concentrations of Rhodamine B only increased the light absorption to a minor extent).

The following factors were also considered: (a) the effect of time on the intensity of the color (very small for Ca dips) and the age of the stock solution; and (b) adsorption of Ca dips on the walls of the glass vessels used. It was established that in solutions of $1\text{--}2 \mu\text{moles/l.}$ about $0.5 \mu\text{mole/l.}$ could be adsorbed, and in solutions containing from 10 up to $2000 \mu\text{moles/l.}$, about $2 \mu\text{moles/l.}$ This has been taken into account.

RESULTS

The determinations were carried out in the upper layer of the centrifuged suspension containing 0.1% carbon.

Adsorption of Calcium Diisopropyl Salicylate and Tiap When Added Separately

The following data were obtained for the suspensions with calcium diisopropyl salicylate (see Table IV).

The higher concentrations could not usefully be determined because of the relatively large experimental error (difference between two large figures).

The above results are plotted in Fig. 4.

These results will be discussed together with the following of the adsorption of tiap, given in Table V.

The above results are plotted in Fig. 5.

In Figs. 4, 5, and 6 are plotted: (a) the electrophoretic velocity against the amount of electrolyte added; (b) the amount of electrolyte adsorbed against the amount in solution; and (c) the electrophoretic velocity against the amount of electrolyte in solution.

TABLE IV

Ca dips added to suspension $\mu\text{moles/l.}$	Ca dips found in equilibrium liquid $\mu\text{moles/l.}$	Quantity adsorbed by carbon (1 g.) = difference μmoles
0	0	0
10	0	10
20	0	20
60	9 ± 0.5	51 ± 0.5
140	62 ± 2	78 ± 2
200	135 ± 5	65 ± 5
600	540 ± 12	60 ± 12
2000	(1950 ± 40)	(50 ± 40)

Discussion of Results of Adsorption of Tiap and of Ca Dips Separately

Beginning with the simpler case of tiap, the adsorption is relatively small; the adsorption curve in the graph is nearly linear when plotted against the square root of the concentration. This means that an adsorption isotherm according to Freundlich is obtained in which the exponent

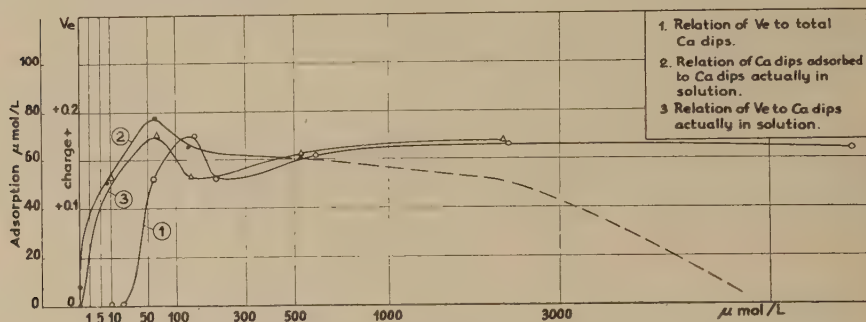


FIG. 4. Electrophoretic velocity v_e and adsorption as functions of concentration (Ca dips).

$1/n$ is ca. $\frac{1}{2}$. Because of the relatively small adsorption the v_e curve against actual concentration is not much different from that against added concentration.

An entirely different picture is obtained in the case of calcium diisopropyl salicylate.

The first interesting point is that when up to 20 μ moles is added it is all adsorbed; when 60 μ moles is added 9 μ moles is available in the solution.

TABLE V

Tiap added to suspension μ moles/l.	Tiap found in equilibrium liquid μ moles/l.	Quantity adsorbed by carbon (1 g.) = difference μ moles
0	0	0
1.3	0.7 ± 0.2	0.6 ± 0.2
1.9	1.2 ± 0.2	0.7 ± 0.2
5.7	4.2 ± 0.2	1.5 ± 0.2
13	11.7 ± 0.2	1.3 ± 0.2
19	16.7 ± 0.2	2.3 ± 0.2
57	53 ± 0.6	4 ± 0.6
130	121 ± 3	9 ± 3
190	180 ± 5	10 ± 5
570	(555 ± 15)	(15 ± 15)

It is at that point that electrophoretic motion sets in. It appears therefore that for obtaining electrophoretic motion a certain concentration of ions must be present in the continuous phase. This is confirmed by the electric conductivities of the continuous phases. When 20 μ moles/l. had been added to the suspension the clear centrifugate showed a specific conduc-

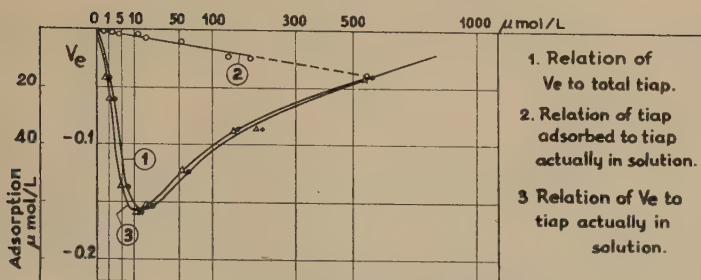


FIG. 5. Electrophoretic velocity v_e and adsorption as functions of concentration (tiap).

tivity of below $10^{-14} \Omega^{-1} \text{ cm}^{-1}$, a value which was also obtained for pure benzene, whereas when 60 $\mu\text{moles/l.}$ had been added the conductivity rose to 0.5×10^{-12} . (This latter value was also obtained by adding 10 $\mu\text{moles/l.}$ of Ca dips to the centrifugate of the suspension of the carbon black in pure benzene.) The concentration of Ca dips in the continuous

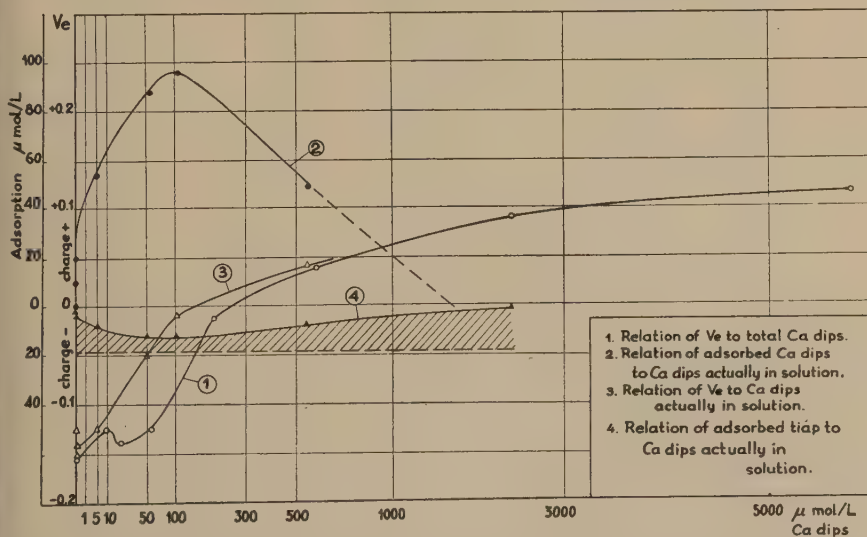


FIG. 6. Electrophoretic velocity v_e and adsorption as functions of concentration (Ca dips and tiap combined).

phase necessary for electrophoretic motion of the carbon particles may even be smaller than 9 or 10 $\mu\text{moles/l.}$

The second interesting point is that adsorption of Ca dips reaches a maximum at Ca. 140 $\mu\text{moles added} = 62 \mu\text{moles actually in solution.}^2$

² The experimental error here is rather large (see Table IV). However, on repetition the same maximum was obtained. Moreover with another carbon black (MPC) a maximum was also clearly present (also with another metal salt, namely zinc diisopropyl salicylate).

From then on increasing the concentration in the solution reduces the adsorption. Also, exactly at this same point v_e is at its maximum, and at higher concentrations it diminishes.

Results of Adsorption Determination in the Case That Calcium Diisopropyl Salicylate and Tiap Are Added Together

This aspect has been studied in detail in relation to one of the curves of Fig. 2 (Table III), namely that in which 19 μ moles tiap and varying amounts of the calcium soap have been added.

Results are tabulated in Table VI.

These data are plotted in Fig. 6.

In this graph the adsorbed amounts are plotted against the actual concentration in the solution; also the v_e values are plotted against the

TABLE VI

Ca dips added μ moles/l.	Ca dips found in equilibrium liquid μ moles/l.	Tiap found in equilibrium liquid μ moles/l.	Amounts adsorbed by 1 g. carbon	
			Ca dips μ moles	Tiap μ moles
0	0	18 ± 0.2	0	1 ± 0.2
10	0	16.5 ± 0.2	10	2.5 ± 0.2
20	0	16 ± 0.2	20	3 ± 0.2
60	5 ± 0.4	11 ± 0.2	55 ± 0.4	8 ± 0.2
140	53 ± 1	7 ± 0.2	87 ± 1	12 ± 0.2
200	104 ± 2	8 ± 0.2	96 ± 2	11 ± 0.2
600	550 ± 12	12 ± 0.2	50 ± 12	7 ± 0.2
2000	Not detd.	18 ± 0.2	Not detd.	1 ± 0.2

actual concentration of the calcium soap. The curve originally determined is also given.

The adsorption of Ca dips is virtually the same as in the case without tiap, as far as the rising branch is concerned, perhaps somewhat higher. The carbon particles are negative in the presence of tiap and they remain negative even when relatively large amounts of Ca soap are adsorbed. A change to a positive charge only sets in when relatively large amounts of Ca soap become available in solution. The carbon particles seem to be reluctant to acquire a positive charge and this is even the case at 2000 μ moles Ca soap.

The absorption of tiap is very much fostered by the addition of Ca dips. Originally only 1 or 2 μ moles, it rises to *ca.* 12 μ moles, i.e., 60% of the total quantity present. At higher concentrations of Ca dips (2000 and 6000 μ moles/l.) the adsorption of tiap is markedly diminished. The experimental error in the adsorption determination of Ca dips at these high concentrations is large, but indications are available that adsorption here is smaller than at lower concentrations (and even may be nil).

In the region up to 100 μ moles of Ca soap (actual concentration) both electrolytes seem to promote each other's adsorption. At 100 μ moles/l.

the adsorption of both is at a maximum and it is remarkable that at or near that point (100–200 μ moles) electrophoretic velocity is at a minimum. Above that concentration the adsorption of both electrolytes is diminished.

GENERAL DISCUSSION AND CONCLUSIONS

From the experiments with calcium diisopropyl salicylate (Ca dips) on electrophoresis and adsorption measurements it is concluded that:

1. No electrophoresis occurs unless a sufficient number of ions are present in the solution (see Fig. 4).

In the case where a very low concentration of Ca dips was present in the continuous phase (below 0.2 μ mole/l. as determined by electric conductivity) no electrophoresis occurred, whereas in the case where 9 μ moles/l. was present it did occur.

This is understandable if one considers that in the transport of the particle relative to the liquid the double layer is constantly being stripped off and ions from the liquid are constantly needed to rebuild it. If such ions are not available in the liquid, electrophoresis cannot continue. To put it another way, the displacement of the particle represents a certain electric conductivity, and if the liquid around the particle does not have a sufficient conductivity no movement can occur.

It must be added that, as shown in Part I [Ref. (2), p. 614], if no ions are present in the continuous phase and electric conductivity is zero, no electric field can be formed in an electrophoretic apparatus having a small capacitance in respect to the surroundings.

From early data on electroendosmosis by Coehn (5) and from later data by Fairbrother and Balkin (6), it was known that in various organic liquids glass showed a distinct negative ζ -potential. However, in the liquids with a dielectric constant of 2.3, such as benzene, toluene, xylene, and carbon tetrachloride, no ζ -potential was found. Coehn ascribed this to the absence of conductivity, and rightly so as is pointed out above in relation to the kindred phenomena of electrophoresis. However, what charge the glass or other substances acquire depends entirely on what kinds of ions are added to increase the conductivity. Quartz or carbon particles are charged positively by calcium soap and negatively by tiap. The dielectric constant of the solutions is hardly different from that of benzene, and therefore Coehn's rule that the sign (and magnitude) of the charge depends on the difference in magnitude of the dielectric constants of the two phases is entirely without foundation. This needs to be stated because too much is still heard about Coehn's so called "rule."

The other conclusions are, briefly, the following:

2. Calcium diisopropyl salicylate gives a positive charge to the carbon particles, and tetraisoamylammonium picrate, a negative charge. This

is the explanation for the antagonism between these two electrolytes. A critical potential for stability of *ca.* 21–24 mv. is found from data (critical electrophoretic velocity is 0.07–0.08 μ /sec./v./cm.).

3. The concentration of electrolyte necessary for increasing or decreasing the ζ -potential is remarkably small compared with what is required in aqueous systems. In the latter a concentration of say 20–100 μ moles/l. of a 1:1 electrolyte is required for flocculation. In benzene 400 μ moles/l. of tetraisoamylammonium picrate is required, about 100 times less. Ionic concentrations are much lower still because the degree of dissociation of the electrolyte is about 10^{-5} to 10^{-6} as against unity for water. Ionic concentrations necessary for a 1:1 electrolyte to cause flocculation in benzene are therefore 10^{-7} to 10^{-8} times less than in water. The mechanism will be entirely different in the two cases; the concept of compression of the double layer, assumed for water, is entirely out of the question at the low concentrations occurring in benzene. The explanation of the flocculation at the higher concentrations of the picrate must be sought in the diminished preferential adsorption of negative ions (see also 4).

4. The adsorption isotherm of calcium soap on carbon shows a maximum at the same point (concentration) where the ζ -potential on carbon and on the quartz wall show a maximum. The adsorption isotherm of tiap shows a normal behavior. When calcium soap and tiap are both present adsorption of both is at a maximum at about this same concentration (ζ -potential is very low at that point). The explanation of the above peculiarities is surmised to be the presence of various complicated association products of the electrolytes which are known from the work of Walden, of La Mer and Downes, (7) and of Fuoss and Kraus (3) to exist in electrolyte solutions in hydrocarbons. Increase of concentration is known to increase the degree of association strongly. The above mentioned peculiarities may possibly be explained on the assumption that certain of these association products and their ions are less adsorbed than the unassociated ones.

REFERENCES

1. MINNE, J. L. VAN DER, *Rec. trav. chim.* **65**, 549 (1946).
2. MINNE, J. L. VAN DER, AND HERMANIE, P. H. J., *J. Colloid Sci.* **7**, 600 (1952).
3. FUOSS, R. M., *Chem. Revs.* **17**, 27 (1935); STRONG, L. E., AND KRAUS, C. A., *J. Am. Chem. Soc.* **72**, 166 (1950).
4. ARKIN, L., AND SINGLETERRY, C. R., *J. Am. Chem. Soc.* **70**, 3965 (1948).
5. COEHN, A., *Ann. Physik* **66**, 217 (1898); COEHN, A., AND RAYDT, V., *Ann. Physik* **30**, 777 (1909); see ABRAMSON, H. A., *Electrokinetic Phenomena*, p. 58. New York, 1934.
6. FAIRBROTHER, F., AND BALKIN, M. J., *J. Chem. Soc.* **1931**, 389, 1564.
7. LA MER, V. K., AND DOWNES, H. C., *J. Am. Chem. Soc.* **53**, 888 (1931); *ibid.* **55**, 1840 (1933); *Chem. Revs.* **13**, 47 (1933).

ON MONOLAYER PENETRATION

R. Matalon¹

University of Cambridge, Department of Colloid Science, Cambridge, England

Received June 4, 1952

INTRODUCTION

The phenomenon of penetration of an insoluble monolayer by a water-soluble amphipathic compound was discovered by Schulman and Hughes in 1935, and has since been investigated by several authors.

The monolayer experiments led to the conception that penetration resulted in a new type of compound (1) displaying properties which could not be found in either of the constituents. This conclusion had been supported in bulk experiments, e.g., sodium cetyl sulfate, although strongly hemolytic on its own, was observed to lose its lytic activity when mixed with cholesterol in equimolecular amounts (2).

Furthermore, it was found that, unlike sodium cetylsulfate, the equimolecular cetyl sulfate/cholesterol mixture was not precipitated by the addition of silver nitrate (3).

A great deal of work has since been done (4,5) on the properties of analogous complexes in bulk solution. That penetration leads to true stoichiometric associations is still disputed. Some authors question the validity of the basic experiments, which have been claimed to demonstrate their existence. For example, Harkins and co-workers (6) applying the monolayer technique concluded that no evidence can be produced in the case of the cetyl alcohol/cetyl sulfate system. Recently Hutchinson (7), by application of the Gibbs equation to the surface tension concentration curve of (γ -c) of a mixed solution of octyl alcohol and sodium dodecyl sulfate reached the same conclusion.

Information regarding the phenomenon of penetration has been obtained from the study of (a) the compression curve of the monolayer after penetration; (b) the ejection curve, in which the pressure of the penetrated monolayer is fixed and the area reduction with time noted; and (c) the expansion of the monolayer under a constant piston oil pressure after injection of the solute. In addition, penetration has been followed by recording the rise in pressure as a function of time, keeping the area of the insoluble monolayer constant throughout the experiment. This method was first used by Schulman and Stenhagen (1), then by Harkins

¹ Present address: Department of Physical Chemistry, King's College, University of London, London, W.C.2, England.

et al. (6), and latterly by Matalon and Schulman (8). Using this technique it was shown (8) that for a given pair of compounds displaying the phenomenon of monolayer penetration, the properties of the penetrated monolayer depend on the composition of the bath into which the solute is injected, and on the concentration of the solute in the bulk and in the surface.

Since penetration is produced by injection of an amphipathic compound under an insoluble monolayer, it follows obviously that the composition of the penetrated monolayer, and thus its mechanical properties, must be markedly dependent on the relative number of molecules of the two species present at the surface. This will depend on the concentration of the solute. It is clear, therefore, that as adsorption of the injected solute is relatively slow at the concentration generally used, the composition and the mechanical properties of the monolayer will vary with time. Furthermore, penetration reorientation and adlineation of the solute in the insoluble monolayer are also slow, particularly when the monolayer is initially held at high pressures. Therefore, in any compression (or ejection) curve, the time interval between injection of the solute and compression should always be specified. Furthermore, the compression curve, as well as depending on the relative concentration of the two components in the monolayer at the start of compression, will also depend upon the rate at which the water-soluble molecules leave the monolayer. This means in practice that before equilibrium at any given pressure is reached some considerable time may elapse, and therefore the compression technique is rendered tedious and uncertain.

These difficulties may be overcome by using the technique of monolayer expansion at constant pressure to study the penetration phenomenon. Schulman, Stenhagen, and Rideal (1,9) followed the expansion of monolayers under constant piston oil pressure and characterized complexes by noting the area at which the film apparently stopped expanding. They observed that a change in the piston oil pressure from 32 to 23 dynes/cm. could alter the composition of a complex from 1:1 to 1:2. Their result contradicts the concept of a well-defined stoichiometric complex which should be stable over an appreciable range of film pressure and solute concentration. Using this technique these authors recorded only one point on the expansion at a region coinciding with 50 or 100% increase in the area of the original monolayer.

A new technique has now been developed which permits the monolayer to be maintained at any desired surface pressure during the course of the penetration experiment. The kinetics of the interaction are followed by measuring the expansion as a function of time under constant pressure. The experiments have been carried out varying the film pressure and also

the solute concentration in order to establish whether a complex of constant composition exists over a range of different conditions.

DESCRIPTION OF THE APPARATUS

The apparatus used in these studies was a Langmuir trough fitted with the device previously described for the compensation of pressure due to the slow adsorption of the injected solute on the free water side (10). Furthermore, two platinum wires were attached at the end of the horizontal arm fixed on the center of the torsion balance. One wire dipped in a mercury cup, the other contacted a mercury drop as soon as the arm was tilted by a slight pressure excess acting on the monolayer. The platinum mercury contact set a relay in motion which controlled a motor. The movement of this motor was transmitted to the glass slide which expanded the monolayer. The rate of expansion was so adjusted that the monolayer stopped expanding as soon as the platinum mercury contact was broken. By this means the surface pressure of the monolayer was kept constant during the penetration and did not vary by more than 0.2–0.3 dyne/cm. throughout the experiments.

The whole balance was enclosed in a box so as to avoid any floating impurities present in the atmosphere. The box was double-walled and was thermostated during operation.

EXPERIMENTAL

The injection technique used is the same as that described previously (8). This technique was found satisfactory and was adequate for a first approach. To enable a quantitative study of the reaction kinetics of penetrations to be carried out, certain improvements in the technique are still necessary.

After injection, two to three points are recorded per minute for a period of *ca.* 30 min. For longer periods the rate of expansion decreases, and an hour after the injection readings are taken at *ca.* 2-min. intervals and are found to lie on a straight line. This linear expansion with time has been observed for periods of 2 or 3 hr. and has remained unchanged. Each curve given in this paper results from many readings, upward of 50 individual points carried out during the course of a monolayer expansion. (See as an example Fig. 1, in which every observation is shown!)

In all cases, the expansion of the interacting monolayer was carried out at pressure values greater than the equilibrium pressure of the injected solute. The curves show the expansion of cholesterol monolayers as a function of time due to penetration by an interacting solute. The experiments were carried out using sodium cetyl sulfate and saponin, varying the injected amounts from 1.5 to 7 mg., and 3–10 mg., respectively. Seven hundred milliliters of quartz-distilled water, containing 100 mg.

NaCl to mitigate the effect of any accidental impurity was used as the underlying solution.

The injection process was of $2\frac{1}{2}$ min. duration, and readings were started at the moment of injection.

RESULTS

In all cases the injection of the interacting solute species resulted in an expansion of the film, the rate of which decreased with time and subsequently became constant. The results obtained show that variations of surface pressure and the amount of injected solute markedly influence the expansion curves, which, nevertheless, all possess the following important features:

(a) Extrapolation of the linear portion of the expansion curve back to zero time gives an area whose value generally lies between 20 and 27 A.²/mole (for the cholesterol-sodium cetyl sulfate system), unless the surface pressure is too high, i.e., above 30 dynes/cm., or the amount of sodium cetyl sulfate injected is too large, i.e., 7 mg. Similarly for the cholesterol-saponin system the same extrapolation gives a value of 54 A.²/mole. In both cases the increase in area is related to the cross-sectional area of the penetrating molecule, and the total extrapolated area corresponds to the area of the stoichiometric 1:1 association between cholesterol and sodium cetyl sulfate, cholesterol and saponin.

(b) The extrapolated areas are identical with the collapse areas found on compression of those films which have previously been allowed to expand for 90 min. The mixed film collapses as a unit.² The systems studied here differ from those described by Adam, Askew, and Pankhurst in 1939, where on compression the solute molecule is ejected from the mixed film, thus giving at the collapse pressure the area of the insoluble compound alone. The latter systems thus show no complex formation.

It follows that the expansion curves described here are the result of two processes:

(a) Interaction of the solute with the film-forming molecules as indicated by the value of the extrapolated areas, defining the stoichiometric associations.

(b) Solution of the injected solute in the surface structure as demonstrated by the linear expansion.

During the first 20 min. both processes occur simultaneously and a rapid expansion is observed. In the later stages when a linear relationship is obtained on the expansion curve, solution in the monolayer occurs exclusively, and a slow expansion is observed.

² The compression film experiment will be published later.

In order to characterize the first process, i.e., the interaction, the expansion areas must be corrected for the solution effect. Such corrections are shown in the curves marked by the suffix *a* in the diagrams. These curves are obtained by subtracting from the total expansion area the ordinate on the parallel of the linear expanding portion passing through the origin. The corrected curves, in all cases, follow the relationship:

$$\log_{10} (a_e - a_t) = kt + \text{constant},$$

where a_e is the limiting expansion area reached by the system, i.e., the area reached by extrapolation of the linear part back to zero time; a_t is

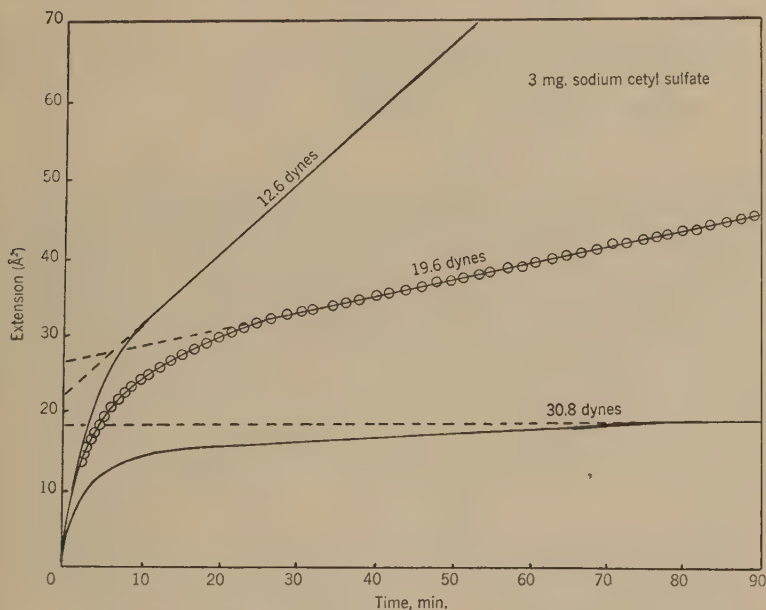


FIG. 1. Effect of pressure on the expansion of cholesterol monolayers by sodium cetyl sulfate at 21°C. At 30.8 dynes/cm. the linear expansion appears 80 min. after the injection and has been followed for over 100 min. Only the extrapolated line is represented in the figure.

the area at time t , and k is a constant, depending on different parameters. For a given system k depends on the concentration of the solute in the substrate, the pressure at which the experiment is carried out, and the temperature. We may now consider each system individually.

A. Study of the Cholesterol-Sodium Cetyl Sulfate System

1. *Effect of Surface Pressure on Monolayer Interaction.* Figure 1 shows some typical results obtained for cholesterol expansion after injection of 3 mg. of cetyl sulfate. The expansions were carried out at three different

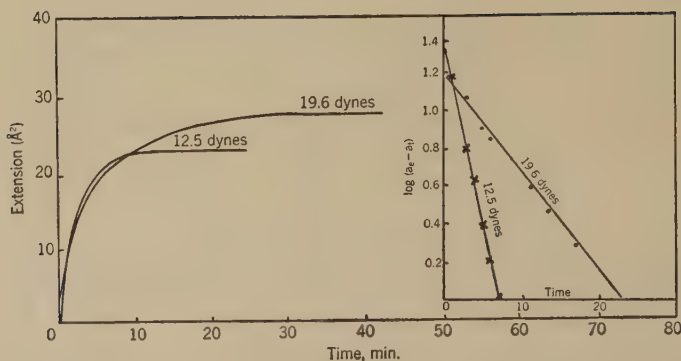


FIG. 2. Effect of pressure in the rate of cholesterol-sodium cetyl sulfate interaction at 21°C . At 30.8 dynes/cm. the first-order law is not obeyed, this pressure value being presumably too close to the stability pressure of the complex.

pressures, i.e., 12.6, 19.6, and 30.0 dynes/cm. Figure 2 shows the expansion of a monolayer due to the interaction process only. The curves shown are obtained after correction for the solution effect. Such curves follow a first-order law as shown by the linearity of the logarithmic plot. It appears also that the rate coefficient decreases as the pressure in the monolayer increases, showing that the interaction can be slowed down markedly by steric effects.

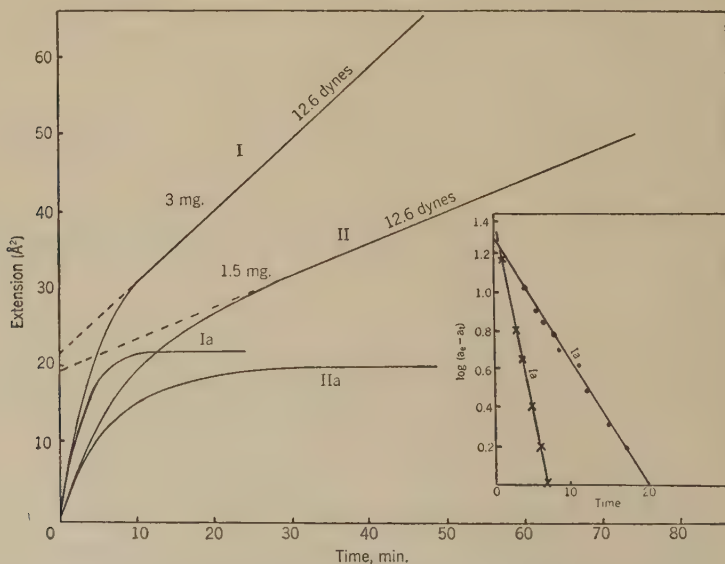


FIG. 3. Effect of sodium cetyl sulfate concentration on the rate of cholesterol-sodium cetyl sulfate interaction at 21°C .

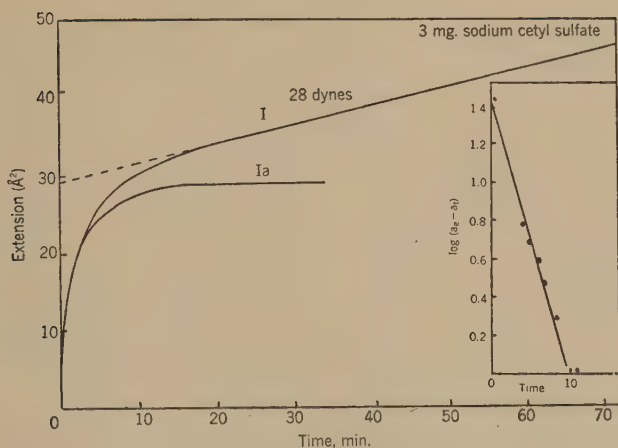


FIG. 4. Cholesterol-sodium cetyl sulfate interaction at 21°C.

2. *Effect of Concentration.* Figures 3 and 4 show the expansion characteristics when different quantities of the solute are injected into the underlying solution. By using 1.5 mg. instead of 3 mg. at 12.6 dynes/cm. the rate constant is reduced by more than half; this is possibly due to the fact that, in the former case, the pressure due to the adsorbed monolayer of cetyl sulfate, is much less than when 3 mg. is used. Therefore a greater energy barrier is presented to the cetyl sulfate molecules during monolayer penetration at the same pressure.

Figure 4 shows the behavior of the monolayer when 7 mg. is present

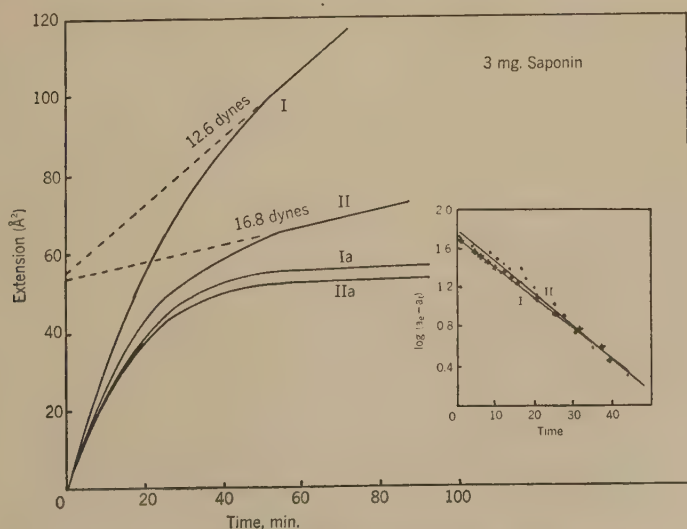


FIG. 5. Effect of pressure on cholesterol-saponin interaction at 21°C.

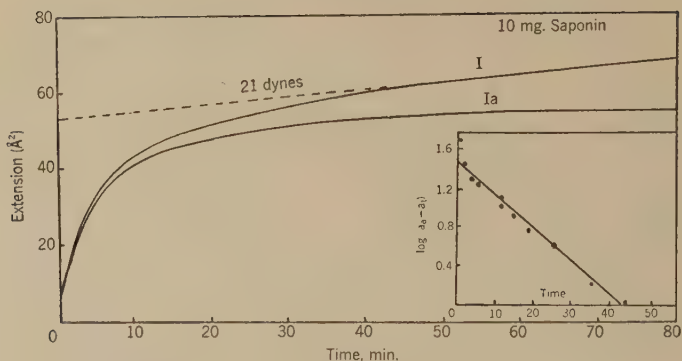


FIG. 6. Cholesterol-saponin interaction at 21°C.

in the underlying solution. Increasing the concentrations results in an increase in the value of the reaction rate coefficient k . For example, k is greater when 7 mg. is injected under the monolayer at 28 dynes than when 3 mg. is injected at 19.6 dynes.

In all cases investigated, it appears that varying the pressure under which monolayer expansion is carried out, or varying the amount of injected solute, does not alter greatly the value of the extrapolated area increase.

B. Study of the Cholesterol-Saponin Interaction

In contrast to the previous system, this interaction leads to a much greater increase in area of the cholesterol monolayer.

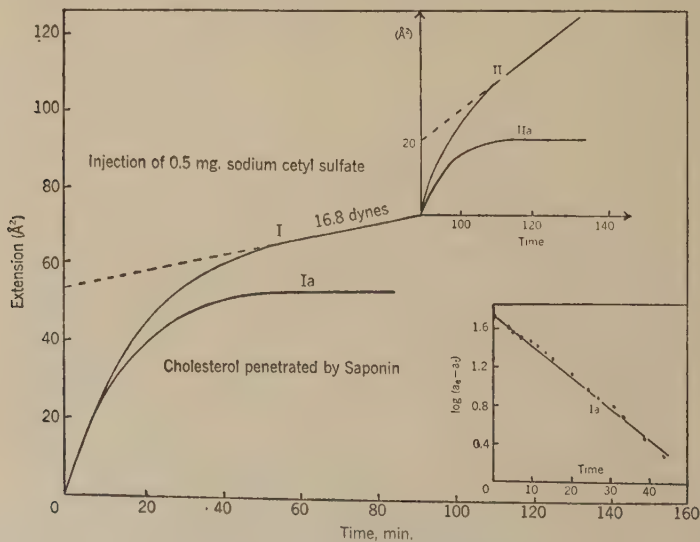


FIG. 7. Effect of saponin on cholesterol-sodium cetyl sulfate interaction at 21°C.

The results of Figs. 5 and 6 show that the monolayer expansion due to the interaction also follows a first-order law, and it appears that, in the range investigated, the rate of interaction is practically independent of the pressure and of the concentration of the solute in the substrate.

C. Mechanism of Formation of Tricomplexes

This technique has also been used to investigate the process of tri-complex formation in which the interaction of three substances with each other results in the formation of a stable structure. The investigation has been carried out with saponin, cholesterol, and cetyl sulfate. Figure 7 shows some experimental results. Whereas injection of 0.5 mg. of cetyl sulfate under cholesterol monolayers maintained at 16.8 dynes/cm. produces a very small effect, a previous penetration by saponin enhances very markedly the penetration of the cetyl sulfate. Indeed, the complex saponin-cholesterol-cetyl sulfate is formed completely 20 min. after injection of a minute quantity of cetyl sulfate.

It is interesting to note that if cetyl sulfate is previously injected under cholesterol, injection of saponin under the expanded monolayer results in a much smaller expansion than when cetyl sulfate is absent.

DISCUSSION

The results described clarify the mechanism of monolayer expansion. The corrected curves shown in the figures obey the relationship $\log (a_e - a_t) = kt + \text{constant}$. As the experiments are carried out at constant pressure, the solute molecules occupy the same area throughout the expansion, and consequently the increase in area is proportional to the number of penetrating molecules, x . The above relationship is therefore equivalent to $\log (x_e - x_t) = kt + \text{constant}$. This is compatible with the view that the interaction between species A present in the monolayer, and B in the solute molecules follows the equation $A + B = AB$. Since B is present in great excess the interaction leading to the formation of the stoichiometric complex follows a pseudo-unimolecular law.

The solution phenomenon described here extends over periods greater than 4 hr. after injection. This phenomenon is responsible for the very slow rise in pressure of mixed films which was observed by Harkins and co-workers (6) and later by Matalon and Schulman (10).

This is possibly due to an activated adsorption since it occurs at pressures greater than the equilibrium pressure of the injected solute. The results show that the rate of solution into the monolayer for a given system decreases as the pressure in the monolayer increases. This reduction in the effect of the solution factor indicates that the formation of the stoichiometric complex has been partially prevented, as has been verified in a study of monolayer-lipoprotein associations (11).

Hence it appears that when interaction between two species results in the complete formation of a stoichiometric complex, excess solute molecules continue to expand the monolayer and are stabilized in it.

The results shown in Figs. 1, 2, and 3 for cholesterol-sodium cetyl sulfate give values for a_e between 20 and 27 \AA^2 , an area close to the cross-sectional area of the cetyl sulfate molecule. Hence it is apparent that the interaction leads to a stoichiometric 1:1 association. Instances of deviation from the range of 20–27 \AA^2 are found when the solution factor has been depressed by working at high pressures (Fig. 1), and also when excess sodium cetyl sulfate has been injected into the underlying solution (Fig. 4).

Using saponin instead of sodium cetyl sulfate, a_e is found to be equal to 54–56 \AA^2 , which is 14–16 \AA^2 higher than the area of cholesterol. This is probably due to the presence of the glucoside residues in saponin.

It follows that with both systems the molecular interaction leads to a stoichiometric 1:1 association, and that this complex is found over a range of pressure and concentration. That a difference exists between the cholesterol-sodium cetyl sulfate and the cholesterol-sodium saponin interaction is shown since the rate of interaction of the latter system is independent of variations of pressure. This is probably due to the great similarity of structure between cholesterol and saponin, both being of the phenanthrene type, and possessing similar cross-sectional areas. These two substances can therefore pack together in a mixed structure in the surface. In the latter case the ion/dipole association is responsible for the complex formation. Dervichian (12) has shown that such an association in bulk destroys the crystalline structure of cholesterol, and results in the formation of liquid mixed crystals as shown by myelinic figures.

The application of the monolayer expansion technique to investigate tricomplices indicates that molecular interaction can be partially suppressed, as well as sensitized. When cholesterol is previously associated with sodium cetyl sulfate it becomes more difficult to pack saponin into this new structure, and the expansion area resulting from the saponin injection beneath this film is decreased. Quite the reverse is found when saponin is first associated with cholesterol; a very rapid expansion then takes place upon injection of a minute amount (0.5 g.) of sodium cetyl sulfate, and the interaction is complete within 20 min. Under similar conditions, the injection of this quantity of sodium cetyl sulfate beneath a pure cholesterol monolayer expands the monolayer by 8 \AA^2 only.

The present results have been interpreted on the basis of two concurrent processes, solution and complex formation. The stoichiometric association has been demonstrated by eliminating the solution factor from the expansion curves. It has also been assumed that the solution phenomenon manifests itself as soon as injection begins.

The experimental results have also shown that when this solution is prevented, association is only partial.

It is apparent, therefore, that the two processes are by no means so independent as might be suggested by the treatment given in this work, and that both must be considered in problems of molecular interaction in monolayers.

It is hoped to make a more precise analysis of the relation between these two phenomena.

SUMMARY

The techniques used for the study of the penetration phenomenon have been discussed in the light of recent work, and a new method of investigation, based on monolayer expansion and using the automatic compensating balance, is described.

Two processes have been found to occur, solution and complex formation. For the two systems investigated, cholesterol-sodium cetyl sulfate and cholesterol-saponin, a 1:1 association between monolayer and water-soluble compounds occurs.

The cause of the very slow variation in pressure in mixed films has been found to be due to a solution process of the injected molecules into the monolayer.

The technique has also been shown to be applicable to the study of micelle complex films. It has also been found that the interaction can be sensitized or partially prevented.

REFERENCES

1. SCHULMAN, J. H., AND STENHAGEN, E., *Proc. Roy. Soc. (London)* **B126**, 356 (1939); SCHULMAN, J. H., *Trans. Faraday Soc.* **39**, 412 (1943).
2. SCHULMAN, J. H., AND RIDEAL, E. K., *Proc. Roy. Soc. (London)* **B122**, 29 (1937).
3. SCHULMAN, J. H., *Trans. Faraday Soc.* **33**, 1116 (1937).
4. SCHULMAN, J. H., AND COCKBAIN, E. G., *Trans. Faraday Soc.* **36**, 651 (1940).
5. ALEXANDER, A. E., AND SCHULMAN, J. H., *Trans. Faraday Soc.* **36**, 960 (1940).
6. HARKINS, W. D., COPELAND, L. E., AND GORDON, B., *Surface Chemistry. Am. Ass. Adv. Sci. Publication* **21**, p. 79, 1943.
7. HUTCHINSON, E., *J. Colloid Sci.* **3**, 413 (1948).
8. MATALON, R., AND SCHULMAN, J. H., *Trans. Faraday Soc.* **43**, 479 (1947).
9. SCHULMAN, J. H., STENHAGEN, E., AND RIDEAL, E. K., *Nature* **141**, 785 (1938).
10. MATALON, R., AND SCHULMAN, J. H., *J. Colloid Sci.* **4**, 89 (1949).
11. MATALON, R., AND SCHULMAN, J. H., *Discussions Faraday Soc.* **6**, 27 (1949).
12. DERVICHIAN, D. G., *Trans. Faraday Soc.* **42B**, 180 (1946).

VISCOSITY AND ELECTROVISCIOUS EFFECT OF THE AGI SOL. I. INFLUENCE OF THE VELOCITY GRADIENT AND OF AGING OF THE SOL.

G. J. Harmsen, J. van Schooten and J. Th. G. Overbeek

van't Hoff Laboratory, University of Utrecht, Utrecht, Netherlands

Received May 29, 1952

INTRODUCTION

Although the relation between viscosity and the concentration of macromolecular solutions has already been investigated extensively and successfully, this subject causes greater difficulties with hydrophobic sols, and the small amount of experimental material can only very partly be fitted into the picture (1).

The Einstein (2) relation

$$\eta_{\text{rel}} = 1 + 2.5 \varphi \quad [1]$$

was derived for very dilute suspensions of rigid, spherical uncharged particles. It has been extended to higher concentrations by different investigators, usually by adding a term in φ^2 , the coefficient of which, unfortunately, is given differently by every investigator, varying between 2.5 and 75.

As our investigation is carried out with roughly spherical particles, the influence of deviating shapes of the particles will not be considered here.

The influence of the charge of the particles was considered by Smoluchowski (3) who published in 1916 his equation on the so-called electroviscous effect:

$$\eta_{\text{rel}} = 1 + 2.5 \varphi \left[1 + \frac{1}{\sigma \eta_0 a^2} \left(\frac{\epsilon \zeta}{2\pi} \right)^2 \right] \quad [2]$$

In Eqs. [1] and [2] η_{rel} is the relative viscosity of the suspension; φ , the volume fraction of suspended particles; σ , the specific conductance; η_0 , the viscosity; ϵ , the dielectric constant of the dispersion medium; a , the radius of the particles, and ζ , the potential of the double layer at the slipping plane between particles and liquid. A derivation of this equation was given by Krasny-Ergen (4), who found a slightly deviating numerical factor.

Booth (5) recently published a theory about the electroviscous effect, arriving at a much smaller correction term

$$\eta_{\text{rel}} = 1 + 2.5 \varphi \left[1 + q^* \left(\frac{e\xi}{kT} \right)^2 (1 + \kappa a)^2 Z(\kappa a) + \dots \right] \quad [3]$$

with

$$q^* = \frac{\epsilon k T \sum n_i z_i^2 \rho_i}{\eta_0 e^2 \sum n_i z_i^2} \quad \text{and} \quad \kappa^2 = \frac{4\pi e^2 \sum n_i z_i^2}{\epsilon k T}$$

in which equation e is the elementary charge; n_i the number of ions, i , per unit volume; z_i the valency, and ρ_i the frictional constant of the ion i ; k Boltzmann's constant; and Z a certain function of κa .

The equations of both Smoluchowski and Booth are restricted to very dilute suspensions. Smoluchowski's equation is moreover restricted to thin double layers, that is to relatively high concentrations of electrolytes, whereas Booth's equation applies to any thickness of the double layer.

The equations for the electroviscous effect were only tested in a few cases, from which it appeared that the effect found was much smaller than that predicted by the equation of Smoluchowski (5,6).

The object of the present investigation was to examine experimentally the electroviscous effect at different sol concentrations with a well-defined hydrophobic sol. The AgI sol was chosen, which has been extensively studied by Kruyt and his co-workers.

AGING OF THE AgI SOL

A fresh silver iodide sol, prepared (7,8) by mixing solutions of AgNO_3 and KI (with a slight excess of KI), followed by electrodialysis and elec-

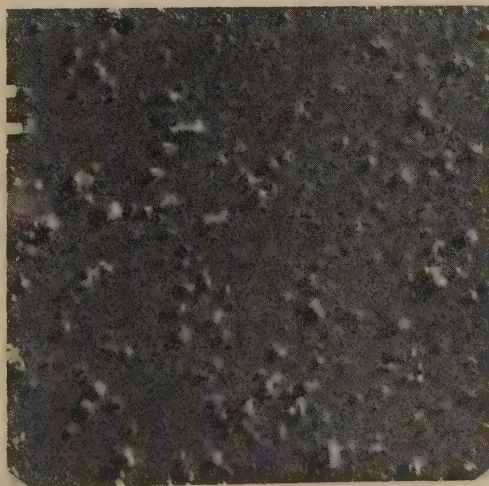


FIG. 1. (a) Fresh AgI sol. Pt-shadowed. 1:10,000.



(b) Aged AgI sol. Pt-shadowed. 1:10,000.

trodecantation, shows aging phenomena as, e.g., an increase in conductivity and in the activity of I^- ions (9). The viscosity also changes by this aging. This decrease in viscosity may, in principle, have several causes: (a) change in form of the particles; (b) change in size of the particles owing to recrystallization or slow flocculation; and (c) liberation of electrolyte.

The increase in the conductivity and increase in the concentration of I^- ions indicate that case (c) actually occurs.

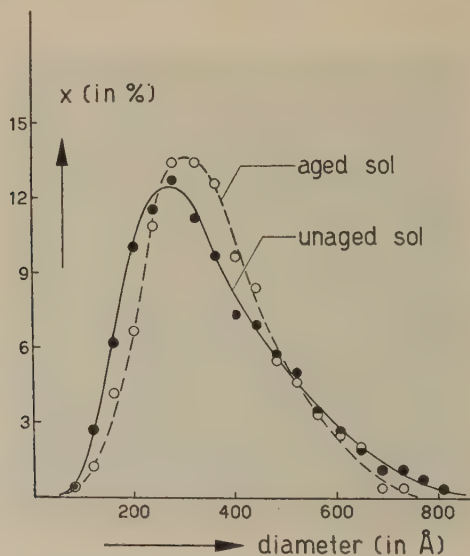


FIG. 2. Distribution of diameters of particles of a fresh and an aged AgI sol.

Taking into account the preparation of the sol in which the *gegenions* have been exchanged against H^+ ions by the electrodialysis, liberation of occluded KNO_3 and of adsorbed HI can be expected.

In order to test how far one or the other of the above-mentioned factors plays a part, an electron micrograph of an unaged sol was compared with one of the same sol that had been aged by heating for 24 hr. at $85^\circ C$. (see Figs. 1a and b, respectively).

On the basis of some pictures made at smaller magnifications, the distribution curves of the diameters for the two sols were determined (see Fig. 2). It is clear that from these pictures hardly any difference can

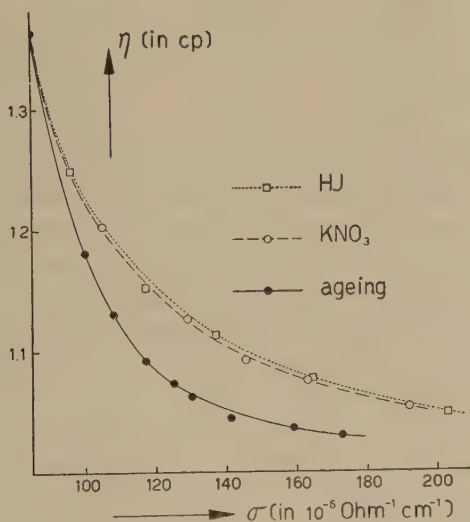


FIG. 3. Relation between viscosity and specific conductivity of an AgI sol. $\varphi = 2.33\%$.

be found between the aged and the unaged sol. Moreover, it appears from the length of the shadows (the particles have been shadowed with platinum at an angle $\tan^{-1} 4$) that the particles are nearly spherical.

In order to examine how far the liberated electrolyte may explain the change in viscosity, a $0.06 N KNO_3$ solution was added dropwise to a portion of an unaged sol ($\varphi = 2.33\%$) and the viscosity and the specific conductance were measured. The same was done with another part of this sol and a $0.015 N HI$ solution. The influence of those additions on the sol concentration φ was negligible.

Figure 3 shows the viscosity as a function of the conductivity. These curves were compared with a similar curve of the aging AgI sol. The aging was performed at $45^\circ C$.; the measurements were made, however, at 25° . The last point was measured 500 hr. after the starting point. The specific resistance as well as the viscosity decreased regularly.

TABLE I
Data for Ostwald Viscometers Used

No.	Viscometer constant, k	Mean gradient of velocity for water of 25°C. $\left(\frac{dv}{dr}\right)_{av} = \frac{HdgR}{3\eta l}$	Diameter of the capillary, $2R$	Time of efflux for water of 25°C.
		sec.^{-1}	cm.	sec.
I	0.002656	700	0.038	338.2
II	0.01176	1000	0.055	76.9
III ^a	<i>ca.</i> 0.00665	<i>ca.</i> 900	0.050	<i>ca.</i> 135
IV	0.00775	900	0.050	116.3
V ^a	<i>ca.</i> 0.00692	<i>ca.</i> 900	0.050	<i>ca.</i> 130

^a No exact values are given for viscometers III and V, as the latter had to be repaired between times. They were fairly equal to viscometer IV. After each reparation the viscometer was calibrated anew.

If we compare the three curves we see that the viscosity decreases more rapidly than might be expected on the basis of the conductivity and the KNO_3 and HI curves. So our conclusion must be that the liberation of electrolyte is, in fact, the most important, but not the only cause of the decrease in viscosity. In this case we think of a perfecting of the AgI crystals which, though not growing into larger, do grow into more compact particles and thus might cause a decrease of the viscosity.

TABLE II
(a) Electrolyte: HNO_3 39.0 mmoles/l. + HI 0.035 mmole/l.

vol. %	Viscometer									
	I		II		III		IV		V	
	η	K	η	K	η	K	η	K	η	K
0.476	0.9142	4.41	0.9120	3.89	0.9130	4.14	0.9126	4.05	0.9135	4.23
1.09	0.9340	3.95	0.9310	3.64	0.9338	3.94	0.9311	3.65	0.9331	3.86
2.11	0.9672	3.80	0.9648	3.67	0.9651	3.68	0.9650	3.68	0.9658	3.73
2.95	1.0038	4.10	0.9953	3.78	0.9965	3.83	0.9934	3.71	0.9973	3.87
4.87	1.0743	4.10	1.0676	3.95	1.0685	3.97	1.0667	3.94	1.0686	3.97

(b) Electrolyte: HI 0.035 mmole/l.

0.411	0.9099	4.41	0.9088	4.11	0.9069	3.60	0.9071	3.66	—	—
0.797	0.9270	4.68	0.9245	4.33	0.9248	4.37	0.9256	4.46	0.9245	4.33
1.58	0.9668	5.18	0.9615	4.80	0.9665	5.16	0.9661	5.12	0.9664	5.15
2.99	1.1089	8.05	1.0915	7.40	1.1016	7.78	1.1007	7.74	1.0994	7.70
6.37	1.9330	18.26	1.8516	16.82	—	—	1.8834	17.40	1.8934	17.54

INFLUENCE OF THE RATE OF SHEAR ON THE VISCOSITY OF AgI SOLS

The viscosity measurements were carried out in a number of Ostwald viscometers all having the same outward dimensions but different capillary diameters. The data for the viscometers used have been collected in Table I.

All viscosities have been determined at $25 \pm 0.01^\circ\text{C}$.

The kinematic viscosity, ν , was calculated in centistokes, according to

$$\nu = \frac{\eta}{d} = kt - \frac{0.6}{t},$$

in which t is the time of efflux, and d the density. The factor 0.6 has been derived from Sprokel's work (10).

In order to test whether the AgI sol behaves as a Newtonian liquid, viscosity measurements were carried out on two series of sol concentrations in all five viscometers, the one series containing considerable electrolyte, the other one only a small amount. The aqueous solutions in which the AgI was suspended contained only HNO_3 and HI, while in both cases the p_I ¹ amounted to 4.6. The viscosity of each sol was calculated in centipoises and from it the value of $K = (\eta_{\text{rel}} - 1)/\varphi$. The results have been recapitulated in Tables IIa and b. They show that with a higher electrolyte concentration (Table IIa) the effect of the time of efflux on viscosity is very slight. For the low electrolyte concentration, on the other hand, and with the higher sol concentrations, the viscosity is clearly dependent on the time of efflux. Evidently, the deviation from Newtonian behavior increases with increasing interaction between the double layers, and the viscosity increases with decreasing rate of shear.

The flow pattern in the capillary obeys the equation

$$\frac{1}{r} \frac{dv}{dr} = - \frac{Hdg}{2l\eta}$$

in which g is the acceleration of gravity. For all our viscometers H/l has the same value. Therefore, for one definite sol the profile of flow is given by

$$\frac{1}{r} \frac{dv}{dr} = - \frac{\text{const.}}{\eta}$$

where the constant is independent of the viscometer used.

If, as a first approximation, η is also taken as constant, then the mean gradient will be proportional to the radius of the capillary. Extrapolation to a velocity gradient $\frac{dv_{\text{av}}}{dr} = \text{zero}$, is consequently obtained by extrapolating to a capillary radius $R = 0$. In Fig. 4 the values of K obtained for

¹ p_I = negative logarithm of concentration of I^- ions.

the viscometers I, II, and IV in the last three rows of Table IIb have therefore been plotted against R .

It is true that the observations do not admit accurate extrapolation to $R = 0$, but the points indicated do show that the influence of the rate of shear on the value of K is not very large. Qualitatively, the effect of the sol concentration and the electrolyte concentration will therefore not be different from the extrapolated value, if measured at a finite rate of shear.

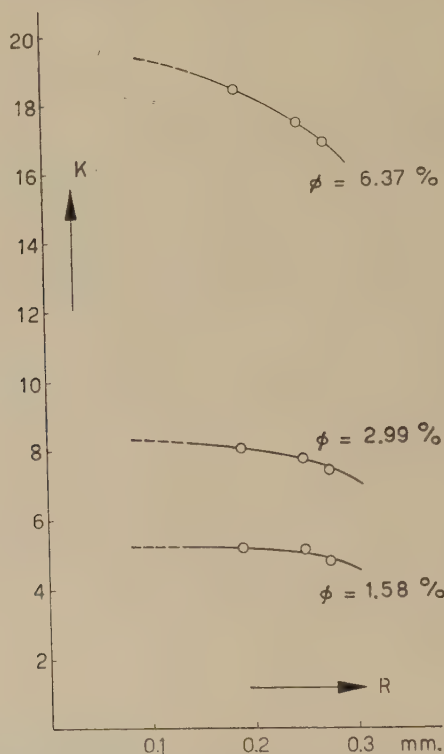


FIG. 4. Dependence of K on the radius of the capillary of the viscometer (\sim rate of shear).

In order to restrict the number of measurements, we continued our investigation [see next paper (11)] with viscometers III, IV, and V, thus working with an average gradient

$$\left(\frac{dv}{dr}\right)_{av} = \frac{HdgR}{3l\eta}$$

or of $8/\eta$, that is of 500–1000/sec.

For details on the preparation of the AgI sols we refer to our second paper (11).

SUMMARY

It was shown that the change of the viscosity of silver iodide sols during aging was mainly, but not exclusively, caused by the liberation of electrolytes.

The viscosity of AgI sols was shown to decrease with increasing rate of shear, the more so as the concentration of the sol was higher and that of the electrolytes lower. For the investigation of the influence of these concentrations on the viscosity, a rate of shear of 500-1000/sec. was considered sufficiently low, and extrapolation to zero rate of shear was deemed unnecessary.

REFERENCES

1. A survey with references to the literature can be found in: KRUYT, H. R., *Colloid Science*, Vol. 1, Chap. 9. New York and Amsterdam, 1952; PHILIPPOFF, W., *Viskosität der Kolloide*. Dresden and Leipzig, 1942; *Handbuch der Kolloidwissenschaft in Einzeldarstellungen*. Bd. 9.
2. EINSTEIN, A., *Ann. Physik* **19**, 289 (1906); *ibid.* **34**, 592 (1911).
3. SMOLUCHOWSKI, M. V., *Kolloid-Z.* **18**, 194 (1916).
4. KRASNY-ERGEN, W., *Kolloid-Z.* **74**, 172 (1936).
5. BOOTH, F., *Proc. Roy. Soc. (London)* **A203**, 533 (1950).
6. DOBRY, A., *J. chim. phys.* **47**, 402 (1950); *ibid.* **48**, 28 (1951).
7. DE BRUYN, H., AND TROELSTRA, S. A., *Kolloid-Z.* **84**, 192 (1938).
8. DE BRUYN, H., AND OVERBEEK, J. TH. G., *Kolloid-Z.* **84**, 186 (1938).
9. VERWEY, E. J. W., AND KRUYT, H. R., *Z. physik. Chem.* **A167**, 137, 149 (1933).
10. SPROKEL, G. J. M., Thesis. University of Utrecht, Utrecht, Netherlands, 1952.
11. HARMSSEN, G. J., SCHOOTEN, J. V., AND OVERBEEK, J. TH. G., *J. Colloid Sci.* **8**, 72 (1953).

VISCOSITY AND ELECTROVISCIOUS EFFECT OF THE AgI SOL. II. INFLUENCE OF THE CONCENTRATION OF AgI AND OF ELECTROLYTE ON THE VISCOSITY

G. J. Harmsen, J. van Schooten and J. Th. G. Overbeek

van't Hoff Laboratory, University of Utrecht, Utrecht, Netherlands

Received May 29, 1952

INTRODUCTION

In our previous paper (1) we showed that the AgI sol does not entirely behave as a Newtonian liquid. In order to be able to continue the investigation of the electroviscous effect on a comparative basis, observations were made in viscometers of nearly identical construction, with an average velocity gradient of about 1000/sec. for water of 25°.

It was also shown that the AgI sol, when aging, exhibits a decrease in viscosity, which can be explained for the greater part by liberation of electrolyte.

In this paper the electroviscous effect will be further investigated. On theoretical grounds it is expected to be dependent on the structure of the electrical double layer. This structure is determined by the concentration of the potential-determining ions, i.e. the I^- ions, and by the concentrations of the neutral electrolyte determining the quantity $1/\kappa$, thus, the dimensions of the double layer.

The influence of the latter being our main point of interest, we always took care to have one and the same p_I in our sols.

EXPERIMENTAL

Preparation of the Sols

The AgI sol was prepared in portions of 800 ml. by adding a solution of 50 mmoles of $AgNO_3$ in 400 ml. water to a solution of 55 mmoles KI in 400 ml. water under continuous agitation. By electrodialysis the KNO_3 formed and the excess KI were removed (2). At the same time the K^+ gegenions are exchanged against H^+ ions, so that finally a so-called acid sol remains that can be represented schematically as $[AgI] I^- H^+$. This sol is concentrated by electrodecentration, after which it is aged by heating it for 24 hr. at 85°C. After the aging the liberated electrolytes are removed by electrodialysis and electrodecentration. In this way an aged AgI sol was obtained with a concentration of ca. 1800 mmoles AgI/l., which showed no more change in viscosity with time.

From this sol eight series of 7 to 8 sol concentrations, varying from 5 to 1800 mmoles AgI/l. were prepared. Each series was dialyzed against an HNO_3 solution of a certain concentration. Moreover, care was taken, by adding HI, that all these electrolyte solutions at the termination of the dialysis had a $p_I = 4.6$. By this method we obtained that

TABLE I
Composition of Equilibrium Solution

No.	C_{H^+} mg. ion/l.	Thick- ness of double layer, $1/\kappa$ Å.	Conduc- tivity, σ $\times 10^6$ mho/cm.	Viscosity, η_0 centipoise
1	0.035	500	19	0.8937
2	0.12	278	55	0.8937
3	0.49	138	200	0.8937
4	2.3	64	1200	0.8938
5	8.2	34	3200	0.8942
6	15.0	25	5700	0.8943
7	25.6	19	9500	0.8949
8	39.0	16	14400	0.8954

each series consisted of a number of perfectly comparable sols of different sol concentrations, while moreover the properties of the dispersion medium like electrolyte concentrations, conductivity and p_I could be measured without running the risk of complications caused by the presence of sol particles (3).

Next, the kinematic viscosity of each of the sols was measured in viscometers (1) III, IV, and V at 25°C., and from these results the average was taken. The AgI content was determined by evaporation and weighing. The density of the sol, necessary in the

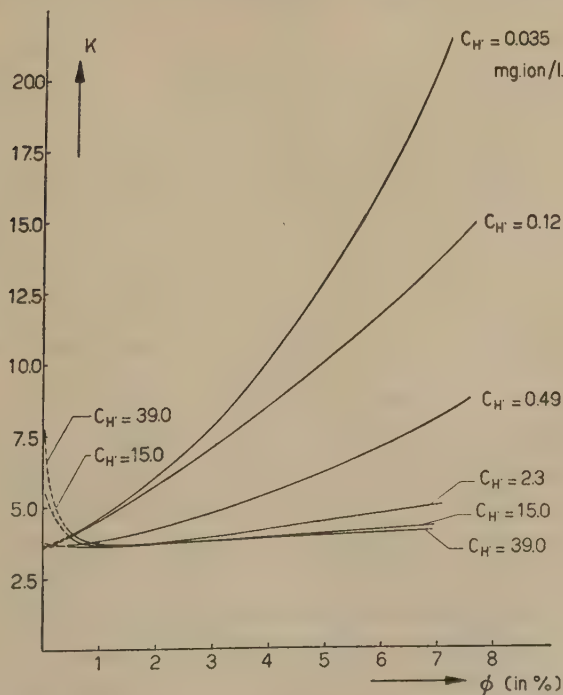


FIG. 1. The value of $K = \eta_{sp}/\phi$ for the AgI sol with different HNO_3 concentrations as a function of the volume fraction ϕ .

calculation of the dynamic viscosity, η , was calculated from the AgI content and the densities of the equilibrium liquid and of the solid AgI. The correctness of the density thus found was confirmed by some pycnometric determinations.

From the viscosity determinations and the volume fraction φ , the value of $K = (\eta_{\text{rel}} - 1)/\varphi$ was calculated.

RESULTS

Measurements

The data obtained have been collected in Tables I and II and are represented graphically in Figs. 1 and 2. Table I gives the composition of the eight equilibrium liquids. Tables II-1 to II-8 give, each for a different equilibrium liquid, the corresponding values of the volume fraction φ , the viscosity η , and the value of K .

Figure 1 shows how K changes as a function of sol concentration and Fig. 2 how it depends on the thickness of the double layer $1/\kappa$.

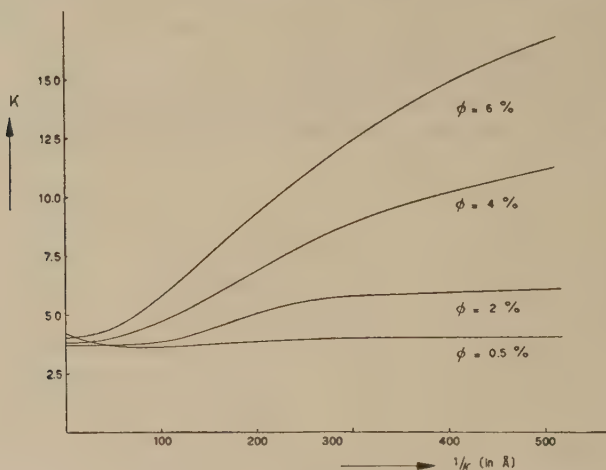


FIG. 2. Relation between $K = \eta_{\text{spec}}/\varphi$ and thickness of double layer, $1/\kappa$.

Accuracy of the Measurements

It appeared that for the lower sol concentrations ($\varphi < 1\%$) the standard deviation of the value of η , averaged from three measurements was about 0.05%. The accuracy of K was of course much smaller. The standard deviation was 20% and higher for $\varphi \leq 0.1\%$, 5–10% for $\varphi \sim 0.2\%$, and reached only 1–2% when $\varphi > 1\%$. For the greater values of φ somewhat larger deviations in η occurred owing probably to deposition of AgI in the viscometers. But even the largest errors in η , which are of the order of 0.2%, do not give rise to deviations in K of more than 1%.

As for the effect of the non-Newtonian behavior of the sols on the systematic error in the measurements we refer to our first paper (1).

TABLE II

Relation between Volume Fraction φ ,^a Viscosity η ,^b and K

II-1			II-2			II-3		
$C_{H^+}=0.035$			$C_{H^+}=0.12$			$C_{H^+}=0.49$		
φ	η	K	φ	η	K	φ	η	K
0.107	0.896 ₂	2.6	0.111	0.896 ₃	2.7	0.095	0.897 ₁	4.0
0.209	0.901 ₀	3.9	0.215	0.901 ₄	4.0	0.198	0.899 ₀	3.0
0.411	0.907 ₀	3.6 ₃	0.418	0.908 ₄	3.9	0.403	0.906 ₉	3.7
0.797	0.925 ₀	4.3 ₉	0.830	0.926 ₈	4.4 ₄	0.831	0.92 ₁	3.7
1.58	0.966 ₃	5.1 ₄	1.61	0.96 ₈	5.1 ₃	1.68	0.95 ₆	4.1 ₇
2.99	1.10 ₁	7.7 ₄	4.85	1.31 ₉	9.8 ₂	3.34	1.034 ₅	4.7 ₂
6.37	1.88 ₉	17.4 ₇	7.08	1.76 ₁	13.7 ₀	4.82	1.152 ₇	6.0 ₁
						7.38	1.45 ₃	8.4 ₇
II-4			II-5			II-6		
$C_{H^+}=2.3$			$C_{H^+}=8.2$			$C_{H^+}=15.0$		
φ	η	K	φ	η	K	φ	η	K
0.101	0.897 ₅	4.1	0.160	0.899 ₁	3.4	0.075	0.898 ₁	5.6
0.206	0.899 ₉	3.3	0.324	0.904 ₇	3.6	0.162	0.901 ₅	5.0
0.382	0.906 ₃	3.7	0.635	0.914 ₄	3.6	0.312	0.905 ₉	4.4
0.773	0.918 ₈	3.6 ₂	1.50	0.943 ₅	3.6 ₈	0.678	0.917 ₀	3.7 ₅
1.59	0.946 ₀	3.6 ₇	2.74	0.987 ₄	3.8 ₁	1.34	0.938 ₀	3.6 ₅
3.04	1.002 ₈	4.0 ₂	4.29	1.049 ₈	4.0 ₆	2.69	0.985 ₅	3.7 ₉
4.54	1.069 ₈	4.3 ₃	6.60	1.15 ₇	4.4 ₅	4.27	1.04 ₅	3.9 ₅
6.53	1.179 ₂	4.8 ₉				6.35	1.13 ₅	4.2 ₅
II-7			II-8					
$C_{H^+}=25.6$			$C_{H^+}=39.0$					
φ	η	K	φ	η	K			
0.021	0.896 ₃	7 ± 3	0.037	0.898 ₂	8 ± 2			
0.049	0.897 ₂	5 ± 1	0.103	0.901 ₂	6.3			
0.113	0.899 ₇	4.7	0.225	0.905 ₄	5.0			
0.384	0.907 ₄	3.6	0.476	0.913 ₀	4.1			
1.14	0.932 ₆	3.6 ₉	1.09	0.93 ₃	3.8			
1.82	0.955 ₈	3.7 ₃	2.11	0.965 ₄	3.7 ₀			
2.68	0.985 ₅	3.7 ₈	2.95	0.99 ₆	3.8 ₀			
			4.87	1.06 ₈	3.9 ₆			

^a In volume per cent.^b In centipoises.

DISCUSSION OF RESULTS

(a) *Very Low Sol Concentrations*

If, for the present, we forego the deviating behavior at higher electrolyte concentrations, extrapolation to $\varphi = 0$, gives a value for K lying between 3.4 and 3.6. The deviation of the value 2.5 from the Einstein equation is probably caused by a slight deviation of the spherical form, which is not visible on the electron microscope picture, but which is in accord with the crystalline character of AgI.

The extrapolated value of K is evidently not noticeably dependent on the electrolyte concentration. It is of interest to compare this result with the theories of Smoluchowski and Booth, which hold only for very dilute sols [see our first paper (1)].

For this purpose the value of the ζ -potential has to be known. From the work of Mackor (4) on the structure of the double layer of AgI it can

TABLE III

Equilibrium solution no.	$1/\kappa$	Electrolyte content	Correction factor f according to Smoluchowski		Correction factor f according to Booth	
			$\zeta = 200$ mv.	$\zeta = 100$ mv.	$\zeta = 200$ mv.	$\zeta = 100$ mv.
	<i>A.</i>	<i>mmoles/l.</i>				
1	500	0.035	1.70	0.43	0.010	0.003
2	278	0.12	0.59	0.15	0.008	0.002
3	138	0.49	0.16	0.04	0.006	0.001
4	64	2.3	0.03	0.01	0.004	0.001
6	25	15.0	0.006	0.001	0.003	0.001

be inferred, that at $p_I = 4.6$ the total double layer potential is about 350 mv., from which at the electrolyte contents used by us, 100–200 mv. is located in the diffuse layer.

The equations of Smoluchowski and Booth both have the form $K = 2.5 (1 + f)$, whereby, in our case, the numerical value 2.5 will have to be replaced by 3.6. Calculating now f for ζ -potentials of 100 and 200 mv., we find the values shown in Table III.

Taking into account that the equation of Smoluchowski may only be applied when the dimension of the double layer is small in respect to the particle diameter, only the equilibrium solutions 4 and 6 may be used for testing the equation of Smoluchowski in this table.

It then appears that in these cases the correction term according to Smoluchowski is smaller than 0.03. Thus, Smoluchowski's equation is not in conflict with our observations, provided that the conditions under which the equation is valid are not disregarded. The equation of Booth

gives for all electrolytic liquids very small correction terms, which come entirely within the error of our observation. It may therefore be concluded that the theory of Booth is not contradicted by our experiments either.

When looking at Fig. 1, one is struck by the anomalous behavior at higher electrolyte concentrations. Here the question arises as to whether this anomaly is characteristic for the sol, or whether it is due to a systematic error in calculation or measurement.

Since an abnormally high viscosity of the sol with higher electrolyte concentrations does not seem probable, we are inclined to look for the cause in an incipient orthokinetic flocculation in the sol or perhaps more in the slight flocculation on the wall of the capillary that is practically independent of the sol concentration. Considering that the times of efflux are proportional to the fourth power of the capillary diameter and assuming that without flocculation phenomena the value of $K = 3.6$ would have been found, then this would signify, with solution 8, a narrowing of the capillary of about 0.07%. The radius of the capillary being 0.25 mm. this would turn out to be an AgI layer of about 1500 Å., thickness. As this is only a few times the particle diameter, our supposition seems quite reasonable. That this flocculation is not noticeable with higher sol concentration is for the simple reason that the small increase in the time of efflux then causes only a very slight error in η_{spec} . In our further considerations, this increase has therefore been left out of account.

(b) Higher Sol Concentrations

For the highest two electrolyte concentrations (25.6 and 39.0 mmoles/l.) the relation between K and φ is given by two fairly coinciding straight lines. For these cases the relative viscosity may be written

$$\eta_{\text{rel}} = 1 + k_1\varphi + k_2\varphi^2 \quad [1]$$

in which $k_1 = \text{ca. } 3.55$ and $k_2 = \text{ca. } 8$.

For lower electrolyte concentrations the relation between K and φ is at least of the second degree; that between η and φ is therefore at least of the third degree.

$$\eta_{\text{rel}} = 1 + k_1\varphi + k_2\varphi^2 + k_3\varphi^3 + \dots \quad [2]$$

Here also k_1 can be put at *ca.* 3.55, while the best-fitting values of k_2 and k_3 greatly increase with decreasing electrolyte concentration, as is presented by Table IV.

As the different points of one curve are mutually not entirely comparable, because of unequal deviations from Newtonian behavior (cf. our previous paper), too much importance should not be attached to the exact value of the constants k_2 and k_3 . Table IV is merely intended to illustrate the trend in these constants.

Theoretical Interpretation of the New, Higher Order, Electroviscous Effect

That the rapid increase in viscosity with decreasing electrolyte concentration finds expression only in the constants k_2 and k_3 , and not in k_1 ,

shows that, at least in this case, the electroviscous effect is based on an interaction between the sol particles.

The particles which are carried away in the laminar flow have to pass each other. This passing is only possible if the particles are also displaced perpendicularly on the streamlines of the liquid. This displacement is the source of an extra dissipation of energy and consequently manifests itself in an extra contribution to the viscosity proportional to the number of meetings between particles, that is to the second and higher powers of the concentration. For uncharged particles, the displacement will be over a distance of the order of the radius of the particles; when the particles are charged the displacement is expected to cover distances of the order of the thickness of the double layer. An important electroviscous effect is therefore only expected when the thickness of the double layer is of the same order of, or larger than, the particle radius. Figure 2 shows that this is in good agreement with our results, the particle radius being of the

TABLE IV
Constants from Equation [2]

No.	Electrolyte concentration mmoles/l.	k_1	k_2	k_3
1	0.035	3.40	80	2200
2	0.12	3.60	100	600
3	0.49	3.40	30	525
4	2.3	3.55	10	160
5	8.2	3.55	10	50
6	15.0	3.55	8	50
7	25.6	3.55	8	—
8	39.0	3.55	8	—

order of 150 Å. (see previous paper). With larger particles the effect will be quite difficult to detect owing to the difficulty of having a value of $1/\kappa$ larger than 1000 Å.

The non-Newtonian behavior of sols showing this higher order electroviscous effect is also easily explained. The displacement of the particles in passing is caused by the repulsive force, and the total displacement will be smaller the more rapid the passing. Consequently at high rates of shear the extra dissipation of energy and its influence on the viscosity will be smaller.

As the viscosities in solutions 7 and 8 (25.6 and 39.0 mmoles/l.) do not differ mutually and are only slightly smaller than the solution 6 (15 mmoles/l.) it may be assumed that in these cases the interaction has been reduced to a merely hydrodynamic one. Theories for that case have been developed by Guth (5) and Vand (6) among others, who found for k_1 2.5 and for k_2 14.1 and 7.349, respectively. So the order of magnitude of k_2 is the same as in our Eq. [1]. Further conclusions cannot be made as

long as we do not know how to account exactly for the greater hydrodynamic volume which is reflected in $k_1 = 3.55$.

SUMMARY

Viscosity measurements were carried out on silver iodide sols with different sol concentrations and electrolyte concentrations. Independent of the electrolyte concentration the measurements extrapolated to a value of $K = \eta_{\text{rel}}/\varphi$ of 3.55 for a volume concentration $\varphi = 0$.

At higher sol concentration and with low electrolyte concentration, the interaction of the double layers gave rise to an increased viscosity (electroviscous effect). With electrolyte concentrations above 25 mmoles/l. the electroviscous effect has practically disappeared. The remaining excess viscosity can be explained by hydrodynamic interaction. So, an electroviscous effect is not measurable at $\varphi = 0$. This is in accord with Booth's theory but does not conflict either with the theory of Smoluchowski, within the range of application of the latter (thin double layer).

A theoretical explanation of the electroviscous effect at high concentrations is given, based upon the repulsive forces between particles passing each other in the laminar flow.

REFERENCES

1. HARMSSEN, G. J., SCHOOTEN, J. V., AND OVERBEEK, J. TH. G., *J. Colloid Sci.* **8**, 64 (1953).
2. DE BRUYN, H., AND TROELSTRA, S. A., *Kolloid-Z.* **84**, 192 (1938).
3. For the sol concentration effect see e.g., DE BRUYN, H., Thesis. University of Utrecht, Utrecht, Netherlands, 1938; *Rec. trav. chim.* **61**, 12 (1942); LOOSJES, R., Thesis. University of Utrecht, Utrecht, Netherlands, 1942.
4. MACKOR, E. L., *Rec. trav. chim.* **70**, 763 (1951).
5. GUTH, E., AND GOLD, O., *Phys. Rev.* **53**, 322 (1938).
6. VAND, V., *J. Phys. & Colloid Chem.* **52**, 277 (1948).

ULTRAVIOLET ABSORPTION OF AQUEOUS SULFUR SOLUTIONS

Henry L. Friedman and Milton Kerker

Department of Chemistry, Clarkson College of Technology, Potsdam, New York

Received June 2, 1952

INTRODUCTION

The kinetics of the formation of monodispersed sulfur hydrosols by the acid decomposition of sodium thiosulfate has been extensively studied by La Mer and others (1-5). The homogeneous part of the reaction can be followed by optical absorption measurements at 300 $m\mu$. If the absorption is interpreted as due to molecular sulfur, it is necessary to know the extinction coefficient of sulfur in water in order to determine the concentration of sulfur at any stage of the reaction.

The extremely low solubility of sulfur in water precludes the direct determination of the extinction coefficient. La Mer and Kenyon (1) have measured the absorption of sulfur in carbon tetrachloride, chloroform, and acetone and have used the average of the extinction coefficients in these solvents as an approximation to the value in water.

We have determined the extinction coefficient of sulfur in ethanol-water mixtures as well as a number of transparent organic solvents and will present an empirical relation between extinction coefficient and solvent refractive index which will permit us to estimate the extinction coefficient of sulfur in water.

EXPERIMENTAL PROCEDURE

Optical densities of sulfur solutions were measured for wavelengths of 225-380 $m\mu$ using a Beckman model DU quartz spectrophotometer with 1-cm. and 10-cm. quartz cells. The sulfur solutions, whose concentrations varied from 0.00012 to 0.012 g. atoms of sulfur/l., were compared with the pure solvents as standards of absorption. The solvents used were chloroform, ethanol, ethanol-water mixtures, glycerol, *n*-hexane, and methanol.

The solutions were prepared by adding small amounts of sulfur to the solvents and heating. It was found inexpedient to determine the concentrations by direct weighing because of the small quantities of sulfur to be handled. Furthermore, sulfur did not dissolve completely in the cases of chloroform and *n*-hexane. Preparations in which a suspension appeared

were filtered. The extinction coefficients for the glycerol solutions are not reported because such small amounts of sulfur dissolved that analysis was unsuccessful. Aliquot portions of the solutions were used for making dilutions. It was found that much of the solubility data in standard

TABLE I
Extinction Coefficients of Sulfur in Various Solvents

λ $m\mu$	Extinction coefficients						
	CHCl ₃	C ₂ H ₅ OH	95% C ₂ H ₅ OH	90% C ₂ H ₅ OH	n-Hexane	CH ₃ OH	Water
380	2.2	2.3	2.3	3.6	2.2	3.2	2.6
370	5.5	4.7	4.7	6.2	4.5	5.8	5.2
360	11.8	10.4	10.1	12.2	9.8	11.2	10.9
350	25.0	21.6	21.3	23.8	20.7	20.8	20.9
340	51.9	43.3	42.9	46.2	42.7	41.3	41.6
330	102	83.2	82.9	86.0	83.2	80.2	80.7
320	186	154	154	158	156	149	150
310	314	264	263	270	276	257	258
300	494	428	426	431	451	411	414
295	615	536	540	544	571	521	524
290	727	649	658	658	696	637	640
285	818	739	755	752	796	732	735
280	864	790	807	800	845	789	792
275	875	812	824	819	860	802	805
270	895	828	830	832	864	812	815
265	920	842	847	848	880	829	832
260	904	820	830	827	859	813	816
258	869	795	805	801	831	790	792
256	846	764	769	772	797	761	763
254	818	732	735	740	766	724	727
252	803	707	708	710	738	699	702
250	823	698	690	693	718	680	683
248	854	703	692	697	725	676	682
246	883	732	717	722	756	697	702
244	—	775	766	770	810	745	749
242	—	844	836	839	892	806	812
240	—	936	935	932	987	901	907
235	—	1182	1191	1182	1256	1161	1166
230	—	1363	1378	1375	1435	1351	1357
225	—	1458	1477	1474	1504	1435	1440

references was not reliable. Brooke (6) has pointed this out and has suggested this topic for undergraduate research projects.

The solutions were analyzed for sulfur content both by evaporation and by gravimetric analysis of sulfur as barium sulfate. The sulfur was first oxidized to sulfate by bromine and then precipitated and weighed as

BaSO₄ (7). The analysis was the largest source of error, for the quantities of sulfur and BaSO₄ were quite small. A microbalance was used for all weighings.

The spectrophotometer was thermostated at 25°C. by circulating water in order to keep the cells from being heated by the hydrogen lamp, thus minimizing evaporation and thermal currents. Narrow slit widths were used for maximum sensitivity and reproducibility. Sulfur was purified by the method of Bacon and Fanelli (8). Commercial 95% alcohol was used for the 90 and 95% ethanol runs. The absolute ethanol was prepared by the method of Weissberger and Proskauer (9). Hexane from

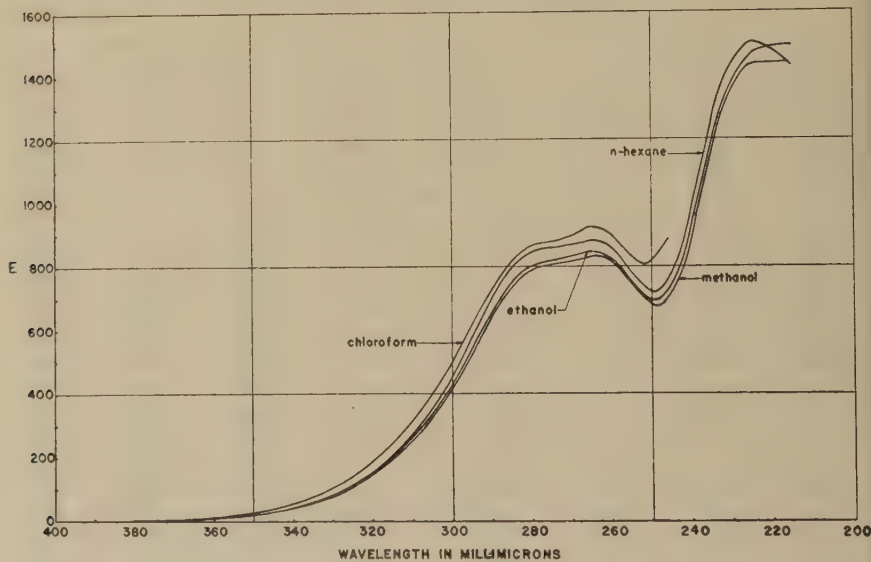


FIG. 1. Absorption curves for sulfur in various solvents. Extinction coefficient, $E = \log_{10} (I_0/I)$ for 1 *M* concentration and 1-cm. path length.

petroleum was purified for optical use by the method of Weissberger and Proskauer. A hydrocarbon mixture whose index of refraction was 1.3815, rather than 1.3750 for pure *n*-hexane, was produced. Merck's reagent-grade chloroform and Baker's c.p. reagent-grade methanol were used. All refractive indexes are for the sodium D line and 20°C.

RESULTS AND DISCUSSION

The extinction coefficients¹ are found in Table I and are plotted as a function of wavelength in Fig. 1. The curves show a maximum in the

¹ The extinction coefficient, E , is defined by $\log_{10} (I/I_0) = -Elc$, where I/I_0 = transmission, c = molar concentration, and l = light path in centimeters. This differs from the value of La Mer and Kenyon (1) by the factor 2.303.

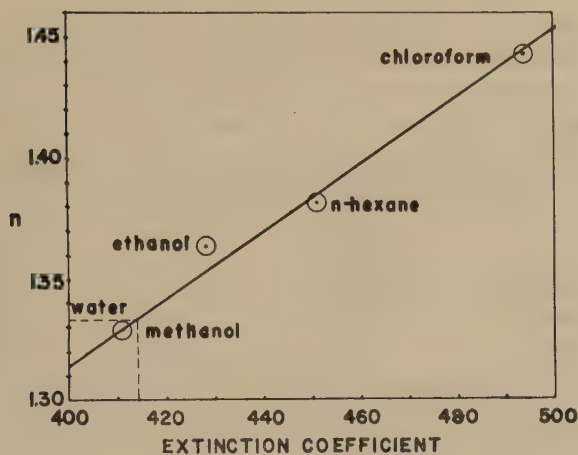


FIG. 2. Variation of extinction coefficient at 300 $m\mu$ with the index of refraction of the solvent (sodium D line).

vicinity of 265 $m\mu$ and a minimum in the region of 250 $m\mu$. This is in agreement with the findings of Ford and La Mer (10).

An examination of the results reveals that the extinction coefficients vary linearly with the index of refraction of the solvent. A plot of extinction coefficient at 300 $m\mu$ against solvent index of refraction (sodium D line) is shown in Fig. 2. A value of 414 for the extinction coefficient of a water solution (index of refraction, 1.33) was obtained by interpolation. When divided by the conversion factor 2.303, the average value obtained

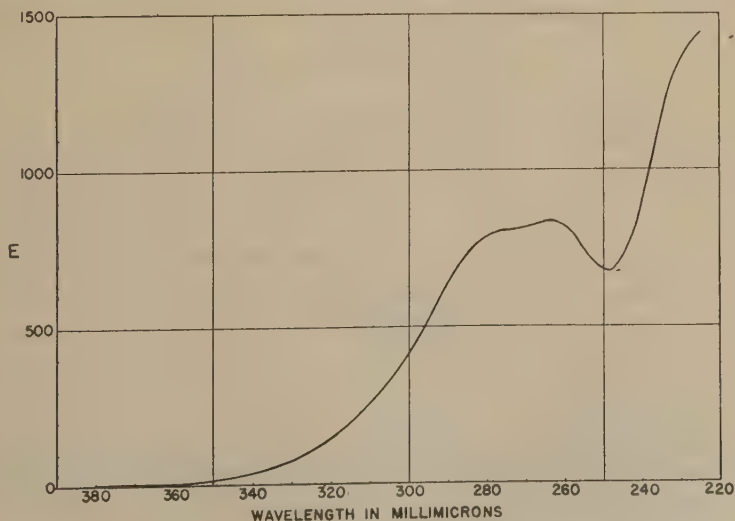


FIG. 3. Absorption curve for sulfur in water.

by La Mer and Kenyon for 300 $m\mu$ is 551. By similar interpolations the extinction coefficients of sulfur in water were obtained at other wavelengths and are tabulated in the last column of Table I. The extinction curve for sulfur in water is plotted in Fig. 3.

Variation of Wavelength of Maximum and Minimum of Absorption Curves with Solvent Refractive Index

Solvent	Maximum	Minimum	Refractive index ^a
Glycerol	266.0	251.0	1.4729
Chloroform	265.5	250.5	1.4432
<i>n</i> -Hexane	264.5	249.8	1.3815
Ethanol	264.0	249.3	1.3618
Methanol	263.5	249.0	1.3290

^a The index of refraction data were obtained from the International Critical Tables, Vol. VII. McGraw-Hill Book Company, Inc., New York, 1933. The index of refraction of the *n*-hexane mixture was measured. All refractive indexes are for sodium D line and 20°C.

The addition of water to the ethanol solutions had no apparent effect upon the extinction coefficient. This is consistent with the above results since the index of refraction of 90 and 95% ethanol is very close to that of pure ethanol.

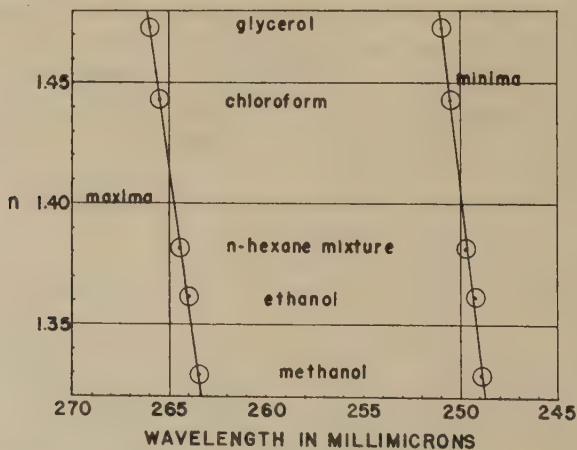


Fig. 4. Variation of position of maximum and minimum of absorption curves with solvent refractive index.

Beer's law was found to hold within the experimental limits. Each solvent was examined at at least three concentrations over at least a ten-fold concentration range. There was an apparent failure of Beer's law in the range 340–380 $m\mu$ and at the lower wavelengths where the solvents absorb appreciably. The former can be attributed to the inaccuracy of the spectrophotometer in the region of low optical density. The apparent

failure of Beer's law near the transmission limits of solvents was studied by Vandenbelt, Henrich, and Bash (11) and is attributed to the influence of stray light.

The positions of the maximum and minimum of the absorption curves move toward higher wavelengths with solvents of increasing index of refraction. This is in agreement with Kundt's Rule (12) and the work of Le Rosen and Reid (13). The data are tabulated in Table II and plotted in Fig. 4.

The two principal sources of error in this research were in the analysis for sulfur concentration and the optical density readings. The average deviations of the analyses were about 2%. The average deviations of the optical density readings were within $\pm 1\%$ except in cases of very low optical density and near the transmission limit of the solvents.

ACKNOWLEDGMENT

The authors are indebted to Dr. Vladimir Gordieyeff for suggesting this problem.

SUMMARY

Absorption curves of sulfur in the solvents chloroform, ethanol, ethanol-water mixtures, *n*-hexane, and methanol were obtained for the range 225–380 $m\mu$. The curves were found to be quite similar, but were displaced toward higher wavelength and extinction coefficients as the index of refraction of the solvent increased. The average of all extinction coefficients at 300 $m\mu$ was $440 \pm 4.9\%$. Examination of these extinction coefficients with respect to solvent index of refraction permits estimation of a value of 414 for water solutions at 300 $m\mu$. Beer's law holds for these solutions.

REFERENCES

1. LA MER, V. K., AND KENYON, A. S., *J. Colloid Sci.* **2**, 257 (1947).
2. ZAISER, E. M., AND LA MER, V. K., *J. Colloid Sci.* **3**, 571 (1948).
3. KERKER, M., *J. Chem. Phys.* **19**, 1324 (1951).
4. ZAISER, E. M., *J. Chem. Phys.* **20**, 538 (1952).
5. DINEGAR, R. H., SMELLIE, R., AND LA MER, V. K., *J. Am. Chem. Soc.* **73**, 2050 (1951).
6. BROOKE, M., *J. Chem. Education* **28**, 434 (1951).
7. SCOTT, W. W., *Standard Methods of Chemical Analysis*, 5th Ed., Vol. II, p. 2003. D. Van Nostrand Co., Inc., New York, 1925.
8. BACON, R. F., AND FANELLI, R., *Ind. Eng. Chem.* **34**, 1043 (1942).
9. WEISSBERGER, A., AND PROSKAUER, E. S., *Organic Solvents*. Oxford University Press, London, 1935.
10. FORD, F. P., AND LA MER, V. K., *J. Am. Chem. Soc.* **72**, 1959 (1950).
11. VANDENBELT, J. M., HENRICH, C., AND BASH, S. L., *Science* **114**, 576 (1951).
12. KUNDT, A., *Ann. Phys. u. Chem. (Jubelband)*, p. 615 (1874); *ibid.* **4**, 34 (1878).
13. LE ROSEN, A. L., AND REID, C. E., *J. Chem. Phys.* **20**, 233 (1952).

SOLUBILIZATION AND MICELLE FORMATION IN A HYDROCARBON MEDIUM ¹

Martin B. Mathews and Ernestine Hirschhorn

R. R. Street & Co. Inc., Chicago, Illinois

Received June 6, 1952

INTRODUCTION

Such typical colloidal phenomena as abnormally low osmotic pressure, light scattering, and solubilization have been observed in nonaqueous, as well as aqueous, solutions of low-molecular compounds (i.e., soaps and detergents). A recent review (1) summarizes the data which have led to the conclusion that the solute molecules associate or form micelles in these systems.

From measurements of viscosity and flow birefringence on solutions of sulfonates in hydrocarbons, van der Waarden (2) concluded that the micelles possessed a platelike shape with axial ratio between 10 and 50. Previous studies by means of x-ray scattering of similar systems containing water had led to the assumption of solubilization into a spherical aggregate in one case (3) and into a lamellar aggregate in another (4). Using both x-ray and light-scattering techniques, Schulman and co-workers (5,6) reported that a concentrated four-component system of the oil-continuous type contained closely packed spherical water droplets surrounded by a mixed monolayer of soap and alcohol molecules. The diameter of the micelle was a function of the composition of the system and could be calculated from surface chemical data. However, the presence in some compositions of micelles in the shape of short cylinders or of lamellae was considered possible. Since the problem appeared complicated by the conceivable simultaneous presence of a variety of sizes and shapes of micelles in concentrated solution, it appeared desirable to investigate micellar size and shape at low concentration where less involved conditions might be expected to prevail.

EXPERIMENTAL

1. *Materials and Methods*

A purified grade of *n*-dodecane was purchased from Humphrey-Wilkinson, Inc., North Haven, Conn. It had a refractive index of 1.4220 at 20°. At 30°, it had a density of 0.7419, and a viscosity of 0.01244 poise. The manufacturer claimed a minimum purity

¹ Presented at the 121st National Meeting of the American Chemical Society, Buffalo, N. Y., March 23-27, 1952.

of 95%. Solid di(2-ethylhexyl) sodium sulfosuccinate (Aerosol OT) was purchased from American Cyanamid Corp. The manufacturer claimed 99% purity with 1% water. The material was further dried in a finely divided condition in a vacuum desiccator over P_2O_5 for 2 weeks. The substantial purity of the material is indicated by the analytical data in Table I.

Densities were determined at $30 \pm .03^\circ$ in a pycnometer of about 30 ml. capacity fitted with a capillary neck. Viscosity measurements were carried out at the same temperature in Ubbelohde viscometers calibrated with water at several temperatures to obtain the calibration equations, including the correction for kinetic energy (7). Solutions were prepared by adding a weighed amount of water to a stock solution of Aerosol OT in *n*-dodecane and diluting with *n*-dodecane as required. Measurements on these solutions were completed within 8 hr. after preparation. Changes in viscosity were not observed during this period of time, although a slow decline of about 1% per week was noted for some solutions. The most concentrated solutions with different water to Aerosol OT ratios on which data are reported here were also examined in a capillary viscometer modeled after one described by Fox, Jr. *et al.* (8). The relative viscosities were found to be independent of the pressure head in the range of 10 to 30 cm. of solution.

Conductance measurements on solutions were made by measuring the current with a Radio Corp. of Amer. Ultrasensitive Meter when the potential due to three 67.5-v.

TABLE I

Analysis of Di(2-ethylhexyl) Sodium Sulfosuccinate

Sample	Water ^a %	Carbon ^b %	Hydrogen ^b %	Ash (as Na_2SO_4) ^c %
Theoretical	0.1	52.1	8.54	15.70
	0.0	54.0	8.39	15.97

^aBy distillation according to A.S.T.M. Designation D500-45.

^bPerformed by Microtechnical Laboratories, Evanston, Ill.

^cIgnition with sulfuric acid.

radio B-batteries was applied to the bright platinum electrodes of an Ostwald-type conductance cell. The cell constant was obtained by indirect comparison, using an Aerosol OT solution, with a cell, containing platinized electrodes, previously standardized by means of 0.1 *N* KCl in the usual manner (i.e., using a Wheatstone bridge with alternating current). The microammeter had a sensitivity of 0.0004 μ a. Measurements were carried out at 30° and at 240 v./cm. A fresh concentrated solution was prepared for each series of measurements and the solutions of lower concentration were prepared from it by appropriate dilutions with *n*-dodecane. Each series of measurements was completed within 8 hr.

Ultracentrifugal runs were made with a Spinco (Specialized Instrument Corp.) analytical ultracentrifuge at 59,780 r.p.m. This speed produces a gravitational field of about $240,000 \times g$ at the meniscus and about $300,000 \times g$ at the base. Calculation of sedimentation and diffusion constants were performed by standard procedures (9). Diffusion results were calculated by the formula $D = A^2 / (4 \pi t H_m^2)$ where A is the area under the curve, H_m is the maximum ordinate, t is the time in seconds, and D is the diffusion constant.

2. Viscosity Measurements

Einstein (10) derived theoretically the following relationship for the viscosity of suspensions of rigid spheres at low concentration under ideal

conditions of flow.

$$(\eta - \eta_0)/\eta_0 = \eta_{sp} = kC;$$

here η and η_0 are, respectively, the viscosity of solution and solvent. When C , the concentration, is expressed as volume per cent, $k = 0.025$, a value which has since been confirmed by experiment (11).

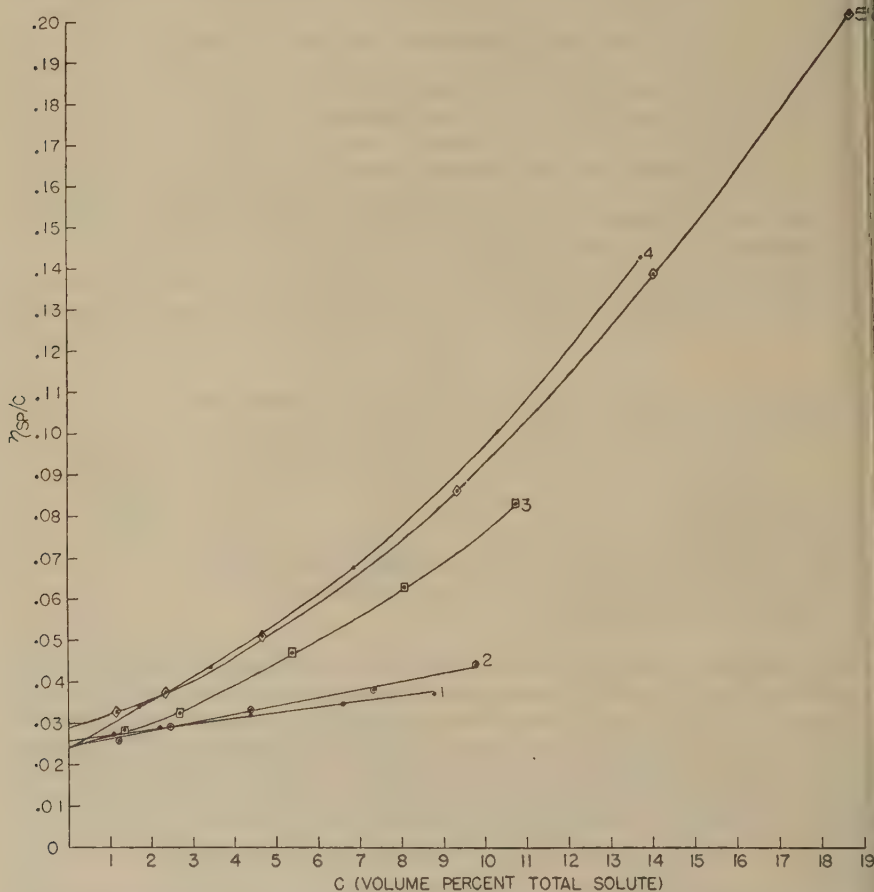


FIG. 1. Viscosity vs. concentration for dodecane solutions of different water/OT ratio. The volume ratio of water to Aerosol OT is 0.00 for curve 1, 0.114 for curve 2, 0.228 for curve 3, 0.570 for curve 4, and 1.14 for curve 5.

In order to obtain information as to the shape of the micelles in solutions of Aerosol OT in *n*-dodecane containing solubilized water, measurements were made of the viscosities of a series of solutions at various concentrations for different ratios of water to Aerosol OT. The data are shown in Fig. 1 with the values at zero concentration obtained by linear extrapolation of a semilogarithmic plot. The agreement (curves 1-4) with

theory obtained for, as shall be seen later, particles of different size, implies not only near sphericity, but also close conformance of the hydrodynamic units to the flow behavior of ideal spheres assumed by Einstein.

The curve for the solution with the largest water to Aerosol OT ratio (curve 5) shows distinct deviations from the pattern set by the remaining curves. As will be seen later, this difference is retained when other properties of these solutions are examined.

3. Apparent Specific Volume of Water

Density measurements were made on a series of solutions prepared by mixing varying amounts of water with 10 g. of Aerosol OT dissolved in

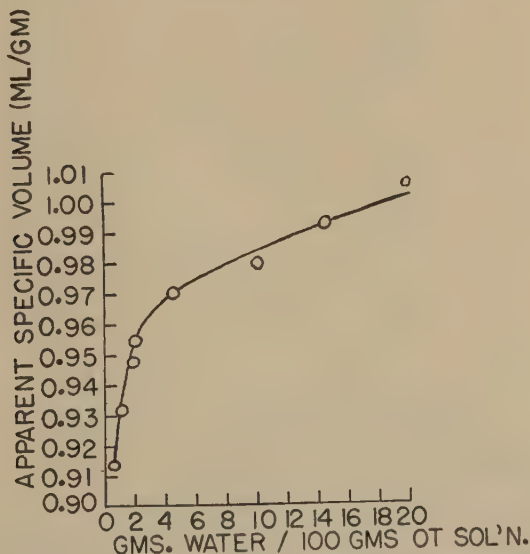


FIG. 2. Apparent specific volume of water vs. weight of water added to 100 g. dodecane solution containing 10 g. of Aerosol OT in 90 g. dodecane.

90 g. *n*-dodecane. The difference in volume between the final solution and the original Aerosol OT solution divided by the weight of water added is the apparent specific volume of the water. The data of Fig. 2 show that the apparent specific volume is below the bulk value for water at low water/OT ratios and approaches the bulk value with increase in water/OT ratio. A similar phenomenon had been noted for solubilized oils in aqueous systems (12).

The apparent specific volume of Aerosol OT was obtained from density measurements on solutions containing 99 g. *n*-dodecane, 1 g. water, and 1–10 g. Aerosol OT and found to be relatively constant at 0.880 ml./g.

The influence of solubilized water upon micelle structure is also reflected in the viscosity data of Fig. 3. As is most evident from curve 5

for 8.80% Aerosol OT, the viscosity increment due to addition of water is least where the ratio water/OT is lowest (less than 0.1).

4. Conductance Measurements

An earlier observation (3) of these systems revealed that the solute behaved as positively charged particles in an electric field. It might be expected that conductance measurements, in conjunction with other data, would contribute to an understanding of the nature of these particles. The data represented in Fig. 4 show a complex dependence of conductance upon solute concentration. In general, the conductance per unit solute

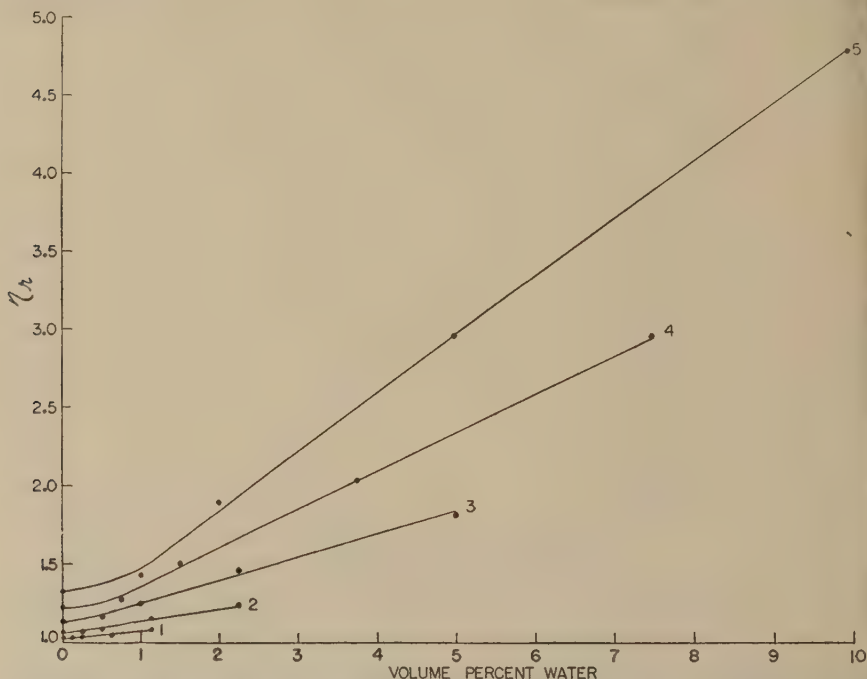


FIG. 3. Relative viscosity vs. volume per cent water for various dodecane solutions of different Aerosol OT content. The volume per cent of Aerosol OT is 1.10 for curve 1, 2.20 for curve 2, 4.40 for curve 3, 6.60 for curve 4, and 8.80 for curve 5.

concentration increases with concentration and with increase in water/OT ratio for curves 1-4. Here again must be noted a striking divergence in behavior of the solution of highest water/OT ratio (curve 5) from the pattern set by the remaining solutions of lower water/OT ratio.

5. Ultracentrifugal Measurements

The ultracentrifuge is a powerful tool for the determination of the particle size of large molecules or of stable aggregates containing small

molecules. It is also capable of revealing nonuniformity of sizes in a mixture. When solutions containing 1 g. Aerosol OT with varying amounts of water in 100 ml. of *n*-dodecane solution were run in the ultracentrifuge, the patterns shown in Fig. 5 were obtained.

For 0.0, 0.2, 0.5, and 0.75 g. of water, a single sedimenting peak may be taken to indicate monodispersity¹ of size and shape (or else, rapid equilibrium between particles of different size and shape). In sharp contrast with the preceding patterns, the pattern for 1.00 g. of water shows the presence of at least three different particles. The inverted peaks of

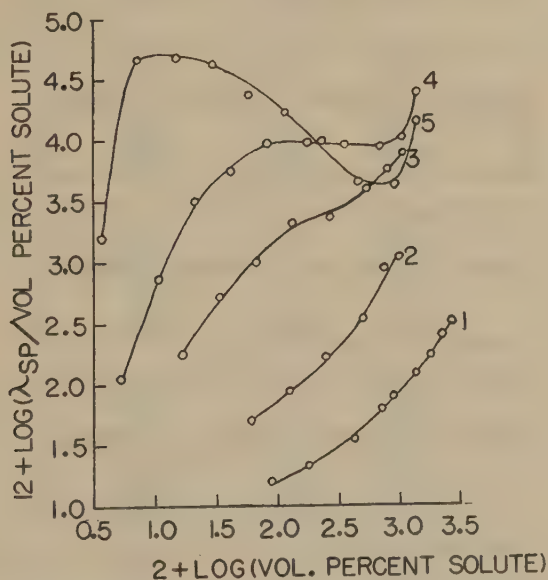


FIG. 4. Dependence of conductance upon total solute concentration for Aerosol OT solutions in dodecane containing solubilized water. The volume ratio of water/OT is 0.00 for curve 1, 0.114 for curve 2, 0.228 for curve 3, 0.570 for curve 4, and 1.14 for curve 5.

some patterns are associated with a lowering of refractive index of the system due to addition of solute.

If the assumption is made that each peak is produced by ideally sedimenting spheres of a single size, particle diameters may be calculated

¹ In order to establish monodispersity it is necessary to show in addition that the shape of a peak is identical with an ideal diffusion curve. According to Neurath (13), this can be reliably accomplished only with diffusion data of the highest accuracy. In view of the known instability of Aerosol OT solutions and the lengthy time required for diffusion experiments, the exact determination of the state of dispersion by this means did not appear feasible. Within experimental limitations, where a single sedimenting peak has been obtained, it has not differed significantly from an ideal diffusion curve. However, this relatively crude comparison cannot be taken to exclude a possible narrow distribution of size and shape.

from the observed rates of sedimentation in the ultracentrifuge. It is also possible to make a completely theoretical calculation of micelle size for each ratio of water to Aerosol OT if the assumption is made that the micelles are uniformly sized spheres with a water core just sufficient to

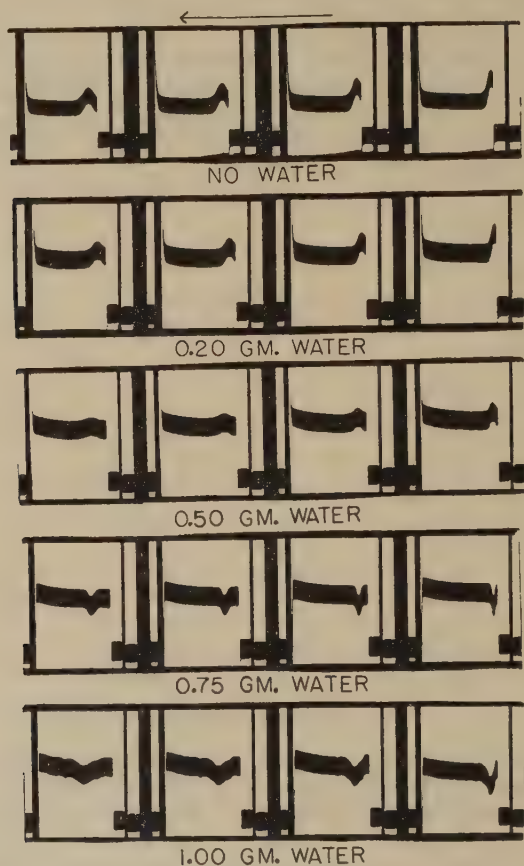


FIG. 5. Ultracentrifugal patterns obtained with solutions containing the amounts of water shown solubilized with 1 g. of Aerosol OT in 100 ml. of dodecane solution. The top three sets show successive pictures taken at 16-min. intervals; the remaining sets at 8-min. intervals.

accommodate a monolayer of Aerosol OT molecules. We may write the equations:

$$(4/3)\pi r^3 N = V, \quad [1]$$

where r , N , and V are, respectively, the radius, number, and total volume of spherical water particles in 100 ml. of solution.

$$\text{Total surface} = 4 \pi r^2 N = 6.06 \times 10^{23} g A/M, \quad [2]$$

where g is grams Aerosol OT in 100 ml. of solution, A is the surface area per Aerosol OT molecule, and M is the molecular weight of Aerosol OT.

Combining Eqs. [1] and [2] and taking the area and length of the Aerosol OT molecule from known surface chemical data (14) as 60 Å.² and 11 Å., respectively, we obtain the diameter (d) of the micelle, for $\gamma = 1$, as

$$d \text{ (in Å.)} = 73.3 V + 22. \quad [3]$$

Micelle particle weight may be calculated by adding the weight of the water core and the weight of Aerosol OT molecules required to cover completely the surface of the water core.

For calculation of experimental molecular weights and diameters of the micelles the basic equation (9) was

$$m = (4/3)\pi r^3/V_{30} = 6\pi r\eta_{30}S_{30}/(1 - \rho_{30}\bar{V}_{30}), \quad [4]$$

where m is the mass of the micelle, η_{30} is the solvent viscosity, ρ_{30} the solvent density, \bar{V}_{30} the specific volume of the solute, and S_{30} the corrected sedimentation rate. The conditions refer to 30° and unit centrifugal force. S_{30} is obtained from experimental data according to the equation

$$S_{30} = S_t \times (\eta_t/\eta_{30}) \times (\eta_o/\eta_{30}), \quad [4a]$$

where S_t is the observed sedimentation rate per unit centrifugal force, η_t is the solvent viscosity at the experimental temperature and unit centrifugal force, and η_o is the solvent viscosity at 30° for the experimental conditions of pressure. The ratio η_o/η_{30} represented a relatively large correction factor, about 1.25. It was obtained by estimation from data on pressure-viscosity functions of related hydrocarbons (15).

The theoretically calculated values and the experimental ultracentrifugal data appear in Table II. For the solution containing 1 g. water in 100 ml., only data on the principal peak have been used. Comparison of the experimental and calculated values of micelle diameter shows good agreement and apparently establishes the validity of Eq. [3]. Further, diameters calculated from diffusion constants obtained by measurements on the patterns for 0.0, 0.2, and 0.75 g. of water are consistent with the assumption that the micelles in a solution may be considered equivalent to uniformly sized spheres. Use of the Sutherland-Einstein equation relating diffusion constant and radius of ideal spheres gives results differing from the calculated values of Table II by not more than 25%, which is probably the experimental error in estimating the diffusion constant.

Yet, it is to be expected that the assumptions necessary to the derivation of Eq. [3] would become increasingly invalid with decrease in water/OT ratio and consequent increase in curvature of the water core. In the absence of added water, a micellar molecular weight of 14,000 is estimated from the ultracentrifugal data. For a spherical particle, the corresponding

diameter is 34 Å. However, a platelike shape, equivalent to an oblate spheroid of axial ratio about 2, is an alternative model also consistent with the viscosity and sedimentation data.

Comparison of the calculated and experimental values of molecular weight shows only fair agreement on the basis of a spherical model. Considerably better agreement is obtained when molecular weights are calculated on the basis of an oblate spheroid model of axial ratio (a/b) of 2 representing the water core of the micelle.

TABLE II
Ultracentrifugal Data for Dodecane Solutions

Grams/100 ml. of solution		Refractive increment	S_{30}^a	Micelle, spherical model				Micelle, oblate spheroid core, axial ratio 2, calculated mol. weight
				Calculated		Experimental		
OT	Water			Diameter	Mol. weight	Diameter	Mol. weight	
		<i>A.</i>		<i>A.</i>				
1	0.00	0.00045	2.0	—	—	34	14,000	—
1	0.20	0.00030	2.0	37	6,000	35	15,000	8,000
1	0.50	0.00008	4.9	59	47,000	57	60,000	62,000
1	0.75	−0.00012	10.1	77	123,000	82	190,000	170,000
1	1.00	−0.00032	14.0	95	250,000	99	310,000	328,000

^a Sedimentation constant in units of 10^{-13} reduced to *n*-dodecane at 30° and normal pressure.

In a manner similar to that used for the calculation with a spherical model, the equivalent of Eq. [3] may be obtained for an oblate spheroid. The value of the semimajor axis a is given by the relation

$$a(\text{in Å.}) = f(a/b)V, \quad [5]$$

where V is, as in Eq. [3], grams water in 100 ml. of solution containing 1 g. of Aerosol OT, and $f(a/b)$ is a function of the axial ratio only. For $a/b = 2$, $f(a/b) = 50.6$.

The deviation from the spherical of the complete micelle is less than that of the water core and is sufficiently slight that on theoretical grounds neither the calculations from sedimentation data nor the conclusions drawn from the viscosity data should be appreciably affected (9,16).

DISCUSSION

The agreement of viscosity data at infinite dilution with Einstein's theory for hard spheres suggests that dilute Aerosol OT solutions with solubilized water contain spherical or near-spherical hydrodynamic units. This conclusion is supported by comparison between calculations of size

based upon spherical and near-spherical models and upon ultracentrifugal data. Both the spherical and the oblate spheroid models require that the linear dimensions of the micelle be a linear function of the ratio of water/OT. This relation was found to hold for concentrated solutions of Aerosol OT with water in hydrocarbons in a study of x-ray scattering by Philippoff (4). Although the increase in long-spacing was linear with an increase in the ratio of water/OT, the slope was 3 or 4 times as much as could be accounted for on a proposed lamellar model.

However, these x-ray findings may be accounted for if it is assumed that the spherical (or near-spherical) model used in the above calculations for dilute solutions is also applicable to much higher concentrations. The probable applicability of a similar spherical model at high concentrations of surface-active agents has already been demonstrated for a more complex, nonaqueous colloidal system (5,6).

The presence of asymmetric particles in some, if not all, of these systems is likely. Viscosity and ultracentrifugal data obtained in the absence of water indicate the presence of a large aggregate which cannot be interpreted on a spherical model. Also, direct evidence (by observation of flow birefringence) of the presence of highly asymmetric aggregates was obtained for high-molecular-weight sulfonates similar to Aerosol OT in a hydrocarbon medium (2). In the presence of water, however, the degree of asymmetry of the micelles appears greatly reduced.

The phenomenon of low apparent specific volume of solubilized water may be interpreted as indicating that the initial increments of water strongly hydrate the polar groups of the detergent. Additional water beyond this stage may be considered to retain its bulk density in the micelle. The sharp change in slope (Fig. 2) which occurs at a water/OT ratio of 1/5, or about 5 moles water/mole detergent, possibly indicates the extent of strong hydration. In addition, an explanation offered for the corresponding effect in aqueous micellar systems appears plausible in this case also. It has been suggested (1) that solubilization may be accompanied by a change from a nonswollen oblate spheroid to the more normal, spherically swollen micelle in which there is a minimum of strain.

The viscosity and sedimentation data give information only as to the average shape and size of the micelles and cannot exclude the possible existence of an equilibrium mixture of micelles. Winsor has recently published (17) an interpretation of present x-ray data on solubilized systems (nonaqueous as well as aqueous types) on the basis of the coexistence in equilibrium of three forms of micelles, viz., the spheroidal lipophilic, the spheroidal hydrophilic, and the lamellar. He believes that these three types are present at all times, the relative amounts of each type depending upon the composition and temperature of the system. There is no evidence from diffusion in most of the solutions investigated here

for any extreme distribution of particle sizes and shapes. The sedimentation patterns for the solution containing equal weights of water and Aerosol OT, however, show multiple peaks and directly demonstrate that polydispersity of size and/or shape does occur in this one solution. Although it appears probable that only lipophilic micelles are present to any appreciable extent in these dilute solutions, further study is necessary before more definite conclusions can be drawn.

ACKNOWLEDGMENTS

We are indebted to Dr. Frank Putnam of the Department of Biochemistry, the University of Chicago, for making available a Spinco Ultracentrifuge and for technical assistance in its operation. We are grateful to R. R. Street & Co. Inc., for permission to publish this work.

SUMMARY

Viscosity and ultracentrifugal data on dilute solutions of di(2-ethyl-hexyl) sodium sulfosuccinate (Aerosol OT) in *n*-dodecane containing solubilized water support the view of the lipophilic micelle as consisting of a spherical or near-spherical water core surrounded by a monolayer of detergent molecules. In the absence of water, the detergent molecules exist as large aggregates, probably of platelike shape. Solutions with a low ratio of water to detergent appear to contain micelles of uniform size and shape. However, the presence in these solutions of an equilibrium mixture of micelles with a relatively narrow distribution of sizes and shapes cannot be excluded. When equal weights of water and detergent are present the solution appears in the ultracentrifuge to be polydisperse with respect to particle size and/or shape.

REFERENCES

1. KLEVENS, H. B., *Chem. Revs.* **47**, 1 (1950).
2. WAARDEN, M., VAN DER, *J. Colloid Sci.* **5**, 448 (1950).
3. MATTOON, R. W., AND MATHEWS, M. B., *J. Chem. Phys.* **17**, 496 (1949).
4. PHILIPPOFF, W., *J. Colloid Sci.* **5**, 169 (1950).
5. SCHULMAN, J. H., AND RILEY, D. P., *J. Colloid Sci.* **3**, 383 (1948).
6. SCHULMAN, J. H., AND FRIEND, J. A., *J. Colloid Sci.* **4**, 497 (1949).
7. SWINDELLS, J. I., *J. Colloid Sci.* **2**, 177 (1947).
8. FOX, T. C., JR., FOX, J. C., AND FLORY, P. J., *J. Am. Chem. Soc.* **73**, 1901 (1951).
9. SVEDBERG, T., AND PEDERSEN, K. O., *The Ultracentrifuge*. Oxford Press, London, 1940.
10. EINSTEIN, A., *Ann. Physik* **19**, 289 (1906).
11. EIRICH, F., BUNZL, M., AND MARGARETHA, H., *Kolloid-Z.* **74**, 276 (1936).
12. HARKINS, W. D., MATTOON, R. W., AND CORRIN, M. L., *J. Colloid Sci.* **1**, 105 (1946).
13. NEURATH, H., *Chem. Revs.* **30**, 357 (1940).
14. CARYL, C. R., *Ind. Eng. Chem.* **33**, 731 (1941).
15. BRIDGMAN, P. W., *Proc. Am. Acad. Arts Sci.* **61**, 57 (1926); *ibid.* **77**, 115 (1949).
16. MEHL, J. W., ONCLEY, J. L., AND SIMHA, R., *Science* **92**, 132 (1940).
17. WINSOR, P. A., *J. Phys. Chem.* **56**, 391 (1952).

EFFECT OF DEGREE OF ESTERIFICATION ON VISCOSITY AND GELATION BEHAVIOR OF PECTIN

E. L. Pippen, T. H. Schultz and H. S. Owens

*Western Regional Research Laboratory, Albany, California*¹

Received September 8, 1952

ABSTRACT

Pectin was esterified with diazomethane so that degradation did not occur. The intrinsic viscosity was found to decrease with increasing degree of esterification. Maximum shear modulus of high-solids content gels containing 0.3% pectin of nearly constant chain length was obtained near a degree of esterification of 40%. The significance of these findings to the theory of pectin gel formation is discussed.

INTRODUCTION

Pectin, a polymeric galacturonide in which 60 to 80% of the acid groups are esterified with methanol, is widely used to prepare high-solids content (60–65%) gels. The main sources of pectin are citrus pulp and apple pomace, although sugar-beet pulp has been used in Germany. Sugar-beet pectin differs in the respect that it contains acetate groups and more nonuronide material, such as arabinose and galactose, than citrus or apple pectin. For years, sugar-beet pectin was considered a nongel former, but recent work (1,2,3) has shown that the acetate groups are responsible, and after their removal by acid hydrolysis beet pectin forms high-solids gels.

Because it is now possible to prepare many pectic derivatives without depolymerization, further information on the relationships of $-\text{OH}$, $-\text{COOH}$, and $-\text{COCH}_3$ groups to the formation of pectin gels appears desirable. The effect of acetyl in preventing gel formation and in increasing the solubility of pectic acid (4) may be due to a change in the polar nature of the molecule or to a change in the degree of regularity which influences cross linking along the chain. Introduction of methyl ester groups has been reported to yield products that form gels at pH values as high as 5.8 (5), as compared to the usual maximum pH of 3–4 (6,7). The gels produced from these completely esterified products are reported to be stronger than those made with the original pectin (5). Earlier work (7,8), however, has shown that stronger gels are obtained with pectins that have a degree of esterification (DE) near 60% than with those near

¹ Bureau of Agricultural and Industrial Chemistry, Agricultural Research Administration, U. S. Department of Agriculture. Article not copyrighted.

75%. The apparent contradiction is so important to the evaluation of the function of the carboxyl and ester groups in pectin gel formation that its re-examination is necessary.

This paper deals with the preparation of methyl esters of pectin and their use in high-solids gels. In addition, certain features of the viscosity behavior of the methyl esters are reported.

MATERIALS AND METHODS

The pectins and pectate used were commercial products prepared from citrus peel or apple pomace. The results, however, are applicable to

TABLE I
Analytical Data on Samples Used in This Investigation

Sample No.	Ash ^a	Anhydrouronic acid %	Methoxyl		Method of esterification
			Ether %	Ester %	
1869	0.5	86	0	8.9	—
1872	2.9	86	0	6.3	—
1872-1	2.5	80	—	13.6	^b
1872-2	2.7	84	1.8	8.6	^b
1872-3	2.7	87	—	9.2	^b
1873	0.45	89	0	10.6	—
1873-1	0.30	86	—	11.6	^c
1873-2	0.11	84	—	12.5	^c
1873-3	0.18	83	—	14.6	^d
1874	0.38	75	0	0.0	—
1875	1.47	86	0	10.5	—
1875-1	1.41	85	1.1	11.3	^d
1875-2	1.46	84	—	13.1	^d
1875-3	1.27	82	1.6	14.4	^d
1875-3A	0.86	86	1.7	10.9	^d
1876	0.10	80	0	10.3	—
1876-1	0.05	78	1.3	13.6	^d

^a Mainly silica.

^b Esterified in 80% methanol at -23°.

^c Esterified in 80% methanol at room temperature.

^d Esterified by Vollmert's method (10).

deacetylated beet pectin. They were deashed either by ion-exchange resins, or by precipitation in acidified alcohol, or by both. Extraneous acid was removed with neutral 70% ethanol. The pectic substance was dehydrated in acetone, and further dried *in vacuo* at 60°C. The dried samples were humidified at room temperature and humidity for at least 48 hr. and then analyzed. Analytical data in Table I are corrected to a moisture- and ash-free basis.

Sample 1872 was prepared by acid hydrolysis at 40°C. (9) of a sample of commercial citrus pectin, while 1875-3A was similarly prepared from

1875-3. Samples 1876 and 1876-1 were the only ones prepared from apple pectin.

Diazomethane was used to prepare methylated samples of pectin, following essentially Vollmert's procedure (10) in which pectin is precipitated from aqueous solution with methanol, washed free of water with methanol, and freed of methanol with ether. Esterification at -20° or less is recommended. Exceptions to this procedure are noted in Table I.

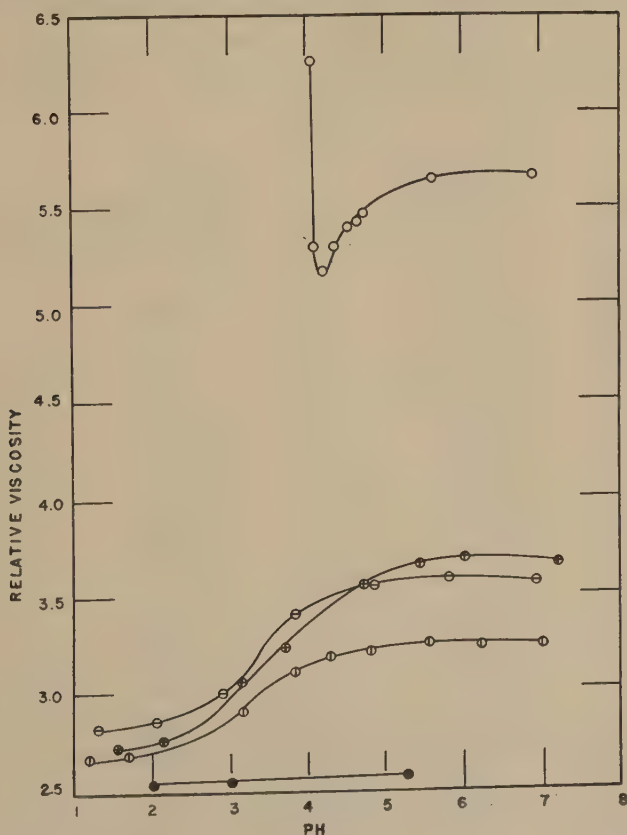


FIG. 1. Effect of pH on relative viscosity of 0.3% solutions of 1874 (DE 0)○; 1873 (DE 68)⊖; 1873-2 (DE 85)⊕; 1873-3 (DE 100)●; and 1869 (DE 59)⊕.

Analyses for ester and total methoxyl content, intrinsic viscosity, and number-average molecular weight were made by procedures already outlined (11). The rigidometer (7) was used to measure the shear modulus of gels. The use of Bull osmometers (12) with thin-walled size 18/32-in. regenerated cellulose casing, and with no less than 15 days allowed for establishment of equilibrium, has given more reliable measurements of osmotic pressure than those previously reported (13). The molecular

weights are believed to be accurate within $\pm 10\%$. They are about 20% higher than the earlier values and are in better agreement with those obtained after propionylation and measurement in organic solvents (14).

RESULTS AND DISCUSSION

The viscosity of fully esterified pectin is only slightly dependent on pH, but as the number of carboxyl groups increases, the viscosity becomes markedly pH-dependent, as shown in Fig. 1. It increases sharply with increase in pH in the range of pH 2.5–4.5 and levels off below and above that range. The increase may be attributable primarily to repulsion effects

TABLE II
Physical Constants of the Samples Used

Sample No.	Degree of esterification %	$[\eta]$ dl./g.	Number-average molecular weight ^a	Shear modulus ^b g./cm. ²
1869	59	3.6	—	3.1
1872	41	4.7	—	4.5
1872-1	98	3.1	39,000	0.1
1872-2	58	4.2	—	2.7
1872-3	60	4.1	—	2.4
1873	68	3.8	37,000	2.4
1873-1	77	3.7	—	1.3
1873-2	85	3.5	34,000	0.9
1873-3	100	3.4	—	Ppt.
1874	0	5.4	—	—
1875	69	7.1	46,000	4.0
1875-1	80	6.2	—	—
1875-2	90	5.5	—	—
1875-3	99	4.6	45,000	Ppt.
1875-3A	72	4.0	—	2.1
1876	73	5.4	39,000	3
1876-1	99	4.4	40,000	Ppt.

^aThe molecular weights have been calculated to a pectic acid basis.

^b Shear modulus of 0.3% pectin gels containing 65% soluble solids at pH 2.2 ± 0.1 .

along the chain, with some elongation of the polymeric molecule. At low pH values, ionization of the carboxyl groups is suppressed and intrinsic viscosities measured at such pH's are the same as those measured in the presence of salt at high pH values (15). The important point to this discussion is that below pH 2.5 electrostatic repulsions are so much reduced that they should have little influence on jelly formation. Additional evidence is given by the viscosity-pH curve for pectic acid. There is an abrupt rise in the viscosity of its solutions below pH 4, in contrast to the decrease noted for the pectinic acids shown in Fig. 1. This increase must be due to association, despite the fact that the degree of ionization of the pectic acid is about 50%, at that pH.

Data on intrinsic viscosities and molecular weights in Table II confirm the finding that intrinsic viscosity decreases with increasing degree of esterification (16). The decrease appears fairly regular throughout the examined range of DE values when the intrinsic viscosity is measured in salt solution. This finding is of interest in the preparation of samples of varying DE's for comparative tests, because it proves that molecular weight rather than viscosity measurements are necessary, to assure that the chain length is constant. Figure 2 indicates the change in slopes of

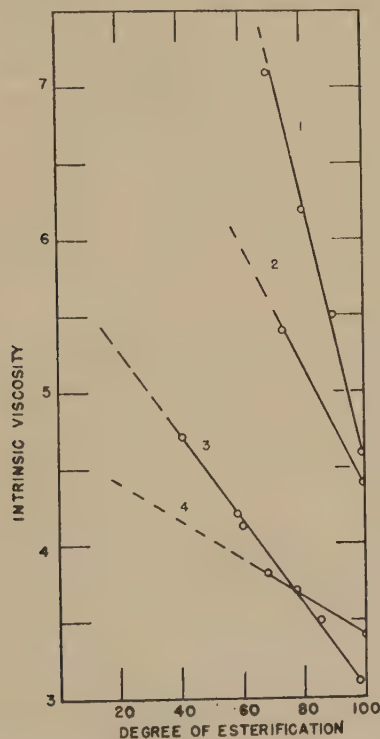


FIG. 2. Relation of intrinsic viscosity to degree of esterification: 1, 1875 series; 2, 1876 series; 3, 1872 series; and 4, 1873 series.

the lines relating intrinsic viscosity to degree of esterification with increase in chain length. The fact that two lines cross requires further examination. There may be a marked difference in molecular weight distribution, which could explain the different slopes. The observation of Deuel and Neukomm (17) that viscosity increases with increasing ester content is probably due to the method used to compare molecular weights. Their method requires the assumption that pectin is de-esterified by alkali without degradation. Pectin, however, is known to be labile to alkali (15,17). Thus the assumption is invalidated.

The molecular weight data show that Vollmert's method of esterification does not cause degradation, while esterification at room temperature decreases the molecular weight.

Results of gelation tests on a series of pectate esters are given in Table II. As the DE approaches 100%, the pectates lose their ability to form gels prepared by the usual method for standardization in this country. In Fig. 3 are plotted some of these and earlier data (7) to show that shear modulus approaches a maximum at a DE of 40%. The lower curve represents a series of pectins of nearly constant intrinsic viscosity and, therefore, of increasing molecular weight with increase in DE. The upper curve is an attempted representation of pectins with a chain length corresponding to 1872. It includes pectins 10.1 and 8.0 A. (7) and an arbitrary adjustment (see next paragraph) for the presence of ether

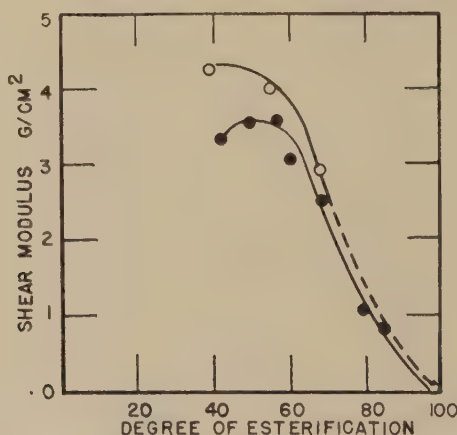


FIG. 3. Variation of shear modulus of 65% solids gels containing 0.3% pectins of different degrees of esterification. The shadowed circles are pectins with intrinsic viscosities of 3.6 ± 0.2 , while the top line represents results adjusted for ether methoxyls in pectins of approximately the same chain length.

methoxyl in 1872-2. Because no pectins without ether groups but with a DE above 70% were available, the curve is purely hypothetical at higher DE's. These results were obtained with citrus pectins, but those with apple pectins indicate the same trend. Because fully esterified methyl pectates are not very soluble in solutions of 65% sugar, 60% solutions were tried, with no improvement. Sample 1872-1 was soluble in both gel media but formed only very weak gels, indicating that lack of solubility is not the controlling factor in the poor gelling quality of the fully esterified pectin.

The percentage of ether methoxyl introduced by diazomethane is apparently the same regardless of the temperature of the reaction within the time limits used. An esterified pectate (1875-3) containing 1.6% ether

methoxyl was acid hydrolyzed from a DE of 99 to 72%. The shear modulus of a gel prepared from it was 2.1 g./cm.², compared to about 3.0 g./cm.² expected for a pectin of similar DE and intrinsic viscosity but not containing ether methoxyl. The ether methoxyl, therefore, does not account for the poor gelling qualities of the fully esterified pectins. We cannot compare the effect of our method of preparing gels to that of Deuel *et al.* (5) because of the low solubility of our methyl pectates.

These data yield a further inkling of the mechanism of pectin gel formation. It appears that there is an optimum for the degree of regularity along the galacturonide chain in pectin. If the DE is too high, association, possibly because of the hydrophobic nature of the ester groups, becomes sufficiently strong to cause precipitation. This tendency may explain why high-ester pectins are rapid-setting or have a higher setting temperature. If the DE is too low, cross bonding through the carboxyl groups causes association and production of irregular gels as soon as acid is added to the gel medium. In between (at DE's between 40 and 75) uniform gels with high gel strengths and elastic moduli can be prepared with small amounts of pectin.

On this basis, it is no longer necessary to assume that alcohol-to-alcohol bonds in pectin play a prominent part in the formation of gels. Esterification of alcohol groups with acetyl may prevent close approach between pectin molecules required for interaction of carboxyl or carboxyl and alcohol groups. A further implication is that sucrose does not form a bridge between pectin molecules because its bulk is so great that it should mask small amounts of acetyl groups.

The proposed mechanism of pectin gel formation is that at high temperatures association between pectin molecules begins because of the presence and hydrophobic nature of ester groups. As the temperature decreases, hydrogen bonds form between the polar carboxyl and alcohol groups, which gives the gel its elastic properties. Control of pH is necessary to reduce electrostatic repulsion and increase the ability of the carboxyl groups to form hydrogen bonds. Sucrose, glycerol, or other hydrophilic substance is necessary to desolvate the pectin, thus permitting the close approach required for bond formation. Sucrose may play a supplemental role, as it is known that the viscosity of its solutions increases rapidly at concentrations greater than 45%. At 65% its rheological properties would reinforce those of pectin.

The findings reported here also suggest that a more versatile pectic product could be made by partly acetylating or etherifying pectic acid. The side groups would offer the necessary irregularity while the greater pH stability of pectic acid would permit use of higher pH values in preparing gels. In this case cross bonding with multivalent cations might be necessary.

ACKNOWLEDGMENT

The authors appreciate the many stimulating discussions on this subject with Dr. K. J. Palmer of this laboratory.

REFERENCES

1. BERGLUND, D. T., Belg. Pat. 482,585, May 20, 1948; *C. A.* **44**, 8018 (1950).
2. PIPPEN, E. L., MCCREADY, R. M., AND OWENS, H. S., *J. Am. Chem. Soc.* **72**, 813 (1950).
3. HENGLEIN, F. A., *Forschungen u. Fortschr.* **26**, 184 (1950).
4. SOLMS, J., AND DEUEL, H., *Helv. Chim. Acta* **34**, 2242 (1951).
5. DEUEL, H., HUBER, G., AND LEUENBERGER, R., *Helv. Chim. Acta* **33**, 1226 (1950).
6. HINTON, C. L., *Biochem. J.* **34**, 1211 (1940).
7. OWENS, H. S., AND MACLAY, W. D., *J. Colloid Sci.* **1**, 313 (1946).
8. BAKER, G. L., AND GOODWIN, M. W., *Univ. Del. Agr. Expt. Sta. Bull.* No. 234 (1941).
9. SPEISER, R., EDDY, C. R., AND HILLS, C. H., *J. Phys. Chem.* **49**, 563 (1945).
10. VOLLMERT, B., *Makromol. Chem.* **5**, 101 (1950).
11. AIC-340, Methods Used at the Western Regional Research Laboratory for the Extraction and Analysis of Pectic Materials (mimeographed), Bureau of Agricultural and Industrial Chemistry, U. S. Department of Agriculture, July, 1952.
12. BULL, H. B., *J. Biol. Chem.* **137**, 143 (1941).
13. OWENS, H. S., LOTZKAR, H., SCHULTZ, T. H., AND MACLAY, W. D., *J. Am. Chem. Soc.* **68**, 1628 (1946).
14. OWENS, H. S., MIERS, J. C., AND MACLAY, W. D., *J. Colloid Sci.* **3**, 277 (1948).
15. OWENS, H. S., LOTZKAR, H., MERRILL, R. C., AND PETERSON, M., *J. Am. Chem. Soc.* **66**, 1178 (1944).
16. VOLLMERT, B., *Makromol. Chem.* **5**, 110 (1950).
17. DEUEL, H., AND NEUKOMM, H., *J. Polymer Sci.* **4**, 759 (1949).

STUDY OF DILUTE AQUEOUS SOLUTIONS OF SODIUM OLEATE

B. D. Flockhart and H. Graham

Chemistry Department, Queen's University, Belfast, Northern Ireland

Received May 21, 1952; revised September 10, 1952

INTRODUCTION

Aqueous solutions of unhydrolyzed paraffin-chain salts exhibit a more or less abrupt change in physical properties over a relatively short concentration range. Such solutions are characterized by the association of the solute into colloidal aggregates or micelles, the concentration at which the transition occurs being designated "the critical concentration for the formation of micelles." Careful measurements with aqueous fatty acid soap solutions also show an inflection in many of the physical property-concentration plots. These solutions have not, however, been extensively studied, probably on account of the complicating effects of hydrolysis. The position is particularly unsatisfactory in the case of sodium oleate. Ekwall was unable to detect a break point in the equivalent conductance-concentration curve for this soap (1). According to recent statements in the literature "its critical concentration of micelle formation is not well established" and "correlation . . . has been poor with sodium oleate, perhaps because of the ill-defined breadth of the concentration band over which it transforms into micellar form" (2).

The object of the present investigation was to examine in some detail dilute aqueous solutions of sodium oleate by measuring the electrical conductance and viscosity of the solutions. A sharp arrest has been observed in the equivalent conductance-concentration plot. An anomalous viscosity-concentration curve has been obtained. The significance of these and of other experimental observations is briefly discussed.

EXPERIMENTAL

Materials

British Drug Houses' redistilled oleic acid was purified according to the method of Brown and Shinowara (3). The product was colorless, almost odorless, and had an iodine value of 88.1. Sodium oleate was prepared by dissolving sodium hydroxide (A.R.) in absolute alcohol and slowly adding slightly less than the calculated weight of oleic acid. A recently

boiled mixture of alcohol and water (3:1) was added and final adjustment to neutrality was made by adding the oleic acid drop by drop with phenolphthalein as external indicator. The neutral solution was evaporated down at about 40°C. under reduced pressure, and the product was crystallized from ethanol and dried for a week *in vacuo* over potassium hydroxide. The sodium oleate thus obtained was a pure white powder.

A sample of sodium oleate was prepared from oleic acid supplied through the courtesy of Imperial Chemical Industries (I.C.I.). The acid

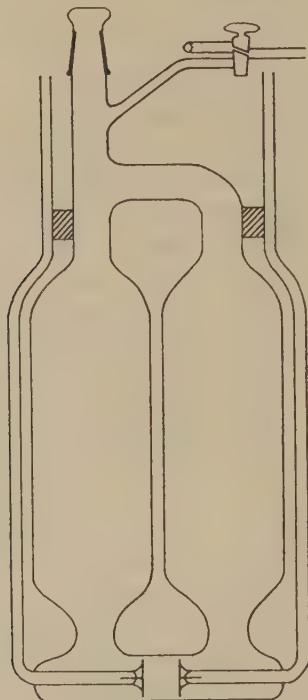


FIG. 1. Conductance cell.

was estimated to be about 96.5% pure, the main impurity probably being palmitic acid. Lever Bros., & Unilever Ltd., kindly made available a sample of sodium oleate, which had been prepared from an acid having the following constants:

Iodine value, 90.0; SCN value, 89.7; m.p. 12.9°C. (lower melting form).

Distilled water from the laboratory supply was redistilled in a Pyrex glass still, which had been well conditioned. Only the middle fraction was collected. The specific conductance ranged between 1.0 and 1.5×10^{-6}

ohm⁻¹. As precautions had been taken to exclude carbon dioxide, the conductance was only partly due to this impurity.

Apparatus

Alternating current with a frequency of 1000 cycles was supplied by a valve oscillator to a direct reading conductance bridge of conventional design. The null point was determined with a cathode-ray tube indicator, the circuit being a modification of the one described by Hovorka and Mendenhall (4). These workers used an input transformer giving a step-up ratio of approximately 1:64 and one stage of amplification. An instrument with a superior performance was obtained by employing a shielded transformer which had a 1:20 step-up ratio and adding a 6J5 amplification stage. Using the detector the bridge could be set to 0.1 ohm for

TABLE I

Conductance of Sodium Oleate in Water

\sqrt{C}	Λ at 25°C.	Λ at 40°C.
0.0145	77.	110.
0.0206	74.	105.
0.0264	70.7	101.2
0.0315	69.7	97.1
0.0372	69.7	97.5
0.0393	69.7	97.5
0.0423	69.2	97.7
0.0453	67.8	97.0
0.0551	56.4	81.6
0.0666	47.9	69.4
0.1012	36.9	53.6
0.1412	31.4	45.5

resistances up to about 1000 ohms. At 10,000 ohms a difference of 1 ohm in the setting could be detected, while at 50,000 ohms the precision was a few tenths of a per cent.

Two Pyrex glass cells were used. The cell constants were determined with several solutions of potassium chloride (A.R.). The platinum electrodes were platinized and then heated to redness to form grey platinum in order to minimize adsorption. At the glass-platinum seal the glass was made to flow slightly over the plates to make a more rigid joint. A Washburn cell of the pipet form was used for the solvent measurements. The design of the other cell is shown in Fig. 1. Usually some flask-type cell is used when increasing concentrations are built up or series of dilutions made in the cell itself. The contents are mixed by rotating the electrodes, ordinary stirring, or by removing the cell from the bath and shaking. This cell was mechanically rocked in the thermostat; the contents were mixed rapidly and quickly attained a steady temperature (about 15

min.). Howell and Handford (5), who used a flask-type cell, record that over an hour is required for temperature equilibrium. The capacity of the cell was slightly over 1 l. The electrodes were 1.5 cm. in diameter. All conductance measurements were made at $25^{\circ} \pm 0.02^{\circ}\text{C}.$; measurements in pure water were also carried out at $40^{\circ} \pm 0.03^{\circ}\text{C}.$

Procedure

Using a long glass lead, a strong current of pure nitrogen was passed through the cell for about 15 min. During the addition of the soap solution

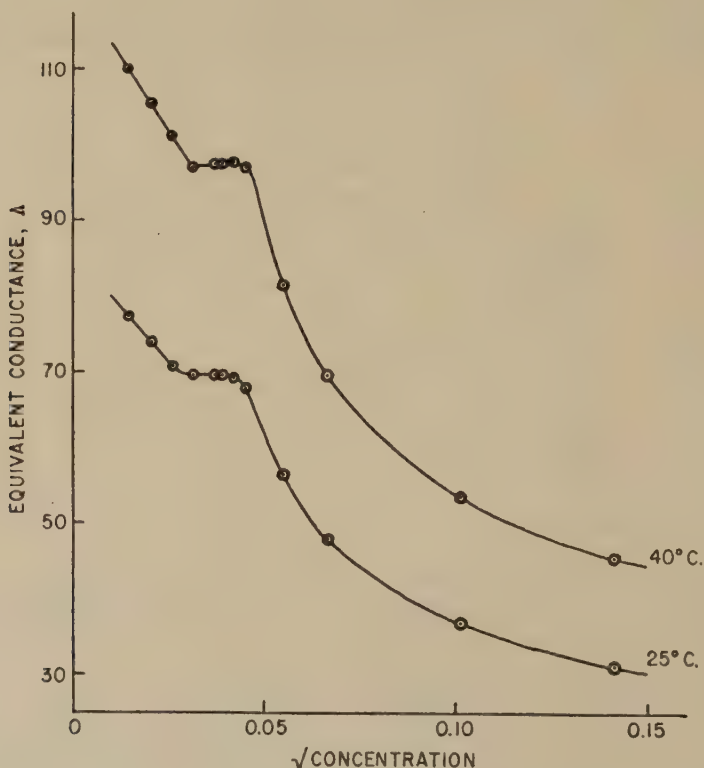


Fig. 2. Equivalent conductance vs. square root of the concentration for sodium oleate in water.

a stream of nitrogen, primed with the solvent, was passed through the cell via the tap. The cell, mounted on a stand, was supported in the thermostat and connected to a large brass disk on the spindle of a low-g geared motor. By adjusting a resistance in series with the motor the shaking could be reduced to a very low rate. Conductance measurements

were made after about 15 min. and again after about 25 min. The solution was diluted by adding weighed amounts of solvent.

A solvent correction was made by subtracting the specific conductance of the aqueous solvent from the specific conductance of the solution. At the highest dilutions it ranged between 4 and 9%. In the case of the alkaline solutions the specific conductance of the excess base was found by carrying out runs under exactly similar conditions to those when soap

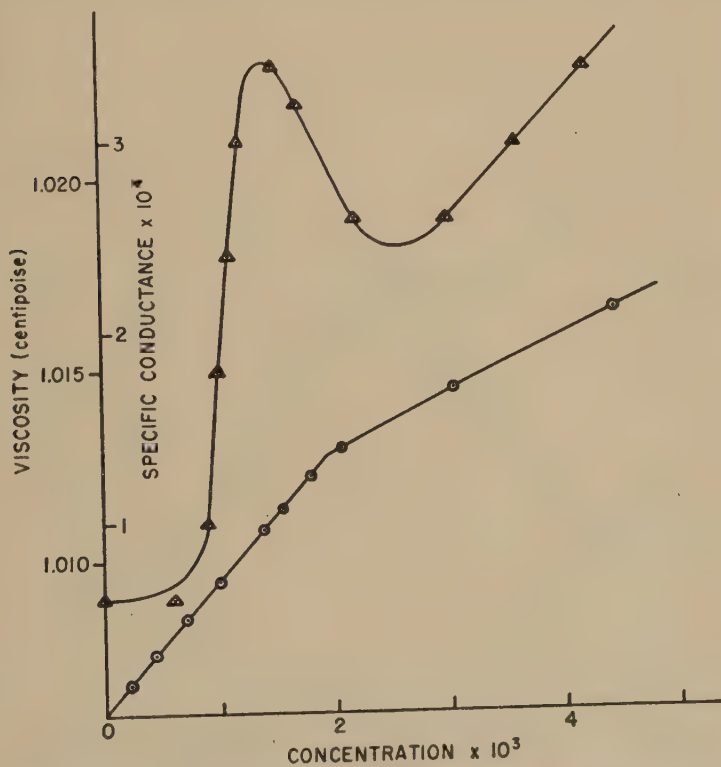


FIG. 3. Viscosity vs. concentration at 20°C. (Δ) and specific conductance vs. concentration at 25°C. (○).

was present. The conductance by difference was calculated by subtracting the specific conductance of the base from the specific conductance of the solution containing the base and the soap.

Viscosity Measurements

The measurements were made with an Ostwald-type viscometer, the standardization being accomplished through the known viscosity of water. Five determinations of the time of flow of each solution were made.

These agreed within 0.2%. The solutions were maintained at $20^{\circ} \pm 0.02^{\circ}\text{C}$.

RESULTS

In Table I selected values are given of the equivalent conductance (Λ) as a function of the square root of concentration (in moles per liter) for sodium oleate in water. On account of the large solvent corrections the values in the most dilute solutions may be uncertain by a few per

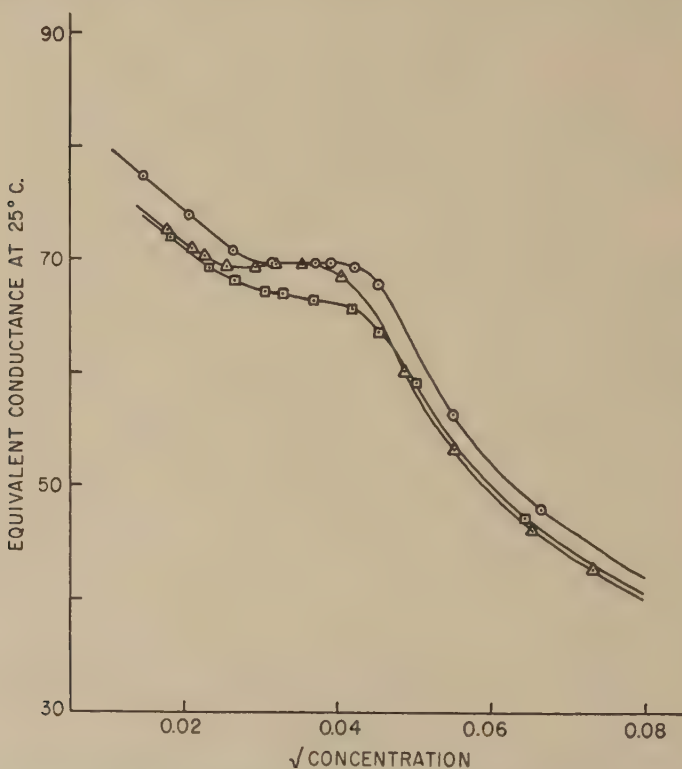


FIG. 4. Equivalent conductance vs. square root of the concentration for sample A (\odot), sample B (Δ), and sample C (\square).

cent. The $\Lambda - \sqrt{C}$ curve (Fig. 2) exhibits a pronounced arrest commencing at about $0.9 \times 10^{-3} M$ and ending at approximately $1.8 \times 10^{-3} M$. Only the latter break point shows clearly in the specific conductance-concentration plot (Fig. 3). At 40°C . the values are slightly higher.

In Fig. 4 the $\Lambda - \sqrt{C}$ curve for the present sample of sodium oleate (A) is compared with the curves for Lever Bros.' sample of soap (B) and for the sample prepared from I.C.I. oleic acid (C). It will be noted

that the curves for samples *A* and *B* are in fairly close agreement. The arrest is not so pronounced for sample *C*, where the acid was estimated to be 96.5% pure. An oxidized sample of sodium oleate exhibited no arrest, but a slight inflection at the same concentration as that found for the end of the arrest.

Values of the viscosity as a function of concentration for aqueous solutions of sodium oleate at 20°C. are plotted in Fig. 3. An abrupt rise

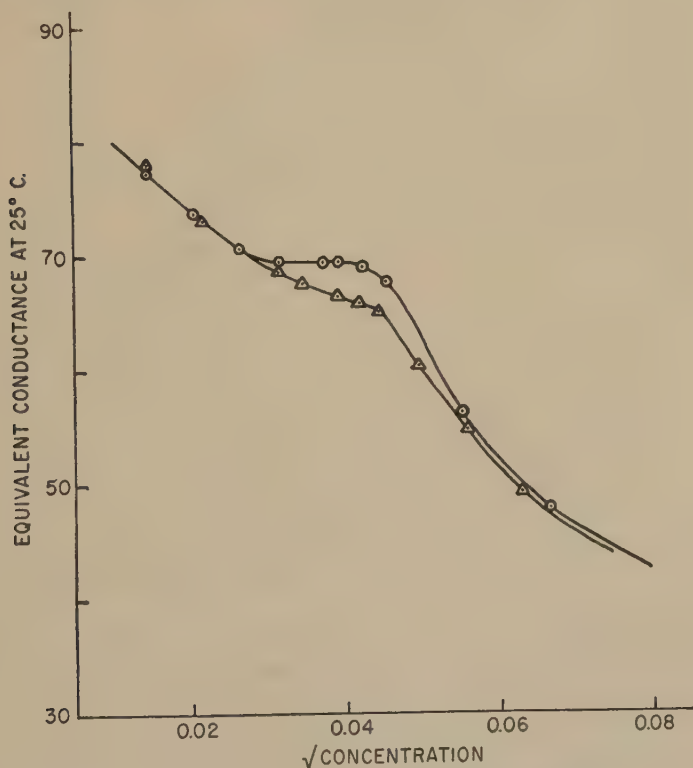


FIG. 5. Equivalent conductance vs. square root of the concentration on the addition of 0 mole-% (○) and 3.4 mole-% oleic acid (Δ).

is observed at about $0.9 \times 10^{-3} M$, a maximum value being reached in the region of $1.5 \times 10^{-3} M$. A minimum value is recorded at approximately $2.5 \times 10^{-3} M$.

The $\Lambda - \sqrt{C}$ plot for sodium oleate in water is compared in Fig. 5 with the plot for sodium oleate in water on the addition of 3.4 moles of oleic acid per 100 moles of soap. In the presence of the acid the arrest is less pronounced, the end of the arrest occurring at a rather higher concentration.

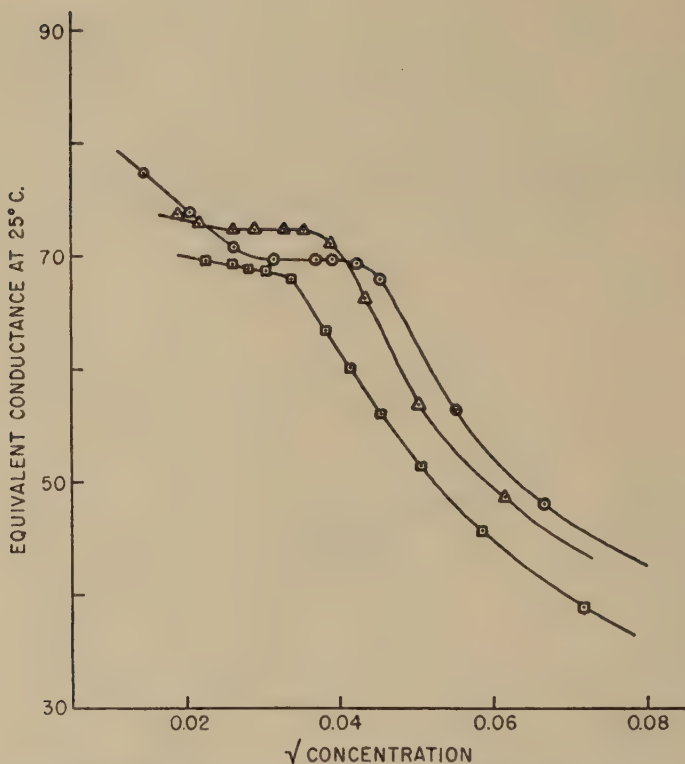


FIG. 6. Equivalent conductance vs. square root of the concentration on the addition of 0 mole-% (○), 6 mole-% (△), and 16.7 mole-% sodium hydroxide (◻).

The results of measurements with sodium oleate in water on the addition of 6 mole-% and 16.7 mole-% of sodium hydroxide (again based on the soap) are graphed in Fig. 6. The curves show only one break point. In the presence of 6 mole-% of alkali this occurs at about $1.5 \times 10^{-3} M$ and for 16.7 mole-% at approximately $1.2 \times 10^{-3} M$.

DISCUSSION

While the position of the "critical micelle concentration" of non-hydrolyzable paraffin-chain salts is clearly defined, the possible existence of aggregates at lower concentrations is still a matter of dispute. It is the opinion of Hartley that, in general, below the critical concentration these salts are *ordinary* strong electrolytes. McBain, on the other hand, has postulated that ionic micelle formation begins in very dilute solution before this concentration is reached.

In the case of the fatty acid soaps the position of the critical concentration is also a subject of controversy. Ekwall (1) observed an arrest in

the equivalent conductance-concentration curve for sodium myristate in water; for sodium palmitate the curve passes through a minimum and maximum, while for sodium oleate no break point was detected. According to this investigator the arrest for sodium myristate can be attributed to the formation of acid soap, the renewed fall at the end of the arrest heralding colloid formation. Hartley (6), however, has suggested that the arrest itself is due to micelle formation.

The degree of hydrolysis of a number of fatty acid soaps in water has been measured by Powney and Jordan (7). Plots of the degree of hydrolysis against soap concentration exhibit very pronounced minima and maxima. Stainsby and Alexander (8) have accounted quantitatively for the essential features of these curves on the assumption that mixed micelle formation occurs between fatty acid molecules (formed by hydrolysis) and soap ions. In their opinion aggregation to fatty acid micelles sets in just before the minimum in the hydrolysis curve. As the total soap concentration is increased, the ratio of soap ions to fatty acid molecules in the micelle increases.

According to their calculations the concentration at which the hydrolysis maximum occurs is equal to twice the critical concentration as normally measured. For a number of soaps these calculated values are in reasonably good agreement with the experimental values. Now from Powney and Jordan's data the hydrolysis maximum for sodium oleate at 25°C. occurs at $3 \times 10^{-3} M$. This would indicate a value of $1.5 \times 10^{-3} M$ for the critical concentration, which is approximately the value at which the conductance arrest ends and the viscosity-concentration curve shows a maximum. It is also the concentration at which the break point is observed in the $\Lambda - \sqrt{C}$ curve in the presence of 6 mole-% excess of alkali. The presence of the added electrolyte will, of course, tend to lower the critical concentration. But on the basis of the results of Corrin and Harkins (9), it is unlikely that the error so introduced will exceed several per cent. McBain and Fineman (10), who added 4 mole-% of alkali to suppress hydrolysis, also obtained the value of $1.5 \times 10^{-3} M$ for the critical concentration at 25°C. from study of the osmotic behavior of the soap.

Both the equivalent conductance-concentration curve and the viscosity-concentration curve show the initial inflection at $0.9 \times 10^{-3} M$. Ulmann (11) observed a density change at $0.986 \times 10^{-3} M$. The explanation for this break remains obscure. According to Stainsby and Alexander, aggregation to fatty acid micelles sets in just before the minimum in the hydrolysis curve, i.e., below $1 \times 10^{-4} M$ for sodium oleate at 25°C. On the other hand, it is unlikely that it can be taken as the critical concentration. In the presence of 6 mole-% and 16.7 mole-% excess of sodium hydroxide, the break point occurs at a higher soap concentration.

Accepting the end of the arrest as the critical concentration, the falling conductance suggests that the decrease in Λ resulting from the atmospheric and inclusion effects is now greater than the increase in Λ due to the Stokes's law effect of aggregation plus the conductance due to the hydroxyl ions. The fall in viscosity at soap concentrations above the maximum may also possibly be attributed to the increasing micellar charge. It is not improbable that at lower soap concentrations the fatty acid aggregates undergo flocculation to a limited extent. As the percentage of soap ions in the aggregates increases rapidly above the critical concentration, the electrostatic repulsion will produce separation, possibly yielding a system having a rather lower viscosity.

Stainsby and Alexander have suggested that the effect of normal alcohols in decreasing the hydrolysis of soap is due to a simple competition between free fatty acid (formed by hydrolysis) and alcohol molecules for the limited number of sites in the micelles. If the alcohol is in great excess, no increase in the total amount of fatty acid can be obtained by solubilization, and the hydrolysis, therefore, remains at a normal value. On the same basis it can be suggested that in the presence of added oleic acid a rather greater excess of acid may be left in solution and the hydrolysis accordingly reduced (Fig. 5). It is significant that at concentrations lower than the initial inflection the added oleic acid does not affect the conductance.

SUMMARY

Conductance measurements have been made with sodium oleate in pure water and in the presence of oleic acid and sodium hydroxide at 25°C. The viscosity of aqueous solutions has been measured at 20°C.

1. The equivalent conductance (Λ) vs. $\sqrt{\text{concentration}}$ curve for sodium oleate in water exhibits a distinct arrest in dilute solution. This behavior parallels that of sodium myristate in water.

2. There is an anomalous increase in viscosity in the region of the arrest, followed by a decrease.

3. The addition of oleic acid modifies the arrest. In the presence of sodium hydroxide only one break point is observed.

4. The critical concentration for sodium oleate at 25°C. appears to be about $1.5 \times 10^{-3} M$.

REFERENCES

1. EKWALL, P., *Kolloid-Z.* **101**, 135 (1942); *Z. physik. Chem.* **A161**, 195 (1932).
2. PRESTON, W. C., *J. Phys. & Colloid Chem.* **52**, 84 (1948).
3. BROWN, J. B., AND SHINOWARA, G. Y., *J. Am. Chem. Soc.* **59**, 6 (1937).
4. HOVORKA, F., AND MENDENHALL, E. E., *J. Chem. Educ.* **16**, 239 (1939).
5. HOWELL, O. R., AND HANDFORD, C., *Trans. Faraday Soc.* **29**, 640 (1933).

6. HARTLEY, G. S., Aqueous Solutions of Paraffin-Chain Salts, p. 29. Hermann et Cie., Paris, 1936.
7. POWNY, J., AND JORDAN, D. O., *Trans. Faraday Soc.* **34**, 363 (1938).
8. STAINSBY, G., AND ALEXANDER, A. E., *Trans. Faraday Soc.* **45**, 585 (1949).
9. CORRIN, M. L., AND HARKINS, W. D., *J. Am. Chem. Soc.* **69**, 683 (1947).
10. FINEMAN, M. N., AND MCBAIN, J. W., *J. Phys. & Colloid Chem.* **52**, 881 (1948).
11. ULMANN, M., *Z. physik. Chem.* **A182**, 18 (1938).

THE RHEOLOGY OF PRINTING INKS. II. TEMPERATURE CONTROL STUDIES IN THE ROTATIONAL VISCOMETER

George W. Lower, William C. Walker and Albert C. Zettlemoyer

National Printing Ink Research Institute, Lehigh University, Bethlehem, Pennsylvania

Received July 31, 1952; revised November 19, 1952

ABSTRACT

The use of the rotational viscometer has become well accepted in fundamental studies of the rheological properties of non-Newtonian materials such as printing inks. It is very important, therefore, that the behavior characteristics of this instrument be well known.

One of the most important variables in rheological studies is the temperature since small temperature changes greatly affect viscosities. The present studies indicate that in previous work in this field this point has not been adequately treated. At low energy inputs, the viscometer bath itself is found to be effective in keeping the sample at constant temperature. In the medium range of 60,000–300,000 ergs/sq. cm./sec., the temperature can be controlled by lowering the bath temperature to keep the bob temperature constant. In the high range above 250,000 ergs/sq. cm./sec., the temperature can best be controlled by keeping the mean temperature of the cup and bob constant. These energy input ranges are given per square centimeter of bob surface so that they can be related to various precision rotational viscometers.

Contrary to previous findings reported in the literature, ordinary mineral oils, vegetable oils, and litho varnishes show no evidence of thixotropy when measured by the new technique. Furthermore, the equilibrium flow curves of several oil-based printing inks were found to be linear above the low stress range. Therefore, well-defined values of the plastic viscosity and yield value can be reported for such printing inks.

INTRODUCTION

In order to determine the equilibrium flow curves for oils and printing inks, it is essential to employ an instrument that is capable of exerting a homogeneous shearing stress at a uniform rate of shear upon the sample under investigation. Furthermore, it is desirable to use an instrument in which the rate of shear can be readily changed over a wide range. These requirements are satisfied in the concentric-cylinder, rotational viscometer.

In addition, the flow-curve measurements should be made under isothermal conditions since viscosity decreases very rapidly with increasing temperature. In a material undergoing shear, the internal frictional resistance produces heat. If this heat is not removed from the material, the temperature of that material will rise. This temperature rise will lead to a decrease in the shearing stresses developed and thus to a decrease in

viscosity. As a result, the equilibrium flow curve will be nonlinear. In fact, earlier workers (3,8) have reported such curves as measured in a rotational viscometer to be nonlinear at moderate and high shearing stresses.

In the past, much work with the rotational viscometer has been done by the hysteresis-loop method of Green and Weltmann (4,5). This method has now been discarded by many rheologists. One of its difficulties is the fact that the viscosities and yield values of many systems measured with it are functions of the top rate of shear. In addition, Weltmann¹ (9,10) has reported that even ordinary mineral and vegetable oils appear thixotropic when measured by the hysteresis-loop method. It should be mentioned, however, that Green's work has been extremely helpful in developing the field of printing ink rheology.

In the usual hysteresis-loop method (4) the rate of shear is increased from zero to the top rate chosen, and then decreased rapidly to zero. This method of making viscosity measurements has been discarded because the curve measured is not an equilibrium flow curve and because the size of the loop has little real meaning. If the internal structure of the suspension breaks down at the slightest application of stress, for example, the size of the hysteresis loop will not indicate the amount of structure present. This appears to be the situation in some printing inks.

To put it precisely, the hysteresis-loop method is a mixture of kinetic and thermodynamic measurements. These two fundamentally different characteristics are usually best considered separately. The measurement of a true equilibrium flow curve characterizes the system thermodynamically. This type of measurement has been made in the work reported here and in the study of simple calcium carbonate suspensions to be reported in a paper which will follow. Work on the kinetics of thixotropic breakdown is in progress.

In order to determine accurately the flow characteristics of oils and pigment suspensions, the foremost problem was to determine the most suitable experimental method of measuring the flow curve. The influence of stress-induced temperature had to be determined. Thereafter, the exact shape of the isothermal flow curves of oils and printing inks could be determined. The results reported here indicate that a considerable amount of precaution must be observed in order to keep the temperature of the sample constant as the rate of shear is increased.

In view of earlier work (6,7) on heat effects in lubricating films, it is somewhat surprising that the temperature effect in rotational viscometry had been considered negligible (9) until recently (1).

¹ Recently, after discussing the work presented here, Weltmann and Kuhns [*J. Colloid Sci.* **7**, 218 (1952)] calculated temperature distributions in the rotational viscometer, and confirmed some of the conclusions drawn here.

EXPERIMENTAL

Description of Viscometer

The viscometer used is one described by Buchdahl *et al.* (2). The moving parts consist of a rotating cylindrical cup driven by a variable-speed transmission to a top speed of 550 r.p.m. The stationary inner cylinder or bob is mounted on a special sealed bearing designed to give minimum static friction. The clearance between the cup and bob is approximately 0.05 cm.; with this clearance a maximum rate of shear of 660 sec^{-1} can be obtained. The bob is suspended on a torsion wire which can be calibrated directly with weights. Angular deflection of the bob is read on a vernier dial mounted at the lower end of the wire. A series of wires with constants ranging from 252 to 30,450 dyne-cm./deg. is available. The cup is surrounded by a water bath containing a stirrer and thermoregulator so that the bath temperature can be controlled to $\pm 0.02^\circ \text{C}$. over a range from 20 to 50°C .

Figure 1 is a diagrammatic cross section of the bob, and of the cup and bath on one side. The sample is contained in the narrow annular space between the cup and the bob. The cup is connected thermally to the wall of the bath by a film of thin oil.

What is desired are measurements of the actual temperatures of the ink samples under shear. Of course, a thermocouple placed in the sample would disturb the flow pattern so that homogeneous shearing stress would not be produced; therefore, the next best possibility is to place thermo-

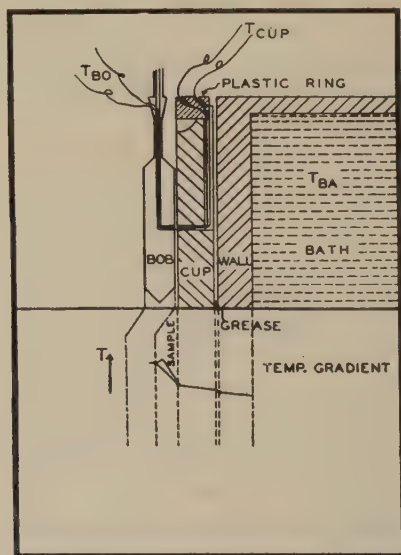


FIG. 1. Cross-sectional diagram of the cup and bob arrangement.

couples in the walls of the cup and bob. Measurements made with these thermocouples led to a refutation of earlier claims that temperature effects in rotational viscometry are negligible. An example of the temperature gradient existing in this system under normal operating conditions is sketched also in Fig. 1. Most of the temperature gradient occurs in the sample. The temperature is probably highest at a point near the bob as indicated by the full line through the sample region.

The values of the rate of shear, D , and the shearing stress, S , are calculated from the following equations:

$$D = \frac{R_1 R_2 \text{ (r.p.m.)}}{15(R_2^2 - R_1^2)} = 1.212 \text{ (r.p.m.)} \quad [1]$$

$$S = \frac{K\theta}{2\pi h R_1 R_2} = 0.1106 K\theta, \quad [2]$$

where: R_1 = radius of bob = 0.5499 cm.; R_2 = radius of cup = 0.5954 cm.; h = length of bob = 4.365 cm.; K = wire constant in dyne-cm./deg.; θ = angular deflection of bob in degrees; S = shearing stress in dynes/sq. cm.; and D = rate of shear in sec.⁻¹. The viscosity of Newtonian liquids is then calculated from the slope of the S - D curve by:

$$\eta = S/D. \quad [3]$$

The plastic viscosity of non-Newtonian materials is calculated from the slope of the linear part of the S - D curve by:

$$U = dS/dD. \quad [4]$$

Method of Obtaining the Flow Curve

The flow curve is obtained by measuring the angular deflection θ at various cup speeds. The variable-speed transmission is set at a particular point and the revolutions per minute (r.p.m.) are determined with a stopwatch. The instrument is run at that r.p.m. value until a steady deflection of the wire is attained. Then the r.p.m. are increased to the next point desired and the resulting deflection is obtained in the same manner. Using this procedure the points on the flow curve are read in the following order: 1, 2, 1, 3, 2, 4, 3, 5, 4, 6, etc. In this manner each point is approached from both above and below. If the readings are taken at true equilibrium, the values should be the same whether approached from higher or lower rates of shear. If the angles of the deflections agree within 0.2°, it is assumed that equilibrium has been reached. The rate of attainment of equilibrium is nearly instantaneous with Newtonian liquids such as mineral oils and vegetable oils, but with thixotropic materials equilibrium is reached more slowly.

Temperature Measurement

In order to measure the temperature rise within the sample, a bob was first constructed containing an iron-constantan thermocouple² marked

² After the work reported here was completed, a thermistor was incorporated in the bob and connected to a microammeter through an electronic circuit. This more elegant arrangement is preferred.

T_{BO} in Fig. 1. This thermocouple is inserted in the bob so that the junction is at the face of the bob in direct contact with the liquid. The wire leads come up through the interior of the bob and out at the top where they dip into two mercury wells. From the mercury wells the leads are connected to the reference junction contained in an external water bath. The temperature of the bath is controlled to within $\pm 0.02^\circ\text{C}$. by means of a thermoregulator and relay. The bob thermocouple is connected electrically to the rest of the circuit through a pair of mercury wells to allow free movement of the bob without breaking the electrical circuit.

Finally, a thermocouple T_{cup} is placed in the wall of the cup so that the temperature can be measured on either side of the sample. This thermocouple junction does not actually contact the liquid directly but is placed so that only a thin section of the cup wall separates it from the liquid. The leads from this thermocouple are taken out to the measuring circuit through a pair of mercury slip rings in a piece of plastic mounted at the top of the cup. Thus readings can be taken while the viscometer is in operation. (For usual work it has been found that the cup thermocouple is unnecessary because the plastic viscosity can be established at low energy inputs where control of the bob temperature is sufficient.)

The resulting current is measured on a Leeds and Northrup D'Arsonval-type galvanometer using a light beam reflected on a meter scale. The thermocouple was calibrated using a Beckmann thermometer and a water bath. The calibration was such that a 1-cm. deflection was approximately equal to 0.1°C . with the reference junction held at $30 \pm 0.02^\circ\text{C}$. The accuracy of these thermocouple temperature readings was about $\pm 0.05^\circ\text{C}$.

In addition to the above changes, the viscometer bath is modified so that cooling water can be admitted and the excess removed through an overflow. In this manner the temperature of the bath can be lowered as desired.

As is well known, viscosity is extremely sensitive to temperature variations so that temperature control during measurements is extremely important. For Newtonian materials such as mineral or vegetable oils the viscosity may vary several per cent per degree centigrade.

In order to discuss the control of temperature in the rotational viscometer it is convenient to consider three ranges of energy input. These energy input ranges are defined as follows: (a) low energy input range, 0–75,000 ergs/sq. cm./sec.; (b) medium energy input range, 60,000–300,000 ergs/sq. cm./sec.; and (c) high energy input range, 250,000 ergs/sq. cm./sec. and above. Energy input rather than stress was chosen because the former is the more significant quantity with regard to temperature control. The energy inputs were put on the basis of square centimeters of bob area or shearing area so that these ranges would be more meaningful with regard to any other similar precision rotational vis-

cometer. The division between the ranges is necessarily not precise; therefore the ranges were made to overlap.

RESULTS

Temperature Effects in the Low Energy Input Range

When the viscosities were determined at energy inputs below 75,000 ergs./sq. cm./sec. (generally below stresses of 16,000 dynes/sq. cm. for the materials tested here), the temperature could be controlled to about $\pm 0.02^\circ\text{C}$. That is, the viscometer bath could effectively control the temperature of the sample at the low stresses.

Temperature Control

The efficiency of temperature control and the over-all accuracy of the instrument was checked against two Bureau of Standards oils in the low energy input range. The viscosities of these standard oils had been determined in capillary viscometers to an accuracy of 0.1% relative to the absolute viscosity of water. With this instrument, viscosity measurements relative to the Bureau of Standards values can be determined with an accuracy of about 4% and a precision of about $\pm 1.5\%$.

Temperature Effects in the Medium and High Energy Input Ranges

Upon investigating the flow curves of oils with the bath temperature held constant it was found that they deviated from linearity at energy inputs of approximately 60,000 ergs/sq. cm./sec. or greater. This is shown in Figs. 2-BA and 3-BA for two polybutene oils with viscosities of 138 and 483 poises, respectively. In this figure the designation BA indicates that the bath temperature was held constant.

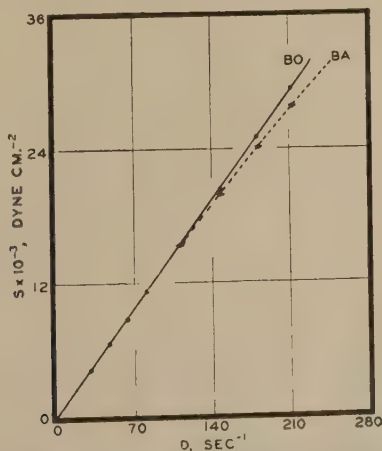


FIG. 2. Flow curve for polybutene No. 24: BO = bob temp. constant; BA = bath temp. constant.

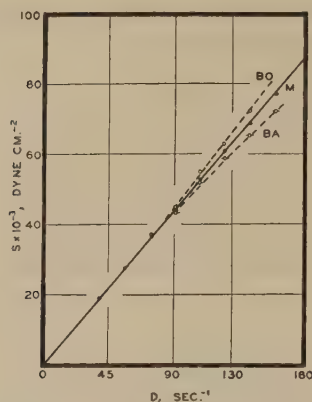


FIG. 3. Flow curve for polybutene No. 32: BO = bob temp. constant; BA = bath temp. constant; M = mean temp. constant.

This curvature indicates either that the oils are thixotropic or that some other phenomenon is occurring. One of the possible explanations for the curvature could be an increase in the sample temperature as the shear rate is increased.

To investigate this curvature the temperature rise at the bob face was measured with the bob thermocouple for two polybutene oils, a litho varnish, and a yellow-lake ink. The results are shown in Table I. The bath temperature and reference junction temperature were maintained at 30.0°C .

As can be seen from these data, the temperature rises as the rate of shear increases, that is as the energy input increases, and is greater for the more viscous oils. For low-viscosity oils, the temperature rise was not

TABLE I
Temperature Rise at Bob^a

Polybutene No. 24A $\eta = 145$ poises		No. 5 litho varnish $\eta = 146$ poises		Polybutene No. 32 $\eta = 485$ poises		Yellow-lake ink $\eta = 285$ poises	
D	ΔT	D	ΔT	D	ΔT	D	ΔT
<i>sec.</i> ⁻¹	$^{\circ}\text{C}$.	<i>sec.</i> ⁻¹	$^{\circ}\text{C}$.	<i>sec.</i> ⁻¹	$^{\circ}\text{C}$.	<i>sec.</i> ⁻¹	$^{\circ}\text{C}$.
77.4	0.11	76.8	0.13	92.8	0.40	81.0	0.16
148	0.51	119	0.28	144	1.1	123	0.58
216	1.1	148	0.45	180	1.5	152	0.58
289	1.9	217	0.8	263	3.1	178	0.26
364	2.8	287	1.3	349	4.8	220	1.1
440	4.0	363	2.0			263	1.6
		438	2.8			291	2.0

^a ΔT means temperature rise at D rate of shear.

very great; for instance, No. 3 litho varnish with $\eta = 31.9$ poises gave a temperature rise of only 0.7°C . at a rate of shear of 531 sec.^{-1} .

In order to determine whether the temperature rise, as measured at the bob face, would account for the decrease in viscosity with increasing energy input the following experiment was conducted:

From the measured temperature coefficients of viscosity and the measured viscosity at any particular rate of shear the temperature rise necessary to decrease the viscosity to the observed value was calculated. This calculated temperature rise was compared at a number of rates of shear to that measured at the bob face.

The viscosity-temperature curves for polybutene No. 24A and polybutene No. 32 were determined and the temperature coefficients calculated. The relationships could be adequately expressed by the usual

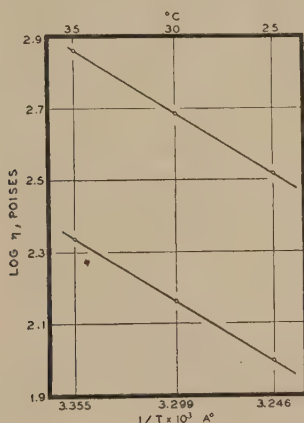


FIG. 4. Variation of viscosity with temperature: polybutene No. 25 (lower curve); polybutene No. 32 (upper curve).

equation:

$$\log \eta = \frac{A}{T} + B, \quad [5]$$

where T is the absolute temperature and A and B are constants. The validity of Eq. [5] is shown in Fig. 4 where the plot of $\log \eta$ vs. $1/T$ is linear.

The viscosities of these polybutene oils were measured at shear rates below 30 sec.^{-1} at three different temperatures: 25, 30, and 35°C . The values of A and B in Eq. [5] are, respectively, 3146.5 and -8.2234 for No. 24A, and 3187.4 and -7.8327 for No. 32.

From these temperature coefficients of viscosity and the measured viscosity at any particular rate of shear, the temperature rise necessary to decrease the viscosity to the observed value was calculated. These

calculated values are shown in Table II for polybutene No. 24A along with the experimentally measured values.

It may be seen from the figures tabulated in Table II that the observed temperature rise is generally nearly as great as the rise calculated to be necessary to account for the deviation of the flow curve from linearity. Apparently a considerable amount of this deviation, then, can be attributed to inadequate dissipation of heat. Thus, if we are to be concerned with accurate determination of the shape and slope of isothermal flow curves, it is essential that the sample temperature be more closely controlled than can be done by thermostating the surrounding water bath.

Weltmann (9,10) stated that temperature rise was a second-order effect in the hysteresis-loop method of measuring viscosity. On the basis of this loop she postulated that oils are thixotropic. A rapid flow curve was run on polybutene No. 32 to test this effect. In order to minimize the temperature rise, no up curve was made. The viscometer was started at a top rate of shear of 349 sec.^{-1} , and the down curve was measured as rapidly as possible. The results are shown in Fig. 5. The low energy input

TABLE II

Calculated and Observed Temperature Rises for Polybutene No. 24A at 30.0°C.

D sec.^{-1}	$\Delta T_{\text{calcd.}}$ $^{\circ}\text{C.}$	$\Delta T_{\text{obs.}}$ $^{\circ}\text{C.}$
77.4	0.10	0.11
148	0.90	0.51
216	1.4	1.1
289	2.3	1.9
364	3.2	2.8
440	4.1	4.0

range viscosity of this oil was 485 poises. The time necessary to make this rapid down curve was 1.4 min., and the maximum measured temperature rise was 2.6°C. The measured viscosity from the rapid run was 364 poises, whereas the viscosity calculated from the maximum temperature rise was 396 poises. From this evidence it can be seen that even in this rapid type of measurement the temperature rise is considerable. This temperature rise, although a variable quantity throughout the run, is sufficient to account for a considerable decrease in viscosity. It seems probable that it was this temperature rise which led Weltmann to believe that oils are thixotropic.

Temperature Control in Oils: Medium Energy Input Range

In order to compensate for the temperature rise in the sample, a series of runs was made at a constant bob temperature of 30.0°C. This was accomplished by cooling the external bath until the thermocouple at the

bob face registered 30.0°C. At this point the torque reading was taken. The flow curves obtained by this method are shown in Fig. 2-BO for polybutene No. 24B ($\eta = 133$ poises); similar results were obtained with a No. 7 litho varnish ($\eta = 113$ poises). The designation *BO* indicates that the bob temperature was held constant. The flow curves for polybutene No. 24B and No. 7 litho varnish are linear and pass through the origin. That is, these oils have a constant viscosity and show no thixotropy in the low or medium range of energy input. The viscosity calculated from the slope of the flow curve agrees with the low energy input viscosity. This method of temperature control appears to be adequate for materials where the shearing stresses lead to energy inputs in the medium energy input range.

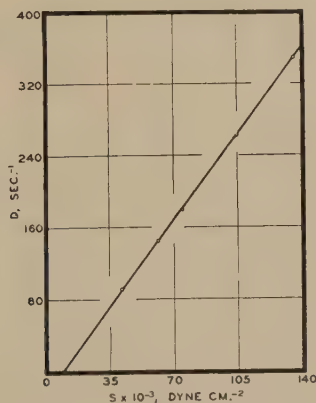


FIG. 5. Rapid flow curve for polybutene No. 32.

Temperature Control in Oils: High Energy Input Range

The flow curve for polybutene No. 32, as shown in Fig. 3-BO, curves upward in the direction of increasing viscosity in the high energy input range when the bob temperature is controlled. This indicates that the effective temperature of the sample using this type of control is actually lower than 30.0°C., when the energy inputs developed are above about 250,000 ergs/sq. cm./sec. (stresses above about 50,000 dynes/sq. cm. for this material).

In order to overcome this effect, the flow curves of heavy oils were run at a mean temperature by using the cup thermocouple in conjunction with the bob thermocouple. Using both thermocouples it was possible to adjust the viscometer bath temperature so that the mean of the bob and bath temperatures was kept at the temperature of the reference junction. According to the temperature gradient diagram in Fig. 1, it is seen that the mean temperature of the cup and bob, on the dotted line, would not

be quite as high as the actual mean temperature of the sample. Actually, the gradient diagrammed in Fig. 1 is somewhat exaggerated. The mean between the cup and the bob is the best, convenient approximation that can be made. That the dotted line lies close to the full line, that is, that the approximation is very close, was confirmed by the self-consistency of the data presented below.

The flow curve of polybutene No. 32 was studied at a mean temperature of 30.0°C. Figure 3-*M*, where *M* designates that the sample was run at a constant mean temperature, shows that this method effectively corrects for temperature rise. The flow curve is linear, and the viscosity agrees with the low shear viscosity.

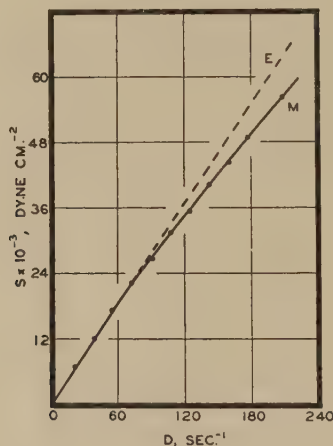


FIG. 6. Flow curve for Dow Silicone Oil No. 200: *M* = mean temp. constant; *E* = extrapolation of low shear points.

Application to Oils

Weltmann based much of her theory for thixotropy in the oils on the fact that a silicone oil apparently exhibited strong thixotropy. Since silicones have a very low temperature coefficient of viscosity, she claimed that temperature rise in the sample could not account for the decrease in viscosity with increased shear. In order to determine if this were true, a Dow Silicone Oil No. 200 of about 300 poises was studied. Figure 6-*M* shows that the flow curve of this silicone oil is not linear when run at a mean sample temperature. In fact, there is very little change in the position of the flow curve no matter how the temperature control is maintained. This persistent curvature away from the extrapolated curve indicates that this silicone oil is definitely thixotropic, but does not necessarily prove that mineral and vegetable oils are also thixotropic. In a private communication, A. Voet reported that silicone oils exhibited streaming

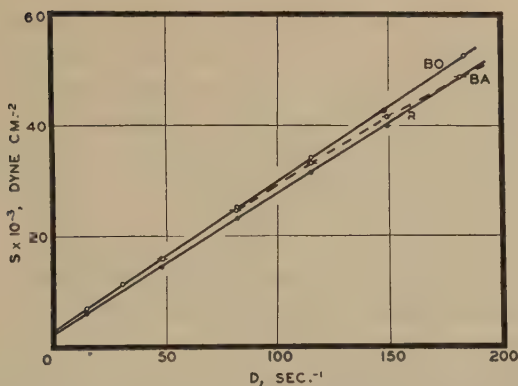


Fig. 7. Flow curve for green-lake ink: BO = bob temp. constant; BA = bath temp. constant; and R = rapid run; bath temp. constant.

birefringence at low shear rates whereas ordinary viscous mineral and vegetable oils did not. The presence of streaming birefringence data confirm the results obtained in this laboratory. That is, silicone oils are thixotropic but ordinary mineral and vegetable oils tested are not.

Temperature Control in Printing Inks

The lower portion of the flow diagram of a pigment suspension is curved provided that any structure is built up in the suspension. The important portion of the flow curve, for the present discussion, is the upper portion as shown in Fig. 7. In general, a linear equation can be written for the flow curve of a printing ink, although an important exception has been observed with certain black inks as indicated in Fig. 8.

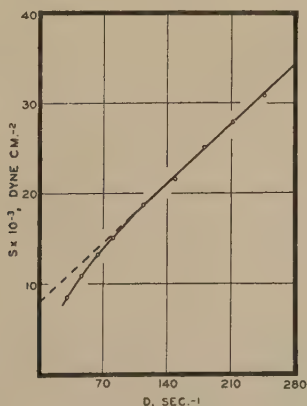


Fig. 8. Flow curve for carbon black ink, bob temp. constant.

For a number of printing inks, the upper part of the flow curve was found to deviate from linearity when the bath temperature was held constant, as shown in the example of the green-lake ink in Fig. 7-BA. When run at constant bob temperature, however, the flow curve was linear, as in Fig. 7-BO. The pronounced curvature at the lower end of the curve for the carbon black ink, Fig. 8, shows the presence of a high yield value or coefficient of thixotropy.

A rapid flow curve was made on the green-lake ink starting from the top equilibrium point and decreasing the shear rapidly as is shown in Fig. 7-R. The plastic viscosity calculated from this curve was found to be 255 poises as compared to 272 poises for the BO equilibrium curve; the yield value was also slightly less. Thus, it is evident that even when the top point is an equilibrium point, the rapid method does not give a true flow curve or a true viscosity.

SUMMARY

Preliminary flow curve measurements of oils and pigment suspensions in the concentric cylinder, rotational viscometer were found to be non-isothermal. This is in sharp contrast to the conclusions of earlier workers. Therefore, this finding prompted a thorough study of temperature control during flow curve measurements. Since isothermal, equilibrium measurements are usually desired, careful modifications had to be made to record and control the temperature rise in the sample as high shear stresses were reached.

The viscometer was modified by carefully inserting thermocouples in the bob and cup to permit the temperature to be recorded. The method of temperature control necessary was found to depend on the magnitude of the shearing stresses developed in the sample. When the stresses are in the low energy input range, below 75,000 ergs/sq. cm./sec., the viscometer bath is effective in maintaining the sample at constant temperature. In the medium energy input range, from 60,000 to 300,000 ergs/sq. cm./sec., however, the temperature must be controlled by altering the bath temperature and keeping the bob temperature constant; and in the high energy input range, above 250,000 ergs/sq. cm./sec., the mean temperature of the cup and bob must be kept constant.

When any doubt exists concerning temperature control, it is always best to attempt to keep the mean temperature between the cup and the bob constant.

When adequate temperature control was maintained, the equilibrium flow curves for ordinary mineral and vegetable oils were linear and passed through the origin. That is, no evidence of thixotropy was found in these oils. The apparent thixotropy reported heretofore in these oils was shown to be due to temperature rise in the sample under test.

The rapid method of determining the flow curve used in some laboratories was shown to give false results owing to an increase in sample temperature.

Flow curves for printing inks based on litho varnishes were linear at high rates of shear when adequate temperature control was maintained. The slope of the linear part of these curves gave a precise measure of the viscosity of the system. The extrapolation of this linear region to the stress axis also gave a well-defined value for the coefficient of thixotropy or yield value. This value can now be considered to be unique.

REFERENCES

1. AMERICAN SOCIETY FOR TESTING MATERIALS, Special Technical Publication No. 111: Symposium on Methods of Measuring Viscosity at High Rates of Shear. Philadelphia, 1951.
2. BUCHDAHL, R., CURADO, J. C., AND BRADDICKS, R., *Rev. Sci. Instruments* **18**, 168 (1947).
3. GOODEVE, C. F., AND WHITFIELD, C. W., *Trans. Faraday Soc.* **34**, 511 (1938).
4. GREEN, H., AND WELTMANN, R., *Ind. Eng. Chem., Anal. Ed.* **15**, 201 (1943).
5. GREEN, H., AND WELTMANN, R., *Ind. Eng. Chem., Anal. Ed.* **18**, 167 (1946).
6. HERSEY, M. D., *Trans. Am. Soc. Mech. Engrs.* **64**, 453 (1943).
7. KINGSBURY, A., *Mech. Eng.* **55**, 685-8 (1933).
8. PHILIPPOFF, I. W., *Viskosität der Kolloide*. Steinkopff, Dresden and Leipzig, 1942.
9. WELTMANN, R., *Ind. Eng. Chem., Anal. Ed.* **15**, 424 (1943).
10. WELTMANN, R., *Ind. Eng. Chem.* **40**, 272 (1948).

RHEOLOGY OF SYNTHETIC LATEX. III. CONCENTRATION DEPENDENCE OF FLOW IN TYPE III GR-S LATEX

Samuel H. Maron and Benjamin P. Madow

*Physical Chemistry Laboratory, Department of Chemistry and Chemical Engineering
Case Institute of Technology, Cleveland, Ohio*

Received September 23, 1952

INTRODUCTION

The second paper in this series (1) described a study of the flow behavior of type V GR-S latex as a function of rate of shear and concentration. This latex is an aqueous dispersion of 70:30 butadiene-styrene copolymer emulsified with a mixture of Dresinate 731 (a rosin soap) and potassium oleate, and has generally a volume to surface average diameter of *ca.* 2000 Å. On the other hand, type III latex is an aqueous dispersion of a 50:50 butadiene-styrene copolymer emulsified with the potassium soap of K-wood rosin, and shows generally a volume to surface average diameter of 800–1100 Å. In view of the differences in the composition, emulsifier, and particle size of the two systems, a comparison of their rheologic behavior is of interest. Hence a study similar to that made on type V latex was also made on type III latex, and is presented in this paper.

EXPERIMENTAL

The type III latex investigated was a standard commercial product concentrated by evaporation from its original *ca.* 39% solids. On receipt this latex had a solids content of 59.50% and a dry rubber content of 55.34% by weight. Analysis (2) showed the soap and free rosin acid contents to be respectively 0.1416 and 0.0093 normal. This latex was concentrated further by evaporation to a solids content of 66.49% and a polymer content of 61.84%, and the latter concentrate was used as a stock solution for preparation by dilution with distilled water of the 20 concentrations studied.

All flow measurements were made at $30.00 \pm 0.01^\circ\text{C}$. in the equipment and by the procedures described before (3). The theoretical methods of analyzing the data have also been given previously (1,3).

RESULTS AND DISCUSSION

Up to *ca.* 40% rubber content, and over the entire range of rates of shear investigated, the solutions of type III latex gave single straight

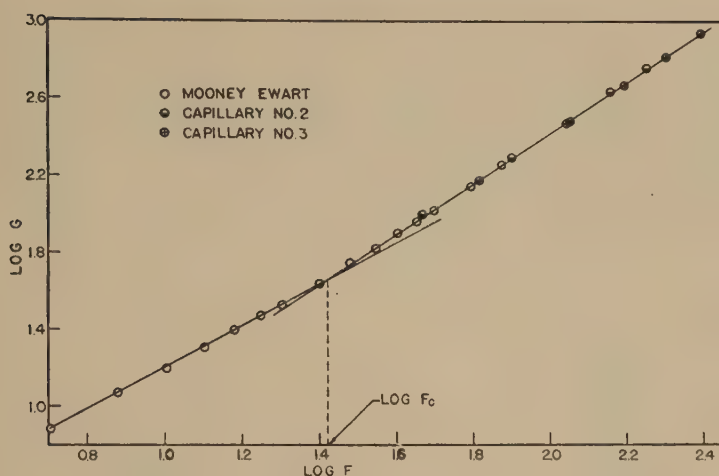


FIG. 1. Flow curves for type III latex at 54.65% solids content.

lines when $\log G$ was plotted against $\log F$. G is the rate of shear in sec.^{-1} , while F is the shearing stress in dynes/sq. cm. These lines could be represented by the equation

$$F^N = \eta' G, \quad [1]$$

TABLE I

Flow Constants for Type III GR-S Latex

Rubber content Wt. %	ϕ	N_1	$\log(\eta'_1/\eta_0)$	N_2	$\log(\eta'_2/\eta_0)$	F_2 dynes/sq. cm.
0	0	1.00	0	—	—	—
9.46	0.0960	1.00	0.142	—	—	—
19.44	0.1970	0.99	0.287	—	—	—
27.81	0.2813	1.01	0.535	—	—	—
32.40	0.3276	1.03	0.675	—	—	—
34.78	0.3515	1.04	0.771	—	—	—
38.03	0.3841	1.05	0.936	—	—	—
41.57	0.4196	1.09	1.167	1.00	1.097	10.4
46.18	0.4658	1.15	1.561	1.00	1.378	15.7
48.37	0.4877	1.19	1.812	1.03	1.615	19.0
50.82	0.5122	1.31	2.284	1.08	1.970	25.6
53.01	0.5341	1.42	2.764	1.17	2.402	30.8
55.34	0.5574	1.62	3.555	1.31	2.920	36.3
56.34	0.5674	1.70	3.910	1.45	3.507	41.1
58.18	0.5859	1.95	4.884	1.76	4.582	42.0
58.69	0.5908	1.98	4.964	—	—	—
59.24	0.5963	2.18	5.698	—	—	—
59.89	0.6028	2.27	6.192	2.53	6.757	151
60.67	0.6106	2.14	6.105	2.56	7.018	214
61.46	0.6184	2.10	6.124	2.61	7.358	278
61.84	0.6222	1.96	5.933	2.64	7.596	291

where N and η' are constants dependent only on the concentration at constant temperature. However, above *ca.* 40% rubber content the plots were of the type shown in Fig. 1, and consisted of two intersecting straight lines. As before, separate equations of the above form were fitted to the upper (subscript 1) and lower (subscript 2) portions of the curves. Values of N and η' for both shearing-stress ranges, as well as F_c , the shearing stress where the lines intersect, are given in Table I as a function of the

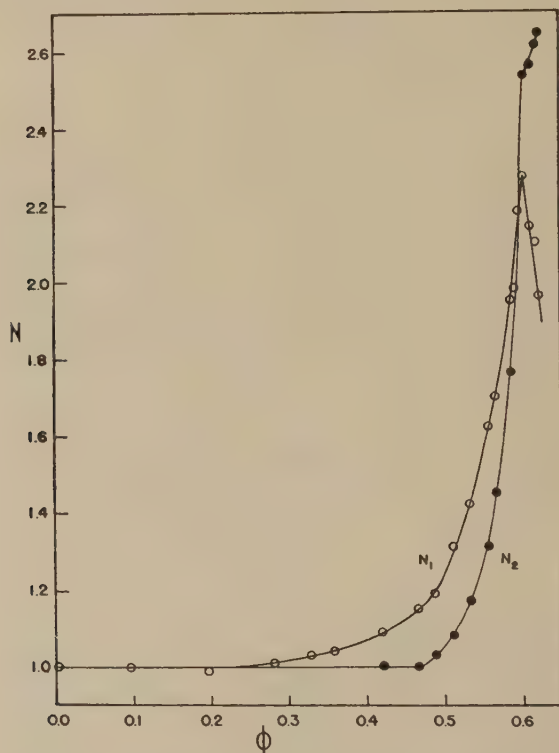


FIG. 2. Variation of N with volume fraction of rubber.

rubber content and the volume fraction of rubber, ϕ . The density for the polymer used to convert rubber content to volume fraction was 0.984.

The data of Table I are plotted in Figs. 2 and 3. From Fig. 2 it may be seen that type III latex is Newtonian ($N = 1$) at all shearing rates investigated up to $\phi = 0.25$, and non-Newtonian above $\phi = 0.47$. Between these concentrations the flow behavior is Newtonian at shearing stresses below F_c and non-Newtonian above them. Again, above $\phi = 0.25$, N_1 increases up to $\phi = 0.60$ and then decreases, whereas N_2 increases continuously and rapidly from $\phi = 0.47$ to $\phi = 0.60$, and then more slowly

thereafter. It should also be observed that between $\phi = 0.25$ and $\phi = 0.595$, N_1 is greater than N_2 , whereas above the latter concentration, N_2 is greater than N_1 . This behavior contrasts with that of type V latex, where over the entire concentration range studied, N_2 was larger than N_1 .

There are several points of interest in Fig. 3. First, η_2' increases continuously with concentration, whereas η_1' increases only up to $\phi = 0.60$ and then drops thereafter. Secondly, the two curves cross at $\phi =$

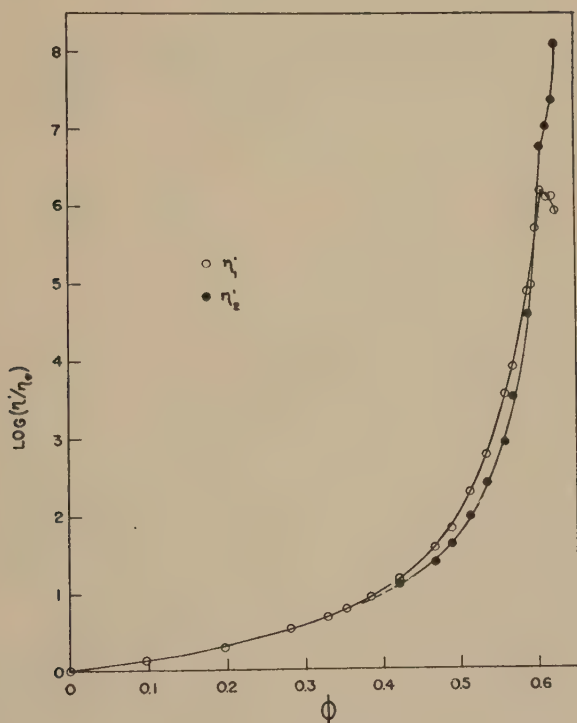


FIG. 3. Variation of η' with volume fraction of rubber.

0.595. Thirdly, below the latter concentration, η_1' is larger than η_2' , whereas above the latter concentration η_2' is larger than η_1' . This behavior of η' is again different from that observed with type V latex. With the latter system, η_1' showed the monotonic increase and η_2' the drop above $\phi = 0.60$; the two curves did not cross, and over the entire concentration range investigated η_2' was larger than η_1' .

As with type V latex, the variation of η' with concentration can be expressed by the equation

$$\log \eta'/\eta_0 = bZ, \quad [2]$$

where η_0 is the viscosity of water, and Z is defined by the relation

$$Z = \frac{\alpha\phi}{1 - \alpha\phi} \quad [3]$$

The constants b and α have to be selected to fit the data. By combining Eqs. [2] and [3] we obtain

$$\frac{\phi}{\log(\eta'/\eta_0)} = \frac{1}{\alpha b} - \frac{1}{b}\phi \quad [4]$$

and hence the constants should follow from the slope and intercept of the expected linear plots of $\phi/\log(\eta'/\eta_0)$ versus ϕ .

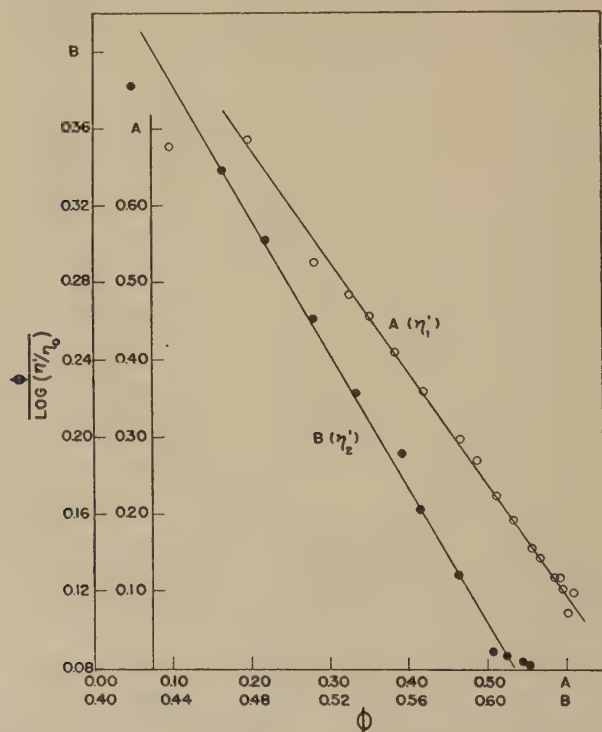


FIG. 4. Graphical determination of α and b .

Such plots are shown in Fig. 4 for η'_1 and η'_2 . These yield the following constants: $\alpha_1 = 1.496$, $b_1 = 0.697$, $\alpha_2 = 1.515$, $b_2 = 0.572$. Using these values of α , plots of $\log \eta'/\eta_0$ vs. Z are obtained (Fig. 5) which are linear up to $\phi = 0.60$. At the latter point, sharp breaks occur of the same character as observed with type V latex. In line with Eq. [2], the slopes of these lines are $b_1 = 0.694$ and $b_2 = 0.575$, values in excellent accord with those evaluated from Fig. 4.

According to Eq. [2] η' should become infinite when $\phi = 1/\alpha$. Using the above values of α we get $\phi_1 = 1/\alpha_1 = 0.668$ and $\phi_2 = 1/\alpha_2 = 0.660$. These values of ϕ_1 and ϕ_2 are low, since close packing of nonuniform rigid spheres should be reached at a volume fraction of 0.74–0.78. As with type V latex, the difference can be ascribed to the monolayer of adsorbed soap. It was shown before (1) that the relation between the observed volume fraction ϕ when $\eta' = \infty$ and that due to rubber plus soap, ϕ_t , is

$$\frac{\phi_t}{\phi} = 1 + \frac{6\Delta}{D_s}, \quad [5]$$

where Δ is the length of the soap molecule and D_s is the volume to surface average diameter. For the type III latex in question, D_s was found by

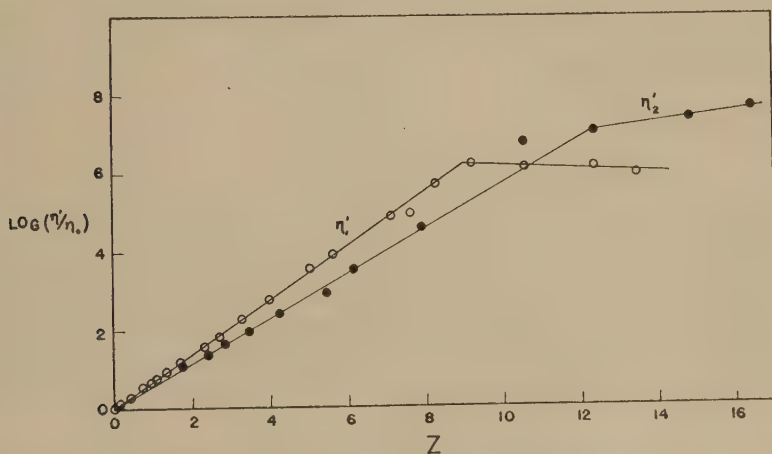


FIG. 5. Plots of $\log \eta'/\eta_0$ vs. Z for type III latex.

soap titration to be 980 Å. The length of the K-wood rosin soap molecule is not known, but it should not be far different from that of abietic acid. Scaling of a Hirshfelder-Fisher model of this molecule gave a maximum length of 17 Å. With this value of Δ , Eq. [5] yields from $\phi_1 \phi_t = 0.74$, and from $\phi_2 \phi_t = 0.73$. These values are in good accord with the volume fraction to be expected for close packing of rigid spheres.

It was also shown before (1) that for the region of low concentrations Eq. [5] reduces to

$$\eta' = \eta_0(1 + 2.303 \alpha b \phi). \quad [6]$$

In line with Einstein's theoretical expression (4) for the viscosity of dilute suspensions of rigid spheres, the quantity $2.303\alpha b$ should equal 2.5. The values of this factor found here were $2.303\alpha_1 b_1 = 2.40$ from the high shear rate data, and $2.303\alpha_2 b_2 = 2.00$ from the low shear rate data.

ACKNOWLEDGMENT

This research was sponsored by the Office of Synthetic Rubber, Reconstruction Finance Corporation, as part of the government Synthetic Rubber Program, and was first reported in March, 1949.

SUMMARY

Type III GR-S latex was found to be Newtonian at concentrations below a volume fraction of $\phi = 0.25$ rubber. Between $\phi = 0.25$ and $\phi = 0.47$, the latex was Newtonian at low shearing rates, but non-Newtonian at higher ones. Above $\phi = 0.47$, the flow was non-Newtonian at all rates of shear.

Up to $\phi = 0.40$, a single exponential flow equation covered the entire range of shearing stresses employed. Above the latter concentration, however, separate exponential flow equations had to be used for the low- and high-stress ranges. The flow constants N and η' varied regularly with concentration, but in a manner more complex than observed with type V latex.

The extension of the Einstein equation used before, namely, $\log(\eta'/\eta_0) = bZ$ where $Z = \frac{\alpha\phi}{1 - \alpha\phi}$, was again found to hold well from 0 to 0.60 volume fraction of rubber. Application of this equation to the low concentration region gave a proportionality constant between η' and ϕ not far different from the Einstein 2.5. Again, extrapolation of the equation to infinite viscosity gave a volume fraction of rubber plus adsorbed soap monolayer equal to 0.73–0.74, a value very close to that expected for close packing of spheres.

REFERENCES

1. MARON, S. H., MADOW, B. P., AND KRIEGER, I. M., *J. Colloid Sci.* **6**, 584 (1951).
2. MARON, S. H., ULEVITCH, I. N., AND ELDER, M. E., *Anal. Chem.* **24**, 1068 (1952).
3. KRIEGER, I. M., AND MARON, S. H., *J. Colloid Sci.* **6**, 528 (1951).
4. EINSTEIN, A., *Ann. Physik* **19**, 289 (1906).

TACKY ADHESION—A PRELIMINARY STUDY ¹

W. H. Banks and C. C. Mill

*Printing, Packaging and Allied Trades Research Association, Randalls Road,
Leatherhead, Surrey, England*

Received April 14, 1952

ABSTRACT

Consideration of the conditions of liquid flow between separating parallel disks suggests that cavitation sets upper limits to the force opposing the separation. On this basis the limiting force should be independent of the liquid and the initial separation of the disks.

Some preliminary measurements appear to be in agreement with this, and the bearing on studies of tacky adhesion is discussed.

INTRODUCTION

The problem of tacky adhesion involves an understanding of the forces or energies involved in the separation of two surfaces in general closely separated by a film of highly viscous liquid. Stefan (1) in a study of adhesiveness in liquids regarded the problem as one of hydrodynamics and calculated that the force F required to increase the separation of two circular disks of radius R from h_1 to h_2 in a time t under conditions of complete immersion in a liquid of viscosity η was given by

$$F = 3\pi\eta R^4[1/h^2 - 1/h_2^2]/4t.$$

Although his experiments with water, alcohol, aqueous salt solutions, and air were not in exact agreement with theory, subsequent study of the data by De Bruyne (2) and Dow [in the light of Bikerman's suggestion of the importance of surface roughness (3)] showed that the discrepancies might be removed if due allowance was made for errors in the initial separation.

Reynolds (4) made a similar calculation for elliptical flat plates which with the appropriate geometry leads to the Stefan relation. Green (5) apparently unaware of these earlier studies made experiments similar to those of Stefan with the object of measuring "tackiness." He found that viscosity was the relevant property of the liquid determining its tack, and indeed showed purely empirically that his data conformed to a rela-

¹ This paper is published by permission of the Director and Council of the Printing, Packaging and Allied Trades Research Association, Randalls Road, Leatherhead, Surrey, England.

tion identical with Stefan's provided the initial separation was increased by a small constant.

It is thus reasonable to infer that the Stefan theory is basically true. Its validity for high rates of separation, for extremely small separations, or for highly viscous liquids has, however, from time to time been questioned, and Voet and Geffken in particular (6) have suggested that viscosity is not fundamentally the tack-determining property of highly viscous liquids. They have provided evidence to show that Stefan's law would predict energies of separation far higher than is in fact observed experimentally.

The present study re-examines the flow of a Newtonian liquid occasioned by separation of Stefan disks with the object of establishing the existence of limits beyond which obedience to Stefan's law may not be expected. It will be shown that there are limits to the speed of separation or applied force above which the flow conditions consistent with the law may be upset by the onset of cavitation. This situation arises through the existence of reduced hydrostatic pressure in the liquid during flow. The importance of the effect is not immediately apparent in the Stefan relation as usually stated because the pressures in the liquid do not appear explicitly in it, but the tension in the liquid can, as we shall show, assume such values (under easily attainable experimental conditions) as to make cavitation a possibility with most viscous liquids and particularly so with any such liquid which has been not specially purified.

THEORETICAL

Consider two completely immersed circular disks of radius R arranged parallel and moving apart under constant force (Fig. 1).

The equation of motion in the liquid of viscosity η is $d^2u/dz^2 = -\frac{dp}{dr}/\eta$, where dp/dr is the pressure gradient at r, z . Integrating and inserting

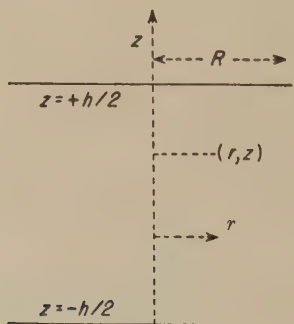


FIG. 1.

TABLE I

$h, \text{cm.}$	10^{-1}	10^{-2}	10^{-3}	10^{-4}
$U\eta$	$1.06 \times 10^{+3}$	1.06	1.06×10^{-3}	1.06×10^{-6}

boundary conditions, $u = 0$ at $z = \pm h/2$,

$$\eta u = \frac{1}{2} \cdot \frac{dp}{dr} [h^2/4 - z^2].$$

The volume of the cylindrical space of radius r between the plates is increasing at a rate given by $\pi r^2 U$, where U is the velocity of plate separation. This equals the volume of liquid flowing into the space, i.e.,

$$2\pi r \int_{-h/2}^{+h/2} u \cdot dz = \pi r^2 U,$$

whence

$$U = \frac{1}{6} \cdot \frac{h^3}{\eta} \cdot \frac{1}{r} \cdot \frac{dp}{dr}. \quad [1]$$

To calculate the hydrostatic pressure at a distance r we rewrite the equation and integrate, obtaining

$$P_r = 3\eta U r^2 / h^3 + I,$$

where I is a constant of integration.

We now assume that the pressure at $r = R$ is atmospheric, A ; hence

$$A - P_r = 3\eta U / h^3 [R^2 - r^2]. \quad [2]$$

Equation [2] predicts that at a sufficiently high value of the product $U\eta$, negative values can be assumed by P_r . Table I shows for a few selected values of h the values of $U\eta$ corresponding to zero pressure in the center of the liquid, calculated for disks of area 1 sq. cm. For $A = 1 \text{ atm.} = 1.013 \times 10^6 \text{ dynes/cm.}^2$ $U\eta = 1.06 \times 10^6 h^3$.

These figures suggest for liquids normally of interest in tacky adhesion (where the viscosities are usually greater than 100 poises) that the conditions for negative pressures are readily attainable and probably often encountered in experiments of the Stefan type.

Except under special conditions of experiment, liquids normally do not sustain large tensions and even where precautions have been taken to remove likely disturbing influences, rupture occurs at negative pressures of a few hundred atmospheres only. For example, Vincent and Simmonds (7) reported rupture in a mineral oil at -119 atm. and the lowest recorded pressure of which we are aware is -300 atm. for water observed by Trevenna (8). Thus generally for ordinary liquids we might expect to realize experimentally a limiting force for separation of Stefan disks so soon as $U\eta$ reaches values of an order given by Eq. [2]. It follows

also that there will be an upper limit to the amount of work which can be expended in separation.

The Limiting Force of Separation

The force to separate the disks is given by

$$\begin{aligned} F &= 2\pi \int_0^R r(A - P_r)dr \\ &= 6\pi\eta U/h^3 \int_0^R (R^2 - r^2)r \cdot dr \quad (\text{from [2]}) \\ &= \frac{3}{2} \pi\eta UR^4/h^3. \end{aligned}$$

Taking the limit of realizable pressure in the liquid at zero atmosphere, then it follows from [2] that the critical values of velocity U_0 and separation h_0 are related by

$$A = 3\eta U_0 R^2/h_0^3,$$

and therefore the force is given by

$$F_0 = \pi \frac{R^2}{2} \cdot A \quad [3]$$

EXPERIMENTAL PROCEDURE

If cavitation occurs the theory predicts an upper limit to the force required to separate two surfaces adhering by means of a thin layer of liquid. This limiting force was shown to be independent of the liquid and the film thickness. A simple experiment was designed to test this aspect of the theory, and although it is to be regarded as a preliminary to a more refined study, the results obtained are sufficiently informative to warrant publication.

The method was to stick two smooth-ended brass cylinders (diameter 1.1 cm.) together with liquid, and with the uppermost cylinder suspended from a spring, the lower one was loaded with weights. By observing the extension of the supporting spring at rupture of the joint, the force acting across the liquid film is determined. The principle of the method is illustrated schematically in Fig. 2. Observation of the limits of extension of the spring was made by means of a nonreturn pointer attached to the scale actuated by the moving-spring pointer. Between each loading the surfaces of the cylinders were cleaned and fresh samples of liquid smeared on them. Considerable care was taken to avoid entrapped air bubbles during this operation. The two surfaces were then wrung together whereby excess liquid was squeezed out to remain as a rib around the joint of the cylinders.

The characteristics of the spring were such that a static load of 1000 g. produced an extension of 17 mm., and its period of oscillation in seconds was given by the relation $T = 8.37 \times 10^{-3} \sqrt{M + 67}$, where M is the load in grams. Thus with the masses used in these experiments (200–4000 g.) the period of oscillation varied from 0.15 to 0.54 sec.

The liquids investigated were medicinal paraffin B.P. ($\eta = 1.2$ poises approx.), a solution of an ethylene glycol ester of rosin (Flexolin) in linseed oil ($\eta = 75$ poises approx.), a glycerol phthalic anhydride condensation product (Paralac 15) ($\eta = 2200$ poises approx.), all of which are Newtonian in behavior, finally a letterpress ink consisting principally of a

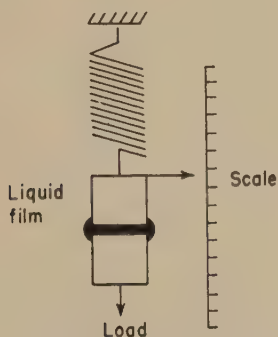


FIG. 2.

dispersion of 16% carbon black and 12% bronze blue in heat-treated linseed oil of viscosity 25 poises—a non-Newtonian substance.

RESULTS

The results are summarized in Table II (and plotted in Fig. 3). The load in grams is shown in col. 2, the mean dynamic extension of the spring (in millimeters) with its standard error calculated from the range ($\pm w/n$) in col. 3, and the confidence limits calculated for a significance level of 95% from $\pm w \cdot t_{0.05}/n$ in col. 4. The calibration data for the spring, obtained by tying the two cylinders together and loading is also shown in Table II. Occasionally with low loads the spring extended first to its maximum value as shown by the nonreturn pointer and returned to its equilibrium extension before rupture. In these cases the minimum (equilibrium) values are given in col. 5.

The spring extensions as a function of load in the absence of a liquid joint are shown as the two full lines (Fig. 3), the upper for dynamic and the lower for static loading. The data for the various liquid joints are shown as vertical lines representing the 95% probability range, and for

TABLE II

Liquid	Load g.	Mean \pm S.E.M. ^a	Confidence limits for 95% ^b	Mean minimum extension (static loading)
Paraffin $\eta = 1.2$ poises	100	2.8 ± 0.16	± 0.72	1.5
	200	6.0		4.2
	500	15.2 ± 0.66	± 2.8	
	1000	23.4 ± 1.7	± 4.7	
	1500	20.4 ± 2.8	± 7.6	
	1870	13.9 ± 2.7	± 7.5	
Flexolin solution $\eta = 75$ poises	200	5.0		3.5
	300	8.0		5.5
	500	14.3 ± 0.25	± 3.2	8.3
	700	19.5		11.0
	1000	24.5 ± 1.0	± 6.4	
	1500	24.2 ± 2.7	± 7.9	
	1870	24		
Paralac 15 $\eta = 2200$ poises	200	5 ± 1.0	± 12.7	4.5
	500	13 ± 1.0	± 3.2	9.5
	1000	24.5 ± 1.0	± 3.2	
	1200	24		
	1500	29.8 ± 3.0	± 8.3	
	1870	36 ± 1.2	± 3.3	
	2370	30 ± 0.66	± 2.8	
	2870	29.7 ± 3.0	± 12.9	
Ink	200	6.1 ± 0.5	± 2.2	4.0
	500	14.6 ± 0.91	± 2.4	
	1000	18.5 ± 2.5	± 8.0	
	1500	25.3 ± 2.0	± 5.6	
	1870	22.5 ± 1.4	± 3.8	
	2870	25.9 ± 2.9	± 8.1	
	3370	26.4 ± 1.6	± 5.1	
Spring calibration	200	5.0		
	500	15.5		8.0
	1000	32.2		17.0
	1500	46.5		25.5
	1870	56.0		31.5

^a S.E.M. (standard error of mean) calculated from w/n .

^b Confidence limits calculated from (S.E.M.) $t_{0.05}$.

clarity are displaced slightly along the abscissa. The few static values observed conform to the static calibration line for the spring.

The theory outlined leads to the conclusion that limiting forces of an order given by Eq. [3] represent the maximum which any liquid film can sustain before rupture. It follows that as the load on the spring is

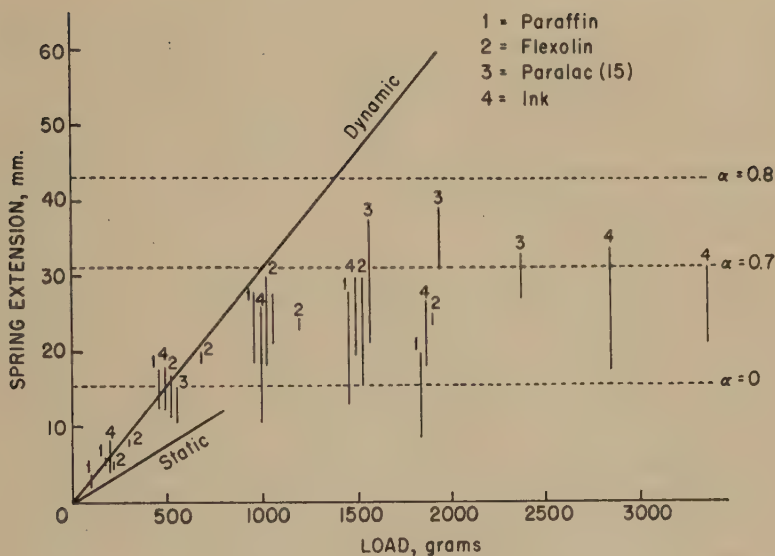


FIG. 3.

increased beyond a certain value the spring should exhibit constant extension, that is to say, the extensions as a function of load should depart radically from the near proportionality with load normally observed when a spring is so loaded. Whether an observed limiting load is in fact due to failure of the liquid or is the natural consequence of separation according to Stefan's law will depend on the various time factors involved in the experiment.

A spring loaded as in these experiments will oscillate about a mean extended position with period T . The maximum extension, twice the static value, will be attained approximately $T/2$ sec. after loading. If the load applied is M , the period T will be given by the relation in the previous section. Following Stefan, the time of separation of two plates under a load M is given by $t = \frac{3\pi R^4}{4Mg} \left(\frac{1}{h_1^2} - \frac{1}{h_2^2} \right)$ which for $h_2 \gg h_1$ reduces to $t = 2.2 \times 10^{-4} \eta / M h_1^2$ sec. for the system used. The value of h_1 is not known but values of t may be estimated for order of magnitude by taking likely values as in Table III.

TABLE III

Viscosity Separation, cm. Load, M , g.	$\eta = 1$		$\eta = 2000$	
	0.01 sec. $\times 10^3$	0.001 sec.	0.01 sec.	0.001 sec./ 10^2
500	4.4	0.44	8.8	8.8
1000	2.2	0.22	4.4	4.4
4000	0.55	0.055	1.1	1.1

Values of t estimated in this way are likely to be minimum values because the load on the plates during the extension of the spring is not M but that consistent with the spring extension at any instant.

If $t > T/2$ then the spring will reach the maximum extension before the plates separate, and since a nonreturn pointer is used on the scale the recorded extension will be that given by the line corresponding to dynamic loading in Fig. 3.

If $t < T/2$ the weight will cease to extend the spring before the full extension is reached and lower values will be recorded.

Reference to Table II shows that at low loads, even with paraffin, the time of separation was greater than $T/2$ and was long enough for the equilibrium extension of the spring to be observed. From Table III it would seem that the appropriate thickness to satisfy this observation would be about 0.001 cm. At this thickness all the liquids tested give separation times greater than the $T/2$ appropriate to the load with the exception of paraffin. In this case the separation time decreases so rapidly that the spring would not extend very much and could explain the tendency to give low values obtained at high loads. For all the other liquids the time of separation would be more than ample for the spring to reach its maximum extension. The fact that at loads greater than 700 g. the maximum extension was not reached is an indication that the separation was not completed according to Stefan's equation. The results summarized in Fig. 3 show clearly how they diverge from the values expected from the spring characteristics shown by the upper full line for dynamic loading.

It has been argued that provided cavitation occurs in the liquid as soon as the pressure at the center of the disks becomes zero, the force for separation is given by Eq. [3]. With this as the lower limit and assuming $A = 1 \text{ atm.} = 1.013 \times 10^6 \text{ dynes/cm.}^2$ and $g = 981 \text{ cm./sec./sec.}$, it follows that for the area of joint used in the experiments (diameter 1.1 cm., area 0.95 cm.²) the lowest limit to be expected is 491 g. which under dynamic conditions corresponds to a spring extension of 15.5 mm. This theoretical lower limit is shown in Fig. 3 as a dotted horizontal line. It is obvious that the majority of the data lies above this line.

The separation of the brass cylinder takes place under accelerating conditions and it is probable that the velocity of separation will increase beyond the critical value before cavitation sets in. Should this be so then clearly the region over which cavitation is possible will extend outward from the center. It follows from Eq. [2] that for zero pressure in the liquid to exist at some distance away from the center, say αR the velocity of separation U_α is related to the critical value for central zero pressure U_0 through $U_\alpha/U_0 = 1/(1 - \alpha^2)$. Thus, for example, a 33% increase in velocity will shift the point of zero pressure a distance equal to one half the radius of the disk.

In the experiments reported, the conditions of acceleration are not highly dependent on the liquid, being determined more by the large loads and spring so that with liquids requiring a low critical velocity it is more probable that it will be exceeded and cavitation will be extended over large regions of the film. For example, at a film thickness of 10^{-2} cm. Table I shows for paraffin ($\eta = 1.2$ poises) a critical velocity of 0.89 cm./sec., while for Paralac 15 ($\eta = 2200$ poises) a velocity of 5.0×10^{-4} cm./sec.

The limiting force for cavitation to occur at a distance R from the center is given from Eq. [3] by

$$F_{\alpha} = \frac{\pi R^2}{2} \frac{A}{1 - \alpha^2}$$

which for $\alpha = 0.7$ is approximately double the lower limiting force. This limit is shown in terms of spring extension by the dotted horizontal line in Fig. 3. The limit corresponding to $\alpha = 0.8$ is also shown.

It is apparent that all the data are accommodated between the lower limit and that corresponding to $\alpha = 0.8$.

Yet another consideration is the effect of viscosity of the liquid on the rate of bubble expansion, and this could affect the measured extension of the spring.

These considerations are believed to account for the variations observed in the extension at a given load and the tendency to extension in excess of the lower limit.

DISCUSSION

The conclusion that the forces operating in tacky adhesion are subject to upper limits imposed by cavitation has an important bearing on theories of tackiness² in liquids. It is clear for Newtonian liquids (at least as viscous as 2200 poises) that provided the critical values of force or velocity are not exceeded, Stefan's law is relevant for an experimental definition of tackiness (due account being taken of the necessity for complete wetting of the adherends) and that the decisive liquid property is viscosity. Under conditions in excess of these critical values, forces observed will be very much smaller than predicted by the law; furthermore, differences between liquids will be reduced and dependent only on those properties of liquids which determine rate of cavitation in such a way that factors retarding cavitation might be expected to increase tackiness. We have here an analogy with the strength of solids where the actual cohesive strength always falls short of the theoretical because of the presence of discontinuities or singularities in the system. Bikerman (9) has indeed empha-

² We make here a clear distinction between tackiness as measured and the subjective quantity assessed by craftsmen, which may well be different in concept.

sized this principle in a general way as a necessary concept for the understanding of adhesion in relation to laws for an idealized system.

The inability of Stefan's law to account for observed energies involved in film "rupture" has been discussed principally by Voet (6) who, finding energies of a very much smaller order than so predicted, concludes that rapid film separation involves viscoelastic rupture. It is necessary to recall that Voet proceeds to argue from observations on the separations involved when a cylinder rolls over a plane covered with a film of liquid but, accepting the validity of deductions from such systems for the movement apart of parallel plates, his low energies may well be accounted for by the existence of forces limited by cavitation.

We have indeed shown that similar limits to hydrodynamical theory exist for a system consisting of a liquid film confined between two rollers rotating externally to one another and have directly observed cavitation in the liquid film at regions near the line of closest approach. Further, the discontinuities so produced lead to the filamentation of the liquid at the meniscus, a phenomenon studied by L. H. Sjodahl and quoted by Voet in illustration (Fig. 1 of his paper) (6). Voet describes this process of filamentation as preceding film splitting, from which point of view he argues in favor of an elastic response by the filaments of liquid.

In the experiments described earlier we made no direct observation of cavitation, but we are of the opinion that the fernlike patterns which are so characteristic of the rapid separation of two surfaces confining a liquid film is a manifestation of it. De Bruyne refers to these characteristic patterns too (2), but of particular interest are the observations of Kumler (10) on the figures in thin layers of various greases and oils arising from the release of pressure after squeezing the materials between glass plates. His conclusions were briefly:

- (a) The figures were holes in the grease or oil and the holes had curved sides.
- (b) The cavities were completely enclosed by the film material, i.e., there was no solid boundary.
- (c) They could be formed in the absence of entrapped air.
- (d) The only property observed to have any bearing on their formation was that of "stickiness" and viscosity.

All these observations are consistent with cavitation.

Finally, although we must emphasize that our studies have been limited to three liquids known to be Newtonian, and one dispersion characterized by a yield value and a plastic viscosity, we have no evidence which would require us to invoke either special properties of liquids or any modification in the behavior of liquids in thin films as a means of understanding tackiness in such materials.

REFERENCES

1. STEFAN, J., *Sitzber. Akad. Wiss. Wien, Math.-naturwiss Kl., Abt. II*, **69**, 713-35 (1874). (Quoted by J. J. Bikerman in Ref. 9.)
2. BRUYNE, N. A. DE, *Paint Technol.* **9**, 106, 217 (1944).
3. BIKERMAN, J. J., *J. Soc. Chem. Ind.* (London) **62**, 41 (1943).
4. REYNOLDS, O., *Phil. Trans.* **177**, 190 (1886).
5. GREEN, H., *Ind. Eng. Chem., Anal. Ed.* **13**, 632 (1941).
6. VOET, A., AND GEFFKEN, C. F., *Ind. Eng. Chem.* **43**, 1614 (1951).
7. VINCENT AND SIMMONDS, *Proc. Phys. Soc.* (London), 380 (1943).
8. TREVENNA, *Proc. Phys. Soc.* (London) **65**, 46 (1952).
9. BIKERMAN, J. J., *J. Colloid Sci.* **2**, 163 (1947).
10. KUMLER, W. D., *J. Phys. Chem.* **44**, (5), 612 (1940).

DIELECTRIC PROPERTIES OF THE SYSTEM POLYVINYL CHLORIDE-DIMETHYLTHIANTHRENE

Edwin R. Fitzgerald¹ and Robert F. Miller

B. F. Goodrich Company Research Center, Brecksville, Ohio

Received July 15, 1952

INTRODUCTION

Variations of complex dielectric constant with temperature and frequency have been previously adduced for polyvinyl chloride combined with varying amounts of plasticizers (1-3), but there have been no reported studies of systems in which dielectric data for plasticizer concentrations from 0 to 100% are given. A method is described here for determining the dielectric behavior of liquids, gels, and solids of the type encountered in plasticizer-polymer systems over the entire range of plasticizer concentration. A combination dielectric cell with plane, parallel electrodes and a guard ring suitable for use over a frequency range of 15 to 15,000 cycles/sec. at temperatures from -100 to $+150^{\circ}\text{C}$. has been constructed and used for dielectric measurements on the system polyvinyl chloride-dimethylthianthrene, where the physical state of the sample (at room temperature) varies from that of a hard, glassy material such as molded polyvinyl chloride to that of an oily liquid like the plasticizer. Included in the range of sample types are those of a gelatinous nature obtained by dissolving small amounts (up to 15% by volume) of polymer in plasticizer.

The variation of complex dielectric constant with frequency and temperature for polyvinyl chloride (PVC) combined with dimethylthianthrene (DMT) is given for 0, 10, 20, 40, 60, 80, and 100% PVC by volume, and the apparent activation energy for dipole rotation is determined as a function of concentration. The activation energy of viscous flow is compared with that for dipole rotation for the pure solvent (DMT). A consideration of the electrical properties of the pure solvent and low-polymer concentrations indicates that the generally accepted view as to the role of the polymer constituent in such systems, predicated on the basis of the incomplete data previously available, must be revised.

¹ Present address: Department of Physics, Pennsylvania State College, State College, Pa.

DETERMINATION OF COMPLEX DIELECTRIC CONSTANT

Alternating current measurements of dielectric constant (ϵ') and loss factor (ϵ'') were made by means of a Schering bridge circuit using a General Electric² No. 716177 alternating-current bridge with its amplifier modified to secure an extended frequency range from 15 to 15,000 cycles/sec. A General Radio³ type 713A beat-frequency oscillator was used to supply 100 v. across the bridge. The oscillator drift after a 2-hr. warm-up was not appreciable during the measuring time, and presented frequency values can be considered correct to within 1%. The calibration of the oscillator dial was relied upon at frequencies above 60 cycles/sec., but frequencies below this were set by comparison with a 60-cycle source on a cathode-ray oscilloscope. The standard air capacitor was a Leeds and Northrup⁴ No. 1160 cylindrical air capacitor with a rated value of $101.0 \pm 0.2\%$ $\mu\mu\text{f}$. For samples where the tangent of the loss-factor angle is greater than one, the Schering bridge is converted into a resistance bridge by rearranging the bridge and introducing a standard resistance of 100,000 ohms.

In order to check the accuracy and precision of the bridges, a set of readings was taken on "standard" samples made up of an air capacitor and a noninductive resistance in parallel. A General Radio type 722 variable air capacitor was used to provide a range of capacitances, and a number of noninductive resistances were combined with different settings of the capacitor to "synthesize" a series of standard samples having the same range of values as encountered in actual sample testing. On the basis of tests of this kind it was established that values of capacitance (and hence ϵ') can be determined to an accuracy of 0.5% or 1 $\mu\mu\text{f}$, whichever is larger, and values of $\tan \delta$ ($\tan \delta = \epsilon''/\epsilon'$) to within 2% or 0.0002 whichever is larger in the frequency range 15 to 15,000 cycles/sec. Bridge readings at balance were found to be reproducible, by the same and different observers, to within 0.5%.

Description of Dielectric Cell

Samples of the material to be tested are introduced into the bridge circuit by means of the combination dielectric cell (for liquids and solids) shown in cross section in Fig. 1. The cell has a disk-shaped electrode surrounded by a guard ring and insulated from it by a backing plate, and a parallel unguarded electrode which is recessed to hold liquid dielectrics or fitted with a plate and spring to press solid samples against the upper electrodes (Fig. 1). Metal parts are of hard rolled steel, chrome plated; all electrode surfaces and parts which contact liquid or solid samples are

² General Electric Company, Schenectady, New York.

³ General Radio Company, Cambridge, Massachusetts.

⁴ Leeds and Northrup Company, Philadelphia, Pennsylvania.

gold plated. The cell is sealed by gaskets between guard ring and guarded electrode cover plate, and unguarded electrode and guard ring. This makes possible the immersion of the cell in a constant-temperature bath of a high electrical resistivity liquid, e.g., mineral oil or hexane, at high and low temperatures. The sealing gasket in addition to being a good insulator must be resistant to the bath liquids and capable of withstanding large temperature variations. Gaskets made from either Hycar OR or Neoprene FR stocks have been used with success; these have a fairly short life and

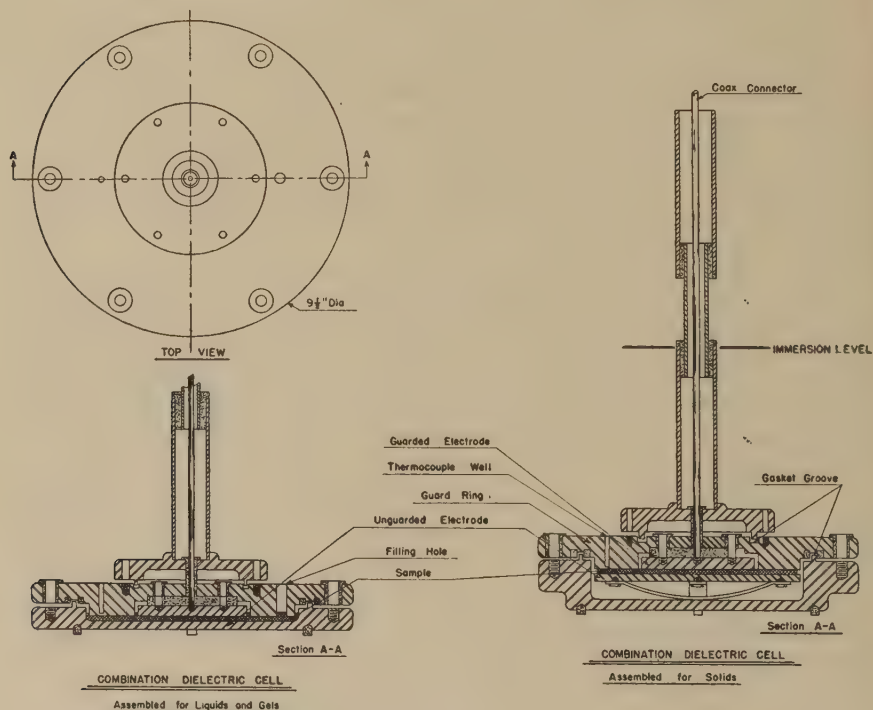


FIG. 1. Combination dielectric cell.

must be replaced after three or four complete temperature cycles have been traversed.

The guarded electrode lead is brought out of the cell in a shielding tube made up of three parts, overlapped, and joined with thermal insulators to prevent undue heat exchange between the cell and surroundings. The electrical connection between insulated sections is maintained by a thin wire, while the overlapping insures adequate electrostatic shielding. Tests with surface thermocouples indicated that the upper section of this tube remained essentially at room temperature with the immersed end at -80°C . This has the advantage of preventing moisture condensation

across the insulation between guard ring and guarded electrode when the cell is at low temperatures.

For liquid or gel-like samples the cell is assembled as shown in Fig. 2. The guarded electrode has a diameter of 3.500 ± 0.001 in. while the inside diameter of the guard ring is 3.580 ± 0.001 in.; thus the cross-sectional area of the sample is defined by these dimensions to within 2%. The thickness of liquid or gel tested depends on the thickness of the outer sealing gasket and is usually about 0.1 in. The inside diameter of the bottom electrode is 6.380 in. so that about 60 ml. of sample is required.

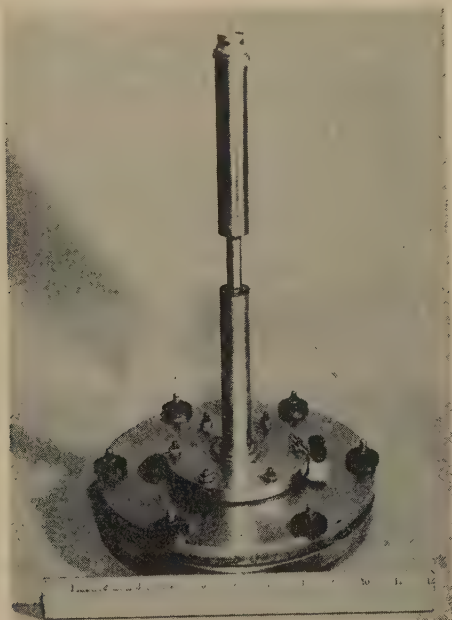


FIG. 2. Combination dielectric cell assembled for immersion in constant-temperature bath.

The actual cell coefficient, A/h , (cross-sectional area/thickness) is determined by measuring the capacitance of the assembled cell when empty, taking the dielectric constant of air as 1.000. The dielectric is then poured into the filling hole. For extremely viscous liquids or low polymer concentrations in solvent this is facilitated by heating the sample and cell before filling. This procedure for determining cell coefficient was checked using hexane and benzene as standard samples; the observed agreement with the standard values of dielectric constants for these materials⁵ was within 1%.

⁵ International Annual Table of Constants and Numerical Data Vol. XI, pp. 22-29. McGraw-Hill, New York, N. Y. Values at 200 kc. and 25°C.; for hexane, $\epsilon' = 1.878$; for benzene, $\epsilon' = 2.272$.

Values of cell coefficient (from 200 to 230 cm.) found in this way are virtually independent of cell dimensional changes due to temperature variation. This was verified by measuring the capacitance of the empty cell at 20-degree intervals from -70 to $+150^{\circ}\text{C}$. No significant change in capacitance (i.e., greater than 1%) was found, indicating at the same time that no anomalous effects peculiar to the cell itself occur as the temperature is varied over this range.

For solid samples the alternate unguarded electrode housing is used as shown in Fig. 1. A conducting layer of colloidal graphite (Aquadag) painted on the sample surface insures good electrode contact. A ruling compass is used to form a guard gap of about 0.05 in., and the diameter of the painted electrode is measured on the sample with a rule to 0.01 in.; for a usual diameter of about 3.50 in. this results in an accuracy in area determination of $\pm 1.5\%$. The sample thickness is measured with a micrometer to 0.001 in. and the average of five measurements spaced over the electrode area used; even with molded samples, thickness measurements made in this way are not more accurate than 2% (for a sample thickness of about 0.10 in.). The coefficient for solid samples is thus known to about 3%.

Temperature Control and Measurement

Two bath liquids are used to secure the desired properties of high resistivity and low viscosity: hexane from -100 to 20°C . and mineral oil from 20 to $+150^{\circ}\text{C}$. Cooling is accomplished by means of four narrow cold pockets around the edge of the bath and two auxiliary pockets inserted above the cell after it is in position. These pockets are filled with Dry Ice and hexane for temperatures from 25 to -75°C . or with liquid nitrogen for temperatures from -75 to -100°C . Four 250-w. knife-blade immersion heaters are used for heating and temperature regulation. Two of the heaters are operated on-off by a direct-current relay activated by a De Khotinsky type bimetallic thermoregulator placed in the bath. The number of cold pockets used varies from one at room temperature to four at -100°C ., while the additional pockets are used for rapid decreases between temperature steps. The bath liquid is stirred by a 1/25 horsepower induction motor operating at 1200 r.p.m. The temperature distribution in the region surrounding the cell was investigated at -50 , $+25$, and $+70^{\circ}\text{C}$., and the temperature differential was found to be less than 0.5°C .; the variation at any one spot was less than $\pm 0.25^{\circ}\text{C}$., and because of the large mass (12 kg.) of steel surrounding the thin sheet of sample, the temperature variation within the sample is probably less than 0.1°C .

A thermocouple is sealed into the guard ring with the junction at the bottom of a hole drilled to within 0.050 in. of the inner face of the electrode

to insure a temperature measurement close to the sample. This temperature is taken as that of the sample after sufficient time for establishment of thermal equilibrium has elapsed. For 5-degree steps, equilibrium is essentially established about 15 min. after the cell temperature becomes constant, when the electrode arrangement for liquids is used. For the solid-sample electrode arrangement, because of the poor thermal contact to the electrode housing furnished by the unguarded electrode spring, from 45 to 60 min. is required for the same degree of equilibrium.

An iron-constantan thermocouple (wire diameter 0.0201 in.) is used with a Leeds and Northrup temperature indicator potentiometer system to read temperatures to $\pm 0.25^\circ\text{C}$.

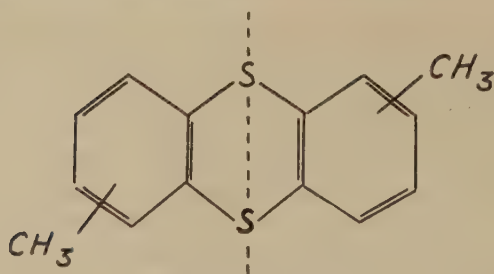
MATERIALS STUDIED

Polyvinyl chloride (PVC) of weight-average molecular weight 63,000 ± 3000 was combined with dimethylthianthrene (DMT) to form the series of samples used for electrical testing. PVC in the form of a fine powder was mixed with liquid DMT on a mill and then molded under pressure into disks about 6 in. in diameter and 0.1 in. thick. A small amount of lead silicate was added as an electrical stabilizer to combine with any hydrogen chloride formed from the PVC during molding or testing at high temperatures. This reduces the ionic (sometimes called the direct-current) conductivity, since the lead silicate combines with any HCl present to give lead chloride of much less mobility than HCl. Without stabilizer the free charge or ionic conductivity may completely obscure the conductivity due to bound charge or dipole loss in which our chief interest lies. Samples containing from 20 to 100% by volume of PVC can be made in this way.

Gels are formed by dissolving PVC powder in DMT at 130 to 150°C . to give, at room temperature, a clear nonflowing sample of gel-like consistency. Up to 15% by volume of PVC has been combined with DMT by this means. The gel is poured into the dielectric cell while hot, as previously mentioned, although it is possible to form a sample disk by molding as was done with "solid" samples.

The dimethylthianthrene used contained as its chief impurity from 1 to 3% ditolyl sulfide. However, a redistilled sample was also measured and values of complex dielectric constant were identical, except at high temperatures where the redistilled sample had a lower loss factor due to decreased ionic conductivity. A sample of DMT with 1% lead silicate added was also tested.

The dipole moment of DMT arises from the molecule not being flat but folded back along the dotted line shown below—corresponding to a valence angle for sulfur between 110 and 120° (4).



Dimethylthianthrene

Polarization measurements on DMT in dilute solution of benzene at 25°C. (8) give a value of 1.62×10^{-18} e.s.u. for the dipole moment of DMT, which compares with values of 1.54 and 1.57×10^{-18} e.s.u. reported for thianthrene.⁶

TABLE I

Compounding Data and Description of Electrical Samples

Sample No.	E1	E2	E3	E4	E5	E6	E7	
							^a	^b
Per cent PVC by volume ^b	100	80	60	40	20	10	0	0
Description at 25°C.	Hard glassy solid	Stiff solid	Leathery solid	Rubbery solid	Soft rubbery	Soft gel	Viscous liquid	Viscous liquid
Density g./cc. at 25°C.	1.40	1.41	1.38	1.34	1.31	1.25	1.22	1.22
<i>Parts by weight</i>								
Polyvinyl chloride	100	100	100	100	100	100	0	0
Dimethylthianthrene	0	22.4	60.0	137	387	785	100	100
Lead silicate	0.5	6.02	8.06	12.3	26.0	14.3	0	0
Molding or heating time, min.	5	15	15	15	15	15	Not molded or heated before testing	
Molding temp., °C.	160	160	160	160	160	150		

^a Redistilled.

^b Calculated assuming additivity of component volumes as verified from measurements on density.

⁶ Bennet and Glasstone (4) give 1.54×10^{-18} e.s.u. for the dipole moment of thianthrene measured in carbon tetrachloride solution at 24.9°C., while LeFevre (5) lists a value of 1.57×10^{-18} e.s.u. measured in benzene solution. Assuming that the methyl groups contribute little to the moment, measurements on thianthrene and DMT should be roughly equivalent, and the moment of DMT somewhat larger, as is, indeed, the case.

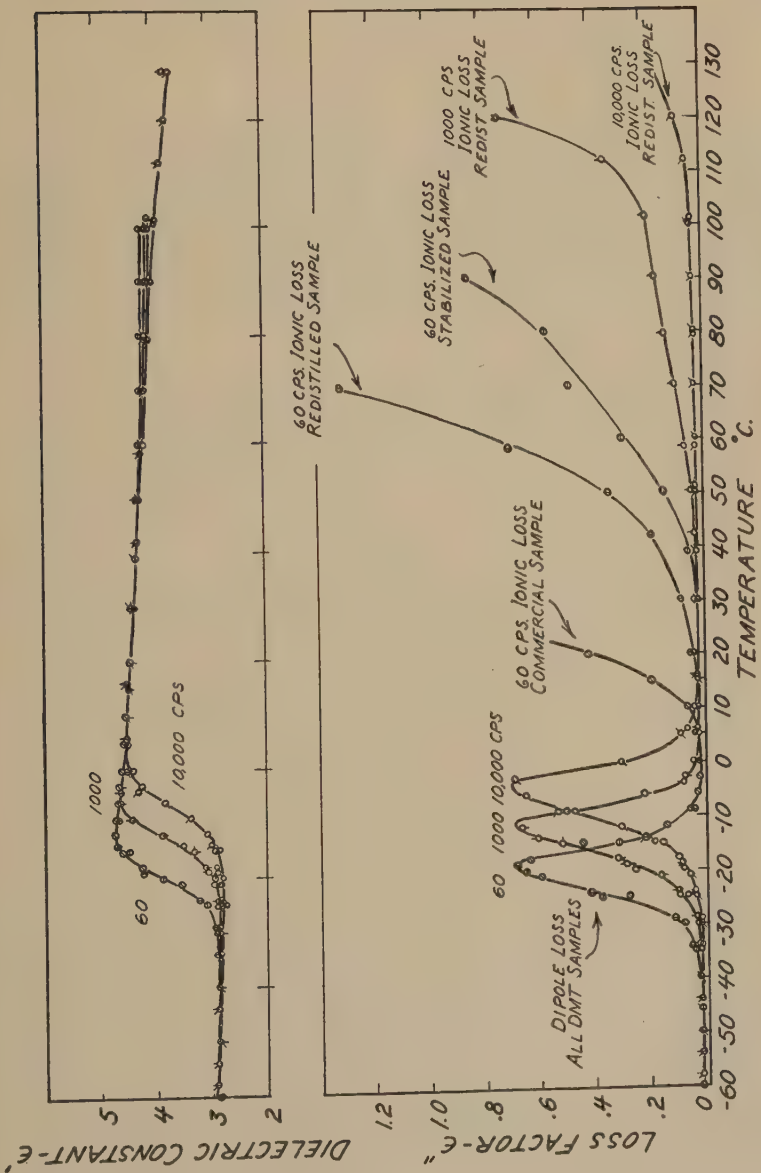


Fig. 3. Variation of complex dielectric constant with temperature for dimethylthianthrene at 60, 1000, and 10,000 cycles/sec.

Since the presence of even a small amount of water will cause changes in electrical properties, all solid samples were dried over phosphorus pentoxide for one month or longer after the Aquadag electrode coating was applied. A summary of compounding data and description of the samples is given in Table I.

EXPERIMENTAL RESULTS

The temperature variation of the complex dielectric constant, ($\epsilon^* = \epsilon' - i\epsilon''$), for dimethylthianthrene at 60, 1000, and 10,000 cycles/sec. is shown in Fig. 3. Data on three samples of DMT are given, including a sample with 1% lead silicate added and a redistilled sample. As can be seen from the values of ϵ'' for the redistilled sample, the rise in loss factor

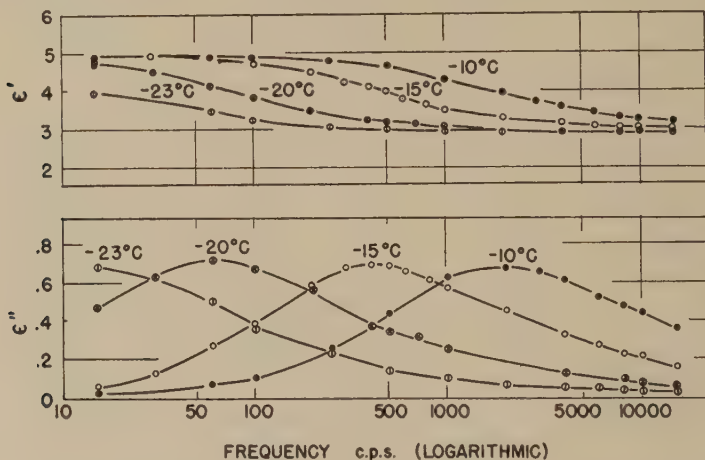


FIG. 4. Variation of complex dielectric constant with frequency for dimethylthianthrene.

at high temperatures is not characteristic of the material but of the impurities in it and cannot be taken as a fixed property of the material. On the other hand, the locations of the loss-factor maxima and increases in dielectric constant are exactly reproducible for different samples so long as the ionic losses are negligible in the region where the maxima occur.

By selecting temperatures in the correct region (Fig. 3) it is possible to obtain frequency dispersion within the audiofrequency range as is demonstrated in Fig. 4. From the shape of the dispersion curves obtained, qualitative agreement with the Debye theory for polar molecules is evident. The loss-factor maxima occur at the temperatures or frequencies where the slopes of the corresponding dielectric-constant curves are the greatest, and while the observed loss-factor maxima are less than the values predicted by the single relaxation time Debye theory, this type

TABLE II

Summary of Frequency and Temperature Dispersion Data for Dimethylthianthrene^a

f_m cycles/sec.	T_m °C.	ϵ_0'	ϵ_{∞}'	$\frac{\epsilon_0' + \epsilon_{\infty}'}{2}$	ϵ_m' , obs.	$\frac{\epsilon_0' - \epsilon_{\infty}'}{2}$	ϵ_m'' , obs.	$\frac{\epsilon_m''(\text{obs.})}{\epsilon_m''}$	Type of dispersion
56	-20	4.85	2.93	3.89	4.20	0.960	0.710	0.740	Frequency
60	-19	4.80	2.91	3.85	4.11	0.945	0.700	0.741	Temperature
380	-15	4.85	2.90	3.88	4.20	0.975	0.700	0.718	Frequency
1000	-11	4.72	2.84	3.78	4.00	0.940	0.700	0.745	Temperature
1800	-10	4.85	2.90	3.88	4.05	0.975	0.690	0.708	Frequency
10,000	-4	4.70	2.80	3.75	4.00	0.950	0.700	0.737	Temperature

^a f_m and T_m are the relaxation frequency and relaxation temperature, respectively, i.e., corresponding to a maximum value of observed loss factor.

ϵ_0' = low frequency or high temperature value of dielectric constant before dispersion.

ϵ_{∞}' = high frequency or low temperature value of dielectric constant after dispersion.

$(\epsilon_0' + \epsilon_{\infty}')/2$ = predicted value of ϵ_m' for Debye theory assuming a single mean

relaxation time $\tau_m = \frac{1}{\omega_m}$.

$(\epsilon_0' - \epsilon_{\infty}')/2$ = predicted value of loss factor maximum ϵ_m'' for Debye theory assuming as above.

of discrepancy has been accounted for in terms of molecular association and a distribution of relaxation times. A summary of temperature and frequency dispersion data for DMT is given in Table II.

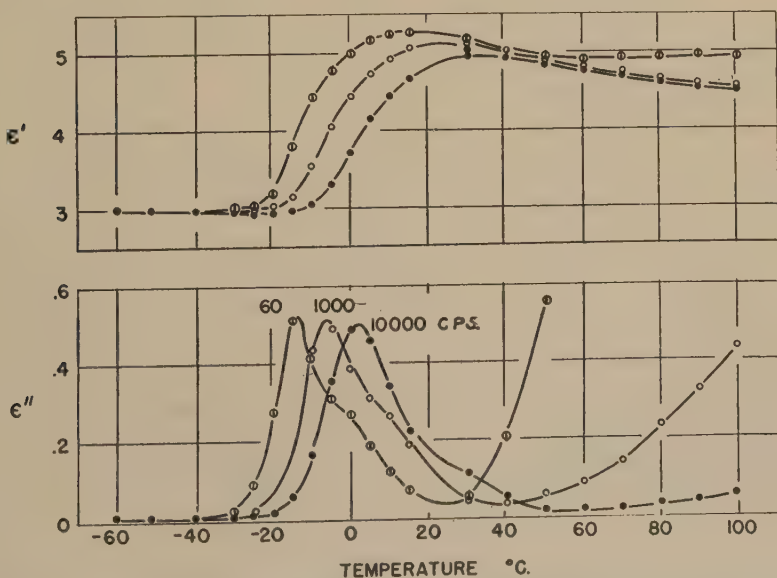


FIG. 5. Variation of complex dielectric constant with temperature for a polyvinyl chloride (PVC)-dimethylthianthrene gel (10% PVC by volume).

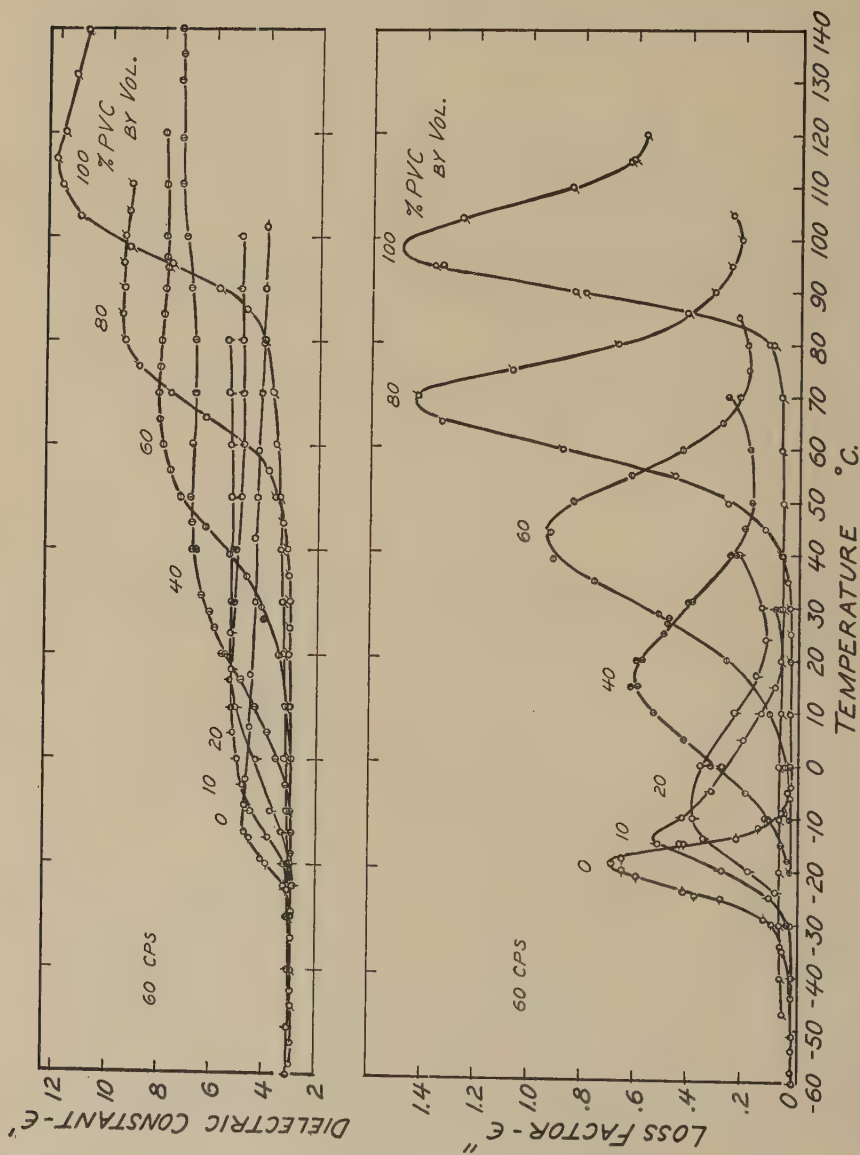


Fig 6. Variation of complex dielectric constant with temperature for 7 polyvinyl chloride-dimethylthianthrene concentrations at 60 cycles/sec.

The variation of complex dielectric constant with temperature for a gel (10% PVC by volume) stabilized with lead silicate is shown in Fig. 5. The dielectric constant increase observed at high temperatures may be a result of Maxwell-Wagner polarization (9) due to the lead silicate or polarization at the electrodes. This rise of dielectric constant beyond the region of dispersion due to dipole rotation has been observed for other compounds, notably tricresyl phosphate (8) and various rubbers (7,8). The rise occurs in a region of high ionic loss or when an added constituent is present. DMT showed this effect when stabilized with lead silicate or when its ionic losses were high; a redistilled sample did not.

TABLE III

Summary of Loss-Factor Maxima (ϵ_m'') and Corresponding Values of Dielectric Constant (ϵ_m') for Stabilized Polyvinyl Chloride-Dimethylthianthrene Systems

Sample No.	E1	E2	E3	E4	E5	E6	E7
Per cent PVC by volume	100	80	60	40	20	10	0
60 cycles/sec.							
Relaxation temperature, $T_m, ^\circ\text{C.}$	97	69	44	17	-6.0	-15	-19
ϵ_m' (obs.)	8.8	7.3	6.2	5.1	3.9	3.9	4.1
ϵ_m'' (obs.)	1.50	1.43	0.940	0.60	0.38	0.525	0.700
1000 cycles/sec.							
$T_m, ^\circ\text{C.}$	105	79	54.	30.	5.0	-7.0	-11
ϵ_m' (obs.)	9.0	7.3	5.9	5.2	4.2	3.90	4.00
ϵ_m'' (obs.)	1.50	1.43	0.980	0.645	0.38	0.52	0.700
10,000 cycles/sec.							
$T_m, ^\circ\text{C.}$	113	88	63	39	14	2.0	-4.0
ϵ_m' (obs.)	8.2	6.7	5.7	5.1	4.1	3.9	4.0
ϵ_m'' (obs.)	1.56	1.42	1.00	0.70	0.38	0.50	0.700

The appearance of a hump on the high-temperature or low-frequency side of the loss-factor curve for this gel indicates the presence of some PVC which has not been dissolved to the same extent as the bulk of the material.

The variation of complex dielectric constant with temperature at 60, 1000, and 10,000 cycles/sec. for samples containing 0, 10, 20, 40, 60, 80, and 100% PVC by volume is given in Figs. 6-8. As the percentage of polymer is increased, the temperature of the loss-factor maximum at any frequency shifts regularly from that of DMT to that of PVC. A summary of dielectric data for all samples at 60, 1000, and 10,000 cycles/sec. is given in Table III.

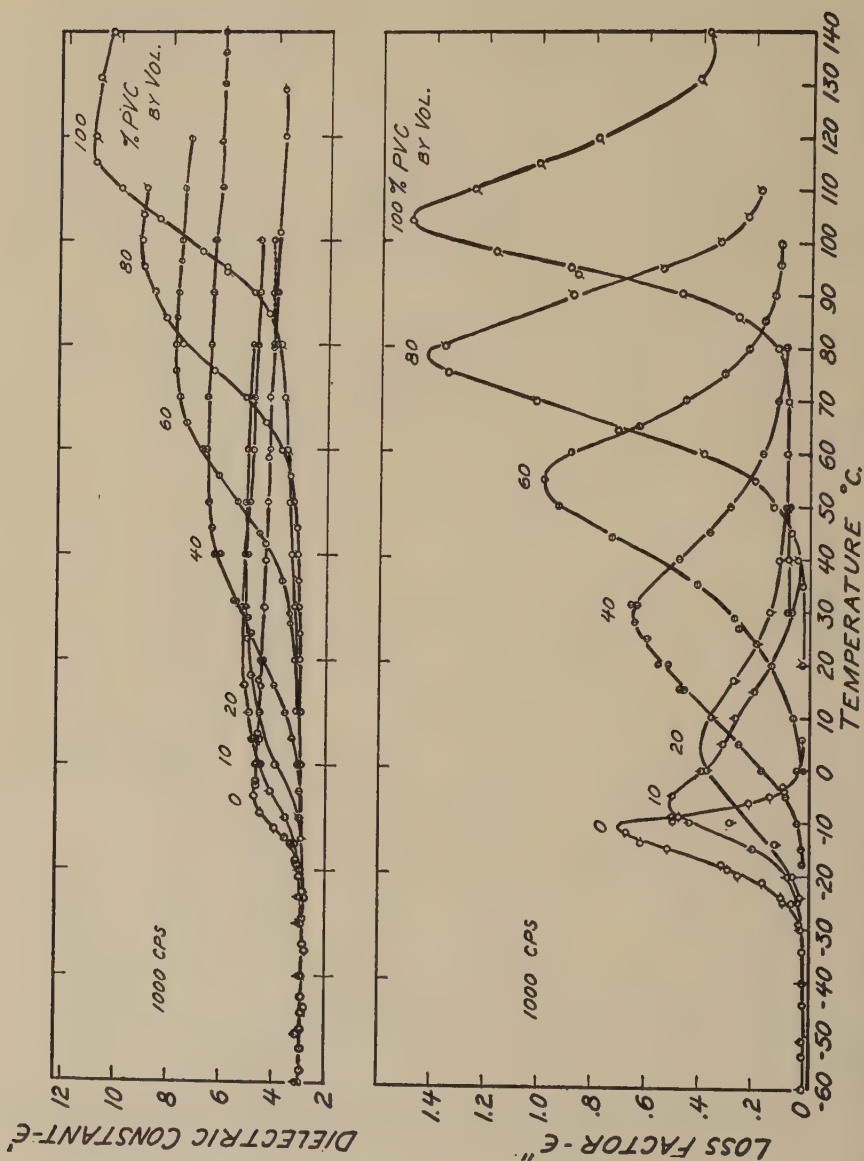


Fig. 7. Variation of complex dielectric constant with temperature for 7 polyvinyl chloride-dimethylthianthrene concentrations at 1000 cycles/sec.

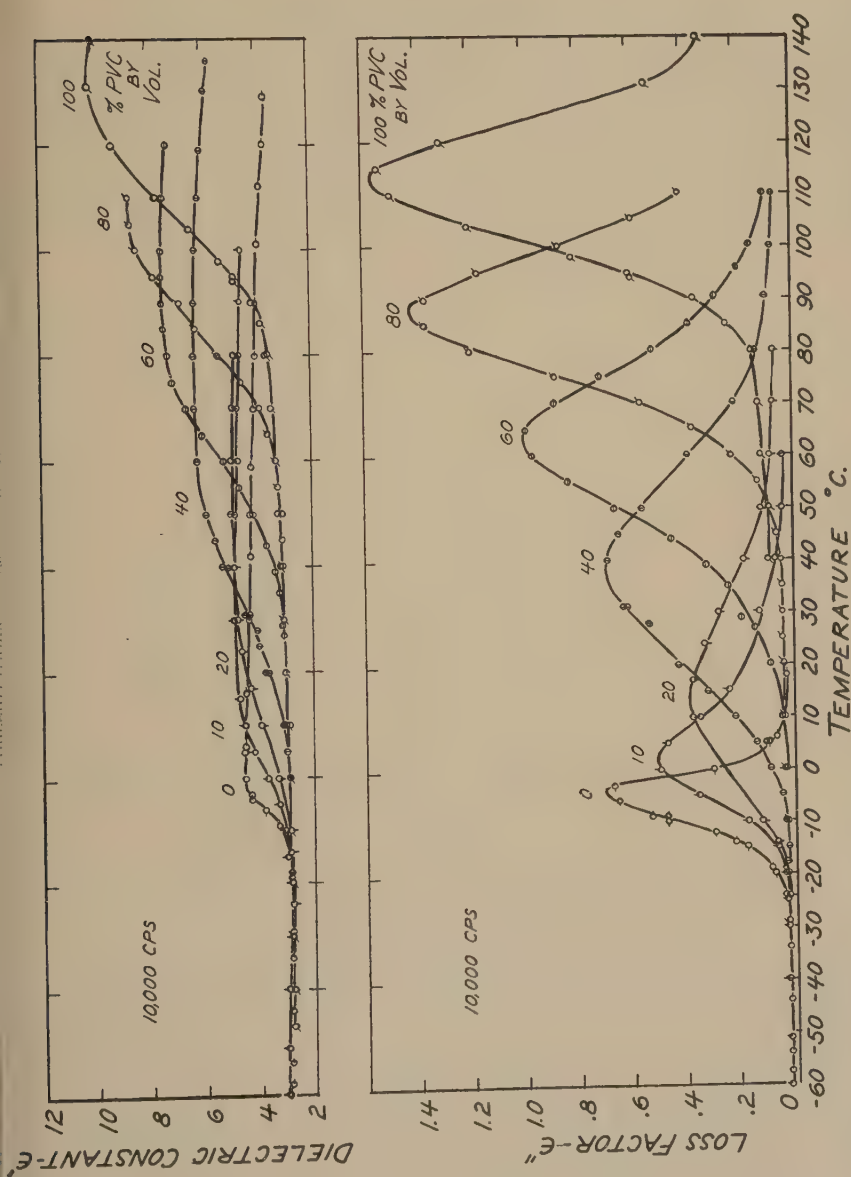


Fig. 8. Variation of complex dielectric constant with temperature for 7 polyvinyl chloride-dimethylthianthrene concentrations at 10,000 cycles/sec.

From the data presented it is evident that changes in polymer concentration, temperature, or frequency can be used to produce roughly equivalent effects on the complex-dielectric-constant curves. For temperature dispersion, an increase in frequency or PVC concentration shifts the region of high-energy loss to higher temperatures, while for frequency dispersion an increase in temperature or decrease in PVC concentration shifts the region of maximum energy loss to lower frequencies. In addition, the regular shift of loss-factor maxima at a given frequency as the PVC volume concentration increases corresponds to a regular change in the

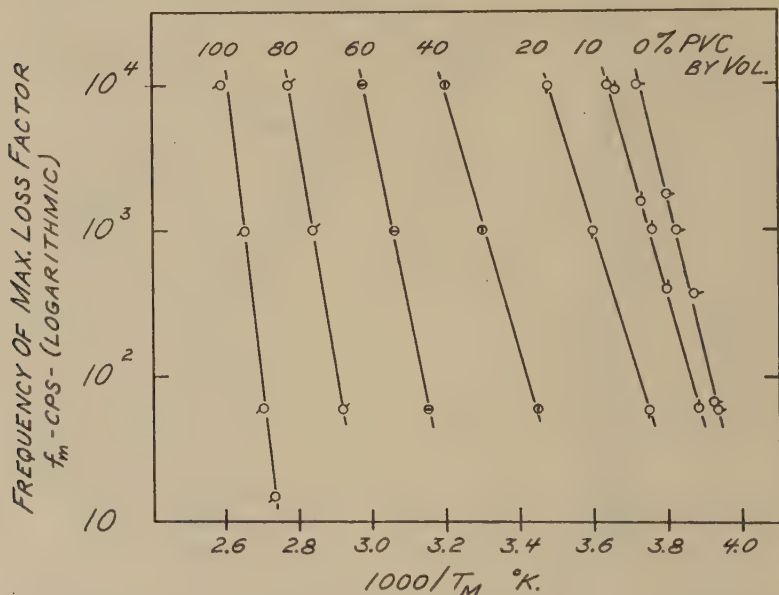


FIG. 9. Frequencies of loss factor maxima vs. reciprocal absolute temperatures for 7 polyvinyl chloride-dimethylthianthrene concentrations.

static mechanical properties of the samples [cf. Table I and (1)], which indicates some prospect of correlation between mechanical and electrical properties.

ACTIVATION ENERGIES OF DIPOLE ROTATION AND VISCOUS FLOW

The apparent molar activation energy Q_D needed to permit dipole rotation in an electric field can be found from the relation (1,13) $T\tau = \tau_0 \exp Q_D/RT$ where τ is the relaxation time of the dipole molecule, T is the absolute temperature in °K., R is the molar gas constant, and τ_0 is a constant. In the PVC-DMT system a distribution of relaxation times is undoubtedly present so that the original meaning of τ will not be valid.

However, using a mean relaxation time τ_m defined as $\tau_m = (\frac{1}{2})\pi f_m$ where f_m is the frequency at which the loss-factor maximum occurs, we have $-\ln f_m = Q_D/RT_m + \ln 2\pi \tau_0/T_m$. For a small range in the variation of T_m , the expression $\ln 2\pi \tau_0/T_m$ can be considered a constant, so that by plotting $\ln f_m$ vs. $1/T_m$ values of Q_D can be obtained. The results of plotting $\log f_m$ vs. $1/T_m$ for each PVC concentration are given in Fig. 9.

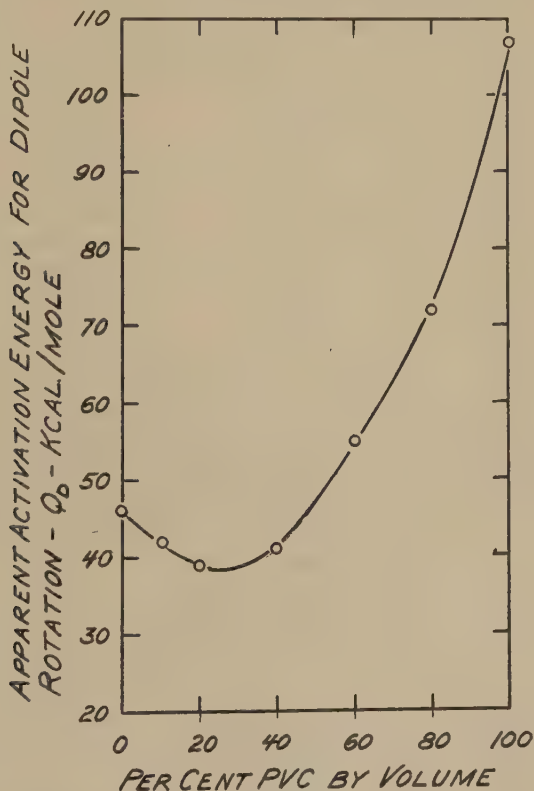


FIG. 10. Apparent activation energy of dipole rotation as a function of polymer concentration for the system polyvinyl chloride (PVC)-dimethylthianthrene (DMT).

The straight lines indicate constant values of Q_D within the observed temperature ranges. The variation of Q_D with concentration is shown in Fig. 10 and Table IV, where it can be seen that a minimum value of 39 kcal./mole occurs at a concentration of 20% PVC by volume, with values of 46 and 108 kcal./mole found for DMT and PVC, respectively.

The steady-flow viscosity, η , of DMT can be expressed approximately by the equation $\eta = A \exp (Q_V/RT)$ where Q_V is the apparent molar activation energy, and A is a constant. Thus by plotting $\ln \eta$ vs. $1/T$,

values of Q_V can be obtained. Actually this plot does not give a straight line over a wide temperature range, however, indicating a temperature dependence of the apparent activation energy. Values of η and Q_V at various temperatures from -5 to $+40^\circ\text{C.}$ are given in Table V.⁷ From Tables IV and V it is clear that the apparent activation energy for dipole

TABLE IV
Apparent Activation Energy Q_D of Dipole Rotation for Polyvinyl Chloride-Dimethylthianthrene Systems

% PVC by vol.	Q_D kcal./mole	Temperature range $^\circ\text{C.}$
0	46	-19 to -4
10	42	-15 to 2
20	39	-6 to 14
40	41	17 to 39
60	55	44 to 63
80	72	69 to 88
100	108	97 to 113

rotation of DMT (46 kcal./mole) is the same as that for viscous flow within the same temperature range. This indicates that the size of the moving unit in dipole rotation is the same as that for viscous flow. This also has been found to be true for di-2-ethylhexylphthalate ($Q_V = Q_D = 24$ kcal./mole at -50 to -70°C.) and tricresyl phosphate ($Q_V = Q_D$

TABLE V
Viscosity, η , and Apparent Activation Energy of Viscous Flow, Q_V , for Dimethylthianthrene

T $^\circ\text{C.}$	η poises	Q_V kcal./mole
40	1.45	18
30	4.40	25
21	18.0	31
13	100	35
5	560	38
-3	5500	46
-5	12,000	—

$= 40$ kcal./mole at -4 to -20°C.) (8). All three of the liquids cited here solidify into hard, glassy states as the temperature is lowered (due to the presence of isomers), and the activation energies given are at temperatures where solidification is nearly complete.

⁷ As previously reported by Fitzgerald and Miller (8), the viscosity of DMT was determined independently by means of a rotating-cylinder method (1-1000 poises) and a falling-ball method (10-10,000 poises). The results of both methods agree well in the region where they overlap.

DISCUSSION

Molecular Association in DMT

The summary of temperature and frequency dispersion data given for DMT in Table II indicates the presence of more than one relaxation time for this liquid. The observed values of loss-factor maxima, for example, are about 0.74 of the values predicted by Debye's single relaxation time theory, and the corresponding values of dielectric constant are greater than those predicted by the theory. The basis for this disagreement may be found in the intermolecular forces existing in a polar liquid. The molecules exert forces of mutual attraction and repulsion and will tend to take up positions relative to each other such that the potential energy of any combination is a minimum. This tendency toward association will be opposed by thermal motion, and hence can be expected to be greatest at low temperatures such as encountered here. The type and degree of association at any temperature depend upon the shape of the DMT molecule and the location and magnitude of its permanent moment; in most cases the molecules evidently tend to orient in such a way that the average resultant moment of the associated groups is less than the moment of an isolated molecule.

The presence of associated groups of molecules clearly can lead to a number of relaxation times corresponding to varying degrees of interaction and result in a broader dispersion of complex dielectric constant than that expected from a single relaxation time. At the same time it should be mentioned that the presence of an apparent distribution of relaxation times does not necessarily guarantee that association exists.

Comparison of Dispersion at Different Concentrations

Previous work on dielectric properties of plasticized polar polymers has been confined largely to the concentration range 50 to 100% polymer with the result that the true importance of a polar plasticizer in determining dielectric dispersion has been overlooked. Thus the view is widely held that the addition of plasticizer merely lowers the internal viscosity (supposedly related to macroscopic viscosity) in a polymer and shifts the dispersion region at a given frequency to lower temperatures. The dielectric loss is attributed to rotation of chain segments resulting from the presence of dipoles in the polymer chain. The distribution of relaxation times, deduced from a broadening of the temperature- or frequency-dispersion curves, is likewise cited as a consequence solely of the structure of the long-chain polymer, in which the length of the cooperating segment necessary to allow orientation of a dipole will vary over a wide range of values.

There can be no doubt that the addition of plasticizer shifts the dispersion regions, as found by Davies, Miller, and Busse (1), by Fuoss

(2), by Mead, Tichenor, and Fuoss (3), and as also shown in Figs. 6-8 and Fig. 11. However, this shift is certainly not the only result, *nor the most important consequence* of adding a polar plasticizer. Remarkable changes take place in the loss factor-temperature curves which change from high, steep to low, broad, and then back to high, steep curves as the percentage of polymer varies from 0 to 100%. Thus while previous investigators (1-3, and 10) have been concerned with the effect of plasticizer on the dipole action of the polymer because of the particular concentration region which they studied, we could just as well imagine ourselves confined by experimental limitations to the range 0 to 20% polymer.

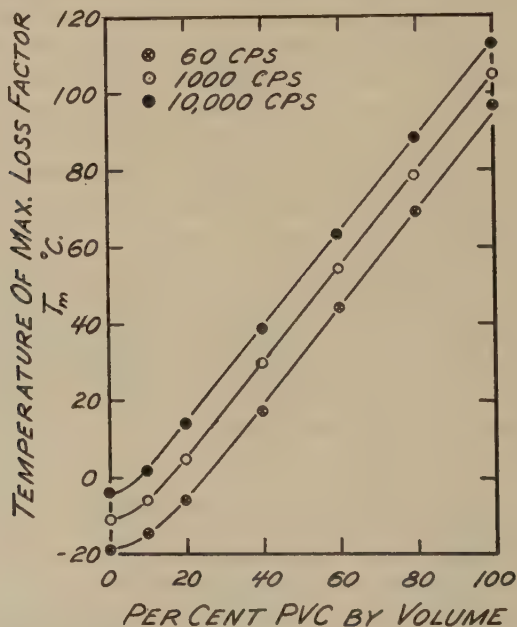


FIG. 11. Temperatures of loss-factor maxima vs. polymer concentration for the system polyvinyl chloride-dimethylthianthrene.

The polymer then would be thought of as a thickening or stiffening agent for the plasticizer. It could also be logically concluded that the observed dielectric dispersion (Figs. 6-8) is due to the dipole moment of the plasticizer molecule, and that the addition of polymer, by increasing internal viscosity, merely shifts the region of dispersion to higher temperatures or lower frequencies. The same type of behavior as indicated in Figs. 6-8 has also been observed for PVC plasticized with di-2-ethylhexylphthalate (DOP) as reported by Miller *et al.* (11). In this case the importance of the plasticizer is even more pronounced. At 1000 cycles/sec., for example, the loss-factor maximum for DOP is 1.57 at -60°C . (compared

to 1.50 at 105°C. for PVC), and the lowest, broadest loss factor-temperature curve occurs at a concentration of 50% by volume of PVC. In this system, therefore, we could study the concentration range 0 to 50% by volume of polymer and again conclude that the dielectric loss results from the presence of the DOP molecule; the addition of polymer serves only to increase the internal viscosity of the plasticizer and shift the dispersion region. Similar behavior for PVC plasticized with tricresyl phosphate (TCP) is found if the complex dielectric constant-temperature curves of Davies, Miller, and Busse (1) are combined with the temperature dispersion for TCP alone as reported by Fitzgerald and Miller (8). The loss-factor maximum of TCP is 2.17 at -37°C. and 1000 cycles/sec.; again a substantial contribution to the dielectric loss can be expected from the plasticizer molecule.

In measurements on PVC plasticized with TCP made at 40°C. and 20 to 10,000 cycles/sec., Fuoss (10) lists for 100% TCP values of ϵ' only, and at 60, 500, and 1000 cycles/sec. where (at 40°C.) no dispersion exists. In a later publication Mead, Tichenor, and Fuoss (3) recognize that polar plasticizers at 40 and 60°C. may have an absorption peak at much higher frequencies, but apparently do not consider that this region of dispersion can be shifted to lower frequencies by the addition of polymer. However, they do consider that a shift of the dispersion region in the polymer is accomplished through the action of the plasticizer in decreasing the internal viscosity of the PVC.

In view of the data shown in Figs. 6-8 and that cited above, it must be concluded that the dielectric dispersion observed in a polar polymer combined with a polar plasticizer is the result of dipole rotation of chain segments of the polymer *together with dipole rotation of the plasticizer molecules*. The relative importance of each type of rotation will depend on the relative concentration of polymer in plasticizer, but the dielectric dispersion will not, in general, be a result of only dipole rotation of segments of the polymer chain. It certainly cannot be argued, for example, that the chief contributions to the dipole loss for a 10% PVC gel arise from the PVC molecule (cf. Figs. 6-8).

If we accept the view of Fuoss and Mead (2,3,10) that plasticization is essentially a separation of chain molecules by the plasticizer molecules, we can account for the observed dielectric behavior of polar polymers combined with polar plasticizers as follows: (a) The plasticizer decreases the internal viscosity of the polymer and shifts the dispersion region to lower temperatures or higher frequencies; (b) at the same time the polymer increases the internal viscosity of the plasticizer and shifts *its* dispersion region to higher temperatures or lower frequencies; and (c) the observed dispersion results from the dipole rotation of polar segments of the polymer chain (e.g., C-Cl for PVC) and the dipole rotation of the plasticizer

molecule, where each rotation is influenced by mutual interaction of polymer and plasticizer. This explanation may not be complete. For a polar polymer and nonpolar plasticizer, (a) is a plausible explanation, as is (b) for a nonpolar polymer with a polar plasticizer;⁸ but when a polar plasticizer and polar polymer are combined there is a possibility that a very strong association between plasticizer and polymer may occur as a result of dipole-dipole interaction. If this association is pronounced, rotation of an associated plasticizer chain segment complex may take place in addition to individual orientations of segments of the chain and the plasticizer molecules. This view is supported by the recent work of Curtis *et al.* (12) who find that in the microwave region the critical wavelength (wavelength at which ϵ'' is a maximum) of a pure polar liquid may be longer than that in a nonpolar solvent (such as viscous paraffin oil) even when the viscosity of the solution is the same as that of the pure liquid. This is attributed to hindrance of molecular rotation by dipole-dipole interaction which is present to a greater extent in the pure liquid than in the solution. Strong dipole-dipole coupling between plasticizer and polymer may likewise be an important factor in determining the dispersion region in plasticized polymers.

ACKNOWLEDGMENTS

Discussions with J. M. Davies, D. L. Loughborough, and W. L. Davidson were of great value during the course of this work. We are grateful to the B. F. Goodrich Company for permission to publish the results of this investigation.

SUMMARY

A method is described for determining the dielectric behavior of liquids, gels, and solids at frequencies from 15 to 15,000 cycles/sec., and over a temperature range from -100 to $+150^{\circ}\text{C}$. Included in the range of sample types are those of a gelatinous nature obtained by dissolving small amounts of polymer in plasticizer. The variation of complex dielectric constant with frequency and temperature for polyvinyl chloride (PVC) combined with dimethylthianthrene (DMT) is given for 0, 10, 20, 40, 60, 80, and 100% PVC by volume, and the apparent activation energy for dipole rotation is determined as a function of concentration.

A consideration of the dielectric dispersion of the pure plasticizer and low polymer concentrations indicates that a polar plasticizer may contribute materially to the loss mechanism in a plasticized polymer. In view of the data presented here, and that cited for PVC plasticized with di-2-ethylhexylphthalate and tricresyl phosphate, it is concluded that

⁸ While these explanations seem plausible, the term "internal viscosity" is somewhat ambiguous unless it can be definitely related to some measurable quantity such as macroscopic viscosity.

the dielectric dispersion observed in a polar polymer combined with a polar plasticizer is a result of *dipole rotation of the plasticizer molecule together with dipole rotation of chain segments of the polymer*. The relative importance of each type of rotation will depend on the relative concentrations of polymer and plasticizer and the magnitude of their permanent dipole moments. Dipole-dipole coupling between plasticizer and polymer may also play a part in determining the dielectric dispersion in plasticized polymers.

REFERENCES

1. DAVIES, J. M., MILLER, R. F., AND BUSSE, W. F., *J. Am. Chem. Soc.* **63**, 361 (1941).
2. FUOSS, R. M., *J. Am. Chem. Soc.* **63**, 2410 (1941); *ibid.* **63**, 378 (1941).
3. MEAD, D. J., TICHENOR, R. L., AND FUOSS, R. M., *J. Am. Chem. Soc.* **64**, 283 (1942).
4. BENNET, G. M., AND GLASSTONE, S., *J. Chem. Soc.* **1934**, 128.
5. LEFEVRE, R. J. W., *Dipole Moments*, pp. 70-74. Methuen and Co., Ltd., London, 1938.
6. DEBYE, P., *Polar Molecules*. Dover Publications, New York, 1945.
7. CARTER, W. C., MAGAT, M., SCHNEIDER, W. C., AND SMYTH, C. P., *Trans. Faraday Soc.* **42A**, 213 (1946).
8. FITZGERALD, E. R., AND MILLER, R. F., presented at the 305th Meeting of the American Physical Society at Washington, D. C., April 27, 1951.
9. YAGER, W. A., *Physics* **7**, 434 (1936).
10. FUOSS, R. M., *J. Am. Chem. Soc.* **61**, 2334 (1939).
11. MILLER, R. F., FITZGERALD, E. R., DAVIES, J. M., AND SEARS, W. C., presented at the 312th Meeting of the American Physical Society, Columbus, Ohio, March 20, 1952.
12. CURTIS, A. J., MCGEER, P. L., RATHMANN, G. B., AND SMYTH, C. P., *J. Am. Chem. Soc.* **74**, 644 (1952).
13. KAUZMAN, W., *Revs. Modern Phys.* **14**, 12 (1942).

FORCE-AREA CURVES OF SURFACE FILMS OF SOLUBLE SURFACE-ACTIVE AGENTS

Arthur L. Meader, Jr. and Dean W. Criddle

California Research Corporation, Richmond, California

Received December 1, 1952

ABSTRACT

The Langmuir film balance was used to determine the cross-sectional areas of a number of surface-active agents of different molecular structure. Use of 95% saturated sodium nitrate solution as a substrate effectively prevented films of the detergents from dissolving, and enabled reproducible force-area curves to be obtained even on the most soluble compounds. Results were expressed in terms of compressibility of the films and area occupied per molecule at a given film pressure.

INTRODUCTION

In the study of the fundamental physicochemical properties of surface-active agents, it is desirable to know the dimensions of the molecules, the manner in which they pack together in surface films, and something about the attractive and repulsive forces between the individual molecules in the films. This information is useful in identification of unknown materials and in partial determination of structure. In addition, when sufficient knowledge of this sort is obtained, it should be possible to obtain from it a better insight into the actual performance properties of surface-active agents, such as foam stability, emulsifying power, wetting ability, and possibly detergency. The Langmuir film balance offers a convenient method of determining cross-sectional areas of molecules of materials insoluble in water, such as fatty acids, barium soaps, long-chain alcohols, and the like (1), but until recently has not been applied to the study of very soluble materials, such as detergents and wetting agents.

Some of the sodium 1-alkylbenzene sulfonates have a very low solubility in cold water, of the order of a thousandth of a per cent, and consequently, might be expected to form monomolecular films on water. These did, indeed, form films on distilled water, but the films were very unstable and dissolved rapidly on even a small amount of compression. Brady (2) has recently described a method for overcoming this difficulty by using a salt solution as the substrate instead of water. Because of the instability of the films, he used an automatic machine for advancing the barrier and a recording device for indicating the film pressure; he was thereby able to obtain reproducible force-area curves. The substrates

he used were sodium chloride solutions of concentrations from 0.5% to 16.6% and dilute calcium and barium chloride solutions. His films on barium chloride solutions, however, were too fragile to give reproducible results.

A 6% sodium chloride solution as substrate was first tried in our work. This gave films which were only slightly more stable than those on distilled water. Saturated sodium chloride solution gave more stable films from which reproducible force-area curves could be obtained. However, these films were unstable at film pressures above 30 dynes/cm., and the saturated sodium chloride solution was difficult to work with because of its tendency to crystallize on the barriers and the edges of the trough. In order to increase the concentration of ions in solution and thereby decrease still further the solubility of the surface-active agents, the substrate was changed to sodium nitrate solution. Sodium nitrate is considerably more soluble than sodium chloride, so a higher concentration could be obtained without going to a saturated solution, thus avoiding the problem of crystallization. A 95% saturated solution of sodium nitrate was found to be a satisfactory substrate upon which reasonably stable films were formed. Even the most soluble detergents, such as sodium 6-dodecylbenzene sulfonate and sodium polypropylene benzene sulfonate, formed films which were relatively stable at compressions up to 30 dynes/cm. Accordingly, 95% saturated sodium nitrate was selected as the substrate for all future work, and force-area diagrams were obtained on a large number of compounds.

EXPERIMENTAL

Apparatus

The apparatus used was a Cenco Hydrophil Balance without modifications. The torsion wire had a sensitivity of 3.26°/dyne/cm.

Materials

All of the detergents used in this study were 100% active material which had been either synthesized or purified in these laboratories. All of the 1-alkylbenzene sulfonates, the 2-dodecylbenzene sulfonate, and the 2-methyl-2-hendecylbenzene sulfonate were recrystallized from 95% ethanol. The 6-dodecylbenzene sulfonate was recrystallized from acetone. The above materials are believed to be principally *para*-sulfonates. The polypropylene benzene sulfonate and the two samples of dodecylbenzene sulfonate prepared from 1-dodecene were not recrystallized, but were deoiled by extraction with isopentane of their solutions in 70% aqueous ethanol. They probably consisted of a mixture of *ortho*- and *para*-isomers. The alkylphenyl polyglycol ether was a laboratory preparation from commercial alkylphenol; the isopropyl alcohol was Baker's c.p. It was

necessary to test each bottle of isopropyl alcohol before using by spreading a few drops on the substrate and moving the barriers together. If it showed an appreciable film pressure, the bottle was rejected.

Procedure

Samples of the detergents were dried to constant weight *in vacuo* at 100°C., and portions were weighed out and made up to 10^{-3} *M* solutions with 50% aqueous isopropyl alcohol. Aliquots of the solutions (except the non-ionic) were titrated with a standard solution of cetylpyridinium bromide according to the procedure of Epton (3) as a check on the molarity.

After the detergent had been spread on the surface, the film was allowed to age for 1 min. The movable barrier was then advanced 1 or 2 cm. at a time and the film pressure noted each time. When the film became

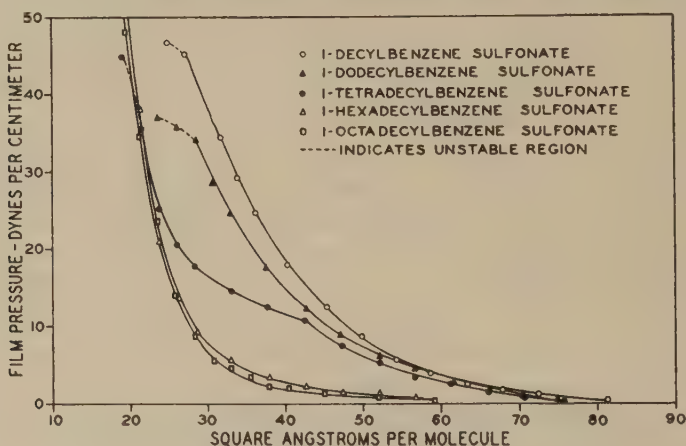


FIG. 1.

unstable or collapsed, the readings were discontinued. The readings obtained on compression were reproducible, but hysteresis occurred on expansion, and the same readings could not be obtained until the film was compressed again to the point at which it had been allowed to expand. At film pressures above about 30 dynes/cm. many of the films started to become unstable; i.e., they showed a decrease in film pressure with time at a constant area. At pressures of about 45–50 dynes/cm. most of the films either collapsed entirely or spilled over the sides of the trough. In this procedure, measurements were made every 15 to 20 sec., and the entire run was made in about 5 min. Duplicate runs on the same compound could be reproduced to within ± 3 dynes/cm. at the smallest areas, if this procedure was followed.

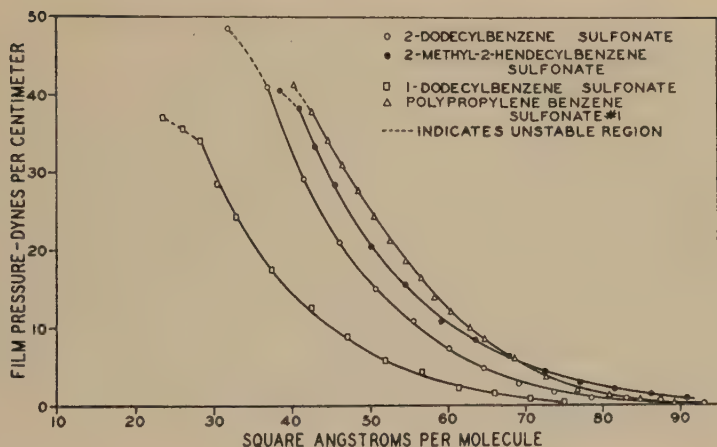


FIG. 2.

All of the experiments were performed at room temperature ($24 \pm 2^\circ\text{C}$).

RESULTS AND DISCUSSION

The first series to be run in the present work was a number of sodium 1-alkylbenzene sulfonates having side chains from C_{10} to C_{18} . The set of curves obtained, shown in Fig. 1, followed a logical sequence, with the area per molecule decreasing to a limit of about 20 \AA^2 as the molecular weight of the compounds increased. This is due to the fact that the electrostatic repulsive force between the head groups is the same for each compound, but the attractive van de Waals' forces between the hydrocarbon tails increase with the length of the chain. The over-all result is

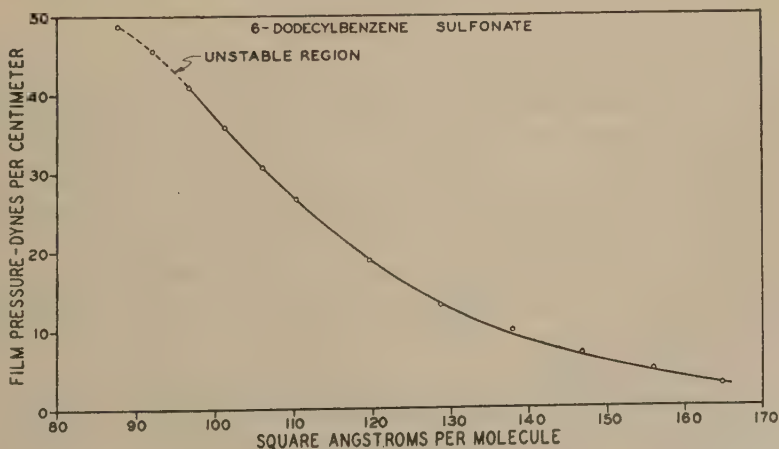


FIG. 3.

that the longer-chain compounds are more easily compressed to their limiting value than are the short-chain compounds.

Figures 2 and 3 show the effect of structure on the force-area curves of compounds of the same molecular weight. The sodium 1-dodecylbenzene sulfonate was found to have the smallest area per molecule of the compounds in this group. Sodium 2-dodecylbenzene sulfonate, sodium 2-methyl-2-hendecylbenzene sulfonate, and sodium polypropylene benzene sulfonate were grouped closely, with the area increasing in the order named. Sodium 6-dodecylbenzene sulfonate, with the hydrophilic group in the center of the hydrocarbon chain, occupied a much larger area. This set of curves gives some indication of the structure of the polypropylene side chain, showing that the benzene sulfonate group is located near, but not at, the end of the hydrocarbon chain.

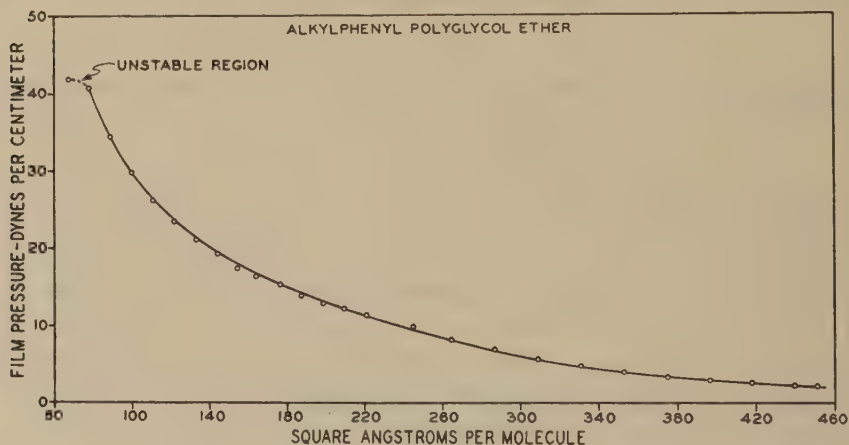


FIG. 4.

All of the detergents so far described have been of the anionic type, and all have been sodium salts, so that, in addition to the salting-out effect of electrolytes, there has been a common-ion effect tending to reduce still further the solubility of the detergent in the substrate. The non-ionic detergent, an alkylphenyl polyglycol ether, is not subject to the common-ion effect. Nevertheless, it formed a film on the sodium nitrate solution very similar to the others except that it had a very large area per molecule and an extremely high rate of change of area with pressure (Fig. 4). This material showed a small but significant film pressure at an area per molecule well over 400 \AA^2 , but on compression to a pressure of 25 dynes/cm., the area was decreased to 116 \AA^2 . This indicates that at low film pressures the hydrophilic polyethylene oxide portion of the molecule lies flat on the surface and that, as compression takes

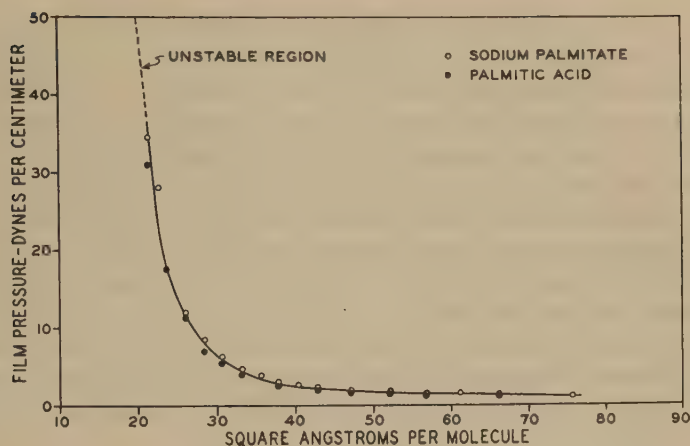


FIG. 5.

place, more and more of it is forced out of the surface until finally at some point, corresponding to an area of about 80 Å.² per molecule, the film collapses.

Runs with palmitic acid and sodium palmitate on the sodium nitrate substrate were indistinguishable from each other (Fig. 5). They showed a limiting area of about 20 Å.² per molecule, which is in good agreement with values recorded in the literature.

TABLE I

Properties of Films on 95% Saturated Sodium Nitrate

	Compressibility $\frac{1}{A} \left(\frac{dA}{dF} \right)_{F=25}$ $10^3 \times \text{cm./dyne}$	Area per molecule at 25 dynes/cm. Å. ²
Sodium 1-decylbenzene sulfonate	15.6	36
Sodium 1-dodecylbenzene sulfonate	17.3	33
Sodium 1-tetradecylbenzene sulfonate	9.6	24
Sodium 1-hexadecylbenzene sulfonate	7.8	23
Sodium 1-octadecylbenzene sulfonate	7.8	23
Sodium 2-dodecylbenzene sulfonate	12.9	43.5
Sodium 2-methyl-2-hendecyl-benzene sulfonate	12.0	47.5
Sodium 6-dodecylbenzene sulfonate	9.9	112
Polypropylene benzene sulfonate No. 1	13.0	50
Polypropylene benzene sulfonate No. 2	14.1	51
Sodium palmitate	8.4	22.5
Palmitic acid	8.4	22.5
Alkylphenyl polyglycol ether	34.6	116
Dodecylbenzene sulfonate from 1-dodecene (hygroscopic)	14.9	51.0
Dodecylbenzene sulfonate from 1-dodecene (nonhygroscopic)	14.4	41

There is some difference of opinion on how best to report the results of these experiments. To avoid ambiguity, the whole force-area curve for each compound should be presented. For purposes of tabulation, however, numerical values are desirable. Some workers give as values of area per molecule that area obtained by extrapolating back to zero pressure the straight upper portion of the force-area curve. With substances such as fatty acids and long straight-chain alcohols, this method is quite satisfactory because the curves for these materials show a sharp break, and a long straight portion in which a large change in film pressure results in a small change in area per molecule. With the detergents, however, there is no such sharp break in the curve, and many of the curves have no straight portions whatsoever. Consequently, any extrapolation to zero pressure would have to be done in an arbitrary manner, and the values

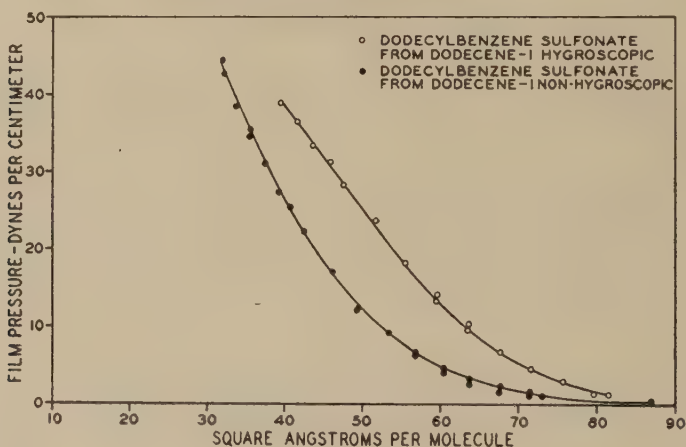


FIG. 6.

obtained would be subject to considerable uncertainty. A better method would be to give the area per molecule at two different surface pressures, or alternatively, give the area per molecule at one pressure, and the compressibility at that point. Table I summarizes the results with all the detergents tested by giving the compressibility of the film and the area per molecule at 25 dynes/cm. film pressure.

Applications

It has been shown that compounds of different structure give different force-area curves, so it was thought that this might be used as a tool for identification of certain unknown materials or for detecting the presence of certain types of structures in mixtures of surface-active agents. The first example of this kind involved two preparations of sodium dodecyl-

benzene sulfonate made from 1-dodecene. These two preparations had been made under very similar conditions and showed identical physical properties except that one was very hygroscopic, and the other one was not. In view of previous experience with pure compounds, we knew that pure sodium 2-dodecylbenzene sulfonate was nonhygroscopic, while pure 6-dodecylbenzene sulfonate was very hygroscopic and became gummy on absorption of moisture. The force-area curves for these two substances are quite different. Accordingly, force-area curves were run on the two preparations of dodecylbenzene sulfonate from dodecene, and it was found that the hygroscopic preparation had a larger area per molecule than the other (Fig. 6). This indicates the presence of some 3-, 4-, 5-, or 6-dodecylbenzene sulfonate in the mixture and may be the explanation of its hygroscopicity. These materials probably resulted from a migration of the double bond of the original 1-dodecene during the alkylation reaction.

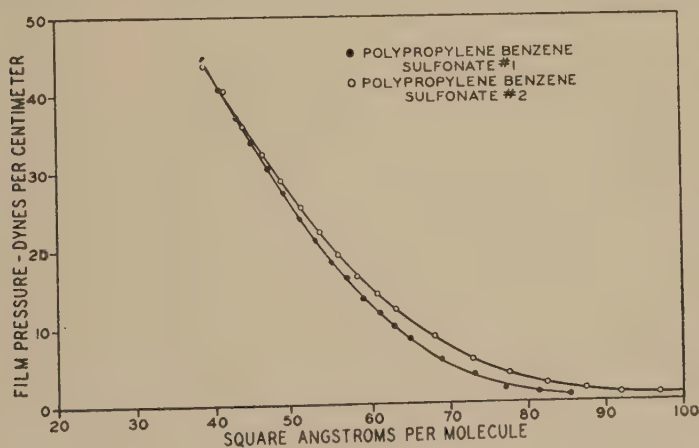


FIG. 7.

The two commercial detergents of the polypropylene benzene type gave nearly identical force-area curves (Fig. 7). The film balance, then, together with force-area curves of several known structures, shows promise as a means of at least partially identifying the structure of detergents of unknown composition.

SUMMARY

The technique of the film balance has been modified so that it is applicable to the rapid and easy measurement of force-area curves of films of soluble detergents. The use of 95% saturated sodium nitrate solution as a substrate prevents even the most soluble detergents from passing into the bulk of the solution at film pressures as high as 30 dynes/cm. Detergents of different structures give markedly different

force-area diagrams, and it is thus found possible to tell something about the structure of a detergent or mixture of detergents by studying their force-area curves. A convenient method for tabulating data on these curves is suggested. It is recommended that the area per molecule and compressibility at 25 dynes/cm. be reported rather than the area per molecule extrapolated to zero pressure. A complete description of the experimental procedure is included.

ACKNOWLEDGMENT

The writers are greatly indebted to Dr. A. H. Lewis for many helpful suggestions.

REFERENCES

1. ADAM, N. K., *The Physics and Chemistry of Surfaces*. The Clarendon Press, Oxford, 1938.
2. BRADY, A. P., *J. Colloid Sci.* **4**, 417 (1949).
3. EPTON, S. R., *Nature* **160**, 795 (1947).

LETTER TO THE EDITORS

SOME REMARKS CONCERNING THE MEASUREMENT OF ION ACTIVITIES IN COLLOIDAL SYSTEMS AND THE SUSPENSION EFFECT

The recent discussion (1-6) on the measurement of ion activities in colloidal systems in general, and the important "Suspension Effect" in particular, brings to mind a considerable body of earlier, germane contributions to this problem which, though neglected by the authors cited, should not be omitted from the consideration of this still highly controversial problem.

Thus, the gist of a somewhat involved discussion by Rabinovitch and Kargin in 1934 (7) concerning the measurement of ion activities in colloidal solutions may be paraphrased as follows: Imagine two "micro-electrodes" responding to the compensating ions, one of the electrodes being immersed in the intermicellar liquid, the other being situated in the double layer of some particle. The electromotive force of the resulting chain must be zero, notwithstanding the fact that the concentration of the compensating ions is much higher in the double layer. In other words, the Guggenheim-Brönsted electrochemical potentials of any given species of ions must be the same in all parts of a system in equilibrium (8). Rabinovitch and Kargin conclude that potentiometric measurements in colloidal solutions characterize only the equilibrium activities in the intermicellar liquid of the respective ion and do not allow any conclusion as to the situation in the double layer. However, Rabinovitch and Kargin implicitly take it for granted that truly meaningful electrometric measurements can be made in colloidal solutions. They do not consider the all important question whether or under what conditions adequate experimental techniques exist; in particular the difficulties and uncertainties involved in the use of salt bridges are not evaluated.

In a subsequent discussion (pp. 66-80 and 302-304) many of the arguments recently brought forward (1-6) were clearly stated. The same cleavage between the needs of the practical colloid chemist and his desire for easy and reliable, or at least phenomenologically meaningful methods on the one side, and the more rigorous and critical, strictly physico-chemical treatment on the other side, was apparent then as it is today.

Somewhat later (1938) Du Rietz (9), in discussing the acidity of dispersions of acidic fibers, states (p. 99; free translation by K. S.): ". . .

the hydrogen-ion concentration in the interior of the solid phase is enormously higher than in the free, outside solution; this difference, however, is compensated by the existing Donnan potentials. The position of the electrode with respect to the suspended particles must therefore be without significance and, indeed, it is without significance as the experiment shows. . . ."

"Entirely different, however, is the situation which arises at the contact point of the KCl bridge. This method of taking off a potential ("Potentialableitung") does not involve a reversible process; the solution of KCl serves only the purpose of equalizing the potential ("Potentialausgleich") with respect to the most nearby parts of the solution. Suppose that two KCl bridges were introduced in the same suspension, the one making contact in the free solution, the other one being introduced in some manner into the interior of a solid fiber. Under these conditions a potential difference of the magnitude of the aforementioned Donnan potential must become measureable." Du Rietz, thus, clearly states the core of the problem, but he does not come up with either a practical or a theoretical solution which would seem satisfactory to the present writer.

Loosjes (10), in a thesis containing numerous pertinent references, summarized the current (1942) state of the problem as follows (p. 91): ". . . a working hypothesis is developed starting from the thermodynamically established fact that a reversible electrode cannot produce a suspension effect (Rabinovitch and Kargin, Du Rietz). It is concluded that the effect must be due to the liquid junction and the problem reduces to the question as to what electrical potential arises at the contact of a concentrated solution (KCl) and a dilute solution (intermicellar liquid) in a capillary system (the suspension)." Loosjes' work deserves close attention, though much of it seems controversial.*

The difficulty encountered in measuring ion activities in colloidal systems in general, and of the suspension effect in particular, stems from several roots, some primarily psychological and some essentially conceptual. The former should be recognized before the latter are examined.

From a practical point of view, e.g., that of the soil chemist, the important parameter, after all, might be not so much electrometrically determined ion "activities" expressed in terms of ordinary aqueous reference solutions, but rather the actual ionic concentrations in the system which can be determined—though in some instances perhaps with limited accuracy only—by appropriate physicochemical methods.¹ The counter

* Since this letter was accepted for publication, a critical presentation (in English) of Loosjes' work by J. Th. G. Overbeek has become available (*Colloid Science*, Vol. 1. Edited by H. R. Kruyt, Elsevier Publishing Company, 1952, pp. 184–187)—The Editor.

¹ Numerous instances are known of the coexistence in equilibrium of two truly liquid aqueous phases. Which one is the proper reference solution? Or is it preferable to describe the different phases of such systems in terms pertaining to the individual phases themselves?

ions in a gel or sediment might be in a state of complete dissociation and have a degree of electrolytic mobility, similar to that which the same species of ions has in free aqueous solution; being present in an essentially aqueous medium, these ions might have about the same effect on chemical reactions which occur in the gel phase, e.g., on the rates of such reactions, as the same ions have at the same concentration in a common, liquid, aqueous solution.² In describing the individual phases (particularly for practical purposes) "let us make sure that there is no misunderstanding of the way in which we are to use the term activity," etc. [G. N. Lewis (13)].

The physicochemical difficulties could be reduced if technical terms were more precisely defined (e.g., the altogether too loosely used terms, activity and pH!), and particularly if detailed statements were made concerning the conditions which arise at the various phase boundaries and liquid junctions in the real or hypothetical experiments under consideration.

The commonly neglected but serious limitation of the meaningful use of salt bridges obviously needs a careful re-examination both from the experimental and theoretical side. With concentrated gel phases the errors due to salt bridges, in spite of all argument to the contrary, are important (1,6); in limiting cases, gel phases virtually assume the electromotive properties of reversible electrodes!

Another set of difficulties, of a conceptual nature, arises from the microheterogeneous character of many of the systems which were discussed. Certain difficulties involved in visualizing the fundamentals of the problem can seemingly be eliminated if a treatment were initiated—more consistently than was attempted in the past—from a consideration of two coherent macrophases in equilibrium, a liquid phase and a gel phase. This approach would bring to the discussion a considerable body of experimental data from the literature on ion exchangers and membranes.

It might be indicated here that many of the currently prevalent ambiguities and apparent difficulties might be resolved by a careful analysis of the concept of the Guggenheim-Brönsted electrochemical potential and by its judicious application to the case on hand. The lucid exposition of the physical meaning of this concept by Brönsted (8) may prove to be particularly helpful in this connection.

A meeting of minds could be facilitated by a series of (invited) papers and a subsequent round table conference of colloid chemists and theoretical electrochemists. This would offer an opportunity of stating and

²Correspondingly, in microheterogeneous and colloidal systems one might expect a low activity of a particular ion when an electrometric method is used, and a high activity if, e.g., the catalytic action of the system is studied. This situation, found by Rice and Osugi (11), was studied in some detail by Wiegner and Pallmann (12) in their investigations on the "Suspension Effect."

discussing in greater detail than heretofore the various points of view. The *Journal of Colloid Science* could do a great service by providing leadership in this direction.

REFERENCES

1. JENNY, H., NIELSEN, T. R., COLEMAN, N. T., AND WILLIAMS, D. E., *Science* **112**, 164 (1950).
2. COLEMAN, N. T., WILLIAMS, D. E., NIELSEN, T. R., AND JENNY, H., *Soil Sci. Soc. Am., Proc.* **15**, 106 (1951).
3. MARSHALL, C. E., *Science* **113**, 43 (1951); *ibid.* **115**, 361 (1952); *idem*, *Soil Sci. Soc. Am., Proc.* **15**, 110 (1951).
4. ERIKSSON, E., *Science* **113**, 418 (1951); *Ann. Agr. Coll. Sweden* **17**, 92 (1951).
5. PEECH, M., AND SCOTT, A. D., *Soil Sci. Soc. Am., Proc.* **15**, 115 (1951).
6. MYSELS, K. J., *Science* **114**, 424 (1951).
7. RABINOVITCH, A. J., AND KARGIN, V. A., *Trans. Faraday Soc.* **31**, 50, 284 (1935).
8. BRÖNSTED, J. N., *Physical Chemistry*, pp. 275 ff., 304 ff. The Chemical Publishing Company, New York, 1938.
9. DU RIETZ, C., *Über das Ionenbindungs-Vermögen fester Stoffe*. Thesis, Stockholm, 1938.
10. LOOSJES, R., pH-meting in Suspensies. Scheltema en Holkema's Boekhandel en Uitgeversmaatschappij N. V. Amsterdam, 1942; *Chem. Weekblad* **46**, 902 (1950).
11. RICE, F. E., AND OSUGI, S., *Soil Sci.* **5**, 333 (1918).
12. WIEGNER, G., AND PALLMANN, H., *Z. Pflanzenernähr. Düngung u. Bodenk.* **A 16**, 1 (1930); PALLMANN, H., *Kolloidchem. Beihefte* **30**, 334 (1930).
13. LEWIS, G. N., AND RANDALL, M., *Thermodynamics and the Free Energy of Chemical Substances*, pp. 257-8. McGraw-Hill, New York, 1923.

Laboratory of Physical Biology,
National Institute of Arthritis and Metabolic Diseases,
National Institutes of Health, Public Health Service,
Federal Security Agency, Bethesda 14, Maryland
Received October 10, 1952

KARL SOLLNER

Book Reviews

Advances in Catalysis. Vols. I, II, and III. Edited by W. G. FRANKENBURG, V. I. KOMEREWKY, AND E. K. RIDEAL. Academic Press Inc., Publishers, New York. Vol. I (1948), 321 pp., Price \$7.80; Vol. II (1950), 292 pp., price \$6.80; and Vol. III (1951), 360 pp., price \$7.80.

Advances in Catalysis is a collection of papers by outstanding authorities in the various fields of catalysis. They differ from the usual types of papers found in published symposia inasmuch as they are in the nature of reviews or surveys and are reasonably detailed. In several cases the authors have presented some hitherto unpublished material. The papers are representative of the various approaches to the subject of catalysis and treat the material from points of view which might be categorized as follows:

(a) Surface Chemistry: "Heterogeneity of Catalyst Surfaces" by Hugh S. Taylor; and "Catalysis and the Adsorption of Hydrogen on Metal Catalysts" by Otto Beek.

(b) Surface Physics: "Surface Area Measurements. A New Tool for Studying Contact Catalysis" by P. H. Emmett; and "The Application of X-Ray Diffraction to the Study of Solid Catalysis" by M. A. Jellinek and I. Fankuchen.

(c) Unit Catalytic Processes: "Alkylation of Isoparaffins" by V. N. Ipatieff and Louis Schmerling; and "Chemical Characteristics and Structure of Cracking Catalysts" by A. G. Oblad, T. H. Millikan, and G. A. Mills.

(d) Catalyst Types: "Nickel Sulfide Catalysts" by Wm. J. Kirkpatrick; and "Hydrogen Fluoride Catalysts" by J. H. Simons.

The first three volumes have eight such papers in each volume, averaging about forty pages per paper.

The editors have purposely omitted matter related to biocatalysis since this subject matter is adequately covered elsewhere. In studying heterogeneous catalysis whether it be liquid-liquid, gas-solid, or any of the other combinations in which more than one phase is involved, it is usual to consider some sequence of events such as diffusion to the interface, adsorption, formation of a chemical complex, reaction, desorption, and finally diffusion back into the main body of reactants and products. All these steps or modifications of them, depending upon the phase relationships, should be considered in any rate study involving heterogeneous catalysis. It is therefore felt that major sections on diffusion, heat, and mass transfer could, very profitably, have been included in an early volume. While these phenomena are not catalytic in themselves they have an important relationship to the subject especially where one is interested in the interpretation and application of rate data. The advances made in this field during the past few years certainly warrant recognition, summary, or review. Diffusion and flow are very briefly mentioned by G. M. Schwab, and diffusion in catalyst pores is extensively covered by A. Wheeler. Acid-base catalysis is another subject which could be profitably covered in an early volume. It was felt, in one or two instances, that the editors had selected papers which, while worthy of publication, do not properly belong in a collection under the title *Advances in Catalysis*, but on the whole they have accomplished the difficult task of selecting suitable material with notable success.

As is usually the case with such collected works, there is no uniformity of style, use of symbols, and in some cases there is an unnecessary overlap of material coverage. The style of the section entitled "Catalysis and the Adsorption of Hydrogen on Metal

Catalysts" by O. Beek has much to recommend it for a reference work of this type. Each section is headed by an italicized abstract which clearly informs the reader as to what is to be found in that section of the paper. Needless to say, this method of presentation considerably enhances, the ease with which the subject matter can be assimilated and its usefulness as a reference article.

The preface of the collection correctly summarizes the status of our understanding of catalysis, the difficulties involved, and the necessity for presenting the subject from many points of view.

Advances in Catalysis is a worth-while contribution to the chemical literature and should help speed the day when the foundations of catalysis will have been laid so that a science of catalysis can be erected.

CHARLES POTTER, New York, New York

Hydrogen Ion Concentration. New concepts in a systematic treatment. By JOHN E. RICCI. Princeton University Press, Princeton, N. J., and Oxford University Press, London, England, 1952. xxxvi + 460 pp. Price \$10.00.

This is an advanced, mathematical treatise developed on the author's thesis that: "The quantitative relations determining the hydrogen ion concentration of aqueous solutions constitute a purely mathematical problem subject to exact and systematic treatment and capable of simple and uniform presentation."

Two virtues of this book are: (a) It repeatedly reminds the reader of the distinction between postulates that are necessary and sufficient for a particular mathematical treatment and postulates that may involve more than the adequate, mathematical requirements; and (b) it gives detailed mathematical treatments of a large number of problems.

With regard to the first virtue it should be said that some readers may object to certain statements in the introductory chapter if these statements are not read with appreciation of the author's apparently exclusive concern for the mathematics involved. For example, Dr. Ricci chooses to regard hydrogen and hydroxyl ions as exclusively "water ions" in the sense that "they are never 'contributed' by solutes" (such as acids). "Solute ions (acids, bases and ampholytes) contain the solute molecule unbroken." For example, the hydrated chloride ion, formally represented by $[\text{Cl} \cdot \text{H}_2\text{O}]^-$, cannot be distinguished (analytically) from the ion formed by capture of OH^- by HCl , formally the ion $[\text{HCl} \cdot \text{OH}]^-$. In the opinion of the reviewer such views should be construed with regard for what Dr. Ricci considers convenient for his mathematics, most of his equations being oriented from the difference between the concentrations (or activities) of hydrogen and hydroxyl ions as affected by "solutes," and matters of mechanism being secondary. When, however, he uses classical equilibrium equations, such as

$$\frac{[\text{H}^+][\text{CH}_3 \cdot \text{COO}^-]}{[\text{CH}_3 \cdot \text{COOH}]} = K,$$

something will appear to be missing. Also, it will appear that the author has cut himself off from an easy transition to systems in those nonaqueous solutions where it has proved convenient to retain the concept of proton exchange and definitely from extension to Lewis acids and bases. The first transition is not impossible but would require considerable reformulation of "species."

With regard to the second virtue it should be said that the owner of this book will have assembled in one monograph somewhat special treatments of problems, discussions of which are widely scattered in the literature. While more references would have been welcomed, the book remains a valuable compilation for the specialist. As the reader will find, it is impracticable to examine all detail without the expenditure of a great deal of

time. The parts that the reviewer has examined in detail have not fulfilled the implied promise of simplicity.

The reader will find the going hard for the following reasons. He must gain familiarity with symbols and abbreviations, the list of which occupies more than seven pages. If the reader has not digested much that precedes the topic in which he is interested, he may have difficulty in tracing the derivation of the equation in which the discussion of that topic centers. Symbols and remarks distinguish: ideal, classical relations; relations currently regarded as "applicable" at infinite dilution; relations of the latter class that are numerically standardized (because of the impossibility of dealing experimentally with ions of one kind only); and "apparent" relations (which are limited to a narrow range of physical conditions). However, the reader will have to watch his step lest in overlooking these distinctions he apply incorrectly a mathematical relation. This is because the author is preoccupied with his mathematics rather than with those experimental relations that require constant attention to the distinctions.

Dr. Ricci says little regarding experimental methods and nothing regarding techniques, the excellence of which must match the elegance of the mathematics if data and their formulation are to be refined together. Thus the monograph remains a very special one, severely restricted to a mathematical treatment and to aqueous solutions.

W. MANSFIELD CLARK, Baltimore, Maryland

ERRATA

In the article entitled "The Surface Tension and Surface Potential of Aqueous Solutions of Normal Aliphatic Alcohols," by A. M. Posner, J. R. Anderson and A. E. Alexander, which appeared in Volume 7, No. 6, December, 1952, the following corrections should be noted:

1. P. 637, delete " \square acids, vapor to surface" from caption to Fig. 6.
2. P. 629, footnote to Table II should read "Based on the two values at 12°C., the mean value for $\alpha_n/\alpha_{n-1} = 3.38$ and $\beta_n/\beta_{n-1} = 2.51$ ".
3. P. 627, right hand ordinate of Fig. 1 should be " π (dynes/cm.)" instead of " π (dynes/mg.)".
4. P. 638, ordinate of Fig. 7 should be " $-\Delta H^\circ$ (k.cal./mole)".
5. P. 639, ordinate of Fig. 8 should be " $-\Delta S^\circ$ (E.U./mole)".

CRITICAL SUPERCOOLING OF PURE WATER DROPLETS BY A NEW MICROSCOPIC TECHNIQUE¹

G. M. Pound, L. A. Madonna and S. L. Peake

Metals Research Laboratory

Carnegie Institute of Technology, Pittsburgh 13, Pennsylvania

Received December 11, 1952

ABSTRACT

Very pure water droplets of 10–50 μ in diameter were condensed in silicone oil to form an emulsion. A portion of this emulsion was placed on the specially designed cold stage of a Bausch and Lomb Research Metallograph and cooled to a low temperature. Temperature of the emulsion was measured by a small thermocouple, and freezing of the droplets was detected by observation with polarized light.

The supercooling that is critical for ice formation was observed to be $-40 \pm 2^\circ\text{C}.$, in agreement with the results of Schaefer and of Cwilong. There was usually no marked change in shape of the droplets upon solidification.

INTRODUCTION

The supercooling of a liquid that is critical for rapid nucleation of the thermodynamically stable crystalline phase is an experimental quantity of considerable significance in the study of phase-transition kinetics. This measurement can be used to test nucleation theory and to estimate liquid-crystal interfacial free energy, a quantity that is difficult to evaluate by any other method (1,2). Tammann (3) has reported critical supercoolings for a number of bulk liquids, but many of these figures are questionable because of the possibility of contamination by small solid impurity particles which may serve as foreign nuclei or "seeds."

Vonnegut (4) showed that much of the effect of contamination could be eliminated by dispersing the bulk liquid into many small droplets, thereby sequestering the foreign nuclei in a small fraction of the total droplets. Pound and La Mer (5) measured nucleation rate in tin dispersions, and Turnbull (6) studied the freezing of mercury dispersions.

Pound and La Mer (5) suggested a technique similar to Vonnegut's in which the droplets to be studied are produced by a condensation method (7) instead of by mechanical dispersion. They found that the very pure liquid sulfur droplets, produced as an aerosol by this method could be supercooled to $-45^\circ\text{C}.$ without crystallization.

¹ The research described in this paper was sponsored by the Geophysics Research Division, Air Force Cambridge Research Center, Cambridge, Mass., under Contract No. AF 19(122)-185.

The supercooling of water droplets that is required for rapid nucleation of ice is a quantity of great importance in experimental meteorology (8). However, there is wide disagreement in the literature on the value of critical supercooling for pure water. On the basis of various experiments in cold chambers, Cwilog (9) and Schaefer (10,11) reported that ice crystals were formed spontaneously in air saturated with respect to water at about -35°C . From more precise measurements using an expansion cloud chamber and "dust-free" air, Cwilog (12) found the value of this critical temperature to be -41.5°C . However, he concluded that the process was one of direct sublimation from the vapor, because he could observe no minimum supersaturation required for the formation of ice crystals. Actually, one would expect a minimum supersaturation for the formation of ice crystals just as much as for the formation of water droplets (13). Further, the fact that no minimum supersaturation was required for the formation of ice crystals in these experiments indicates that some nucleating impurities were present. Accordingly in interpreting Cwilog's data, there are at least three possibilities: (a) Sublimation nuclei that are active at -41.5°C . caused the solidification. (b) First, droplets formed on condensation nuclei, and then freezing nuclei that are active at -41.5°C . caused the solidification. (c) First, droplets formed on condensation nuclei, and then froze homogeneously at -41.5°C . without the assistance of freezing nuclei.

Rau (14) has stated that he has supercooled water to -72°C ., but these results are now questioned (15). Mason and Ludlam (16) suggested that they failed to detect a critical temperature.

Probably the most unambiguous work on the critical supercooling of liquid water is that of Schaefer (17) who used a continuous cloud chamber to determine a critical temperature for droplet solidification of -38.5°C . This measurement was made by noting the level in the chamber at which the droplets transformed to spherical or slightly angular crystals.

However, some expansion cloud chamber work has been done using very pure carrier gases, and no ice formation could be observed at or near -40°C . Upon measuring the critical supersaturation for water-droplet or ice-crystal formation from the vapor in pure air as a function of temperature, Sander and Damköhler (13) reported that only droplets were observed to form above -62°C ., while crystals were always seen at lower temperatures. In the course of similar work on other carrier gases and vapors, the present authors (18) found that the condensate particles from water vapor in very pure nitrogen appeared to be droplets for all terminal temperatures above -63°C . Below -63°C . the condensate particles were obviously angular and crystalline. In this connection, Cwilog (12) reported mixed fogs down to -70°C . Further, he stated that at all temperatures below -41°C . the majority of the water droplets in the mixed fogs

evaporated readily, as indicated by the visible decrease in density of the mixed cloud in the first minute after expansion.

Accordingly, there was some reason to think that very pure water droplets might be cooled considerably below -40°C . before spontaneous solidification occurred. Inasmuch as cloud chambers are not designed to measure critical supercoolings but to measure critical supersaturations of vapors, it was decided to apply a dispersion technique to the problem of how far pure water can be supercooled before it freezes spontaneously. Further, it was desired to investigate the degree to which water droplets can retain their sphericity and apparent homogeneity upon freezing. This would shed light on the possibility of having spherical ice particles that are indistinguishable from water droplets in some of the cloud chambers mentioned above.

EXPERIMENTAL METHOD

1. *Preparation of Specimens*

An emulsion of water droplets was used for microscopic study instead of an array of droplets on a glass slide, because the silicone oil of the emulsion served to protect the droplets from solid nucleating impurities. Such impurities could come from the air or be in the glass slide itself. In preliminary experiments it was found that emulsions obtained by dispersing water in silicone oil with a homogenizer could be supercooled only about 25°C . Accordingly, the emulsions used in this work were obtained by a condensation technique. The emulsion was prepared by passing Air Reduction Corporation dry nitrogen over warm (not boiling) distilled water and then bubbling the warm, moist gas through a capillary tip immersed in cool (20°C .) Dow-Corning silicone oil (DC 200, 2000 centistokes) to condense water droplets in the oil. By this method, no freezing nuclei were transferred from the liquid water to the emulsion. Further, it is probable that not many freezing nuclei were transferred from the nitrogen into the water droplets of the emulsion, because the equipment was operated at temperatures and nitrogen rates such that no fog was formed. This means that the droplets condensed on the silicone oil-bubble interface and not on condensation nuclei in the nitrogen gas which might later serve as freezing nuclei. Preliminary experiments showed that filtering of the nitrogen through a cotton filter did not affect the results. There is the possibility that freezing nuclei present in the original oil could have contaminated the droplets. In order to reduce the likelihood of this source of contamination, the oil was exposed to the air of the room as little as possible. The silicone oil had been carefully washed with distilled water to remove any water-soluble materials. The washing had been done slowly (several days) and without excessive agitation in order to avoid introduction of freezing nuclei from the wash water into the oil. The emulsion

obtained by this method usually had to be diluted with washed silicone oil in order to get a concentration of water droplets suitable for study under the microscope.

2. The Cold-Stage Microscope Technique

A Bausch and Lomb Research Metallograph was found to be convenient for observing solidification, because it is equipped for polarized illumination and has accessory equipment for photography. Further, the

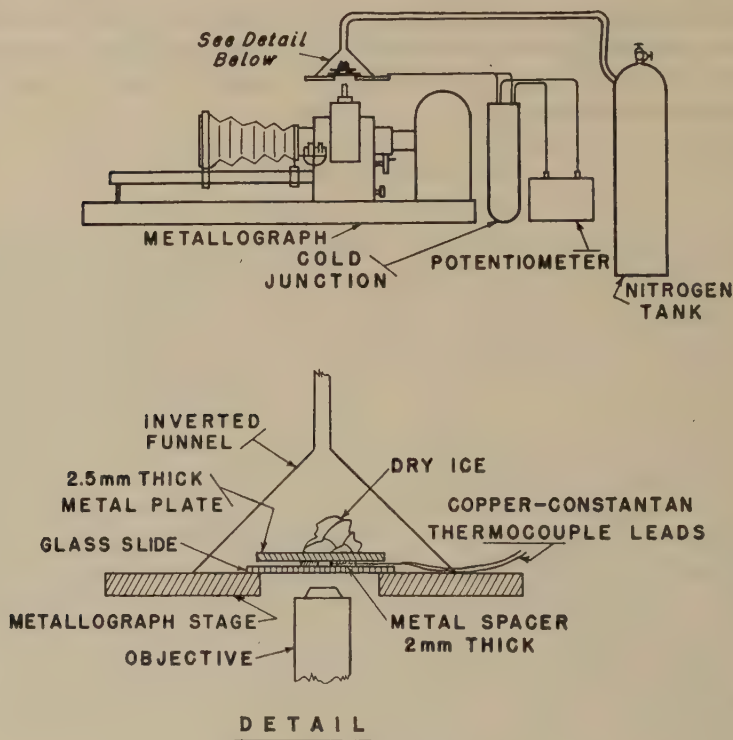


FIG. 1. Diagram of apparatus.

horizontal specimen stage of this reflected-light microscope is above the objective, and hence this instrument may be conveniently adapted to cold-stage operation. A diagram of the cold-stage adaptation is given in Fig. 1.

A drop of emulsion specimen was sandwiched between an ordinary 3-in. microscope slide below and a 2.5-mm. thick aluminum plate above. The slide was separated from the plate by a 2-mm. thick steel washer ($\frac{1}{2}$ in. in diameter), which encircled the specimen and lessened its annoying tendency to flow across the slide while exposures were being made. The

two-strand, calibrated, copper-constantan thermocouple (33-gage wire) was inserted through a small radial cut in the washer. Cooling was accomplished by placing a piece of Dry Ice on the aluminum plate. All but the central portion of the aluminum plate was lacquered to reduce undesired heat transfer from the surrounding atmosphere. Rate of cooling could be conveniently changed by using metal plates of different thermal conductivity. Condensation of moisture on the cold slide and microscope objective was prevented by the flow of dry nitrogen through the funnel placed over the specimen assembly and out the objective hole in the stage. While the specimen was cooling, suitable droplets were located in the microscope field, the temperature was read, and the droplets were photographed. Just as soon as the droplets solidified, the temperature was quickly noted and the droplets were photographed again.

RESULTS

Although prismatic crystals were never observed, solidification could usually be detected by the rather sudden appearance of cracks in the spheres and roughness in their profiles. Widening of the dark periphery of the image of the sphere and a "dirty" appearance in the light, central portion of the image were also observed. All of these effects were more readily observed with polarized light. However, polarized illumination required considerably more exposure time than ordinary light (15 sec. vs. 5 sec.). Accordingly, only a few of the photomicrographs were taken with polarized light.² The rest were taken with ordinary yellow light. In general, the photomicrographs are not as clear as the directly observed images, because the binocular eyepiece provides better vision than the single lens of the camera and finer focusing is possible on direct observation.

The character of the solidification and the temperature at which it occurred were not strictly a function of droplet size, but general trends for particular sizes were noticed. The temperature of solidification was higher for larger droplets, and the changes accompanying freezing were more evident than for the smaller droplets. The larger droplets (30–50 μ) frequently exhibited cracks upon freezing. Of the 50 observations on droplets having diameters from 20 to 50 μ , about 20% froze above -36°C . and about 70% froze between -36° and -42°C . The freezing temperatures of the remainder were uncertain, because of the difficulty in observing solidification.

For most of the droplets smaller than 10 μ , no evidence of solidification was apparent. This was probably because the resolution and magnification

² Owing to the difficulties in reproducing photographs, the photomicrographs are omitted from this publication. These photomicrographs are included in Scientific Report No. 1, Contract No. AF 19(122)-185, of the Air Force Cambridge Research Center, Cambridge, Mass.

used were not sufficient to study these smaller droplets. The resolution in the present experiment ($0.5\ \mu$) was limited because the specimen-to-objective distance had to be greater than the thickness of the slide plus emulsion drop (about 3 mm.). An objective of 0.4 numerical aperture was required, and the optimum magnification for this objective was 300.

It is believed that the measured temperatures of the emulsion drops were correct, because different cooling rates (from 10 to 20 min. for cooling to $-40^{\circ}\text{C}.$) gave essentially the same freezing temperature. Also, frozen specimens were frequently observed as their temperatures rose again to above $0^{\circ}\text{C}.$ The frozen spheres were always seen to lose their irregularities and assume the appearance of liquid droplets when the temperature read $0^{\circ}\text{C}.$

DISCUSSION

It is clear from the results that the maximum supercooling observed for the pure water droplets was $40 \pm 2^{\circ}\text{C}.$ This is in agreement with the results of Schaefer (17) and of Cwilong (12). It is certain that the droplets which froze at temperatures higher than $-40^{\circ}\text{C}.$ were contaminated with foreign freezing nuclei. As in all nucleation experiments, there is a possibility that even the droplets assumed to be free of foreign nuclei were in reality contaminated. Perhaps with even more elaborate purification measures, an emulsion could be prepared whose droplets could be supercooled appreciably below $-40^{\circ}\text{C}.$ However, it would seem a coincidence if the droplets of Schaefer and of Cwilong and of the present authors, all prepared by different methods, each contained the same impurity that catalyzed freezing at $-40^{\circ}\text{C}.$

Prismatic crystals of ice were never obtained in this work. The crystals formed as nearly perfect spheres. These spheres of $10\text{--}50\ \mu$ in diameter were of the same order of magnitude as the "droplets" observed in cloud chamber work. Without the aid of a good microscope, it would be impossible to tell whether the "droplets" seen in the cloud chambers were liquid or solid. Accordingly, visual observation of "droplets" in a cloud chamber below $-40^{\circ}\text{C}.$ cannot be interpreted as evidence that water may be supercooled below $-40^{\circ}\text{C}.$ Probably such "droplets" are in reality spheres of ice.

Of course, the water droplets used in this work were surrounded and protected by a silicone oil medium, whereas the droplets in a cloud chamber are suspended in a gas. It would be desirable to determine directly whether the spheres observed in a cloud chamber at terminal temperatures between -40° and $-63^{\circ}\text{C}.$ are liquid or solid. Attempts to do this have been unsuccessful thus far.

It might be argued that the critical freezing temperature of pure water is appreciably lowered as droplet size is decreased, simply because the volume available for incidence of homogeneous nucleation is limited.

However, it has been shown (19) that the increase of homogeneous nucleation frequency with decrease in temperature is very great. This may be calculated from Volmer's (1) equation:

$$J = \text{crystalline nuclei/cm. sec.} = C \exp\left(\frac{-16\pi\gamma^3}{3kT\Delta F_v^2}\right) \quad [1]$$

where C = the kinetic coefficient,

γ = crystal-liquid interfacial free energy/sq. cm., and

ΔF_v = bulk free-energy change/unit volume.

The increase in nucleation frequency with supercooling is so great that an additional 4° of supercooling will offset a decrease in droplet diameter from 1 mm. to 0.01 mm. (corresponding to a millionfold decrease in nucleation probability). Accordingly, the only appreciable effect that droplet size can have on critical supercooling is through its effect in determining the probability of the presence of a foreign freezing nucleus. This has been amply demonstrated by Pound and La Mer (5) and by Turnbull (6).

REFERENCES

1. VOLMER, M., *Kinetik der Phasenbildung*. Edwards Bros., Ann Arbor, Mich., 1945; see also LA MER, V. K., *Ind. Eng. Chem.* **44**, 1268 (1952) and POUND, G. M., *Ind. Eng. Chem.* **44**, 1278 (1952).
2. HOLLOMON, J. H., TURNBULL, D., MEHL, R. F., AND QUENAU, B. R., *The Solidification of Metals and Alloys*. Am. Inst. of Metallurgical Eng., New York, 1951.
3. TAMMANN, G. (translated by R. F. Mehl), *The States of Aggregation*. D. Van Nostrand, New York, 1925.
4. VONNEGUT, B., *J. Colloid Sci.* **3**, 563 (1948).
5. POUND, G. M., AND LA MER, V. K., *J. Am. Chem. Soc.* **74**, 2323 (1952).
6. TURNBULL, D., *J. Chem. Phys.* **20**, 411 (1952).
7. FORD, G., AND LA MER, V. K., *J. Am. Chem. Soc.* **72**, 1959 (1950).
8. HEVERLY, J. R., *Trans. Am. Geophys. Union* **30**, 205 (1949).
9. CWILONG, B. M., *Nature* **155**, 361 (1945).
10. SCHAEFER, V. J., *Science* **104**, 457 (1946).
11. SCHAEFER, V. J., *Bull. Am. Meteorol. Soc.* **29**, 175 (1948).
12. CWILONG, B. M., *Proc. Roy. Soc. (London)* **A190**, 137 (1947).
13. SANDER, A., AND DAMKÖHLER, G., *Naturwissenschaften* **31**, 460 (1943).
14. RAU, W., *Schriften deut. Akad. Luft.* **8**, 65 (1944).
15. BREWER, A. W., AND PALMER, H. P., *Proc. Phys. Soc. (London)* **B64**, 765 (1951).
16. MASON, B. J., AND LUDLAM, F. H., *Progr. in Physics* **14**, 147 (1951).
17. SCHAEFER, V. J., *Ind. Eng. Chem.* **44**, 1300 (1952).
18. POUND, G. M., AND MADONNA, L. A., to be published.
19. FISHER, J. C., HOLLOMON, J. H., AND TURNBULL, D., *Science* **109**, 168 (1948).

THE SPREADING OF LIQUIDS ON LOW-ENERGY SURFACES. VI. BRANCHED-CHAIN MONOLAYERS, AROMATIC SURFACES, AND THIN LIQUID FILMS

H. W. Fox, E. F. Hare and W. A. Zisman

Naval Research Laboratory, Washington, 25 D. C.

Received October 13, 1952

ABSTRACT

A study has been made of the wettability of adsorbed monolayers of branched-chain and cyclic molecules. It is shown that such monolayers are nonwetted by organic liquids with surface tensions higher than a critical value characteristic of the monolayer. Oleophobicity is therefore not restricted to monolayers whose surfaces comprise close-packed methyl groups, the latter merely representing an extreme case. It is shown, further, that adsorbed layers of nonpolar liquids behave, as regards wettability, like low-energy solids with the same atomic groups exposed in the surface. It is concluded that the free surface energy of adsorbed liquid or solid films depends only on the atomic groups in the surface and their packing.

INTRODUCTION

Recent research has shown that many liquids lose their ability to spread on high-energy surfaces such as metals when there are dissolved in them minor concentrations of certain types of amphipathic polar compounds. When the liquid is water the variety of polar solutes which inhibit spreading is extensive; when an organic liquid such as a hydrocarbon is the solvent, the solutes (or oleophobic additives) which inhibit spreading were thought to be restricted to polar compounds having an aliphatic structure with a terminal $-\text{CH}_3$ group, with no branching and no *cis*-unsaturated configuration (1-3).

More recent studies (3,4) on the wettability of high-energy surfaces covered with an adsorbed monolayer of an oleophobic compound showed a similarity in the wetting properties of the coated solid with those of organic solids (i.e., low-energy surfaces) having the same atomic groups in the surface. Thus, platinum coated with an adsorbed monolayer of *n*-octadecylamine behaved like the surface of a single crystal of *n*-hexatriacontane (5); when coated with a monolayer of *n*-perfluorodecanoic acid it was even less wettable than the surface of polytetrafluoroethylene (4). Furthermore, close analogies in wettability could be drawn between surfaces comprising analogous atomic groupings; e.g., the differences found between $-\text{CF}_3$ and $-\text{CF}_2-$ were analogous to those found for $-\text{CH}_3$ and $-\text{CH}_2-$.

While developing ingredients for synthetic nonspreading oils for clocks, Barker and co-workers (6,7) discovered that certain organic liquids were nonspreading on brass, steel, and synthetic ruby. In a discussion with Barker late in World War II, we suggested that these liquids were nonspreading because of the presence of oleophobic, unbranched, polar compounds which might have been present as deterioration products in the base liquid or as additives. Although in some instances this is believed to be the correct explanation, in others another mechanism appears to be operative since the most probable impurities were branched or cyclic polar compounds. To decide this point, a group of these compounds (e.g., benzyl phenylundecanoate and dipropylene glycol dicaproate) were synthesized and rigorously purified for us (8). Despite all precautions to prevent contamination and deterioration during the investigations of the spreading properties, the persistency of the nonspreading behavior and the reproducibility of the contact angles made it apparent that the nonspreading property of these liquids was either inherent in the liquid molecule or was caused by slight and uncontrollable hydrolysis occurring at the liquid/solid interface during these measurements. If either were true, it would be necessary to recognize that oleophobicity is not restricted to adsorbed films of unbranched, aliphatic, polar molecules. Evidence for the latter conclusion will be given here.

Since a number of organic liquids were found to be nonspreading on solid polyethylene (5), the question arose as to whether *n*-hexadecane can be adsorbed as a thin film on a high-energy surface such as platinum to produce a surface similar to polyethylene in wetting properties. It would be expected that *n*-hexadecane would adsorb with its long axis parallel to the surface, since in the absence of permanent dipoles, the adsorptive forces which would be operative would be van der Waals' forces along the carbon-carbon chain (9). Experimental evidence for this kind of behavior is given below.

Since a critical surface tension (γ_c) had been found for every low-energy surface studied (3-5,10), it was believed that there might also be a critical surface tension for each high-energy surface coated with a monolayer of branched-chain or cyclic polar molecules. The value of γ_c for the latter surfaces should be higher than those found for straight-chain compounds in our earlier studies (i.e., a surface covered with a branched-chain monolayer should be more wettable than one covered with a straight-chain monolayer). Furthermore, to isolate such branched-chain films on solid surfaces by using the oleophobic property, it was conjectured that the branched-chain polar compound could be adsorbed from its solution in a less adsorbable liquid having a surface tension greater than γ_c . The fact that such phenomena had not been observed in much of our earlier work may have been because hexadecane, which was usually

employed as a solvent, has a surface tension (27.7 dynes/cm. at 20°) less than the critical surface tension of surfaces covered with hydrocarbon groups other than methyl.

MATERIALS AND PROCEDURES

The surface used as a substrate for the low-energy films was polished platinum because of the ease of freeing this substance from organic contamination by flaming. Platinum, in the form of disks 1 mm. thick and 7 mm. in diameter, was polished with γ -alumina on a silk lap to give specularly smooth and flat surfaces, scratch-free to the naked eye. Measurements were also made on single crystals of naphthalene and anthracene. One-centimeter cubes of these materials were cleaved along the 001 plane exposing the β -hydrogen atoms in each case (11). A number of contact-angle measurements were made for various liquids on freshly sublimed naphthalene crystals. These yielded somewhat lower values than obtained on the cleaved surfaces, probably because the latter were smoother.

In observing the contact angles, a drop of the liquid under study was placed on the surface with a fine platinum wire, and small increments of liquid were added to the drop until the contact angle became constant. It was thus assured that the contact angle measured in this way represented a reasonable approximation to the equilibrium advancing angle. Contact angles of the nonspreading liquid were measured with the special goniometer described in earlier publications (1,2). The drops were initially 1–2 mm. in diameter and at equilibrium assumed a diameter which was a function of the spreading tendency of the liquid and the amount of liquid in the drop before small increments were added. The contact angles were independent of the diameter of the drop, and the agreement between the measurements for a set of drops (6 values) was $\pm 2^\circ$. All measurements were made at 20° and 50 per cent relative humidity.

RESULTS AND DISCUSSION

Spreading on a Surface Coated with a Monolayer of Branched-Chain or Cyclic Polar Compounds

The clean surface of a platinum disk was coated with an adsorbed monolayer of the polar compound of interest by immersing the metal in a saturated solution of the adsorbate in water (12,13) and then slowly withdrawing it. Monolayers free of adhering solution could readily be deposited in this way using each of the following polar compounds as the solute: 2-ethylhexylamine, α -amylmyristic acid, *p*-dodecyloxybenzoic acid, sebacic acid, aniline, and α -naphthoic acid. The observed contact angle (θ_E) of each of the liquids studied for each type of polar monolayer on platinum is given in Table I. Liquids are listed in decreasing order of

their surface tension. As in our previous studies of the wetting of low-energy surfaces (3-5,10), $\cos \theta_E$ is plotted against the liquid surface tension (γ_{LV}). The experimental curves for the wetting behavior of platinum coated with these polar compounds are given in Figs. 1a, 1b, and 1c. Because of the high values of γ_C for these surfaces, the number of liquids which are nonspreading is severely restricted, so that the number of points delineating each curve is not so large as in our previous reports. The outermost portion of each of these adsorbed polar monolayers is not composed solely of close-packed methyl groups, yet it is now seen that

TABLE I

Contact Angles of Various Liquids on Thin Films Adsorbed on Platinum (20°C.)

Liquid	Surface tension	Surface coated with adsorbed monolayer of:						Surface coated with thin film of nonpolar liquid	
		2-Ethyl-hexyl-amine	α -Amyl-myristic acid	p-Dodecyloxy-benzoic acid	Seba-cic acid	Ani-line	α -Naph-thoic acid	Hexa-decane	Perfluoro-alkane
	<i>dynes/cm.</i>								
Water	72.8	77	79	79	54	55	58	79	—
Glycerol	63.4	66				47	57	42	—
Methylene iodide	50.8	53			36		37		—
Tetrabromoethane	49.7	49	55	49	35				—
α -Bromonaphthalene	44.6	41	47	42	25	28		31	—
Aroclor 1248	44.2					26	33		—
Bis(2-phenylethyl) β -methyladipate	41.3	42	48	50	23				—
Tricresyl phosphate	40.9	40	44	49	22	20	31	38	—
Hexachlorobutadiene	36.0					2			—
Bis(cyclohexylethyl) α -methyladipate	35.8	31	34	34			19	21	—
Bis [2-(2'-ethylbutoxy) ethyl] azelate	34.3	26	30					23	—
tert-Butylnaphthalene	33.7			30		5	10	21	—
Bis(2-ethylhexyl) sebacate	31.1	ca. 9						15	—
Bis(2-ethylhexyl) adipate	30.2							13	—
Dibutyl pyrotartrate	29.3							10	—
Hexadecane	27.7								63
Tetradecane	26.7								60
Dodecane	26.4								55
Decane	23.9								49
Octane	21.8								39
Heptane	20.3								33
Hexane	18.4								25

they are oleophobic (or are not perfectly wetted) by liquids having surface tensions above some critical value. These surfaces, however, are more wettable than surfaces comprising only close-packed methyl groups.

It is interesting to compare the values of γ_C for these monolayers with $\gamma_C = 22$ dynes/cm. for an octadecylamine monolayer adsorbed on platinum (3) and $\gamma_C = 31$ dynes/cm. for solid, smooth polyethylene (5). The former represents a nearly close-packed methyl surface and the latter a methylene surface. It would be expected then that the branched-chain monolayers would have some intermediate value of γ_C since, if close-packing is not possible, the surface will contain methyl groups and some

exposed methylene groups. The values of γ_c found are about 29 dynes/cm. for the 2-ethylhexylamine monolayer (see Fig. 1a); about 26 dynes/cm. for α -amylmyristic acid (see Fig. 1b); and about 26 dynes/cm. for *p*-dodecyloxybenzoic acid (see Fig. 1c). The lower values are associated

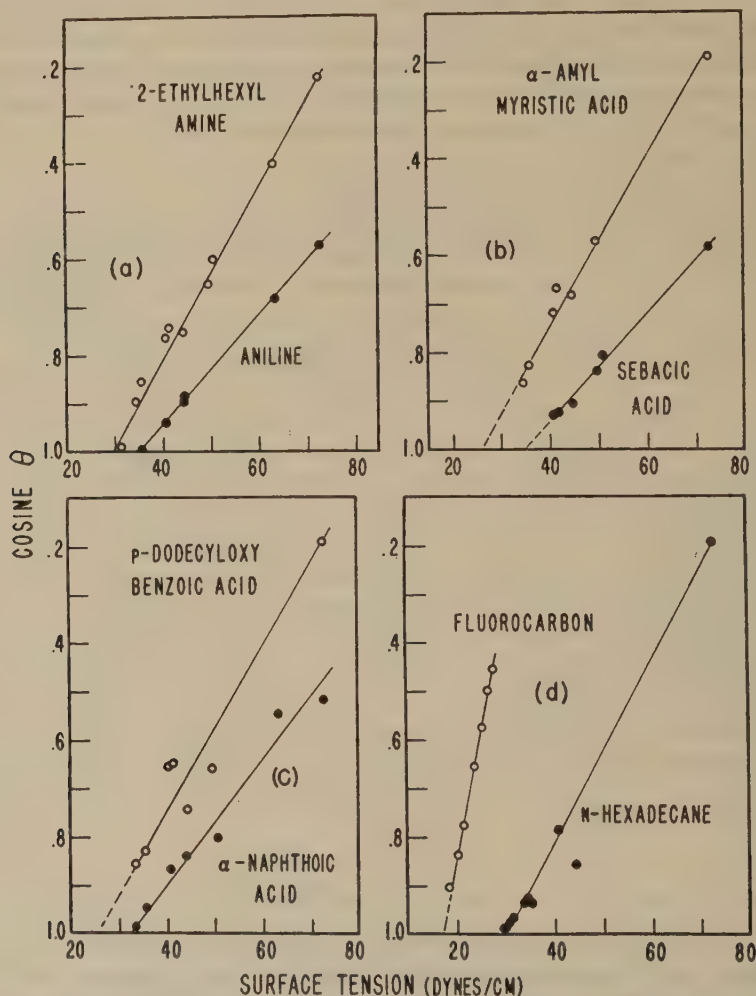


FIG. 1. Liquid surface tension versus contact angle of liquids on various monolayers and thin liquid films at 20°C.

with the long-chain compounds because relatively more methyl groups must be present in the surface, the degree of packing and the average lifetime of adsorption being increased by the action of the van der Waals' forces along the chain.

Sebacic acid monolayers (see Fig. 1b) have γ_c equal to about 35

dynes/cm. This value is a consequence of the presence of both methylene and carboxyl groups in the surface. If the closest possible packing occurred, it would be expected that as the chain length of the dicarboxylic acid increased, the value of γ_c would approach that of polyethylene (31 dynes/cm.) since both carboxyl groups are adsorbed at the metal surface (13).

Aniline and α -naphthoic acid (see Figs. 1a and 1c) adsorb to give monolayers which expose aromatic atomic groups in the surface rather than aliphatic. Both molecules are essentially planar and when close-packed could be expected to adsorb with the planes normal to the surface, thus exposing the edges of the benzene ring. The contact angles of water of 58° on monolayers of α -naphthoic acid and of 55° on aniline are to be compared with the value of 53° found on monolayers of benzoic acid (13). The three surfaces should be nearly identical except for small differences in packing.

It was of interest to compare the wetting properties of the above monolayers with those of the cleavage planes of naphthalene and anthracene.

TABLE II

Contact Angles of Some Pure Liquids on Single Crystals of Naphthalene and Anthracene (20°C.)

Liquid	Surface tension dynes/cm.	Cleaved anthracene	Cleaved naphthalene	Sublimed naphthalene
Water	72.8	94	95	92
Glycerol	63.4	77	79	80
Formamide	58.2	73	77	72
Ethylene glycol	47.7	62	65	60

Unfortunately, these crystals are too soluble in most of the weakly polar or nonpolar liquids used. From the data on four polar liquids, however (see Table II), the indications are that γ_c for surfaces comprising the edges of aromatic rings is about 25 dynes/cm., a value significantly lower than the 36 and 33 dynes/cm. found for monolayers of aniline and α -naphthoic acid. This is attributable to the looser packing of the molecules in the monolayers than in the single crystals, just as in our previous comparison of the contact angles of liquids on octadecylamine monolayers with those on *n*-hexatriacontane crystals (5). Since anything less than close packing would expose the faces of some benzene rings, it is concluded that the faces are more wettable by most liquids than the edges.

Since a comparison of relative wettabilities can only be made under similar conditions of packing, the following comparison is valid only for hydrocarbons in the solid state: as indicated by γ_c , the order of wettability for hydrocarbon surfaces is methyl < aromatic ring, edge exposed; < methylene < aromatic ring, face exposed.

Spreading on Surfaces Coated with Nonpolar Liquid Films

In order to determine whether a permanent dipole moment in the molecule is necessary in forming low-energy surfaces by adsorption upon a high-energy surface, two nonpolar liquids (*n*-hexadecane and perfluorokerosene) were each spread on clean, polished platinum and were lightly wiped with grease-free tissue paper until the resulting thin films showed interference colors. Drops of various liquids were placed on these surfaces giving the contact angles listed in the last two columns of Table I and also plotted in Fig. 1*d*. It is seen that γ_c for the liquid *n*-alkanes upon the fluorocarbon film is about 17 dynes/cm., just a little below the 18.2 dynes/cm. found for polytetrafluoroethylene with the same liquids (10). This is a reasonable difference and in the right direction, for although both surfaces are made up essentially of $-\text{CF}_2$ groups, the liquid surface has a high proportion of $-\text{CF}_3$ groups, is smoother than the solid, and must therefore give higher angles according to Ref. (10) and to Wenzel's rule (14). The *n*-hexadecane film on platinum had a critical surface tension of about 29 dynes/cm. or 2 dynes/cm. less than that found earlier for polyethylene. A similar argument can rationalize this lower value for the liquid film and the solid polymer.

It is of interest that γ_c for the hexadecane film is 1.5 dynes/cm. greater than the surface tension of hexadecane, while γ_c for the fluorocarbon liquid film is some 5.0 dynes/cm. smaller than the surface tension of the fluorocarbon liquid (22.0 dynes/cm.). These differences indicate that the interfacial tensions between the liquid fluorocarbon film and the test liquids are larger than those between the hydrocarbon films and the test liquids.

It should be noted that liquids ordinarily miscible with hexadecane (for example *tert*-butylnaphthalene) did not appear to dissolve the thin film within the time taken to make the measurements (perhaps 15 min.). Bangham and Saweris (15) have described a number of cases where two miscible liquids placed upon a clean mica surface repelled each other because they apparently had "abnormal properties" when in the act of spreading. This suggests that these liquid films in contact with solid substrates are in a different state of aggregation than bulk liquids. The molecules in the adsorbed layer must, in fact, be in a state of lower energy than those in the bulk liquid because of the heat of adsorption lost to the system under isothermal conditions.

Spreading of Mixtures of Nonpolar Compounds on Platinum

Both *sym*-tetrachloroethane (TCE) and hexadecane spread freely on clean platinum. Mixtures of these two liquids, however, do not spread, the contact angle depending on the proportion of each liquid in the

REFERENCES

1. BIGELOW, W. C., PICKETT, D. L., AND ZISMAN, W. A., *J. Colloid Sci.* **1**, 513 (1946).
2. BIGELOW, W. C., GLASS, E., AND ZISMAN, W. A., *J. Colloid Sci.* **2**, 563 (1947).
3. SHAFRIN, E. G., AND ZISMAN, W. A., *J. Colloid Sci.* **7**, 166 (1952).
4. SCHULMAN, F., AND ZISMAN, W. A., *J. Am. Chem. Soc.* **74**, 2123 (1952).
5. FOX, H. W., AND ZISMAN, W. A., *J. Colloid Sci.* **7**, 428 (1952).
6. BARKER, G. E., U. S. Patent 2,355,616, Aug. 15, 1944.
7. BARKER, G. E., ALTER, G. E., JR., MCKNIGHT, C. E., MCKLVEEN, J. R., AND HOOD, D. M., *ASTM Bull. No. 133*, 25 (Mar. 1946).
8. O'REAR, J. G., Naval Research Lab. Report 3891, Synthesis and Characterization of Esters and Ethers for Nonspreading Lubricants. Dec. 14, 1951.
9. DEBOER, J. H., *Advances in Colloid Sci.* **3**, 27 (1950).
10. FOX, H. W., AND ZISMAN, W. A., *J. Colloid Sci.* **5**, 514 (1950).
11. BRAGG, W. H., *Proc. Roy. Soc. (London)* **34**, 33 (1921).
12. SHAFRIN, E. G., AND ZISMAN, W. A., *J. Colloid Sci.* **4**, 571 (1949).
13. BAKER, H. R., SHAFRIN, E. G., AND ZISMAN, W. A., *J. Phys. Chem.* **56**, 405 (1952).
14. WENZEL, R., *Ind. Eng. Chem.* **28**, 988 (1936).
15. BANGHAM, D. L., AND SAWERIS, R., *Trans. Faraday Soc.* **34**, 554 (1938).
16. ADAM, N. K., *Physics and Chemistry of Surfaces*. Oxford University Press, 1941.
17. JURA, G., LOESER, E. H., BARFORD, P. R., AND HARKINS, W. D., *J. Chem. Phys.* **14**, 117 (1946).

sterically impossible so that methylene groups or aromatic structures (as the case may be) are exposed to the wetting liquid. Our earlier work (*loc. cit.*) has shown that optimum nonwetting is obtained when packing is closest, and that for a given packing, methyl groups are less wetted than methylene groups.

An additional fact uncovered in this investigation is that monolayers comprising the edges of aromatic rings are more wettable than those comprising methyl groups. For such surfaces it is again true that close packing reduces wettability, since it was shown that γ_c for naphthalene is smaller than for an adsorbed layer of aniline or α -naphthoic acid. The large discrepancy in wettability for the latter surfaces compared to naphthalene indicates that the "faces" of aromatic rings are considerably more wettable than the edges, making the former the most wettable of all solid hydrocarbon surfaces, i.e., the surface with the highest free surface energy.

It is also evident that the presence of carboxyl groups in the surface of an adsorbed monolayer contributes strongly to the wettability. Adam (16) showed this to be true for water on stearic acid surfaces by measuring the contact angle on stearic acid crystals cleaved so as to expose the $-\text{CH}_3$ surface in one instance and $-\text{COOH}$ groups in another; our results on sebacic acid monolayers show that this conclusion is general for liquids other than water.

The conclusion that *n*-hexadecane adsorbs on metals with its long axis in the surface agrees with the results for *n*-heptane on ferric oxide reported by Harkins *et al.* (17) from their study of the adsorption of the vapor. Our results on the wettability of films of nonpolar liquids show that low-energy surfaces may be formed by adsorption of high-boiling liquids through van der Waals' forces only.

This is another example to support our conclusion that adsorbed films only one molecule thick behave very much like solids with the same atomic groups in the surface; and that therefore the free surface energy of adsorbed liquid or solid films depends only on the atomic groups in the surface of the film and their packing.

These generalizations have been useful in elucidating the spreading behavior of a large number of pure organic liquids on high-energy surfaces (to be reported elsewhere). Furthermore, they establish a method of isolating monolayers of branched or cyclic polar molecules on solid surfaces: it is only necessary to choose a solvent with a surface tension sufficiently greater than the critical surface tension of the monolayer so that the solid surface coated with the adsorbed monolayer emerges dry from the solution of adsorbate. This will generally occur if the solvent exhibits a contact angle as high as 35° on the monolayer.

REFERENCES

1. BIGELOW, W. C., PICKETT, D. L., AND ZISMAN, W. A., *J. Colloid Sci.* **1**, 513 (1946).
2. BIGELOW, W. C., GLASS, E., AND ZISMAN, W. A., *J. Colloid Sci.* **2**, 563 (1947).
3. SHAFRIN, E. G., AND ZISMAN, W. A., *J. Colloid Sci.* **7**, 166 (1952).
4. SCHULMAN, F., AND ZISMAN, W. A., *J. Am. Chem. Soc.* **74**, 2123 (1952).
5. FOX, H. W., AND ZISMAN, W. A., *J. Colloid Sci.* **7**, 428 (1952).
6. BARKER, G. E., U. S. Patent 2,355,616, Aug. 15, 1944.
7. BARKER, G. E., ALTER, G. E., JR., MCKNIGHT, C. E., MCKLVEEN, J. R., AND HOOD, D. M., *ASTM Bull. No.* **138**, 25 (Mar. 1946).
8. O'REAR, J. G., Naval Research Lab. Report 3891, Synthesis and Characterization of Esters and Ethers for Nonspreading Lubricants. Dec. 14, 1951.
9. DEBOER, J. H., *Advances in Colloid Sci.* **3**, 27 (1950).
10. FOX, H. W., AND ZISMAN, W. A., *J. Colloid Sci.* **5**, 514 (1950).
11. BRAGG, W. H., *Proc. Roy. Soc. (London)* **34**, 33 (1921).
12. SHAFRIN, E. G., AND ZISMAN, W. A., *J. Colloid Sci.* **4**, 571 (1949).
13. BAKER, H. R., SHAFRIN, E. G., AND ZISMAN, W. A., *J. Phys. Chem.* **56**, 405 (1952).
14. WENZEL, R., *Ind. Eng. Chem.* **28**, 988 (1936).
15. BANGHAM, D. L., AND SAWERIS, R., *Trans. Faraday Soc.* **34**, 554 (1938).
16. ADAM, N. K., *Physics and Chemistry of Surfaces*. Oxford University Press, 1941.
17. JURA, G., LOESER, E. H., BARFORD, P. R., AND HARKINS, W. D., *J. Chem. Phys.* **14**, 117 (1946).

ADSORPTION OF DYES FROM AQUEOUS SOLUTIONS ON PIGMENTS¹

Warren W. Ewing and Fred W. J. Liu

Wm. H. Chandler Chemistry Laboratory, Lehigh University, Bethlehem, Pennsylvania

Received June 23, 1952, revised January 19, 1953

INTRODUCTION

Certain organic molecules are preferentially adsorbed from solutions on specific solid surfaces. Successful studies have been made by Harkins and Gans (1) in adsorbing oleic acid from a benzene solution on titanium dioxide, by Ewing (2) in adsorbing methyl stearate and glycol dipalmitate from benzene on zinc oxide, and by Smith and Fuzek (3) in adsorbing various fatty acids from organic solvents on nickel and platinum catalysts. Even a trace of water leads to erratic results, so it was necessary to scrupulously dry both solution and solid in such studies.

The use of aqueous solutions should eliminate the tedious drying procedures. Ewing and Rhoda (4) obtained the relative surface areas of seven zinc oxide pigments by the adsorption of a wetting agent, Daxad 11, from aqueous solution. Their work suffered from the drawback that the Daxad 11 was probably a mixture of various molecular species of unknown composition and that the cross-sectional area of the adsorbed molecules was unknown. Corrin, Lind, Roginsky, and Harkins (5) have studied the adsorption of long-chain electrolytes from aqueous solutions on graphite and on polystyrene.

The use of dye molecules as the adsorbate offers certain advantages: (a) Single molecular species of many dyes can be obtained and readily purified. (b) The molecular structures have been carefully studied. (c) The concentration of dyes can be determined readily by spectrophotometric methods. Rather indifferent success has been achieved beginning with the classical work of Freundlich in 1900 (6). Marc (7) observed the saturation tendency in the adsorption of methylene blue on barium sulfate. Paneth and co-workers (8-10) attempted to correlate the surface area of lead sulfate with the amount of the dye Ponceau 2R adsorbed. Schmidt and Durau (11) studied the adsorption of methyl violet and Diamond Fuchsin on glass powders. The lack of success in these early

¹ Taken in part from a dissertation submitted by Fred W. J. Liu to the Graduate Faculty of Lehigh University in partial fulfillment of the requirements for the Ph.D. degree, June, 1952.

studies may be attributed to (a) lack of reliable reference surface area, (b) failure to take into account the influence of pH as found by Bancroft and Barnett (12), and (c) failure to allow sufficient time to attain equilibrium.

In the present work the adsorption of crystal violet monochloride on titanium dioxide and of Orange II on titanium dioxide and on zinc oxide has been studied, after preliminary studies showed that they were preferentially adsorbed.

MATERIALS

Pigments

The TiO_2 and the ZnO samples were donated by the New Jersey Zinc Co. of Pennsylvania. The ZnO samples were the ones used by Ewing and Rhoda (4). Data on the samples are tabulated in Table I.

TABLE I

Pigment Samples and Surface Areas
(In square meters per gram)

Sample No.	N. J. zinc identification	Electron microscope ^a	N_2 - area ^a	N_2 - area ^b	Area by crystal violet ^c	Area by Orange II ^d
Anatase-X		—	—	6.6	—	—
Anatase-1	S74A	9.5	10.3	11.0	8.4	7.6
Anatase-2	S130A	8.3-9.7	7.0		8.6	9.0
Anatase-3	S17A	6.7	5.6		7.5	6.2
Rutile-1	C133EK	e	7.0	8.6	5.8	4.5
Rutile-2	C133EO	e	6.2		5.8	6.3
Rutile-3	C128DP	e	4.4		8.3	4.5
ZnO-1	U.S.P. 12	4.3	4.2		f	4.0
ZnO-2	Kadox 15	8.9	7.9		f	7.8

^a Determined by New Jersey Zinc Co. (Pa.).

^b Determined by Lehigh University.

^c One milligram Crystal Violet equivalent to 1.27 sq. m.

^d One milligram Orange II equivalent to 1.21 sq. m.

^e Particles too irregular and aggregated for estimation—N. J. Zinc Co.

^f Dye decomposed by ZnO.

Crystal Violet Chloride (CVCl) is the monochloride of the dye base N,N',N'' -hexamethyltriaminotriphenylmethylcarbinol. A sample of crystal violet, Extra Pure, Special TLA-141 was donated by E. I. du Pont de Nemours and Company. This dye was further recrystallized twice from water. Analysis for chloride, by precipitation as AgCl in 50% alcoholic solution, gave 8.56% chloride (theoretical for monochloride is 8.71%). For further confirmation of the purity of this dye, the molar extinction coefficient was measured using the Beckman model DU spectrophotometer. The value found was 96,200 at 585 $m\mu$. Adams and Rosenstein (13) reported 85,600 at 583 $m\mu$.

Orange II is the sodium salt of *p*-(2-hydroxyl-1-naphthylazo)benzenesulfonic acid. It was a Calco product previously purified by Justice (14) by the sodium acetate method.

EXPERIMENTAL PROCEDURE

The procedure was to attain equilibrium between dissolved and adsorbed molecules by agitating 5 g. of pigment in 25 ml. of dye solution. This was carried out in 75-ml. tubes having ground-glass stoppers. The stoppers were sealed in with paraffin wax, because vaseline absorbed the dyes. The high temperature runs were made in tubes sealed by fusion. Enough agitation to keep the pigment suspended was sufficient. Rolling, tumbling, and supersonic vibration (frequency, 75 kc./sec.) were equally efficient. Time and temperature were the important variables in attaining equilibrium. The amount of dye adsorbed on the pigment was obtained by determining the concentrations of the solutions before and after adsorption. The concentration measurements were made with a Coleman universal model No. 11 spectrophotometer by comparing the per cent transmission of light, at the wavelength of maximum absorption, 585 $m\mu$ for the crystal violet and 485 $m\mu$ for the Orange II, with the values from a calibration chart. A concentrated dye solution (about 4 g./l.) was prepared by dissolving the dye in distilled water and then filtering through a sintered-glass filter. The concentration was accurately determined by drying 10-ml. portions and weighing the residue (15). The calibration curve was made by diluting this solution to $4 \times 10^{-6} M$ and measuring the per cent transmission. This concentration is in the region of validity of Beers law for crystal violet (16). Because crystal violet was strongly adsorbed on glass, there was an appreciable error in concentration at the dilutions at which transmission measurements could be made (16). This error was minimized by rinsing the volumetric ware with the appropriate solutions and by coating the spectrophotometer cuvettes with paraffin wax, leaving windows in the light path, and taking the readings as soon as possible.

The apparent adsorption, x/m , in milligrams of dye adsorbed per gram of adsorbent, was found by $x/m = V/S (C_i - C_f)$, where C_i and C_f are the initial and final concentrations of the dye in grams per liter, V is the volume of the dye solution in liters, and S is the weight of the adsorbent in grams. The chief source of error, assuming that true equilibrium is reached, was in the determination of the dye concentration. The error in the spectrophotometer reading was 1.6% at 37% transmission. It was necessary to dilute the working solutions to about 1.5 mg./l. to get 37% transmission. It was estimated that the maximum relative error in x/m would amount to 10% in a solution containing 5 g./l.

RESULTS

Adsorption Isotherms

Adsorption isotherms have been obtained at room temperature for the adsorption of CVCl on four samples of anatase and three samples of rutile. CVCl is not a suitable dye for adsorption on zinc oxide because at the high pH of the zinc oxide solution ($\text{pH} = 7.5$) some of the dye is converted to the color base. Adsorption isotherms have been obtained also for the adsorption of Orange II on three samples of anatase, three samples of rutile, and two samples of zinc oxide. Additional isotherms were obtained at 60° and 93° with CVCl on Anatase-X. Typical isotherms

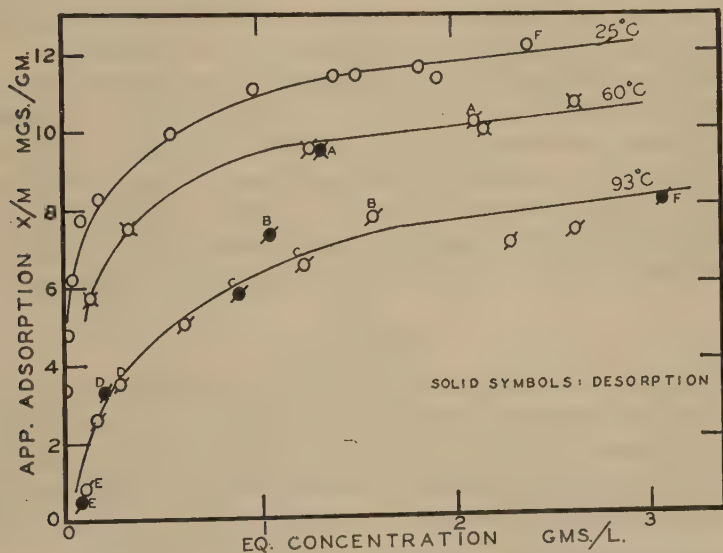


Fig. 1. Adsorption of crystal violet on Anatase-X. Letters indicate the origin of desorption experiments.

are plotted in Fig. 1 showing the adsorption of CVCl on Anatase-X at the three temperatures.

Most isotherms obtained do not appear to flatten out entirely, but show a tendency to rise with increasing concentration. A sigmoid curve would be obtained if adsorption could be determined in the more concentrated regions.

In Fig. 1 the solid points are the results of desorption experiments. The fact that the adsorption and the desorption data lie on the same line indicates that the adsorption is physical in nature. Furthermore the adsorption at the three different temperatures is in the correct order as that expected from physical adsorption.

Time studies showed that 7-9 days were required to establish equi-

librium in the CVCl-TiO₂ system at room temperature. At 60° and 93°, 1 day was sufficient. With Orange II, adsorption on ZnO was rapid, but slow on TiO₂.

Studies were made on the adsorption of NaCl, HCl, mixtures of HCl and CVCl, and mixture of NaCl and CVCl on anatase. Results indicated that the NaCl is not adsorbed, since an equimolecular amount of NaCl did not effect the adsorption of CVCl. However, hydrogen ion is adsorbed strongly. In the case of the mixture of HCl and CVCl the adsorption of the latter rose to a maximum as the pH reached 6-7, indicating that at this pH the adsorption of hydrogen ions is at a minimum. It is noteworthy that in adsorbing CVCl from water solutions the pH invariably rose to 6.5. Bancroft and Barnett (12) similarly found that adsorption of methylene blue on BaSO₄ is at a maximum at a pH of 5.8-7.1.

Adsorption from solution is complicated by the presence of micelles, as indicated by the work of Corrin and co-workers (5). It is probable that the equilibrium concentration used in depicting the results should be the concentration of the dispersed molecules. Hence conductance studies were made over the dilution range of the dye solutions used in this work. The straight-line relationship obtained in the conductance-concentration plot indicated the absence of micelles and the strong ionic character of the dye.

DISCUSSION

The validity of the data obtained can be illustrated by attempting to use it in calculating the surface areas of the pigments. In order to do this it is necessary to know (a) the configuration of the adsorbed layer and the cross-sectional area of the adsorbate in this configuration, and (b) the amount of adsorbate present in a monomolecular layer of adsorbate.

Theoretical Cross-Sectional Area of the Dye Molecules

The adsorption of the dyes has been shown to be a physical process. Therefore the amount of dye adsorbed would be a function of surface area rather than active sites. As there is good reason to suppose that large organic molecules lie flat on the surface, the theoretical cross-sectional area of the dye molecules can be approximated from a constructed molecular model.

The cross-sectional area of CVCl calculated from the projections of a model is about 160 sq. Å. and 1 mg. of the dye would occupy 2.48 sq. m. As the dye is hydrated, it would be more valid to employ crystallographic data of the hydrate. Recent x-ray studies (17) on CVCl indicate that CVCl·9H₂O crystallized from water has a C₃⁴ space group (trigonal pyramidal) with 2 molecules per unit cell, and $a = 16.0$ Å. and $c = 7.8$ Å. The cross-sectional area for such a unit cell is 171 sq. Å. One milligram of

the enneahydrate would cover 1.85 sq. m. As the data are expressed as anhydrous dye, 1 mg. would cover 2.54 sq. m.

The cross-sectional area of Orange II calculated from the projections of a model is about 140 sq. A., or 1 mg. of the dye equivalent to 2.42 sq. m.

The adsorption of the large organic ion is accompanied by the adsorption of the gegenion. As the gegenion is relatively small, its orientation

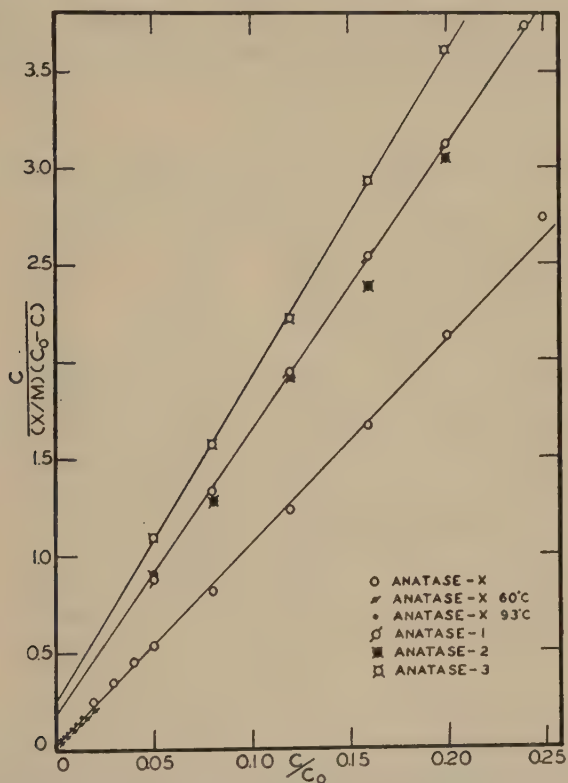


FIG. 2. A BET plot: adsorption of crystal violet on anatase.

on the surface would probably not affect appreciably the theoretical calculations. The position of the Cl^- is on top of the central carbon of CV^+ , as indicated by crystallography.

Evaluation of Monolayer Coverage

The adsorption equations of Freundlich and of Langmuir were applied to our data, but without success.

Rather successful attempts have been made recently by Bartell and co-workers (18-20) in modifying the Brunauer-Emmett-Teller (BET)

equation to apply to adsorption from solutions, although no attempt was made by them to correlate the monolayer coverage with surface area. Their modified BET equation was found to be applicable to the data obtained in this work.

The BET multimolecular adsorption equation became:

$$\frac{C}{(x/m)(C_0 - C)} = \frac{1}{(x/m)_m k} + \frac{k - 1}{(x/m)_m} \frac{C}{C_0}$$

when suitable terms were substituted into the original equation for gaseous adsorption. Notation k is used instead of their c , in order to avoid confusion with the concentration term C . x/m is milligrams of dye ad-

TABLE II

Evaluation of $(x/m)_m$ and $E_1 - E_L$ from Application of the BET Equation

Adsorbent	Temp. °C.	Adsorption of crystal violet		Adsorption of Orange II	
		$E_1 - E_L$ cal./mole	$(x/m)_m$ mg./g.	$E_1 - E_L$ cal./mole	$(x/m)_m$ mg./g.
Anatase-X		4140	9.5		
	60	4630	9.5		
	93	5080	9.5		
Anatase-1		2800	6.6	1950	6.3
Anatase-2		2690	6.8	2480	7.4
Anatase-3		2510	5.9	2350	5.1
Rutile-1	93	2000	4.6	1820	3.7
		2410	4.7		
Rutile-2		2250	4.6	1820	5.2
Rutile-3		2300	6.5	1860	3.7
ZnO-1				2080	3.3
ZnO-2				1990	6.4

sorbed per gram of pigment; $(x/m)_m$ is x/m at monolayer coverage. Determination of the solubility of the dye, C_0 , presents some difficulty. Solubility of CVCl at 25°C., if approached from the undersaturated side, was 7.4 g./l., but was 10–13 g./l. from supersaturated solutions. It was decided to use a value of 10 g./l. for C_0 at 25°C. The solubility at 60°C. was found to be 120 g./l. Solubility at 93°C. can only be estimated to be about 200 g./l. The solubility of Orange II at 25°C. was determined to be 40 g./l. As Orange II was not adsorbed at 93°C. by rutile at all, it is believed that the solubility must be very great at high temperatures, and therefore, no attempt was made to determine the solubility at high temperatures.

A sample BET plot is given in Fig. 2. Very good straight lines are obtained in most cases. Values of $(x/m)_m$ and the BET heats, $E_1 - E_L$,

were evaluated from the plot and are tabulated in Table II. It is remarkable that $(x/m)_m$ found for Anatase-X and for Rutile-1 are the same for the different temperatures, although the values of C/C_0 are very low at high temperatures.

In Fig. 3 $(x/m)_m$ values from our data calculated by means of the BET equation are plotted against the nitrogen values (open symbols), and against the electron microscope values (closed symbols). Line A is the

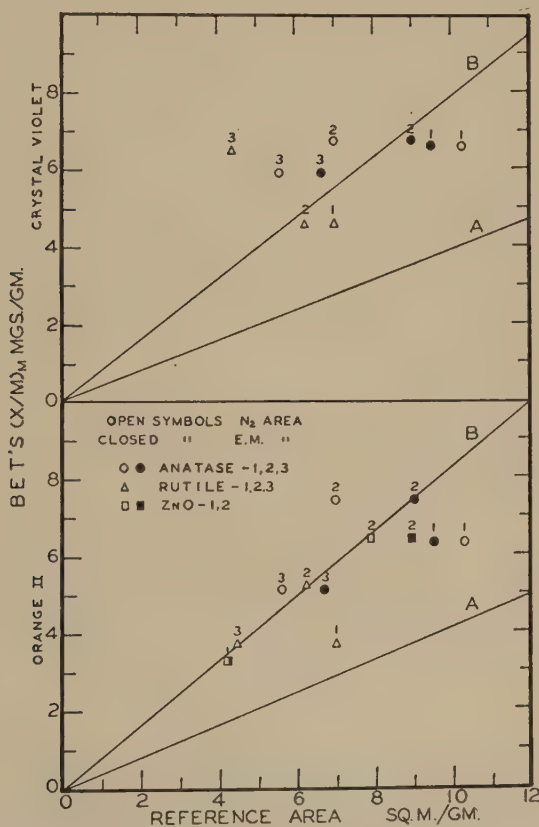


FIG. 3. Correlation of BET's $(x/m)_m$ values with nitrogen and electron microscope area. Curve A, unimolecular adsorption; curve B, bimolecular adsorption.

theoretical curve assuming unimolecular adsorption. The best line that can be drawn through the points and to the origin is found to be the same as the theoretical curve B for bimolecular adsorption. Thus, assuming that the BET monolayer corresponds to a layer of dye two molecules in thickness, the theoretical area covered by 1 mg. of dye would be one half of the amount previously estimated. Then 1 mg. of CVCl is equivalent to 1.27 sq. m., and 1 mg. of Orange II to 1.21 sq. m. By multiplying

these two factors with the respective values for $(x/m)_m$, the surface areas of the pigments were obtained and tabulated in Table I. The correlation with both the N_2 data and electron microscope data is as good as can be expected. For the adsorption of CVCl , only Rutile-3 is out of line. The adsorption data of Orange II agrees to within 10%, with the exception of Rutile-1. Unfortunately, electron microscope area is not available for the rutile samples.

The possibility of having an $(x/m)_m$ value corresponding to two layers can now be discussed. Without employing the linear form of the BET equation, approximate monolayer coverage can be found from the so-called point *B* in a type II adsorption isotherm. Point *B* indicates a sharp change of slope in the isotherm, which in turn indicates a sharp change of the heat of adsorption. According to the multimolecular adsorption theory, this sharp change of rate signifies the completion of a statistical unimolecular layer. In the derivation of the BET equation, it was assumed that E_1 , the heat of adsorption for the first layer, is different from E_2 ; but $E_2 = E_3 = \dots = E_L$. Now, if it is assumed $E_1 \approx E_2$, but $\gg E_3$, then point *B* in the isotherm would be shifted to the upper part of the isotherm and correspond to the two statistical layers indicated by applying the equation to our data.

The proof of the applicability of an adsorption equation lies not only in the evaluation of consistent $(x/m)_m$ values, of which evidence has just been given, but also in the reasonable values of heat of adsorption. The consistency of the $E_1 - E_L$ evaluated from the BET equation can be noted in Table II. In this work E_L , the heat of condensation in gaseous adsorption, would be the heat of crystallization of the dye, which we will notate as E_c . The experimental calorimetric value for E_c is not available. It was, therefore, estimated by means of van't Hoff's equation:

$$\ln \frac{C_2}{C_1} = \frac{-\Delta H}{R} \left(\frac{1}{T_2} - \frac{1}{T_1} \right),$$

where C_1 and C_2 are the solubility of the solute at T_1 and T_2 , respectively; and ΔH is the heat of solution of the solute, and is equal to $-E_c$.

By using the solubility data of CVCl at 25° and 60°C., E_c is calculated to be -14,000 cal./mole. If a mean value of -2400 cal./mole for $E_1 - E_c$ is used, then E_1 , the heat of adsorption of CVCl on TiO_2 , can be readily calculated to be -16,400 cal./mole. This value appears to be rather high for a physical adsorption. According to de Boer (21), adsorption energies can be approximated from the various contributing factors. The contribution due to the adsorption of a phenyl group alone amounts to 3400 cal./mole. The adsorption of crystal violet, a triphenylmethane dye, would have an adsorption energy of 10,200 cal./mole from the contribution of the three phenyl groups, which are believed to lie flat on the sur-

face. Any additional contribution in adsorption energy arising from the polarization of the dielectric adsorbent TiO_2 would certainly raise the value. Thus, the value of E_1 , $-16,400$ cal./mole, from an application of the BET equation is theoretically reasonable.

SUMMARY

The adsorption of two ionic dyes, crystal violet and Orange II from aqueous solutions on anatase, rutile, and zinc oxide has been investigated.

It was found that up to 9 days of agitation were required to attain true equilibrium, and that high temperatures hastened the process.

The adsorption has been found to be physical in nature.

The Brunauer-Emmett-Teller multimolecular adsorption equation has been found to apply to the data. Rather consistent $(x/m)_m$ and $E_1 - E_L$ values were evaluated. By assumption of planarity and close packing of the adsorbed dye molecules, the area found corresponds to twice that determined by the nitrogen and electron microscope methods. A bimolecular layer is suggested.

REFERENCES

1. HARKINS, W. D., AND GANS, D. M., *J. Phys. Chem.* **36**, 86 (1932).
2. EWING, W. W., *J. Am. Chem. Soc.* **61**, 1317 (1939).
3. SMITH, H. A., AND FUZEK, J. F., *J. Am. Chem. Soc.* **68**, 229 (1946).
4. EWING, W. W., AND RHODA, R. N., *Anal. Chem.* **22**, 1453 (1950).
5. CORRIN, M. L., LIND, E. L., ROGINSKY, A., AND HARKINS, W. D., *J. Colloid Sci.* **4**, 485 (1949).
6. FREUNDLICH, H., *Colloid and Capillary Chemistry*. E. P. Dutton, New York, 1922.
7. MARC, R., *Z. physik. Chem.* **75**, 710 (1911).
8. PANETH, F., AND RADU, A., *Ber.* **57**, 1221 (1924).
9. PANETH, F., AND THIMANN, W., *Ber.* **57**, 1215 (1924).
10. PANETH, F., AND VORWERK, W., *Z. physik. Chem.* **101**, 480 (1922).
11. SCHMIDT, G. C., AND DURAU, F., *Z. physik. Chem.* **108**, 128 (1924).
12. BARNCROFT, W. D., AND BARNETT, C. E., *Colloid Symposium Monograph*, Vol. 6. Chemical Catalog, New York, 1928.
13. ADAMS, E. Q., AND ROSENSTEIN, L., *J. Am. Chem. Soc.* **36**, 1452 (1914).
14. JUSTICE, J. D., AND EWING, W. W., *Am. Dyestuff Reporter* **41**, 668 (1952).
15. HANTZSCH, A., AND OSWALD, G., *Ber.* **33**, 278 (1900).
16. TURGEON, J. C., AND LA MER, V. K., *J. Am. Chem. Soc.* **74**, 5988 (1952).
17. KREBE, H., *Fortschr. Mineral.* **26**, 79 (1947); *C. A.* **44**, 9767 (1950).
18. FU, Y., HANSEN, R. S., AND BARTELL, F. E., *J. Phys. & Colloid Chem.* **52**, 374 (1948).
19. HANSEN, R. S., FU, Y., AND BARTELL, F. E., *J. Phys. & Colloid Chem.* **53**, 769 (1949).
20. BARTELL, F. E., AND DONAHUE, D. J., *J. Phys. Chem.* **56**, 665 (1952).
21. DEBOER, J. H., *Advances in Colloid Sci.* **3**, 27 (1950).

HYSTERESIS OF CONTACT ANGLE OF WATER ON PARAFFIN. EFFECT OF SURFACE ROUGHNESS AND OF PURITY OF PARAFFIN¹

B. Roger Ray² and F. E. Bartell

Department of Chemistry, University of Michigan, Ann Arbor, Michigan

Received October 24, 1952

INTRODUCTION

Many investigators have measured the contact angles of water on paraffin with considerable variation in results. It is nevertheless a common belief that the system has a unique characteristic value which is easily reproducible and free of complications. The system has been much used as a standard for calibration and for experiment as well as for theoretical calculations pertaining to surface forces. Fowkes and Harkins (1) reported no hysteresis for the contact angle of water on a sample of paraffin solidified in air and examined by the tilting-plate method, but before reading the instrument they permitted evaporation to take place for several minutes or else shook the cell "to produce equilibrium." Similar experiments carried out in this laboratory under conditions where evaporation and mechanical jarring were carefully prevented have invariably shown the occurrence of hysteresis. Thiessen and Schoon (2) reported the absence of hysteresis on single crystals of paraffin but based their conclusions on rather variable results. The objective of the present research was to extend earlier studies of hysteresis in the paraffin-water system by investigating the effect of purification of the paraffin and of the gross physical character of the paraffin surface, and to attempt to show conclusively either the permanent nature of hysteresis or the conditions under which hysteresis might be induced or might be eliminated.

EXPERIMENTAL PROCEDURE

Methods Used for Contact-Angle Measurements

Contact angles were measured by four methods, the choice of method depending upon the conditions of the experiment. All measurements were carried out in an air thermostat regulated to $25.0 \pm 0.1^\circ$. The contact-

¹ The data in this paper were taken from a portion of the thesis of B. Roger Ray, submitted to the School of Graduate Studies of the University of Michigan in partial fulfillment of the requirements for the Ph.D. degree, December, 1945.

² Present address: Department of Chemistry, University of Illinois, Urbana, Illinois.

angle device and cell were supported independently of the thermostat so as to eliminate vibration.

For the vertical-rod (VR) method (3) and the tilting-plate (TP) method (4), a contact-angle device was constructed which consisted, in the main, of a sample holder attached to a circular disk graduated in degrees. The elements were so mounted that with the fine rack-and-pinion device the glass rod or plate could be moved easily and accurately in both horizontal and vertical directions, and could be rotated about a point so fixed that the center of rotation remained exactly at the solid-water-air interface.

The controlled-drop-volume (CDV) method, a modification of the usual drop-on-plate method (5), made use of a pipet with a very fine tip (approx. 0.02 mm. outside diameter) from which water was either forced out to increase the volume of the small drop when forming an advancing angle or sucked back in when forming a receding angle. Sensitive and positive control of the drop volume was achieved, and the fine tip did not appreciably distort the drop. A greatly magnified silhouette of the drop was projected onto a ground-glass screen and the tangent erected upon the image.

The drop-on-capillary-tip (CT) method employed an apparatus developed by Bartell and Smith (6) for their studies on the wetting of metal surfaces. The capillary tip was sealed into an all-glass contact-angle cell; the absence of all stopcocks, grease, rubber, corks, and sealing compositions insured freedom from contamination. A fresh paraffin surface could be formed in a vacuum on the flat tip in the cell either by melting a lump of paraffin previously placed on the tip (using a resistance coil suspended above the tip) or by volatilization onto the tip from a drop of paraffin held within the resistance coil by capillarity. Water could then be introduced to saturate the vapor space (in some cases air or nitrogen was also introduced). Finally, water could be forced onto the tip to form a drop.

Measurement of Contact Angles

All parts of the apparatus coming into contact with paraffin or water were freshly cleaned in hot chromic acid, followed by soaking in water or by flaming. Thermal equilibrium and aqueous saturation of the vapor space surrounding the paraffin surface were achieved in each case before the formation of the interface.

For all the water-paraffin systems examined, both stable advancing and stable receding angles were found. The angles quickly reached stable values and no appreciable changes with time were observed. Ordinarily, angles were measured at 2, 5, and 15 min. Receding angles were formed after the paraffin had been covered with water for at least 2 min. The reproducibility of measurements varied, depending first upon the physical

character of the paraffin surface, and secondly upon the method used. The tilting-plate method proved inferior to the other methods in accuracy and convenience.

Materials

Double-distilled water was stored in Pyrex, and portions were withdrawn from the interior by siphon. The surface tension was frequently

TABLE I
Contact Angles in Air of Water on Surfaces of Paraffin
(Surfaces formed in air)

Experiment	Method of formation of surface ^a	Appearance of surface	Method used	Contact angle values			Hysteresis $\Delta\theta$
				θ^a	θ^r	Av.	
				deg.	deg.	deg.	deg.
Sample I ^b							
I-A	A	Heavy, opaque, rough	TP	120 \pm 3			
I-B	B	Thin, opaque, waxy-like	VR	112 \pm 1	104 \pm 2	108	8
Sample II ^c							
II-A	B	Same as in I-B	VR	111 \pm 2	102 \pm 3	106	9
Sample III ^d							
III-A	B	More crystalline than I-B	VR	115 ^f	106 ^f	110	9
III-B	B	Same as III-A	CT	112 \pm 1	105 \pm 1	108	7
Sample IV ^e							
IV-A	C	Heavy, coarse, crystalline, transparent	VR	132 \pm 4	97 \pm 2	114	35
IV-B	D	Thin, crystalline, nearly transparent	VR	115 \pm 1	110 \pm 2	113	5

^a Method of formation of surface: A, microscope slide quickly dipped into and out of sample held at 110°. Paraffin solidified on contact; B, glass rod immersed a few seconds in sample held at 100° and slowly withdrawn. Paraffin solidified in few seconds; C, glass rod quickly dipped as in I-A. Paraffin solidified on contact; D, glass rod heated in sample at 100° and then withdrawn. Paraffin solidified in 1 min.

^b Commercial paraffin, specially filtered, m.p. 56–58°.

^c Commercial paraffin: Parowax.

^d First purification product from Parowax, b.p. 191–198° at 2 mm.

^e Final purification product from Parowax, b.p. 185–188° at 1 mm.

^f Single determination.

checked with a ring tensiometer. Two commercial samples of paraffin from two different companies were examined and are designated as sample I and sample II.

Most of the measurements were made on a purified sample, a narrow-boiling fraction of paraffin freed of nonhydrocarbon substance and of contaminants by the following procedure. Fifteen hundred grams of

Parowax (sample II) was stirred for several hours with warm concentrated sulfuric acid. This was repeated twice. The paraffin, tan in color, was washed free of acid with several portions of warm water. This product and 500 g. of clean sodium metal were placed in a three-necked flask. After flushing with nitrogen, the temperature was raised to 110°C. and the contents were stirred. After 4 hr., the paraffin, now brown in color, was forced into the flask of the distillation apparatus by a stream of nitrogen gas. This apparatus had previously been flushed with nitrogen

TABLE II

Contact Angles of Water on Surfaces of Purified Paraffin
(Surfaces formed in vacuum and in nitrogen)

Experiment	Method of formation of surface ^a	Appearance of surface	Composition gas phase	Method used	Contact angle values			Hysteresis $\Delta\theta$
					θ^a	θ^r	Av.	
Sample IV					deg.	deg.	deg.	deg.
IV-C	A	Fairly transparent, crystal formation, cracks	Water vapor	CT	114 \pm 2	110 \pm 1	112	4
IV-D	B	Same as in IV-C.	Nitrogen + water vapor	CT	114 ^b	110 ^b	112	4
IV-E	C	Opaque, similar to deposit of white smoke	Nitrogen + water vapor	CT	121 ^b	108 ^b	115	13
IV-F	D	Film invisible except interference pattern	Nitrogen + water vapor	CDV	112 \pm 1	112 \pm 1	112	None approx.
IV-G	E	1. Opaque, similar to that in IV-E	Air + water vapor	CDV	120-140	96-110		27 approx.
		2. Transparent, barely detectable	Air + water vapor	CDV	116 ^b	108 ^b	112	8
		3. Film similar to that in IV-F	Air + water vapor	CDV	112 \pm 1	112 \pm 1	112	None approx.

^a Method of formation of surface: A, contact-angle cell sealed to distillation receiver. One drop of distillate, at 1 mm. N₂, caused to fall onto tip in cell. Cell evacuated to 10⁻⁴ cm. and sealed off; B, small lump placed on tip in contact-angle cell. Cell flushed with H₂ and evacuated. Paraffin was caused to vaporize by heat from resistance coil above tip; C, same as B except N₂ was used as inert gas; D, same as C except only small amount of paraffin vaporized; E, similar to C except condensation was on glass plates and coatings of different thicknesses were obtained.

^b Single determination.

by evacuating and filling twice in succession. The nitrogen pressure was reduced to 2 mm. and the paraffin slowly distilled, the fraction boiling at 191-198°C. being labeled sample III. This fraction was re-treated with molten sodium metal (no color developed) and redistilled at less than 1 mm. Sample IV, used for contact-angle measurements, was that portion collected at 185-188°C.

The distillate was caused to flow from the condenser tube into a glass spout which swiveled at its upper end and contained a sealed-in iron strip

by means of which, through manipulation of a magnet outside the glass walls, the paraffin melt could be directed into a receiving flask or directly into the contact-angle apparatus so positioned as to permit drops of distillate to fall onto the capillary tip in the cell.

RESULTS

In Tables I and II are presented the values of the contact angles of water on various paraffin surfaces (advancing angles = θ^a and receding angles = θ^r). Each experiment noted in the first column of each table summarizes the measurements made under one particular set of conditions which is outlined in the accompanying column. Also indicated is the physical appearance of the surface as it appeared to the eye. Table I deals with surfaces formed in the presence of air and upon which the contact angles were measured with the vapor space filled with air saturated with water vapor. Table II deals with purified paraffin (sample IV) the surfaces of which were formed in vacuum or at a low pressure of nitrogen, and on which the contact angles were measured with the vapor space filled as noted in col. 4.

Contact Angles on Surfaces Formed from Melts in Air

The results of Expts. I-A through II-A are typical for ordinary paraffin surfaces. When the rate of solidification of the paraffin was rapid and the coating thick and rough, as in I-A, the advancing angle was found to be as high as 120° . When the rate of solidification was slow and the thickness of the layer reduced, the surface became smoother and the angle dropped to 112° . Values intermediate between these limits were obtainable depending, it appeared, upon the roughness of the surface.

This roughness, to a major extent, is the result of crystallizing forces that lead to a surface composed of the planes, edges, and corners of crystals with many holes and fissures due to the high degree of imperfection. The commercial paraffins, being a mixture of constituents, were observed to solidify from melts as typical, white, opaque masses (presumably microcrystalline). Under comparable conditions the purified paraffin, represented by the narrow fraction designated as sample IV, solidified from melts as practically transparent surfaces with what appeared to be cleavage planes between relatively large crystals. Evidence of roughness effects in what may be called the limiting cases, is seen by comparing Expts. I-A and IV-A. The advancing contact angle for I-A was 120° while the very coarse crystalline character of the surface of sample IV gave an advancing angle of 132° . Angles between 132° and 115° could be obtained by varying the dipping procedure and, thereby, the physical character of the surface.

The receding angles decreased with increasing surface roughness as can be seen by comparing Expts. IV-A and IV-B. Although the measurements for them are not shown, intermediate type surfaces gave receding angles between 97° and 110° .

Without exception, the surfaces described in Table I showed significant differences between the values of the advancing and receding angles. The magnitude of this hysteresis effect seemed, on the one hand, to be in proportion to the gross roughness of the surface, as illustrated by the $\Delta\theta$ value of 35° in Expt. IV-A. On the other hand, for surfaces formed under similar conditions the magnitude of hysteresis decreased with increasing purity of the paraffin, as illustrated by Expts. I-B and II-A, in which $\Delta\theta$ averages 9° , and Expt. IV-B in which $\Delta\theta$ is 5° . Although the factors of surface roughness and surface purity could not be quantitatively distinguished, it was evident that the purified material was characterized by the largest as well as by the smallest hysteresis effects depending upon the physical nature of the surface.

It can be observed that the contact angles for the samples listed in Table I increased very slightly with purification. Comparing surfaces similar as to conditions of formation, we find the following approximate values:

Commercial paraffins, contact angles, $\theta^a = 112^\circ$ and $\theta^r = 103^\circ$.

First purification product, contact angles, $\theta^a = 113^\circ$ and $\theta^r = 106^\circ$

Final purification product, contact angles, $\theta^a = 115^\circ$ and $\theta^r = 110^\circ$

The increase, however, is only of significant magnitude for the receding angles. The trend may be due to traces of polar impurities that are removed in purification with a resulting increase in the free energy of the water-paraffin interface.

The average values of the angles for each sample as given in the next to last column of Table I are found to fall within the range 106 – 114° despite the quite varied hysteresis effects. This indicates that the main factor or factors responsible for hysteresis operate to increase the advancing angles and to decrease the receding angles by about the same amounts. In Expts. IV-A and IV-B the hysteresis effects were 35° and 5° , respectively, yet the average angles were 114° and 113° .

The fairly good agreement between results obtained with the vertical-rod and drop-on-capillary-tip methods is shown by Expts. III-A and III-B. The tilting-plate method was found to give less reproducible results and to be more difficult to manipulate than the other methods.

Contact Angles on Surfaces of Purified Paraffins

The smallest hysteresis effect listed in Table I is 5° . This was for the purified material when the coating was as thin as could be produced by a

simple dipping technique. According to certain theories of hysteresis, one might consider the persistence of the hysteresis effect to be due to the presence of air which led either to a certain polar heterogeneity of the surface by trace oxidation on the surface or to an adsorption of constituents from the surroundings. A second explanation might be that surfaces formed from melts, under the best of conditions, were of sufficient thickness and crystallinity, or surface roughness, to give rise to a measurable hysteresis effect. To furnish information on these points the experiments presented in Table II were carried out.

In Expt. IV-*C* the tip in the contact-angle cell was coated with sample IV by causing a drop of this distillate, under 1 mm. pressure of purified nitrogen, to fall directly from the condenser tube onto the tip. This drop solidified to form a thin coat similar in appearance to that formed in Expt. IV-*B*. The cell was saturated with water vapor and the contact angle measured by the drop-on-capillary-tip method. In this experiment, at no time was the paraffin exposed to air. The measured contact angles of 114° and 110° agreed very well with the angles in air found in Expt. IV-*B*.

Further confirmation of the inertness of the paraffin was furnished by Expt. IV-*D*. A small lump of sample IV, broken from the mass that had been exposed to air for several days, was caused to flow over the tip in the evacuated contact-angle cell by the procedure outlined. After cooling, the cell was filled with pure nitrogen at 1 atm., saturated with water vapor, and the contact angles were measured. They were the same as before.

An evaporation technique was employed to investigate the wettability of films of paraffin thinner than those that could be produced from a melt. After placing a small lump of sample IV in the coil of resistance wire, the cell was sealed, evacuated, and a portion of the paraffin volatilized at a controlled rate by regulation of the current through the coil. That portion of the vapor striking the tip condensed thereon. A considerable amount of paraffin was volatilized in Expt. IV-*E*, the first carried out with this technique, and a fairly heavy coat was produced which, in contrast to a coat formed from a melt, was completely opaque and was amorphous and velvet-dull in appearance. A single determination of the contact angles showed a considerable hysteresis effect.

In the next experiment, IV-*F*, only a very small amount of paraffin was vaporized. The thinness of the film produced can be judged from the fact that the appearance of the tip was unaltered except for interference patterns seen when the surface was observed at an angle. An attempt to measure the contact angles on this surface by the drop-on-capillary-tip failed because the water extruded onto the tip instantly displaced the film. The experiment was repeated with success using the controlled-

drop-volume method. This was accomplished as follows: After the film was deposited, the cell was filled with nitrogen and saturated with water vapor. The top of the cell was broken off while a positive flow of water-saturated nitrogen was supplied. The long glass tube with the very fine capillary point used for this method was lowered into position above the film and the drop was formed. The averages of the measured angles were 112° advancing and 112° receding. That is to say, a film of purified paraffin prepared in this manner exhibited no measurable degree of hysteresis. A residual hysteresis of less than 1° would have remained undetected. Such a film was very fragile and, to avoid rupturing it, great care had to be taken in the placement and movement of the very small water drops.

The final experiments, outlined under IV-G, further confirmed the dependence of the hysteresis effect upon the character of the film. Angles as high as 140° and as low as 96° were recorded. When, however, the film was reduced in thickness to a few molecular diameters, the hysteresis effect disappeared. Since the measurements were carried out in the presence of air, it was established that the very thin films were, like thicker films, inert toward air, having the same contact angles in air as when surrounded by nitrogen. The practice was to measure the contact angles within a few minutes after the disposition of the film upon the glass plate. In one case a plate covered with a very thin film was allowed to age for 1 hr. in air at room temperature. The average of the advancing angles on this plate was $113 \pm 1^\circ$ and for the receding angles $110 \pm 2^\circ$. The optical appearance of this film had changed. It seems probable that surface crystallization was taking place.

Significance of the "Average" Contact Angle

Although the hysteresis effects on the purified paraffin varied in magnitude, the average angles for a number of the surfaces were nearly the same, 112° approximately. The concept of physical roughness of surface can be postulated to explain the relationship observed. Adam (7), Wenzel (8), Coghill and Anderson (9), and Cassie and Baxter (10) have discussed surface roughness from various points of view.

Roughness, which stems from the fundamentally crystalline nature of solids, is presumed to be the result of a complex variety of peaks, planes, edges, holes, and fissures, which altogether comprise the surface. Various orders of roughness, from the macroscopic, to the microscopic, to the submicroscopic, or even to the molecular, exist. Within limits it may be permissible to consider that along any line on the macroscopic plane surface of a given solid the same average roughness exists and that a liquid caused to advance across the solid surface, or to recede, can be considered to flow up and down the slopes of a continuous series of peaks and depressions. Any effect of the angle these slopes make with the hori-

zontal would be the effect of the resultant angle of all the actual irregularities.

If a liquid having a contact angle against a solid surface of, say, 60° for the case in which the surface was ideally plane and smooth is caused to advance over the same material in roughened form, say with a roughness angle of 15° , then the experimentally observed apparent angle should be 75° . If, on the other hand, the liquid is caused to recede, the observed apparent angle should be 45° . These are the two limiting conditions characteristic of the system which must be exceeded if movement of the liquid periphery is accomplished; all apparent angles between these values can exist. These predictions are based upon (a) the assumption that a true and single-valued equilibrium of surface forces exists at all times along the liquid-solid-gas line of contact; (b) the fact that the observed angle is measured from the macroscopic plane of the solid; and (c) the absence of other factors which might influence the hysteresis effect (adsorption, polar heterogeneity, liquid friction).

It is obvious that this simplified picture of physical roughness necessitates that the "average" angles, which are the arithmetic means of the pairs of advancing and receding angles for a given solid, be constant and be equal to the "true" angle. In the present work it was found that the contact angles of water against purified paraffin did give an average angle which was constant. In contrast, contact-angle data on many other systems have indicated that other factors, or additional factors, must be involved. The surfaces of solid, saturated hydrocarbons such as paraffin may, because of their complete and uniform nonpolar character, represent the limiting relationship between hysteresis of the contact angle and physical roughness.

SUMMARY

The experimental results show that when very thin films of purified paraffin were formed in vacuum by volatilization on smooth glass surfaces and water drops were placed upon them, the advancing and the receding contact angles were sensibly the same, 112° ; that is, hysteresis effects did not exist on these very thin and very smooth surfaces.

Measurable hysteresis effects from 5° to 35° were found for less smooth films, and coatings of appreciable thickness formed in vacuum, in nitrogen, or in air, whether from a melt or by volatilization.

The magnitude of the hysteresis effects appeared to be closely associated with the microscopic roughness of the surfaces, the roughness adding to the magnitude of the advancing angle but subtracting from the receding angle to the same degree, so that the average angle remained the same for paraffin films of different roughnesses but of the same degree of purification. The average contact angle for purified paraffin was slightly larger than the average angle for unpurified paraffin.

REFERENCES

1. FOWKES, F. M., AND HARKINS, W. D., *J. Am. Chem. Soc.* **62**, 3377 (1940).
2. THIESSEN, P. A., AND SCHOON, E., *Z. Elektrochem.* **46**, 170 (1940).
3. BARTELL, F. E., CULBERTSON, J. L., AND MILLER, M. A., *J. Phys. Chem.* **40**, 881 (1936).
4. ADAM, N. K., AND JESSOP, G., *J. Chem. Soc.* **127**, 1863 (1925).
5. BARTELL, F. E., AND ZUIDEMA, H. H., *J. Am. Chem. Soc.* **58**, 1449 (1936).
6. BARTELL, F. E., AND SMITH, J. T., *J. Phys. Chem.* **57**, 165 (1953).
7. ADAM, N. K., *The Physics and Chemistry of Surfaces*, 3rd Ed., p. 186. Oxford University Press, New York, 1941.
8. WENZEL, R. N., *Ind. Eng. Chem.* **28**, 988 (1936); *J. Phys. Chem.* **53**, 1466 (1949).
9. COGHILL, C. O., AND ANDERSON, C. O., *U. S. Bur. Mines Tech. Paper No. 262*, 47 (1923).
10. CASSIE, A. B. D., AND BAXTER, S., *Trans. Faraday Soc.* **40**, 546 (1944).

MECHANICAL AND ELECTRICAL RELAXATION DISTRIBUTION FUNCTIONS OF TWO COMPOSITIONS OF POLYVINYL CHLORIDE AND DIMETHYLTHIANTHRENE

John D. Ferry and Edwin R. Fitzgerald

Department of Chemistry, University of Wisconsin, Madison, Wisconsin

Received September 8, 1952

INTRODUCTION

It has been recognized for some time that the dynamic mechanical and electrical properties of polymers and their solutions must be related, since they both involve configurational changes of flexible molecules. Attempts have been made to correlate dielectric constant and dielectric loss, and their dependence on frequency and temperature, with mechanical measurements obtained under static conditions (1) or dynamic conditions at some arbitrary frequency (2,3). It is impossible, however, to draw conclusions about the relations between mechanical and electrical properties unless both types of data are available over wide ranges of frequency and temperature.

The dielectric measurements of Fitzgerald and Miller (4) and dynamic mechanical measurements of Fitzgerald and Ferry (5) provide for the first time the necessary information on two compositions of polyvinyl chloride and dimethylthianthrene: a gel containing 10% polymer by volume, and a plastic containing 40% by volume. These data have been briefly compared in a previous paper (5); there it was shown that the shifts of loss-tangent maxima with temperature were the same for both mechanical and electrical losses, but the magnitudes of the maxima were very much greater for the mechanical case. The present paper furnishes a more extensive analysis of the data. The temperature dependence of relaxation times is derived by the method of reduced variables (6). Distribution functions of relaxation times and retardation times are calculated and compared. Fundamental similarities and differences in the responses to mechanical and electrical stress are discussed.

APPLICATION OF THE METHOD OF REDUCED VARIABLES

On the assumption that the magnitudes of all elastic mechanisms are proportional to absolute temperature and density, and that all relaxation times depend identically on temperature, the following reduced variables G_p' and G_p'' should each yield a single composite curve for dynamic

mechanical measurements on an undiluted polymer, or a polymer solution or gel of constant composition (6,7):

$$G_p' = G' (T_0 \rho_0 / T \rho), \quad [1a]$$

$$G_p'' = G'' (T_0 \rho_0 / T \rho), \quad [1b]$$

$$\omega_p = \omega a_T. \quad [1c]$$

Here G' and G'' are the real and imaginary parts of the complex modulus of rigidity, and a_T is the factor by which all relaxation times are multiplied for a change in temperature from T_0 to T ; ρ_0 and ρ are the densities at T_0 and T , and ω is the circular frequency. The subscript p denotes reduction to a reference state for the actual composition at T_0 (in contrast to the subscript r which is used (6) for a hypothetical reference state of unit density and unit viscosity at T_0 , in connection with polymer solutions). The corresponding equations for compliance are

$$J_p' = J' (T \rho / T_0 \rho_0), \quad [2a]$$

$$J_p'' = J'' (T \rho / T_0 \rho_0), \quad [2b]$$

$$\omega_p = \omega a_T, \quad [2c]$$

where $J' - iJ'' = 1/(G' + iG'')$. In this case a_T is a factor expressing the change in all *retardation* times; it is identical with that of Eq. [1c].

Extension of Reduced Variables to the Transition Region

At frequencies sufficiently high that configurational changes in the flexible molecules are slight and the consistency of the polymer approaches that of a hard glass, it is obvious both theoretically and, as it turns out, experimentally that the factor T/T_0 should not be used to reduce J' . It is the configurational elasticity which is proportional to T (compliance inversely proportional), and if this is not operative the so-called ordinary elasticity changes very slightly with temperature in the opposite direction. It is necessary, therefore, to provide a somewhat more complicated method for reducing dynamic mechanical data in the frequency range of transition from rubbery to glassy consistency. This can be achieved by supposing that the compliance is the sum of a glassy compliance, J_∞ , which is attained at high frequencies and is independent of temperature, and a series of configurational compliances which conform to the assumptions stated above. The use of such a separate term, J_∞ , is common in most discussions of viscoelastic properties (8,9). In this case, $J_p' = J_\infty + (J' - J_\infty) (T \rho / T_0 \rho_0)$. By rearrangement, the reduction equations take the following form:

$$J_p' = J' [T \rho / T_0 \rho_0 + (J_\infty / J') (1 - T \rho / T_0 \rho_0)], \quad [3a]$$

$$J_p'' = J'' (T \rho / T_0 \rho_0). \quad [3b]$$

For this purpose, J_∞ must be known, but only roughly. When J_∞/J' is small, the reduction factor in Eq. [3a] is the same as that in [2a]; when J_∞/J' approaches unity, the reduction factor approaches unity, as it should. It should be noted that J_p''/J_p' is equal to J''/J' as long as $J' \gg J_\infty$, but this is not true in the transition region where J' approaches J_∞ in magnitude.

Because this reduction method cannot be applied directly to G' and G'' , and also because compliance rather than rigidity is analogous to

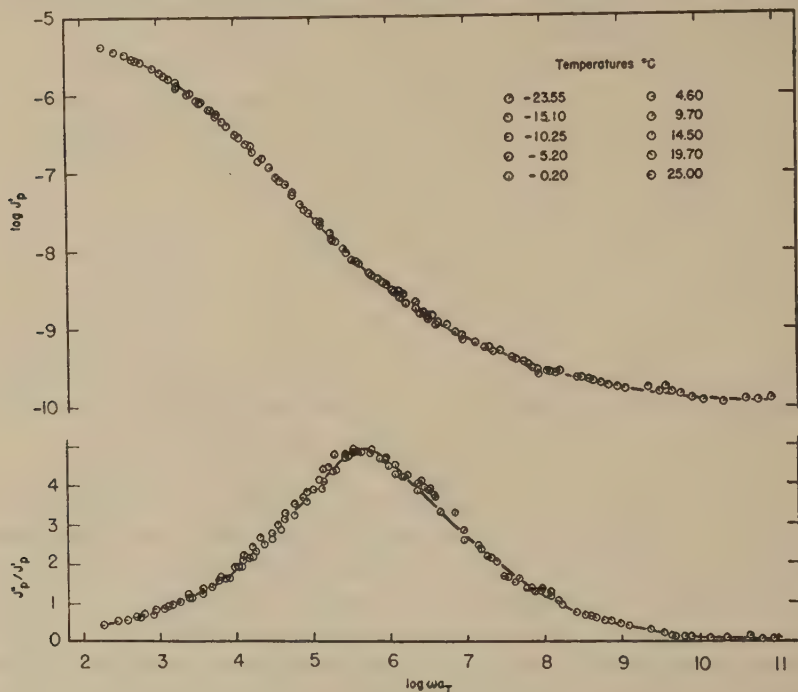


FIG. 1. Logarithm of reduced dynamic compliance J_p' and loss tangent J_p''/J_p' plotted against reduced frequency for 10% gel of polyvinyl chloride in dimethylthianthrene at ten different temperatures identified as shown. (Compliance in sq. cm./dyne)

dielectric constant, the mechanical data are treated here in terms of J' and J'' rather than the more familiar rigidities.

Reduced Variables for the Dielectric Constant

The orientation polarization is inversely proportional to the absolute temperature, and, to the extent that the polarization is a linear function of the dielectric constant (10), the temperature dependence of individual contributions to the dielectric constant associated with molecular configurational changes is therefore exactly analogous to the case of mechanical compliance. However, the density dependence is opposite; the more

molecules per unit volume, the *less* the mechanical compliance, but the *greater* the electrical polarization. For the sake of simplicity, we assume the orientation contributions to the dielectric constant to be directly proportional to the density, leading to the reduction factor $T\rho_0/T_0\rho$ instead of $T\rho/T_0\rho_0$. (Actually, the density ratio is never very far from unity.) Finally, the limiting dielectric constant at high frequencies, ϵ_∞ , is analogous to J_∞ in being independent of temperature (except for the slight influence of the change of density with temperature, which in the case of ϵ_∞ is ignored here). The reduction equations for the real and imaginary

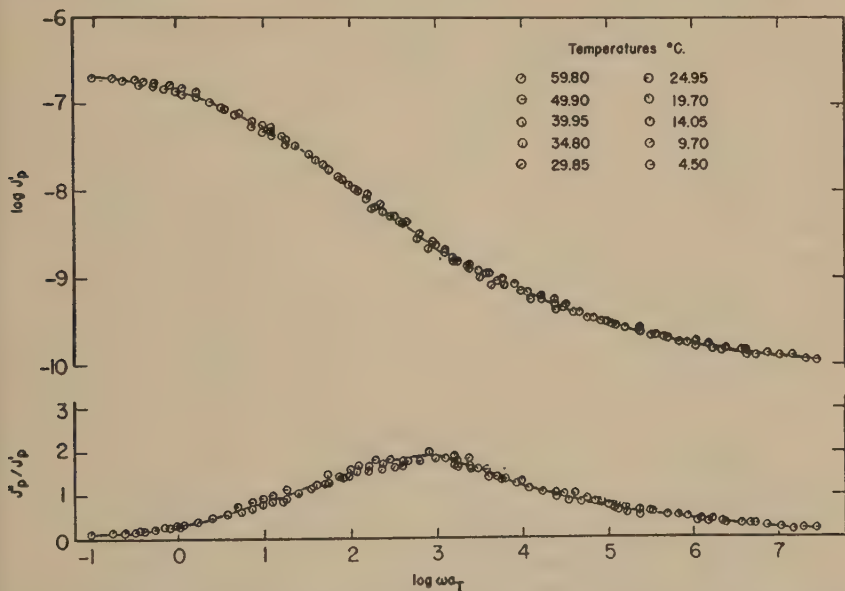


FIG. 2. Logarithm of reduced dynamic compliance J_p' and loss tangent J_p''/J_p' plotted against reduced frequency for 40% plastic of polyvinyl chloride in dimethylthianthrene at ten different temperatures identified as shown. (Compliance in sq. cm/dyne)

parts of the dielectric constant, ϵ' and ϵ'' , are therefore:

$$\epsilon_p' = \epsilon' [T\rho_0/T_0\rho + (\epsilon_\infty/\epsilon') (1 - T\rho_0/T_0\rho)], \quad [4a]$$

$$\epsilon_p'' = \epsilon'' (T\rho_0/T_0\rho), \quad [4b]$$

$$\omega_p = \omega b_T, \quad [4c]$$

where b_T is the factor by which all electrical relaxation times are multiplied for a change in temperature from T_0 to T .

Application to Experimental Data

Equations [3] were applied to dynamic mechanical data (5) on a gel of polyvinyl chloride in dimethylthianthrene containing 10% polymer by

volume over frequency and temperature ranges of 30 to 5000 cycles/sec. and -23 to $+25^{\circ}\text{C}.$, respectively; and on a plastic containing 40% polymer by volume over ranges of 30 to 5000 cycles/sec. and 5 – $60^{\circ}\text{C}.$ For reduction of J' , the value of J_{∞} was estimated from the measurements at lowest temperatures and highest frequencies to be $10^{-9.95}$ sq. cm./dyne for both compositions. The values of a_T for reduction to $25^{\circ}\text{C}.$ were obtained empirically by trial shifts of plots of J_p' , or J_p''/J_p' , against the

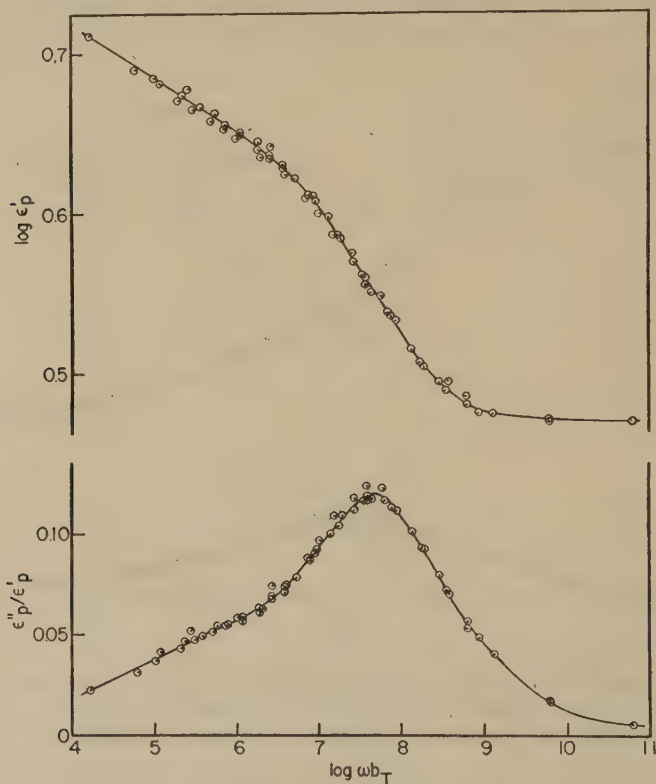


FIG. 3. Logarithm of reduced dielectric constant ϵ_p' and loss tangent ϵ_p''/ϵ_p' plotted against reduced frequency for 10% gel of polyvinyl chloride in dimethylthianthrene at seven different temperatures. Pip upper left, $-20^{\circ}\text{C}.$; successive 45° rotations counter-clockwise, -15° , -10° , -5° , 0° , 5° , 10° .

logarithm of the frequency. The results are shown in Figs. 1 and 2, where $\log J_p'$ and J_p''/J_p' are plotted against the logarithm of the reduced frequency. The same choice of a_T makes both the real part and the imaginary to real ratio conform to single composite curves, showing that all the mechanical retardation times have the same temperature dependence.

Equations [4] were applied to dielectric data (4) on the same compositions: the 10% gel over ranges from 15 to 15,000 cycles/sec. and -20

to $+10^\circ\text{C.}$, respectively; and the 40% plastic from 60 to 10,000 cycles/sec. and $5\text{--}60^\circ$, respectively. The value of ϵ_∞ was taken as 2.79 for both compositions. This is identical with the square of the refractive index of the pure solvent at 25°C. The values of b_T were determined empirically. To reduce the data for the gel from the highest temperature of measure-

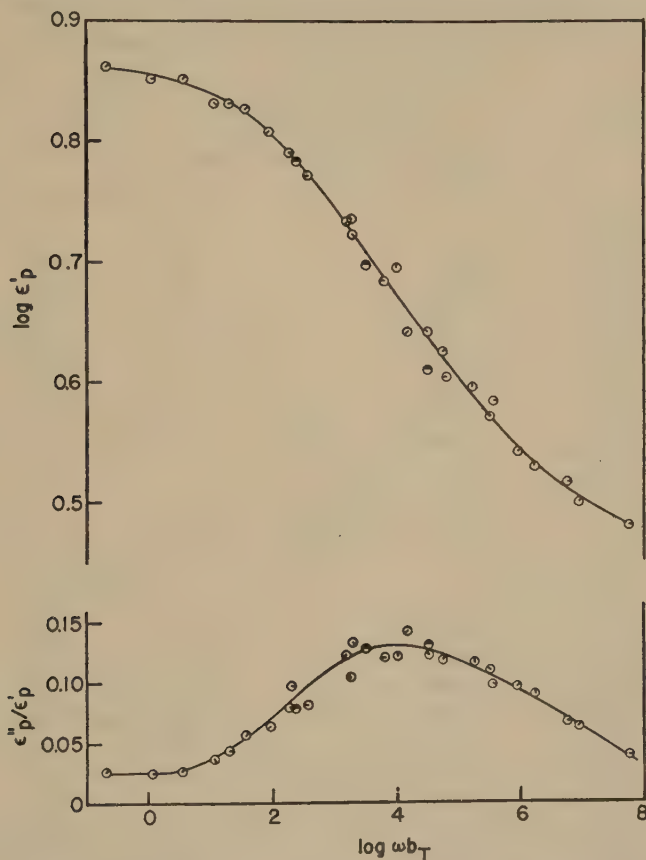


FIG. 4. Logarithm of reduced dielectric constant ϵ'_p and loss tangent ϵ''_p/ϵ'_p plotted against reduced frequency for 40% plastic of polyvinyl chloride in dimethylthianthrene at ten different temperatures. Pip right, 5°C. ; successive 45° rotations counterclockwise, 10° , 15° , 20° , 25° , 31° ; pip lower left, 40° ; successive 45° rotations counterclockwise, 50° , 60° ; half shaded, 28° .

ment, 10° , up to 25°C. , the value of a_T for 10° from the mechanical data was employed—a procedure well justified by conclusions to be drawn below. The results are shown in Figs. 3 and 4, where $\log \epsilon'_p$ and ϵ''_p/ϵ'_p are plotted against the logarithm of the reduced frequency. Again the conformity of both real part and of imaginary to real ratio to the single

composite curves shows that all the electrical relaxation times have the same temperature dependence.

The values of a_T and b_T are listed in Table I and plotted in Fig. 5 against the reciprocal absolute temperature. It is a striking conclusion that for each polymer composition the values of a_T and b_T are identical. Thus the mechanical retardation (and relaxation) and the electrical relaxation processes have the same temperature dependence.

TABLE I
Reduction Factors

Ten per cent polyvinyl chloride

Temp. °C.	Mechanical log a_T	Temp. °C.	Electrical log b_T
-23.55	7.03	-20	6.00
-15.10	5.30	-15	5.00
-10.25	4.40	-10	4.15
- 5.20	3.60	- 5	3.49
- 0.20	2.80	0	2.79
4.60	2.25	5	2.21
9.70	1.55	10	1.64
14.50	1.00		
19.70	0.49		
25.00	0		

Forty per cent polyvinyl chloride

Temp. °C.	Mechanical log a_T	Temp. °C.	Electrical log b_T
4.50	3.06	5	2.95
9.70	2.24	10	2.15
14.05	1.48	15	1.42
19.70	0.69	20	0.70
24.95	0	25	0
29.85	-0.62	28	-0.30
34.80	-1.20	31	-0.62
39.95	-1.78	40	-1.52
49.90	-2.88	45	-2.02
59.80	-3.31	50	-2.50
		60	-3.25

Although the curves in Fig. 5 are far from linear, the apparent activation energies for relaxation, ΔH_a , may be calculated at various temperatures, as in the treatment of temperature dependence of viscosity of polymers (11). The results of such calculations are shown in Fig. 6, together with values of the apparent activation energy for viscous flow of the pure solvent calculated from viscosity measurements (4). The activation energies for relaxation and flow are closely related (7) and should differ by only the order of 0.5 kcal. in this temperature range.

The apparent activation energy increases markedly with decreasing temperature, just as does the activation energy for flow in polymers (11) and liquids of low molecular weight (12) or the activation energy for dielectric orientation in liquids (13) when a glass transition is approached. It is of particular interest that the curves for the pure solvent, which itself goes into a glass transition below $-20^{\circ}\text{C}.$, and the 10% gel are so closely similar. Thus the *temperature dependence* of the properties of the the gel is determined almost wholly by the solvent.

The curves of Figs. 1-4 represent predictions of the mechanical and electrical properties of the 10% gel and 40% plastic at $25^{\circ}\text{C}.$ over very

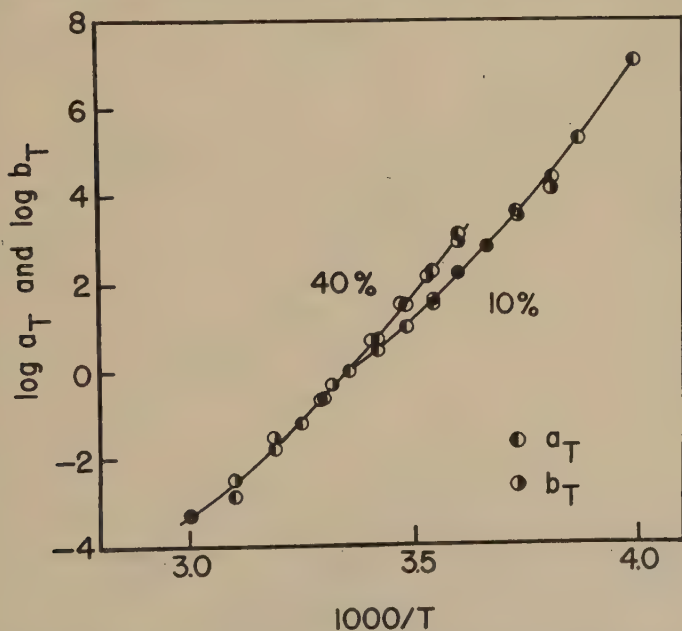


FIG. 5. Frequency reduction factors a_T (mechanical) and b_T (electrical) plotted against reciprocal absolute temperature for two polyvinyl chloride compositions.

extended frequency ranges. In spite of the identity of temperature dependence, there is no obvious correlation between the mechanical and electrical properties themselves, other than the existence of dispersion in both. The magnitudes of the loss tangents are much greater in the mechanical case, as previously noted from examination of the original data (5), and the electrical maximum occurs at a frequency which is higher by two or more powers of ten than that of the mechanical maximum. The real part of the elastic compliance ranges over several powers of ten, whereas the real part of the dielectric constant ranges over only a factor of about two. These differences are partly due to the fact that in the dielectric case the

frequency-independent (optical) contribution is a much higher proportion of the total, but there are more fundamental differences which are revealed by the distribution functions of relaxation times, as described below.

Since the real and imaginary parts of the complex modulus of rigidity, G' and G'' , are somewhat more familiar than J' and J'' , the reduced mechanical data for the 10% composition are plotted in this form in Fig. 7, together with the real part of the complex dynamic viscosity, η' ($= G''/\omega$). The static rigidity, determined in a coaxial cylinder appa-

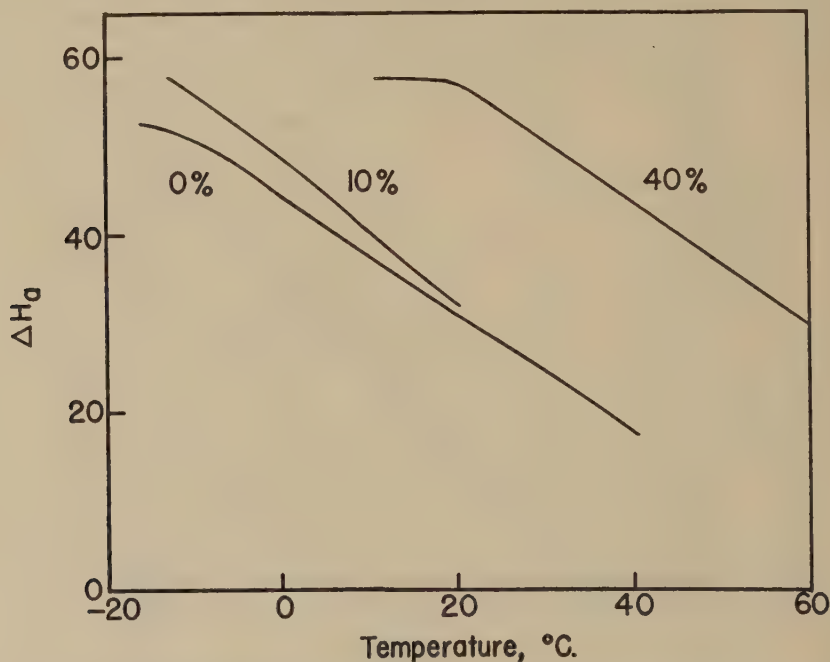


FIG. 6. Apparent energy of activation for relaxation in two polyvinyl chloride compositions (10 and 40%), and for viscous flow in dimethylthianthrene (0%), plotted against temperature.

ratus (14) as $10^{4.97}$ dynes/sq. cm., is also shown. At low frequencies G' should approach this value, and it appears likely that it will do so.

The static rigidity depends on the number of effective cross-links represented by the crystallites which form a permanent three-dimensional network in a polyvinyl chloride gel or plastic (15). However, the dynamic properties (except at very low frequencies) are believed (5) to be determined primarily by the amorphous regions, which comprise most of the polymer mass; just as in butyl rubber, for example, where the dynamic properties in the frequency range corresponding to the transition from

rubbery to glassy consistency differ very little from those of polyisobutylene (7), which possesses no cross-links at all.

It is of particular interest that η' varies so little with frequency, being of the order of 10^2 poises over a considerable range. The viscosity of the pure solvent is about 10 poises at 25°C. (4).

DISTRIBUTION FUNCTIONS

The distribution function of mechanical relaxation times, $\Phi d \ln \tau$, representing the differential contribution to instantaneous rigidity associated

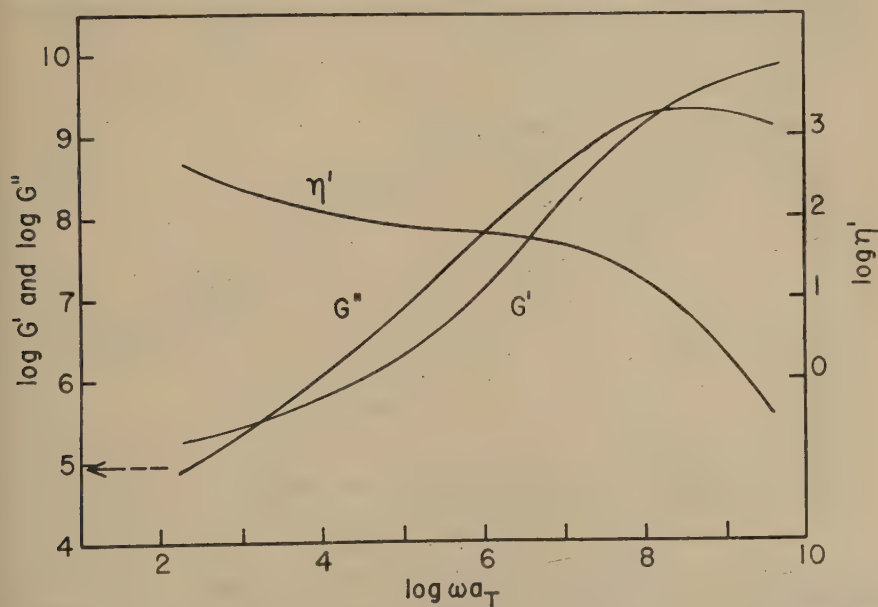


FIG. 7. Real and imaginary parts of the complex rigidity, and real part of the complex viscosity, for the 10% polyvinyl chloride gel, all reduced to 25°C. Arrow denotes static rigidity.

with relaxation times whose logarithms lie between $\ln \tau$ and $\ln \tau + d \ln \tau$, may be calculated from the following second-approximation equations (16):

$$\Phi(\tau = 1/\omega) = AG' (d \log G' / d \log \omega), \quad [5a]$$

$$\Phi(\tau = 1/\omega) = BG'' (1 - |d \log G'' / d \log \omega|). \quad [5b]$$

Here A and B are numerical factors which depend upon m , the negative slope of a logarithmic plot of Φ against τ determined from a first-approximation calculation. (The use of the absolute value of $d \log G'' / d \log \omega$ in Eq. [5b] is a recent improvement (17), which must be associated with the use of $|m|$ to determine the value of B from the previously published table.) Values of Φ , reduced to 25°, calculated thus from data interpolated

from the curves of Fig. 7 and similar curves for the 40% plastic, are shown in Fig. 8, plotted logarithmically. The agreement between the calculation from G' and that from G'' is gratifying and represents an internal test of the accuracy of the experimental data as well as the method of calculation. The distribution functions for the two compositions are similar in shape, though that for the 40% plastic is somewhat broader; and the latter lies in a time region higher by several powers of ten than that of the 10% gel.

As mentioned previously, it is the compliance, rather than the rigidity, which is analogous to the dielectric constant, representing a measure of

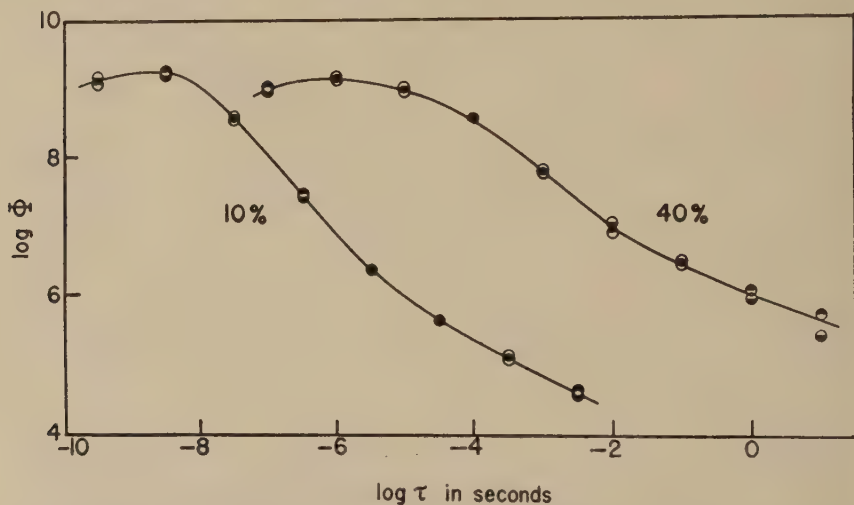


FIG. 8. Distribution functions of mechanical relaxation times for two polyvinyl chloride compositions, reduced to 25°C. Top shaded, calculated from G' ; bottom shaded, calculated from G'' .

the ease rather than the difficulty of molecular configurational changes under applied forces. Hence the function which has long been known in the dielectric literature as the distribution function of electrical relaxation times (18) cannot be compared with the distribution function of mechanical relaxation times but rather with what is usually called the distribution of mechanical *retardation* times (9).¹ The terminology is confusing but too well established to change.

The function $Ld \ln \tau$, representing the differential contribution to static (or steady-state) compliance associated with retardation times

¹ Alternatively, a distribution function can be calculated from the electrical elastivity or a related quantity, for comparison with the distribution of mechanical relaxation times, as mentioned in an earlier abstract (19). However, this introduces a wholly unfamiliar concept.

whose logarithms lie between $\ln \tau$ and $\ln \tau + d \ln \tau$, is obtained from the following second-approximation equations (17):

$$L(\tau = 1/\omega) = -AJ'(d \log J'/d \log \omega), \quad [6a]$$

$$L(\tau = 1/\omega) = BJ''(1 - |d \log J''/d \log \omega|). \quad [6b]$$

The factors A and B are the same as those appearing in Eqs. [5]; the value of m which determines them is the positive slope of a logarithmic plot of L against τ .

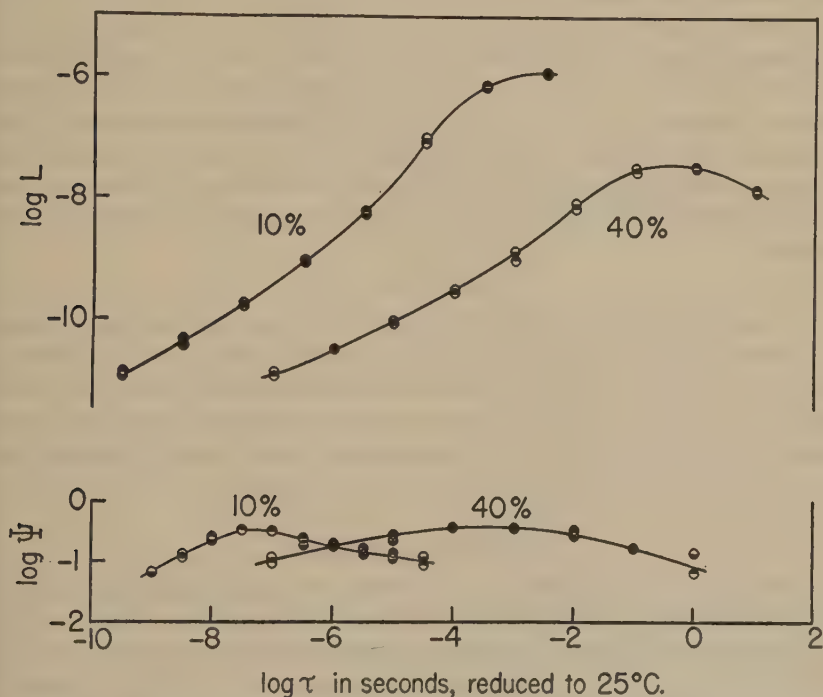


FIG. 9. Distribution functions of mechanical retardation times and electrical relaxation times for two polyvinyl chloride compositions, reduced to 25°C. Top shaded, calculated from real part of J or ϵ ; bottom shaded, calculated from imaginary part of J or ϵ .

The corresponding equations for $\Psi d \ln \tau$, the differential contribution to static dielectric constant associated with relaxation times in the usual logarithmic range, are as follows (17):

$$\Psi(\tau = 1/\omega) = -A\epsilon'(d \log \epsilon'/d \log \omega), \quad [7a]$$

$$\Psi(\tau = 1/\omega) = B\epsilon''(1 - |d \log \epsilon''/d \log \omega|). \quad [7b]$$

The value of m which determines the factors A and B is the slope of a logarithmic plot of Ψ against τ .

Values of L and Ψ calculated from interpolated data of Figs. 1-4, and corresponding to the reduced temperature of 25°C., are plotted logarithmically in Fig. 9. Again there is very satisfactory agreement between the calculations from the real and imaginary parts. (This agreement is not attained without the second-approximation factors; the dielectric distribution, in particular, is much improved by these corrections.)

Like Φ , the function L is broader for the 40% than for the 10% composition, and lies at longer times. The Ψ functions for the two compositions are similarly related.

In comparing Ψ with L , it is seen that the electrical distribution is very much broader than the mechanical. The absolute magnitudes of these functions provide no basis for comparison, of course, since they represent different physical quantities with different dimensions. The logarithmic plots show, however, that relatively Ψ varies by only a factor of 5 over a frequency range where L varies over 10^4 to 10^5 . The maxima in the L functions lie at much longer times than the maxima in the Ψ functions.

DISCUSSION

The use of reduced variables permits description of either mechanical or electrical properties by two master functions²—one a function of time, L or Φ or Ψ , and the other a function of temperature, a_T or ΔH_a . The degree of variation of observed mechanical or electrical properties with temperature will depend on the steepness of both these functions. For purposes of interpretation it is highly advantageous to be able to discuss them separately.

Temperature Dependence

The equivalence of temperature dependence for dielectric relaxation and viscous-flow processes has been shown by several investigators (21, 13, 4); and similarly the equivalence of temperature dependence for mechanical relaxation and viscous-flow processes (6,7,22,23). Figure 5 now shows directly the identity for mechanical and electrical processes. All three processes are evidently closely related.

The strong temperature dependence of the apparent activation energy, shown in Fig. 6, is no doubt caused by the rapid relative decrease in free volume as the glass-transition temperature is approached, as discussed by Fox and Flory (11). It may be inferred by comparison of the curves of Fig. 6 that the presence of 10% of polyvinyl chloride alters the free volume of the solvent only slightly, whereas 40% reduces it considerably and causes the glass transition to occur at a higher temperature. Direct measurements of the glass-transition temperatures are not yet available.

² The use of two master functions has also been emphasized recently by Tobolsky (20). For the dependence on time he uses stress relaxation rather than a distribution function.

In any case, the temperature dependence of all the processes considered here is probably largely determined by the free volume, and therefore the local structure of the solution, which in turn depends largely on the solvent. These relations may be responsible for the correlations reported between plasticizing effectiveness and plasticizer viscosity (24).

Mechanical Distributions

The dependence of mechanical properties on time can be expressed by either Φ or L , and in fact these functions are explicitly related (25), though in a complicated manner which makes direct interconversion difficult. For comparison with mechanical properties of other polymers, Φ is the more useful, since the extensive existing data on stress relaxation (20,26) can be readily expressed in this form.

From stress-relaxation measurements in the transition region, between rubbery and glassy consistency, Tobolsky has recently shown that the relaxation functions (stress/strain ratio following sudden strain) of two very dissimilar polymers, polymethyl methacrylate and a GR-S vulcanizate, are quite similar in shape but widely separated in time scale (20). For convenience in comparing their properties, he has introduced a characteristic relaxation time K at which the relaxation function attains a value equal to the geometric mean of the moduli characteristic of the glassy and rubbery consistencies. It is of interest to compare the Φ functions from Fig. 8 with similar functions derived from Tobolsky's relaxation curves.

The latter³ were converted to Φ by the formula $\Phi = -(M/3)dE(t)/d \ln t$, where M is a second-approximation factor (16), $E(t)$ is the stress/strain ratio in elongation reduced to a standard temperature, and the factor of 3 is the ratio of elongation modulus to shear modulus. (This value will be 3 over most of the range of consistency; at the glassy end, Poisson's ratio may be as low as 0.3 and the above value may thus drop to 2.6, but on a logarithmic scale this difference is slight.) Neither of Tobolsky's curves can be reduced to 25°C., one being at much higher and one at much lower temperatures, but by plotting $\log \Phi$ against $\log (t/K)$ the shapes of the functions can be compared without considering the absolute time scale. From the definition of K , it can be shown that the value of τ at which Φ is the geometric mean of the moduli of rigidity in the glassy and rubbery states is equal to K except for a small correction. On this basis, $\log K$ in seconds at 25°C. was estimated to be -6.5 for the 10% polyvinyl chloride gel and -3.6 for the 40% plastic; and for polyisobutylene, also included for comparison, -6.0 .

³ We are indebted to Professor Tobolsky for large-scale copies of his figures, from which numerical values were interpolated.

The distribution function $\log \Phi$ is plotted in Fig. 10 against $\log \tau/K$ for all five of these systems, the polyisobutylene curve being taken from data from this laboratory on a sample supplied by the National Bureau of Standards (27). They are all similar in shape except for the 10% polyvinyl chloride, which is sharper. The GR-S rubber is somewhat sharper than the polymethyl methacrylate (as is apparent (20) from the relaxation data), and the 40% polyvinyl chloride and the polyisobutylene are intermediate between these. Evidently, except for minor differences, the shape of the relaxation distribution function and the molecular processes which underlie it are characteristic of flexible molecules and do not depend on their chemical composition—whether polar or nonpolar; whether uncross-

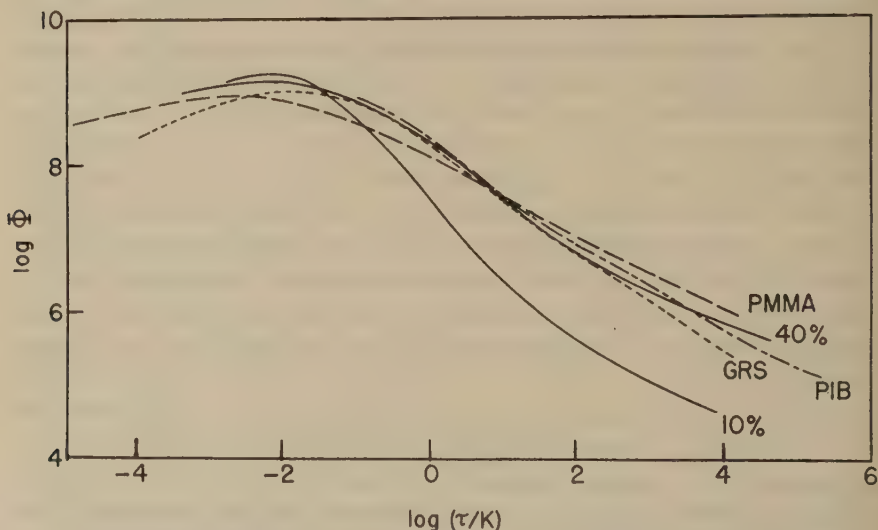


FIG. 10. Comparison of mechanical relaxation distribution functions of five polymer systems.

linked, cross-linked by primary bonds, or cross-linked by crystalline regions; or, within a wide range, whether diluted by solvent.

Electrical Distributions

The complex plane plot of Cole and Cole (28) has been widely used to represent dielectric dispersion of both polymer systems and liquids of low molecular weight. Data interpolated from Figs. 3 and 4 are so plotted in Fig. 11. The results for the 40% plastic are quite well represented by a circular arc whose center lies below the real axis, as found for several other concentrated polymer systems (1). Those for the 10% gel deviate from such an arc at high dielectric constants, however.

The circular arc implies a certain analytical form for the function (29). Another analytical expression is given by the theory of Kirkwood and Fuoss (30): $\Psi = 4 \Psi_0(\tau/\tau_0)/(1 + \tau/\tau_0)^2$, where Ψ_0 is the maximum value and τ_0 is the corresponding value of τ . The latter expression gives a curve symmetrical about $\log \tau_0$ which is somewhat sharper than the experimental curve for the 10% composition in Fig. 9 and considerably sharper than that of the 40% composition. These comparisons are similar to those made by Fuoss on mixtures of polyvinyl chloride and biphenyl (29). They are difficult to interpret in the present case, however, because dielectric measurements at other polymer concentrations in dimethylthianthrene (4) show that the solvent is contributing appreciably to the polarization and that both its orientation and that of the polymer are strongly influenced by mutual interaction.

Comparison of Mechanical and Electrical Distributions

The functions L and Ψ are independent of the values of J_∞ and ϵ_∞ , and the fact that the latter is a much higher proportion of the total

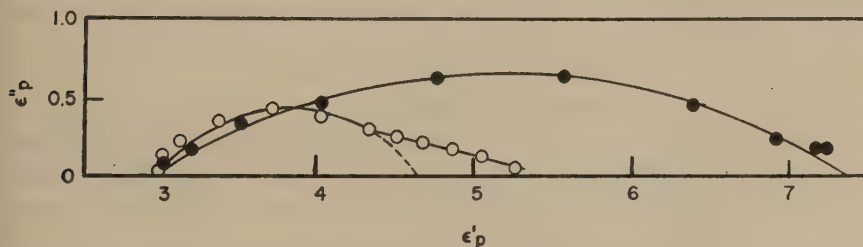


FIG. 11. Cole plots of data of Figs. 3 and 4, with centers of arcs as follows: 10% gel (open circles), (3.80, -0.57); 40% plastic (solid circles), (5.15, -3.46).

response than the former does not influence comparison of the distribution functions as it does, for example, the loss tangents. The observations that the maximum of L lies far to the right of the maximum of Ψ , and the left side of the L curve is far steeper than that of Ψ , both mean that short-time mechanisms contribute relatively less to L than to Ψ .

Kirkwood has shown that the electrical and mechanical distributions⁴ should be identical for a cross-linked system in which mechanical stress is applied only to the ends of network strands (31). However, in brief deformations stresses act all along the strands; and, for an assembly of chains with an assortment of effective lengths, the individual electrical and mechanical contributions do not add up in the same way.

⁴ The mechanical relaxation-time distribution function of Kirkwood corresponds to our retardation-time distribution; his $\Phi(\tau)$ is equal to $L/\tau J_0$, where J_0 is the static compliance.

Electrically, the magnitude of the maximum polarization does not depend on chain length, and the maximum contributions of individual molecules (per unit mass) are the same. Thus, for example, the static dielectric constant is independent of molecular weight; and the shape of the distribution function Ψ is actually quite insensitive to molecular-weight distribution, as shown by both theory and experiment (30,29).

Mechanically, on the other hand, the maximum contribution of an individual chain (per unit mass) to the compliance is directly proportional to its length. Thus, for example, the equilibrium compliance of a cross-linked rubbery polymer is directly proportional to the average chain length between cross-links. Therefore the distribution function L , unlike Ψ , is strongly influenced by the assortment of effective chain lengths. In the transition region between rubbery and glassy consistency, these lengths have little or nothing to do with the spacing of permanent cross-links or whether there are any cross-links at all (7) (cf. Fig. 10); they are related to various modes of coordinated motion of the chains, as analyzed by Rouse (32). The influence of the distribution of effective lengths is qualitatively what would be expected; the compliance contributions with short relaxation times are relatively smaller than the corresponding polarization contributions, and as a result L falls off far more rapidly with decreasing τ than does Ψ .

Thus the data analyzed here reveal a fundamental difference between the mechanical and electrical distribution functions. Further quantitative interpretation is complicated by the polar nature of the solvent. It would be of great interest to compare the two functions, for a polar polymer should be studied in a non-polar solvent.

ACKNOWLEDGMENTS

This work was supported in part by a grant from Research Corporation, and in part by the Research Committee of the Graduate School of the University of Wisconsin from funds supplied by the Wisconsin Alumni Research Foundation. Since March, 1951, these investigations have been part of a program of research on the physical structure and properties of cellulose derivatives and other polymers supported by the Allegany Ballistics Laboratory, Cumberland, Maryland, an establishment owned by the United States Navy and operated by the Hercules Powder Company under Contract NOrd 10431.

SUMMARY

Dynamic mechanical and electrical data on two compositions of polyvinyl chloride and dimethylthianthrene, containing 10% and 40% polymer by volume, covering a wide range of frequencies and temperatures, have been treated by the method of reduced variables. The reduced real part of the complex compliance and the reduced mechanical loss tangent fall on single composite curves when the frequency scale is reduced by a temperature-dependent factor a_T . The reduced real part of the dielectric

constant and the reduced electrical loss tangent fall on single composite curves when the frequency scale is reduced by a temperature-dependent factor b_T . The factors a_T and b_T are identical, but the mechanical and electrical composite curves are very different. The apparent activation energy for mechanical and electrical relaxation increases rapidly with decreasing temperature, and the values for the 10% polymer composition are not far from those for the apparent activation energy for viscous flow of the solvent. The frequency-dependent properties have been expressed as distribution functions of mechanical relaxation and retardation times and of electrical relaxation times. The mechanical relaxation distribution for the 10% composition is sharper and lies at shorter times than that for the 40% composition. The latter is similar in shape to distributions in the transition range between soft and glassy consistency for several other widely different polymer systems. The maximum in the mechanical retardation distribution is, for each composition, at a much longer time than the maximum in the electrical relaxation distribution, and the mechanical curves are much steeper on the short-time side of the maximum. It is concluded that the mechanical properties are strongly influenced by a distribution of effective chain lengths.

REFERENCES

1. FUOSS, R. M., *J. Am. Chem. Soc.* **63**, 378 (1941).
2. PONOMAREV, L. T., *J. Tech. Phys.* (U. S. S. R.) **10**, 588 (1940).
3. NIELSEN, L. E., BUCHDAHL, R., AND LEVREAU, R., *J. Applied Phys.* **21**, 607 (1950).
4. FITZGERALD, E. R., AND MILLER, R. F., *J. Colloid Sci.* **8**, 148 (1953).
5. FITZGERALD, E. R., AND FERRY, J. D., *J. Colloid Sci.* **8**, 1 (1953).
6. FERRY, J. D., *J. Am. Chem. Soc.* **72**, 3746 (1950).
7. FERRY, J. D., FITZGERALD, E. R., JOHNSON, M. F., AND GRANDINE, L. D., JR., *J. Applied Phys.* **22**, 717 (1951).
8. ALEKSANDROV, A. P., AND LAZURKIN, Y. S., *Acta Physicochim. U. R. S. S.* **12**, 647 (1940).
9. ALFREY, T., *Mechanical Behavior of High Polymers*. Interscience Publishers, New York, 1948.
10. WYMAN, J., JR., *J. Am. Chem. Soc.* **58**, 1482 (1936).
11. FOX, T. G., JR., AND FLORY, P. J., *J. Applied Phys.* **21**, 581 (1950).
12. TAMMANN, G., AND HESSE, W., *Z. anorg. allgem. Chem.* **156**, 245 (1926).
13. DAVIDSON, D. W., AND COLE, R. H., *J. Chem. Phys.* **19**, 1484 (1951).
14. HECKLER, G. E., Ph.D. Thesis, University of Wisconsin, 1952.
15. ALFREY, T., WIEDERHORN, N., STEIN, R., AND TOBOLSKY, A. V., *Ind. Eng. Chem.* **41**, 701 (1949).
16. FERRY, J. D., AND WILLIAMS, M. L., *J. Colloid Sci.* **7**, 347 (1952).
17. WILLIAMS, M. L., AND FERRY, J. D., *J. Polymer Sci.* (submitted).
18. WAGNER, K. W., *Ann. Physik* **40**, 817 (1913).
19. FERRY, J. D., AND FITZGERALD, E. R., *Phys. Rev.* **86**, 645 (1952).
20. BISCHOFF, J., CATSIFF, E., AND TOBOLSKY, A. V., *J. Am. Chem. Soc.* **74**, 3378 (1952).
21. KOBOKO, P. P., KUVSHINSKII, E. V., AND SHISHKIN, N., *Tech. Phys. U. S. S. R.* **5**, 413 (1938).

22. DAHLQUIST, C. A., AND HATFIELD, M. R., *J. Colloid Sci.* **7**, 253 (1952).
23. LEADERMAN, H., AND SMITH, R. G., *Phys. Rev.* **81**, 303 (1951).
24. JONES, H., *Trans. Inst. Rubber Ind.* **21**, 298 (1946).
25. GROSS, B., AND PELZER, H., *J. Applied Phys.* **22**, 1035 (1951).
26. McLOUGHLIN, J. R., AND TOBOLSKY, A. V., *J. Colloid Sci.* **7**, 555 (1952).
27. FITZGERALD, E. R., GRANDINE, L. D., JR., AND FERRY, J. D., *J. Applied Phys.* (in press).
28. COLE, K. C., AND COLE, R. H., *J. Chem. Phys.* **9**, 341 (1941).
29. FUOSS, R. M., *J. Am. Chem. Soc.* **63**, 2401 (1941).
30. KIRKWOOD, J. G., AND FUOSS, R. M., *J. Chem. Phys.* **9**, 329 (1941).
31. KIRKWOOD, J. G., *J. Chem. Phys.* **14**, 51 (1946).
32. ROUSE, P. E., JR., *J. Chem Phys.* (submitted).

VISCOSITY AND INITIAL PHASE SEPARATION STUDIES ON SOLUTIONS OF CELLULOSE ACETATE

W. R. Moore and J. Russell

Department of Chemistry and Dyeing, Technical College, Bradford, England

Received September 5, 1952

INTRODUCTION

This paper presents the results of viscosity and initial phase separation studies on solutions of cellulose acetate and attempts to relate them to solvent power and some properties of the solvent. While relationships between solvent power and the viscosities of dilute solutions of flexible, predominantly nonpolar polymers are well established (1,2), similar relationships are less definite in cases involving polar and less flexible polymers such as cellulose derivatives. Thus, the value of k' in the Huggins equation (3),

$$\eta_{sp}/c = [\eta] + k'[\eta]^2c$$

where η_{sp} is the specific viscosity, c the concentration, and $[\eta]$ the intrinsic viscosity, does not appear to decrease with increasing solvent power. Spurlin, Martin, and Tennent (4), using ethyl cellulose, found the slope of the Martin equation,

$$\ln(\eta_{sp}/c) = \ln[\eta] + k[\eta]c$$

divided by $[\eta]$, decreased with increasing solvent power. One of us (5), using nitrocelluloses, found that, in a homologous series of solvents, both intrinsic viscosity and the initial slope of η_{sp}/c versus c plots increased with solvent power, as estimated from the volume of hexane required to cause initial phase separation from solution. The Huggins and Spurlin relationships did not apply. Frith (6), using cellulose acetate in a few mixed solvents, found the initial slopes of η_{sp}/c vs. c plots to increase with solvent power.

While the best estimates of solvent power would appear to be obtained from the results of osmotic-pressure or light-scattering studies, such data are not generally available for most of the solvents for cellulose derivatives. Solvent power is often related to the volume of precipitant liquid required to cause initial phase separation from solution. This method suffers from a number of disadvantages, some of which have been pointed out (5,7). With cellulose derivatives different precipitants may give differing orders

of solvent power in a range of solvents (8,9). It would seem desirable that the precipitant should not interact with the polymer, in the sense of causing swelling or possessing latent solvent power. Alcohols and some aromatic hydrocarbons may interact with cellulose derivatives in this way (10), but such interaction does not seem to occur with saturated aliphatic hydrocarbons. For this reason hexane has been used as a precipitant in the present work. Since toluene is often used as a precipitant for cellulose derivatives, it has also been used in order to compare values with those obtained with hexane.

Among the factors likely to affect the solvent power of solvents for cellulose derivatives are polarity, chemical type determining acidity or basicity, and the cohesive energy density of the solvent. For nitrocellulose, homologous series of solvents exist. In such a series, polarity and chemical type are essentially the same for all members, and intrinsic viscosities, initial slopes of η_{sp}/c vs. c plots, and the volumes of hexane required for initial phase separation can be related to the cohesive energy density of the solvent (11). No homologous series of solvents for cellulose acetate appears to exist, and in a range of solvents the effects of chemical type and polarity may be marked.

EXPERIMENTAL METHODS

The cellulose acetate used was an unfractionated fibrous sample, acetic acid yield 53.7%. Its weight-average molecular weight, obtained from the intrinsic viscosity in acetone at 25° using the data of Philipp and Bjork (12), was 49,000. Before use it was dried for 3 hr. at 110°C. and stored over phosphorus pentoxide. The following solvents: *o*-cresol, *m*-cresol, *p*-cresol, acetic acid, acetone, methyl acetate, methyl formate, dioxane, nitromethane, pyridine, α -picoline, β -picoline, γ -picoline, and aniline, were purified and dried by appropriate methods and fractionated just prior to use. The hexane used was *n*-hexane, boiling range 67–69°, freed from aromatic hydrocarbons by shaking with fuming sulfuric acid for several hours, followed by washing with caustic soda solution, drying, and distillation over solid caustic soda. Spectroscopic examination showed this method to be effective. The toluene was sulfur-free, shaken with sulfuric acid, washed with dilute caustic soda solution, dried, and fractionally distilled, the fraction boiling at 109–109.5° being collected.

Solutions were prepared by dissolving exactly 1 g. of cellulose acetate in about 50 ml. of solvent with the aid of mechanical agitation, the resulting solution being diluted to 100 ml. These solutions were used for initial phase-separation studies, less concentrated solutions used for viscosity measurements being obtained by careful dilution. All solutions were filtered before use. Preliminary experiments showed that the viscosities of the solutions, unlike those of some solutions of nitrocellulose (13),

did not change with time. Viscosity and initial phase-separation measurements were made after the solutions had stood at room temperature for 60 hr., it being considered that complete dispersion would be obtained in this time.

Viscosities were determined using Ostwald-type capillary viscometers at $25 \pm 0.05^\circ\text{C}$. Kinetic-energy corrections were made where applicable. Preliminary experiments using viscometers of differing flow times showed viscosities to be independent of rate of shear. Viscosities were determined for concentrations within the range 0.05–0.5 g./100 ml. The volume of precipitant required for initial phase separation was obtained by running

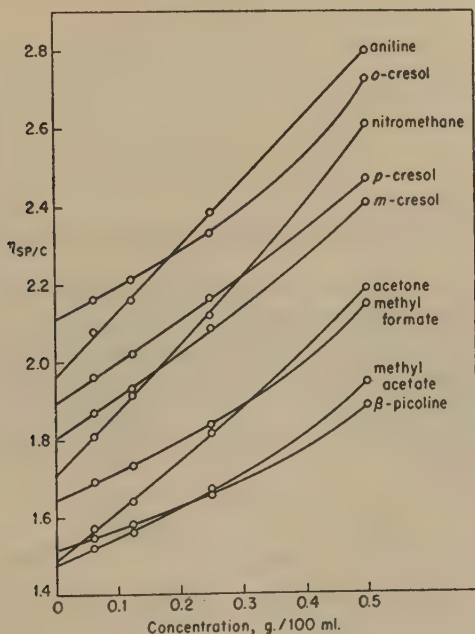


FIG. 1. Viscosities of cellulose acetate solutions.

the precipitant from a microburet into 5 ml. of the 1% solution with constant agitation at 25° . The point of initial phase separation was usually indicated by a faint but permanent turbidity, but in some cases by the deposition of particles of gel on the walls of the vessel.

RESULTS

Figure 1 illustrates viscosity results obtained with most of the solvents. Plots appear to be initially linear, but in most cases upward curvature occurs at higher concentrations. Figure 2 shows results obtained with pyridine, α -picoline, and γ -picoline. Downward curvature of the η_{sp}/c vs. c plots is seen at concentrations below about 0.1 g./100 ml. Open and

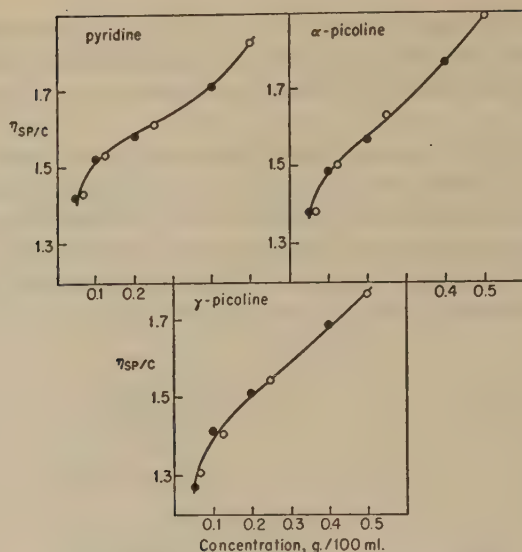


FIG. 2. Viscosities of cellulose acetate solutions.

closed circles represent two separate series of measurements. In Fig. 1 extrapolation to zero concentration is by free-hand drawing. Extrapolation of Martin plots of $\ln(\eta_{sp}/c)$ against c was also carried out, using the method of least squares to obtain values of $[\eta]$ and slope. Intrinsic viscosities and initial slopes of η_{sp}/c vs. c plots were also obtained by a method previously used by one of us (5). Expressing the relationship between η_{sp}/c and c by

$$\eta_{sp}/c = A + Bc + Cc^2,$$

TABLE I

Viscosity Data and Volumes of Precipitants Required for Initial Phase Separation

Solvent	$[\eta]$	Initial slope	k'	k_s	Hexane ml.	Toluene ml.
γ -Picoline	1.30	1.34	0.81	0.21	2.09	6.67
α -Picoline	1.37	1.04	0.54	0.19	1.08	3.08
Pyridine	1.46	0.44	0.22	0.14	2.06	6.53
Methyl acetate	1.48	0.60	0.28	0.18	0.25	0.58
Acetone	1.49	1.36	0.61	0.23	0.39	1.68
β -Picoline	1.55	0.12	0.05	0.13	1.94	5.87
Methyl formate	1.66	0.38	0.14	0.15	0.60	1.75
Dioxane	1.70	1.14	0.39	0.18	0.70	1.32
Nitromethane	1.73	1.46	0.48	0.22		2.06
<i>m</i> -Cresol	1.82	0.84	0.27	0.14	8.30	34.75
Acetic acid	1.83	0.76	0.23	0.17	1.25	3.50
<i>p</i> -Cresol	1.90	0.96	0.27	0.12	10.30	35.80
Aniline	1.95	1.75	0.45	0.16		6.65
<i>o</i> -Cresol	2.12	0.54	0.12	0.11	7.00	23.00

the initial slope B and intrinsic viscosity A are evaluated graphically. In all methods of extrapolation the lowest concentration terms have been ignored with solvents showing downward curvature. Intrinsic viscosities obtained by the three methods differed only slightly. Table I gives values of $[\eta]$; initial slopes of viscosity plots, both obtained graphically; calculated values of Huggins k' ; the Spurlin slope of Martin plots divided by $[\eta]$ (denoted by k_s); and the volumes of precipitants required for initial phase separation. With the exception of dioxane, the same order of volumes of precipitant is obtained with both hexane and toluene.

DISCUSSION

Most of the viscosity plots show upward curvature at concentrations above about 0.2 g./100 ml., in contrast to the results obtained with more flexible polymers which give linear plots up to considerably higher concentrations. The upward curvature may arise from marked hydrodynamic interaction (14) which, with extended chains such as those of cellulose derivatives, should occur at lower concentrations than with flexible chains capable of coiled or contracted forms. Downward curvature at low concentrations, similar to that shown in Fig. 2, has been reported by Howlett, Minshull, and Urquhart (15) for cellulose acetate in acetone and for solutions of polyethylene oxide, polystyrene, and other polymers by Cutler and Kimball (16) who account for the downward curvature by absorption of polymer on the viscometer. As previously pointed out by us (17), other factors such as aggregation and extensive coiling of chains might, below a certain critical concentration, lead to a considerable decrease in hydrodynamic interaction and a more rapid decrease of η_{sp}/c with dilution. The influence of these factors and of adsorption is likely to be greater in poor solvents and it may be significant that the three solvents showing downward curvature give the lowest intrinsic viscosities although, as indicated later, intrinsic viscosity and solvent power do not appear to be simply related. Of the factors mentioned, any marked coiling of cellulose acetate chains is unlikely, but both adsorption and aggregation may occur.

The variation of intrinsic viscosity with solvent is small compared with that shown by flexible high polymers in a range of solvents. This is likely to be due, at least in part, to the relatively rigid nature of the chains. Badger and Blaker (18) suggest that coiling of nitrocellulose chains does not occur for degrees of polymerization less than about 100, and Doty and Stein (19) conclude that chains of cellulose acetate in acetone are rather extended up to molecular weights of 80,000. Even in poor solvents extended configurations are likely.

There would appear to be no general relationship between the volumes of either of the two precipitants and intrinsic viscosity, initial slope of

η_{sp}/c vs. c plot, and Huggins k' or the Spurlin k_s ; although with the aliphatic solvents, $[\eta]$ increases with the volume of precipitant. No general relationship is apparent between the different suggested measures of solvent power and the cohesive energy density of the solvent, values of which, expressed as $(E/V)^{\frac{1}{2}}$, are given in Table II. $E = L_e - RT$, where L_e is the molar latent heat of vaporization at the absolute temperature T , and V is the molar volume. Values of $(E/V)^{\frac{1}{2}}$ have been taken from Hildebrand and Scott (20), obtained from the Hildebrand rule (20) or from vapor-pressure data. The same method of obtaining $(E/V)^{\frac{1}{2}}$ has been used for solvents of the same type.

Spurlin (7) has suggested that solvents for a polar polymer might be divided into three classes corresponding to a balance in cohesive energy

TABLE II
Values of Solvent $(E/V)^{\frac{1}{2}}$ and Dipole Moment at 25°

Solvent	$(E/V)^{\frac{1}{2}}$ (cal./ml.) ^½	Debye units
Acetic acid	13.1	0.8
Nitromethane	12.6	3.0
<i>o</i> -Cresol	11.4	1.41
<i>m</i> -Cresol	11.5	1.54
<i>p</i> -Cresol	11.5	1.57
Aniline	10.8	1.55
Pyridine	10.4	2.2
α -Picoline	9.6	
β -Picoline	10.0	
γ -Picoline	10.0	
Acetone	9.8	2.9
Methyl acetate	9.5	1.9
Methyl formate	10.2	1.9
Dioxane	10.0	0.4

density, solvation by an acid, and solvation by a base, the terms acid and base being used in the Lewis sense. This concept has been successfully applied to polymethyl methacrylate (2,21) and polyvinyl acetate (21). The solvents used for the cellulose acetate can be divided into three groups: acidic: acetic acid, nitromethane, *o*-, *m*-, and *p*-cresols; basic: aniline, pyridine, α -, β -, and γ -picolines; and more neutral: acetone, methyl acetate, methyl formate, and dioxane. Through acetone and esters might be regarded as basic, such character will be less marked than that of relatively strong aromatic bases. A plot of volumes of toluene required for initial phase separation against solvent $(E/V)^{\frac{1}{2}}$ (Fig. 3) suggests that a relationship similar to that suggested by Spurlin may apply. Although the lines drawn for basic and more neutral solvents are speculative, there would seem to be a distinct separation of the three groups. A plot of volumes of hexane against $(E/V)^{\frac{1}{2}}$ shows a similar

separation, but $[\eta]$ against $(E/V)^{1/2}$ is more random, although, as indicated in Table I, basic solvents other than aniline tend to give lower values of $[\eta]$ than the more neutral, whereas the acidic solvents give higher values. These results somewhat resemble those obtained by Alfrey, Goldberg, and Price (2) with polymethyl methacrylate. There would appear to be no relationship, within either of the three groups, between measures of viscosity or volumes of precipitants and the dipole moment of the solvent, some values of which, taken mainly from Le Fevre (22), are included in Table II.

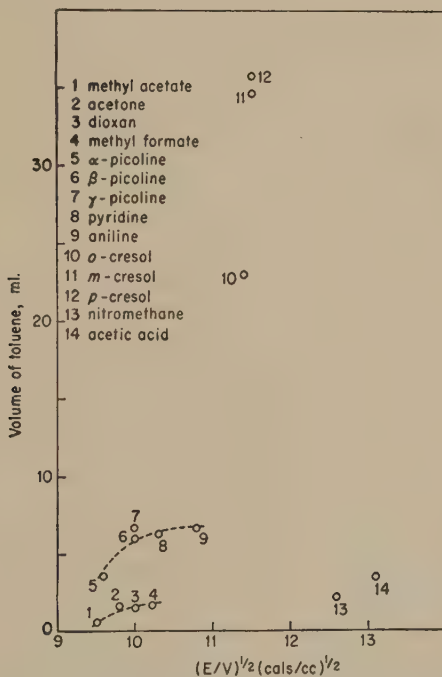


FIG. 3. Variation of volumes of toluene required for initial phase separation with cohesive energy density of solvent.

It would thus appear that the volumes of hexane or toluene may be qualitatively related, within the restricted range of solvents, to the acidic, basic, or more neutral character of the solvent. There may be a relationship, within each group, between volume of precipitant and solvent $(E/V)^{1/2}$, but this is less definite, particularly with the acidic solvents. The volumes of precipitants required to cause initial phase separation from solution in the cresols are much greater than those required for the other acidic solvents. This may be due to strong solvation effects arising from the marked hydrogen-bonding power of the cresols. It should be

noted that initial phase separation will presumably occur when, for a particular solvent, the cohesive energy density of the solvent-precipitant mixture reaches a certain value. $(E/V)^{1/2}$ values for associated solvents such as acetic acid and cresols will include a marked contribution from dipole in addition to those from dispersion forces. To what extent dipole contributions will persist in solvent-precipitant mixtures is doubtful, and the values of $(E/V)^{1/2}$ for certain solvents may not represent those effective in determining the cohesive energy density of the mixture.

Any relationship between $[\eta]$ and acidic, basic, or more neutral character of the solvent is much less definite, and there would appear to be no simple relationship, within each group, between $[\eta]$ and $(E/V)^{1/2}$. This may be due to the differing types of solvents used. A number of factors, related to the solvent and possibly its type, may affect the viscosities of dilute solutions of cellulose acetate. Among such factors is solvation which will affect the axial ratio of the chains and hence the intrinsic viscosity, which is a measure of the shape and size of the chains in solution. Evidence for the solvation of cellulose acetate in solution has been reviewed by Howlett and Urquhart (23). Qualitative evidence is very strong, but the exact number of molecules of a particular solvent which are bound to each glucose residue is doubtful. More quantitative knowledge is required before the effect of solvation on viscosity can be assessed. It should also be noted that while solvation may be an essential part of cellulose acetate-solvent interaction a good solvating agent may not be a good solvent from the thermodynamic point of view.

Other factors affecting viscosity may be more directly related to solvent power. Though the chains may be regarded as extended, slight variations in the kinking of solvated chains might, as suggested by Frith (24), affect both $[\eta]$ and the initial slope of η_{sp}/c vs. c plots. Aggregation of chains in poorer solvents is also possible. Doty, Wagner, and Singer (25) have shown that cellulose acetate may be associated in Methyl Cellosolve (2-methoxyethanol) and in 10:23 acetone-methanol. The formation of aggregates might lead to decreased hydrodynamic interaction and to a lower viscosity than that obtained in the absence of aggregation. Doty, Wagner, and Singer found, however, that specific viscosities of polyvinyl chloride solutions were little affected by association. In view of these factors that may affect the viscosities of dilute solutions of cellulose acetate, relationships between viscosity and solvent power are unlikely to be simple.

It is, of course, not clear to what extent the volumes of precipitants required for initial phase separation can be regarded as measures of solvent power in the thermodynamic sense. For a better understanding of relationships between solvent power and the volumes of precipitants or measures of viscosity, values of the Huggins interaction constant

for the solvents, together with more quantitative data on solvation and aggregation, are desirable. Further work with these aims in view is being carried out.

ACKNOWLEDGMENT

We wish to gratefully acknowledge a Courtaulds Research Scholarship to one of us (J. R.).

SUMMARY

Specific viscosity/concentration versus concentration plots and volumes of hexane and toluene required to cause initial phase separation from solution have been obtained at 25° using a cellulose acetate (acetic acid yield 53.7%, $\bar{M}_w = 49,000$) in 14 solvents of differing types. The volumes of precipitants appear to be qualitatively related to acidic, basic, or more neutral character of the solvent and, less definitely, to its cohesive energy density. Relationships between such properties of the solvent and measures of viscosity are less clear. Some of the factors affecting the viscosities of dilute solutions of cellulose acetate are briefly discussed.

REFERENCES

1. ALFREY, T., JR., BARTOVICS, A., AND MARK, H., *J. Am. Chem. Soc.* **64**, 1557 (1942).
2. ALFREY, T., JR., GOLDBERG, A. I., AND PRICE, J. A., *J. Colloid Sci.* **5**, 251 (1950).
3. HUGGINS, M. L., in E. Ott, ed., *Cellulose and Cellulose Derivatives*, p. 943. Interscience, N. Y., 1943.
4. SPURLIN, H. M., MARTIN, A. F., AND TENNENT, H. G., *J. Polymer Sci.* **1**, 63 (1946).
5. MOORE, W. R., *J. Polymer Sci.* **7**, 175 (1951).
6. FRITH, E. M., *Trans. Faraday Soc.* **41**, 90 (1945).
7. SPURLIN, H. M., *J. Polymer Sci.* **3**, 597 (1948).
8. MOORE, W. R., *Trans. Faraday Soc.* **43**, 543 (1947).
9. DOOLITTLE, A. K., *Ind. Eng. Chem.* **36**, 229 (1944).
10. MARDLES, E. W. J., in Alexander, *Colloid Chemistry*, Vol. 4, p. 94.
11. MOORE, W. R., *J. Polymer Sci.* **5**, 91 (1950).
12. PHILIPP, H. J., AND BJORK, C. F., *J. Polymer Sci.* **6**, 383 (1951).
13. CAMPBELL, H., AND JOHNSON, P., *J. Polymer Sci.* **5**, 143 (1950).
14. SIMHA, R., *J. Colloid Sci.* **5**, 386 (1950).
15. HOWLETT, F., MINSHULL, E., AND URQUHART, A. R., *Mem. Shirley Inst.* **18**, 251 (1941).
16. CUTLER, M., AND KIMBALL, G. E., *J. Polymer Sci.* **7**, 445 (1951).
17. MOORE, W. R., AND RUSSELL, J., *J. Polymer Sci.* **9**, 472 (1952).
18. BADGER, R. M., AND BLAKER, R. H., *J. Phys. & Colloid Chem.* **53**, 1056 (1949).
19. DOTY, P., AND STEIN, R. S., *J. Am. Chem. Soc.* **68**, 159 (1946).
20. HILDEBRAND, J., AND SCOTT, R. L., *The Solubility of Non-Electrolytes*. Reinhold, N. Y., 1950.
21. DAOUST, H., AND RINFRET, M., *J. Colloid Sci.* **7**, 11 (1952).
22. LE FEVRE, R. J. W., *Dipole Moments*. Methuen, London, 1948.
23. HOWLETT, F., AND URQUHART, A. R., *Chemistry & Industry* (1951), 82.
24. FRITH, E. M., *Trans. Faraday Soc.* **41**, 17 (1945).
25. DOTY, P., WAGNER, H., AND SINGER, S., *J. Phys. & Colloid Chem.* **51**, 32 (1947).

THE POLYMERIZATION OF AQUEOUS POTASSIUM SILICATE SOLUTIONS¹

A. P. Brady, A. G. Brown and Harriette Huff

Stanford Research Institute, Stanford, California

Received September 2, 1952; revised January 19, 1953

ABSTRACT

The molecular weight of the silicate ion in aqueous solutions of potassium silicate ($\text{SiO}_2\text{:K}_2\text{O}$ mole ratio of 3.8:1), both alone and in the presence of various salts and acids, was investigated by means of light-scattering techniques. Angular-dependence data are given for solutions with molecular weight greater than about 10^6 (results at lower molecular weights did not appear to be meaningful in terms of the main solute). The time dependence of the molecular weight of the silicate ion was determined at one or two concentrations for NH_4Cl , $(\text{NH}_4)_2\text{SO}_4$, $(\text{NH}_4)_2\text{CO}_3$, H_3BO_3 , CH_3COOH , H_3PO_4 , NaHCO_3 , KHCO_3 , $(\text{NH}_4)_2\text{C}_2\text{O}_4$, isopropyl alcohol, KH_2PO_4 , K_2HPO_4 , NaH_2PO_4 , Na_2HPO_4 , $\text{NH}_4\text{H}_2\text{PO}_4$, $(\text{NH}_4)_2\text{HPO}_4$, Na_2SO_4 , K_2SO_4 , NaCl , KCl , and LiCl . The effects of different temperatures and concentrations were studied for KCl and for acetic acid. The influence of additions of various amounts of alkali or of excess acid, alone or in the presence of salt, on the molecular weight of the silicate ion was also determined. The results of the present investigation are discussed in terms of those of other investigators and in relation to possible models for the method of polymerization.

INTRODUCTION

Aqueous solutions of alkali metal (usually sodium) silicates have been of both scientific and industrial interest for a great number of years. Despite this interest in silicates and in the influence of salts and acids on the properties of their solutions, information as to the physical state of the silicate ion is surprisingly meager. Numerous workers have studied the rate of gelation under certain conditions of pH and added electrolytes. None of this work, however, gives a basis for estimating either the molecular weight during the course of the reaction leading to a gel or the molecular weight of the silicate before the salts or acids were added. Many theories are predicated on the original solution being a high polymer. However, the existence of stable monomeric silicate ions in aqueous solution under certain conditions has been postulated from physico-chemical evidence [e.g., diffusion (1,2), and cryoscopy (3)]. It was not until 1949 that the light-scattering results of Debye and Nauman (4)

¹ For detailed paper (or extended version or material supplementary to this article) order Document 3889 from American Documentation Institute, c/o Library of Congress, Washington 25, D. C., remitting \$2.50 for microfilm (images 1-in. high on standard 35-mm. motion picture film) or \$6.25 for photostat readable without optical aid.

showed that sodium metasilicate is essentially a monomer. In 1951 the same authors (5) showed that the silicate ions in solutions in which the mole ratio of $\text{SiO}_2:\text{Na}_2\text{O}$ was 3.75:1 were still, at the most, only low polymers.

The present paper is concerned with light-scattering measurements on potassium silicate solutions. The principal objective of the work was to investigate the rate of polymerization, and if possible the shape of the polymer, in the presence of various salts and acids. In the course of this investigation, information was gained concerning the silicate before such additions, as well as some idea of under what circumstances the polymerization process is reversible.

Potassium silicate was chosen for study primarily because of its interest to the television industry in screen application. In addition, the material presents advantages over sodium silicate from an experimental standpoint. First, because of the deleterious effect of certain multivalent ions on phosphorescence, the commercial material is quite pure in this regard. Secondly, even at high $\text{SiO}_2:\text{K}_2\text{O}$ ratios, the commercial solutions show none of the gross turbidity characteristic of similar sodium preparations. It will be shown that the molecular weight of the potassium silicate used here is of the order of magnitude of weights reported (5) for very carefully prepared sodium silicate solutions.

MATERIALS

The potassium silicate used was Kasil No. 1, manufactured by Philadelphia Quartz Co. It was an aqueous solution with a mole ratio of $\text{SiO}_2:\text{K}_2\text{O}$ of 3.83:1, containing 7.78% alkali calculated as K_2O . All other reagents used were of reagent-grade quality.

In light-scattering measurements, freeing the solutions from traces of foreign particles is generally a more important concern than is the chemical purity of the starting materials. Initial attempts to remove particulate matter involved the use of a special high-speed attachment to an International centrifuge. Speeds up to 15,000 r.p.m. (average force up to $25,000 \times g$) were employed. Despite precautions in deceleration and the use of special pipets to prevent remixing, the results were generally unsatisfactory, apparently owing to the presence of low-density particulate matter in the solutions. The final procedure adopted was relatively simple and, as judged by the results, at least as effective as other reported procedures. Each solution was filtered twice through a $5\text{-}\mu$ pore-size stainless steel filter and once through a bacteriological-grade fritted-glass filter under nitrogen pressure. New filters had to be "broken in" by filtering through them a large quantity of conductivity water; thereafter they were quite satisfactory. Filtering did not appreciably change the concentration of the solutions.

All glassware was cleaned chemically with hot nitric-sulfuric acid, rinsed repeatedly in conductivity water, and finally rinsed by condensing steam, generated from conductivity water, passed through a series of Kjeldahl traps. This system of vapor-phase washing is similar to that used by Blaker, Badger, and Gilman (6).

APPARATUS AND CALIBRATIONS

Two instruments were used to determine light scattering. One of these was the Lumetron colorimeter equipped with a turbidimeter attachment. This instrument is too insensitive by several orders of magnitude for absolute measurements, but by using white light it was found to be quite useful for crude exploratory measurements and for some rate measurements (on a strictly comparative basis) at relatively high molecular weights. For absolute measurements and for angular exploration a microphotometer constructed in these laboratories was used. The principle of the instrument is the same as that described by Zimm (7), although it differs considerably in constructional and operational details. Since these details are important only from a convenience standpoint, the description here will be limited to a brief outline of the principles of the instrument. In this type of instrument, dark-current corrections and small variations in incident light are canceled by utilizing the natural 120-cycle modulation of the mercury arc, and causing the current from a RCA 1P21 photomultiplier tube picking up scattered light to oppose the current (through a potentiometer) from a reference phototube (RCA 929) which is picking up a portion of the incident beam. The potentiometer is adjusted to a null point. The unbalance is amplified by an alternating-current amplifier and gated rectifier tuned to the 120-cycle modulation of the mercury arc source. The sample cell, designed to minimize reflection into the photomultiplier tube, consisted of a special, small, thin-walled Erlenmeyer flask (about 15-ml. capacity) contained in an ordinary 250-ml. Erlenmeyer flask. The space between the two flasks was filled with isopropyl alcohol. In Zimm's apparatus, in which the internal flask is much smaller, the photomultiplier tube "sees" the whole of the inner Erlenmeyer; we found it more satisfactory to arrange stops so that only a narrow strip was seen. This required a correction for the different volume of solution seen as the angle of observation relative to the incident beam was changed. This correction was experimentally determined using very dilute fluorescein solution in the cell, but was very close to the expected proportionality to $\text{cosec } \theta$. The optical system was otherwise similar to that described by Zimm. The mercury 546 $m\mu$ line, polarized perpendicular to the plane of observation, was used with this system.

In many cases, including the present investigation, only an approximate calibration of the instrument readings in terms of the absolute

intensity of the scattered light is necessary. This is fortunate, because an accurate calibration presents a formidable problem that is too often glossed over. The reduced intensity of benzene, for example, has been variously reported (for unpolarized 546 m μ illumination) as 11×10^{-6} (8), 12.4×10^{-6} (9), and 16×10^{-6} (10). The last two values are fairly recent. Similarly, values reported for carbon disulfide range from 39.6×10^{-6} to 47.8×10^{-6} (6). In order to avoid troublesome refractive-index corrections, it was desirable to calibrate with an aqueous solution. The calibration problem was greatly simplified by use of a dilute polymer latex, kindly supplied by Professor Bruno H. Zimm, and determined by him, in comparison to absolute measurements, to have a reduced intensity at 90° for polarized incident light of 1.37×10^{-3} . A similar, somewhat more dilute latex served as a convenient working standard for checking the sensitivity of the photomultiplier tube after each reading. Comparison with the latex supplied by Zimm gave the reduced intensity of this working standard as 4.90×10^{-4} . In order not to be in a position of basing all conclusions on this single reference, a further check was made utilizing the turbidity data of Halwer (11) for sucrose solutions. In comparison with a charcoal-extracted solution of sucrose, the working standard had a reduced intensity of 4.4×10^{-4} . For present purposes this agreement, although only to 10%, was considered satisfactory, especially in view of the difficulty in obtaining sucrose sufficiently pure for a scattering standard.

The results of the present investigation are largely presented in the form of $I_{\theta p}$, the intensity at the angle θ expressed as a percentage of the 90° intensity of the working standard latex. This we know with good accuracy, and comparisons can be made with some confidence, whereas, as pointed out above, the absolute value of the scattered intensity is known only to, say, 10%. Nevertheless, it will occasionally be useful to talk in terms of molecular weights. In terms of reduced intensity, the molecular weight of the solute is given by

$$M = \lim_{c \rightarrow 0} \left[\frac{N\lambda^4 R_{op}}{4\pi^2 c n_0^2 (dn/dc)^2} \right]$$

where M denotes the gram molecular weight, N Avogadro's number, λ the wavelength of the incident light, R_{op} the reduced intensity of light scattered in the forward direction with vertically polarized incident light, c the concentration, n_0 the refractive index of the solvent, and n that of the solution. Taking the working standard latex as having a reduced intensity of 4.90×10^{-4} (as determined by comparison with Zimm's latex), and combining with $dn/dc = 0.131$ (determined by a Zeiss white-light interferometer) for our sample of potassium silicate and the other

appropriate constants, the equation for conversion to molecular weights is

$$M = \lim_{c \rightarrow 0} \frac{2.11}{c} I_{op} \times 10^3.$$

The extrapolation to zero concentration, indicated by the above equation, will in general be completely impractical in the systems studied here because of their change with time. Therefore, most conclusions will be based on measurements at a finite concentration, usually about 1%, although a partial check on the validity of this will be afforded in the last section. Theory would predict, and we have experimentally confirmed, that the presence of the electrolytes of the types and concentrations used here will lead to no significant alteration in this relationship. Because of the uncertainty in the calibration, no attempt was made to correct for depolarization.

RESULTS AND DISCUSSION

Potassium Silicate Alone

Figure 1 presents the 90° scattering results, using the microphotometer, for several concentrations of potassium silicate with no other solute present. It can be seen that the molecular weight of the original solution (26.8% in potassium silicate) can be estimated only roughly, owing to the aging phenomena in the more dilute solutions. Solutions higher than 12% in potassium silicate were not tested because their viscosity made filtration too difficult. It is evident from the figure that the more dilute solutions show the greater time effect upon molecular weight—at 12% concentration, the molecular weight is fairly stable, and it would be inferred that the 26.8% solution is quite stable, with a molecular weight in the neighborhood of 2000. The same general phenomenon was reported by Nauman and Debye (5) for sodium silicate with a mole ratio of $\text{SiO}_2:\text{Na}_2\text{O}$ of 3.95. The aging is not due to carbon dioxide; Nauman and Debye kept their solutions under nitrogen. Although a very long diffusion path was relied upon to maintain purity in the runs shown in Fig. 1, a sample of 1% potassium silicate which was sealed off from all contact with the air gave a curve identical to that shown in the figure.

Despite the rather elaborate purification train through which all solutions were put, sufficient "cleanliness" for angular-dependence measurements could not be obtained when the molecular weight was low. The same phenomenon was reported for sodium silicates by Nauman and Debye. The excessive low-angle scattering undoubtedly arises, at least in our case, from a small amount of material that is small enough to escape the filter, but nevertheless is very much larger than the main solute. This conclusion is based not only upon the inordinate length calculated from slope-intercept relations (the slope-intercept relation, which will be

used and discussed in more detail below, gives a Z -average square of the length, whereas the intercept gives the weight-average molecular weight), but also upon the form of the angular-dependence curve. A plot of c/I_{θ} should be straight or convex to the abscissa (see for example, Fig. 5); instead, it is strongly concave.² In practice, it turns out that the scattered intensity at 90° will give a truer picture of the main solute than will the extrapolated value to 0° , until the specific scattered intensity becomes about 100% (on our scale), whereupon the scattering of the main solute at the lower angles submerges the 1–4% given by chance particulate

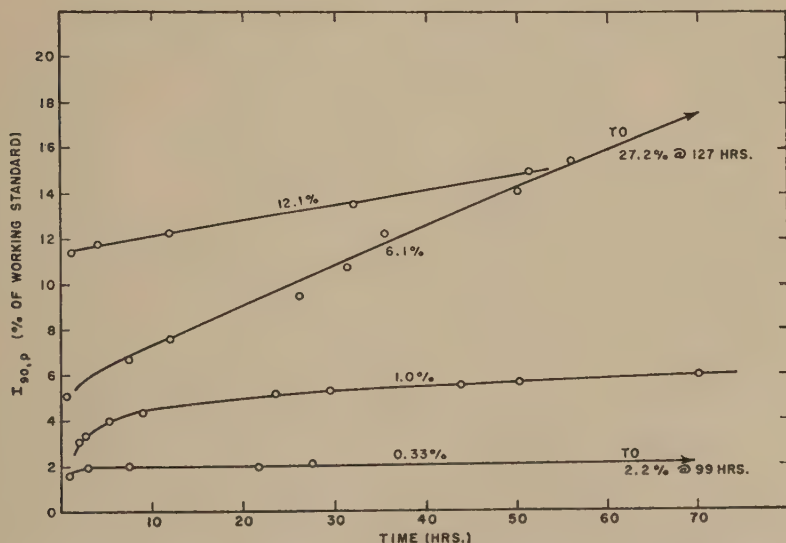


FIG. 1. Scattering from aqueous solutions of K silicate; wt. % solids as indicated on curves.

matter. The use of 90° scattering in investigating relatively low molecular weight materials is quite common—usually for the same reason.

Effect of Various Electrolytes on the Molecular Weight

Table I gives the results of crude light-scattering results (using the Lumetron colorimeter). These exploratory results are crude not only in measuring but also in temperature control (25 – 33°C). Nevertheless, they serve to illustrate several effects that are of such magnitude as to overshadow the crudity of the measurements. In general, these effects observed on scattering parallel the observations of others on rate of gelation.

² An example of such a curve as well as other curves not reproduced in this paper but used for drawing conclusions or parallels can be obtained from the American Documentation Institute (see footnote 1).

TABLE I

Exploratory Light-Scattering Results on the Lumetron Photometer
(pH values from Hydrion pH paper except for glass-electrode values marked with an asterisk)

Substance added	Concn. <i>M</i>	pH	<i>T</i> , time to reach 100% of standard <i>min.</i>	Slope at time <i>t</i> , %/min.
A. K silicate concentration $\frac{1}{3}\%$ (0.020 <i>N</i> in alkali)				
(NH ₄) ₂ SO ₄	0.125	—	21.4	12
(NH ₄) ₂ CO ₃	0.15	—	13	15
CH ₃ COOH	0.08	5	^c	
B. K silicate concentration 1% (0.0615 <i>N</i> in alkali)				
<i>Ammonium salts</i>				
NH ₄ Cl	0.10	8.5-9	68	2
	0.15	8-8.5	7 $\frac{1}{2}$	21
	0.20	7.5-8	2 $\frac{1}{2}$	57
(NH ₄) ₂ SO ₄	0.075	—	11	9
	0.125	—	3	60
(NH ₄) ₂ CO ₃	0.075	8.5	48	3
	0.15	—	2 $\frac{1}{2}$	60
(NH ₄) ₂ C ₂ O ₄	0.075	7.5-8	19	7
	0.10	7.5-8	6	23
(NH ₄)H ₂ PO ₄	0.15	6.5-7	12	20
	0.5	5	32	6
(NH ₄) ₂ HPO ₄	0.075	9	20	6
	0.25	8	$\frac{2}{3}$	150
<i>Acids</i>				
CH ₃ COOH	0.059	8.3*	29	6
	0.061	7.7*	16	12
	0.077	5.7*	96	4
	0.083	5.5*	225	1.4
	0.278	5	^c	
H ₃ PO ₄	0.019	9.2*	^b	
	0.030	7.9*	79	1 $\frac{1}{2}$
	0.034	7.3*	9	7 $\frac{1}{2}$
	0.038	6.9*	14	14
	0.057	5.9*	28	9
	0.075	3.1*	9	11
	0.136	2	20	12
H ₃ BO ₃	0.0625	9-9.5	^b	
	0.125	8.5-9	^a	
	0.25	8	182	$\frac{1}{2}$
	0.35	7.5	^a	
	0.45	7	^a	

^a Little reaction apparent in 1 hr.

^b No reaction apparent in 1 hr.

^c No reaction apparent in 1 day.

TABLE I—*Continued*

Substance added	Concn. <i>M</i>	pH	<i>T</i> , time to reach 100% of standard <i>min.</i>	Slope at time <i>t</i> , %/min.
<i>Bases</i>				
NH ₄ OH	0-4.0		<i>c</i>	
<i>Acid salts</i>				
NaH ₂ PO ₄	0.15	7	15	15
	0.5	6	54	4½
KH ₂ PO ₄	0.15	6.5-7	8	19
	0.5	5.5-6	34	5
NaHCO ₃	0.15	9-10	68	1½
	0.25	9	26	4½
	0.50	9	4	45
KHCO ₃	0.25	9	3½	42
	0.50	8-9	1	—
<i>Other salts</i>				
Na ₂ HPO ₄	0.075	10-11	<i>a</i>	
	0.25	10-11	23	2½
K ₂ HPO ₄	0.25	10-11	6	8
	0.45	10	1	175
Na ₂ CO ₃	1.35	11	60	5½
K ₂ CO ₃	0.25		<i>b</i>	
	0.45	11	<i>a</i>	
	2.25		80	2½
LiCl	0.5	—	40	1
NaCl	0.5	—	23	11
KCl	0.5	—	28	6
	1.0	—	4	45
K ₂ SO ₄	0.05	—	<i>c</i>	
	0.25	—	100	1
	0.40	—	26	5
	0.45	—	24	8
<i>Nonelectrolyte</i>				
Isopropyl alcohol	1.8	10	<i>a</i>	
	2.8	10	42	1
	3.0	10	31	2
	3.6	10	½	300

It is evident that two types of electrolytes may be distinguished: those that operate to cause polymerization through changing pH, and those that operate through some other mechanism, possibly dehydration. Acetic acid, for example, shows a very sharp maximum, near the equivalence point, in its concentration dependence on the rate of promoting

polymerization. On the other hand, with ammonium chloride or sodium bicarbonate, there is no evidence of such a maximum; these, however, are far weaker acids than acetic. The double maximum for phosphoric acid, corresponding roughly to concentrations at which the first and the first plus the second hydrogen could be used, cannot be explained by the usual concept of the maximum rate of polymerization occurring at a pH just low enough to form free silicic acid.

The various neutral electrolytes and the one nonelectrolyte tried show quite different behavior. Much higher concentrations are necessary (the concentration dependence will be examined in more detail below) to initiate polymerization, and there is no evidence of an optimum concentration. Still another important difference will be discussed under "reversibility." It is of interest to note that, as has been found in the case of gelation rates, sodium salts give more rapid polymerization than do potassium salts (strangely enough, lithium salts are slower than either—a possibility not explored is that an optimum concentration exists for the lithium ion). At electrochemically equivalent concentrations, chlorides are more rapid than sulfates, although at equal molalities the opposite is true. This relation between the cations holds only for the neutral salts, not necessarily for salts in which change of pH also plays a role (e.g., compare KHCO_3 with NaHCO_3 , and KH_2PO_4 with NaH_2PO_4).

Figure 2 presents microphotometric results, in which some rates of reaction with lithium, sodium, and potassium chlorides and sodium and potassium sulfate are examined in more detail. Similar curves were obtained for CH_3COOH , H_3PO_4 , H_3BO_3 , NH_4Cl , $(\text{NH}_4)_2\text{SO}_4$, $(\text{NH}_4)_2\text{CO}_3$, $(\text{NH}_4)_2\text{C}_2\text{O}_4$, NaHCO_3 , KHCO_3 , $(\text{NH}_4)_2\text{HPO}_4$, $(\text{NH}_4)\text{H}_2\text{PO}_4$, Na_2HPO_4 , NaH_2PO_4 , K_2HPO_4 , KH_2PO_4 , and isopropyl alcohol. These curves may be obtained by the procedures indicated in the footnote on page 252. The temperature in these experiments was $27 \pm 1^\circ\text{C}$. The scattering at an angle of 90° and extrapolated values for 0° are given. The general conclusions concerning relative rates of reactions derived from the crude experiments of Table I are borne out by these more accurate experiments.

The semilogarithmic type of plot was chosen only for convenience, but the nearly exact linearity of sodium chloride and sulfate on this plot, and the gentle curvature exhibited by many other additives, are worthy of mention. If the polymerization of the silicate were simply elimination of water to form a pyroxene-type linear chain, then the statistics of bifunctional condensation of Flory (12) should be applicable. According to this, however, the molecular weight should be linear with time, which is not even approximately true. On the contrary, the nearly linear semilogarithmic plot implies that the rate of formation of new bonds is nearly unaffected by the degree of polymerization of the molecules doing the bonding. This implies in turn that the number of functional groups avail-

able is also roughly independent of the degree of polymerization, so the silicate ions must be behaving as multifunctional groups. This is not surprising, in view of silicon's well-known ability to attain coordination numbers up to six. Further evidence on this question is presented in the following sections.

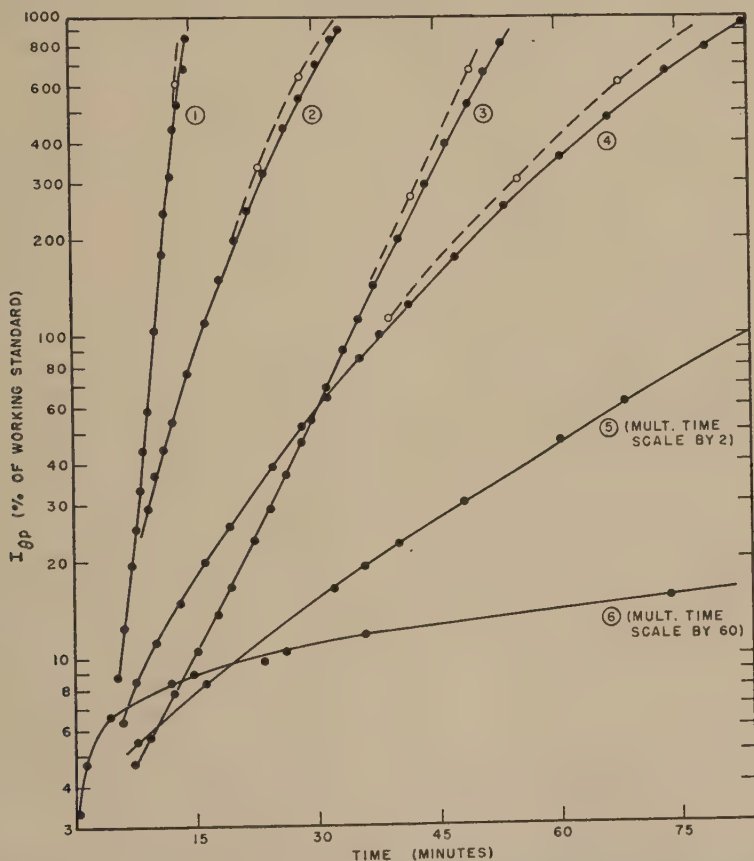


FIG. 2. Scattering from K silicate plus neutral salts. All solutions 1% in K silicate. Solid curves I_{sp} ; broken curves I_{op} (extrapolated). Curves (1) 0.5 M in Na_2SO_4 ; (2) 0.5 M in K_2SO_4 ; (3) 0.5 M in NaCl ; (4) 0.5 M in KCl ; (5) 0.5 M in LiCl ; (6) 0.05 M in K_2SO_4 .

Effect of Electrolyte and Silicate Concentrations

In some cases Table I gives an estimate of the effect of electrolyte concentration and pH on the rate of polymerization of the silicate. As previously pointed out, however, these experiments were of an exploratory nature, and so it was desirable to examine two systems in somewhat more detail and with better control of temperature. The two systems chosen were KCl-silicate and acetic acid-silicate.

For determining the effect of concentration on the rate of increase of molecular weight in these systems, the Lumetron colorimeter was used. This choice precluded studies at the very start of the reaction, because of the stray light and inherent insensitivity of the instrument, but proved extremely convenient at molecular weights of 100,000 and above, because readings could be made rapidly. In this series of experiments the silicate and electrolyte solutions were prepared separately and filtered through

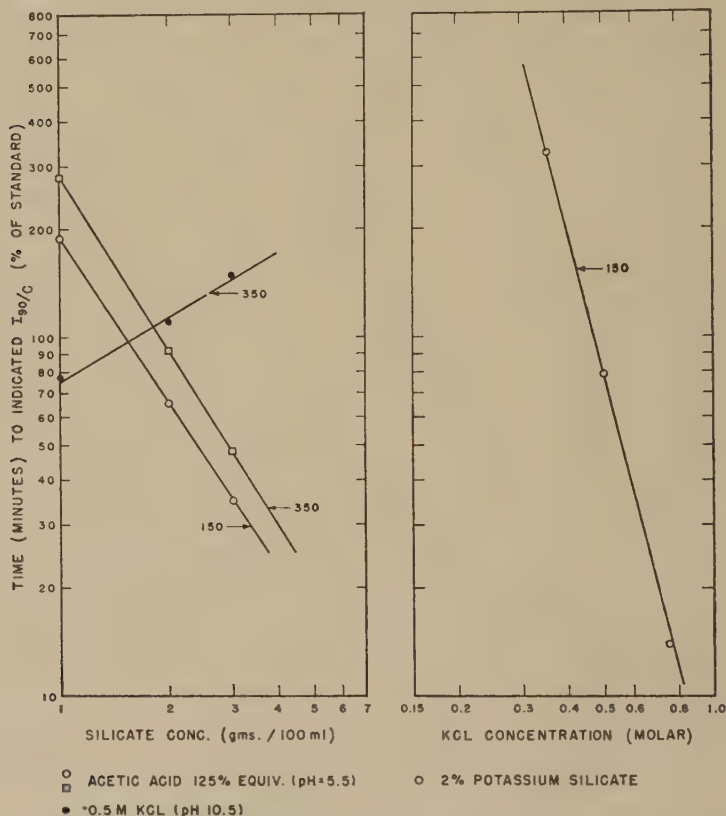


FIG. 3. Summary of effects of concentration for K silicate, KCl, and acetic acid. Left: ○, ◻ acetic acid 125% equiv. (pH = 5.5), ● 0.5 M KCl (pH = 10.5). Right: ○ 2% potassium silicate.

a 5- μ pore-size stainless steel filter, brought to temperature (to $\pm 0.01^\circ\text{C}.$), and then thoroughly mixed to start the reaction. Samples were then periodically withdrawn, and the scattering was determined.

The data presented in Table I on salt systems suggest a power law for the dependence of polymerization rate upon concentration of salts at 1% potassium silicate. Examination of the data of Fig. 3 shows that a power law is obeyed with accuracy at a concentration of 2% potassium

silicate; further, the rate of polymerization is almost exactly proportional to the fourth power of the potassium chloride concentration. We have no explanation for this at this time, but it serves as a useful, and surprisingly accurate, tool for predictions. From Fig. 2, for example, it is evident that at equal molalities potassium sulfate induces polymerization of 1% K silicate at a rate almost exactly 2.5 times as fast as potassium chloride, over the whole range studied. At 0.5 *M*, potassium chloride takes 13 min. to produce scattering of 15% of the working standard, and the polymerization rate is approximately 10%/min. For 0.1 *N* K₂SO₄, then, one would predict 4%/day. This is quite close to the observed rate of 6½%/day (also Fig. 2) when one considers that the extrapolation has been over a factor of 10⁴ in rate of reaction.

The effect of varying the silicate concentration at constant potassium chloride concentration is also given in terms of a log-log plot in Fig. 3. The data can be represented fairly well by taking the rate to be proportional to the inverse square root of the silicate concentration.

The data summarized in Fig. 3 also provide information as to the order of the reaction in an acid medium. In this case, the logarithm of the time to a given reduced intensity plotted against the silicate concentration for constant acetic acid *ratio* (125% of equivalence) is also a straight line. This is essentially a plot at constant pH (around 5.5), since the threefold variation in concentration of the excess acetic acid represents, at most, a change of 0.5 pH unit. The slope of the line indicates that under these conditions the rate of polymerization is proportional to the three-halves power of the silicate concentration.

Similar experiments, made at an acetic acid ratio of 84% of the free alkali of the silicate (pH about 8.5), might be expected to give information as to the order of the reaction in "neutral" systems. However, this system is very close to the optimum pH for polymerization, and a change of 0.5 pH unit, resulting as indicated above from the threefold change in concentration of the system, can change the rate of polymerization by an appreciable factor. The calculated order of the reaction with respect to silicate concentration is 5.5 between 3 and 2% silicate and, for all practical purposes, infinity between 2 and 1%. These values probably have little significance other than that the system is very sensitive to pH and that the mechanism of the reaction may be going through a change.

Effect of Temperature

Temperature-dependence data, obtained on the Lumetron in a manner similar to that described in the last section, are summarized in an Arrhenius type plot in Fig. 4. All reactions were run at 2% potassium silicate: pH 5.5 was obtained by adding acetic acid in an amount equal to 125% of the available alkali of the silicate; pH 8.5 was obtained by 85% equiva-

lence of acetic acid; and the reaction at pH 10.5 was induced by 0.5 *M* KCl.

In theory, one should plot the rate of change of the logarithm of the reduced intensity at 0° from the incident beam against the reciprocal of the absolute temperature, because of the possibility of a change in nature of the controlling reaction and the shape of the polymer as the tempera-

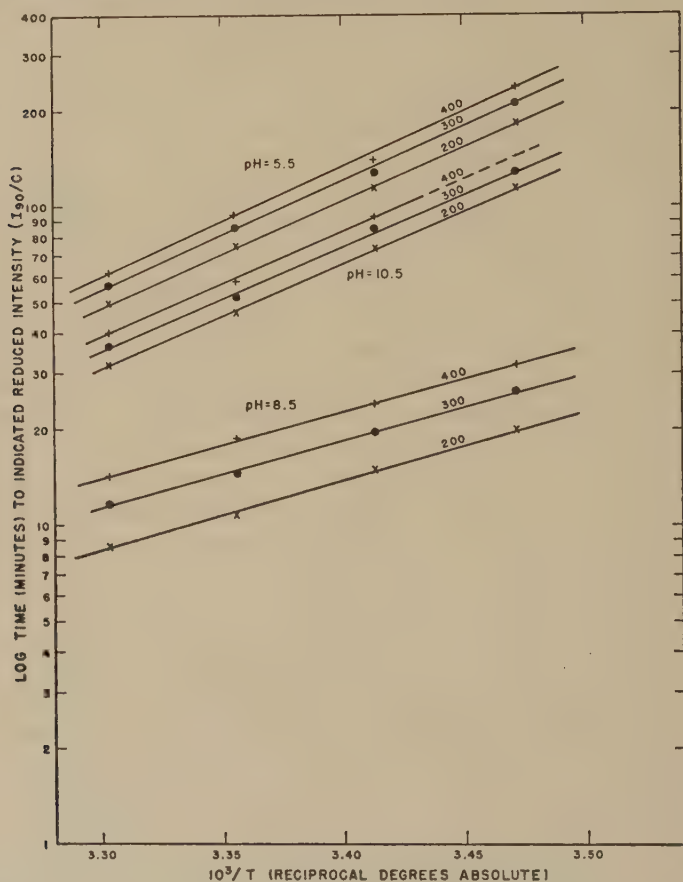


FIG. 4. Summary of temperature dependence of rate of polymerization as a function of pH.

ture is changed. However, it is evident from Fig. 4 that the slope of a plot of the logarithm of the time to reach a given intensity (as read on the Lumetron) vs. $1/T$ is largely independent of the extent of reaction. Therefore, unless there is an extremely fortuitous combination of compensating errors, the time to reach a given reading should be a dependable measure of the rate of reaction.

The calculated activation energies, in kilocalories per mole, are 15.5 ± 0.5 for the acid system (pH 5.5), 9.6 ± 0.3 for the "neutral" system (pH 8.5), and 14.6 ± 0.5 for the alkaline potassium chloride system (pH 10.5). It is instructive to compare these activation energies for the actual polymerization reaction with similar values calculated by other workers from gel times for sodium silicate systems. Thus, for acetic acid-catalyzed formation of gels from commercial sodium silicate, activation energies of 16.4–16.7 kcal. are reported on the acid side by Hurd and Miller (13) and 16.9 kcal. for slightly on the alkaline side by Hurd and Letteron (14). For highly alkaline solutions (above pH 10) those workers report that no activation energies can be calculated because gel times go through a minimum at 35°C. Munroe and co-workers have improved somewhat the technique of measuring gel times by determining times to a specified Young's modulus of the gel. On this basis, the most recent data (15) yield activation energy values of 9.4 at pH 8.2 and 15.2 at pH 5.6, in remarkably close agreement with those found in the present work by light-scattering measurements.

The above data suggest that in the pH region 5–9, gel formation develops when the molecules have reached a certain size, and this size is independent of pH. On the other hand, in more alkaline systems, where both Hurd and Munroe found negative activation energies for gel formation, our Arrhenius plots appear quite linear, at least to 30°C. It therefore appears that in this region the gelation occurs at varying molecular weights, and gel times are no longer a measure of the rate of reaction.

Angular-Dependence Results

Figure 5 gives some angular-dependence results obtained with the microphotometer. The results for ammonium sulfate are presented because they cover the greatest range of molecular weights. In all other cases, however, six angles (30°, 45°, 60°, 90°, 120°, and 135°) were examined rather than the three shown in Fig. 5. As mentioned before, angular-dependence results are meaningful only at the higher molecular weights. In a plot such as Fig. 5, α , the limiting slope (at $\theta = 0$) divided by the intercept, is related to the mean-square radius of this molecule from its center of gravity, \bar{R}^2 , by

$$\alpha = \frac{16\pi^2 \bar{R}^2}{3\lambda^2}.$$

In terms of molecular models, for a random coil the root-mean distance between the ends of the chain is given by $\sqrt{6} \bar{R}$; for a sphere the diameter is given by $\sqrt{20/3} \bar{R}$; for a thin rigid rod the length is given by $\sqrt{12} \bar{R}$; and for a thin disk the large diameter is given by $\sqrt{8} \bar{R}$.

Table II lists the results from Fig. 11 together with results on the other substances for which data are available, obtained from similar

plots. On inspecting the slopes listed in the third column of Table II, it is evident that the various substances fall into three main classes: all those that require high concentrations to induce the silicate to polymerize (including isopropyl alcohol) have slopes in the region $0.5\text{--}0.6 \times 10^{-3}$; all acid anions, all ammonium salts, and boric acid, have slopes in the region $0.9\text{--}1.0 \times 10^{-3}$, and the acetic and phosphoric acid slopes are in the region $1.2\text{--}1.4 \times 10^{-3}$. It may further be noted that in the case of the ammonium

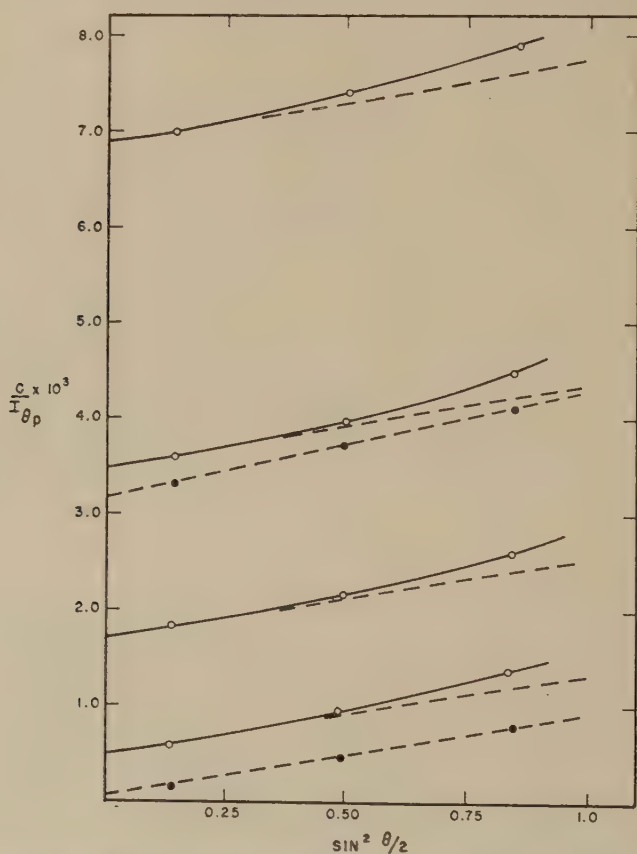


Fig. 5. Typical angular-dependence data. Open circles are for K silicate 1%-(NH_4) $_2\text{SO}_4$ 0.15 *N* at successive times (reading from top to bottom). Solid circles are for K silicate $\frac{1}{3}$ %-(NH_4) $_2\text{SO}_4$ 0.25 *N*. Broken curves indicate limiting slopes.

salts the slope is independent of the molecular weight, and in the case of neutral salts any dependence on molecular weight is slight.

Constancy of the slope as the molecular weight changes means that the molecular weight is varying linearly with the mean-square radius. The particle cannot under these circumstances be growing either as a sphere or as a rigid rod. Ammonium sulfate, the substance for which

angular-dependence data over the widest molecular-weight range are available, shows a very nearly constant slope (the one point out of line, at $I_{90}/c = 267$, probably should not have been included anyway, since it was obtained with $\frac{1}{3}\%$ Kasil, and the actual scattered intensity at 90°

TABLE II

Results from Angular Dependence of Scattered Intensity
(All with 1% K silicate, 0.0615 *N* in alkali, except as noted)

Substance added	Limiting tangent intercept ⁻¹			Mol. wt., ^b $\times 10^{-3}$	Root-mean-square radius, \bar{R}
	$I_{90}, \text{ } \mu/c$	$\alpha c/I_{90}, \times 10^3$	I_{90}/c		
<i>Ammonium salts</i>					A.
$\text{NH}_4\text{Cl}, 0.15 \text{ } M$	125	0.5	127	268	180
	325	0.92	387	816	450
$(\text{NH}_4)_2\text{SO}_4, 0.075 \text{ } M$	135	0.88	145	306	270
	250	0.89	287	606	380
	267 ^a	1.13	313	660	550
	454	0.89	592	1,250	550
	1,000	0.90	2,000	4,200	1,010
	2,010 ^a	0.89	20,000	4,200	3,170
$(\text{NH}_4)_2\text{CO}_3, 0.075 \text{ } M$	500	1.08	690	1,455	650
$(\text{NH}_4)_2\text{C}_2\text{O}_4, 0.075 \text{ } M$	119	0.92	125	264	255
	250	1.15	294	620	440
	570	1.13	883	1,860	750
$(\text{NH}_4)\text{H}_2\text{PO}_4, 0.15 \text{ } M$	289	1.0	340	718	440
	550	1.03	776	1,635	670
$(\text{NH}_4)_2\text{HPO}_4, 0.075 \text{ } M$	120	0.8	124	262	235
	226	0.89	253	534	360
	507	1.04	700	1,475	640
<i>Acids</i>					
$\text{CH}_3\text{COOH}, 0.062 \text{ } M$	350	1.2	446	941	550
$\text{H}_3\text{PO}_4, 0.036 \text{ } M$	116	1.2	126	266	270
	255	1.29	311	666	475
	484	1.40	739	1,560	760
$\text{H}_3\text{BO}_3, 0.25 \text{ } M$	126	1.0	135	285	275
	290	0.95	339	715	420
	360	0.97	442	933	490
	418	1.02	543	1,145	560

^a K silicate, 1/3%.

^b Number of significant figures for comparison purposes only. See text.

TABLE II—*Continued*

Substance added	Limiting tangent intercept ⁻¹			Mol. wt., ^b × 10 ⁻³	Root-mean-square radius, \bar{R}
	$I_{90}, \text{p/c}$	$\alpha c/I_{90}, \times 10^3$	I_{90}/c		
<i>Acid salts</i>					A.
<chem>NaH2PO4</chem> , 0.15 <i>M</i>	268	1.1	319	673	445
	531	1.03	758	1,600	665
<chem>KH2PO4</chem> , 0.15 <i>M</i>	140	0.96	151	319	285
	367	1.05	459	970	520
<chem>NaHCO3</chem> , 0.25 <i>M</i>	251	1.0	289	610	405
	525	0.98	729	1,540	846
	850	0.93	1,453	3,070	1,160
<chem>KHCO3</chem> , 0.15 <i>M</i>	110	0.8	116	245	230
	231	0.91	271	572	375
	494	0.81	619	1,310	530
<i>Other salts</i>					
<chem>Na2HPO4</chem> , 0.25 <i>M</i>	254	0.41	271	572	250
	495	0.50	576	1,215	405
<chem>K2HPO4</chem> , 0.25 <i>M</i>	263	0.7	291	614	340
	562	0.52	665	1,400	440
<chem>LiCl</chem> , 0.5 <i>M</i>	305	0.68	346	730	365
	680	0.62	872	1,840	550
<chem>NaCl</chem> , 0.5 <i>M</i>	250	0.5	269	567	275
	550	0.65	679		500
<chem>KCl</chem> , 0.5 <i>M</i>	110	0.55	113	238	185
	283	0.55	306	646	310
	525	0.59	625		455
<chem>Na2SO4</chem> , 0.45 <i>M</i>	500	0.55	600	1,265	430
<chem>K2SO4</chem> , 0.5 <i>M</i>	300	0.62	333	703	335
	550	0.52	650	1,370	435
<i>Nonelectrolyte</i>					
Isopropyl alcohol, 3.2 <i>M</i>	302	0.63	337	711	345
	559	0.50	665	1,405	435

was only 87% of that of the standard latex) over a molecular weight range of 140-fold. If the particle were growing as a rigid rod the slope should increase 140-fold in this region; if as a sphere, it should decrease

5-fold. Both such changes seem to be considerably in excess of experimental error.

Two reasonable shapes that would account for the linearity of \bar{R}^2 with the molecular weight are a disk, growing only at the edges, and a random coil. The random coil model appears at first attractive since the root-mean-square radius is about the same as that of polystyrene of the same molecular weight, and the lesser extension in salt and alcohol solutions could be explained as the usual effect noted in poor solvents. This model, however, is unlikely to represent the true state of affairs for two reasons. The first is the unreasonable kinetics if the molecule is only bifunctional, already noted. The second is the relatively low viscosity exhibited by these solutions. Measurement of the viscosity with sufficient accuracy in rapidly polymerizing systems is impractical. However, there are ways to stop the polymerization at a prechosen molecular weight. Some of these will be presented in the next section, but one has already been noted. If a 2% solution of potassium silicate is aged in the presence of 85% equivalence of acetic acid for 18 min. at 30°C., the molecular weight is about 10^6 ; if the solution is now diluted with an equal volume of water, the rate of polymerization becomes extremely slow. The specific viscosity divided by the concentration (η_{sp}/c) for a solution so prepared was found to be 25. Similarly, using data to be presented in the next section, a 2% solution of potassium silicate was aged in the presence of 125% equivalence of acetic acid and then diluted with an equal volume of $N H_2SO_4$. The final solution, at pH 3, again contains silicate with a relatively stable molecular weight of 10^6 . For this material η_{sp}/c was found to be 31.2, independent of silicate concentrations between 0.1 and 1.0%. Comparing these values with the value for spheres of 2.5, we may, following Nauman and Debye (5), calculate an effective "density" for the silicate of about 0.1 and 0.06, respectively, for the two cases. This may be compared with 0.6 reported for relatively compact soap micelles and 0.001 for polystyrene of molecular weight of 10^6 . These "densities" are not to be taken too seriously in a physical sense, but the conclusion seems inescapable that the silicate ion is very extended in relation to a sphere, but not nearly so extended as the random coil of polystyrene. If the disk model is accepted (by default), then approximating it by an oblate ellipsoid, and taking the true density of the ion as about 1.0, the relation given by Simha (16) leads to a calculated axial ratio of 42 for $\eta_{sp}/c = 30$. This calculated axial ratio is probably only indicative, since such a platelet would certainly not be very rigid.

Another observation may be made on these systems, with particular reference to the one containing ammonium sulfate. For purely geometrical reasons it can be shown that $I_{90}/c = 2/\text{slope}$. Hence in the ammonium sulfate system, with its slope of 0.89×10^{-3} , I_{90}/c cannot exceed 2250, no

matter how high the molecular weight. For $\frac{1}{3}\%$ potassium silicate this limiting value corresponds to $I_{90,p} = 750$. In Fig. 6 results obtained with ammonium carbonate and ammonium sulfate systems show that both do indeed approach this limiting value. That the molecule has not ceased growing is evident, because its scattering in the forward direction is still increasing with time; only the 90° scattering is no longer increasing. Indeed, at still larger diameters the 90° scattering will become propor-

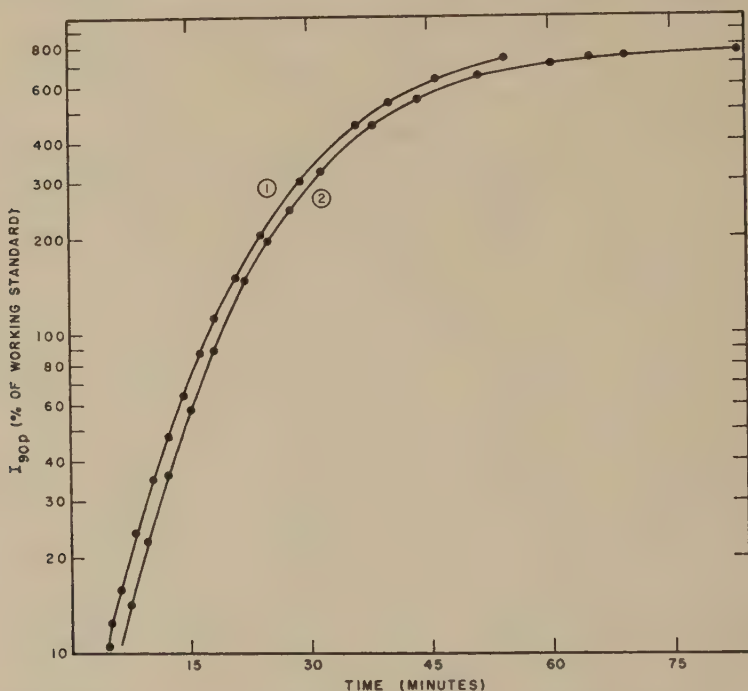


FIG. 6. Scattering from K silicate solutions. All solutions $\frac{1}{3}\%$ in K silicate. Curves (1) 0.17 M $(\text{NH}_4)_2\text{CO}_3$; (2) 0.13 M $(\text{NH}_4)_2\text{SO}_4$.

tional to the total surface area of the particles, and hence would presumably decrease with time.

Stopping and Reversing the Polymerization

Investigation of methods of stopping or reversing the polymerization appeared appropriate, not only because the success of different methods might furnish some insight into the similarities and differences between the different types of polymerization-inducing additives, but also because certain measurements are impractical or unmeaningful on rapidly polymerizing systems. Viscosity measurement, already referred to, is a case in point. In addition, solutions of stable, but high molecular weight permit

estimation of the effect of concentration and (limited) changes in environment upon the apparent size and shape of the polymer.

The most obvious method to try was the addition of alkali to an acid-induced polymerization. Figure 7 gives the scattering results, as measured in the Lumetron, for 2% silicate solutions aged in acetic acid equal to

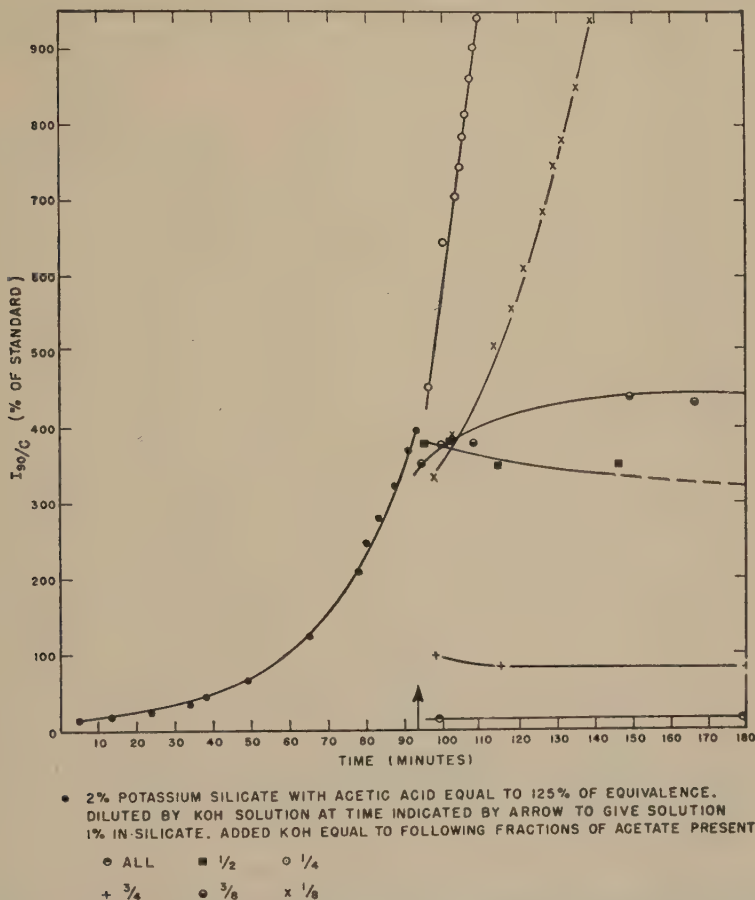


FIG. 7. Effect of dilution and added alkali on acetic acid-aged silicate solutions. Two per cent K silicate with acetic acid equal to 125% of equivalence. Diluted by KOH solution at time indicated by arrow to give solution 1% in silicate. Added KOH equal to the following fractions of acetate present: ● all, ■ $\frac{1}{2}$, ○ $\frac{1}{4}$, + $\frac{3}{4}$, ● $\frac{5}{8}$, × $\frac{1}{8}$.

125% equivalence of the alkali present. The solution was allowed to age until the molecular weight was about 0.6×10^6 , and then the solution was diluted to 1% potassium silicate with water containing various amounts of potassium hydroxide. It is evident that the reaction can indeed be stopped or reversed. If the added alkali is equivalent to the

acetic acid originally present, the depolymerization is almost immediate; if the alkali is equal to only three-quarters of the original acetic acid, only partial depolymerization is obtained, and there is evidence that the depolymerization reaction is slower. When the alkali was equivalent to one-half the original acetic acid, the polymerization was essentially

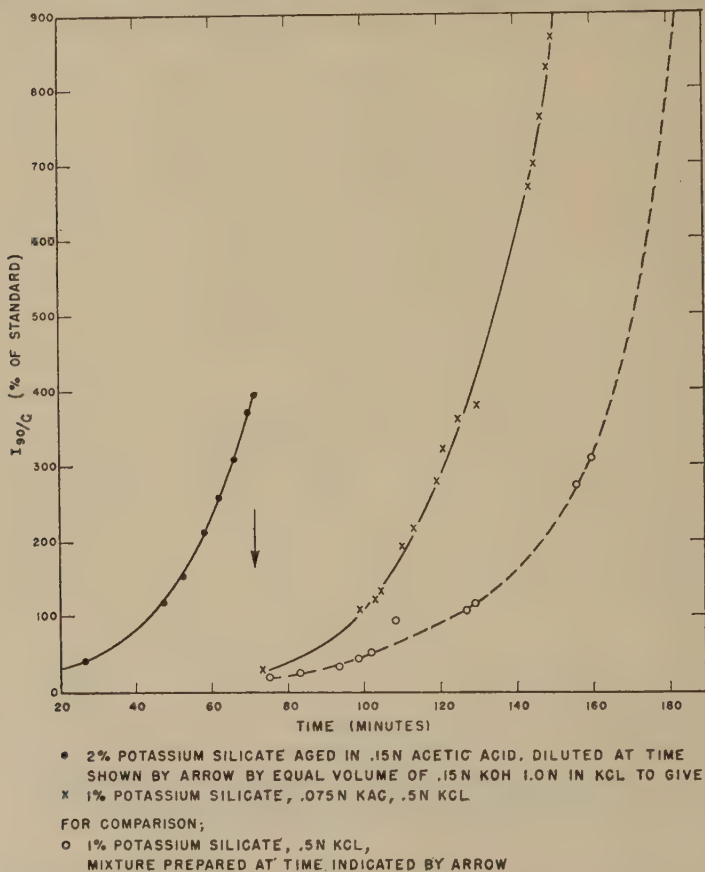


FIG. 8. Effect of simultaneous addition of KOH and KCl. Two per cent K silicate aged in 0.15 *N* acetic acid. Diluted at time shown by arrow by equal volume of 0.15 *N* KOH, 1 *N* in KCl to give (crosses) 1% K silicate, 0.075 *N* potassium acetate, 0.5 *N* KCl. For comparison, open circles are 1% K silicate, 0.5 *N* KCl, mixture prepared at time indicated by arrow.

stopped. Lesser amounts of alkali allowed the reaction to proceed. If the alkali added was equal to one-fourth the original acetic acid, the diluted solution reacted even faster than the original. This is to be expected, since the pH in this case should be that for maximum polymerization rate.

Similar results were obtained when the original polymerization was induced by an acid salt. Here, however, dilution with water alone decreased the reaction rate markedly. It had previously been found that the rate of polymerization is very sensitive to ammonium chloride concentration, probably since both the increase in pH and the decrease in electrolyte concentration decrease the reaction rate in alkaline solutions. Potassium hydroxide in an amount equal to half of the ammonium chloride originally used produced a slow depolymerization, with a half-life of about 30 min.

Results which point to a fundamental difference between the acid- and salt-induced reactions are shown in Fig. 8. A 2% potassium silicate solution was aged as usual with acetic acid. When the desired molecular weight was reached, the solution was diluted to 1% silicate with an equal volume of 1.0 *N* potassium chloride solution containing potassium hydroxide equivalent to all the acetic acid originally present. Complete and immediate depolymerization was first observed. This was then followed by a repolymerization. The rate of this new, salt-induced reaction was somewhat greater than would be expected from the concentration of potassium chloride alone, but of course some additional potassium acetate is also present. The experiment leads to the apparently inescapable conclusion that the bonds formed in the acid-induced polymerization are quite different from those produced in the alkaline, salt-induced polymerizations. The alkali is capable of breaking the acid-induced bonds in the presence of the salt, yet, obviously, is incapable of preventing the salt-induced polymerization from proceeding.

In the final experiment in this series it was found that the acetic acid-induced polymerization could be stopped (but not reversed) by adding strong acid (sulfuric) to bring the pH of the 1% silicate solution down to 2 or 3. A pH of 4 slowed the reaction very noticeably but did not quite stop it. At pH 3, the addition of potassium chloride even in amounts sufficient to give a 1.0 *M* solution, did not produce any evidence of polymerization. In contrast to the alkali, then, the strong acid was capable of preventing formation of the bonds necessary for salt-induced polymerization.

Table III presents the results of examination in the microphotometer of systems similar to those given in Fig. 7. The results in Table III illustrate the effect of adding various amounts of alkali to acetic acid-aged solutions. The solutions in each case were aged to I_{90}/c of approximately 440 (as monitored in the Lumetron) at 2% K silicate and 125% of equivalence acetic acid, and then diluted as noted in the table. In many cases this required considerable handling after the cleanup sequence, and the chances of contamination so introduced make the results in this table considerably less accurate than those of Table II. However, several con-

clusions seem safe. The results are in general similar to those found with the Lumetron. The solution diluted with water continued to polymerize slowly, whereas the one in which half the acetic acid was neutralized was relatively stable over a 24-hr. period at a molecular weight of about a million. This stability affords an opportunity to assess roughly the effect of silicate concentration on apparent molecular weight (i.e., that calculated by assuming $I_{op}/c = \lim_{c \rightarrow 0} I_{op}/c$). No appreciable difference in apparent molecular weight was found in the range $\frac{1}{4}$ –1% K silicate concentration. It is also worthy of note that the addition of alkali decreased

TABLE III

Microphotometer Results for Diluted Acetic Acid-Aged Systems

Aging conditions: 2.0% K silicate, 125% of equivalence acetic acid, aged to approx. 440% of standard, then diluted as indicated with water or KOH solution

Type of dilution	Time from dilution	$I_{90}, \nu/c$	Limiting slope $\times 10^3$	I_{op}/c	Mol. wt., $\times 10^3$
1. To 1% K silicate: with water alone	12 min.	362	1.3	476	1000
	18 min.	401	1.1	521	1100
	24 min.	434	1.2	581	1245
	55 min.	643	0.8	893	1880
2. To 1% K silicate, CH_3COOH all neutralized	45 min.	16.9	"	ca. 17	36
	5 hr. 15 min.	23.1	"	23	49
	149 hr.	53.9	"	54	114
3. To 1% K silicate, CH_3COOH $\frac{1}{2}$ neutralized	29 min.	442	0.9	549	1160
	37 min.	439	0.9	549	1160
	2 $\frac{1}{2}$ hr.	408	0.9	500	1055
	33 $\frac{1}{2}$ hr.	438	0.9	515	1085
4. No. 3 diluted to $\frac{1}{2}$ % K silicate with water at 24 hr.	10 min.	429	0.9	538	1135
	2 $\frac{1}{4}$ hr.	429	0.9	538	1135
5. No. 4 to $\frac{1}{4}$ % K silicate with water at 3 hr.	10 min.	404	0.9	493	1040

" Too low for measurement.

the extension of the molecule, as measured by the limiting slope in a c/I_θ vs. $\sin^2\theta/2$ plot, but not down to the level found in salt-induced polymerization.

In the case where all the acetic acid was neutralized, it can be seen from Table III that the polymerization reaction was reversed, although the molecular weight was not reduced quite to that of the original silicate.

ACKNOWLEDGMENT

The authors wish to thank the Radio Corporation of America, whose financial support made this work possible.

SUMMARY

An investigation was carried out on the light scattering of aqueous solutions of potassium silicate alone and in the presence of various salts and acids. The molecular weight of the potassium silicate ($\text{SiO}_2:\text{K}_2\text{O}$ mole ratio of 3.8:1) could not be determined accurately because of aging effects in dilute solutions, but was in the neighborhood of 2000.

From a study of the various factors influencing the rate of polymerization it was found that:

1. The rate of the salt-induced polymerization is nearly exactly proportional to the 4th power of the concentration of the added salt, and approximately proportional to the inverse square root of the silicate concentration. The rate of the acid-induced polymerization goes through a sharp maximum at a pH of approximately 8 (in agreement with previous "gel-time" studies).

2. The activation energy of the polymerization reaction goes through a minimum at a pH of about 8, as judged from temperature-dependence studies on reactions induced by various concentrations of acetic acid and potassium chloride. The activation energies in neutral and acid solutions agree very well with those calculated by others from "gel times." However, that for the alkaline, salt-induced reaction does not, possibly because in these solutions the molecular weight at a given yield point varies with temperature.

3. The angular dependence of the intensity of scattered light was not meaningful for the low molecular weight silicates, apparently because of the presence of a small amount of high molecular weight material not removed by the cleanup procedures. When the molecular weight is over about 10^5 , however, the effect of the main solute masks the effect of the impurities. From investigation of solutions in which the molecular weight of the silicate is above this value, it was found that (a) the extension (as measured by the root-mean-square radius) of the polymer is less in salt-induced polymerization than in those cases where pH is the controlling factor, and (b) in either case the extension varies as the square root of the molecular weight.

4. The acid-induced polymerization may be slowed, stopped, or reversed by the addition of alkali, or stopped (but not reversed) by the addition of excess acid. In studying the reversal of acid-induced polymerization by the addition of alkali, it was found that if the alkali solution added to reverse the reaction also contains salt, the polymerization reverses as usual, but this reversal is followed by a relatively rapid repolymerization. It thus appears as an inescapable conclusion that the bonds formed in the acid-induced polymerization are different from those formed in the alkaline, salt-induced polymerization.

REFERENCES

1. RAY, R. C., GANGULY, P. B., AND LAL, A. B., *Trans. Faraday Soc.* **38**, 104 (1942).
2. JANDER, G., AND HJUKESHOVEN, W., *Z. anorg. u. allgem. Chem.* **201**, 361 (1931).
3. TREADWELL, W. D., AND KÖNIG, W., *Helv. Chim. Acta* **16**, 54 (1933).
4. DEBYE, P., AND NAUMAN, R. V., *J. Chem. Phys.* **17**, 664 (1949).
5. NAUMAN, R. V., AND DEBYE, P., *J. Phys. & Colloid Chem.* **55**, 1 (1951).
6. BLAKER, R. H., BADGER, R. M., AND GILMAN, T. S., *J. Phys. & Colloid Chem.* **53**, 794 (1949).
7. ZIMM, B. H., *J. Chem. Phys.* **16**, 1099 (1948).
8. CABANNES, J., AND DAURE, P., *Compt. rend.* **184**, 520 (1927).
9. HADOW, H. J., SHEFFER, M., AND HYDE, J. C., *Can. J. Research* **27B**, 791 (1949).
10. OUTER, P., CARR, C. J., AND ZIMM, B. H., *J. Chem. Phys.* **18**, 830 (1950).
11. HALWER, M., *J. Am. Chem. Soc.* **70**, 3985 (1948).
12. FLORY, P. J., *J. Am. Chem. Soc.* **58**, 1877 (1936).
13. HURD, C. B., AND MILLER, P. S., *J. Phys. Chem.* **36**, 2194 (1932).
14. HURD, C. B., AND LETTERON, H. A., *J. Phys. Chem.* **36**, 604 (1932).
15. MUNROE, L. D., McNAB, J. G., AND OTT, W. L., *Can. J. Research* **27B**, 781 (1949).
16. SIMHA, R., *J. Phys. Chem.* **44**, 25 (1940).

BOOK REVIEW

Comité International de Thermodynamique et de Cinétique Electrochimiques. *Comptes rendus de la IIIe réunion*. Berne, 1951. Carlo Manfredi, Milano, 1952. 499 pp. Price 8000 liras.

This is a report on the conference held in August, 1951 by the International Committee of Electrochemical Thermodynamics and Kinetics. It contains three main divisions: (a) original papers on the electrochemical behavior of metals and nonmetals, (b) original papers on the electrical double layer, and (c) papers on electrochemical definitions and nomenclature. The contents of the first two divisions differ from those of an average conference of the Electrochemical Society by the emphasis placed on theory, especially on the thermodynamical theory. Everyone interested in the fundamentals of electrochemistry will profit by reading these parts of the volume. The third division was a little disappointing to the reviewer who believes that definitions should be closely related to the experiments by which the quantity defined can be measured.

In the second division, which would be of the most immediate interest to the readers of this Journal, five papers report experimental work (on electrocapillarity, AgI electrodes, centrifugation potentials, electrodialysis, and polarography) and three are theoretical contributions.

The major part of the book is in French but there are also papers in English and in German.

J. J. BIKERMAN, New York, New York

THE INTERFACIAL ACTIVITY OF MESOPORPHYRIN IX AND SOME DERIVATIVES¹

H. N. Dunning

*Surface Chemistry Laboratory, Petroleum Experiment Station, Bureau of Mines,
Bartlesville, Oklahoma*

Received December 1, 1952

ABSTRACT

The pendent-drop method has been used to study the interfacial aging of solutions of mesoporphyrin IX, its dimethyl ester, and the vanadium complex of the dimethyl ester.

Mesoporphyrin IX dimethyl ester in benzene or chloroform exhibited moderate interfacial activity at the water interface. The free acid and the vanadium complex in benzene solutions were considerably more active than the ester.

The interfacial activity of the esters increased with the alkalinity of the aqueous phase. This increase is attributed to alkaline hydrolysis of the ester to form the more active acid.

Mesoporphyrin IX and the vanadium complex formed complete solid films after short aging periods at the benzene-water interface. Mesoporphyrin IX dimethyl ester formed no solid film at the water-chloroform interface and little solid film upon extended aging at the benzene-water interface.

INTRODUCTION

The influence of interfacially active substances upon the displacement, from a solid surface, of one fluid phase by another has been recognized for many years. A more recent development is the application of the methods of surface chemistry to the production of crude petroleum. The properties of interfacially active substances indigenous to crude petroleum are of prime importance to research in this field.

Treibs (17) isolated several porphyrins from crude petroleum. Skinner (15) reports that much of the vanadium in Santa Maria Valley crude petroleum is complexed with porphyrins. Therefore, studies of the interfacial properties of the porphyrins are of immediate practical importance to research on methods for more efficient production of crude petroleum. It should be emphasized that the porphyrins may be only one of many types of interfacially active substances in crude petroleum.

Relatively few investigations of the surface and interfacial properties of these substances have been reported. Alexander (1) has studied the

¹ Presented before the Colloid Division, American Chemical Society, Atlantic City, N. J., September 15, 1952.

porphyrins as monolayers on aqueous substrates. Although studies of porphyrin films at the oil-water interface may have greater biological significance, they are much more difficult to conduct. The pendent-drop apparatus (2) is well adapted for studying interfacial activity and film formation, since problems of diffusion are minimized and it is possible to determine values of interfacial tension without disturbing the system.

Mesoporphyrin IX, its dimethyl ester, and the vanadium complex of the dimethyl ester were selected as typical examples of the porphyrins and their complexes. The structure of mesoporphyrin IX and its orientation at an oil-water interface are illustrated in Fig. 1. Since the esters may be hydrolyzed under some conditions, the effect of pH on the interfacial tensions of these substances was investigated.

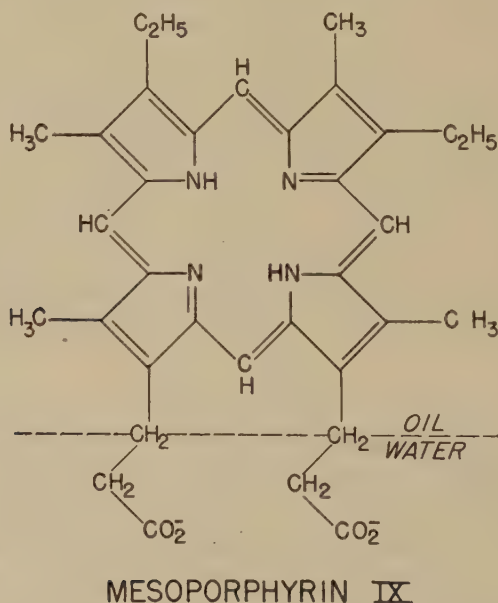


FIG. 1. Orientation of mesoporphyrin IX at oil-water interface (8).

MATERIALS

Porphyrins

Mesoporphyrin IX was prepared from hemin by the method of Corwin and Erdman (6) and esterified in a chloroform suspension, using diazomethane. The vanadium complex of mesoporphyrin IX dimethyl ester was prepared by the method of Treibs (18). The esterified porphyrin and vanadium complex were recrystallized from a methanol-chloroform solution. The mesoporphyrin IX used in the interfacial-tension studies was prepared from the ester by alkaline hydrolysis.

Solvents

The water, chloroform, and benzene were purified carefully prior to use. These three liquids were judged to be free of surface-active impurities, since the values of interfacial tension of benzene and chloroform at the water interface showed no measurable decrease on aging. These values of interfacial tension agreed closely with those recorded in the literature (3,12,16). The densities of the purified solvents and mutually saturated phases also agreed closely with literature values (7,9,11,14).

Buffers

The buffer solutions were prepared from double-distilled water and Coleman pH tablets. The sodium hydroxide used for preparing basic solutions was A.C.S. reagent-grade standard.

EXPERIMENTAL

The values of interfacial tensions that were the major objective of this study were determined by the pendent-drop method (2). Interfacial tensions between pure liquids may be determined very precisely with the pendent-drop apparatus. However, the precise reproduction of aging

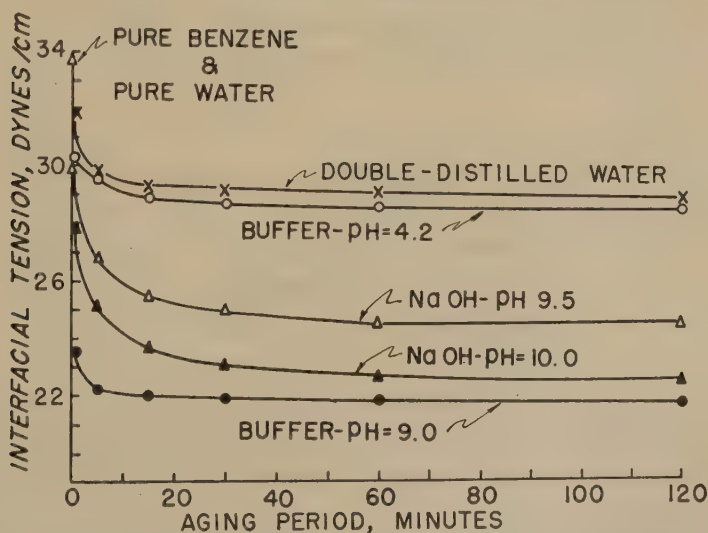


FIG. 2. Effect of pH on interfacial tensions of 0.031 wt. % solutions of mesoporphyrin IX dimethyl ester at benzene-water interface.

curves involving interfacially active substances is extremely difficult owing to various phenomena (10,19), which may disturb the rate of establishment of equilibrium in the system. The values recorded for the aging curves exhibited maximum variations of about ± 0.2 dyne/cm.

The effect of pH on the interfacial tensions of 0.031 wt. % solutions of mesoporphyrin IX dimethyl ester in benzene at aqueous interfaces is shown in Fig. 2. Using an aqueous phase buffered to a pH of 4.2 caused only a slightly larger interfacial tension decrease than that observed when the aqueous phase consisted of distilled water. The electrolyte effect is not appreciable in this case. When the aqueous phase was made basic by the addition of sodium hydroxide, the interfacial tension decrease was greater than when an acidic or neutral aqueous phase was involved. The change in interfacial tension increased with the concentration of sodium hydroxide and approached the change in interfacial tension observed with an aqueous phase buffered to a pH of 9.0. Where the interfacial tension decrease is considered a function of available hydroxyl ion concentration

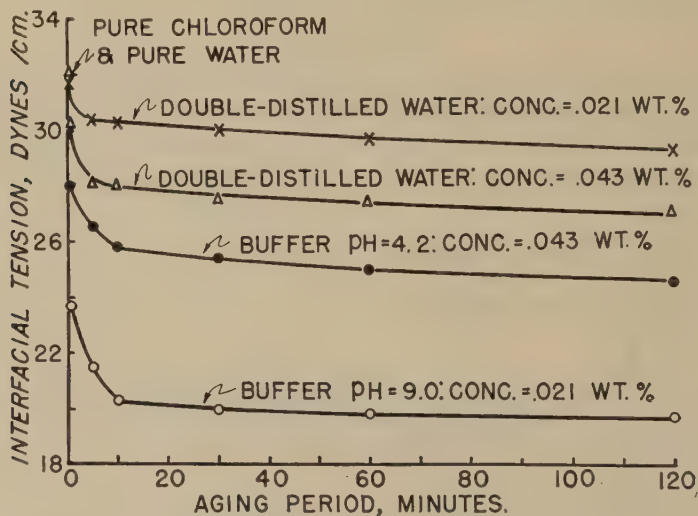


FIG. 3. Effect of pH on interfacial tensions of solutions of mesoporphyrin IX dimethyl ester at chloroform-water interface.

these results might be expected. The buffered solution presents a reservoir of available hydroxyl ion and hence is not so readily depleted in a region near the interface as the sodium hydroxide solutions of relatively low concentration.

The effect of pH on the interfacial tensions of solutions of mesoporphyrin IX dimethyl ester in chloroform at aqueous interfaces is shown in Fig. 3. The decrease in interfacial tension caused by buffering the aqueous phase to a pH of 4.2 was somewhat larger than in the case of the benzene solutions. However, with the aqueous phase buffered to a pH of 9.0 and the use of a more dilute solution, the interfacial tension decrease was about five times as large as that for a solution buffered to a pH of 4.2.

The *interfacial excess* at the chloroform–water and benzene–water interfaces for solutions of mesoporphyrin IX dimethyl ester was calculated from the Gibbs adsorption equation (13). The results are approximations, since values of concentrations rather than activities were used. If the mesoporphyrin film is in the form of a unimolecular layer at the interface, these calculations indicate that in the more concentrated solutions the molecules become vertically arranged rather quickly and that as the drop ages for extended periods enough molecules accumulate at the interface to form a vertically arranged, close-packed film.

The effect of pH on the interfacial tensions of 0.031 wt. % solutions of the vanadium complex of mesoporphyrin IX dimethyl ester in benzene at aqueous interfaces is shown in Fig. 4. The complex was peptized with a

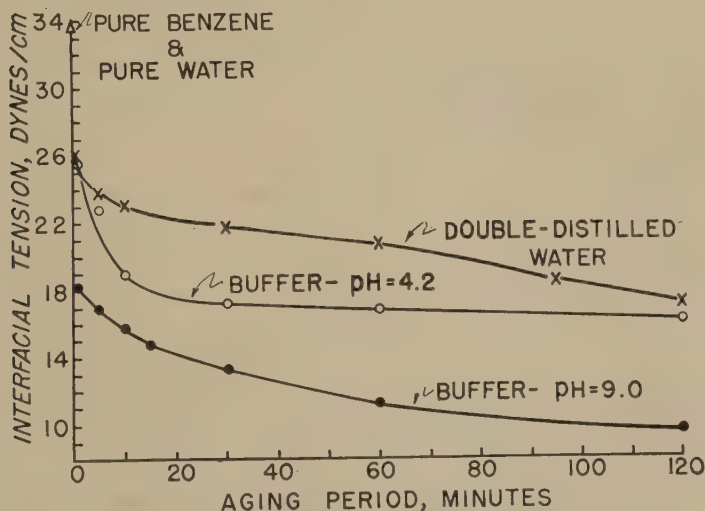


FIG. 4. Effect of pH on interfacial tensions of 0.031 wt. % solutions of vanadium complex at benzene–water interface.

drop of pyridine before adding the benzene. Again, buffering the aqueous phase to a pH of 4.2 caused a slightly larger decrease in interfacial tension than that observed at the water interface. A much larger decrease was caused by buffering the aqueous phase to a pH of 9.0.

A pyridine peptization of the porphyrin before solution in benzene may have a relatively small effect on the interfacial tension values observed during aging. When pyridine was used as a peptization agent, it was observed that, although the interfacial tension decrease was more rapid during the first 5 min. of aging, the values after 1 and 2 hr. were only 0.3 and 0.2 dyne/cm. lower, respectively, than corresponding values determined when the solvent was pure benzene. The effect on film-forming tendencies is more marked. This effect will be discussed below.

The porphyrin ring forms a large planar plate (1,8) which is mainly of a hydrophobic nature. In mesoporphyrin IX the two propionic acid side chains form a hydrophilic portion at the edge of this planar molecule. This duality of structure lends the porphyrins their interfacial activity. Since both the vanadium complex and the uncomplexed ester have the same hydrophilic group (e.g., methyl ester of propionic acid) these results indicate that the presence of vanadium causes better balancing of the hydrophobic-hydrophilic ratio of the molecule to form a substance of greater interfacial activity. This change may be due to lessening of the hydrophobic nature of the porphyrin ring by the addition of vanadium.

The effect of varying pH on the interfacial tensions of the ester solutions may be explained if the porphyrin esters are classified as anionic

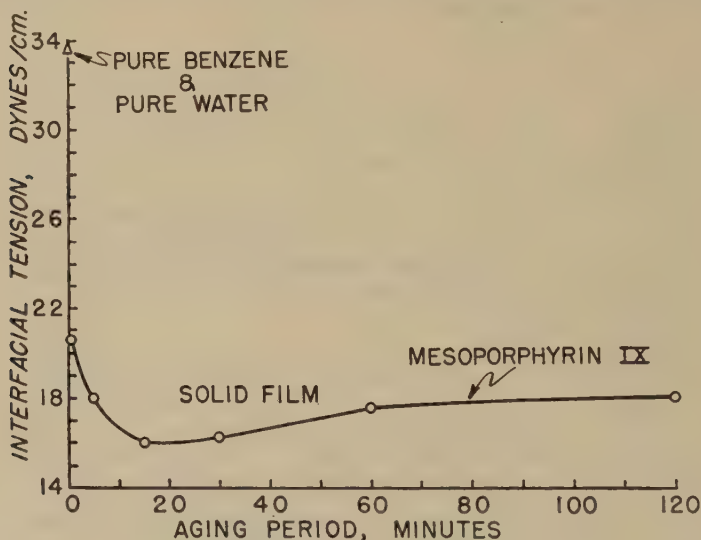


Fig. 5. Interfacial activity of 0.028 wt. % solution of mesoporphyrin IX at benzene-water interface.

surface-active agents of moderate effectiveness. The free acid form of the porphyrin might be expected to be more active interfacially than the ester owing to the more pronounced hydrophilic character of the propionic side chain compared to the esterified form.

The greater interfacial activity of the free acid was demonstrated by determining the interfacial tensions of solutions of mesoporphyrin IX in benzene at the water interface. The results of these studies are shown in Fig. 5. These data show that the free acid form is indeed more active interfacially than the esterified porphyrin. Further, mesoporphyrin IX appears to be the limiting case which is approached by increasing the pH

of the aqueous phase in studies of the interfacial tensions of solutions of mesoporphyrin IX dimethyl ester.

The effect of pH on the interfacial tensions of solutions of the esters of mesoporphyrin IX and the vanadium complex of mesoporphyrin IX may be consistently explained as due to the hydrolysis of the esters, in the presence of hydroxyl ion, to form the free acid (or sodium salt of the free acid) of greater interfacial activity.

The apparent increase (Fig. 5) in the interfacial tensions of solutions of mesoporphyrin IX in benzene at the water interface after about 20 min. has elapsed is attributed to formation of a solid film about the pendent drop. Solid films may lead to several indeterminate errors. Photographs of drops exhibiting this apparent increase in interfacial tension often revealed that the drops were unsymmetrical. This lack of symmetry invalidates the fundamental mathematical treatment of Bashforth and Adams (5). Even with symmetrical drops, the solid film that causes the above observed lack of symmetry may cause other less obvious errors.

Observations of the film-forming tendencies of mesoporphyrin IX, its dimethyl ester, and the vanadium complex of the dimethyl ester were made during the interfacial-tension studies. According to the method of Bartell and Niederhauser (4), film-forming tendency is expressed as the percentage of the original drop length remaining at the first indication of a solid film as the drop is drawn back into the pendent-drop tip.

No solid films were observed with the solutions of mesoporphyrin IX dimethyl ester in chloroform. Some slight formations of solid films were observed with benzene solutions of this substance at the water interface. The film-forming tendency appeared to increase slightly with increasing values of pH. At the interface with double-distilled water after a 16-hr. aging period, the film formation varied from about 0 to 30%. Definite wrinkling of the film was observed after nearly complete retraction of the drop. These wrinkles were unstable. The drop quickly reverted to a rounded shape when retraction ceased.

When the benzene solution was prepared by an initial pyridine peptization of the mesoporphyrin IX dimethyl ester, a film formation of somewhat greater extent was observed. The film formation was about 35% for a drop aged 2 hr. The film was not visibly different from those observed when pure benzene was the solvent.

The film formation exhibited by benzene solutions (prepared by pyridine peptization) of the vanadium complex of mesoporphyrin IX dimethyl ester at aqueous interfaces was much greater than that observed with the uncomplexed porphyrin. These solutions uniformly exhibited a film formation of 100% with a drop aged 2 hr. and about 50% with a drop aged 10 min. These films showed marked wrinkling effects. Owing to the peculiar appearance of these wrinkles, they will be referred to as "shroud

lines." These films are remarkably similar in appearance and behavior to those observed with crude oil or crude-oil extracts at the water interface (4).

Solutions of mesoporphyrin IX in benzene (peptized by pyridine) showed a film formation of an extent equal to or greater than that shown by the solutions of the vanadium complex. Retraction of a drop of the mesoporphyrin IX solution aged 1 min. revealed a film formation of about 45%. A film formation of 100% was observed consistently after a 2-hr. period and often after about 30 min. The solid film formed by the mesoporphyrin IX differed from the films previously observed for the dimethyl ester and the vanadium complex of the dimethyl ester. At no time were shroud lines observed with the free acid. Instead of forming such shroud lines, upon retraction the film wrinkled and then appeared to "jump" up the capillary, leaving a fully rounded drop of smaller size. Small particles of solid material, presumably of the film, were thereupon observed inside the drop. The observation that water sometimes flowed down the capillary beside what appeared to be an elastic sac of the film without breaking the column of the solution is further evidence of the presence of solid films.

It will be necessary to study varied types of porphyrins, prepared from different sources, to determine whether the shroud lines observed with the esters and the conspicuous absence of these shroud lines with the free acid are of a general nature. That such may be the case may be shown if the differences between the hydrophilic natures of the ester and acid side chains of the porphyrin molecules are considered. The formation of a stable wrinkle or shroud line involves the detachment of many of these side chains from the water phase and the folding of these chains back upon a similar layer of side chains. In general, this should be more easily accomplished the weaker the hydrophilic nature of the side chain. These shroud lines might be expected to be formed more readily with the ester side chain than with the acid side chain, since the ester has been indicated to be less hydrophilic than the free acid.

ACKNOWLEDGMENTS

The writer wishes to express his sincere appreciation to Dr. R. I. Walter, who furnished the porphyrin samples and reviewed the manuscript; to Dr. C. G. Dodd, who assembled the pendent-drop apparatus; and to Dr. J. P. McCullough, who reviewed the manuscript.

CONCLUSIONS

The pendent-drop method has been used to study the interfacial activity and film formation of solutions of mesoporphyrin IX, its dimethyl ester, and the vanadium complex of the dimethyl ester.

Mesoporphyrin IX dimethyl ester in benzene or chloroform exhibited moderate interfacial activity at the water interface. The free acid and

the vanadium complex in benzene solutions were considerably more active than the ester.

The interfacial activity of the esters increased with the alkalinity of the aqueous phase. This increase is attributed to alkaline hydrolysis of the ester to form the more active acid or salt of the acid.

Mesoporphyrin IX dimethyl ester formed no solid film at the chloroform-water interface and little solid film upon extended aging at the benzene-water interface. Mesoporphyrin IX and the vanadium complex formed complete solid films after short aging periods at the benzene-water interface. Films formed by the esters gave stable wrinkling effects upon partial retraction of the drops whereas films of the free acid did not. The films formed by the esters are similar in appearance and behavior to those formed from crude oil solutions at the water interface.

The differences in interfacial activity and film formation exhibited by these substances are attributed to variations in the hydrophobic-hydrophilic balance of the molecules. These variations may be caused by a decrease in the hydrophobic nature of the porphyrin ring due to vanadium or to a decrease in the hydrophilic nature of the propionic acid groups upon esterification.

REFERENCES

1. ALEXANDER, A. E., *J. Chem. Soc.* **1937**, 1813.
2. ANDREAS, J. M., HAUSER, E. A., AND TUCKER, W. B., *J. Phys. Chem.* **42**, 1001 (1938).
3. BARTELL, F. E., AND MILLER, F. L., *J. Am. Chem. Soc.* **50**, 1966 (1928).
4. BARTELL, F. E., AND NIEDERHAUSER, D. O., Fundamental Research on Occurrence and Recovery of Petroleum 1946-47, pp. 57-80. American Petroleum Institute, New York, 1949.
5. BASHFORTH, F., AND ADAMS, J. C., An Attempt to Test the Theories of Capillary Action, p. 13. Cambridge University Press, Cambridge, 1883.
6. CORWIN, A. H., AND ERDMAN, J. G., *J. Am. Chem. Soc.* **68**, 2475 (1946).
7. FORZIATI, A. F., GLASGOW, A. R., WILLINGHAM, C. B., AND ROSSINI, F. D., *J. Research Natl. Bur. Standards* **36**, 134 (1946).
8. LEMBERG, R., AND LEGGE, J. W., Hematin Compounds and Bile Pigments, p. 70. Interscience Publishers, New York, 1949.
9. MORGAN, S. O., AND LOWRY, H. H., *J. Phys. Chem.* **34**, 2385 (1930).
10. DU NOUY, P. L., Surface Equilibria of Biological and Organic Colloids, p. 35. Chemical Catalog Company, New York, 1926.
11. OLSON, A. L., AND WASHBURN, E. R., *J. Am. Chem. Soc.* **57**, 303 (1935).
12. POUND, J. R., *J. Phys. Chem.* **30**, 791 (1926).
13. GIBBS, J. W., The Collected Works of J. Willard Gibbs, Vol. I, p. 219. Longmans, Green and Co., New York, 1931.
14. SIMONSEN, D. R., AND WASHBURN, E. R., *J. Am. Chem. Soc.* **68**, 236 (1946).
15. SKINNER, D. A., *Ind. Eng. Chem.* **44**, 1159 (1952).
16. TRANSUE, L. F., WASHBURN, E. R., AND KAHLER, F. H., *J. Am. Chem. Soc.* **64**, 276 (1942).
17. TREIBS, A., *Ann.* **510**, 42 (1934).
18. TREIBS, A., *Ann.* **517**, 192 (1935).
19. WARD, A. F. H., AND TORDAI, L., *J. Chem. Phys.* **14**, 453 (1946).

THE ROLE OF THE SUBSTRATE IN THE DETERGENCY PROCESS¹

Manuel N. Fineman and Phyllis J. Kline

Research Laboratories, Rohm and Haas Company, Bridesburg, Pennsylvania

Received October 6, 1952

ABSTRACT

Experiments are described which demonstrate in a striking fashion the influence of the substrate on the process of removal of soil by a detergent.

When metallic and nonmetallic substrates are coated with an oily-carbon soil, and immersed in solutions of a non-ionic surfactant of the alkylaryl polyether alcohol type, the metals promote rapid removal of the soil in finely dispersed form, whereas the same soil comes off the nonmetallic substrates very slowly and in fairly large clumps.

For metals, fineness of soil dispersion depends upon the electrical character of the substrates, and is roughly proportional to their position in the electromotive series.

The composition of the oily-carbon soil is shown to be unique, and makes these phenomena possible.

INTRODUCTION

Although the process of detergency involves the interaction of soil, surfactant, and substrate, it is surprising that relatively few investigators have examined the role played by the surface being cleaned. Most investigators have concerned themselves with the physical or chemical properties of the detergent solutions. Consequently the literature is replete with reports of unsuccessful attempts to correlate detergency efficiency with such phenomena as surface or interfacial tension, foam capacity, or emulsification efficiency of the detergent (1).

Fifteen years ago Adam (2) and Robinson (3) pointed out that no one factor alone will determine the efficiency of a detergent. The essential conditions involve a combination of three factors, in two of which the substrate plays a major role. These are: high surfactant-substrate adhesion tension, low soil-substrate adhesion tension, and low soil-surfactant interfacial tension.

WETTING PHENOMENA

In their excellent analysis of the performance of diphasic metal cleaners, Reich and Snell (4) emphasized that preferential wetting of the substrate by the detergent solution was a prerequisite to cleaning. However,

¹ Presented at 122nd National Meeting of the American Chemical Society in a general session of the Division of Colloid Chemistry, Atlantic City, N. J., September 16, 1952.

where energy considerations at the interface between soil, solution, and substrate were such as to promote preferential wetting of the substrate by the oil phase, they demonstrated that the detergent would promote soiling rather than cleaning.

These observations have been confirmed in a general way in this laboratory where the response of twenty different substrates to various ionic and non-ionic surfactants has been investigated (5). Our data showed that efficiency of the surfactant depended upon the nature of the surface being cleaned; and that ionic surfactants could indeed interact with that surface to promote soiling rather than cleaning. For example, although anionic surfactants generally cleaned glass and ceramic tile well, they were ineffective—and in some cases caused soil redeposition—on metals. Similarly, cationics promoted soil redeposition on glass. Non-ionic surfactants, however, were effective in cleaning both metal and glass surfaces.

Investigations of the contact angles at the soil-substrate-surfactant interface revealed that anionic and cationic surfactants could cause preferential wetting of metal and glass, respectively, by the soil phase, thus promoting soiling and soil redeposition on these surfaces. The non-ionic surfactants, however, promoted wetting of these substrates by the aqueous phase and, consequently, produced cleaning in both cases. Moreover, the non-ionics were especially good soil-suspending agents, whereas both anionics and cationics were quite poor in this regard.

Although the non-ionics were apparently much less sensitive than the ionics to the characteristics of the substrates, nevertheless, careful observation of the dispersed soil revealed that the non-ionics, too, could interact with the substrates. For example, soil was more readily removed from certain substrates than from others. In addition, degree of dispersion of the soil in the surfactant solution was found to depend upon the substrate from which the soil had been removed.

It will be the purpose of this paper to describe these strange phenomena and to interpret them in terms of the role of the substrate in the detergency process.

EXPERIMENTAL

A standard amount (0.075 g.) of an oily-carbon paste, made by mixing one part of fine carbon black (Philblack 0)² with two parts of aliphatic mineral oil (Atreol 9),³ was applied by spatula to iron and brass washers and to small pieces of glass so that all surfaces were covered. Two soiled and two clean substrates of each type were immersed in 200-ml. solutions of 1.0, 0.3, and 0.1% detergent contained in standard pint Launder-

² Product of Phillips Petroleum Company.

³ Product of Atlantic Refining Company.

ometer jars. The detergent was Triton X-100,⁴ a representative non-ionic surfactant of the alkylaryl polyether alcohol type. The substrates were then agitated in a Launderometer for 10 min. at 60°C. (140°F.). At the end of that period they were removed from the jars and found to be

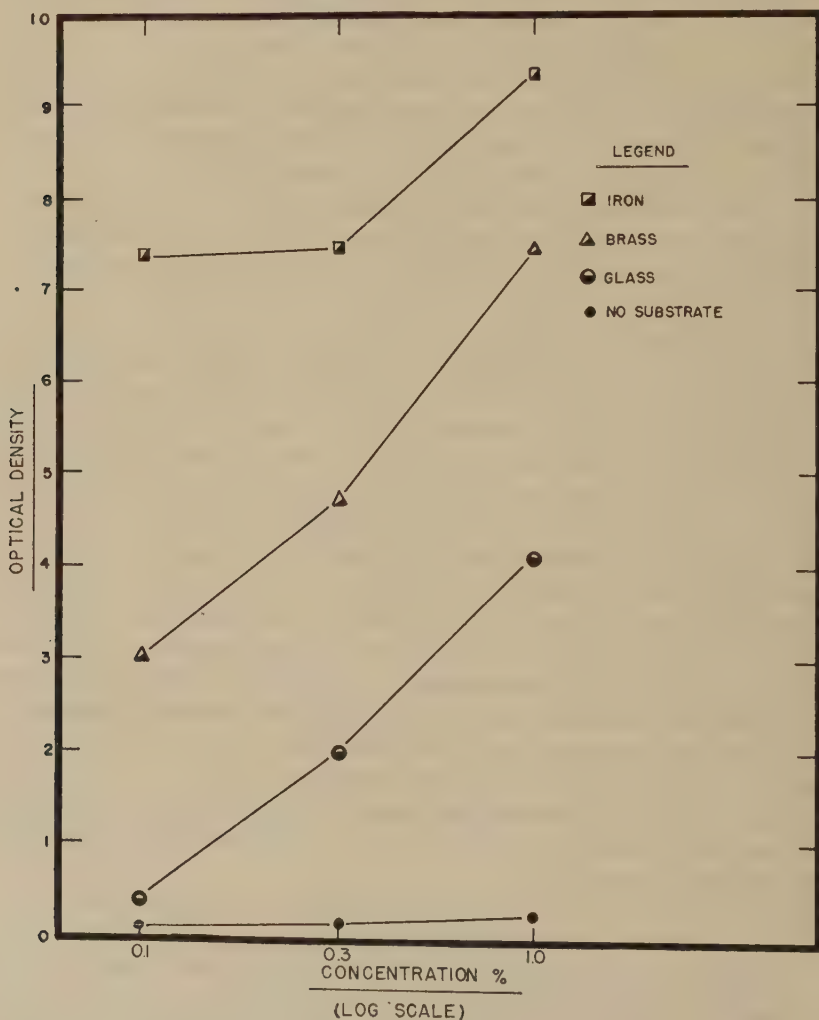


FIG. 1. Dispersion of soil in non-ionic detergent solutions at 60°C. (140°F.).

clean; but the detergent solutions demonstrated wide variations in optical density. The data, obtained with a Coleman spectrophotometer, are shown graphically in Fig. 1.

⁴ Product of Rohm and Haas Company.

Since all of the substrates held equal amounts of soil and were thoroughly cleaned by the detergent solutions, the differences in the optical densities must be attributed to the fact that soil removed from iron was much more finely divided than the same amount of soil removed—by the same detergent—from brass or from glass. This was readily confirmed by microscopic examination of the suspended soil.

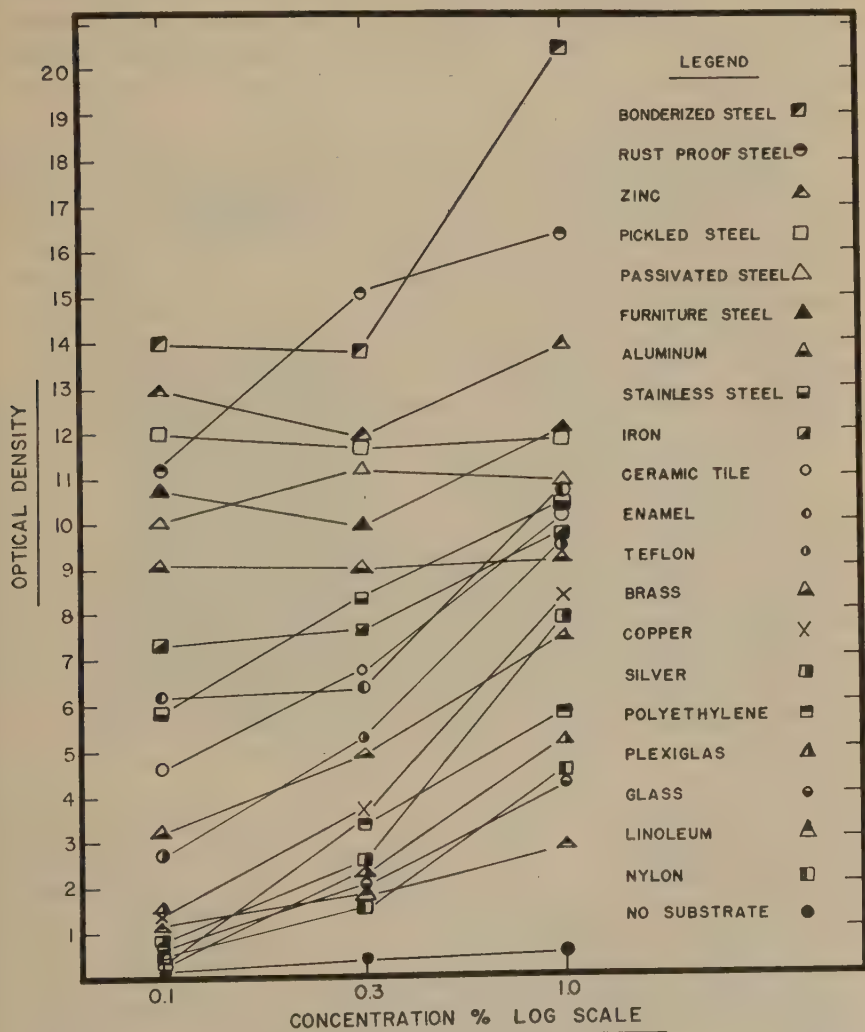


FIG. 2. Characterization of substrates by dispersion of soil in non-ionic detergent solutions at 60°C. (140°F.).⁵

⁵ Teflon is a product of duPont Company.
Plexiglas is a product of Rohm & Haas Company.

Moreover, a lump of oily-carbon paste added to the detergent solution in the absence of any substrate did not disperse. Therefore, optical density was very low. Apparently, in order to be dispersed, the soil must come off a substrate—it will not disperse by itself. This observation suggests that emulsification of the oily-carbon soil by the surfactant must be much less significant as a mechanism for soil removal than had been anticipated. The nature of the substrate from which the soil is removed seems to be the important criterion. The differences in optical density are so great that this technique may be used for characterizing substrates in a very meaningful manner, i.e., in terms of ease of soil removal and degree of dispersion of that soil.

Accordingly, the various metal, glass, and plastic substrates which had been investigated in our extensive studies of detergency were coated with equal amounts of the standard soil and cleaned in the non-ionic detergent solutions as before. All of the substrates were cleaned effectively at the three concentrations of surfactant employed—except pickled steel which retained a thin film of residual soil (6). The optical densities of the solutions are reported in Fig. 2. In terms of degree of dispersion of the removed soil, the substrates demonstrated a wide spectrum of activity ranging from the steels which produced finely dispersed soil suspensions to the plastics which produced rather coarse flocs.

Not only did the substrate affect the degree of dispersion of the soil; at room temperature it also affected the rate of removal of that soil from the surface. This could be readily demonstrated by pouring portions of the same non-ionic surfactant solution over soiled steel and nylon substrates. Within seconds, the surface soil on the steel started to disperse into the solution and, within minutes, the solution became black. However, as shown in Fig. 3, nothing happened to the soil on the nylon. Even after prolonged agitation very little soil was removed—and soil which was dislodged came directly off the nylon in clumps.

This specificity of interaction was independent of the amount of soil applied and was also shown to be independent of the prior location of that soil. For example, soil was removed from steel and transferred manually to a clean panel of nylon; and soil from nylon was transferred to steel. The soil which had come off in clumps from the nylon came off the steel in a finely dispersed form; and soil transferred from the steel to the nylon now came off in clumps.

Small portions of soil were removed from the steel panel and transferred to a fresh solution of detergent. No disintegration of these soil clumps was now noted—even after violent agitation and prolonged immersion in the detergent.

In order to show that the differences between the substrates were real and statistically significant, ten replicate samples of zinc bearing identical

amounts of soil were tumbled in detergent solutions in the usual manner. Optical densities were measured and their coefficient of variation was found to be very low—4.3%. Ten replicate samples of glass produced low optical densities in solution which led to a somewhat higher coefficient of variation—11%.

Assuming that prolonged agitation might cause coarse flocs of soil to break down into finer particles, soiled glass and zinc substrates were agitated for 6 hr. in the Launderometer, and the detergent solutions were examined for changes in optical density at regular intervals during that

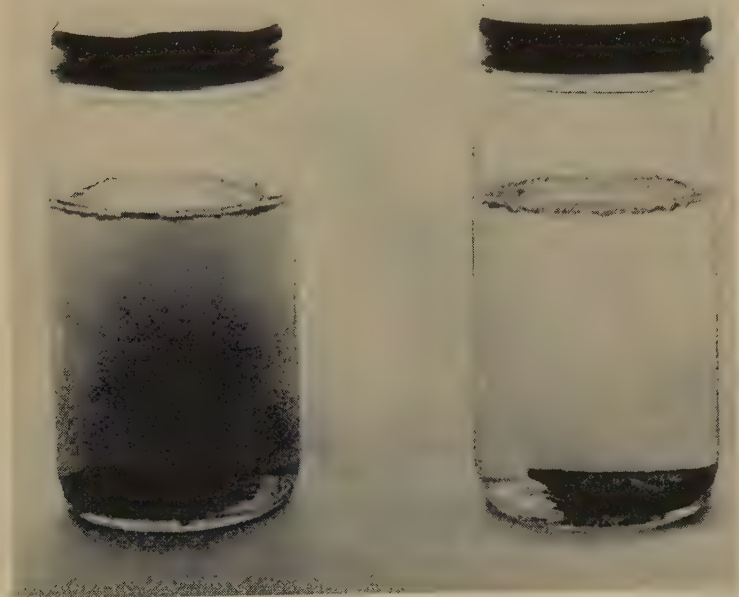


FIG. 3. Soil removal from furniture steel (left) and nylon (right).

time. As shown in Fig. 4, there was little change in optical density of the solution containing the zinc substrates. However, the soil clumps which came off the glass did break down to finer particle size upon agitation and, consequently, produced the high optical density values which were observed. Therefore, although the substrates influence the rate and nature of the soil removal process, agitation can ultimately reduce the size of the soil clumps which may be formed. Assuming that heavy substrates would be more violently agitated in the Launderometer than light ones, a plot of substrate weight against optical density was examined, but no correlation was found. Consequently, the initial soil removal processes, as characterized by optical-density measurements, cannot be attributed to differences in the weights of the substrates.

PROCESSES OF SOIL REMOVAL

As indicated earlier, the substrate is involved in the soil removal process insofar as it affects the relative magnitudes of the surfactant-substrate and soil-substrate adhesion tensions. Since the non-ionic surfactant cleaned all the substrates examined, it must be concluded that

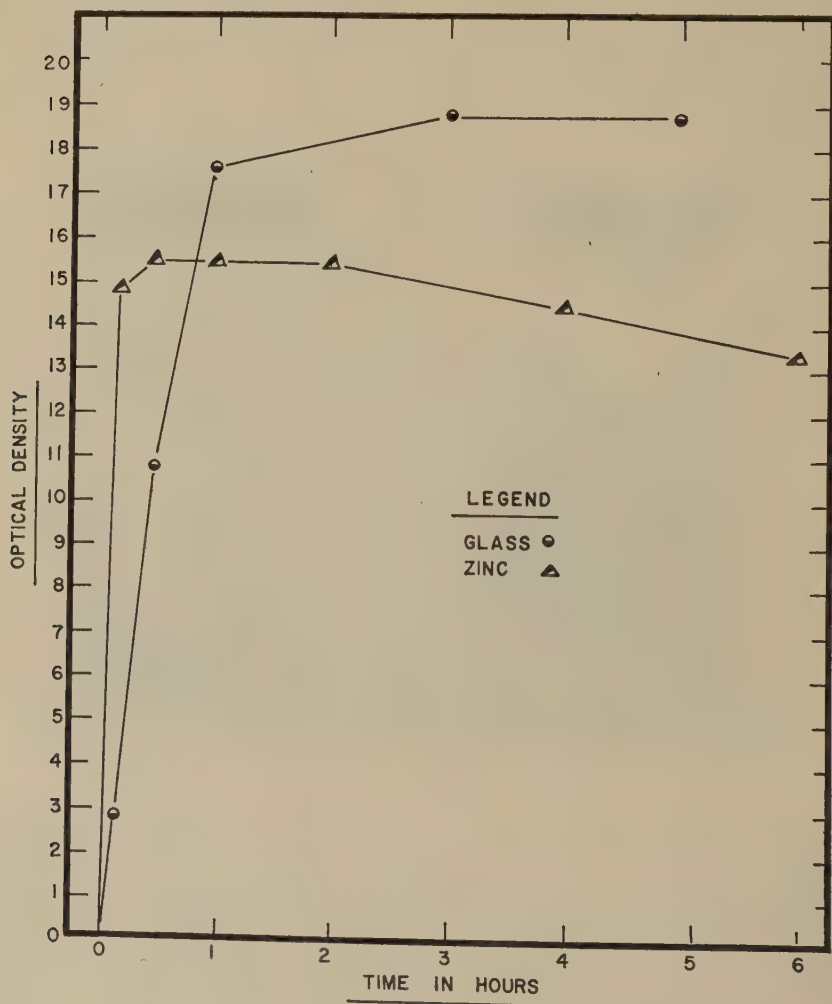


FIG. 4. Dispersion of soil as a function of time of agitation.

the former adhesion tension was generally high—as required for detergency—and the latter, low. In order to explain the mode of soil removal, this low soil-substrate adhesion tension must be compared with the tendency of the soil to cohere.

On glass, for example, cohesion of soil must have been greater than its adhesion to the substrate. Therefore, particles of soil did not separate from the soil surface. Moreover, even though soil-substrate bonds were relatively weak, agitation was required to loosen the soil which then came directly off the substrate—in clumps. This is shown schematically in Fig. 5. A high surfactant-substrate adhesion tension would aid this process.

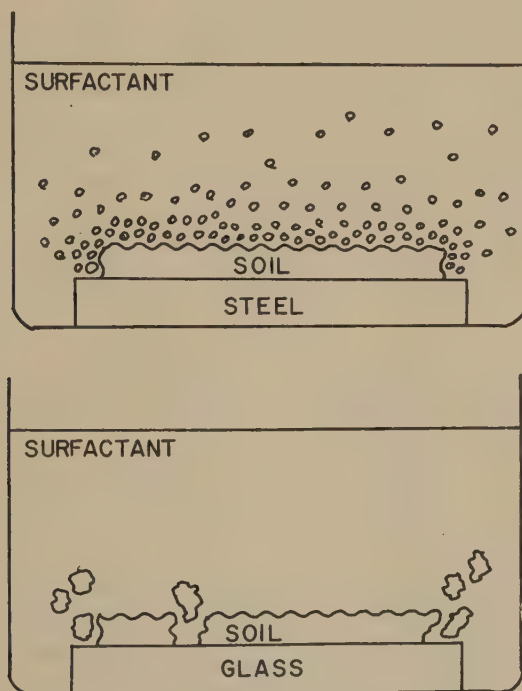


FIG. 5. Picturization of soil removal processes.

That the soil had high cohesion was evident from the fact that, in the absence of substrate, clumps of soil did not disperse in the surfactant solution.

On steel, adhesion of soil to the metal must have been greater than its cohesion. Therefore, when soiled steel was immersed in the detergent solution the surface soil came off first—finely dispersed. As successive layers of surface soil were removed, the surfactant finally reached the particles of soil next to the metal and removed them also. In the case of pickled steel this last layer of soil was held so tenaciously by the metal that the surfactant could not remove it. Rapid removal and dispersion of the *surface* soil suggests that the effect of the steel substrate apparently extended to the outermost soil layer and thus controlled the manner in which that soil was removed.

ELECTRICAL CHARACTERISTICS

Re-examination of the substrates in decreasing order of ease of soil removal or fineness of dispersion of that soil, as listed in Fig. 2, suggests that some correlation may be made between the latter phenomena and the electrical or polar characteristics of the substrates. The polar metals, for example, were high on the list; the nonpolar plastics, low. Moreover, the elements zinc, aluminum, iron, copper, and silver appeared in somewhat the same order as in the electromotive series. Another correlation may be made with the work functions (7) of these metals, that is, the ease with which electrons may be evaporated from their surfaces. Still another correlation may be made with the galvanic series of the metals (8). The latter is based on experience in corrosion testing and is essentially analogous to the electromotive series. However, it takes into consideration the over-all aspects of practical application conditions, in addition to theoretical principles. The four series are listed in Table I.

TABLE I

Electrical Characteristics of the Metals

Soil dispersion series	Electromotive series	Work function series	Galvanic series
Zinc	Aluminum	Zinc	Zinc
Aluminum	Zinc	Aluminum	Aluminum
Iron	Iron	Silver	Iron
Copper	Copper	Copper	Copper
Silver	Silver	Iron	Silver

If the electrical or polar characteristics of the substrate really determine the mode of soil removal, then it should be possible to alter the latter by suitably altering the electrical character of the substrate. This may be accomplished by using the same metal as anode and cathode in a small electrolytic cell containing the detergent, and determining the behavior of the soil on these electrodes.

ELECTROLYTIC EXPERIMENTS

A cell of this type was set up using tap water rather than distilled water in order to get conductivity through the non-ionic detergent solution. Two specimens of the same metal were used as electrodes and were suspended about 1 in. apart. One of these was partly coated with soil. A voltage of 22.5 v. was applied and the electrodes were gently lowered into the detergent solution. The current was found to be about 25 ma. Another specimen of the substrate—not attached to any electrical source—was lowered into a similar solution of the detergent, as a control. Attempts were made to keep agitation of the substrates at a minimum lest this factor interfere with soil behavior. However, it was soon apparent that

agitation had little effect at the electrodes. The current was maintained for 15 min., during which time careful observations were made of the behavior of the soil and of its mode of removal from the electrodes and from the control. Aluminum, copper, and silver were examined in this way, and soil behavior is outlined briefly in Table II.

TABLE II

Results of Electrolytic Cell Experiments

Soil on:	Control	Cathode	Anode
Soil behavior:	Dispersed and suspended	Dispersed, then flocculated	Not dispersed
Phenomena at electrode:	—	Hydrogen gas bubbling	Oxidation of exposed surfaces

As expected, soil came off the control substrates in finely dispersed form and remained suspended in the detergent solution. Rate of soil removal was affected by agitation, but even without agitation almost all of the soil was removed at the end of the test period.

Soil behavior on the two electrodes showed marked differences. When the soiled electrode was made the cathode, soil came off in finely dispersed form in very much the same way as it did from the control. However, after standing for a short time, the particles of soil agglomerated. When the soiled electrode was made the anode, no soil removal was obtained.

These observations confirm that the electrical characteristics of the substrate influence the mode of removal of the soil. When the metal was made the cathode the action of the electric current was such as to raise the activity of the metal in the electromotive series and, therefore, promote soil removal. However, the current also caused flocculation of dispersed soil. That is, it removed whatever factors were promoting stability of the soil suspension—possibly by neutralizing charges on the soil particles. When the metal was made the anode the electric current passivated it, i.e., reduced its electrical behavior to that of a more noble metal. Consequently, no soil removal was obtained.

Some additional phenomena of interest were observed at the electrodes. All of the exposed surfaces of the anode were oxidized. The evolution of hydrogen gas at the cathode introduced the possibility that this gas may have promoted soil dispersion by a scrubbing action. However, repeating the experiment under conditions of low current density, where gas evolution was negligible, did not alter soil behavior.

When zinc was examined in the electrolytic cell it displayed anomalous behavior. Soil dispersed from the anode about as well as from the cathode, and no evidences of oxidation at the anode were observed. Apparently the current density of this cell was less than the minimum required for

passivation of zinc. Increasing this current density by addition of salt passivated the zinc, the electrode surface became etched, and zinc oxide came off the metal together with some clumps of soil which were no longer finely dispersed.

The electrical character of certain plastic substrates can be altered also with subsequent change in the soil removal process. For example, reduction in pH of the detergent solution to less than the isoelectric pH of nylon⁶ caused some dispersion of soil from nylon as evidenced by a measurable increase in optical density. This was not observed with soiled polyethylene, or when acid was added to detergent solution containing a lump of soil and no substrate.

The electrical forces which promote dispersion of the oily-carbon soil may originate from sources other than the substrate. Thus, although a lump of soil could not be dispersed in the detergent solution, passage of an electric current through that solution caused fine particles to separate from the surface of the soil. As before, these particles agglomerated on standing. Dispersion of soil was not obtained by the addition of metallic ions to the detergent solution nor by the mere presence of metallic particles; it was obtained when these particles contacted the soil. Moreover it was independent of the thickness of the soil layer.

COMPOSITION OF THE SOIL

These phenomena depend not only on the nature of the substrate but also on the composition of the soil, and the oily-carbon soil seems to be unique for this behavior. An oily soil containing a nonpolar solid such as sulfur was not dispersed by the detergent, whereas one containing polar TiO_2 was readily dispersed—even in water. The carbon in the oily-carbon soil is also nonpolar, but it must be sufficiently polarizable so that the electrical characteristics of the substrates can extend through the oily paste to its surface.

The means by which this paste becomes a medium for transmission of an electrical potential are not clear, but several possibilities may be considered. The substrate may cause polarization of the carbon so that, by induction, this polarity extends through the paste to the soil surface. Cooperative phenomena may aid this process. Alternatively, a voltaic effect between metal and soil may promote adsorption of metallic ions on the soil surface and favor its dispersion. However, ionic precipitation of dispersed soil cannot be correlated with this hypothesis. Further work will be required for an elucidation of this mechanism.

That carbon is important in the soil is apparent since, in its absence, these soil dispersion phenomena are not observed. Removal of an oil film from substrates does not show differences in size of the oil droplets; it

⁶ Experiment suggested by Mr. R. Bernstein of Philadelphia Naval Shipyard.

does demonstrate that adhesion of oil to metals is greater than its adhesion to nylon or glass.

ACKNOWLEDGMENT

The authors wish to express their sincere appreciation for the many valuable comments and suggestions of Mr. A. C. Nuessle in whose laboratory this work was done.

REFERENCES

1. RUCHHOFT, C. C., AND NORRIS, F. I., *Public Health Repts.* **66**, (21) 655 (1951).
2. ADAM, N. K., *J. Soc. Dyers Colourists* **53**, 121 (1937).
3. ROBINSON, C., *Wetting and Detergency*, p. 137. Chemical Publishing Co., New York, 1937.
4. REICH, I., AND SNELL, F. D., *Ind. Eng. Chem.* **40**, 1233 (1948).
5. FINEMAN, M. N., *Soap & Sanitary Chemicals* **29** (2) 46, (3) 50 (1953).
6. SPRING, S., AND PEALE, L. F., *Metal Progr.* **51**, 102 (1947).
7. UHLIG, H. H., *Corrosion Handbook*, p. 26. John Wiley & Sons, New York, 1948.
8. *Corrosion Testing Bulletin*, p. 17. International Nickel Co., New York, 1944.

RHEOLOGY OF SYNTHETIC LATEX. IV. EFFECT OF POLYDISPERSITY ON FLOW BEHAVIOR

Samuel H. Maron and Benjamin P. Madow

*Physical Chemistry Laboratory, Department of Chemistry and Chemical Engineering,
Case Institute of Technology, Cleveland, Ohio*

Received October 24, 1952

INTRODUCTION

Theoretical study (1,2) of the packing of spheres of uniform size indicates that, dependent on arrangement, the volume fraction of the total available space occupied by the spheres may range from $\pi/6 = 0.5236$ for cubic packing to $\pi/3\sqrt{2} = 0.7405$ for rhombohedral packing. In the case of cubic packing, each sphere is in contact with six others; while in the case of rhombohedral packing contact is made with twelve. Still tighter packing can be obtained in systems containing spheres of non-uniform size, for in such systems the smaller particles can accommodate themselves in the voids between the larger spheres, and thereby fill the available space more completely. For the case of a binary mixture of spherical particles of different homogeneous size but identical voids volume, Furnas (3) showed that the extent of packing depends on the proportion of the two types of spheres in the mixture, and is a maximum when the proportion of the larger constituent is 60–70% by volume. Essentially the same conclusions were reached by Fraser (4), except that according to Fraser the tightest packing is to be obtained above *ca.* 70% of the larger constituent by volume, and that both the extent of and the maximum packing should depend on the diameter ratio of the spheres in the binary mixture. The larger this ratio the tighter is the packing, and the higher is the proportion by volume of the larger constituent at which the maximum packing is attained.

How the packing of spheres and their polydispersity affect rheologic behavior has been considered recently by Mooney (5). Mooney concludes that the crowding action associated with polydispersity should modify the viscosity, but the equation he deduces cannot be readily applied. Further, his treatment is limited to systems exhibiting Newtonian flow.

Synthetic rubber latices are colloidal dispersions of spherical polymer particles in water, and hence they should be suitable for the experimental investigation of the expected effect of polydispersity on flow behavior. Preceding papers in this series (6–8) described the rheology of types III

and V GR-S rubber latices as a function of rate of shear and concentration. The type III latex used had a volume to surface average diameter, D_s , of 980 Å; while for the type V latex, D_s was 1920 Å. Both latices were heterogeneous in particle-size distribution, but it was difficult to ascertain from either latex alone what the effect of this heterogeneity is on the flow behavior and on the extent of the packing attained by the spherical particles in the dispersions when the viscosity becomes infinite. To gain some light on these points, an investigation was made of the flow properties of mixtures of the above two systems at various proportions of the two latices, and at total rubber contents up to 55%. The results of this study are presented below.

EXPERIMENTAL

The type III and type V latices were described before (7,8). These latices were mixed in various proportions to make up concentrated stock solutions from which the various lower rubber contents were obtained by dilution with distilled water. The flow behavior of each solution as a function of shearing stress was measured at $30.00 \pm 0.01^\circ\text{C}$. in the apparatus and by the techniques already given (6).

RESULTS AND DISCUSSION

The various latex mixtures behaved very similarly to the two separate latices. Up to a total rubber content of 25%, the flow was Newtonian. Above a rubber content of 25%, the flow was non-Newtonian and could be represented by the equation

$$F^N = \eta' G \quad [1]$$

where F is the shearing stress, G is the rate of shear, and N and η' are constants dependent on the total rubber content and proportion of the two latices. Below a rubber content of 47% a single equation of the above form sufficed to cover the entire range of shearing stresses employed. Above the latter concentration, however, separate equations of the same form were required for the lower and upper ranges. Since the lower ranges extended only up to *ca.* 20 dynes/sq. cm. at 47% rubber content, and up to *ca.* 50 dynes/sq. cm. at 55.2% rubber content, the following discussion will be limited to the results covering the upper shearing stress range.

In Table I are given the flow constants of the latices and latex mixtures as a function of total rubber content, total volume fraction of polymer ϕ , and the composition parameters f_w and f_v . The quantity f_w is defined as W_5/W_t , where W_5 is the weight of type V polymer and W_t is the total weight of polymer in the mixture. In turn $f_v = V_5/V_t$, where V_5 is the volume of type V polymer and V_t is the total volume of polymer in the mixture. To obtain N_1 and $\log(\eta'_1/\eta_0)$ as a function of f_v at constant ϕ , plots of N_1 and $\log(\eta'_1/\eta_0)$ vs. ϕ at constant f_v were prepared from the

TABLE I

Flow Constants for Mixtures of Type III and Type V Latex

Total rubber content (wt. %)	ϕ	N_1	$\log(\eta_1'/\eta_0)$
$f_w = 0$		$f_v = 0$	
22.50	0.2279	1.00	0.3662
35.00	0.3537	1.04	0.8068
47.00	0.4740	1.18	1.6765
55.20	0.5560	1.60	3.4660
$f_w = 0.1000$		$f_v = 0.1052$	
22.50	0.2288	0.99	0.3495
35.00	0.3550	1.04	0.7725
47.00	0.4755	1.18	1.5867
55.20	0.5574	1.51	3.0105
$f_w = 0.2500$		$f_v = 0.2607$	
22.50	0.2304	0.99	0.3471
35.00	0.3570	1.03	0.7322
47.00	0.4776	1.17	1.5133
55.20	0.5595	1.52	2.8891
$f_w = 0.5000$		$f_v = 0.5141$	
22.50	0.2329	0.99	0.3520
35.00	0.3602	1.04	0.7199
47.00	0.4812	1.17	1.4411
55.20	0.5630	1.50	2.6661
$f_w = 0.7500$		$f_v = 0.7604$	
22.50	0.2354	1.00	0.3471
35.00	0.3635	1.04	0.6988
47.00	0.4847	1.21	1.4392
55.20	0.5665	1.46	2.4929
$f_w = 0.9000$		$f_v = 0.9050$	
22.50	0.2369	1.00	0.3471
35.00	0.3654	1.04	0.6988
47.00	0.4867	1.24	1.4823
55.20	0.5685	1.46	2.5049
$f_w = 1$		$f_v = 1$	
22.50	0.2379	1.00	0.3471
35.00	0.3667	1.05	0.7220
47.00	0.4881	1.26	1.5344
55.20	0.5699	1.62	2.8371

data in Table I, and from these were read the values of these quantities corresponding to selected values of ϕ . The interpolated values of N_1 and $\log(\eta_1'/\eta_0)$ were plotted then versus f_v at constant ϕ to yield Figs. 1 and 2.

From Fig. 1 it may be seen that up to $\phi = 0.25$, N_1 is equal to 1 for all the latex mixtures. Above $\phi = 0.25$, addition of one latex to another

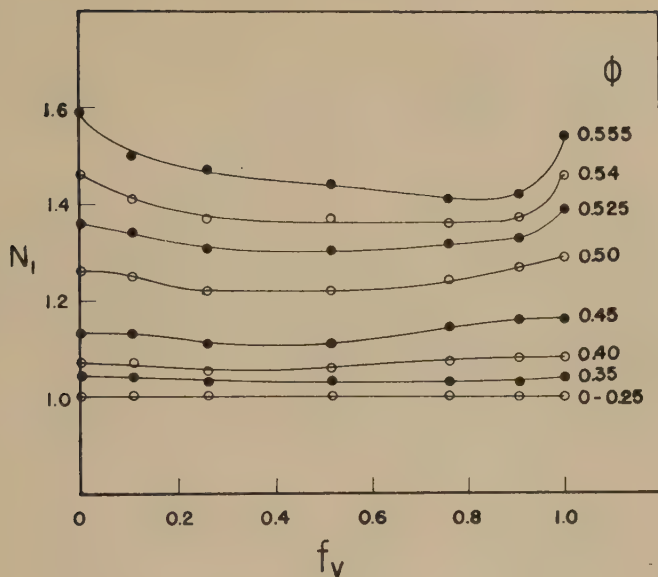


FIG. 1. Dependence of N_1 on f_v at various values of ϕ .

operates to lower N_1 , and to lead to minima in the plots. These minima shift toward higher values of f_v as ϕ increases. A somewhat similar behavior is shown by the plots in Fig. 2. Up to $\phi = 0.30$, the values of $\log(\eta_1'/\eta_0)$ are intermediate between those for the two original latices.

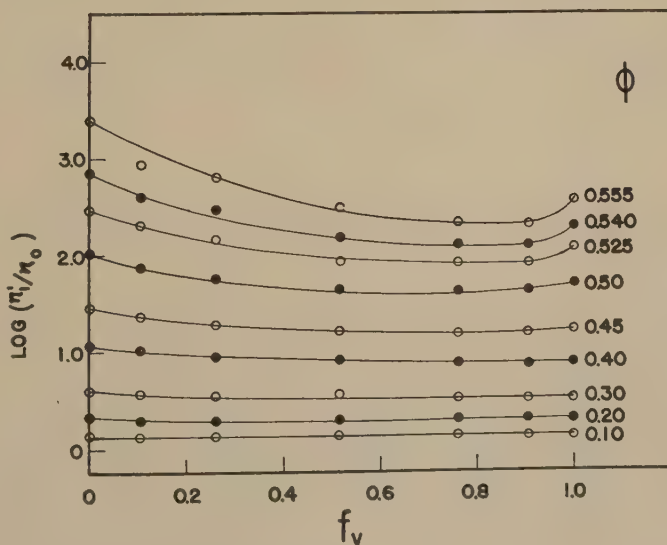


FIG. 2. Dependence of $\log(\eta_1'/\eta_0)$ on f_v at various values of ϕ .

Above $\phi = 0.30$, however, the plots again exhibit minima, and these are the more pronounced the higher the value of ϕ is.

It has been found possible to represent the variation of $\log(\eta_1'/\eta_0)$ with ϕ at constant f_v by means of the relation (7)

$$\log(\eta_1'/\eta_0) = b_1 Z_1 = \frac{\alpha_1 b_1 \phi}{1 - \alpha_1 \phi} \quad [2]$$

where α_1 and b_1 are constants. According to Eq. [2], a plot of $\phi/\log(\eta_1'/\eta_0)$ vs. ϕ should be linear, with slope equal to $-1/b_1$, and y -intercept equal to $1/\alpha_1 b_1$. One such typical plot is presented in Fig. 3. The values of α_1 and b_1 evaluated from the plots at various values of f_v are given in Table II and are shown graphically in Fig. 4.

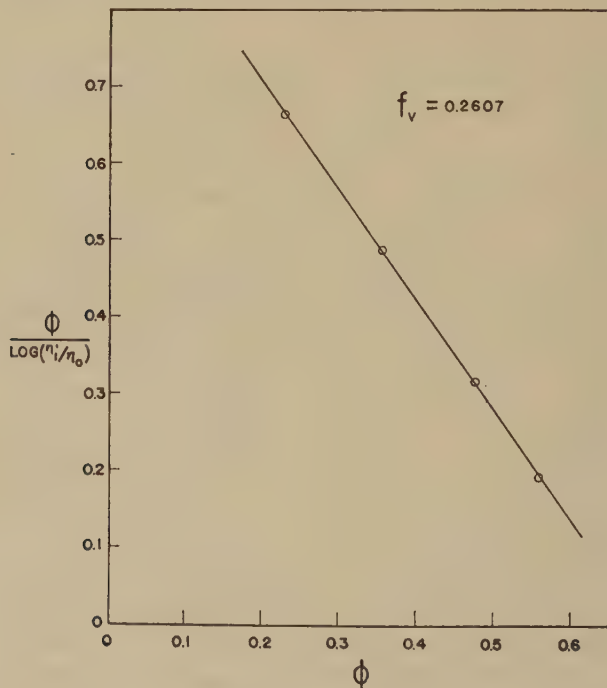
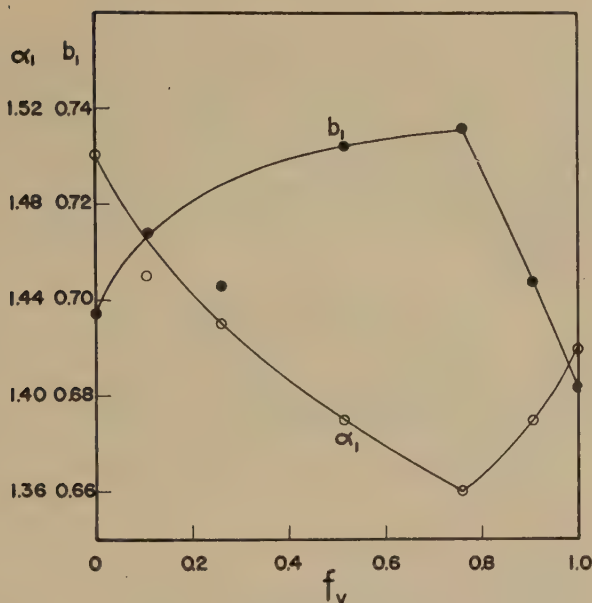


Fig. 3. Typical plot of $\phi/\log(\eta_1'/\eta_0)$ vs. ϕ at constant f_v .

From Fig. 4 it is evident that the addition of one latex to another decreases α_1 and leads to a minimum at $f_v = 0.76$. On the other hand, b_1 increases with f_v to a maximum at $f_v = 0.76$, and then decreases to b_1 of the type V latex. This reciprocal relationship between α_1 and b_1 is not unanticipated. Equation [2] predicts that the quantity $2.303\alpha_1 b_1$ should be equal essentially to the slope of the limiting Einstein relation between η and ϕ , namely, 2.5. Actually the values of this quantity, col. 4 of Table

FIG. 4. Variation of α_1 and b_1 with f_v .

II, range from 2.40 for type III latex to 2.20 for type V latex, with the values for the mixtures varying with f_v between these limits.

Equation [2] also predicts that the viscosity will become infinite when $\phi = 1/\alpha_1$. The values of $1/\alpha_1$, listed in col. 5 of Table II, are the volume fractions of *polymer* at which the viscosity will become infinite, and must be corrected for the volume occupied by the monolayer of adsorbed soap. This correction (7) can be made by means of the equation

$$\phi_t = \phi \left(1 + \frac{6\Delta}{D_s} \right) \quad [3]$$

where ϕ_t is the corrected volume fraction, $\phi = 1/\alpha_1$, Δ is the length of the adsorbed molecule, and D_s is the volume to surface average diameter

TABLE II

Parameters for Concentration Dependence of Flow in Latex Mixtures

f_v	α_1	b_1	$2.303\alpha_1 b_1$	$1/\alpha_1$	$D_s - A$	ϕ_t
0	1.50	0.697	2.40	0.667	980	0.736
0.105	1.45	0.714	2.38	0.690	1030	0.800
0.261	1.43	0.703	2.32	0.699	1120	0.802
0.514	1.39	0.732	2.34	0.719	1310	0.810
0.760	1.36	0.736	2.31	0.735	1560	0.813
0.905	1.39	0.704	2.25	0.719	1760	0.787
1.000	1.41	0.677	2.20	0.709	1920	0.768

of the latex. For the oleate soap present in type V latex, Δ is equal to 27.5 A.(7); while for the K-wood rosin soap in type III latex, Δ may be taken as 17 A.(8). For the mixtures, the greater length of the oleate molecule should be governing, and hence for these Δ should again be 27.5 A.

The volume to surface average diameters of the latex mixtures, D_s , may readily be calculated from the corresponding diameters of the original latices, D_3 and D_5 . It can readily be shown that the relationship among these three diameters is

$$D_s = \frac{D_3 D_5}{f_v D_3 + (1 - f_v) D_5} \quad [4]$$

where f_v has the same significance as before. Using Eq. [4] with $D_3 = 980$ A. and $D_5 = 1920$ A., we obtain the values of D_s listed in the next to

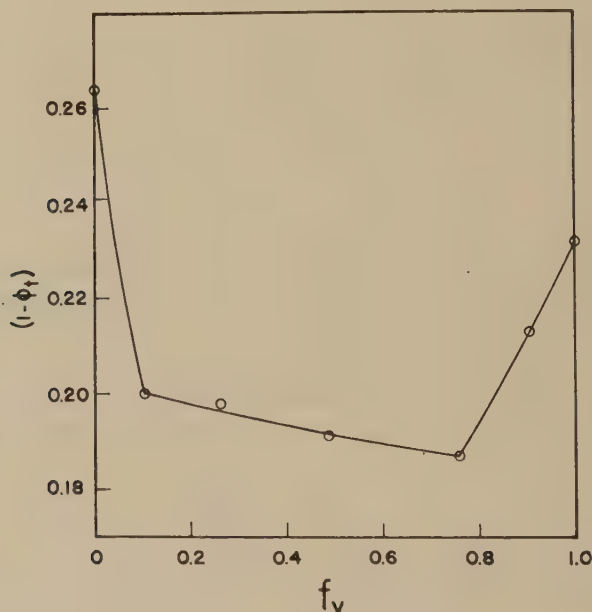


FIG. 5. Dependence of volume fraction of voids on f_v .

last column of Table II. These, along with the Δ 's and $1/\alpha_1$'s lead to the values of ϕ_t given in the last column of Table II.

The fact that the values of ϕ_t are 0.74 or higher indicates that at the point of tight packing, where the viscosity becomes infinite, the arrangement of the larger spheres is rhombohedral, with the smaller particles lying in the voids between these. As a result the void volume is reduced. The extent to which an increase in polydispersity reduces the voids volume is shown in Fig. 5, where the volume fraction of voids, $(1 - \phi_t)$,

is plotted against f_v . From this figure it is evident that the voids volume of each latex is reduced by the addition of the other to it. The rate of this decrease is particularly pronounced at concentrations near the two pure latices, i.e., on addition of relatively small quantities of one latex to another. At higher proportions of the two the rate of decrease is considerably lower. The minimum in the voids volume is observed at $f_v = 0.76$, and hence the tightest packing of the polymer particles occurs at this proportion of the two latices.

These results are in excellent agreement with Fraser's (4) conclusion that tightest packing in a binary mixture should occur at a proportion above 70% of the larger particles by volume. They also show that polydispersity can contribute materially to the tightness of packing of spherical particles in a dispersion, and hence polydispersions should exhibit flow to higher concentrations than monodispersions before infinite viscosity or particle distortion sets in.

ACKNOWLEDGMENT

The work discussed herein was performed as a part of the research project sponsored by the Reconstruction Finance Corporation, Office of Synthetic Rubber, in connection with the Government Synthetic Rubber Program.

SUMMARY

A study has been made of the effect of polydispersity on the flow of synthetic latices by investigating the behavior of mixtures of type III and type V GR-S rubber latex in all proportions and up to total rubber contents of 55%. The two latices differed in volume to surface average particle diameter by a factor of two.

Mixtures of the two latices showed Newtonian flow below total volume fractions of $\phi = 0.25$, and non-Newtonian flow at higher concentrations. Up to $\phi = 0.47$, a single exponential flow equation covered the entire range of shearing stresses used. Above this concentration, separate exponential flow equations had to be used for the low and high stress ranges. The flow constants N and η' were found to depend both upon the total concentration of polymer and the proportion of the two latices in the mixtures.

The equation $\log (\eta'/\eta_0) = \frac{\alpha b \phi}{1 - \alpha \phi}$ again represented well the dependence of η' on the total concentration of polymer, and yielded α 's dependent only on the proportion of the two latices in the mixtures. At low concentrations this equation gave for the proportionality constant between η' and ϕ values ranging from 2.20 to 2.40 as against the Einstein value of 2.5. Again, extrapolation of the equation to infinite viscosity gave volume fractions of rubber plus adsorbed soap which varied with the proportion

of the two lattices, and showed that an increase in heterogeneity of particle-size distribution leads to a considerably tighter packing of the spherical particles. The maximum packing fraction of $\phi_t = 0.81$ was observed at a polymer volume fraction of 0.76 type V latex in the mixture. This is to be compared with $\phi_t = 0.74$ for the type III latex and $\phi_t = 0.77$ for the type V latex.

These results show that at the point of tight packing the larger spheres are arranged rhombohedrically, with the smaller spheres filling the voids between the larger particles. They also indicate that polydisperse systems should exhibit flow to concentrations higher than corresponding monodisperse systems.

REFERENCES

1. GRATON, L. C., AND FRASER, H. J., *J. Geol.* **43**, 785 (1935).
2. HEYWOOD, H., *J. Imp. Coll. Chem. Eng. Soc.* **2**, 9 (1946).
3. FURNAS, C. C., *Ind. Eng. Chem.* **23**, 1052 (1931).
4. FRASER, H. J., *J. Geol.* **43**, 910 (1935).
5. MOONEY, M., *J. Colloid Sci.* **6**, 162 (1951).
6. KRIEGER, I. M., AND MARON, S. H., *J. Colloid Sci.* **6**, 528 (1951).
7. MARON, S. H., MADOW, B. P., AND KRIEGER, I. M., *J. Colloid Sci.* **6**, 584 (1951).
8. MARON, S. H., AND MADOW, B. P., *J. Colloid Sci.* **8**, 130 (1953).

MOLECULAR INTERACTION IN MONOLAYERS.

I. COMPLEX FORMATION

E. D. Goddard and J. H. Schulman

Department of Colloid Science, University of Cambridge, England

Received December 7, 1951; revised December 2, 1952

ABSTRACT

With the aid of a compensated Langmuir balance an investigation of the interaction between insoluble monolayers and soluble surface-active compounds has been undertaken by studying monolayer penetration at constant pressure and constant area, and by mixed monolayer compression. The studies have been limited to cases where the interaction is known to be strong. Compression force-area curves of cholesterol spread on solutions of sodium cetyl sulfate and digitonin, and of eicosylamine spread on sodium cetyl sulfate have shown that 1:1 association mixtures of the soluble and insoluble components are stable up to the collapse point of the mixed film. It is suggested that the film which collapses is, in fact, the 1:1 complex. Monolayer penetration experiments at constant surface area on the above systems have yielded results consistent with the earlier hypothesis that under these conditions 1:1 complexes are formed. Experiments at constant surface pressure on single and mixed films have provided further evidence in support of the existence of complexes between cholesterol and digitonin (or saponin); it is shown, however, that such an interpretation cannot be drawn in the experiments involving sodium cetyl sulfate as penetrant. A mechanism has been suggested in outline to explain the characteristic shape of these expansion curves.

INTRODUCTION

It has been shown in previous work (1,2) that the molecules in insoluble monolayers at the air/water interface may interact or associate with soluble molecules in the underlying solution thus permitting the soluble molecules to enter or "penetrate" the insoluble monolayer. The two species of molecules in the mixed monolayers were considered to form stoichiometric association complexes which are more stable to surface pressure than either of the two components alone. Systems of this type were shown to associate also in bulk phase in the form of complexes in which the two components were in the ratio 1:1. From studies of complex formation it was possible to draw many important analogies between reactions in monolayers and those occurring in various biological processes.

The purpose of the work in the following three papers was to investigate the mechanism and conditions necessary for the formation of stoichiometric complexes in monolayer penetration, and furthermore to investigate the conditions necessary to obtain penetration where there is no direct evidence of stoichiometric association. The association between

the insoluble and soluble molecules in the latter cases are difficult to define and determine in bulk phase. It will be shown that soluble molecules may enter the insoluble monolayer according to the Partial Pressure Law of Dalton, in conditions where there is no association between the insoluble and soluble molecules and where the monolayer is in an expanded state.

The present paper describes an investigation of complex formation in monolayers by four surface chemical techniques; penetration has been measured at constant surface pressure and at constant surface area, force-area curves of mixed monolayers have been obtained, and during all these processes measurements of surface potential have been recorded.

Matalon (3) has recently given a review of monolayer penetration and has examined the penetration of cholesterol monolayers by saponin and sodium cetyl sulfate. The present work confirms Matalon's experimental results but shows that a new interpretation is required to explain the characteristic shape of the monolayer expansion curves.

EXPERIMENTAL

A compensated Langmuir-Adam balance (4) was used in all experiments; for work at constant pressure a contacting device (sensitivity 0.2–0.3 dynes/cm.) was attached to the boom. In this way movements of the boom activated a motor which automatically expanded or compressed the monolayer.

The volume of the trough was 670 ml. except in the initial experiments where the volume was 630 ml. In all experiments freshly distilled water from a quartz still was used. To minimize the effect of adventitious ionic contamination, experiments were carried out with 100 mg. NaCl in the subsolution (3), except in the experiments with eicosylamine in which the subsolution was 10^{-3} *N* HCl.

In carrying out an experiment the insoluble monolayer was spread and compressed to a value of π dynes/cm. which in general exceeded the surface-tension lowering due to the surface-active solute alone; 20 ml. of subsolution was then removed and in its place 20 ml. of the same solution containing the surface-active solute was introduced by means of a wide-mouth pipet (time zero). By gentle inhalation and exhalation (2–3 min.) the subsolution was rendered uniform. At constant surface area the film pressure was measured as a function of time; at constant surface pressure, the change in film area with time was noted, and the resulting curves are referred to as "expansion" curves. Measurements of surface potential (ΔV) were recorded using a vacuum-tube electrometer circuit and polonium ionizing source.

It has been stressed that compression of penetrated monolayers must be carried out slowly (3). Some solute molecules adsorbed at low surface

pressures will be ejected as the pressure is raised, and this is a very slow process. Accordingly the compression curves recorded were, as far as possible, equilibrium curves which allowed a time interval of at least 10 min. at each pressure.

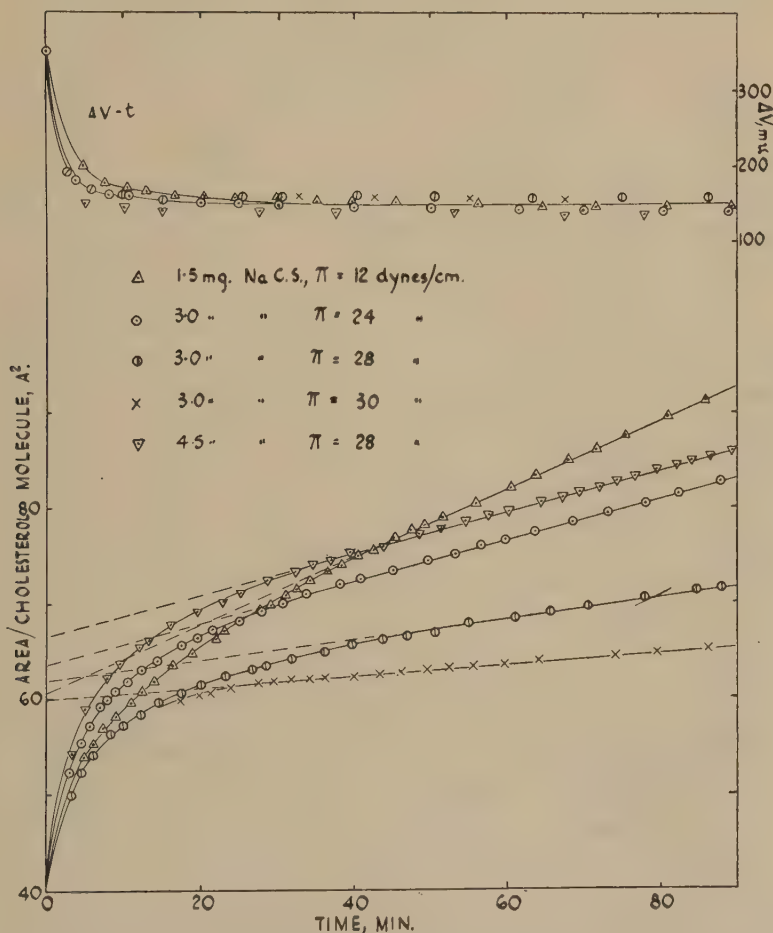


FIG. 1. Sodium cetyl sulfate injected under cholesterol monolayers at constant pressure. Trough volume = 630 ml.

RESULTS

The Cholesterol-Sodium Cetyl Sulfate Association

In Fig. 1 are shown the expansion curves of cholesterol on injection of sodium cetyl sulfate (SCS) into the subsolution. The pattern of the curves was similar to that described by Matalon (3), viz., there was an initial rapid extension of the film the rate of which fell with time and then

became constant. The linear extensions were observed in all the experiments carried out and persisted for the duration of the experiment (3-5 hr.). Extrapolation of these linear portions to zero time gave area values of 60-66 \AA^2 per cholesterol molecule. On Matalon's theory the initial rapid expansion involves the formation of a 1:1 complex between the

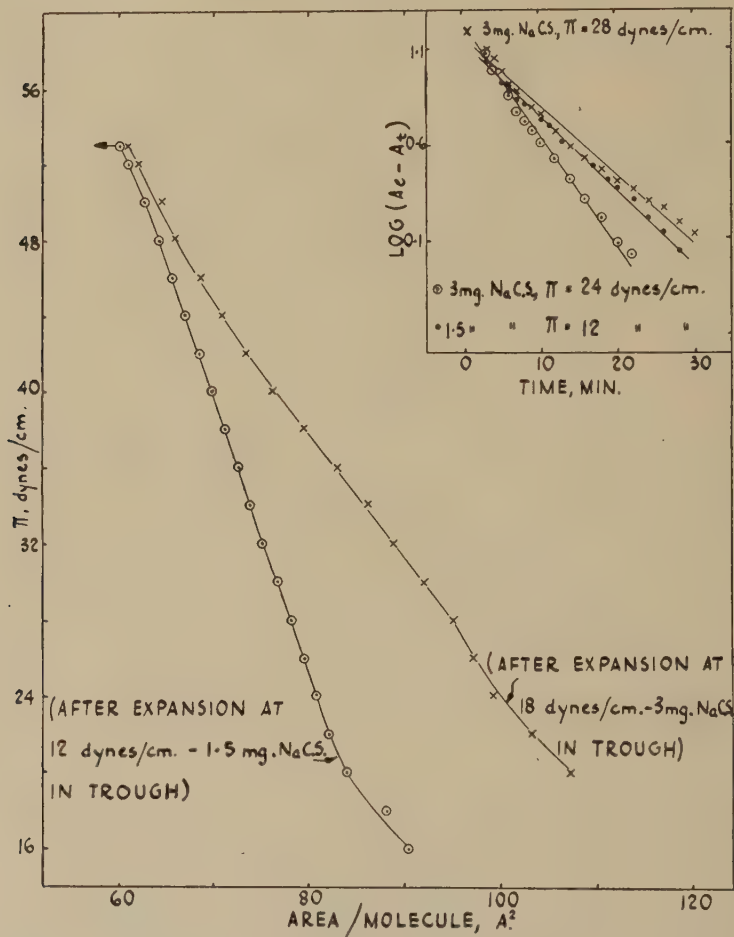


FIG. 2. Compression of cholesterol monolayers previously penetrated by sodium cetyl sulfate.

$\log(A_e - A)$ vs. time for cholesterol expansions

cholesterol and SCS, and the linear extension corresponds to the "solution" of further SCS in the mixed monolayer. For purposes of calculation he considered the two processes to be distinct, both starting at time zero. Accordingly, the extrapolated area value (A_e) was identified with the

area of the 1:1 complex, and if each curve had its "solution" portion subtracted, the resultant curve followed a first-order law of the type:

$$\log (A_e - A_t) = K_t + \log (A_e - A_0)$$

where A_0 = initial area of insoluble monolayer,

A_e = final area of monolayer, and

A_t = area value on "corrected" curve at time t .

In support of this hypothesis, Matalon obtained $(A_e - A_0)$ values of 20–27 A.² for the SCS, and 50–55 A.² for the saponin penetrations into cholesterol. These values are close to those expected for the cross-sectional area of the penetrant molecules. The $(A_e - A_0)$ values obtained by the present authors are in conformity with Matalon's results. In the same way, graphs of $\log (A_e - A_0)$ vs. time (inset Fig. 2) are sensibly linear under varying experimental conditions.

The ΔV value of cholesterol (360 mv.) fell rapidly during the first 10 min. of expansion and then remained reasonably steady at 140–160 mv. during the subsequent adsorption of SCS. This is of interest as the surface potential of SCS alone is considerably different from the latter value. Figure 3 shows the π -time and ΔV -time variations of SCS films adsorbed in the absence of an insoluble monolayer from solutions of varying concentration. All concentrations were below the critical micelle value, and in each case surface "aging" (6) was observed. It is apparent from a study of the π - ΔV relationships during the latter process that certain reorientation effects occur; e.g., with 6.0 mg. SCS in the bath, π reached 16 dynes/cm. in 3½ min. and ΔV had a value of -100 mv.; whereas with 3.0 mg. SCS π reached 16 dynes/cm. after 90 min., but here ΔV was equal to -46 mv. Again, considering the 6.0-mg. curve, corresponding to a π rise of only 2.4 dynes/cm. from $t = 30$ min. to $t = 90$ min., there was a rise in ΔV of almost 70 mv. Although this rise in ΔV was in the direction of increased molecular crowding, it is difficult to ascribe it solely to compression of the monolayer.

Returning to Fig. 1, since (a) continued penetration of the cholesterol-SCS mixed film resulted in little change in ΔV , and (b) this value differed considerably from that of SCS alone, it is concluded either that adsorption into the mixed film involves an appreciably different orientation of the cetyl sulfate or that cetyl sulfate molecules in a sublayer are of importance in determining the ΔV value registered. Some evidence in favor of the existence of such a secondary adsorbed layer is presented in the section on mixed-film penetration.

The results of the investigation of the cholesterol-SCS interaction by the other techniques are given in Figs. 2 and 6. During the compression of penetrated cholesterol films the surface remained fluid and collapse occurred at an area of 60 A.² per cholesterol molecule (Fig. 2). This

strongly suggests that during compression SCS in excess of the 1:1 ratio is progressively ejected and the monolayer which collapses is the 1:1 complex. Similar collapse areas have been obtained by Schulman and Stenhagen (2) and by Matalon (5).

In the constant-area penetration of cholesterol (Fig. 6), there was an immediate pressure rise to 50 dynes/cm. and a fall in ΔV to 180–190 mv.

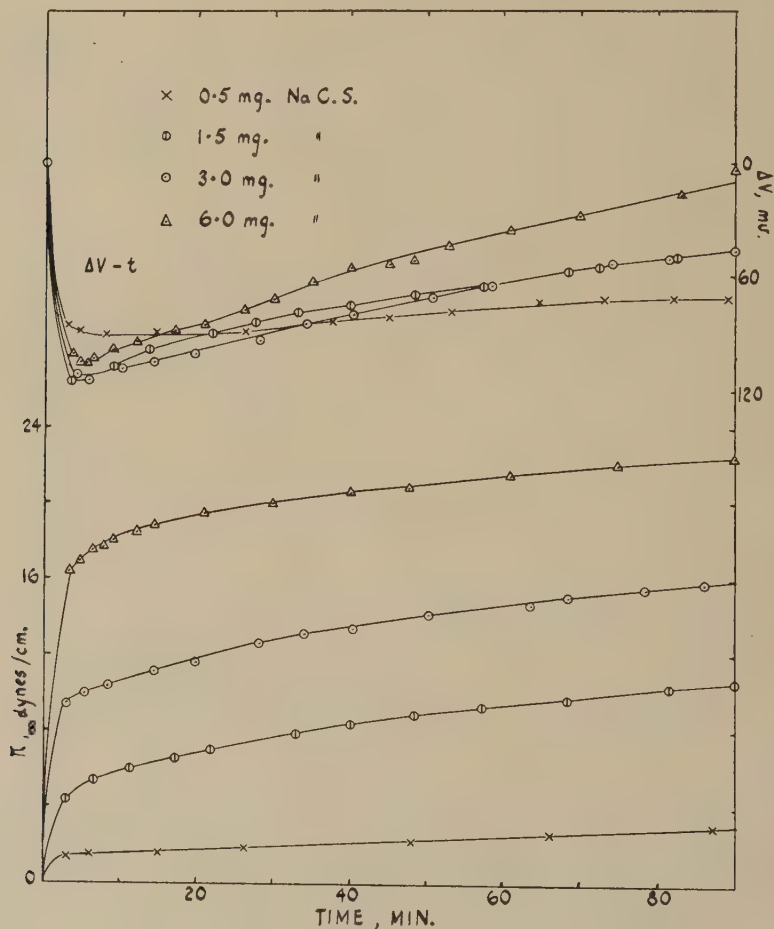


FIG. 3. Injection of sodium cetyl sulfate into trough (630 ml.). Constant area.

which is close to the ΔV value obtained in the constant-pressure penetrations. It is therefore conceivable that in the former penetrations some of the cholesterol is removed from the monolayer to allow the 1:1 association to form (1). This process is analogous to the formation of mixed micelles in solution by the penetration of an alcohol into a soap micelle (7,8).

Insoluble and Penetrating Molecules of Opposite Charge

The results reported above have provided data which favor the hypothesis of surface complex formation. It was therefore deemed desirable to apply the techniques employed to systems where the strongest possible association between the interacting molecules was anticipated, viz., two

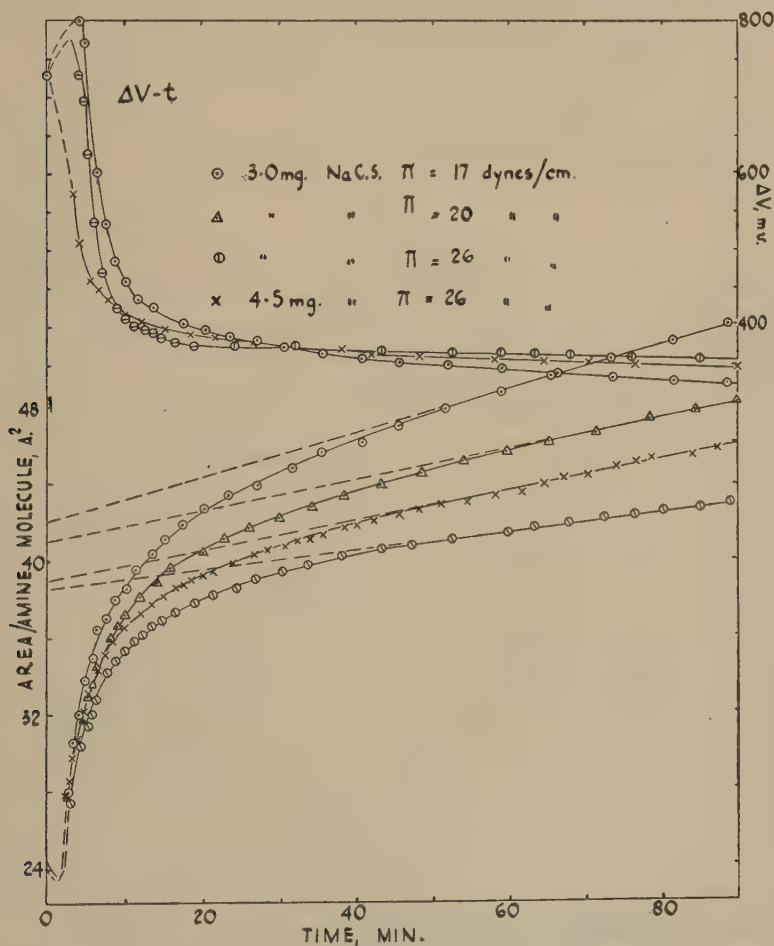


FIG. 4. Sodium cetyl sulfate injected under eicosylamine hydrochloride monolayers at constant pressure.

Trough volume = 670 ml. (0.001 N HCl)

long-chain molecules having ionic head groups of opposite charge. There is abundant evidence that such molecules associate in bulk phase to give 1:1 complexes (9-11).

The authors have investigated emulsions containing ionic long-chain compounds as stabilizing agents. Sodium cetyl sulfate was dissolved in

the aqueous phase, and either octadecylamine hydrochloride or cetyltrimethylammonium bromide (CTAB) in the oil phase (chloroform). Either of these systems should satisfy fully the conditions defined by Cockbain and Schulman (12) for stable water/oil emulsions, viz., an uncharged rigid interface with high molecular crowding. Experiments confirmed these expectations. In the case of the amine, good water/oil

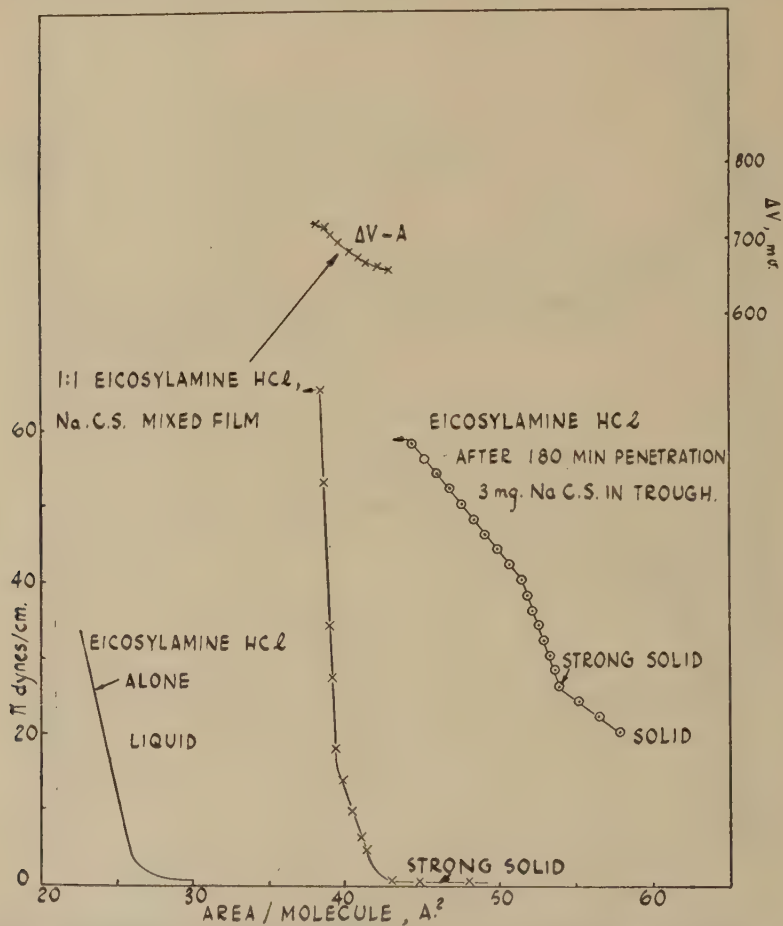


FIG. 5. Compression of eicosylamine hydrochloride-sodium cetyl sulfate mixed films.

emulsions were obtained only where the aqueous phase was acidic. Without acid the charged amine hydrochloride was not formed, adsorbed cetyl sulfate charged the interface, and the emulsions tended to invert. The experiments showed clearly the extent of the interaction at the oil/water interface; attention was therefore turned to studies at the air/water interface.

(a) *Eicosylamine Hydrochloride-Sodium Cetyl Sulfate*. On the 10^{-3} N HCl subsolution the C_{20} amine gave a liquid condensed monolayer of limiting area $26 \text{ \AA}^2/\text{molecule}$ (Fig. 5). It is clear that repulsion between the charged head groups prevents complete close packing in the monolayer.

Expansion curves are shown in Fig. 4. It was expected in these experiments that penetration would result in the formation of a stable 1:1 complex having an area of 40 \AA^2 per amine molecule (see below). Indeed, the area rose rapidly to a value in this region and, as before, this was followed by a linear extension. The curves possessed the common feature of having extrapolated area values (A_e) between 38 and 42 \AA^2 , and appeared, therefore, to support the hypothesis of complex formation already presented (3).

It is interesting that in the first few minutes after injection there was a small *drop* in surface pressure and *rise* in surface potential. It thus appears that the initial adsorption of cetyl sulfate leads to a contraction and immediate solidification of the monolayer by reduction of the repulsive forces acting between the charged amine groups. In the resultant close-packed mixed monolayer the area per individual amine molecule would almost certainly be 20 \AA^2 .

In Fig. 5 is recorded a compression curve of an eicosylamine hydrochloride monolayer after penetration (180 min.) by cetyl sulfate. During compression ΔV rose from 340 to 410 mv., and the area at collapse (44.4 \AA^2 per amine molecule) shows that slightly more than an equimolecular amount of cetyl sulfate was retained in the surface; this, however, might well have been due to the extreme slowness of the ejection process from the strong solid mixed film. An experiment at constant area showed how strong is the association between the amine and SCS. After the initial drop of 2-3 dynes/cm., the pressure rose abruptly to 68 dynes/cm. where it was maintained for *ca.* 15 min. It seems likely that the subsequent fall in π and ΔV corresponds to a slow ejection of excess amine from the rigid film, with replacement by cetyl sulfate molecules from the subsolution to form the 1:1 complex (1).

(b) *Sodium Behenyl Sulfate*¹-*Cetyltrimethylammonium Bromide*. Solutions of cationic detergents are known to render surfaces hydrophobic (9). Clearly, in such solutions, compensation by the Wilhelmy plate will become uncertain. The experiments with CTAB must be regarded as qualitative and are therefore reported in brief. Two points of interest in the expansion curves (not shown) were that (a) the A_e values were much smaller than the anticipated 1:1 association values, and (b) in some experiments the expansions came to a complete halt. Compression curves

¹ In spreading sodium behenyl sulfate from ethanol solution, there is a 25% loss of compound from the monolayer (15). The π - A curve in Fig. 7 was therefore constructed assuming a collapse area of $18.5 \text{ \AA}^2/\text{molecule}$.

also led to small collapse areas (Fig. 7). There was again a close correspondence between the ΔV values of mixed films formed by penetration at constant area and constant pressure. The data did not suggest complex formation; later results on mixed films suggest that the factor responsible is the bulky nature of the quaternary ammonium head group in CTAB.

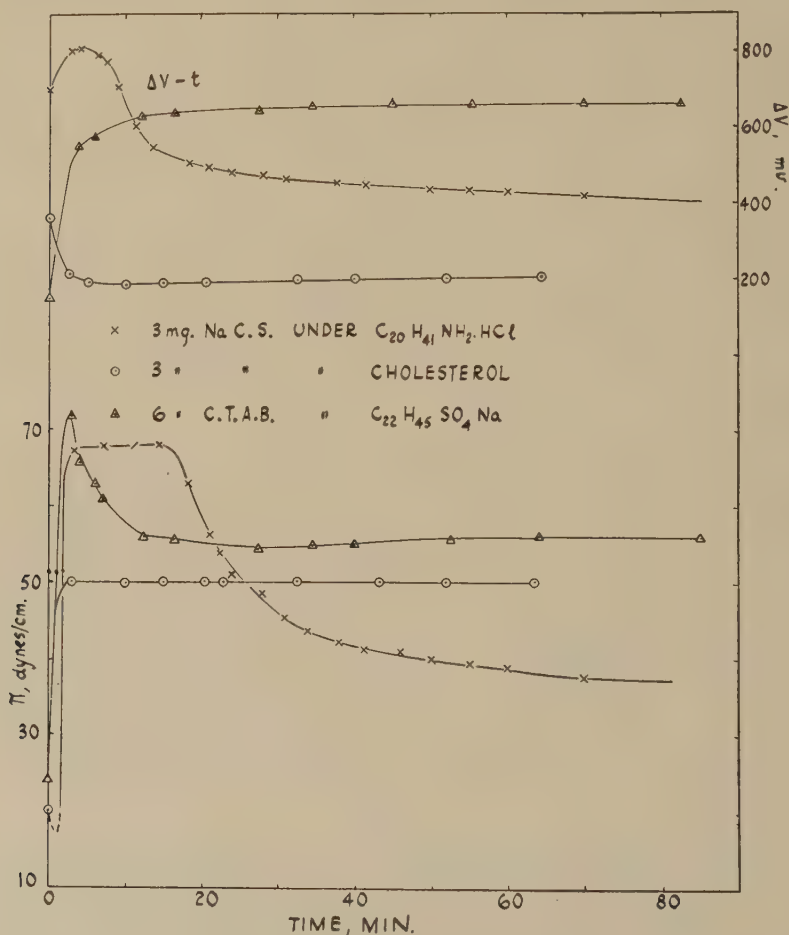


FIG. 6. Constant area penetrations.

The Cholesterol-Digtonin Association

The last of the single-film penetrations involved the well-known cholesterol-digtonin association. Digtonin is the best saponin for precipitating steroids of specific structure (16) e.g., it forms an insoluble complex with normal sterols but not with episterols. Surface-film measurements

(1,2,17) gave results analogous to these bulk phase data, and penetration at constant pressure was found to result in 100% area extension of a cholesterol monolayer.

Pi values for concentrations 4.5, 9, and 13.5 mg. digitonin/l. of $M/700$ NaCl solution were found to be respectively 2.5, 7.4, and 9.0 dynes/cm. after 90 min., and the ΔV values all about 200 mv.

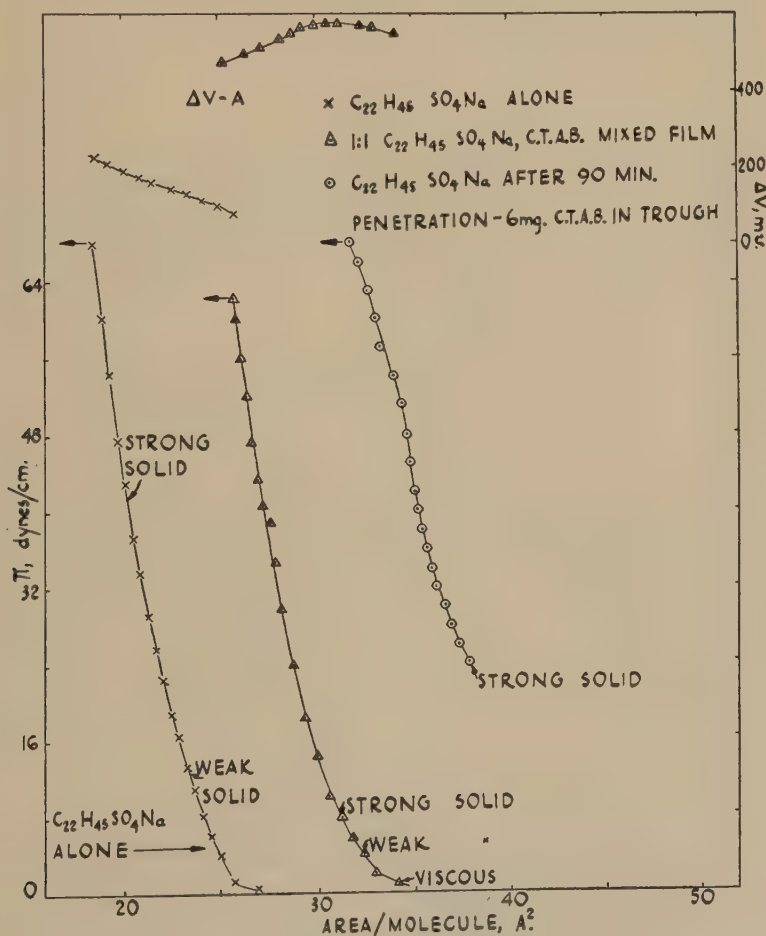


FIG. 7. Compression of sodium behenyl sulfate films.

An interesting feature of the cholesterol-digitonin expansion curves is that the amount of expansion due to the linear portion of the curve was small but definitely present (Fig. 8). Graphs of $\log (A_e - A_i)$ vs. time show that a first-order law was obeyed. Other experiments have shown the effect upon the velocity constant of changes in surface pressure

(between 12 and 20 dynes/cm.) and in digitonin concentration above 9 mg./l. to be small. The values of A_e , 73–75 \AA^2 , are close to that anticipated for the 1:1 complex. Adam (18) gives 36 \AA^2 as the lower limit to cross-sectional area of a steroid molecule. For the cholesterol-saponin complex Matalon (3) obtained an $(A_e - A_0)$ value of 50–55 \AA^2 ; this

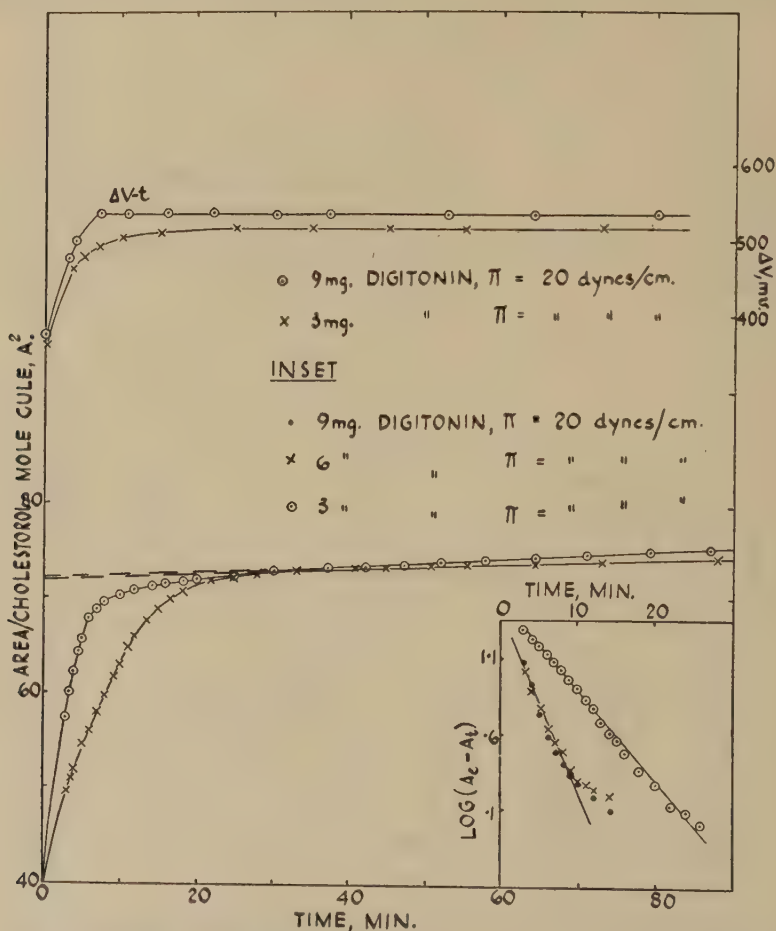


Fig. 8. Digitonin injected under cholesterol monolayers at constant pressure.
Trough volume = 670 ml.

$\log(A_e - A_t)$ vs. time for the expansions.

larger area is probably due to a different spatial arrangement of the sugar molecules in saponin from that in digitonin.

In Fig. 9a the compression curve of a penetrated cholesterol monolayer is compared with compression curves of various cholesterol-digitonin mixtures spread and recorded on an automatic recording balance (19). It is clear that in spreading and compressing the 1:1 mixture meso

digitonin was lost; however, compression of the 1:2 and 1:3 mixtures gave collapse areas close to that obtained for the penetrated cholesterol monolayer, and this suggests ejection of excess digitonin before collapse of the complex.

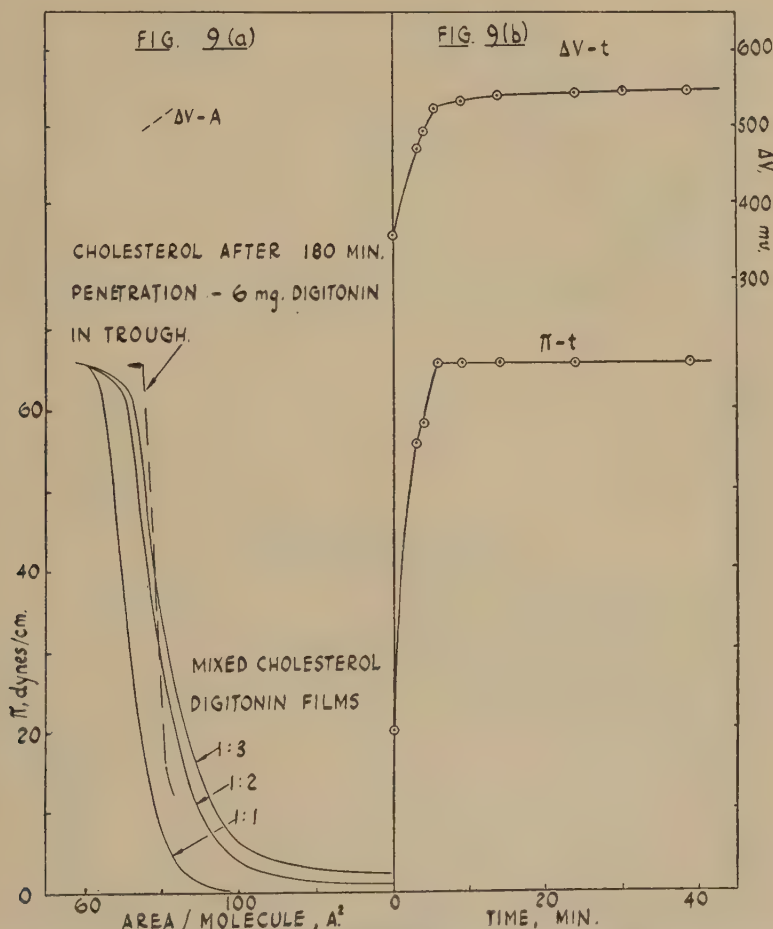


Fig. 9. (a) Compression of cholesterol-digitonin films; (b) digitonin (6 mg./670 ml.) injected under a cholesterol monolayer at 20 dynes/cm. Constant area.

From the results shown in Fig. 9b it is concluded that on injection of digitonin beneath a cholesterol monolayer held at constant area there results a 1:1 mixed monolayer of high stability.

Penetration of Mixed Films

There is a simple method of testing the validity of Matalon's hypothesis, viz., that the rapid progress of monolayer expansion is due to complex formation; for, if a stable 1:1 complex could be formed on the surface by

spreading, injection of the penetrant should result only in a linear extension of the monolayer as interaction to form the complex would already have been accomplished. The systems studied were therefore examined by this method.

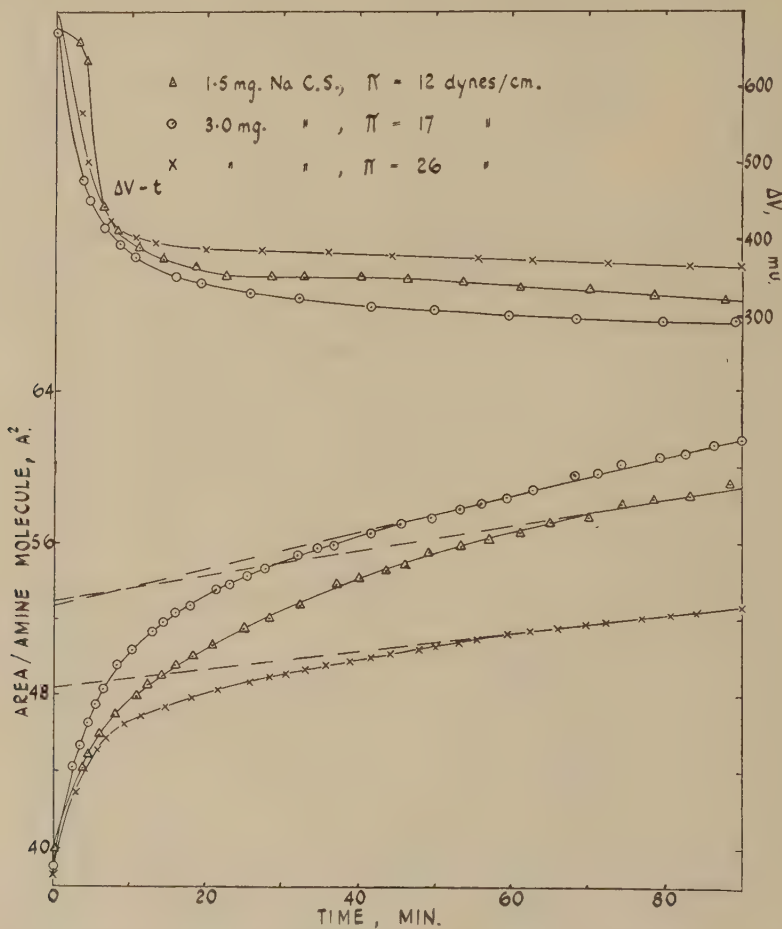


FIG. 10. Sodium cetyl sulfate injected under 1:1 eicosylamine hydrochloride-sodium cetyl sulfate mixed films at constant pressure. Trough volume = 670 ml. (0.001 N HCl).

(a) *Eicosylamine Hydrochloride-Sodium Cetyl Sulfate*. The force-area curve of a 1:1 mixed eicosylamine hydrochloride-SCS film formed by spreading from 1:1 benzene-ethanol solution indicates that little, if any, of the SCS was lost during the spreading and compression of the stable, strong solid film (Fig. 5). It is worthy of note that the surface potential,

ca. 700 mv., of the above film is more than 300 mv. greater than that of a mixed film of the same area formed by penetration.

Injection of SCS below the spread mixed film yielded the unexpected result that the expansion curves obtained were of precisely the same form as before (Fig. 10). Starting at an area of 39–40 $\text{\AA}^2/\text{molecule}$ of amine

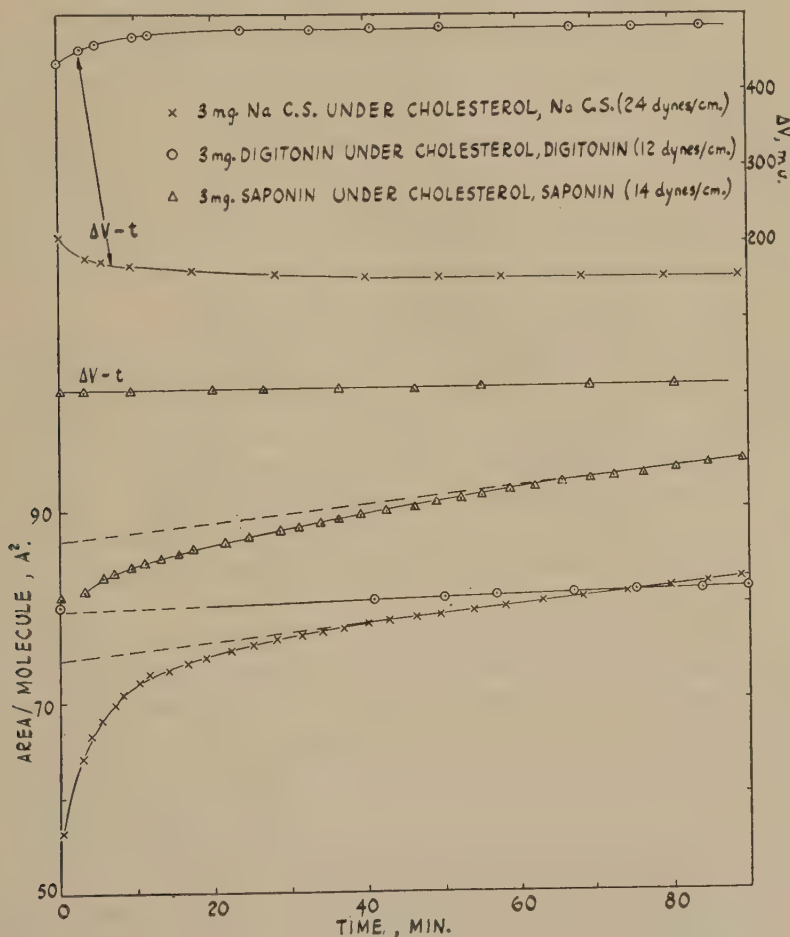


FIG. 11. Penetration of mixed films at constant pressure.

expansion experiments gave rise to A_e values ranging from 48.5 to 53 \AA^2 . The resulting ΔV values (ca. 350 mv.) were much the same as those obtained on penetration of the amine alone by SCS. It emerged that for a given amount of injected SCS at a given surface pressure, the slope of the linear extension was virtually the same, irrespective of whether the initial film was the amine alone or the 1:1 mixed film. It is inferred that after

penetration of the mixed film has proceeded for a time the conditions in the film and bath become identical to those obtaining in the penetration of the amine alone, expanded to the same area. These results obviously cast doubt on the original interpretation given to the expansion curves.

(b) *Cholesterol-Sodium Cetyl Sulfate*. Compression curves of spread 1:1 cholesterol-SCS films showed that on $M/700$ NaCl solution some of the SCS was lost in spreading and some by dissolution at higher pressures. On 1% NaCl, however, the 1:1 film was stable. The 1:1 mixture was spread on the $M/700$ NaCl, rapidly compressed to 24 dynes/cm., and the injection was started when the area/molecule cholesterol was 56.5 \AA^2 . Injection again resulted in an initial extension by the rapid process to an area of 75 \AA^2 (Fig. 11) which is far in excess of the 1:1 complex value. The slope of the linear extension ($0.089 \text{ \AA}^2/\text{min.}$) was observed to be very nearly equal to that obtained in the penetration of cholesterol alone ($0.094 \text{ \AA}^2/\text{min.}$); likewise, the resultant ΔV value (155 mv.) is effectively that obtained in the previous cholesterol penetrations.

(c) *Cholesterol-Digitonin and Cholesterol-Saponin*. A 1:1 cholesterol-digitonin film spread from 1:1 benzene-ethanol solution was reasonably stable at 12 dynes/cm., and occupied an area of 79 \AA^2 . The film was a strong solid, and on injection of 3 mg. digitonin there was *no movement* of the slide until the 25th min., after which there followed the very slow linear extension characteristic of digitonin penetrations (Fig. 11). The surface potential rose to 483 mv., which may be compared with 505 mv., the value obtained in the cholesterol penetration under the same conditions.

As the molecular weight of the saponin used was not accurately known, an approximately 1:2 cholesterol-saponin spreading solution was made assuming a molecular weight of 1000 (16). After injection, there was present a slight expansion of the rapid type, and a linear extension then followed. The important point is that the value of A_e (87 \AA^2) is *not greater than* the value ($90\text{--}95 \text{ \AA}^2$) obtained in the penetration of cholesterol alone. The latter value was obtained by Matalon (3) using the same specimen of saponin. The surface potential of the film was scarcely altered during the expansion. It seems likely that the saponin lost from the surface by dissolution during spreading is replenished by the rapid process on injection of saponin into the bath.

It is seen then that penetration by digitonin or saponin of a cholesterol film, alone or admixed with penetrant, results in the same mixed film, presumably the 1:1 complex.

(d) *Mixed Films with CTAB*. In the compression curve (Fig. 7) of a 1:1 sodium behenyl sulfate-CTAB mixed film the results are plotted as area/molecule values of behenyl sulfate, *no allowance* having been made

for the partial spreading of the latter. In the penetrations of these mixed films the area changes are shown as changes in the distance l between slide and boom (Fig. 12). Injection of CTAB below the mixed film resulted in a *slow* expansion of the film, indicating an absence of the rapid process.

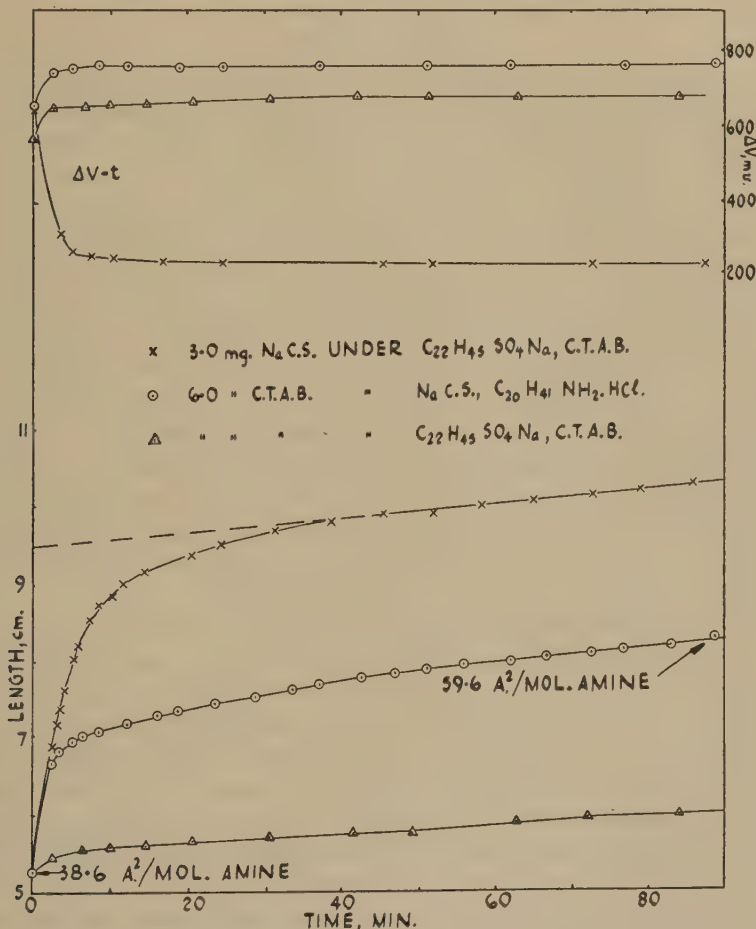


FIG. 12. Penetration of 1:1 mixed films at constant pressure of 24 dynes/cm.

CTAB, however, readily penetrated a 1:1 eicosylamine HCl-SCS mixed film. Like most CTAB penetrations, there was no linear portion of the curve, the rate of extension diminishing with time (Fig. 12). It seems that in the Na behenyl sulfate-CTAB mixed film, the bulky quaternary ammonium head groups "screen" the negatively charged sulfate groups from the CTAB molecules in solution so that penetration is largely restricted. The "screening" effect does not arise when the amine is unsub-

stituted and CTAB molecules are readily adsorbed into the eicosylamine HCl-SCS mixed film.

If these views are correct, then the mixed Na behenyl sulfate-CTAB film should readily be penetrated by SCS. This is, in fact, the case and injection resulted in a very rapid expansion of the film (Fig. 12).

DISCUSSION

The evidence obtained from the experiments with eicosylamine hydrochloride suggests that the first process involved in penetration is the "anchoring" of solute molecules by the insoluble monolayer. This is then followed, after suitable orientation, by adsorption into the monolayer. At constant surface area, penetration in the systems studied results in the formation of an equimolecular mixed film, and this necessitates the ejection of excess of the insoluble component from the mixed monolayer so formed. Further evidence discussed below suggests that a secondary adsorbed layer of solute is part of the ultimate structure of the penetrated film. When a monolayer previously penetrated at constant pressure is compressed, solute molecules in excess of the 1:1 ratio are progressively ejected, and the mixed monolayer eventually collapses as a 1:1 unit. It is interesting that complete ejection of excess solute molecules is not achieved until the collapse pressure of the mixed film is reached. In mixed films studied previously, e.g., long-chain fatty acids and alcohols on acid subsolutions, or long-chain esters and fatty acids, the component in excess was readily ejected at its own collapse pressure (21).

Penetration-expansion curves of these systems proceed in two stages, viz., a rapid initial expansion followed by a slower linear one. Within experimental error the rapid expansion follows a first-order law. In the case of digitonin penetrating a cholesterol monolayer, no marked linear expansion with time was observed and the resultant area was that of the 1:1 complex. The fact that the initial rapid expansion is eliminated when digitonin is injected under a 1:1 cholesterol-digitonin mixed monolayer demonstrates conclusively that the rapid expansion of the single component monolayer corresponds to the formation of the 1:1 complex. The small influence of pressure and concentration on the first-order velocity constant is interesting and is presumably connected with the specificity of the interaction.

In the case of the penetration experiments with SCS the work has shown that no clear-cut evidence of complex formation can be obtained from the expansion curves. The results revealed that the rapid expansion process was still present when SCS was injected below 1:1 mixed films. In this connection it is of interest to examine the difference between 1:1 eicosylamine HCl-SCS films formed (a) by spreading ($\Delta V = ca. 700$ mv.) and (b) by penetration ($\Delta V = ca. 350$ mv.). The surface potential pro-

vides an important clue. Writing

$$\Delta V = 4\pi n\mu + \phi$$

where n is the number of molecules per unit area of surface, μ is their surface moment, and ϕ is a constant depending on the composition of the underlying solution (20) we believe the difference in case (b) to be caused by the building up of an adsorbed double layer of cetyl sulfate in the first 15–30 min. after injection. Clearly, this would alter the value of the term ϕ , and might also influence μ as a result of reorientation in the monolayer. Utilizing the concept of a sublayer, it appears that in the absence of this layer penetration takes place at a greater rate than when it is present, and we suggest that the building up of a double layer is at least one of the factors responsible for terminating the rapid process of the expansions.

The slow linear portion of the expansion curves represents a further penetration of solute molecules into the mixed monolayer. The rate of extension, at a given solute concentration, depends on the pressure of the film, and is the same whether the insoluble component were initially present in the surface alone or in admixture with solute molecules. It would appear that during the rapid expansion process the double layer is built up and that thereafter a sensibly constant potential gradient to adsorption of solute exists. As the rate of the slow expansion is constant, it seems that only those surface collisions which involve the original insoluble molecules are effective in adsorbing the solute molecules. Over the limited pressure range investigated it was observed for the penetrations with SCS that an equation of the following type is obeyed within experimental error:

$$\left(\frac{dA}{dt}\right) \text{ linear extension} = \alpha_1 e^{-\pi\alpha_2}$$

where α_1 and α_2 are constant for a given concentration of solute and a given temperature. The exponential index $(-\pi\alpha_2)$ is usually interpreted in terms of an activation energy. On this basis it seems that the activation energy of the adsorption process is directly affected by the surface pressure of the monolayer. A more precise understanding of the extent to which the rate of interaction is affected by orientation and/or activation energy must await a study of the temperature coefficient of the rate processes involved.

An alternative explanation is that the slow linear expansion process is due to Dalton's Law effects taking place over a time period owing to the condensed nature of the penetrated monolayers. It will be seen in Part III of this series that equilibrium areas are reached very quickly when monolayers are in the vapor state.

It has been observed that steric factors in the polar groups are of importance in limiting penetration. Thus, the large trisubstituted amine

polar group in CTAB can build up a positive potential barrier under a mixed monolayer with a long-chain sulfate, and prevent further CTAB molecules from approaching the monolayer. This brings the expansion process to a halt. In the same way CTAB molecules initially penetrate a mixed long-chain amine-long-chain sulfate film, but as before a potential barrier builds up and limits penetration. It is possible that steric factors of a different type are operating in the case of the cholesterol-digitonin interaction where very strong, solid surface structures are observed; these are such that, after formation of the 1:1 complex, the cholesterol molecules are no longer available to the digitonin in the subsolution.

REFERENCES

1. SCHULMAN, J. H., AND RIDEAL, E. K., *Proc. Roy. Soc. (London)* **B122**, 29, 46 (1937).
2. SCHULMAN, J. H., AND STENHAGEN, E., *Proc. Roy. Soc. (London)* **B126**, 356 (1938).
3. MATALON, R., Ph.D. Dissertation, Cambridge, 1949.
4. MATALON, R., AND SCHULMAN, J. H., *J. Colloid Sci.* **4**, 89 (1949).
5. MATALON, R., private communication, 1950.
6. ALEXANDER, A. E., *Trans. Faraday Soc.* **37**, 15 (1941).
7. SCHULMAN, J. H., AND McROBERTS, T. S., *Trans. Faraday Soc.* **42B**, 165 (1946).
8. HARKINS, W. D., AND OPPENHEIMER, H., *J. Chem. Phys.* **16**, 1000 (1948).
9. HARTLEY, G. S., AND RUNNICLES, D. F., *Proc. Roy. Soc. (London)* **A168**, 420 (1938).
10. EPTON, S. R., *Trans. Faraday Soc.* **44**, 226 (1948).
11. ALEXANDER, A. E., AND SALTON, M. R. J., *Research (London)* **2**, 247 (1949).
12. SCHULMAN, J. H., AND COCKBAIN, E. G., *Trans. Faraday Soc.* **36**, 661 (1940).
13. ADAM, N. K., *Proc. Roy. Soc. (London)* **A126**, 526 (1930).
14. COCKBAIN, E. G., AND SCHULMAN, J. H., *Trans. Faraday Soc.* **35**, 716 (1939).
15. STENHAGEN, E., *Trans. Faraday Soc.* **36**, 496 (1940).
16. FIESER, L. F., AND FIESER, M., *Natural Products Related to Phenanthrene*, 3rd Ed., Reinhold, New York, 1949.
17. LANGMUIR, I., SCHAEFER, V. J., AND SOBOTKA, H., *J. Am. Chem. Soc.* **59**, 1751 (1937).
18. ADAM, N. K., *Physics and Chemistry of Surfaces*, 3rd Ed., Oxford University Press, London, 1941.
19. ALEXANDER, A. E., AND GLAZER, J., unpublished work.
20. SCHULMAN, J. H., AND RIDEAL, E. K., *Proc. Roy. Soc. (London)* **A130**, 284 (1931).
21. SCHULMAN, J. H., AND HUGHES, A. H., *Biochem. J. (London)* **29**, 1243 (1935).

MOLECULAR INTERACTION IN MONOLAYERS. II. STERIC EFFECTS IN THE NONPOLAR PORTION OF THE MOLECULES

E. D. Goddard and J. H. Schulman

Department of Colloid Science, University of Cambridge, England

Received December 7, 1951; revised December 2, 1952

ABSTRACT

The interaction between long-chain alcohols and sodium cetyl sulfate has been examined by the monolayer penetration technique. Molecular association is shown to be strongest when the alcohol possesses a straight hydrocarbon chain and can be weakened considerably by altering the configuration of the chain. The concept of a two-dimensional Dalton's Law has been invoked to explain the results obtained with expanded alcohol monolayers at constant pressure.

INTRODUCTION

In Part I of this series (1), monolayer penetration experiments were reported on systems where there was strong association between the molecules of the insoluble monolayer and the molecules of the surface-active compound dissolved in the underlying solution. Penetration was shown to result in the formation of 1:1 mixed monolayers; the effect on penetration of steric factors involving the polar portion of the molecules was investigated.

In this paper, monolayer penetrations have been measured with special emphasis on the effect of various steric configurations in the nonpolar portion of the molecules. This inevitably leads to the study of penetration where weaker associations are involved, and where the physical forces leading to adsorption are brought into play.

EXPERIMENTAL

The experimental technique was the same as that described in Part I. Monolayer penetration experiments were carried out at constant surface pressure and constant surface area. The duration of the monolayer expansion experiments at constant pressure was usually 3 hr., and, in general, the expansion was allowed to proceed until the slower part of the expansion had been linear with time for at least 2 hr. In carrying out force area determinations on mixed films formed by penetration, the precautions mentioned in Part I were observed. Individual compression curves were of at least 3 hr. duration.

RESULTS

(a) *Penetration of Cetyl Alcohol and 2-Eicosanol by Sodium Cetyl Sulfate*

A monolayer of cetyl alcohol is known to be strongly penetrated by sodium cetyl sulfate (SCS) at constant area (2). Figure 1 shows a series of cetyl alcohol penetrations at constant pressure. Injection of SCS re-

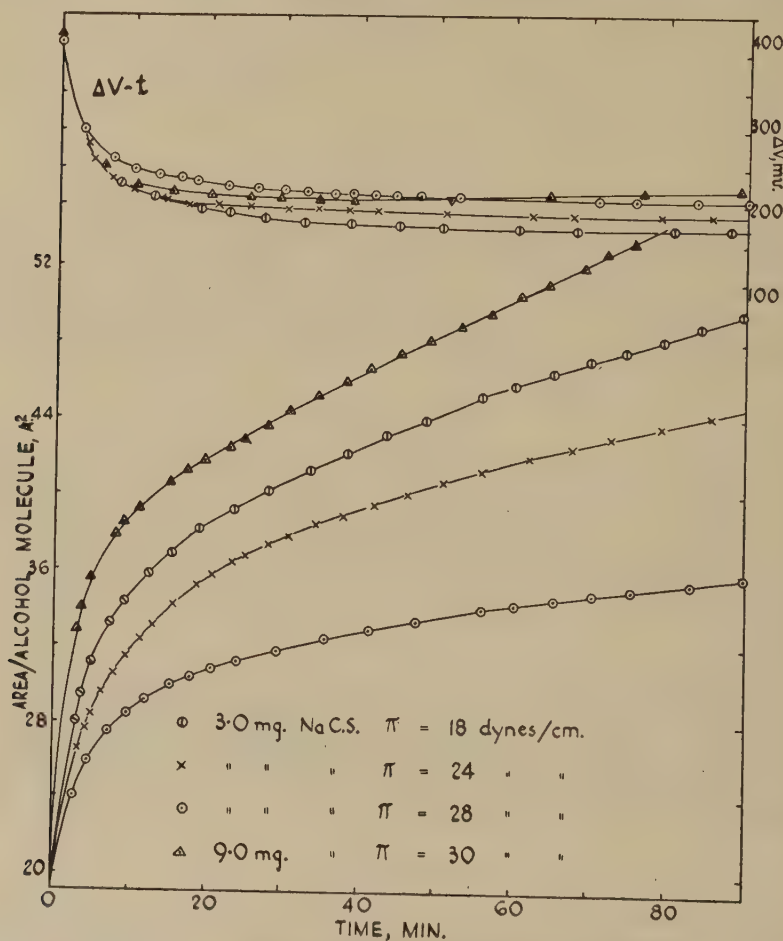


FIG. 1. Sodium cetyl sulfate injected under cetyl alcohol monolayers at constant pressure. Trough volume = 670 ml.

sulted in a fast initial expansion of the condensed monolayer, and, after 30–50 min., the rate of area extension became constant. The pattern of the expansion curves is very similar to that described in Part I. The extent of the expansion and the slope of the linear portion is seen to have

depended markedly on the surface pressure and the concentration of SCS employed.

After injection there was a big change in the surface potential (ΔV), but after 20 min. further changes were very small. In the experiment using 9.0 mg. SCS the surface potential dropped to 207 mv., but on con-

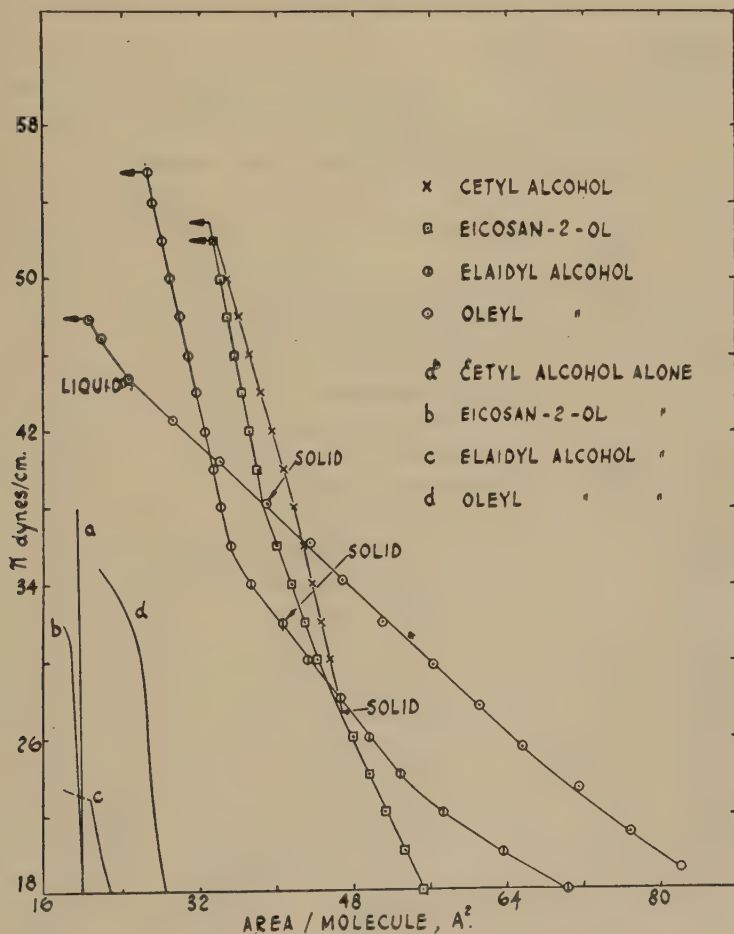


FIG. 2. Compression of alcohol monolayers after penetration by sodium cetyl sulfate (3 mg./670 ml.).

tinued expansion, this value rose to 223 mv. after 90 min. Comparison of this value with that obtained for an adsorbed monolayer of SCS in the absence of an insoluble monolayer, viz., ca. -20 mv., again suggests a difference in orientation of the cetyl sulfate in the mixed monolayer and/or the presence of an adsorbed double layer of sulfate molecules

beneath the mixed film (see Part I). Results very similar to the above were obtained in the experiments on the secondary alcohol, 2-eicosanol. On its own, 2-eicosanol forms a liquid condensed monolayer (Fig. 6).

Compression of a cetyl alcohol-SCS mixed film, formed by penetration at constant pressure, is shown in Fig. 2. Points of interest are (a) the very

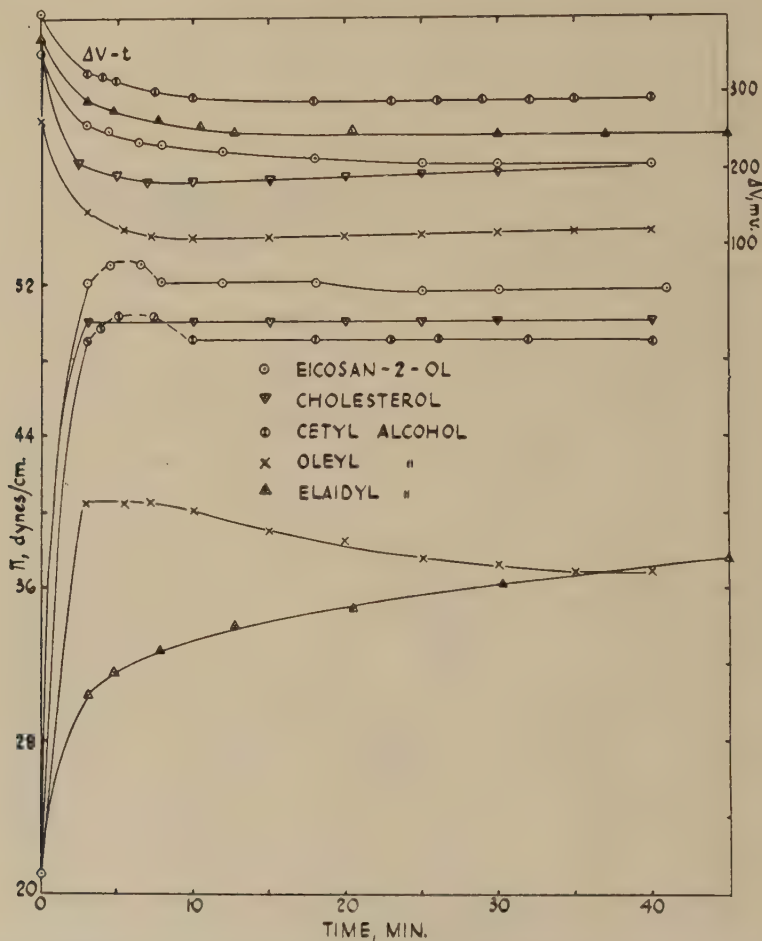


FIG. 3. Sodium cetyl sulfate (3 mg./670 ml.) injected under alcohol monolayers at 21 dynes/cm. Constant area.

high collapse pressure (52 dynes/cm.) at which neither the alcohol nor the sulfate would have been stable on its own, and (b) that the collapse area (34 Å.² per molecule cetyl alcohol) exceeds that of the cetyl alcohol alone (3). Although the collapse area does not correspond to a 1:1 association, it is clear that a considerable quantity of SCS was held and

stabilized in the surface by the cetyl alcohol. The compression of the 2-eicosanol-SCS mixed film resembled the above very closely, both in regard to collapse area and pressure.

In the constant-area penetrations (Fig. 3), injection of SCS beneath cetyl alcohol or 2-eicosanol resulted in an increase in surface pressure to 50 dynes/cm. [cf. (2)]. The differences in the surface potential of the mixed alcohol-cetyl sulfate films formed by penetration at constant pressure and constant area are appreciable. Although it is likely that some alcohol molecules are ejected from the surface in the constant-area penetration, there is little evidence of complex formation.

(b) Effect of Nonpolar Steric Factors on Penetration

(1) *cis-trans Isomerism*. The introduction of a double bond into a long-chain amphipathic compound is known to result in considerable expansion of its monolayers at the air/water interface (4,5). The major factor involved is the reduction in intermolecular cohesion of the hydrocarbon chains. Thus, elaidyl alcohol (*trans*-9-octadecen-1-ol) is observed to form an expanded monolayer at room temperature and to undergo a transition to the condensed state as the surface pressure is raised (6). Under the same conditions oleyl alcohol, the *cis* isomer, is expanded over the entire compression range. Thus elaidyl alcohol exhibits a behavior intermediate between that of the *cis* unsaturated alcohol and the saturated alcohol which gives a condensed monolayer, and this is borne out by the penetration of these films by SCS. The most notable feature of the expansion experiments on the unsaturated alcohols (Fig. 4) was the extraordinarily large rate of area increase, particularly in the case of oleyl alcohol; this was so large at $\pi = 18$ dynes/cm. that it was possible to follow the expansion for only 125 min. For comparison, expansion curves of the three alcohols under the same conditions are shown in the figure.

The above results are unexpected in view of the very much weaker penetrations (as measured by a smaller pressure increase) obtained with the unsaturated alcohols at constant area; these weak penetrations may be related directly to the difficulty in adlineation of the unsaturated alcohol and the cetyl sulfate. It is clear that a new phenomenon must be considered in order to explain the fast and extensive expansion of monolayers when association between the monolayer and the solute is known to be weak.

The ΔV values of the films penetrated at different pressures varied considerably and continued to fall as penetration proceeded. In some cases ΔV fell below zero indicating that cetyl sulfate molecules in the surface region had a different net orientation from that obtaining in the penetrated films studied previously in spite of the operating surface pressure being the same. It was not possible to examine the differences

between mixed films formed by penetration and by spreading because of the instability of the latter.

(2) *Isoalcohols*. Specimens of isohexadecyl alcohol (14-methyl-1-pentadecanol) and isoöctadecyl alcohol (16-methyl-1-heptadecanol) were obtained from Dr. Stenhagen of Uppsala, who has found interesting bulk

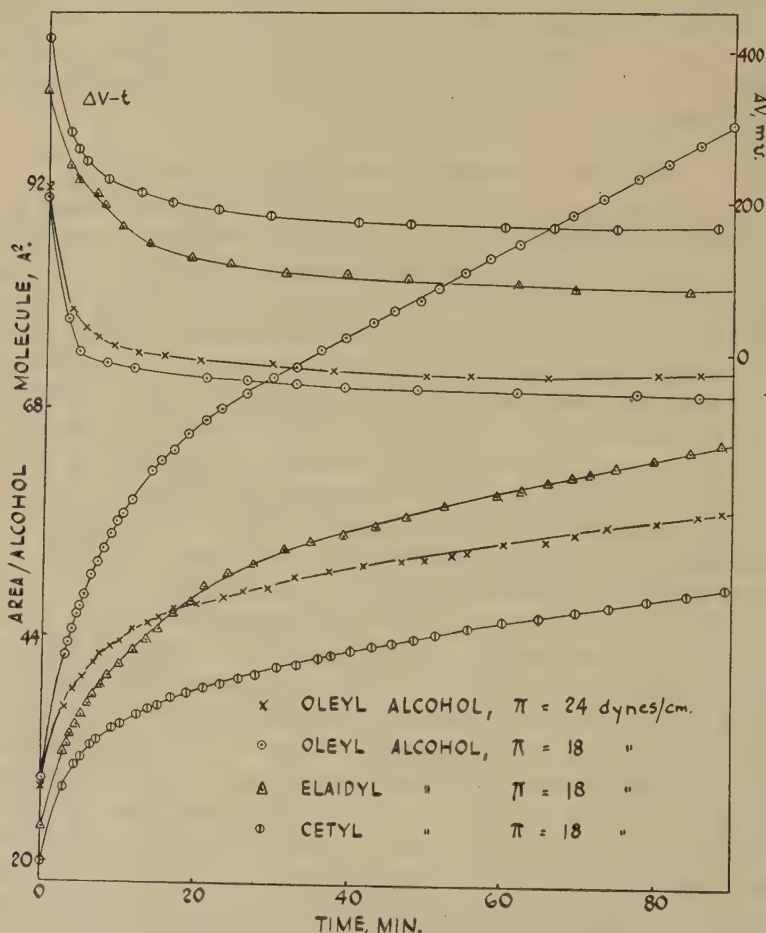


FIG. 4. Sodium cetyl sulfate (3 mg./670 ml.) injected under alcohol monolayers at constant pressure.

relationships with these compounds.¹ Studying the phase diagrams of mixtures of isoöctadecyl alcohol with *n*-octadecanol and *n*-hexadecanol, he obtained results as shown in Fig. 5a. With case (a) the *n*-18-iso-18 alcohols, there was a eutectic mixture; but case (b), the *n*-16-iso-18 mix-

¹ Private communication from Dr. E. Stenhagen, 1950.

ture showed compound formation and gave two eutectics. Clearly this difference arises from steric factors, case (b) allowing far greater ease of packing.

These isoalcohols would therefore be expected to give interesting results on penetration by SCS. By analogy with the above phase diagram,

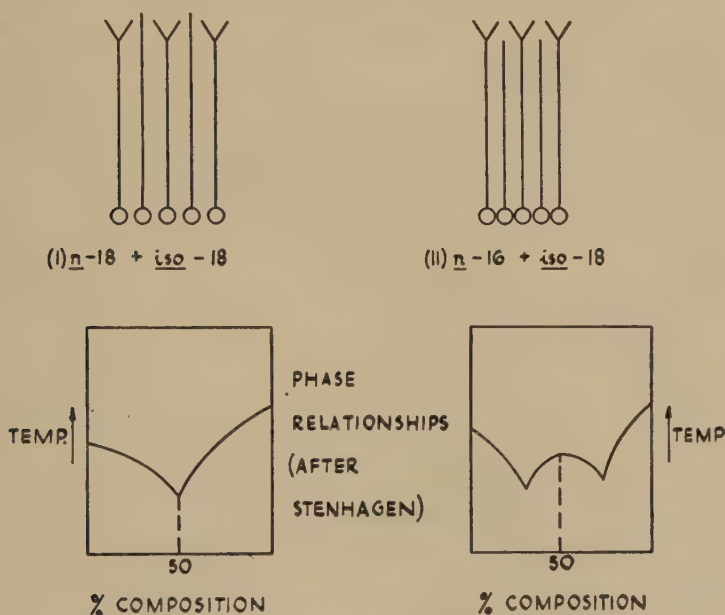


FIG a. MIXTURES OF STRAIGHT CHAIN AND *iso*-ALCOHOLS

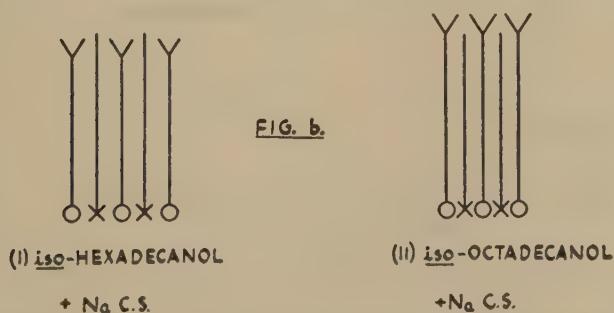


FIG. 5. (a) Mixtures of normal and isoalcohols (diagrammatic); (b) mixtures of isoalcohols and sodium cetyl sulfate (diagrammatic).

strong association would be anticipated with isoöctadecyl alcohol; difficulties in adlineation of the hydrocarbon chains would, however, be expected to render the association between SCS and isohexadecyl alcohol a much weaker one (Fig. 5b).

Π versus A curves for the two isoalcohols are given in Fig. 6; it is seen that terminal branching of the hydrocarbon chains results in expansion of the monolayers. The expansion data are given in Fig. 7. Expansion was faster and more extensive in the case of isohexadecyl alcohol, the more

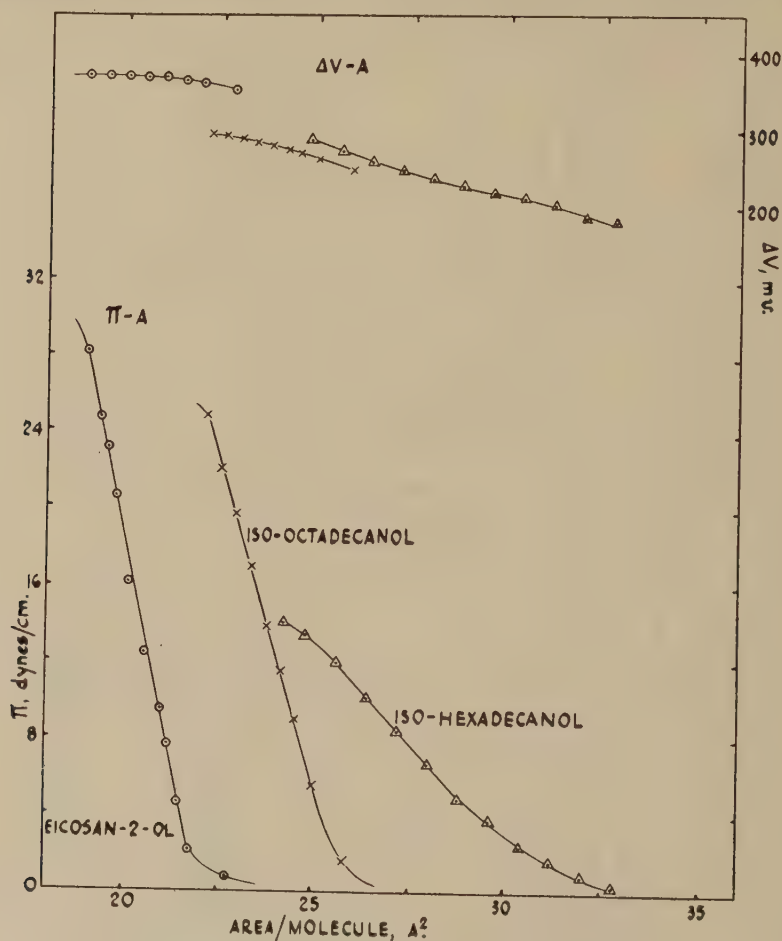


Fig. 6. Force area curves of alcohol monolayers.

expanded monolayer. It is shown below that the isohexadecyl alcohol-SCS association is not a strong one, and that the stability of the mixed film is impaired at higher pressures.

Compression Curves

The oleyl alcohol-SCS mixed film was much more compressible than the cetyl alcohol-SCS mixed film, and compression resulted in complete

ejection of the cetyl sulfate from the surface, the film remaining fluid throughout (Fig. 2). The presence of the cetyl sulfate, however, enabled the oleyl alcohol monolayer to stand a very high pressure [cf. (3)]. The mixed elaidyl alcohol-SCS film collapsed at $27 \text{ \AA}^2/\text{molecule}$ and exhibited

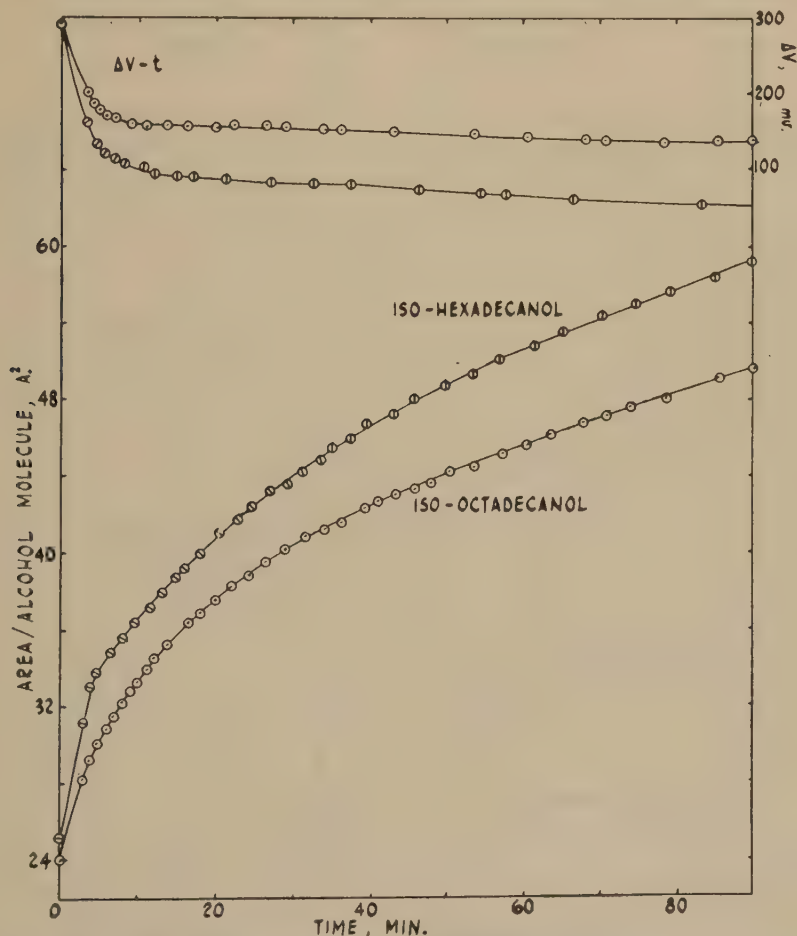


Fig. 7. Sodium cetyl sulfate (3 mg./670 ml.) injected under isoalcohol monolayers at constant pressure of 12 dynes/cm.

a behavior intermediate between that of the *cis*-unsaturated and the saturated alcohol.

Compression of the penetrated isoalcohols followed the expected pattern (Fig. 8a). In both cases the monolayers stood high pressures well above the collapse pressures of the alcohols. In the case of the isohexadecyl alcohol, the cetyl sulfate was almost completely ejected when the

collapse point was reached, and the film remained fluid. The isoöctadecyl alcohol on the other hand behaved very much like cetyl alcohol under these conditions: the mixed film solidified during compression, and cetyl sulfate molecules remained in the monolayer up to the collapse point.

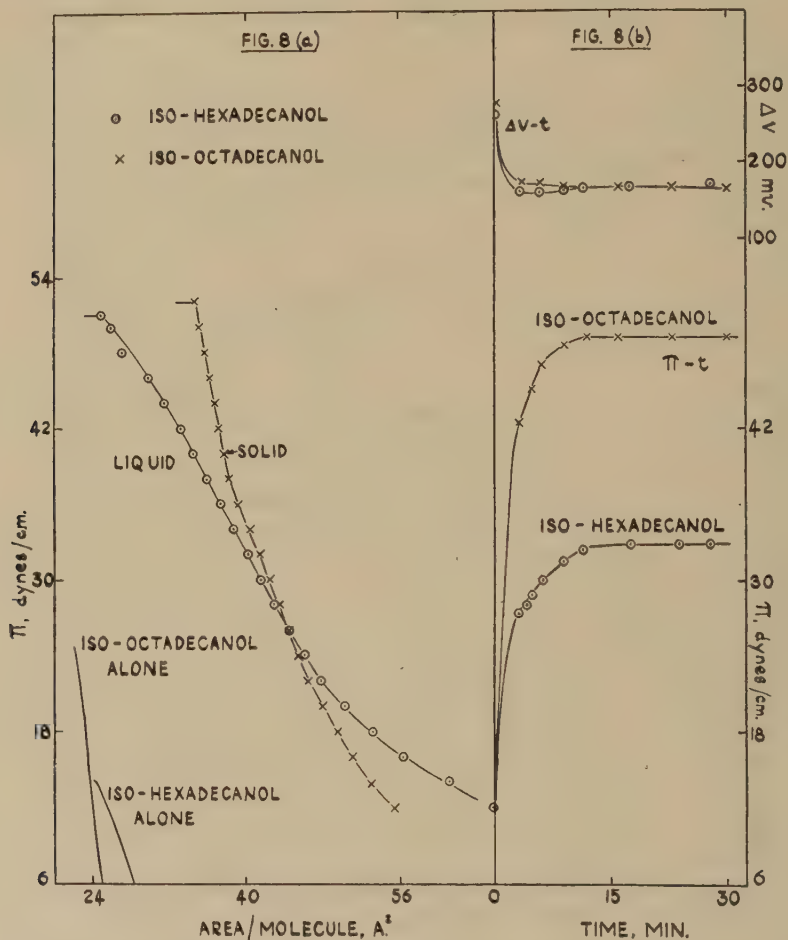


Fig. 8. (a) Compression of isoalcohol monolayers after penetration by sodium cetyl sulfate (1.5 mg./670 ml.); (b) sodium cetyl sulfate (1.5 mg./670 ml.) injected under isoalcohol monolayers at 12 dynes/cm. Constant area.

Constant-Area Penetrations

Further evidence in support of these concepts came from the constant-area penetration of the isoalcohols (Fig. 8b). On injection of 1.5 mg. SCS into the bath, the pressure of isoöctadecyl alcohol rose from 12 to 49 dynes/cm., while the isohexadecyl alcohol increased only to 33 dynes/cm.

These results show the great influence of steric factors on the alcohol-sulfate association.

Figure 3 shows the constant-area penetrations of the other alcohols examined. The saturated alcohols and cholesterol gave very high pressures, characteristic of strong penetration; the unsaturated alcohols gave lower pressures, as expected.

DISCUSSION

The conditions necessary for monolayer penetration, as defined by Schulman and Rideal (2), are twofold: first, there should be a mutual attraction, such as exists between two ions, two dipoles, or an ion and a dipole, between the polar groups of the insoluble and soluble molecules; secondly, the penetrating molecule should possess a long hydrophobic "tail" which will associate by van der Waals' forces with the hydrocarbon chain of the insoluble molecule. These conditions are both satisfied in the systems cetyl alcohol-SCS and 2-eicosanol-SCS and penetration has been shown to be strong in each case; the results do not, however, suggest complex formation under the conditions of the experiment.

In introducing a center of unsaturation or branching into the hydrocarbon chain of the insoluble alcohol molecule the forces of cohesion between the molecules are reduced and the monolayer is expanded; similarly the association between these alcohol molecules and those of adsorbed cetyl sulfate can be reduced so that penetration becomes much weaker and stability of the mixed film is impaired. This is demonstrated most clearly in the experiments at constant area and in the compression of mixed films. The results on the unsaturated alcohols are in general agreement with the data of Cockbain and Schulman (7) on emulsions stabilized by mixtures of SCS and long-chain alcohols.

In order to explain the fast and extensive expansion of the unsaturated and branched-chain alcohols at constant pressure it is necessary to invoke a somewhat modified mechanism of adsorption of cetyl sulfate into the insoluble monolayer. Under conditions where both the insoluble monolayer and the adsorbed monolayer are in a vapor-expanded state it would be expected that a two-dimensional Dalton's Law would hold. On this basis the solute molecules would behave as if the insoluble monolayer were absent, adsorption would occur, and the resultant surface pressure would be the sum of the pressure values of the two components. This, of course, presupposes no interaction between the two components. This concept has been used by Matalon (8) for the oil/water interface and will be enlarged upon in Part III where results on non-associating systems are presented. It will be shown that severe departures from Dalton's Law occur when the insoluble monolayer is in the condensed state. To illustrate this point two results are quoted here: When octyl alcohol is injected

below a monolayer of *cis*-9-dihydroxystearic acid (vapor-expanded on an acid subsolution at room temperature), adsorption occurs and approximate additivity of the partial pressures is obtained; by contrast, octyl alcohol causes no change in surface pressure when injected below a cholesterol monolayer (condensed).

It seems likely that in the case of penetration of expanded alcohols by SCS two processes are in operation. Sodium cetyl sulfate molecules are adsorbed (*a*) by the penetration mechanism which involves surface collisions with the molecules of the insoluble monolayer and (*b*) by the process of ordinary adsorption which depends on the monolayer being in an expanded state. The latter condition is best fulfilled when the expanded alcohol monolayer is maintained at a low surface pressure, and this results in the rapid extensions observed at constant pressure. Extension rate is, therefore, not a measure of the strength of the association or of mixed-film stability.

We believe that an adsorbed sublayer of cetyl sulfate is part of the structure of the penetrated alcohol film; the high pressure stood by oleyl alcohol and isohexadecyl alcohol after complete ejection of cetyl sulfate from the monolayer is advanced as evidence for this.

REFERENCES

1. GODDARD, E. D., AND SCHULMAN, J. H., *J. Colloid Sci.* **8**, 309 (1953).
2. SCHULMAN, J. H., AND RIDEAL, E. K., *Proc. Roy. Soc. (London)* **B122**, 29, 46 (1937).
3. SCHULMAN, J. H., AND STENHAGEN, E., *Proc. Roy. Soc. (London)* **B126**, 356 (1938).
4. ADAM, N. K., *Proc. Roy. Soc. (London)* **A101**, 516 (1922).
5. MARSDEN, J., AND RIDEAL, E. K., *J. Chem. Soc.* **1938**, 1163.
6. GLAZER, J., AND GODDARD, E. D., *J. Chem. Soc.* **1950**, 3406.
7. SCHULMAN, J. H., AND COCKBAIN, E. G., *Trans. Faraday Soc.* **36**, 651 (1940).
8. MATALON, R., Ph.D. Dissertation, Cambridge, 1949.

RHEOLOGICAL APPROACH FOR THE STUDY OF PROTEIN MONOLAYERS¹

Taro Tachibana² and Kiyoshi Inokuchi

Department of Chemistry, Faculty of Science, Ochanomizu University, Tokyo, Japan

Received August 12, 1952; revised January 7, 1953

ABSTRACT

1. A static method of measuring the viscoelasticity of spread monolayers has been presented, and a rheological study has been carried out with the monolayers of proteins and synthetic polypeptides.

2. With ovalbumin films spread on 0.1 *N* hydrochloric acid and 5% ammonium sulfate solution, it has been found that an instantaneous elasticity (Hookean), followed by retarded elasticity and flow, appears at unexpectedly large areas, such as 5 sq. m./mg. Surface shear modulus of the instantaneous elasticity increased linearly with the decrease of surface area, exhibiting several breaks in the slope of the curve.

3. The films of serum albumin and hemoglobin did not exhibit any viscoelasticity until they were compressed down to the area below 1.0 sq. m./mg., where the films became viscous. Further compression down to below 0.8 sq. m./mg. rendered these films viscoelastic. At areas corresponding to such changes of film state, the compressibility-area curve exhibited breaks.

4. Poly-DL- α -aminocaproic acid and poly- γ -methyl L-glutamate showed an instantaneous elasticity (non-Hookean) at the areas larger than that of the close-packed monolayer. The monolayers of poly- ϵ -aminocaproic acid behaved like an ideal elastic body.

5. Concerning the form of the force-area curves, an interesting fact has been found: The films which do not give any instantaneous elasticity have no break point in their force-area curves; whereas, the films which exhibit the distinct instantaneous elasticity show the breaks or plateaus in their force-area curves.

INTRODUCTION

Protein monolayers are characterized by their forming extremely viscous and elastic films. This feature reflects the structure of spread films. Naturally, interest in the study of protein monolayers has emphasized the need for the application of rheological methods to this viscoelastic system. Several investigators have measured the surface viscosity by observing the damped oscillation of floating bodies (3,4,7,10) on the surface, and showed that this method is useful for film studies. Such techniques, however, would be rather inadequate to give information

¹ Presented at the Symposium on Rheology of the Chemical Society of Japan, Tokyo, Japan, Nov. 10, 1951.

² The expense of this work has been defrayed from the Scientific Research Expenditure of the Ministry of Education.

about the structure of films, because the oscillating motion of a floating body may destroy the fine structure of films. On the other hand, surface elasticity has not been subjected to direct measurement for protein monolayers, although the principle of obtaining the film elasticity has been described by Langmuir (11).

The mechanical property of real films is in general neither a purely viscous nor a purely elastic one, but a more complicated one, characterized by the superposition of both viscosity and elasticity. In recent years, the application of modern rheological method to three-dimensional materials has brought a considerable contribution to our knowledge of the structure of materials. It would, therefore, be profitable to study the protein monolayers as viscoelastic films, by the method based on the analysis of the deformation-time relation of the film subjected to a stress. The present study by the authors is a first attempt to describe a new method for use with viscoelastic films and its application to the monolayers of proteins and synthetic polypeptides. A description is also given of the dependence of the rheological character of the protein films on the surface concentration and of the characterization of protein monolayers in mechanical terms.

EXPERIMENTAL³

Apparatus and Procedures

The apparatus used is illustrated in Fig. 1. A metal ring *A*, suspended by a thin torsion wire *B* is in contact with the surface of water. A suspending wire is enclosed by a protector *D* which is fixed to rotate with the torsion head. The rotational angles of the torsion head *C* and the deflection of the ring are measured by means of the mirrors *E* and *F*, respectively, with lamp and scale *G*. Both the torsion constant of a suspending wire and the moment of inertia of the rotating system are chosen small enough so that when the upper torsion head is rotated by a definite angle the turn of the ring may cause an aperiodic motion. For this purpose, a phosphor bronze wire of 25μ in diameter and 30 cm. in length (torsion constant $k = 0.06$ dyne/cm.) and a platinum ring of 3.7 cm. in diameter were chosen. The moment of inertia of the whole rotating system was 0.8 g.-cm.^2 . The shearing stress imposed was within the range from 3×10^{-4} to 6×10^{-3} dynes/cm.

Thus, immediately after the quick turn of the torsion head by a measured angle φ , the deflection ω of the hanging ring during relaxation is measured with time t . When the ring was in contact with the clean surface of the water, the ω - t curve of type *a* in Fig. 2 was obtained. In

³ The authors wish to acknowledge their indebtedness to Dr. T. Nakagawa, of the Chemical Laboratory of Tokyo University, for helpful discussion of the present experimental method.

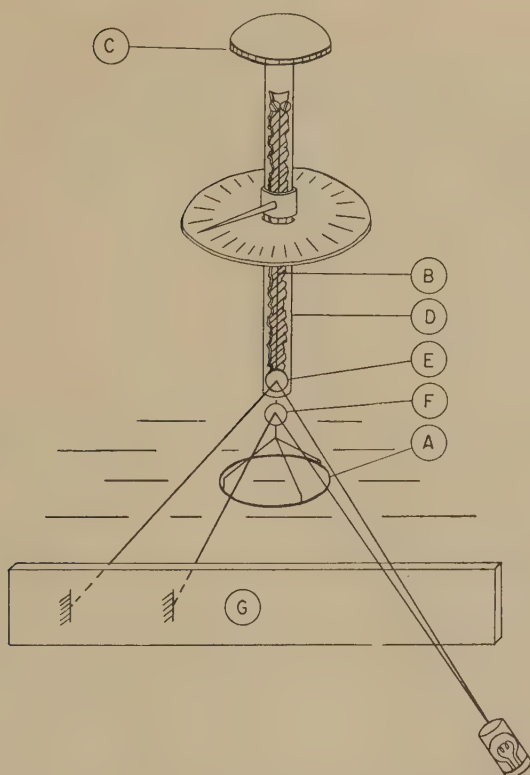


FIG. 1. Apparatus for measuring the film viscoelasticity.

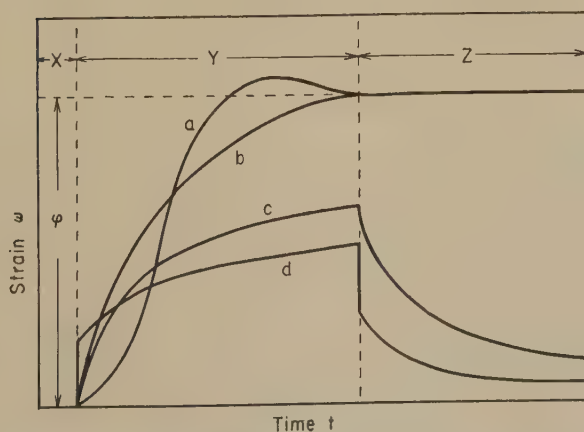


FIG. 2. Various types of strain-time relations. The region of (X) represents the dead time, (Y) the time in which the stress is imposed, and (Z) the time after the stress is removed.

this case, it is seen that the contribution of the moment of inertia of the rotating system to its motion was not so small as could be neglected. However, when a monolayer was spread on water, stressed, and then allowed to relax, three types of the ω - t curve (*b*, *c*, and *d* in Fig. 2) were produced, depending on the species as well as the film state of materials. As ω is considered to indicate a strain of the surface film, its rheological properties are characterized by the ω - t curves which are essentially the deformation-time curves of monolayers under stress. Then the shearing stress imposed is not kept constant, but decreases with the rotation of the ring. However, to the extent that ω is sufficiently smaller than φ , the ω - t curves obtained may be regarded as approximately under constant stress. In Fig. 2, curve *b* shows that the deformation is simple flow, because no elastic recovery occurred on the removal of the stress. If the flow is Newtonian, i.e., the rate of strain, $d\omega/dt$ is proportional to the stress, $\varphi - \omega$, a linear relation should be given between $\log(\varphi - \omega)$ and time t (5). Curve *c* shows that there is a time-dependent elastic deformation, it being delayed by the viscous resistance. In the curve *d*, it is seen that the deformation is divided into three classes: the instantaneous elastic part, the delayed elastic part, and the flow part. These behaviors are quite similar with that of the three-dimensional systems stressed, so that the deformation-time curve (Fig. 2) would be analyzed by the usual method in rheology (1). That is, the rheological behaviors of the spread films would be represented by a mechanical model which consists of the combination of an elastic and a flow element which is represented by a spring and a dashpot, respectively.

When the instantaneous elasticity (curve *d*) is observed, its shear modulus G may be shown by the following equation (10):

$$G = \frac{k}{4\pi} \left(\frac{1}{r_1^2} - \frac{1}{r_2^2} \right) \frac{\varphi - \omega}{\omega} \quad [1]$$

where r_1 is the radius of the ring and r_2 , is the radius of the circular films coaxial with the ring. In the present apparatus, r_2 may be assumed to be 7.3 cm. effective radius of the trough, which is sufficiently large compared with r_1 . In the present study, we have directed chiefly our attention toward the instantaneous elasticity of the films.

We have determined the force-area curve (designated as the F - A curve hereafter) as well as observed the rheological characteristics. The balance used for the measurement of surface pressure F was of the Wilhelmy type, and its sensitivity was 0.01 dyne/cm. The trough was 14.5 cm. wide and 60 cm. long. The balance was enclosed in a cabinet and all the operations were directed from the outside of the cabinet.

Materials⁴

Ovalbumin was prepared from fresh hen egg by the sodium sulfate method, and successive crystallization was done according to Kekwick (8). Horse serum albumin was a crystalline product prepared by the sodium sulfate method (9), and horse hemoglobin by the alcohol method in the Chemical Laboratory of Tokyo University. Samples of unfraktionated polynorleucine (poly-DL- α -aminocaproic acid) and poly- γ -methyl L-glutamate were prepared in the Chemical Laboratory of Osaka University.

RESULTS

1. *Proteins*

(a) *Ovalbumin*.—At first, it seemed necessary to make preliminary study on the rheological behaviors of a well-defined protein, for which ovalbumin has been used. Unless otherwise stated, 0.1 *N* hydrochloric acid was used as the substrate solution. The initial spreading concentration was about 0.2 mg./sq. m. The compression was started about 20 min. after spreading of the film. The mechanical behavior of the film is dependent upon the surface concentration as well as the shearing stress imposed. Under sufficiently large areas, the film resistance against the motion of the ring was negligibly small, resulting in an ω - t curve similar to curve *a* in Fig. 2. With a more compressed film below about 6 sq. m./mg., the film resistance became appreciable, showing non-Newtonian flow or retarded elasticity. Further compression down to the areas below 5 sq. m./mg. resulted in an ω - t curve similar to curve *d* of Fig. 2, i.e., the curve with instantaneous elasticity accompanied by retarded elasticity and flow.

The stress-strain relationships at a definite area were as follows: Under a sufficiently small stress, the instantaneous elastic response with the retarded one alone was observed, and the deformation was recoverable when the stress was removed (curves 1 and 2 in Fig. 3). When the stress was over a certain value, however, the flow being preceded by the above stated elastic deformation, occurred (curves 3 and 4 in Fig. 3). The further increase in the shearing stress, when it exceeded a certain value (breaking strength) made the film one of simple flow, without the instantaneous elasticity (curves 5 and 6 in Fig. 3). From these facts it becomes clear that the structure of the film was broken down under too large a

⁴ It is a pleasure to thank Dr. T. Shimanouchi and Takeda Pharmaceutical Industries Ltd. for a gift of horse serum albumin; Dr. S. Nagakura for a gift of horse hemoglobin; Dr. H. Tani for a gift of polynorleucine and poly- γ -methyl L-glutamate; and Toyo Rayon Co. for a gift of poly- ϵ -aminocaproic acid.

stress. Once the film was broken, the repair of the film structure was found to take appreciable time. In other words, the ovalbumin film shows a "thixotropic" behavior.

In the ω - t curves (curves 1-4 in Fig. 3), the magnitude of the first recovery of the deformation on the removal of the stress is nearly the same as that of the first deformation. A mechanical model representing such rheological behaviors may be made of a four-parameter model (inset

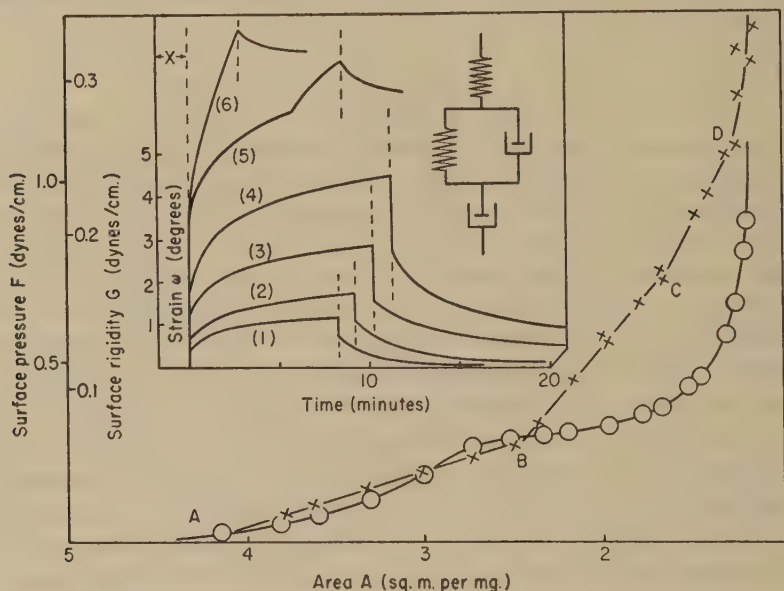


FIG. 3. Rigidity-area curve (crosses) and force-area curve (circles) for ovalbumin film on 0.1 *N* hydrochloric acid, temperature 21°C. Inset shows the strain-time curves under varying shearing stress and the illustration of the corresponding mechanical model. Shearing stress: Curve (1) 2.6×10^{-4} dynes/cm.; Curve (2) 3.4×10^{-4} dynes/cm.; Curve (3) 5.7×10^{-4} dynes/cm.; Curve (4) 8.8×10^{-4} dynes/cm.; Curve (5) 2.3×10^{-3} dynes/cm.; Curve (6) 2.3×10^{-3} dynes/cm., observed 5 min. after the measurement of curve (5). The region of the left side of the dotted lines represents the time in which the stress is imposed, and the right side, the time after the stress is removed. The region of (X) is the dead time.

of Fig. 3), but under sufficiently small stress, it lacks the dashpot corresponding to the flow. Under the shearing stress below breaking strength, the dependence of the magnitude of instantaneous elastic response upon that of the stress was observed. In this case, the relation between the instantaneous elastic deformation and the stress was found to be linear covering almost the whole range of film concentrations. In other words, the instantaneous elasticity of ovalbumin film obeyed

Hooke's law. Under such condition the shear modulus of the instantaneous elasticity G was calculated by formula [1].

A typical example of the shear modulus-area curves (designated as the G - A curves hereafter) is given in Fig. 3. It was found that an instantaneous elastic deformation occurred at the areas above 5 sq. m./mg. Namely, the G - A curve starts at 5 sq. m./mg. (point A), and exhibits breaks in the slope at 2.3 sq. m./mg. (point B), 1.7 sq. m./mg. (point C), and 1.3 sq. m./mg. (point D), respectively. According to the several determinations of the G - A curve under the same conditions, the observed values of G at respective areas were more or less scattered, but breaks were always found and the values of their corresponding areas were progressively more reproducible in the order of A , B , C , and D . These breaks may denote higher-order transformation points of film phase which are hardly capable of being detected by the examination of F - A curves. The F - A curve (circles in Fig. 3) has a break at a certain area which lies in the B - C range of the G - A curve. It is noteworthy that although the pressure is kept nearly constant by compression in this range, shear modulus continues to increase with the decrease of surface area.

Some experiments were carried out to investigate the nature of the observed instantaneous elasticity. It was found that the instantaneous elasticity of ovalbumin film disappears entirely above a certain temperature. Such a transition temperature of film states was around 20°C., and the observed fluctuation was $\pm 3^\circ\text{C}$.

When the spreading solution of ovalbumin containing 10% formaldehyde was used, it was found that the film spread on 5% ammonium sulfate solution, at any temperature, exhibits only simple retarded elastic response without instantaneous elastic deformation. Although the reactions between formaldehyde and protein are complicated, in view of the amino or imino radicals of protein molecules taking a major part in this reaction, it seems probable that these radicals are responsible for the instantaneous elasticity of the film. This elasticity was also affected by the various conditions of the substrate solution. For instance, when spread on 5% ammonium sulfate solution of pH 5.6, ovalbumin films showed the elasticity already at the areas above 15 sq. m./mg., about three times as much area as on 0.1 N hydrochloric acid. This implies that the protein gives a more expanded film on concentrated salt solution than on acid solution.

(b) *Horse Serum Albumin*.—This protein was spread under the same condition as in the case of ovalbumin. It was found that, unlike ovalbumin, horse serum albumin film did not exhibit any perceptible resistance against the rotation of the ring until the film was compressed to considerably small surface areas on 0.1 N hydrochloric acid and at temperatures from 5 to 23°C. Below 1.0 sq. m./mg., however, the film showed appre-

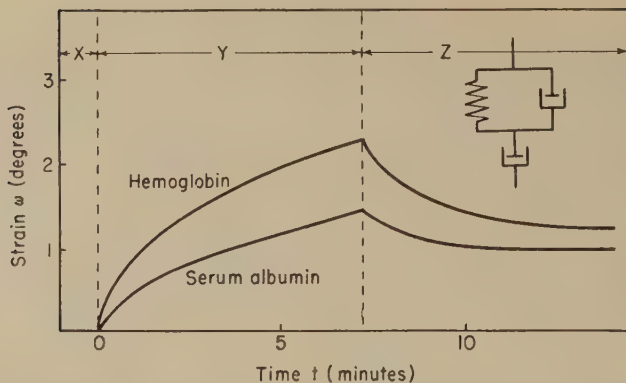


FIG. 4. Strain-time curves for horse serum albumin and horse hemoglobin on 0.1 *N* hydrochloric acid, surface area 0.78 sq. m./mg., surface pressure, 7.8 dynes/cm. (*X*) represents the dead time, (*Y*) the time in which the stress is imposed, and (*Z*) the time after the stress is removed.

ciable viscosity whose values increased gradually with the decrease of area, showing Newtonian behavior. Below 0.8 sq. m./mg., the simple viscous behavior of the film was accompanied by retarded elasticity,

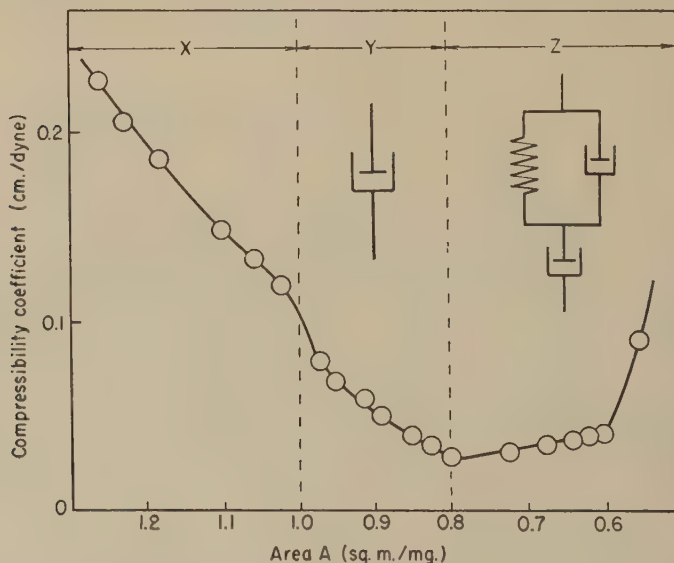


FIG. 5. Compressibility-area curve for serum albumin on 0.1 *N* hydrochloric acid together with the illustration of the mechanical models corresponding to the film states. (*X*) represents the region where the film does not exhibit any perceptible resistance against the rotation of the ring, and (*Y*) the region where the film behaves as simple flow accompanied by the retarded elasticity.

showing no sign of instantaneous elasticity. When the stress was removed thereafter, it resulted in a slight recovery of the strain (Fig. 4). These rheological behaviors were referred to the compressibility⁵ area relation obtained from the F - A curve. Figure 5 shows the compressibility-area curve together with the illustrations of rheological behavior. It is found, from this figure, that the minimum point of the compressibility curve just corresponds to the largest area which the film under shear stress exhibits in the viscous flow accompanied by the retarded elasticity, and the kink point of the compressibility curve at an area of about 1.0 sq. m./

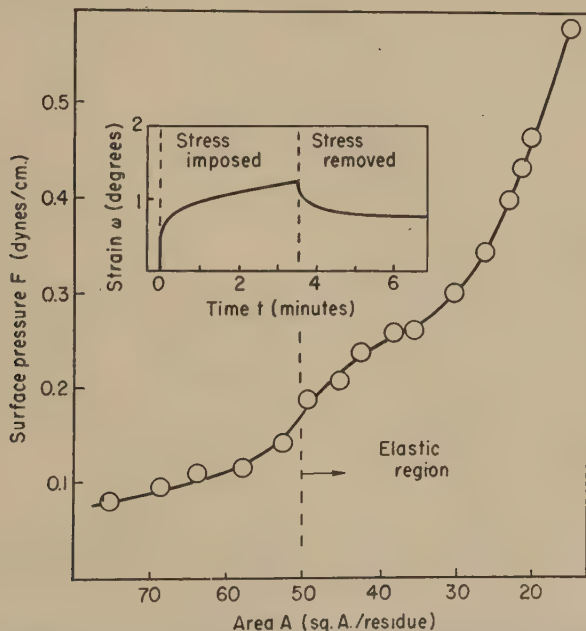


FIG. 6. Force-area curve of poly-DL- α -aminocaproic acid on distilled water. The vertical broken line represents the area where the film starts to exhibit the elasticity (non-Hookean). Inset gives the strain-time curve.

mg. corresponds to the largest area where the ring caught appreciable viscosity of the surface film. The F - A curve did not show any break covering the surface areas involving low pressure region.

(c) *Horse Hemoglobin*.—The sample was spread on 0.1 N hydrochloric acid solution at 14°C. The rheological behavior was nearly similar to that of serum albumin, and likewise it showed no elasticity at larger areas,

⁵ The coefficient of compressibility of the spread film is defined by $(1/A)dA/dF$, where F is the surface pressure expressed in dynes/cm. and A is the surface area in square meters/mg.

while below about 0.9 sq. m./mg., the retarded elasticity appeared, accompanied by viscous flow. At such an area, an example of the ω - t curve together with the corresponding mechanical model is shown in Fig. 4. The correlation of rheological behavior with compressibility of the film was similar to the case with serum albumin and, likewise, no break was observed in the F - A curve.

2. Synthetic Polypeptides

(a) *Polynorleucine*.—Norleucine polymer was spread from its benzene solution on distilled water at 22°C. The F - A curve (Fig. 6) shows that a break appears at the area of about 40 sq. A. per residue. Although

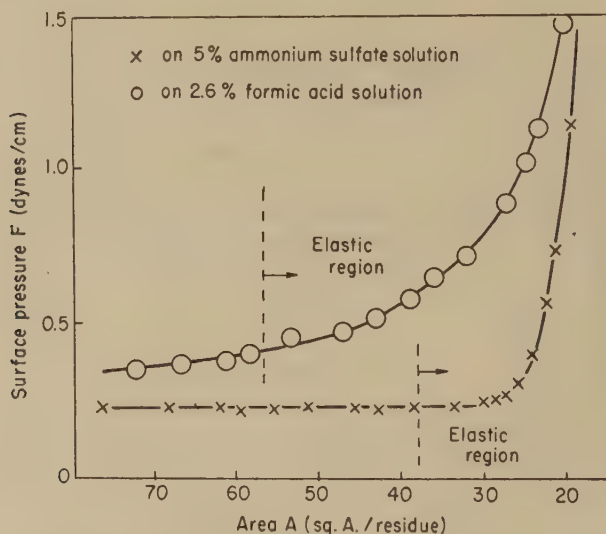


Fig. 7. Force-area curve for poly- γ -methyl L-glutamate. Crosses show the case with 5% ammonium sulfate solution; circles with 2.6% formic acid solution; temperature 29°C. The vertical broken lines represent the area at which the films start to exhibit the elasticity (non-Hookean).

the mechanical behaviors were generally uncertain in the low-pressure region, the instantaneous elastic deformation was clearly observed at the areas above 50 sq. A. per residue. The ω t curve (inset of Fig. 6) gave the incomplete recovery of the instantaneous elasticity on the removal of the stress. Moreover, it was found that the stress-strain relationships deviate from linearity, i.e., this observed elasticity was non-Hookean.

(b) *Poly- γ -methyl L-Glutamate*. This polymer was spread from its pyridine solution. As shown in Fig. 7, it formed a more expanded film when spread on 2.6% formic acid solution than on 5% ammonium sulfate

solution. Instantaneous elastic deformation appeared at smaller areas on ammonium sulfate solution than on formic acid. The deformation, however, was non-Hookean as was the case with polynorleucine.

(c) *Poly- ϵ -aminocaproic Acid*.—This polymer (viscosity-average molecular weight 15,500) was spread from a mixed solution of benzene-phenol (7:3) on distilled water at 31°C. The ω - t curve (the inset of Fig. 8) indicates that this polymer behaves as a simple elastic system showing only instantaneous elastic deformation, without any accompanying flow. The elasticity appeared at the areas below 80 sq. A. per residue, while the Hookean behavior disappeared at the area where the plateau of the F - A curve starts (Fig. 8).

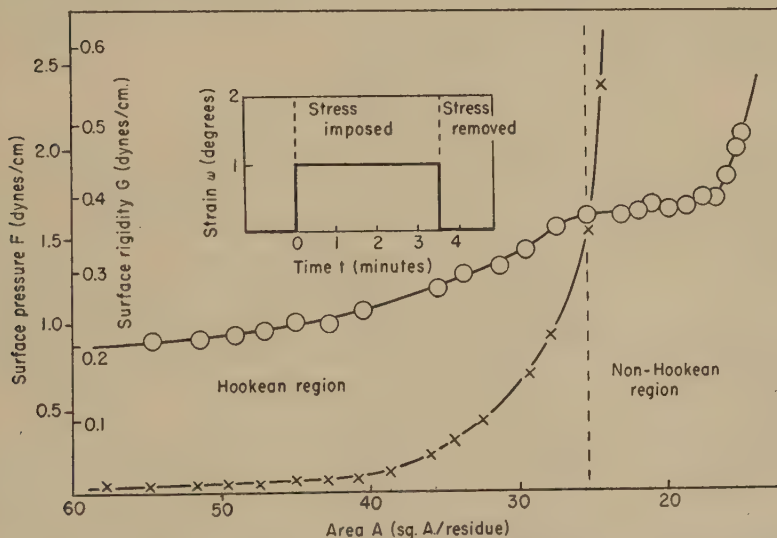


Fig. 8. Rigidity-area curve (crosses) and force-area curve (circles) of poly- ϵ -aminocaproic acid on distilled water, temperature 31°C. The vertical broken line represents the area where the elastic behavior of the film changes from the Hookean to the non-Hookean by compression. Inset gives strain-time curve.

DISCUSSION

It was generally believed that protein films become solid and elastic at areas smaller than about 1 sq. m./mg. (12). The present investigation, however, revealed that ovalbumin film exhibits distinct instantaneous elasticity even at a large area such as 5 sq. m./mg. From such a rather unexpected result, it was thought possible that ovalbumin film was spread only partially on the surface of the substrate. Therefore, the following experiment was undertaken. After the spreading of the ovalbumin film at an area about 5 sq. m./mg., talc powder was dusted on the film and thereafter the barrier enclosing the film was moved. It was, then,

observed that the talc particles, even though they are at a distance from the place where ovalbumin was spread, move with the barrier. This observation confirms that in our spreading condition ovalbumin was spread on the whole surface of the substrate solution.

From the viewpoint of structural theory, the occurrence of the instantaneous elasticity is to be attributed to the existence of intermolecular bondings. The conclusion could, therefore, be drawn that even at a large area such as 5 sq. m./mg., ovalbumin molecules are linked together with each other, making a two-dimensional network covering the whole area of spread film. According to the data of Bull (2), the area of ovalbumin film available in the close-packing state of molecules is not over 2 sq. m./mg. under the best spreading condition. Our experimental result, therefore shows that ovalbumin film forms a two-dimensional network before its spread molecules are closely packed.

TABLE I
Critical Area for Film Elasticity

Materials	Substrate	Critical areas		Areas ^a per residue of polypeptide backbone A_r sq. A.	A_c/A_r
		sq. m./mg.	A_c sq. A./residue		
Ovalbumin ^a	0.1 N HCl	5	95	15.7	6.0
	5% (NH ₄) ₂ SO ₄	15	285	15.7	18.2
Poly-DL- α -amino-caproic acid ^a	Distilled water	2.6	50	15.7	3.2
Poly- γ -methyl L-glutamate ^a	2.6% HCOOH	2.4	56	15.7	3.6
Poly- ϵ -amino-caproic acid ^a	Distilled water	4.7	80	41.8	1.9
Serum albumin ^b (horse)	0.1 N HCl	0.82	15.6	15.7	0.99
Hemoglobin ^b (horse)	0.1 N HCl	0.85	16.2	15.7	1.03

^a A_c values show the critical areas for the instantaneous elasticity.

^b A_c values show the critical areas for the retarded elasticity.

^c A_r values were calculated from the assumption that the side chains are oriented normal to the surface of water.

On the other hand, with serum albumin it is to be noted that the film did not manifest any elastic behavior until it was compressed down to the area about 0.8 sq. m./mg., and that this critical area is just consistent with the area of minimum point of film compressibility. It is commonly said that when the compressed protein film exists in a close-packed state of molecules whose side chains are oriented vertically to the surface, the compressibility-area curve exhibits a minimum point (12). With serum albumin, therefore, it is considered that the closest packing state of film

molecules gives the film viscoelasticity and that the looser packing of them no longer brings any elastic behavior. This shows that the interaction between the film molecules is very weak. Moreover, our experiment with serum albumin shows that no perceptible viscosity of the film was observed until it was compressed to an area of about 1 sq. m./mg. The case is similar with hemoglobin. These facts strongly suggest that the film molecules of serum albumin and hemoglobin have compact form in the uncompressed film state as well as in the compressed one.

In Table I, the critical areas where various films start to exhibit viscoelastic behavior are compared with the area per residue in the close-packing monolayers which can be calculated from x-ray data and a molecular model. From this table, it is seen that the values of the critical areas are, except for hemoglobin and serum albumin, much larger than the area for the close-packing of molecules. Synthetic polypeptides having an elongated configuration might form a two-dimensional network structure on the surface by intermolecular bonding, leading to a critical area (A_c) larger than the area (A_r) for the close-packing of the polypeptide chains. Thus it is suggested that the structure of ovalbumin films bears a resemblance to that of synthetic polypeptides films. Recently, Isemura *et al.* (6) pointed out that the F - A curve for polynorleucine resembles very closely that of ovalbumin.

Cumper and Alexander (3) showed that the area in the close-packed monolayer for polyalanine and polyphenylalanine is in good agreement with the area obtained by extrapolating the surface viscosity-area curve to zero viscosity. The oscillating-needle method for measuring the surface viscosity, which was used by them, is probably inadequate to detect the weak bondings in the films, since it is thought that the rapid oscillation of the needle within the film destroyed its loose structure. If our method be adopted, it may be that with polyphenylalanine, and polyalanine also, viscoelasticity is observed at areas larger than that for close-packed film.

It is interesting to note that poly- ϵ -aminocaproic acid monolayer behaves as a perfect elastic system until it is compressed to 25 sq. A. per residue corresponding to a pressure of 1.5 dynes/cm. and that under further compression the elasticity becomes non-Hookean. It is thus considered that at 25 sq. A. per residue, a structure of poly- ϵ -aminocaproic acid monolayer collapses. This evidence is presented by the fact that at such an area the F - A curve of poly- ϵ -aminocaproic acid monolayer exhibits a conspicuous break point, followed by a high compressibility region. Whether or not the film elasticity is Hookean depends on the strength of formation of the network. The ease of formation of the network is not only dependent upon the strength of the cohesive force between the groups participating in the bond formation, but largely upon

the degree of "fitting" of these groups. It is probable that the instantaneous elasticity in films of synthetic polypeptides arises largely from the hydrogen bonding between —CO— and —NH— groups on adjacent chains. In poly- ϵ -aminocaproic acid, —CO—NH— groups of a chain are separated by five carbon atoms, so that the chain is more flexible than that of poly- α -aminocaproic acid or poly- γ -methyl glutamate. Thus, the film molecules of poly- ϵ -aminocaproic acid could be linked together under more favorable condition for fitting than poly- α -aminocaproic acid or poly- γ -methyl glutamate. Such a condition, though not conclusive, might also be responsible for the fact that the film of the former exhibited Hookean elasticity, while the elasticity of the latter failed to exhibit Hookean behavior.

The instantaneous elasticity of ovalbumin monolayer disappears above room temperature. It results in these film molecules being linked together by very weak bonds.

From the results of the present study, it has been found that the form of the F - A curves is closely related to the rheological behavior: The films which do not exhibit distinct instantaneous elasticity, e.g., the monolayers of serum albumin, of hemoglobin, and of ovalbumin above the critical temperature, have no break point in their F - A curves. On the other hand, with those films of ovalbumin below the critical temperature and with some synthetic polypeptides which distinctly exhibit instantaneous elasticity, a break point or plateau is found in their F - A curves. This is a notable fact for the interpretation of the F - A curve of protein monolayers.

We believe that the rheological method presented here opens a new field for the study of viscoelastic films.

ACKNOWLEDGMENT

We gratefully acknowledge the encouragement of Prof. J. Sameshima.

REFERENCES

1. ALFREY, T., *Mechanical Behaviors of High Polymers*. Interscience Publishers, New York, 1948.
2. BULL, H. B., *J. Biol. Chem.* **185**, 27 (1950).
3. CUMPER, C. W. N., AND ALEXANDER, A. E., *Trans. Faraday Soc.* **46**, 235 (1950).
4. FOURT, L., *J. Phys. Chem.* **43**, 887 (1939).
5. HATSCHKE, V. E., AND JANE, R. S., *Kolloid-Z.* **39**, 300 (1926).
6. ISEMURA, T., AND HAMAGUCHI, K., *Bull. Chem. Soc. Japan* **25**, 40 (1952).
7. JOLY, M., *Surface Chemistry* [Supplement of *Research* (London)] **2**, 157 (1949).
8. KEKWICK, R. A., AND CANNON, R. K., *Biochem. J.* (London) **30**, 227 (1936).
9. KEKWICK, R. A., *Biochem. J.* (London) **32**, 552 (1938).
10. LANGMUIR, I., AND SCHAEFER, V. J., *Chem. Revs.* **24**, 181 (1939).
11. LANGMUIR, I., AND SCHAEFER, V. J., *J. Am. Chem. Soc.* **59**, 2400 (1937).
12. NEURATH, H., AND BULL, H. B., *Chem. Revs.* **23**, 391 (1938).

STUDIES ON POLYELECTROLYTES. III. POLYGLUCOSAMINE HYDROCHLORIDE

Sadhan Basu¹ and Pares Ch. Das Gupta

Indian Association for the Cultivation of Science, Calcutta 32, India

Received December 3, 1952

INTRODUCTION

It has been shown by Basu and Das Gupta (1) that the various physicochemical properties of solutions of sodium carboxymethylcellulose (SCMC) can be explained by the folding-chain theory of Fuoss (2) taking into consideration the polyelectrolyte character of the sodium salt of carboxymethylcellulose. If these properties be attributed to the coiling-uncoiling of the cellulose chain owing to variation in the charge density on the polymer chain, then it may be argued that the nature of the charge will have nothing to do with these properties, which will be governed mainly by the charge distribution on the chain. In the case of SCMC, dissociation of the salt in water leaves the chain negatively charged and the mutual repulsion between the similarly charged centers in the same chain is responsible for the peculiar physicochemical properties of the compound in solution compared to neutral polymers. It may be expected that the polyglucosamine hydrochloride which on dissociation in water leaves the chain positively charged will also behave exactly similarly with respect to its physicochemical properties in solution. With a view to testing this point a series of investigations were undertaken, exactly similar to those reported previously.

Since it is almost impossible to compare the compounds, SCMC and polyglucosamine hydrochloride (PGH) at exactly the same molecular weight, the comparison has been limited to the variation in the physicochemical properties rather than to the absolute values of these quantities. The molecular nature of the PGH solution evidently removes any complications arising from the associated colloidal systems (3).

EXPERIMENTAL

Polyglucosamine hydrochloride was prepared from chitin of carapace of *S. Paeneus* by the alkali hydrolysis method of Clark and Smith (4). The carapace was washed thoroughly with warm water and then treated with nitric acid (dilute) to remove calcium carbonate and coagulate some

¹ Present address: Dept. of Chemistry, Indiana University, Bloomington, Indiana.

of the proteinous matter. The substance was freed of acid and heated with alkali (20%) for about 7 hr. to hydrolyze the acetylamino group of chitin to acetic acid and free amino group. The product was then washed with water and dissolved in 0.1 *N* hydrochloric acid. The solution was dialyzed to free it from residual sodium salts and free chloride ions, filtered, precipitated with acetone, washed free of any hydrochloric acid with acetone, and dried at low temperature. The polyglucosamine hydrochloride thus obtained was a hydrated salt with two molecules of water of crystallization per glucosamine ring (5).

TABLE I
Viscosity of Polyglucosamine Hydrochloride Solutions

Concentration of PGH in g./100 ml. of solution (c)	η_{sp}/c
In water ($\epsilon = 78$)	
0.3120	8.1
0.2080	9.0
0.1387	10.1
0.0925	11.4
0.0619	12.6
0.0309	15.3
0.0155	17.8
0.0077	19.9
In dioxane-water 1:4 ($\epsilon = 62.8$)	
0.1248	9.1
0.0832	10.1
0.0416	12.2
0.0208	13.9
0.0104	15.3
In dioxane-water 1:2 ($\epsilon = 52.7$)	
0.1248	8.0
0.0832	8.9
0.0416	10.4
0.0208	11.7
0.0104	12.7

The equivalent weight of PGH by titration was 220.4 and the nitrogen was 5.76% (Kjeldahl), somewhat lower than the theoretical amount (7.09) on the basis of one amino group per glucosidic ring.

The viscosity measurements were done with an Ostwald viscometer having a flow time of 230 sec. with water at $35 \pm 0.01^\circ\text{C}$. The relative and specific viscosities were calculated from the usual equations (1).

Conductances, measured at $35 \pm 0.01^\circ\text{C}$., on a direct-reading, bridge-type Philoscopic unit, were taken at a cell voltage of 2 v. and at a frequency of 1000 cycles/sec. The conductivity cell was a Kohlrausch-type,

parallel-plate, fixed-electrode cell having a cell constant of 0.6723, checked against 0.01 *N* potassium chloride solution. The conductance of water used in preparing all solutions were 2.2×10^{-6} mho.

RESULTS

The results of viscosity measurements on solutions of PGH at different concentrations in water and dioxane-water mixtures are summarized in Table I and the corresponding η_{sp}/c versus *c* curves are given in Fig. 1 (ϵ represents the dielectric constant of the solvent).

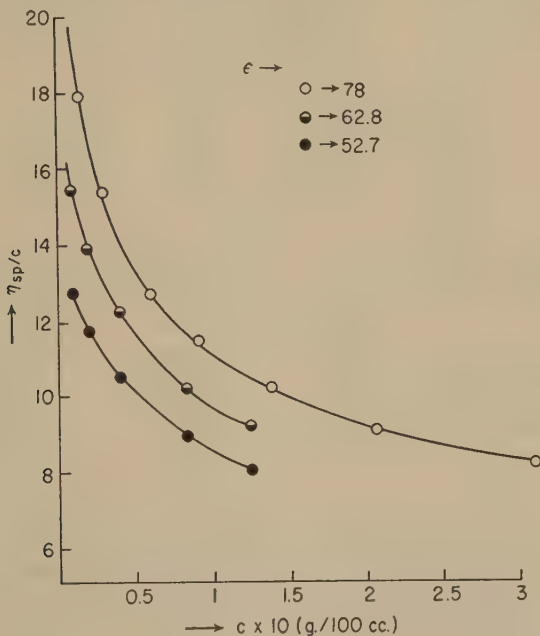


Fig. 1. Change of reduced viscosity of polyglucosamine hydrochloride.

The relative viscosities of PGH solutions were measured at constant solute concentration with increasing and diminishing pH's. The PGH solution (0.162%) had a pH of 4.1. In one experiment the pH of the solution was lowered to pH 1.6 by the stepwise addition of hydrochloric acid, the viscosity being measured at each step. The solution at this pH was divided into two parts: the pH of one was increased step by step by dialysis and of the other by the addition of sodium hydroxide solution, viscosities being measured similarly. In another experiment the pH of the original solution was increased by the addition of sodium hydroxide solution to pH 6.6 and again lowered to its original value with hydrochloric acid, measuring the viscosity in the course. The results are sum-

marized in Table II and the corresponding η/η_0 versus pH curves are given in Fig. 2.

The viscosity measurements were extended to solutions of PGH containing different amount of sodium chloride, sodium bromide, potassium chloride, sodium sulfate and calcium chloride for which the η_{sp}/c versus c curves are given in Figs. 3 and 4. It is evident from these figures that the

TABLE II
Change in Relative Viscosity of PGH Solution with pH

pH diminishing by the addition of HCl		pH increasing by dialysis		pH increasing by the addition of NaOH	
pH	η/η_0	pH	η/η_0	pH	η/η_0
		(In acid region)			
4.10	2.62				
3.55	2.52	1.60	1.48	1.60	1.48
3.05	2.25	1.90	1.58	2.50	1.47
2.58	1.93	2.55	1.92	4.00	1.46
2.15	1.67	3.20	2.37		
1.80	1.53				
1.60	1.48				
pH increasing by the addition of NaOH		pH diminishing by the addition of HCl			
pH	η/η_0	pH	η/η_0		
		(In the alkaline region)			
4.10	2.62	6.60	1.38		
4.80	2.55	6.30	1.39		
5.70	2.00	5.72	1.81		
6.60	1.38	5.23	1.89		
		4.83	1.84		
		4.32	1.92		

maxima in the curves occur at concentrations (all expressed in 10^{-4} g. equiv./l.) 10.89, 27.78, and 48.10 units of PGH with 5.1, 9.28, and 18.56 units of NaCl, respectively. With 7.51 units of KCl the maximum is at 19.05 units of PGH, with 2.91 units of Na_2SO_4 at 21.8 units of PGH, and with 2.5 units of CaCl_2 at 13.6 units of PGH.

The results of conductivity measurements are plotted as graphs of $\Lambda - \sqrt{c}$ in Fig. 5 for the cases of PGH in water and dioxane-water mixtures.

DISCUSSION

It will be evident from Table I and Fig. 1 that the reduced viscosity-concentration relationship in water and water-dioxane mixtures is exactly similar to those of other polyelectrolytes (1,6-9), which can be explained almost uniquely in all cases by the folding-chain theory of Fuoss (2).

The general nature of the pH-viscosity relationship of PGH is also similar to that of SCMC (1). Thus from Table II and Fig. 2 it is evident that the viscosity of a solution of PGH decreases rapidly as the pH of the solution is diminished by the addition of HCl. On bringing the pH back

to its original value with NaOH solution the viscosity did not increase back to its initial value. When, however, the pH is retraced by dialysis, the original viscosity of PGH is regained. If Na ions from added NaOH be held responsible for the lowering of the viscosity of SCMC solution, it is the Cl ion from the added HCl that is responsible for lowering the viscosity of PGH solution by suppressing the dissociation of the hydrochloride. Increasing the pH by neutralizing the excess HCl by NaOH has

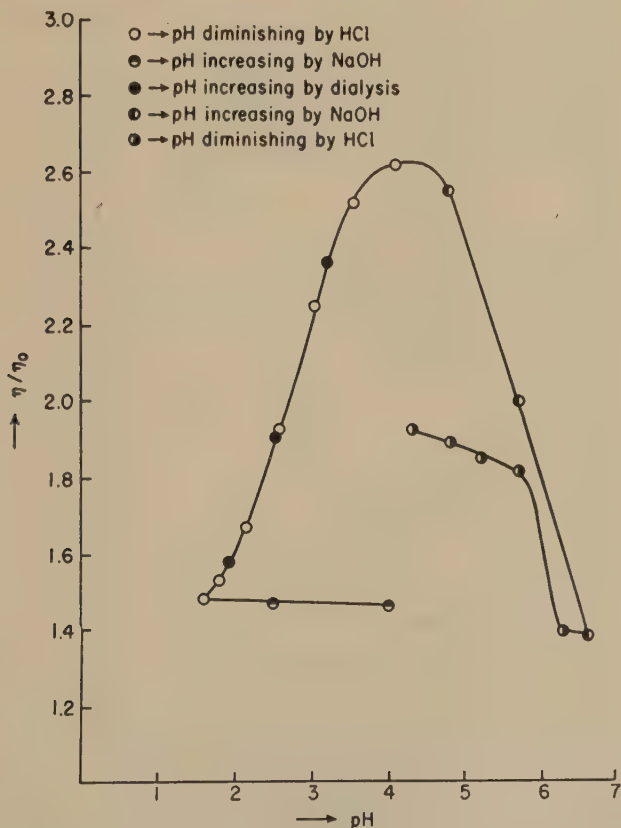


FIG. 2. Effect of pH on the viscosity of a polyglucosamine hydrochloride solution.

no effect on the viscosity of the solution, since the concentration of chloride ion stays the same (as NaCl after partial neutralization). When the pH is increased by dialysis the viscosity increases again since the removal of Cl ion out of the solution causes a better dissociation of the PGH with the subsequent uncoiling of the polymer chain.

When to a PGH solution (pH 4.1) NaOH is gradually added to raise the pH, the viscosity curve (Fig. 4) also shows a similar fall. This is due to

conversion of PGH to polyglucosamine, which remains undissociated and is precipitated if the pH is increased beyond 6.6. When the polyglucosamine thus formed is converted into PGH by lowering the pH again by the addition of HCl, the viscosity of the solution again increases, but it fails to regain its initial value completely. By the addition of HCl the PGH formed increases the viscosity owing to better dissociation of PGH

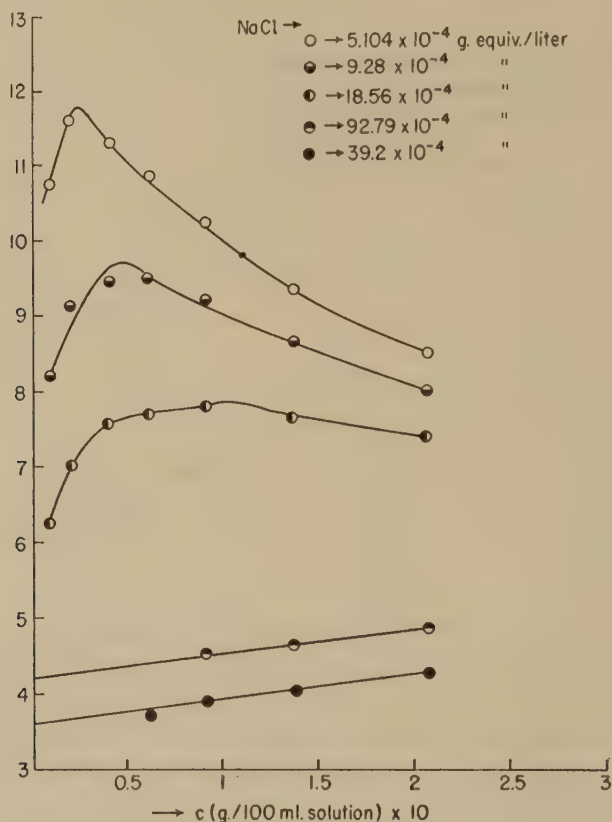


FIG. 3. Viscosity of a polyglucosamine hydrochloride solution in the presence of sodium chloride.

and the subsequent uncoiling of the chain. At the same time, however, the conversion of NaOH to NaCl introduces some amount of free chloride ions in the solution which tend to suppress the dissociation of PGH; as a result the viscosity fails to regain its original value.

The reduced viscosity (η_{sp}/c) of PGH is considerably lowered by the addition of neutral electrolytes, and the η_{sp}/c versus c curves (Figs. 3 and 4) pass through a maximum for small concentrations of added electro-

lytes. On increasing the concentration of added electrolyte, the maximum shifts toward the higher concentration of PGH, and when the concentration of the added electrolyte becomes sufficiently high to keep almost all the polymer molecules in the solution more or less undissociated, the PGH molecule behaves as a neutral polymer and the η_{sp}/c versus c curves are linear. This behavior is exactly similar to that of other polyelectrolytes, especially SCMC, and the explanation put forward in our previous

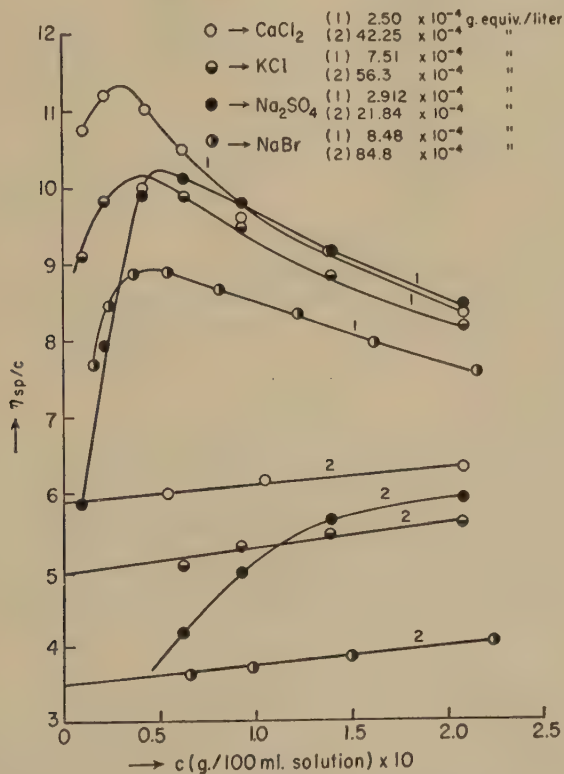


FIG. 4. Viscosity of a polyglucosamine hydrochloride solution in the presence of NaBr, KCl, Na₂SO₄, and CaCl₂.

communication holds in this case as well, with the exception that in the case of SCMC it is the cation that is active whereas in the present case it is the anion. Further, in the case of SCMC it was observed that the maximum in the η_{sp}/c versus c curve occurred at about equal ionic strength, whereas in the present case the maximum occurs at a much lower concentration of added electrolyte. This is due, in all probability, to partial hydrolysis of PGH producing free hydrochloric acid which acts together with the added electrolytes in suppressing the dissociation of

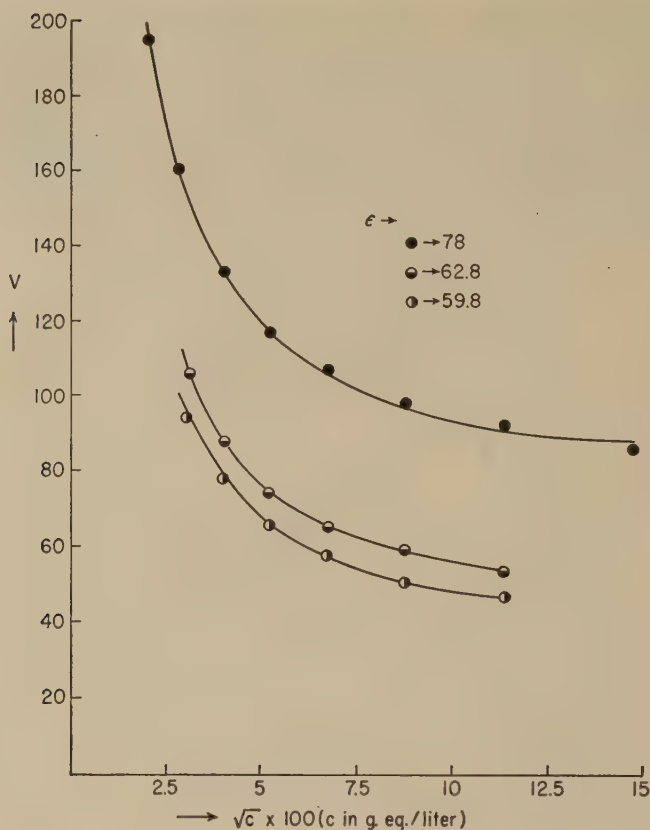


FIG. 5. Conductivity of a polyglucosamine hydrochloride solution.

TABLE III
Conductivity of PGH and NaCl Mixtures in Water^a

Concentration of PGH in g./100 ml. of soln.	$\rho_1 \times 10^4$	$\rho_1 + \rho \times 10^4$ (observed)	$\rho_1 + \rho \times 10^4$ (calculated)	Per cent lowering
Concentration of NaCl soln.: 0.011%				
Specific conductance (ρ): 2.651×10^{-4}				
0.2880	12.030	14.160	14.681	3.55
0.1728	7.649	9.906	10.300	3.86
0.1037	5.034	7.281	7.685	5.26
0.0622	3.301	5.633	5.952	5.36
0.0373	2.254	4.592	4.905	6.38

^a ρ_1 and ρ indicate the specific conductivities of PGH and NaCl solutions, respectively.

PGH; as a result, the maximum occurs at a lower concentration than it would have in the case of no hydrolysis.

The conductivity of PGH, unlike strong electrolytes or colloidal electrolytes but similar to polyelectrolytes (e.g. SCMC), increases with dilution at first slowly and then rapidly, and the $\Lambda-\sqrt{c}$ curves (Fig. 5) are concave upward at low concentration with no obvious tendency to approach a limiting value. The explanation put forward in our previous work also holds in this case. The fact that the dissociation of polyelectrolyte in the presence of a neutral electrolyte is suppressed is evident from the results of conductivity measurements in the presence of added electrolytes. (See Table III.)

It is evident that the sum of the conductances of polyelectrolyte and the neutral electrolyte is greater than that of their mixtures, and their difference increases with a decrease in the polyelectrolyte to neutral electrolyte ratio.

ACKNOWLEDGMENTS

Thanks are due to the Council of Scientific and Industrial Research, Government of India, for financial assistance to one of the authors (P.D.G.) and to Dr. S. R. Palit, Indian Association for the Cultivation of Science, for his keen interest.

SUMMARY

The viscosity, conductivity, and the effect of pH and other neutral electrolytes on the physicochemical properties of polyglucosamine hydrochloride solutions have been measured. The similarity in behavior of polyglucosamine hydrochloride to those of other similarly constituted substances in which the polymer ion is oppositely charged, has been shown. All these properties can be explained by the folding-chain theory of Fuoss.

REFERENCES

1. BASU, S., AND DAS GUPTA, P. C., *J. Colloid Sci.* **7**, 53 (1952).
2. FUOSS, R. M., *Science* **108**, 545 (1948).
3. TACHIBANA, T., AND NOKAGAWA, T., *J. Japan, Chemistry* **1**, 31 (1947).
4. CLARK, G. L., AND SMITH, A. E., *J. Phys. Chem.* **40**, 863 (1936).
5. MEYER, K. H., AND WEHRLI, H., *Helv. Chim. Acta* **20**, 353 (1937).
6. FUOSS, R. M., AND CATHERS, G. T., *J. Polymer Sci.* **2**, 12 (1947); *ibid.* **4**, 96, 121, 457 (1949).
7. PALS, D. T. F., AND HERMANS, J. J., *J. Polymer Sci.* **3**, 898 (1948).
8. HEIDELBERGER, M., AND KENDALL, F. E., *J. Biol. Chem.* **95**, 127 (1932).
9. GOLDACRE, R. J., AND LOCH, I. J., *Nature* **166**, 736 (1951).

THE PRODUCTION OF MONODISPERSE AEROSOLS OF LARGE DROP SIZE

J. H. Burgoyne and L. Cohen

*Department of Chemical Engineering and Applied Chemistry, Imperial College,
London, S.W. 7, England*

Received December 2, 1952

The Sinclair-La Mer aerosol generator (1) is well known for the production of monodisperse aerosols with a droplet diameter less than $2\ \mu$, but appears to have had little application to larger droplet sizes. La Mer and Hochberg (2) produced monodisperse aerosols of sizes up to $20\ \mu$ diameter, but this seems to be the largest value recorded in the literature. The apparatus has, however, proved to be capable of giving aerosols of tetralin up to $55\ \mu$ diameter at high concentrations without departing unduly from monodispersity.

The apparatus used is exactly the same as that described by La Mer and Hochberg (2) with the outlet "chimney" pointing downward. The

TABLE I

Summary of Results^a

Vapor pressure of tetralin at boiler temperature: $110^{\circ}\text{C}.$; 35 mm. Hg

Reference letter, Figs. 1 and 2	Gas flow over liquid and source l./min.	Mass concentration of mist mg./l.	Numerical concentration of mist drops/cc.	Mean droplet diameter, \bar{d} μ	Standard deviation, σ μ	σ/\bar{d}
(a)	1.31	0.7	8.5	53.8	2.69	0.050
(b)	0.92	30.7	942	39.6	7.27	0.184
(c)	1.44	42.5	1.94×10^4	16.1	2.15	0.134
(d)	0.99	69.3	1.37×10^4	21.3	3.44	0.161

^a Gas flow through liquid (l./min.): (a) and (c), 0; (b) and (d), 2.01. Current through nucleus source (amp.): (a) and (b), 1.00; (c) and (d), 2.00.

gas which bubbles through the liquid does so through a sintered-glass disk. The other gas stream which passes over the surface of the liquid first passes over the nucleus source, which is a plug of sodium chloride contained in a coil of wire made from a 3-in. length of 0.0076 in. diameter nichrome wire.

To measure the drop size, a sample of the aerosol was collected on a microscope slide coated with magnesium oxide (3). The actual measure-

ments were done from a photograph of part of the slide, taken by transmitted light. For the purposes concerned with the use of the aerosol, the generator fed into a glass tube 5 ft. long and 2 in. in diameter, and this was used in measuring the mass concentration. The tube was suddenly disconnected from the generator, and the mist contained in it was extracted on to a filter. This gave the weight of mist contained in the known volume of the tube and hence the mass concentration.

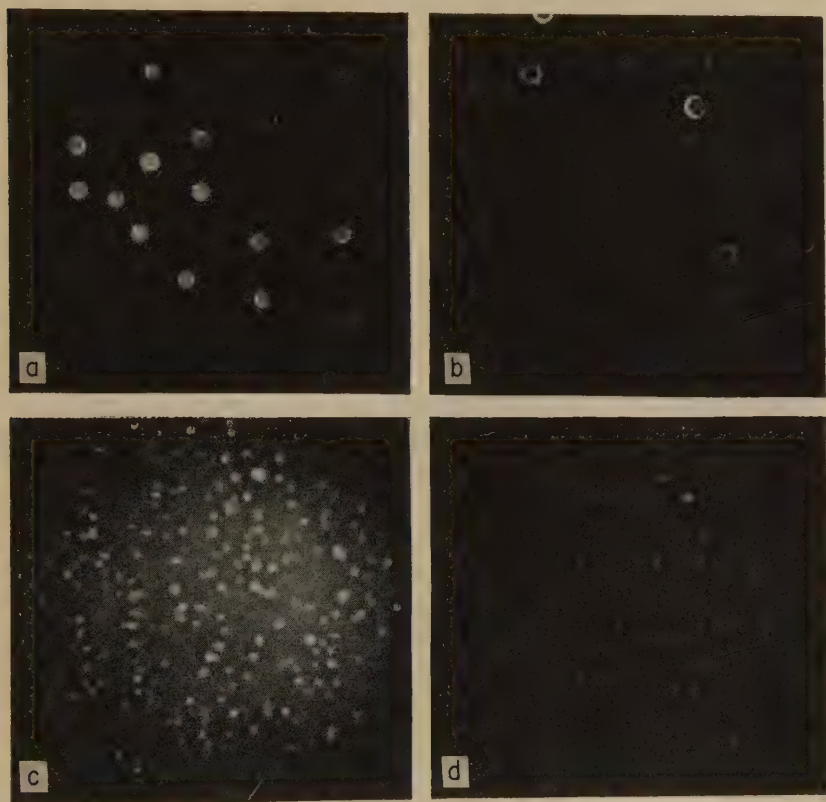


FIG. 1. (a), (b), (c), and (d): Photomicrographs of aerosol samples.

The results of four typical runs with the apparatus are summarized in Table I and illustrated in Figs. 1 and 2. With the present arrangement of the apparatus the highest drop size obtainable is $55\ \mu$ diameter and the lowest $7\ \mu$ diameter; the highest mass concentration measured was 108 mg./l. at a drop size of $13\ \mu$ diameter. These limits could probably be extended by modification to the apparatus.

ACKNOWLEDGMENT

The generator is being used in connection with work sponsored by the British Shipbuilding Research Association, and this note is published with their permission.

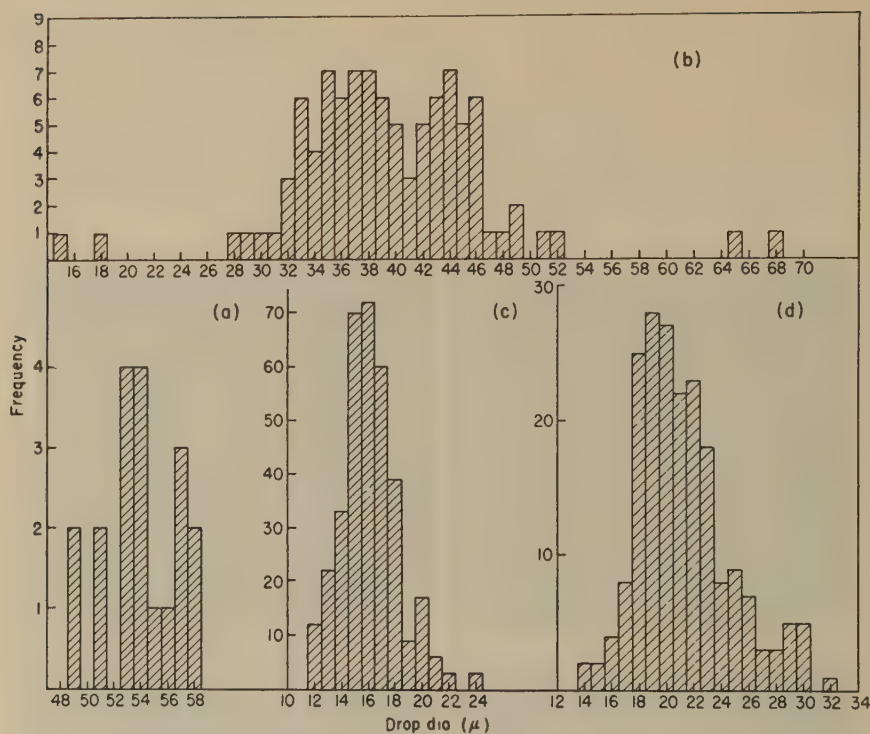


FIG. 2. (a), (b), (c), and (d): Histograms of drop-size distribution.

REFERENCES

1. SINCLAIR, D., AND LA MER, V. K., *Chem. Revs.* **44**, 245 (1949).
2. LA MER, V. K., AND HOCHBERG, S., *Chem. Revs.* **44**, 341 (1949).
3. MAY, K. R., *J. Sci. Instruments* **27**, 128 (1950).

THE FLOW OF EMULSIONS. II

E. G. Richardson

King's College, Newcastle-on-Tyne, England

Received December 8, 1952

INTRODUCTION

In 1950 there was published in this Journal a paper under a similar title (hereinafter referred to as I) in which the author described experiments on emulsions, mainly concerning the formation of emulsions by the injection process, and the variation of their viscosity with concentration and rate of shear (1). The present paper deals firstly with the effect of globule size on the viscosity of emulsions, a few preliminary measurements on the latter effect having been reported at the end of I. There are also described herein some experiments aimed at illustrating the mechanism of the flow of concentrated emulsions.

RESULTS OF VISCOSITY MEASUREMENTS

It has been usual in the past to employ Ostwald or Couette viscometers on emulsions. These have the disadvantage when used on concentrated emulsions that the continuous shearing action over the comparatively long time of flow required to get a reading may result in breakdown of some of the globules. It seemed preferable in this new work to use the falling-sphere viscometer since this causes each portion of the emulsion to be sheared only for the time of passage of the solid in its vicinity. Viscometers of this type have been applied by Cohn (2) and others to viscous fluids. In the present viscometer a vertical glass tube 2.5 cm. in diameter and 30 cm. long was fitted with embracing coils at one-third and two-thirds of its depth. Passage of a steel ball-bearing through each coil was registered, and the interval of time elapsing was recorded electronically. A correction of the Ladenburg type for relative size of sphere and tube was applied to all recorded times, and the instrument was first calibrated by using in it Newtonian liquids of known viscosity.¹

It is true, as with nearly all viscometers, that one gets with such an apparatus an "apparent" coefficient of viscosity pertinent to the average rate of shear which the system suffers during the passage of the sphere, but it is also evident that this average rate of shear increases with the diameter and terminal velocity of the solid sphere.

¹ The viscometer was designed and calibrated by Dr. Azmy Iskander.

Steel ball-bearings of diameter 1.55, 4.73, 6.73, and 8.75 mm. were used. Their terminal velocities in the fluids used were insufficient to cause eddying motion.

Careful control had to be kept on the temperature during a series of measurements which might last several minutes. The experimental tube was therefore enclosed in a water bath. It was confirmed that the electric currents in the detectors were too weak to cause heating of the liquid or glass, considered as dielectrics.

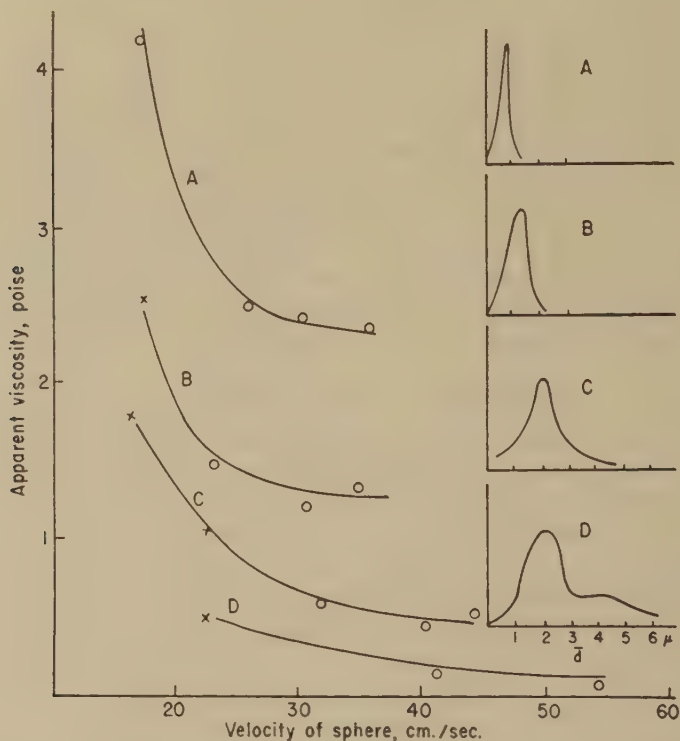


FIG. 1. Apparent viscosities at different rates of shear of emulsions whose size distribution curves are shown as insets.

The emulsions once prepared were placed in the viscometer, and the times of fall of the spheres were determined. After correction for wall effects, these gave the apparent viscosities in terms of values from the calibration curves for homogeneous, aqueous solutions of known viscosities. The mean rate of shear is taken arbitrarily as represented by the velocity of steady fall of the sphere.

While these measurements were going on, a sample of the emulsion was taken and photographed under a microscope. The photographic negative was then analyzed for particle size in another microscope using Kodak graded graticules.

Figure 1 gives typical viscosities at various mean rates of shear—shown as circles—for four 75% oil-water emulsions with the globule size distribution alongside. (Some measurements made in a smaller viscometer giving low rates of shear are shown by crosses.)

As long as the emulsions are fairly homodisperse, as are specimens *A*, *B*, and *C*, the simple relation already cited in I appears to apply, i.e., the viscosity at high rates of shear varies inversely as the mean globule size. When, however, the distribution is rather polydisperse, i.e., when there are fine drops among the large ones, as in sample *D*, the system is less viscous than would be indicated by its mean drop size on this relationship.

When one of these emulsions was prepared and "homogenized" as far as possible and its viscosity at several rates of shear measured, it could then be diluted with more of the continuous phase and the viscosity redetermined, its size distribution being checked in the meantime. At lower concentrations, the variation of viscosity with rate of shear becomes less marked and of course the over-all viscosity diminishes.

MECHANISM OF FLOW OF EMULSIONS

The actual flow of an emulsion must probably involve the slipping or squeezing of small globules through the spaces not occupied by large ones. The emulsion in shear may then be supposed to behave rather like a metal does on the dislocation theory, except that both holes and their occupants must be supposed flexible.

In order to follow up this idea an experiment was devised in which a mixture of paraffin and carbon tetrachloride having the same specific gravity as water at room temperature was allowed to form drops on the tip of a glass tube located along the axis of a wider tube (2 cm. diameter) up which water or other liquid could be made to flow at speeds up to 5 cm./sec. Tap water and water-glycerol liquids were used as conveyors which carried away from the tip equisized and equispaced globules of oil. Further up the tube was a constriction in the form either of a Venturi or of a hole in a thin coaxial metal plate. Under the conditions of the experiment—Reynolds' number 100–500—it was assumed that the resistance of an object passing through the "gate" would be proportional to the first power of the velocity. The flow through the orifice was studied in a subsidiary experiment in which a section of tube containing a number of fine orifices ranging across the diameter was substituted for the oil supply pipe, whereby filaments of color could be introduced into the main tube to mark out lines of flow. It was still possible to observe the configuration of the outer streamlines while oil drops were approaching the gate. In isokinetic flow they did not seem to be disturbed by the presence of the droplet before the constriction, though some disturbance of the flow of the continuous phase appeared to ensue, from the presence of the drop, after the "braking" of the latter.

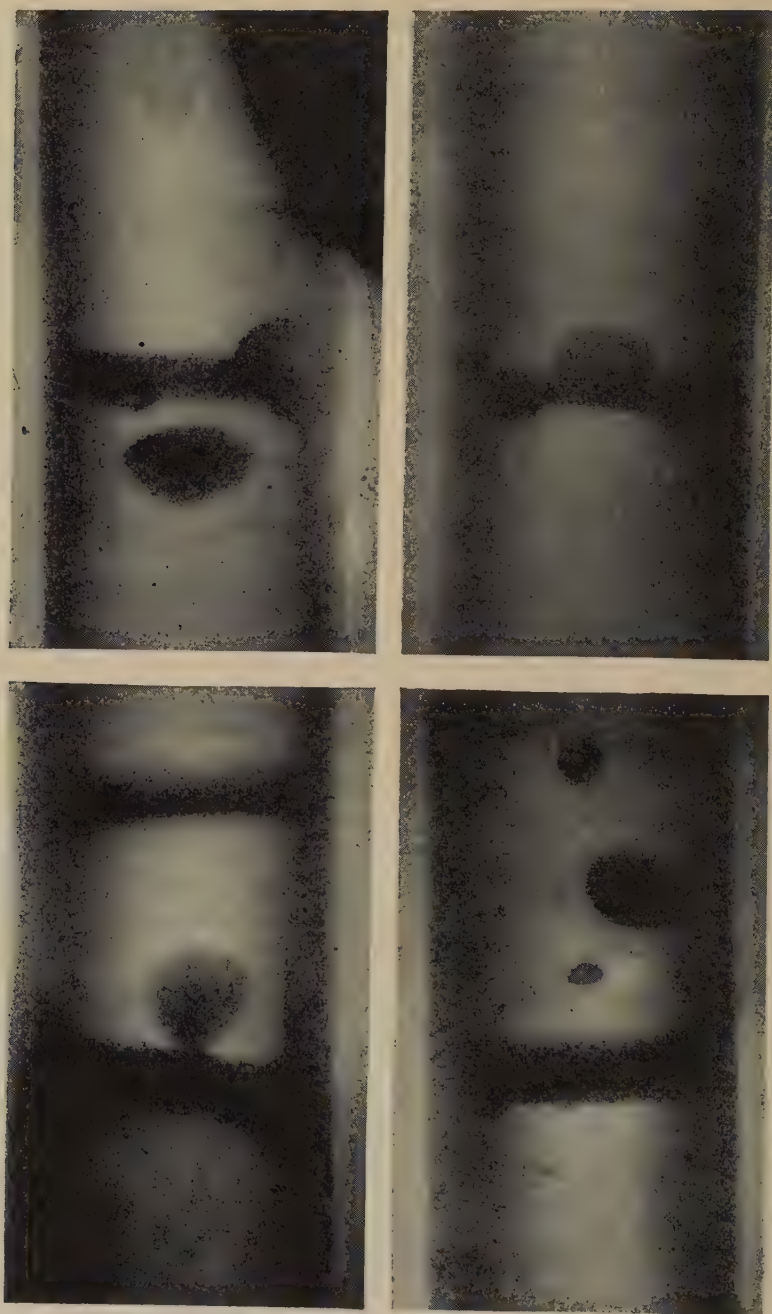


FIG. 2. Photographs of globules (about 7 mm. diameter) passing constriction of 7 mm. diameter.

By taking a cinematograph film of the motion of the globule, it was possible to deduce the velocity to time trajectory of the drop in its passage through the gate. It is also necessary to know the mean velocity of the stream from level to level and this can be calculated from the configuration of the streamlines in the tube.

Next the velocity of the drop relative to the stream is calculated from point to point in its trajectory and plotted against the displacement. On the assumption just made, the area under this curve should give the work done on the globule in forcing it through the constriction and so represent the work done against such resistance when an agglomeration of drops of this size d has to pass through a series of constrictions of size

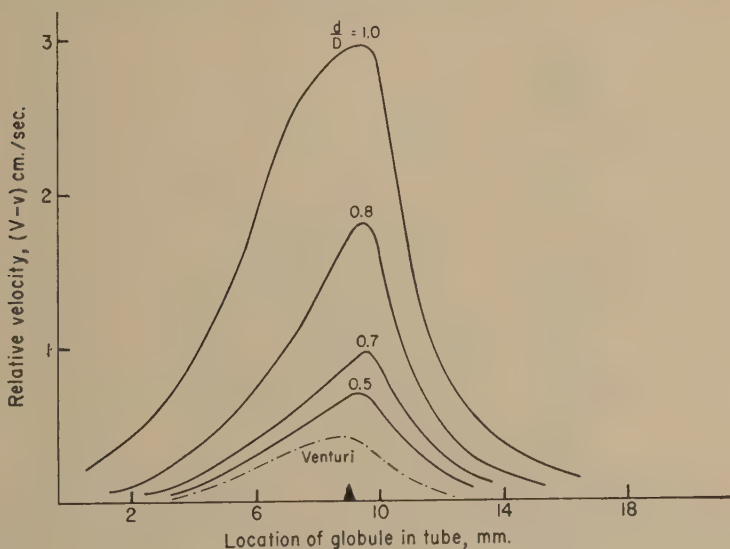


FIG. 3. Relative velocity; displacement curves of globules.
(The constriction is located at 9 mm.)

D. Thus the model is expected to give apparent viscosities typical of an emulsion undergoing such shear with $(d/D)^3$ representing the volume concentration, while the speed of the water through the constriction stands for the shear stress imposed on the drop in the gate, in a similar fashion to the stress imposed by the falling sphere in the viscometer.

It may, perhaps, be objected that this apparatus does not model a real emulsion very closely. For one thing the constrictions through which the small globules have to pass in an emulsion are themselves elastic and, as has been aptly remarked, their portals themselves are in relative motion so that a better model would have the walls of the tube of crinkled pattern, one moving up and one down. This would be too difficult to work. Our model, though perhaps oversimplified, was, however, based on

observation through a microscope of the motion of a small sample of an oil-in-water emulsion placed on a glass slide ever so slightly tilted.

Figure 2 shows some typical "stills" from the films of the drop passing through a hole of nearly equal size, in which some characteristics of the passage can be seen; in particular, the globule becomes ovoid first with its major axis horizontal and later vertical in the "gate," sometimes breaking up as it is sheared. (The photographs are of different "shots.") This change of shape is a factor which complicates our analysis of the trajectory.

Figure 3 shows plots of relative velocity ($V - v$) against displacement for several values of d/D in passing through the coaxial hole and through

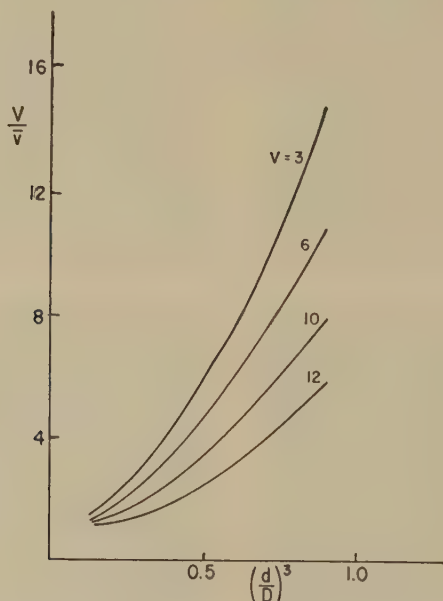


FIG. 4. Viscosity vs. concentration curves in model emulsion.

the Venturi, while Fig. 4 shows V/v —which represents the relative viscosity—plotted against $(d/D)^3$ for several (arbitrary) rates of shear, the lower points corresponding to the higher Reynolds' numbers of flow. It will be observed that the general shape of the curves corresponds to that of the variation of apparent viscosity of an emulsion with concentration (cf. Fig. 5 of I), reckoning that a value $d/D = 1$ represents a concentration of 75% for undistorted spheres of uniform size.

Figure 5 similarly shows \bar{v} against V for different d/D ratios to show how the viscosity represented by the reciprocal slope decreases as the rate of shear (represented by V) increases.

The essential difference between emulsions and solid suspensions is,

of course, that individual globules can be distorted, as the photographs in Fig. 2 show, and that some irreversible work is done during their distortion and subsequent recovery. This is shown especially in Figs. 4 and 5 by the increase in apparent viscosity when the globule is as wide as the gate. Of course, it might happen that the time of compression and relaxation of the globule as it negotiates an obstacle could be comparable with its time period of oscillation, i.e., with $\pi \sqrt{(\rho d^3/16\sigma)}$, where σ stands for the interfacial tension—though such relaxation vibrations were not

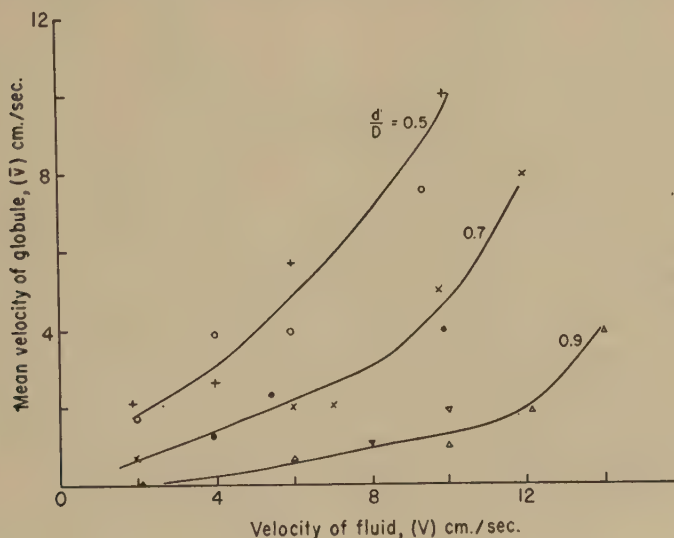


FIG. 5. Mean velocity of globule vs. velocity of fluid curves.

observed on our films and calculation showed that the times of passage through the obstructions were not short enough to excite them.

CONCLUSIONS

The conclusions to be drawn from the work described in this paper are:

1. The apparent viscosity of emulsions having the same concentration and the same size distribution about a mean globule diameter is inversely proportional to this mean diameter.

2. The observed variations of viscosity of a concentrated emulsion with concentration and rate of shear can be explained in terms of the work done in distorting the globules and sliding them past each other.

REFERENCES

1. RICHARDSON, E. G., *J. Colloid Sci.* **5**, 404 (1950).
2. COHN, *Ann. Physik* **21**, 761 (1935).

BOOK REVIEWS

Soil Physical Conditions and Plant Growth. Edited by B. T. SHAW. Academic Press Inc., New York, 1952. 491 pp. Price \$8.80.

This is Vol. II of the Agronomy Monograph Series. It constitutes a collection of articles by members of the *Joint Committee on Soil Tilth* of the American Society of Agronomy and the American Society of Agricultural Engineers. The following broad topics are treated: soil as a physical system; mechanical impedance and plant growth; soil water and plant growth; soil aeration and plant growth; and soil temperature and plant growth. The book has all the advantages and disadvantages of a collection of papers: authoritative treatment of each subject matter by highly qualified specialists, but uneven and often dry and uninspiring presentation. As Hilgard used to say about Agricultural Experiment Station Reports: "Very substantial reading, a good deal like boiled ham or dried beef—very good if you take only a little at a time."

The treatments of soil and plant aspects are largely formalistic; processes and mechanisms are hardly touched upon. For the readers of *Journal of Colloid Science* there is little to gather. Although colloid chemical processes and concepts are basic to an understanding of soil structure, tilth, and plant growth, these aspects are not taken into consideration. Indeed, none of the authors possess a first-hand acquaintance with colloid science. It is a pity that no colloid scientist participated in the symposium.

Consistent theoretical treatment permeates the lengthy chapter on "Soil Water and Plant Growth" by L. A. Richards and C. H. Wadleigh. Soil physics has made great strides in the thermodynamic treatment of soil as a porous body. Arranging the voluminous, seemingly incoherent experimental material on soil water in the light of these new principles, as these two authors have done, is both pleasant and fruitful.

The book is of interest and value primarily to the agriculturist.

HANS JENNY, Berkeley, California

Kinetics and Mechanism. By ARTHUR A. FROST and RALPH G. PEARSON. John Wiley and Sons, New York, 1952. 343 pp. Price \$6.00.

This is a very well written book on homogeneous chemical kinetics in which the emphasis is placed on the mechanism of the reactions rather than on theoretical aspects of chemical reaction theory, although the latter are by no means neglected. It is refreshing and timely to have a text in which this point of view is expounded. The kinetic theory of gases as applied to reaction kinetics, the theory of transition states, potential energy diagrams, etc., is developed in sufficient detail but does not dominate the presentation to the exclusion of fundamental chemical objectives of the mechanism of the reactions they are used to interpret.

By reading this book one can get an up-to-date and reliable survey of the useful and rapidly growing field of chemical kinetics without first having to become an expert in quantum mechanics. The reviewer has found no serious errors of principle, and trivial misprints are uncommon. He recommends this text as a well-balanced and authoritative presentation worthy of the attention of all serious students of kinetics.

VICTOR K. LA MER, New York City



JAMES W. McBAIN

JAMES W. McBAIN, M.A., Ph.D., Sc.D., F.R.S.

James William McBain, advisory editor of this Journal, emeritus professor of chemistry at Stanford University, died at his home on March 12, 1953, after a short illness resulting from a heart attack and culminating in a cerebral hemorrhage.

Dr. McBain was born on March 22, 1882, at Chatham, New Brunswick, and studied at the University of Toronto, from which he graduated with the A.B. degree in 1903. After working with Quincke at Heidelberg during 1904-1905, and receiving the Ph.D. degree from that university, McBain began his long academic career at the University of Bristol, England, in 1906. From 1906 until 1919 he was lecturer in physical chemistry, and from 1919 to 1926 he was the first occupant of the Leverhulme chair of chemistry. In 1926 McBain was invited to become professor of chemistry at Stanford University, and he held this position until he became emeritus professor in 1947. At the personal request of Prime Minister Nehru he accepted the responsibility of building and directing the National Chemical Laboratory at Poona, India, from 1949 to 1952, and had returned home only a few months prior to his fatal illness. He was elected fellow of the Royal Society in 1925, and held membership and office in many scientific societies, including the Society of Rheology, of which he was vice-president. He was awarded an honorary doctorate by Brown University in 1923, and by Bristol University in 1928. In 1939 the Royal Society awarded him the Davy medal.

Dr. McBain was married to Evelyn McBain, who survives him with two children, Janet Quin, and John Keith McBain.

At the outset of McBain's career in colloid science, the little surface chemistry which was then known was commonly held to be a part of classical physics, and colloidal phenomena were an empirical and not very important part of inorganic chemistry. McBain lived to see the field grow both in extent and in scientific stature, and he contributed greatly to its growth; most particularly in the field of adsorption and in the field of colloidal electrolytes which he discovered and made his own. Great as were his scientific contributions, possibly even more important to the growth of colloid science was his youthful and never-failing enthusiasm for the subject which he passed on to all around him, students and professors alike. It is difficult to assess how great his eventual influence on the subject will grow to be through the many students, trained under him, now actively working in this field.

The part of his career which McBain would probably have thought most valuable was his selfless work in building and bringing into vigorous growth the National Chemical Laboratory of India. Always more than willing to do his utmost for his fellow men, McBain characteristically did not hesitate to accept this challenge, which would have overcome many a younger man without his missionary zeal and which he could easily have refused on the grounds of age without losing a single person's respect.

In his personal life McBain was a generous and warm-hearted man who extended to his students not merely all the resources of his intellect but genuine and lasting friendship also. Born the son of a clergyman, McBain went through life with a firm religious faith.

By his death colloid science suffered a grievous loss. By his life all who came into contact with him had their lives enriched.

THE SORPTION OF VAPORS BY MONOLAYERS. VII. THE EFFECT OF ANESTHETIC VAPORS ON SOME MONOLAYERS OF BIOLOGICAL INTEREST¹

Robert B. Dean², Kenneth E. Hayes³, and Roy G. Neville

University of Oregon, Eugene

Received January 19, 1953; revised April 6, 1953

ABSTRACT

The effect of nitrous oxide, ethylene, and vapors of chloroform, divinyl ether, and diethyl ether on monolayers of stearic, pentadecanoic, and oleic acids as well as on cholesterol, ergosterol, lecithin, and cephalin has been investigated. The gases cause slight increases in surface pressure up to 2 dynes/centimeter. The vapors are adsorbed strongly at saturation and behave qualitatively like hexanes on stearic acid monolayers.

INTRODUCTION

The surface properties of anesthetic and other narcotic vapors have been of interest ever since Traube (13) postulated that such vapors exert their physiological effect at cell surfaces. The work reported here deals with the action of various anesthetic vapors and gases on several monolayers of representative lipoidal materials spread on the interface between air and water. Such monolayers might be expected to be reasonable approximations to the lipoidal portion of cell walls (1).

The effects produced by vapors of the isomeric hexanes on stearic acid have been previously reported by Dean (2), Dean and Hayes (3), and Hayes and Dean (8, 9). A preliminary survey of the action of some hexanes, benzene, and CCl_4 was reported by Dean and Li (5). Their work has shown that vapors increase the surface pressure of stearic acid monolayers at constant area or expand it at constant pressure. In favorable cases it has been possible to calculate the quantity of vapor adsorbed. A method for calculating the quantity of vapor adsorbed on a monolayer was developed theoretically by Koenig (10) from the Gibbs equation (6), relating the surface excess Γ of a vapor to the change of surface tension with pressure

¹ Supported by a grant from the United States Public Health Service, National Institute of Neurological Diseases and Blindness. Based in part on material in the master's thesis of Roy G. Neville, deposited in the University of Oregon Library M. S., 1953.

² Present address: The Borden Company, Chemical Division, Bainbridge, N. Y.

³ Present address: Department of Chemistry, Princeton University.

of the vapor $d(\gamma)/dp$. Γ , the surface excess, is the concentration of the adsorbed vapor in moles/square centimeter of surface.

A convenient unit for Γ is the Gibbs, which is equal to 1×10^{-10} moles per square centimeter (2). It is convenient when working with monolayers to use the surface pressure, π , which is the lowering of the surface tension below that of a pure liquid, $\pi = \gamma_0 - \gamma$. For an ideal vapor at a pressure p adsorbed on the surface of a pure liquid

$$\Gamma = \frac{p}{RT} \frac{(d\pi)}{dp} \quad [1]$$

When there are more than two components in the system, i.e., when the liquid is covered by a monolayer, the equation becomes more complicated:

$$\Gamma_1 = \frac{P}{RT} \left(\frac{\partial \pi}{\partial P} - \Gamma_2 \frac{\partial \mu_2}{\partial p} \right) \quad [2]$$

where Γ_1 is the surface excess of the vapor, Γ_2 the surface excess and μ_2 the chemical potential of the substance in the monolayer. Koenig (8, 10) has shown how to compute the last term in the parenthesis for crystalline substances such as stearic acid which form equilibrium monolayers.

In the absence of a monolayer ($\Gamma_2 = 0$) this equation reduces to Eq. [1]. The term in Γ_2 contributes up to 20 % of the value of Γ_1 when hexanes are adsorbed on stearic acid (8). Equation [1] provides a first approximation to the value of Γ_1 and the only approximation possible at present for materials which do not form equilibrium monolayers from a crystal.

In many systems at low vapor pressures the surface pressure varies according to an empirical equation of the type

$$\pi = kp^n \quad [3]$$

Differentiation and substitution in Eq. [1] gives

$$\Gamma_1 = n\pi/RT; \quad [4]$$

at 25° C.

$$\Gamma_1 = 0.40 n\pi \quad [5]$$

if Γ_1 is in Gibbs and π is in dynes/centimeter. Even at low partial pressures it is not possible to determine Γ_1 from a single value of π , since the exponent n must be determined.

Previous work (5, 8) has shown that condensed films of stearic acid are expanded by hexanes, benzene, and CCl_4 . In every case so far investigated the adsorbed vapor converts the condensed stearic acid film to a liquid expanded or transitional film which resembles films formed with lower homologs such as pentadecanoic acid. Figure 1A, redrawn from reference (5), shows the relation between π and the area per molecule for stearic acid

under various vapors, and Fig. 2B, based on this work, shows the π - A curve for pentadecanoic acid under CHCl_3 . The area per molecule $A = 6 \times 10^{23}/\Gamma$. In the absence of organic vapors, stearic acid monolayers exist as crystal-like clumps or micelles on the surface separated by bare patches covered with a very dilute surface gas of stearic acid. An organic vapor is adsorbed on the micelles and dissolves in the hydrocarbon portion

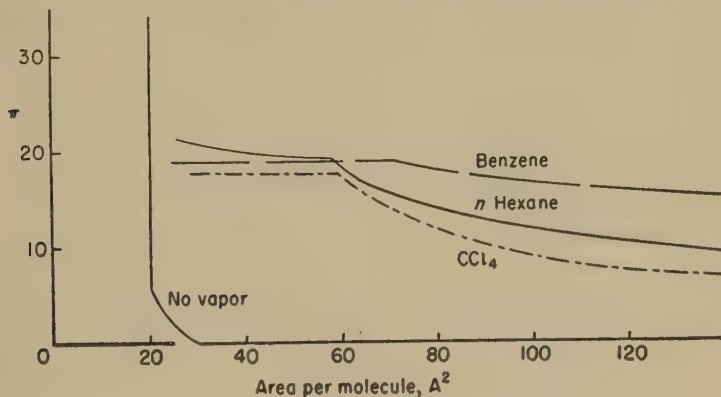


FIG. 1A. Stearic acid

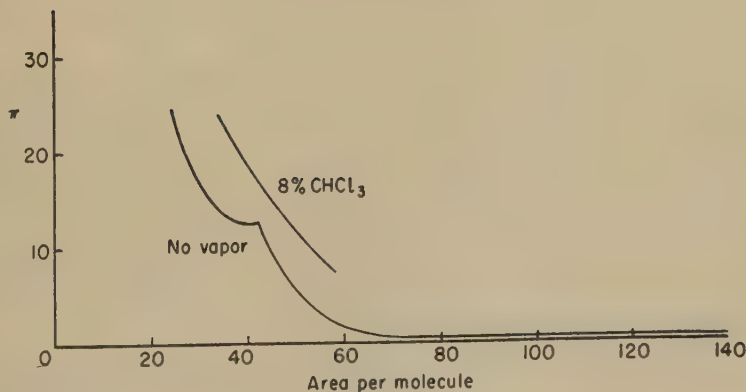


FIG. 1B. Pentadecanoic acid

expanding the micelles to cover the surface completely with a duplex film (4).

EXPERIMENTAL

The preliminary survey with anesthetics was done by measuring the surface tension of a monolayer and the change produced when the vapor or gas was passed over it. A DuNouy tensiometer was used with a 4-cm. ring. The measurements of surface tension were corrected according to Harkins

and Jordan (7) and were routinely checked on the clean water surfaces.

The monolayer was spread on water in a circular Teflon trough having an area of 40.1 cm.². This trough fitted into a 9-cm. glass crystallizing dish. The trough was cleaned before each run in chromic-sulfuric acid and rinsed in distilled water for 15 minutes. The trough was covered by a circular metal plate which fitted loosely in the glass dish about 1 cm. above the water surface and which had a short wide tube in the center through which the organic vapors could be introduced. A platinum wire supporting the ring came in through a small hole in the cap of this tube.

The vapors were introduced in a gas stream at a rate of about 120 cm.³ per minute so that the vapor passed over the monolayer and escaped at the edges of the dish. Nitrous oxide and ethylene were taken from tanks of medical-grade gas, and the flow was measured manometrically. Ether and chloroform were placed in side-arm test tubes partially immersed in water at room temperature, and oxygen was bubbled through the liquids to saturate it with the vapor. Cold water or "dry ice" in acetone was used to cool the liquid when it was necessary to get concentrations of vapor lower than the saturation values at room temperature. Room temperature varied between 22° and 25°C., and temperatures were recorded to the nearest 0.1°C. All the data have been corrected to 25°C., assuming that the change of surface tension with temperature is the same for monolayers as for pure water. In this preliminary survey, surface pressure data are accurate to ± 0.5 dyne/centimeter.

The substances which were to be spread as monolayers were dissolved in benzene or occasionally in di-isopropyl ether, which has a greater spreading pressure than benzene. A measured volume of the solution was placed on the previously cleaned surface a drop at a time, using the same technique reported in our earlier papers (3, 5). Values of the surface concentration or area per molecule are believed to be accurate to $\pm 2\%$. All monolayers were spread on 0.01 *M* H₃PO₄, which has a surface tension negligibly different from that of water and eliminates the interference of heavy metal ions.

The *stearic acid* was Eastman's highest purity.

Pentadecanoic acid was kindly supplied to the senior author by the late A. W. Ralston, Armour and Co., Chicago, and was of exceptional purity (12).

Oleic acid was a 98% pure sample from the Hormel Foundation, Austin, Minnesota.

Crude *cholesterol* was fractionally recrystallized from benzene and methanol, m.p. 148.5°C.

Chemically pure *ergosterol* was recrystallized from methanol, m.p. 163°C.

Lecithin and *cephalin* were supplied by the Glidden Corp., Chicago. They were commercial products extracted from soybeans. Molecular weights assumed for these phospholipids were 791 and 731, respectively.

Diethyl ether C.P. grade was dried over sodium.

Divinyl ether was medical-grade, b.p. 28.3°C.

Chloroform was C. P. grade, b.p. 61.3°C.

Nitrous oxide, *ethylene*, and *oxygen* were all medical-grade gases.

A chamber for investigating monolayers in the presence of vapors has been constructed in this laboratory similar to the one described by Dean and Hayes (3). The important difference lies in the greater length, which permits work with films which are expanded (even in the absence of a vapor). This equipment has been used to study the behavior of penta-

TABLE I

Effects of Various Anesthetic Vapors on the Surface Tension of Pure Water

Surface tension of water: 71.8 dynes/cm.

Anesthetic vapor	Surface tension γ	π
Nitrous oxide, 100%	71.1	0.7
Nitrous oxide, 50% in oxygen	71.1	0.7
Ethylene, 100%	71.1	0.7
Chloroform, satd. (26%) in oxygen	70.0	1.8
Divinyl ether, satd. (85%) in oxygen	61.1	10.7
Diethyl ether, satd. (70%) in oxygen	54.8	17.0

TABLE II

Effects of Anesthetic Vapors on Stearic Acid Monolayers

Surface concentration in Gibbs

	2.0 π	3.0 π	4.0 π	5.0 π	6.0 π	8.0* π
Stearic acid alone	0.0	0.0	0.0	0.0	0.1	0.6
Nitrous oxide, 100%	—	—	—	—	—	0.9
Chloroform, (24%) in O ₂	11.1	—	13.6	14.3	15.0	15.3
Chloroform, (8%) in O ₂	4.1	4.3	4.8	5.0	5.5	6.8
Diethyl ether, (70%) in O ₂	—	—	—	—	—	27.7
Diethyl ether, (24%) in O ₂	20.0	—	20.7	21.2	21.7	22.0
Diethyl ether, (8%) in O ₂	13.6	13.7	13.8	13.9	14.2	16.2

* Nearly close-packed monolayer

decanoic acid at 25°C. in the presence of 8% CHCl₃ vapor. The results of the survey of anesthetic vapors on representative monolayers are presented in Tables I–VI. All of the anesthetics are adsorbed on all of the monolayers tested. In general, the effect of nitrous oxide and of ethylene, both at 100%, is very small, comparable with the limits of accuracy of the data. Chloroform, in agreement with K. H. Meyer (11), has a very low surface activity on water; less than 2 dynes/centimeter. However, chloroform increases the surface pressure of all of the monolayers tested by 7–15 dynes/centimeter. In the case of chloroform on stearic acid one can calculate the approximate amount adsorbed as follows: At 6.0 Gibbs the

surface pressure is approximately a linear function of the partial pressure of chloroform.

$$\pi = 0.83p$$

where p is in per cent by volume ($n = 1$).

Therefore, according to Eq. [5]

$$\Gamma_1 = 0.40 \pi = 0.33p.$$

When $\pi = 15$ dynes/centimeter under 24% chloroform, $\Gamma_1 = 6$ Gibbs, about equal to the concentration of stearic acid. From the data at 8 Gibbs,

TABLE III
Effects of Anesthetic Vapors on Pentadecanoic Acid Monolayers
Surface concentration in Gibbs

	4.15		5.53		6.64	
	π	$\Delta\pi$	π	$\Delta\pi$	π	$\Delta\pi$
Pentadecanoic acid alone	0.5	—	6.9	—	15.4	—
Nitrous oxide, 100%	2.1	1.6	8.6	1.7	17.1	1.7
Chloroform, (26%) in O ₂	11.7	11.2	17.3	10.4	25.9	10.5
Diethyl ether, (70%) in O ₂	33.7	33.2	34.1	27.2	35.7	20.3

TABLE IV
Effects of Anesthetic Vapors on Oleic Acid Monolayers
Surface concentration in Gibbs

	1.0	1.5	2.0	2.5	2.7	3.0*
	π	π	π	π	π	π
Oleic acid alone	0.0	0.0	0.2	0.8	0.8	1.0
Nitrous oxide, 100%	0.6	1.4	1.9	—	1.0	1.7
Ethylene, 100%	0.8	1.1	1.4	—	1.0	1.4
Chloroform, (26%) in O ₂	15.0	15.1	13.1	—	10.2	13.7
Chloroform, (24%) in O ₂	13.3	12.5	14.6	11.7	—	13.5
Diethyl ether, (70%) in O ₂	29.5	29.2	29.3	—	25.2	30.6
Diethyl ether, (24%) in O ₂	21.0	23.9	20.4	16.0	—	17.9

* Condensed monolayer.

where the correction term in Eq. [2] is known to be close to zero (8, 9), and assuming that $\pi = kp^n$, the data give $n = 0.73$ and $\Gamma_1 = 4.3$ Gibbs. The results with chloroform are thus similar to those obtained with isomeric hexanes in the more extensive work previously reported (4, 8, 9). At 8% partial pressure of chloroform, both at 6 and at 8 Gibbs of stearic acid, $\Gamma_1 = 2$ Gibbs. The results with other monolayers, although incomplete, are consistent with a similar adsorption of chloroform.

Nitrous oxide is adsorbed slightly, but the surface concentration is not more than 0.5 Gibbs on any of the monolayers tested. Probably not more than 1.5 Gibbs of ethylene are adsorbed even at saturation on phospho-

lipids, which showed the greatest effect. Ethyl ether is strongly adsorbed even on water, and it is not possible to tell from the data how much additional adsorption takes place when a monolayer is spread on the surface. Divinyl ether has a smaller effect on monolayers than does diethyl ether.

The effect of 8% chloroform on pentadecanoic acid was investigated over a range of surface areas where pentadecanoic acid forms liquid expanded

TABLE V
Effects of Anesthetic Vapors on Sterol Monolayers

	Cholesterol				Ergosterol	
	Surface concentration in Gibbs					
	2.00		4.14*		3.97**	
	π	$\Delta\pi$	π	$\Delta\pi$	π	$\Delta\pi$
Sterol alone	1.0	—	1.0	—	6.7	—
Nitrous oxide, 100%	2.1	1.1	2.0	1.0	6.7	0.0
Nitrous oxide, (50%) in O ₂	1.9	0.9	—	—	—	—
Chloroform, (26%) in O ₂	7.2	6.2	7.1	6.1	15.5	8.8
Divinyl ether, (85%) in O ₂	14.1	13.1	17.3	16.3	—	—
Diethyl ether, (70%) in O ₂	24.5	23.5	27.1	26.1	32.9	26.2

* Close-packed monolayer.

** Nearly close-packed monolayer.

TABLE VI
Effects of Anesthetic Vapors on Phospholipid Monolayers

	Lecithin		Cephalin		Lecithin: Cephalin, 1:1
	Surface concentration in Gibbs				
	1.19 π	1.51* π	1.19 π	1.51* π	1.51 π
Phospholipid alone.....	0.9	0.8	0.2	0.8	0.2
Nitrous oxide, 100%.....	2.2	2.3	0.6	2.1	1.1
Ethylene, 100%.....	3.4	2.4	0.6	2.2	1.2
Chloroform, (26%) in O ₂	10.9	10.0	11.7	11.3	13.2
Diethyl ether, (70%) in O ₂	30.2	30.4	28.1	30.1	29.5

* Close-packed monolayer.

and transitional monolayers. Although the liquid expanded phase is quite common among mixed monolayers and in monolayers at oil-water interfaces, pentadecanoic acid was the only suitable pure material available to us which would give this phase at 25°C. The data presented in Fig. 2B were obtained in the new monolayer trough. The accuracy is believed to be better than 0.5% in area and 0.2 dyne in surface pressure. Chloroform at 8% by volume causes a large expansion in the monolayer but appears to

eliminate the transitional phase. On this system it is not possible to apply Eq. [1] even as an approximation, and we have no method of ascertaining the adsorption of chloroform from this data.

DISCUSSION AND CONCLUSIONS

The data presented here show that saturated anesthetic vapors have a large effect on monolayers similar in kind to the effect of hexanes on stearic monolayers previously reported. However, the anesthetic gases nitrous oxide and ethylene have a relatively slight effect. Extrapolation of our data to anesthetic levels is probably not justified except as to order of magnitude because of the uncertainties in the measurements.

SUMMARY

1. The effect of nitrous oxide and ethylene and the vapors of chloroform, divinyl ether and diethyl ether on monolayers of fatty acids, phospholipids, and steroids has been investigated.
2. The gases have a very slight effect, reducing the surface tension by at most 2 dynes/centimeter.
3. The vapors behave like hexanes on stearic acid and reduce the surface tension by 10–30 dynes at saturation.
4. On a close-packed layer of stearic acid approximately a monolayer of chloroform is adsorbed at saturation. At lower partial pressures, less is adsorbed.

REFERENCES

1. DANIELLI, J. F., *Cell Physiology and Pharmacology*, p. 14 ff. Elsevier, Amsterdam, 1950.
2. DEAN, R. B., *J. Phys. & Colloid Chem.* **55**, 611 (1951).
3. DEAN, R. B., AND HAYES, K. E., *J. Am. Chem. Soc.* **73**, 5583 (1951).
4. DEAN, R. B., AND HAYES, K. E., *J. Am. Chem. Soc.* **74**, 5982 (1952).
5. DEAN, R. B., AND LI, F.-S., *J. Am. Chem. Soc.* **72**, 3979 (1950).
6. GIBBS, J. W., *Collected Works*, p. 55. Yale reprint, New Haven, 1948.
7. HARKINS, W. D., AND JORDAN, H. F., *J. Am. Chem. Soc.* **52**, 1951 (1930).
8. HAYES, K. E., AND DEAN, R. B., *J. Am. Chem. Soc.* **73**, 5584 (1951).
9. HAYES, K. E., AND DEAN, R. B., *J. Phys. Chem.* **57**, 80 (1953).
10. KOENIG, F. O., *Computation of Surface Concentrations from Surface Tension Data*. Academic Press, New York, in press.
11. MEYER, K. H., *Trans. Faraday Soc.* **33**, 1062 (1937).
12. RALSTON, A. W., *J. Org. Chem.* **7**, 546 (1942).
13. TRAUBE, I., *Biochem. Z.* **277**, 39; **279**, 166; **282**, 444 (1935).

COLLOIDAL ASSOCIATION AND BIOLOGICAL ACTIVITY OF SOME RELATED QUATERNARY AMMONIUM SALTS¹

Sydney Ross, C. E. Kwartler² and John Hays Bailey

*Rensselaer Polytechnic Institute, Troy, New York, Winthrop Stearns, Inc., and
Sterling-Winthrop Research Institute, Rensselaer, New York*

Received January 2, 1953

ABSTRACT

Two series of cationic surface-active agents, benzyldimethylalkylammonium chlorides and 4-nitrobenzyldimethylalkylammonium chlorides, where the alkyl group varies from a 6-carbon-atom straight chain to an 18-carbon-atom straight chain, have been prepared. The critical concentration for the formation of micelles has been measured by the dye method for each member of each series. As has been discovered in other cases of long-chain compounds (9, 10), here too there exists a linear relation between the number of carbon atoms in the alkyl group and the logarithm of the critical micelle concentration.

A third series of cationic surface-active agents has been prepared, similar to the series above save that the variation in structure is obtained by varying the nature or position of the substituent in the benzyl group, while the alkyl group is lauryl throughout. The critical micelle concentration of each member of the series has been measured by the dye method. The critical micelle concentration thus obtained varies with the polarity of the benzyl portion of the molecule. Measures of this polarity are provided by the boiling points, melting points, dielectric constants, or dipole moments of the toluene compounds that correspond to the benzyl portions of the quaternary ammonium salts. It is found that the critical micelle concentrations of the quaternary ammonium salts are proportional to the square of the dipole moment of these corresponding substituted toluenes.

Correlations with microbiological activities of these quaternary salts have been attempted.

INTRODUCTION

The relation between molecular structure and critical micelle concentration (CMC) has been investigated for a few types of compounds, such as ordinary potassium soaps and sulfated fatty alcohols. These previous studies have established a logarithmic relation between the CMC and the number of carbon atoms in the aliphatic-chain portion of the molecule. The present work has to do with some related quaternary ammonium salts

¹ Presented in part before the Division of Industrial and Engineering Chemistry at the 122nd Meeting of the American Chemical Society, Atlantic City, N. J., September 17, 1952.

² Present address: Gamma Chemical Co., Great Meadows, N. J.

containing an aliphatic group, a benzyl group, and two methyl groups, and the effect on the CMC of variations in the length of the aliphatic-chain group and of substituents in the benzyl group. The microbiological activities of these compounds have also been measured for comparison with their tendency toward formation of colloidal micelles. A similar comparison has been undertaken by Cella *et al.* (1) for a series of quaternary ammonium salts closely related to those of the present investigation. The conclusions of the earlier work have been verified and extended.

EXPERIMENTAL

(a) Materials

One of the groups of compounds studied was a series of 4-nitrobenzyl-dimethylalkylammonium chlorides. In this series the alkyl group was varied from a normal 6-carbon straight chain to a normal 18-carbon straight chain. The general method of preparation of this series of compounds occurs in two steps:

1. *Preparation of Alkyl-dimethylamines.* This preparation in general proceeded through the reaction of the corresponding alkyl chloride with dimethylamine. This reaction was carried out in a steel autoclave, using an excess of dimethylamine. The tertiary amines were separated by the usual physical means and were then carefully purified, before they were used for the preparation of quaternary ammonium compounds. Our experience indicated that this purification of these intermediates was essential to the preparation of pure quaternary ammonium compounds. Each of the tertiary amines was purified and analyzed prior to their utilization as intermediates.

2. *Reaction with *p*-Nitrobenzyl Chloride.* The analytically pure tertiary amines were then caused to react with purified *p*-nitrobenzyl chloride. This reaction was carried out in conventional solvents such as acetone, ether, isopropyl alcohol, benzyl alcohol, and others. Under the proper operating conditions, the quaternary ammonium compounds frequently settled out as crystalline solids. The further purification of these quaternary ammonium compounds was accomplished by crystallization from such solvents as isopropyl alcohol, acetone, benzene, petroleum ether, or ethyl acetate. All the compounds so prepared have been purified to constant melting point.

The second group of compounds was a series of substituted dodecyl-dimethylamine derivatives. In this series of compounds, various substituted benzyl chlorides have been caused to react with purified dodecyl-dimethylamine. The general method of preparation of this series of compounds occurs in two steps:

1. *The Preparation of Dodecyl-dimethylamine.* This preparation was accomplished by the action of dodecyl chloride with dimethylamine under

pressure in a steel autoclave. This compound was also prepared by the action of formaldehyde and formic acid on dodecylamine. In both methods of preparation, great care was taken to prepare unequivocally pure dodecyl-dimethylamine. It was only after vigorous physical and chemical purification was effected, that the tertiary amine was considered suitable for use in quaternary ammonium compound formation.

2. *Purification.* The various substituted benzyl chlorides were all purified prior to their use. The 2-chloro, 4-chloro, 2,4-dichloro, and 3,4-dichloro-benzyl chlorides were carefully purified by fractional distillation. The 4-nitrobenzyl chloride and 2-hydroxy-5-nitrobenzyl chloride were crystallized prior to use. The 3,4-dimethoxy and 3,4-methylenedioxybenzyl chlorides were crystallized. The quaternization reactions were carried out as described above. In this series, too, extreme care was necessary and extensive purification resorted to in order to obtain pure crystalline compounds.

All of the compounds described in this paper gave satisfactory analyses for nitrogen and halogen. Formulas, analyses, and CMC values in moles per liter for the series of salts are given in Table I.

(b) *Bacteriological Technique*

The minimum killing concentration was determined as follows. Various dilutions of the quaternary ammonium compound in water were prepared, and 5-ml. portions of each were brought to 20°C. in a water bath. A 22-26-hr. broth culture of the test organism was transferred to a sterile 2-oz. serum bottle containing a shallow layer of sterile 3-mm. glass beads, stoppered with a sterile rubber stopper, and shaken in a clinical shaking apparatus for 2 min. After reaching 20°C., 0.5 ml. of culture was added to each of the tubes containing the diluted quaternary compound, and the contents were mixed by gentle twirling of the tubes in the bath. At the end of 5, 10, and 15 min. exposure to the action of the quaternary ammonium compound, one standard 4-mm. loopful of the mixture was removed to culture tubes containing 10 ml. of nutrient broth (peptone 1%, meat extract 0.5%, NaCl 0.5%) and these tubes were incubated at 37°C. for 48 hr. That concentration killing the test organism in 10 min., but not in 5 min., was considered the minimum killing concentration.

The test organisms employed, *Micrococcus pyogenes* var. *aureus* 209 and *Salmonella typhosa* Hopkins, were killed in 10 min., but not in five, by a 1:60 to 1:65 and 1:80 to 1:90 dilution of phenol.

The minimum killing concentrations reported are the average of at least three determinations and, inasmuch as they were obtained in the course of routine phenol-coefficient determinations, are subject to the inaccuracies and limitations of that procedure.

(c) *Titration for CMC Values*

The CMC was measured by the method of Corrin and Harkins (2) using the dye sodium 2,6-dichlorobenzeneindophenol (Eastman No. 3463). The titration in every case was continued until the original red color of the acidified dye solution was just reached.

TABLE I

Formula, Analyses and Critical Micelle Concentration of Certain Substituted Benzyl-dimethylalkylammonium Chlorides

Alkyl	Ring substitution	CMC	Elementary analyses, %			
			Nitrogen		Chlorine	
			Calcd.	Found	Calcd.	Found
		<i>moles/l.</i>				
C ₆ H ₁₃	None	4.34×10^{-2}	5.48	5.37	13.90	13.35
C ₈ H ₁₇	None		4.95	4.86	12.51	12.13
C ₁₀ H ₂₁	None	6.1×10^{-3}	4.50	4.52	11.40	11.08
C ₁₂ H ₂₅	None	2.8×10^{-3}	4.12	4.05	10.43	10.05
C ₁₄ H ₂₉	None	3.7×10^{-4}	3.82	3.89	9.65	9.58
C ₁₆ H ₃₃	None	4.4×10^{-5}	3.54	3.51	8.98	8.95
C ₁₈ H ₃₇	None	7.1×10^{-6}	3.32	3.64	8.39	8.14
C ₈ H ₁₇	4-Nitro	5.7×10^{-2}	4.95	4.86 ^a	12.51	12.13
C ₁₀ H ₂₁	4-Nitro	2.3×10^{-2}	7.88	7.99	10.00	10.06
C ₁₂ H ₂₅	4-Nitro	3.6×10^{-3}	7.28	7.18	9.25	9.06
C ₁₄ H ₂₉	4-Nitro	5.1×10^{-4}	6.78	6.76	8.61	8.63
C ₁₆ H ₃₃	4-Nitro	1.3×10^{-4}	6.36	6.05	8.06	8.31
C ₁₈ H ₃₇	4-Nitro	2.9×10^{-5}	5.98	5.80	7.43	7.50
C ₁₂ H ₂₅	2-Chloro	0.28×10^{-3}	3.74	3.70	9.50	9.47
C ₁₂ H ₂₅	2,4-Dichloro	0.37×10^{-3}	3.44	3.49	8.69	8.74
C ₁₂ H ₂₅	4-Chloro	0.42×10^{-3}	3.74	3.62	9.50	9.42
C ₁₂ H ₂₅	2-Hydroxy-5-nitro	0.69×10^{-3}	6.98	7.23	8.85	8.82
C ₁₂ H ₂₅	3,4-Dichloro	1.1×10^{-3}	3.44	3.42	8.69	8.85
C ₁₂ H ₂₅	3,4-Methylenedioxy	3.8×10^{-3}	3.65	3.61	9.26	9.06
C ₁₂ H ₂₅	3,4-Dimethoxy	3.9×10^{-3}	3.50	3.40	8.88	8.61

^a By TiCl₃ method.

RESULTS

The results for the CMC in moles per liter of both series of quaternary ammonium salts are shown in Fig. 1. In this figure the logarithm of the CMC is plotted versus the number of carbon atoms in the alkyl group. For the 4-nitrobenzyl-dimethylalkylammonium chlorides, the results are fairly well expressed by a single straight line. For the benzyl-dimethylalkylammonium chlorides, two straight lines, intersecting at the point that corresponds to 12 carbon atoms in the alkyl chain, are required to describe the results.

In Figs. 2 and 3 each of the graphs of Fig. 1 is compared with the corresponding antibacterial activities of the compounds. These microbiological activities, expressed as the minimum killing concentration in moles per liter required to kill 0.5 ml. of a 24-26-hr. culture of *M. pyogenes* var. *aureus* or *S. typhosa* in 10 min., are sufficiently close for both organisms to warrant only a single curve through the experimental points. The position of this curve may, of course, be displaced upward or downward because of the merely relative character of the method of comparing antibacterial activities.

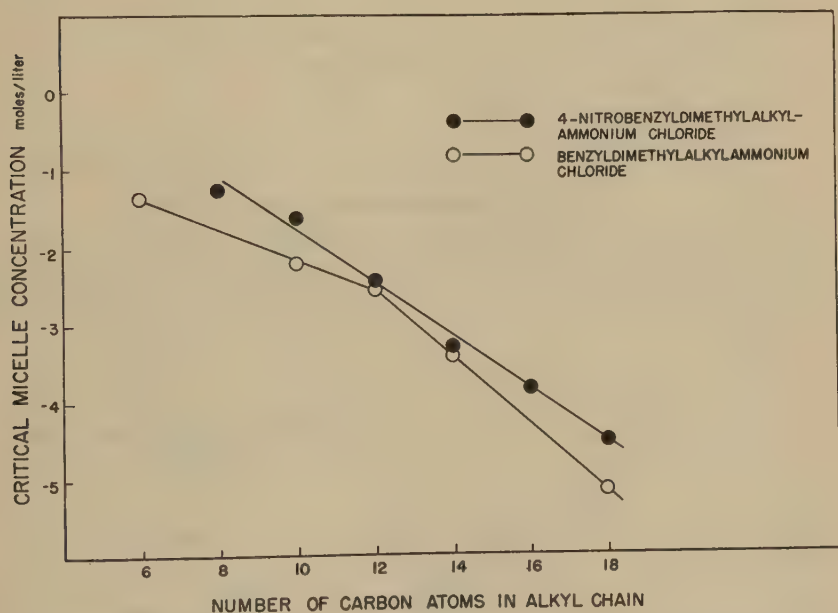


FIG. 1. Logarithm of critical micelle concentrations of 4-nitrobenzyltrimethylammonium chlorides (upper curve) and benzyltrimethylammonium chlorides (lower curve) vs. number of carbon atoms in alkyl chain.

Figures 4 and 5 show a series of curves, similar to the lower curves of Figs. 2 and 3, for the logarithm of the minimum killing concentration in moles per liter versus the number of carbon atoms in the alkyl group. These curves are for compounds in which various substituents are present in the benzyl group. The figures illustrate results obtained using an unsubstituted benzyl group, a 2-chlorobenzyl, a 4-chlorobenzyl, and a 3,4-dichlorobenzyl group. Figure 4 shows the antibacterial action for *M. pyogenes* var. *aureus* and Fig. 5 the antibacterial action for *S. typhosa*. These curves represent a selection from a larger body of data obtained on a variety of quaternary ammonium salts that differed both in the length of

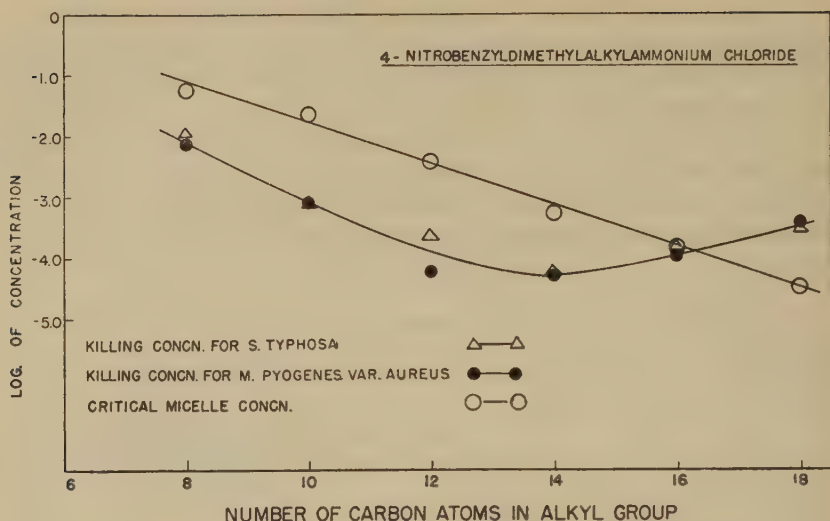


FIG. 2. Comparison of critical micelle concentrations of a series of 4-nitrobenzyltrimethylammonium chlorides and their minimum killing concentrations for *S. typhosa* and *M. pyogenes* var. *aureus*, for varying number of carbon atoms in the alkyl group.

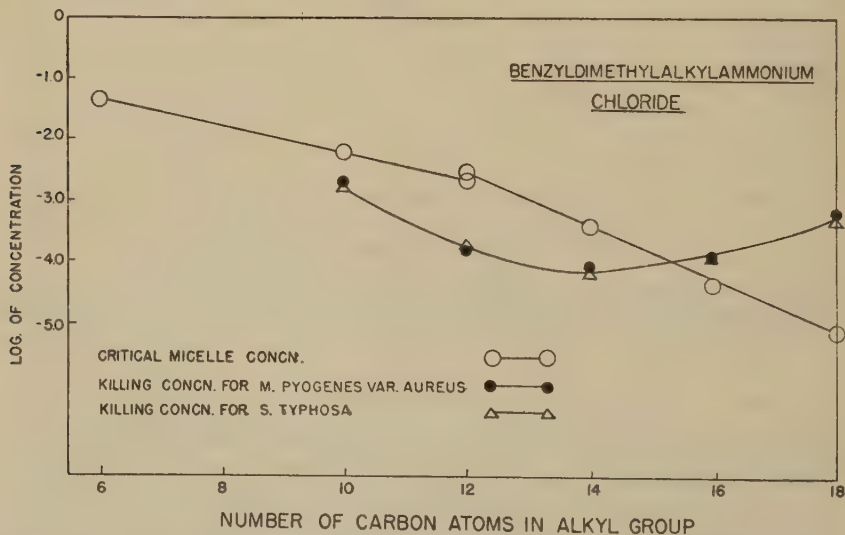


FIG. 3. Comparison of critical micelle concentrations of a series of benzyltrimethylammonium chlorides and their minimum killing concentrations for *S. typhosa* and *M. pyogenes* var. *aureus*, for varying number of carbon atoms in the alkyl group.

the chain and in the nature of the substituent in the benzyl group. Table II presents *in extenso* the results of which Figs. 4 and 5 are representative selections.

DISCUSSION

(a) *Molecular Structure and Critical Micelle Concentration*

The dye method of obtaining the CMC of colloidal electrolytes is always subject to the uncertainty that the presence of the dye may induce the formation of micelles at lower concentrations than they would occur in the absence of the dye. This uncertainty can be resolved only by comparison

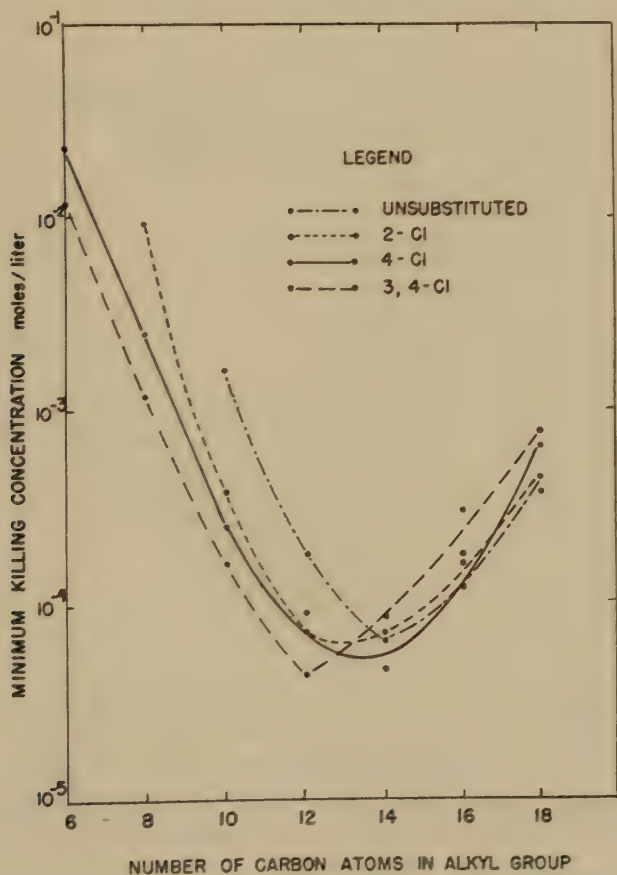


FIG. 4. Relationship between chain length and antibacterial action of certain benzyl-dimethylalkylammonium chloride homologs for *M. pyogenes* var. *aureus*.

of the results of the dye method with those of an independent method, such as that of electrical conductance or refractive index. A wide discrepancy exists between the values of the CMC for benzyldimethyldodecylammonium chloride in this paper (by the dye method) and that given by Cella *et al.* (1), who used electrical conductivity. The values are 0.0028 and 0.0081 mole/l., respectively. The lower value by the dye method

suggests the influence of the dye in the formation of the micelle. The conclusions of the present paper are therefore restricted to comparisons of the compounds here reported, each measured with the same conditions, and cannot be extended to any other substance whose CMC is measured by a different method.

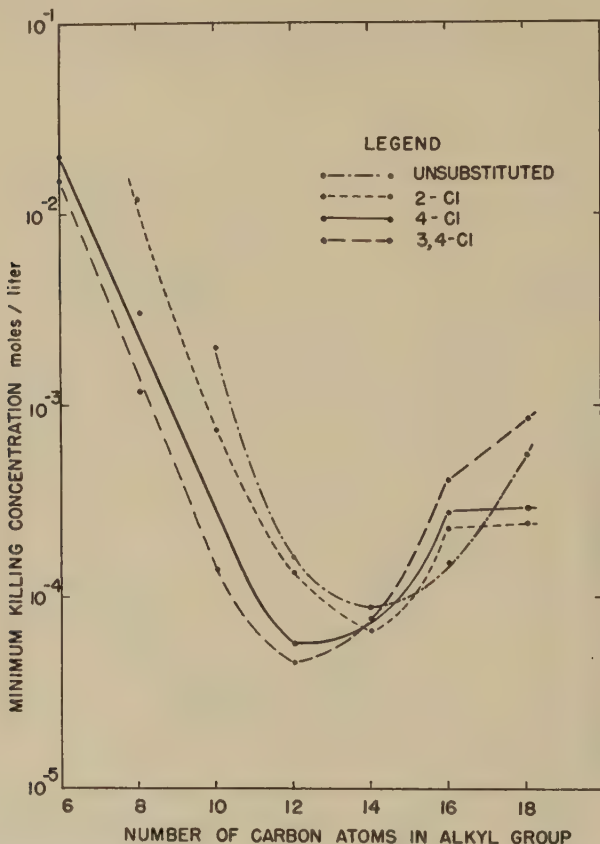

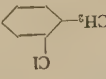
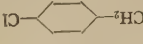
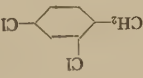
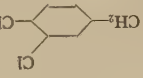


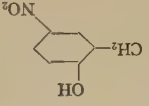


FIG. 5. Relationship between chain length and antibacterial action of certain benzyl-dimethylalkylammonium chloride homologs for *S. typhosa*.

Figures 1 and 2 show the proportionality between the log CMC and the number of carbon atoms in the alkyl group. The 4-nitrobenzyl series gives a single straight line, but the unsubstituted benzyl series gives two straight lines, one below 12 carbon atoms in the alkyl group and the other above 12 carbon atoms. The presence of two straight lines for the same series can be interpreted as evidence for two distinct types of micelle, one for short carbon chains and the other for longer carbon chains. The slope of the line has been used by Debye (3) as the basis for a calculation of the decrease

TABLE II

Minimum Concentration of Unsubstituted and Substituted Benzyltrimethylammonium Chlorides in Moles per Liter Killing *M. pyogenes* var. *aureus* and *S. typhosa* in 10 min.

Organism	Alkyl	Benzyl substituent							
									
<i>M. pyogenes</i> var. <i>aureus</i>	C_8H_{17}	1.6×10^{-3}	9.4×10^{-3}	2.5×10^{-3}	7.6×10^{-3}	2.3×10^{-3}	1.2×10^{-3}	8.7×10^{-3}	
	$C_{10}H_{21}$	1.8×10^{-4}	3.8×10^{-4}	2.5×10^{-4}	7.5×10^{-4}	2.2×10^{-4}	1.6×10^{-4}	8.4×10^{-4}	
	$C_{12}H_{25}$	6.3×10^{-5}	7.0×10^{-5}	8.9×10^{-5}	6.0×10^{-5}	5.4×10^{-5}	4.2×10^{-5}	1.9×10^{-4}	2.0×10^{-3}
	$C_{14}H_{29}$	1.2×10^{-4}	7.0×10^{-5}	4.5×10^{-5}	5.8×10^{-5}	5.1×10^{-5}	8.6×10^{-6}	5.6×10^{-5}	2.3×10^{-3}
	$C_{16}H_{33}$	1.4×10^{-4}	1.8×10^{-4}	1.4×10^{-4}	1.0×10^{-4}	3.8×10^{-4}	4.0×10^{-4}	6.2×10^{-5}	
	$C_{18}H_{37}$	4.4×10^{-4}	3.7×10^{-4}	6.5×10^{-4}	3.4×10^{-4}	4.9×10^{-4}	7.6×10^{-4}	5.7×10^{-4}	
<i>S. typhosa</i>	C_8H_{17}	2.0×10^{-3}	1.2×10^{-2}	1.3×10^{-3}	1.2×10^{-2}	3.1×10^{-3}	1.2×10^{-3}	8.7×10^{-3}	
	$C_{10}H_{21}$	1.6×10^{-4}	7.7×10^{-4}	2.9×10^{-4}	7.7×10^{-4}	2.6×10^{-4}	1.4×10^{-4}	1.2×10^{-4}	1.6×10^{-3}
	$C_{12}H_{25}$	8.6×10^{-5}	1.4×10^{-4}	5.7×10^{-5}	2.2×10^{-4}	7.2×10^{-5}	5.4×10^{-5}	1.4×10^{-4}	2.6×10^{-3}
	$C_{14}H_{29}$	2.2×10^{-4}	6.8×10^{-5}	6.8×10^{-4}	5.4×10^{-5}	7.3×10^{-5}	7.6×10^{-5}	6.6×10^{-5}	
	$C_{16}H_{33}$	1.2×10^{-4}	2.2×10^{-4}	2.8×10^{-4}	1.5×10^{-4}	3.4×10^{-4}	4.0×10^{-4}	1.0×10^{-4}	
	$C_{18}H_{37}$	5.6×10^{-4}	3.4×10^{-4}	2.9×10^{-4}	2.8×10^{-4}	3.2×10^{-4}	8.4×10^{-4}	4.3×10^{-4}	

in free energy per mole per carbon atom in the formation of a micelle. The two types of micelle may therefore have different free energies of micellization, much less below 12 carbon atoms than it is above 12 carbon atoms.

One can measure the slope of these lines and express the results in the same form as was done by Harkins (4), leading to the following statements:

1. For the 4-nitrobenzyl series of these quaternary ammonium salts, a reduction by unity in the number of carbon atoms in the alkyl group multiplies the CMC by a factor of 2.17.

2. For the unsubstituted benzyl series of these quaternary ammonium salts, a reduction by unity in the number of carbon atoms below twelve in the alkyl group multiplies the CMC by a factor of 1.63.

3. For the unsubstituted benzyl series of these quaternary ammonium salts, a reduction by unity in the number of carbon atoms above twelve in the alkyl group multiplies the CMC by a factor of 2.69.

It may be significant that the average of the two factors, 1.63 and 2.69, for the unsubstituted benzyl series is very close to the single value of 2.17 for the 4-nitrobenzyl series.

The factor 2 has been quoted by Harkins for micelles of pure anionic soaps with 7-14 carbon atoms in the chain. From this Debye (3) has calculated the corresponding decrease in free energy in the formation of a soap micelle as 1280 cal./mole/carbon atom.

It has been reported by Hess, Philippoff and Kiessig (5), by Scott and Tartar (6), by Hartley (7), by Stauff (8), and quoted by Harkins (4) that the relation between critical micelle concentration and hydrocarbon chain length for a homologous series of long-chain electrolytes is given by

$$\log \text{CMC} = k_3 N + k_4 \quad 1$$

or, in the equivalent form used by Harkins

$$(\text{CMC})_N / (\text{CMC})_{N'} = B \exp(N' - N) \quad 2$$

where N is equal to the number of carbon atoms in the paraffin chain and k_3 , k_4 , and B are constants. These equations are valid only over a limited range of hydrocarbon chain lengths. The results shown in Fig. 1 add the present quaternary ammonium salts to the growing list of homologs whose behavior can be thus described.

A theoretical model that leads to the equations given above has been developed by Corrin (9). His development is based essentially on the supposition that at the CMC the diffusing tendency of a single molecule inside the micelle is balanced by the gain in surface free energy that would ensue were the molecule removed completely from the micelle. The effect of substituent polar groups in the benzyl ring is to reduce the gain in surface free energy on the separation of the micelle into single molecules. The equilibrium that is represented by the concept of CMC is therefore dis-

placed toward a system of lesser diffusing tendency, i.e., a more concentrated solution. From the viewpoint of molecular structure, the presence of a polar substituent lessens the total hydrophobic character of the molecule and so reduces its tendency to form micelles. The CMC occurs, therefore, at a higher concentration.

The above reasoning leads us to look for some property that measures the degree of polarity of the benzyl portion of the molecule. Measures of this polarity are provided by the boiling points, melting points, dielectric constants, or dipole moments of the substituted toluene compounds that correspond to the benzyl portions of the quaternary ammonium salts. For the compounds studied, these data are collected in Table III.

For a number of these substituted salts, all with 12 carbon atoms in the alkyl group, it was found that the CMC increases as the square of the dipole moment of the corresponding substituted toluene compound (Fig. 6). It is readily seen that variations in the substituent group may do more than merely change the polarity of the total molecule, and the specific action of different chemical groups may account for irregularities when the attempt is made to fit them by the same simple expression. Nevertheless, it is of interest that the 4-nitro substituent should fit so closely to the same relation that describes the monochloro and dichloro substituents. At least for the five compounds shown in Fig. 6, chemical specificity of the substituent group is less significant than the over-all physical polarity of the molecule. The noteworthy exception to the simple relation expressed in Fig. 6 is displayed by the quaternary salt with no substitution in the ring.

The relation depicted in Fig. 6 is expressed by the equation:

$$\text{CMC} = k_1\mu^2 + k_2 \quad 3$$

where k_1 and k_2 are constants and μ is the dipole moment of the substituted toluene compound that corresponds to the benzyl portion of the quaternary ammonium salt. The term in μ^2 is suggestive of a force of interaction between adjacent dipoles, and the trend of the experimental results is in accord with the concept that the greater the force of repulsion between the polar heads of the molecules, the less is the tendency to form micelles.

(b) Molecular Structure and Antibacterial Effect

Figures 4 and 5 for *M. pyogenes* var. *aureus* and *S. typhosa* respectively, have many features in common. They both show the usual optimum antibacterial effect at between 12 and 14 carbon atoms in the alkyl group (10); they both show *increasing* antibacterial effect as more polar substituents are placed in the benzyl group, as long as the alkyl chain is shorter than its optimum value, and they both show a reversal of this trend, namely a *decreasing* antibacterial effect for more polar substitution in the benzyl group, when the alkyl chain is longer than its optimum value. A rationale

TABLE III

Critical Micelle Concentration of Substituted Benzyldimethylaurylammonium Chloride Compared with Physical Properties of the Corresponding Substituted Toluene Compounds

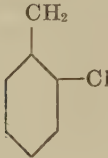


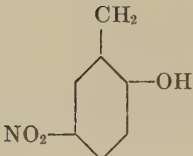
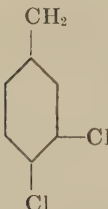

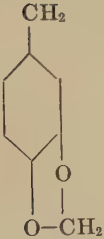
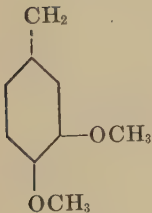

Substitution in benzene ring	Quaternary ammonium salt CMC $\times 10^3$ <i>moles/liter</i>	Corresponding substituted toluenes		
		Melting point °K.	Boiling point °K.	Dipole moment
	0.28	238	432	1.39
	0.37		486	1.78
	0.42	280	435	1.74
	0.69	358		
	1.1		478	2.68

TABLE III—*Concluded*

Substitution in benzene ring	Quaternary ammonium salt CMC $\times 10^3$ moles/liter	Corresponding substituted toluenes		
		Melting point °K.	Boiling point °K.	Dipole moment
	2.43	178	384	0.40
	3.8		471	
	3.9	425	493	
	3.6	324	511	4.40

of this behavior is attempted, based on the colloidal and other physical properties of the substances.

The first of the three characteristic features, i.e., the presence of an optimum antibacterial effect as the length of the alkyl group is varied, is the result of conflicting trends. As the alkyl chain is lengthened, the whole group becomes more hydrophobic. The increasing hydrophobic character of the alkyl group promotes at least two different results. The group itself, and by its action the whole molecule, is increasingly drawn to correspond-

ing hydrophobic interfaces, of which two are closely available. One is the hydrophobic portion of the surrounding molecules and the other is the hydrophobic portion of the bacterial surface. Only the latter attraction conduces to antibacterial action. As the chain length increases, however, the tendency of the molecules to cling together as micelles grows exponentially. The single molecules are increasingly removed from the solution by incorporation in the micelles, presumably at a greater rate than the rate

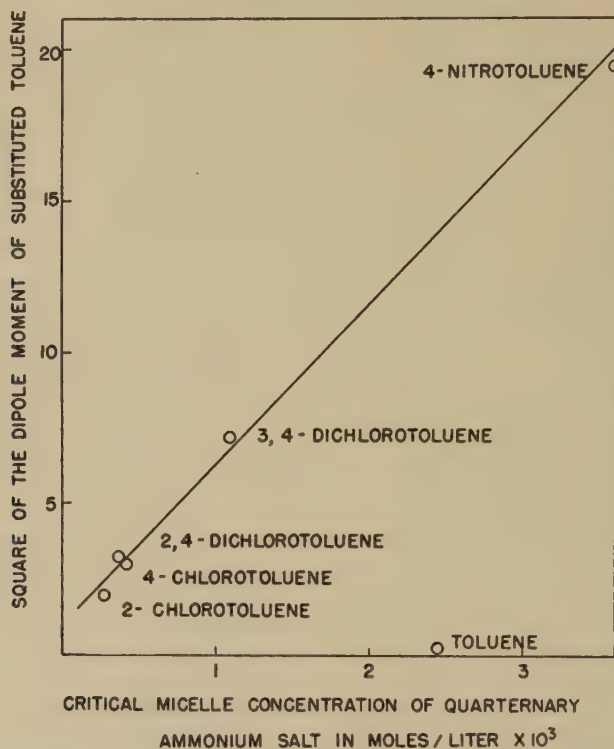


FIG. 6. Relationship between the critical micelle concentration of a series of ring-substituted benzyldimethylalkylammonium chlorides and the square of the dipole moment of the corresponding substituted toluene compound.

of increase of adsorption on a hydrophobic bacterial surface, until the original advantage conferred to the antibacterial properties by lengthening the chain is lost by a concomitant and more active tendency toward association.

The second characteristic feature of the antibacterial effect is the improvement that results from polar substitution in the benzene ring, as long as the alkyl group is shorter than its optimum length. The nature of this effect can be traced in Figs. 4 and 5, but Figs. 7 and 8 give a more striking

demonstration. In these figures the logarithm of the minimum killing concentration is plotted against the logarithm of the dipole moment of the substituted toluene compound that corresponds to the benzyl portion of the quaternary ammonium salt. Toluene itself and its monochloro and dichloro derivatives are included in these figures. The compound that proved exceptional here was not toluene, as happened in Fig. 6, but 4-nitrotoluene,

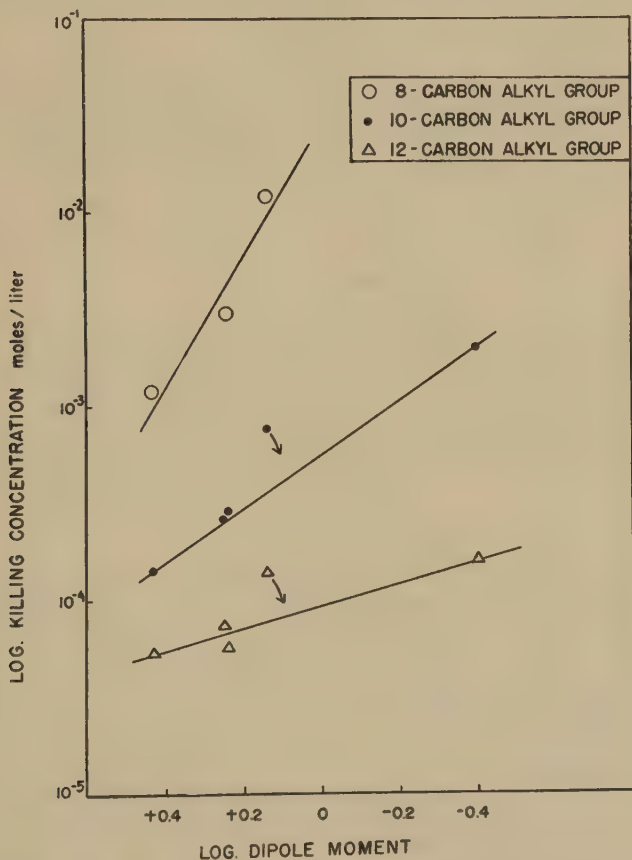


FIG. 7. Relationship between the antibacterial action for *M. pyogenes* var. *aureus* of a series of ring-substituted benzyldimethylalkylammonium chlorides and the dipole moments of the corresponding substituted toluene compounds.

which lies at the opposite extreme of the range of dipole moment values. Figures 7 and 8 also differ from Fig. 6 in the nature of the mathematical function of the dipole moment.

Let us attend for the moment to the similarities between the two types of diagram. We might conclude that by increasing the polar character of the head of the molecule the tendency to form micelles is reduced, and that

this in turn affects the antibacterial action by releasing single molecules to be sorbed by the hydrophobic portions of the bacterial surface. This conclusion makes no claim to be more than a partial explanation. There are unquestionably specific chemical effects that have not been taken into account, as shown, for example, by the unsubstituted benzyl derivative forming fewer micelles than would be predicted by Fig. 6, and by the 4-

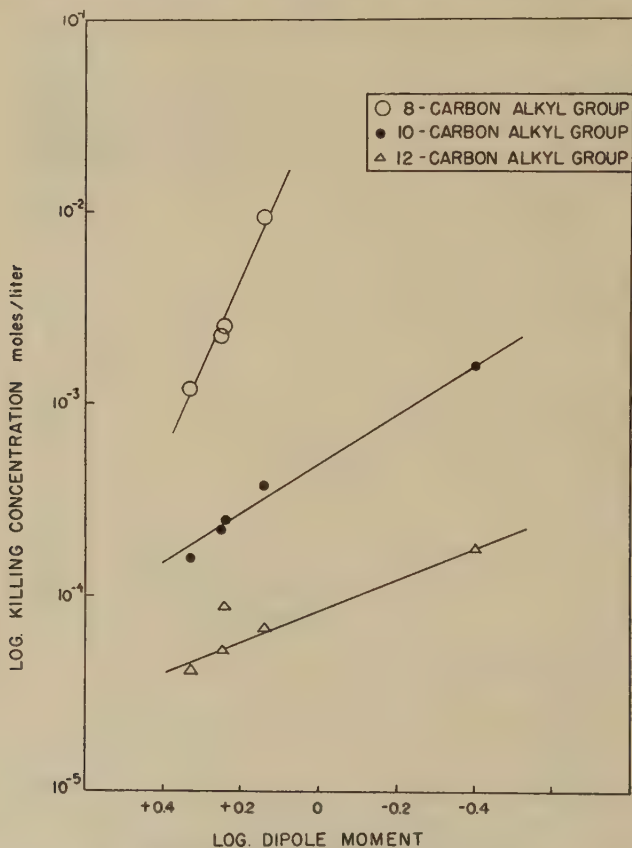


FIG. 8. Relationship between the antibacterial action for *S. typhosa* of a series of ring-substituted benzyldimethylalkylammonium chlorides and the dipole moments of the corresponding substituted toluene compounds.

nitrobenzyl derivative having less antibacterial action than would be predicted by Figs. 7 and 8.

The third characteristic feature of the antibacterial effect occurs with the long alkyl chains, where the extreme degree of micellization has already begun to deprive the substance of its antibacterial action. With these compounds, an increase in the polarity of the benzyl group still

further reduces the antibacterial action. The effect is slight, less pronounced than the reverse tendency noted above for the shorter alkyl chains, but quite definitely present. For the longer chains the effect of polar substituents in the ring on the behavior of the whole molecule must become increasingly less. This is shown in Figs. 7 and 8 by the progressively smaller slopes of the lines as the alkyl chain is lengthened. The cause of the third effect is sought, therefore, not directly in the polarity of the group but in another property that the group acquires with increasing polarity, namely, increasing effective bulk. It is postulated that the long alkyl chains now occupy a relatively large area of the bacterial surface and may prevent, by virtue of their size, other molecules from taking up adjacent adsorption sites. This condition is aggravated by having a bulky benzyl group attached to the nitrogen atom. The polarity of the group is considered to affect the total behavior less significantly than does its effective bulk.

ACKNOWLEDGMENTS

The authors acknowledge the assistance of Mr. E. I. White of the staff of the Sterling-Winthrop Research Institute, who helped with the determination of the minimum killing concentrations, and the following students of Rensselaer Polytechnic Institute, who helped with the determination of the CMC: J. R. Bianchine, P. B. Brock, J. W. Dean, Miss Grace Panza, and A. S. Slowe.

The authors are indebted to Dr. F. C. Nachod, who kindly gave of his time and energy for discussion of the work as it progressed.

REFERENCES

1. CELLA, J. A., EGGENBERGER, D. N., NOEL, D. R., HARRIMAN, L. A., AND HARWOOD, H. J., *J. Am. Chem. Soc.* **74**, 2061 (1952).
2. CORRIN, M. L., AND HARKINS, W. D., *J. Am. Chem. Soc.* **69**, 679 (1947).
3. DEBYE, P., *J. Phys. & Colloid Chem.* **53**, 1 (1949).
4. HARKINS, W. D., *J. Am. Chem. Soc.* **69**, 1428 (1947).
5. HESS, K., PHILIPPOFF, W., AND KIESSIG, N., *Kolloid-Z.* **88**, 40 (1939).
6. SCOTT, A. B., AND TARTAR, H. V., *J. Am. Chem. Soc.* **65**, 692 (1943).
7. HARTLEY, G. S., *Kolloid-Z.* **88**, 22 (1939).
8. STAUFF, J., *Z. physik. Chem.* **183A**, 55 (1938).
9. CORRIN, M. L., *J. Colloid Sci.* **3**, 333 (1948).
10. MOILLIET, J. L., AND COLLIE, B., *Surface Activity*, pp. 287 *et seq.* Spon Ltd., London, 1951.

LIGHT SCATTERING BY SOLUTIONS OF OCTYLTRIMETHYL-AMMONIUM OCTANESULFONATE AND OCTYLTRIMETHYLAMMONIUM DECANESULFONATE

E. W. Anacker

Department of Chemistry, Montana State College

Received October 17, 1952; revised March 13, 1953

ABSTRACT

Molecular weights of micelles of octyltrimethylammonium octanesulfonate in water and octyltrimethylammonium decanesulfonate in water and in aqueous KCl solutions were determined by light scattering. Evidence is presented to show that the aggregates are not spherical.

INTRODUCTION

Light scattering has yielded valuable information concerning the micelles present in solutions of various colloidal electrolytes, such as dodecylammonium chloride (1), *n*-hexadecyltrimethylammonium bromide (2), and sodium dodecyl sulfate (3). Micelles of these substances result from aggregation of either positive or negative paraffin-chain ions. It was thought that an investigation of the light-scattering properties of solutions of colloidal electrolytes consisting of both positive and negative paraffin-chain ions would be of some value in extending our knowledge of micelle structure.

Scott, Tartar, and Lingafelter (4) prepared two double long-chain salts, octyltrimethylammonium octanesulfonate and decyltrimethylammonium decanesulfonate (hereafter designated as C_8-C_8 and $C_{10}-C_{10}$, respectively). They reported that C_8-C_8 is very soluble in water at room temperature and that $C_{10}-C_{10}$ is practically insoluble below 35°C., but that above that temperature it is very soluble, yielding opalescent solutions. Opalescence is an indication of large particles in solution. Its presence in solutions of $C_{10}-C_{10}$ gave added incentive to a study of double long-chain salts by light scattering. Octyltrimethylammonium decanesulfonate (C_8-C_{10}) and decyltrimethylammonium octanesulfonate ($C_{10}-C_8$) were prepared in addition to C_8-C_8 and $C_{10}-C_{10}$, in the hope that they would possess the high solubility at room temperature of the former and the opalescence of the latter.

PREPARATION OF MATERIALS

The long double-chain salts were prepared by mixing equivalent amounts of the appropriate silver alkylsulfonates and alkyltrimethylammonium

bromides dissolved in ethanol or water, filtering off the silver bromide formed, and precipitating the salts by the addition of ethyl ether and cooling. With the exception of C_{10} - C_{10} , the salts were recrystallized at least twice from ethanol-ether mixtures. The C_{10} - C_{10} was recrystallized once from an ethanol-ether mixture and twice from water. Vacuum desiccation and storage over P_4O_{10} completed the preparations.

The silver alkylsulfonates were made from the corresponding sodium alkylsulfonates, which were prepared according to the method of Reed and Tarter (5). Scott and Tarter's method (6) was used to prepare the alkyltrimethylammonium bromides.

The octyl and decyl bromides used to make the silver alkylsulfonates and alkyltrimethylammonium bromides were obtained commercially of

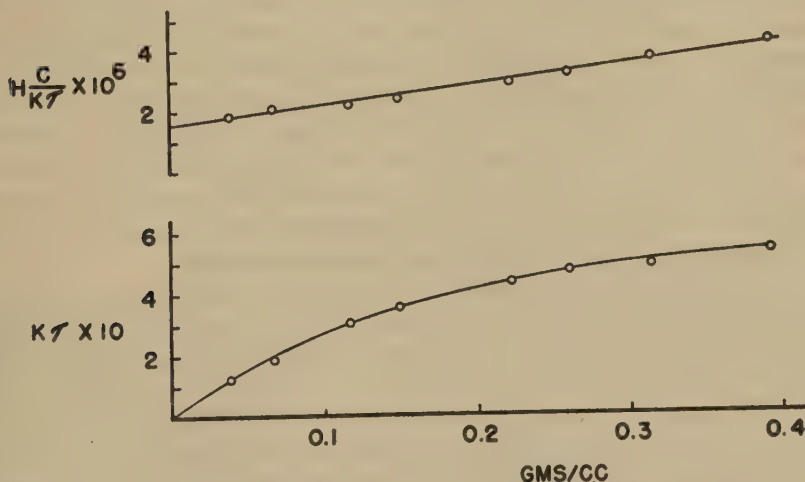


FIG. 1. Calibration of scattering instrument with sucrose solutions.

high purity. Both were further purified by fractional distillation at reduced pressure. The fractions taken had the following boiling points: octyl bromide, 92°C . at 22 ± 2 mm. Hg; decyl bromide, 123°C . at 18 ± 2 mm. Hg.

EXPERIMENTAL METHODS

Except for a few minor differences the scattering instrument used in this work is identical with the one described in an earlier paper (2). The differential refractometer was constructed locally and is similar to the instrument described by P. P. Debye (7).

The scattering instrument was calibrated in the following manner. Aqueous solutions of sucrose were prepared from freshly distilled water and highly purified sucrose (Standard Sample 17—National Bureau of Standards) and filtered through a pyrex, ultrafine, fritted glass funnel.

The 90-degree scattering of each solution was then compared with that of a polished lucite block. Results are plotted in Fig. 1. τ is the solution turbidity minus the water turbidity. C is the sucrose concentration in grams per cubic centimeter. K is the reciprocal "effective" turbidity of the lucite block. A $K\tau$ value for each solution was obtained by dividing the difference in galvanometer readings observed with solution and with water in the scattering cell by the galvanometer reading observed with the reference lucite block in the incident light beam. A galvanometer deflection is proportional to the intensity of the light falling on the phototube of the scattering instrument. From the equation $\frac{1}{342.3} = K \left(H \frac{C}{K\tau} \right)_{C=0}$, K was computed to equal 1.914×10^3 cm.

Solutions of the double long-chain salts were prepared by weighing portions of these substances into volumetric flasks, adding a measured volume of stock KCl solution if the presence of KCl was desired, introducing water, effecting solution, and finally diluting to the mark. After filtration into clean, dust-free test tubes through a pyrex, ultrafine, fritted glass funnel, the solutions were poured as needed and in order of increasing concentration, into the scattering cell. After measurements on a given solution were completed, the cell was drained and the next solution poured in. Prior to use the scattering cell was thoroughly cleaned and continuously rinsed until small-angle scattering had reached a minimum.

As is well known, one transforms light-scattering data into a molecular weight (when no dissymmetry is present) by plotting $H(C/\tau)$ vs. C and taking the intercept of the resulting curve with the ordinate axis as $1/M$. H is the familiar refraction constant (8), C is the concentration of the solute in grams per cubic centimeter, τ is the turbidity, and M is the weight-average molecular weight of the solute particles. With non-electrolytes the plots usually give straight lines. With electrolytes, however, such is not always the case (9, 10), and correct molecular weights may be difficult or impossible to obtain by an extrapolation to zero concentration. Theories pertaining to the scattering of light by solutions of colloidal electrolytes have been advanced by Hermans (11) and Doty and Steiner (12). The point is made that in the conventional theory of light scattering, fluctuations in neighboring volume elements are assumed to be independent. If the solute particles bear a charge, however, this assumption is no longer valid. The long-range coulombic forces tend to establish an ordered distribution, with the result that destructive interference decreases the intensity of the scattered light. If a simple electrolyte is added, the electrical actions of the charged particles will be screened out for long distances, with the result that the long-range order is destroyed and the fluctuation theory again becomes valid. Doscher and Mysels (13) point out that, in the case of association, colloids having a critical micelle concen-

tration, the simple ions present at the critical concentration act as a swamping electrolyte so that molecular weights can be estimated in the conventional manner.

In the present work molecular weights have been determined in the usual manner, with the exception that the reciprocal molecular weight is taken as the intercept of the $H(C - C_0)/\tau$ vs. C plot with a vertical line at the critical micelle concentration, C_0 . The reasoning behind this procedure has been discussed elsewhere (8). Essentially it amounts to designating the solution at the critical concentration as the solvent and the total detergent concentration minus the detergent concentration at the critical concentration as the solute concentration.

A least squares method (originally suggested to the author by Debye) which may be employed to calculate the critical concentration and the best straight-line plot of $H(C - C_0)/\tau$ vs. C from the experimental data is outlined below. The best straight line can be represented by

$$H \frac{C - C_0}{\tau} = A + SC \quad [1]$$

where A is the intercept and S is the slope. Let

$$R_i = H \frac{C_i - C_0}{\tau_i} - A - SC_i \quad [2]$$

where τ_i is the excess turbidity (turbidity of solution minus turbidity of solvent) of a solution of concentration C_i . After squaring both sides of [2] and summing for all¹ experimental points above the critical concentration, we get

$$\begin{aligned} \sum R_i^2 = dH^2 + aH^2C_0^2 + nA^2 + fS^2 + 2bHAC_0 \\ + 2dHC_0S + 2fAS - 2eH^2C_0 - 2dHA - 2hHS \end{aligned} \quad [3]$$

in which n is the number of experimental points used, and

$$\begin{aligned} a = \sum \frac{1}{\tau_i^2}, \quad b = \sum \frac{1}{\tau_i}, \quad d = \sum \frac{C_i}{\tau_i}, \quad e = \sum \frac{C_i^2}{\tau_i^2}, \\ f = \sum C_i, \quad g = \sum C_i^2, \quad \text{and} \quad h = \sum \frac{C_i^2}{\tau_i}. \end{aligned}$$

¹ One can safely choose the points to be used in the least squares calculations from the turbidity versus concentration plot. In general, one uses only those points of the curve which follow the normal trend as typified by similar plots for organic polymer solutions. If the curve exhibits anomalous behavior at high concentrations, data at these concentrations should be excluded from the calculations. When there is a rounding off of the scattering curve in the vicinity of the critical concentration, points in this region are also to be excluded.

If the partial derivatives

$$\frac{\partial \sum R_i^2}{\partial C_0}, \quad \frac{\partial \sum R_i^2}{\partial A}, \quad \text{and} \quad \frac{\partial \sum R_i^2}{\partial S}$$

are taken and set equal to zero and the resulting three equations solved simultaneously, we get

$$C_0 = \frac{e(ng - f^2) - d(bg - fd) + h(bf - nd)}{a(ng - f^2) - b(bg - fd) + d(bf - nd)} \quad [4]$$

$$A = H \frac{a(dg - hf) - b(eg - hd) + d(ef - d^2)}{a(ng - f^2) - b(bg - fd) + d(bf - nd)} \quad [5]$$

$$S = H \frac{a(nh - fd) - b(bh - fe) + d(bd - ne)}{a(ng - f^2) - b(bg - fd) + d(bf - nd)} \quad [6]$$

Since

$$\frac{1}{M} = \left(H \frac{C - C_0}{\tau} \right)_{C=C_0}$$

we have from [1] that

$$M = \frac{1}{A + SC_0} \quad [7]$$

in which C_0 , A , and S are given by [4], [5], and [6].

RESULTS AND DISCUSSION

C_{10} - C_8 and C_{10} - C_{10} "dissolved" in appreciable amounts only at elevated temperatures. Solutions below the critical concentrations were clear and remained so with time. At 40°C. solutions above the critical concentrations were opalescent. The opalescent solutions of C_{10} - C_8 separated rapidly into two clear liquid phases on standing. Opalescent solutions of C_{10} - C_{10} just above the critical concentration separated very slowly into a clear liquid phase and a phase consisting of white cloudy masses. More concentrated solutions of C_{10} - C_{10} remained opalescent on long standing (two weeks or more), but the opalescence became heterogeneous after a day or so. Immediately after preparation, solutions of C_{10} - C_{10} and the water used as a solvent had pH values of 6.5 ± 0.2 . The pH remained unchanged after three days. Opalescent solutions of C_{10} - C_{10} separate into two clear liquid phases on heating above 70°C. Apparently we are concerned with emulsions.

C_8 - C_8 and C_8 - C_{10} were very soluble in water at room temperature. All solutions of these substances were clear.

Transmission measurements at wave lengths ranging from 4000 to 10000 Å. were made with aqueous solutions of C_{10} - C_{10} at $42^\circ \pm 2^\circ\text{C}$. in a

Beckman spectrophotometer. Turbidities were computed from the relationship

$$\tau = -\frac{1}{L} \ln \frac{T}{100}$$

where L is the path length of the primary light beam in the cell (1 cm.) and T is the per cent transmission referred to water at 100 % transmission. Transmission readings were reproducible to within 1 %. After three days standing, solutions above the critical concentration showed signs of phase separation. These solutions after shaking gave transmission values agreeing within 2 % with the values obtained shortly after the solutions were

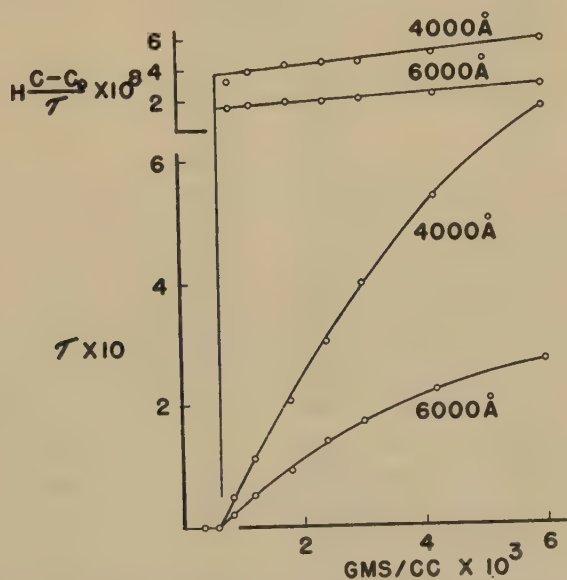


FIG 2. Results of absorption measurements with aqueous solutions of C_{10} - C_{10} .

prepared. Results of measurements made at wave lengths of 4000 and 6000 A. are given in Fig. 2. Since the $H(C - C_0)/\tau$ plots do not have the same intercept, we may conclude superficially that the scattering particles are very large. If the scattering particles consist of emulsion droplets of a liquid phase rich in detergent rather than C_{10} - C_{10} micelles, certain corrections will have to be applied. This can not be done until a phase study of this system is made. Theoretically an extrapolation of $\left(H \frac{C - C_0}{\tau}\right)_{C=C_0}$ values obtained for the different wave lengths to a value for infinite wave length should enable one to compute the particle weight. It is not now clear how this extrapolation should be made. The turbidity curves for the

TABLE I

System	g./100 cc.	$K\tau$	τ (4000 Å.)	τ (6000 Å.)
C ₈ -C ₉ in H ₂ O	0.0551	0.027		
	0.4760	0.002		
	0.8222	0.197		
	1.1400	0.800		
	1.3127	1.08		
	1.7399	1.90		
	1.8750	2.11		
	2.7663	3.22		
C ₈ -C ₁₀ in H ₂ O	0.1374	0.028		
	0.2641	0.314		
	0.4492	1.40		
	0.6196	1.98		
	0.9405	2.67		
	1.1547	2.82		
	1.3080	2.91		
	1.5051	2.91		
	1.7049	2.80		
	2.0243	2.74		
C ₈ -C ₁₀ in 0.0356 <i>M</i> KCl	0.0668	-0.020		
	0.2338	0.121		
	0.2513	0.236		
	0.2893	0.503		
	0.3647	0.979		
	^a 0.4347	1.55		
	0.5816	3.04		
C ₈ -C ₁₀ in 0.178 <i>M</i> KCl	0.0974	0.004		
	0.2001	0.048		
	0.2872	0.745		
	0.3226	1.19		
	0.3834	2.06		
	^a 0.4528	2.95		
	0.5146	4.36		
	0.8263	10.46		
C ₈ -C ₁₀ in 0.265 <i>M</i> KCl	0.0357	0.000		
	0.0770	0.000		
	0.1126	0.000		
	0.1606	0.000		
	0.2527	0.456		
	0.3376	1.43		
	0.3511	1.77		
	0.3849	1.98		
	^a 0.5189	4.89		
	0.6313	6.80		
	0.6577	7.16		
	0.8006	9.63		

TABLE I (continued)

System	g./100 cc.	$K\tau$	$\tau(4000 \text{ \AA.})$	$\tau(6000 \text{ \AA.})$
Sucrose in H_2O	3.927	0.123		
	6.698	0.186		
	11.630	0.305		
	14.877	0.357		
	22.199	0.439		
	26.012	0.471		
	31.431	0.492		
	39.235	0.537		
$\text{C}_{10}\text{-C}_{10}$ in H_2O	0.0359		0.000	0.000
	0.0599		0.000	0.000
	0.0839		0.048	0.020
	0.1198		0.111	0.051
	0.1797		0.206	0.092
	0.2396		0.302	0.139
	0.2995		0.398	0.170
	0.4193		0.540	0.221
	0.5990		0.687	0.270

^a The turbidities of solutions at this concentration and higher decreased somewhat with time immediately after the solutions were introduced into the scattering cell. Final readings were not taken until the scattered intensities appeared to remain constant with time.

longer wave lengths are similar to those appearing in Fig. 2. Calculated turbidities are not as accurate, however, because of the relatively higher transmissions. All turbidity curves show a break at a concentration of 0.00142 M . The critical concentration for $\text{C}_{10}\text{-C}_{10}$ at 40°C . as determined from the conductivity data of Scott *et al.* (4) is 0.00140 M .

A few transmission measurements on solutions of $\text{C}_{10}\text{-C}_8$ at $42^\circ \pm 2^\circ\text{C}$. at a wave length of 4000 \AA . were also made. Because of the rapid separation of phases, reproducible results above the critical concentration could not be obtained. Solutions below a concentration of 0.0050 M , however, were clear and transmitted light as well as did water.

The results of turbidity measurements obtained by 90-degree scattering with solutions of $\text{C}_8\text{-C}_8$ in water and $\text{C}_8\text{-C}_{10}$ in water and aqueous KCl solutions are given in Table I and plotted in Figs. 3 and 4. All runs were made at room temperature ($25\text{--}30^\circ$) and with a wave length of 4358 \AA .

In Fig. 5 are plotted experimental values of $\mu - \mu_0$ as a function of $\text{C}_8\text{-C}_8$ concentration. μ is the refractive index of a solution and μ_0 that of water. The graph consists of two straight lines which intersect at the critical concentration. Since the two straight lines have slopes of approximately the same value, high accuracy in the measurement of $\mu - \mu_0$ is required if a precise determination of the critical concentration is to be obtained from the intersection. Such accuracy was not attained in the present work; accuracy was sufficiently high, however, to show the existence of a break in the curve at or near the critical concentration.

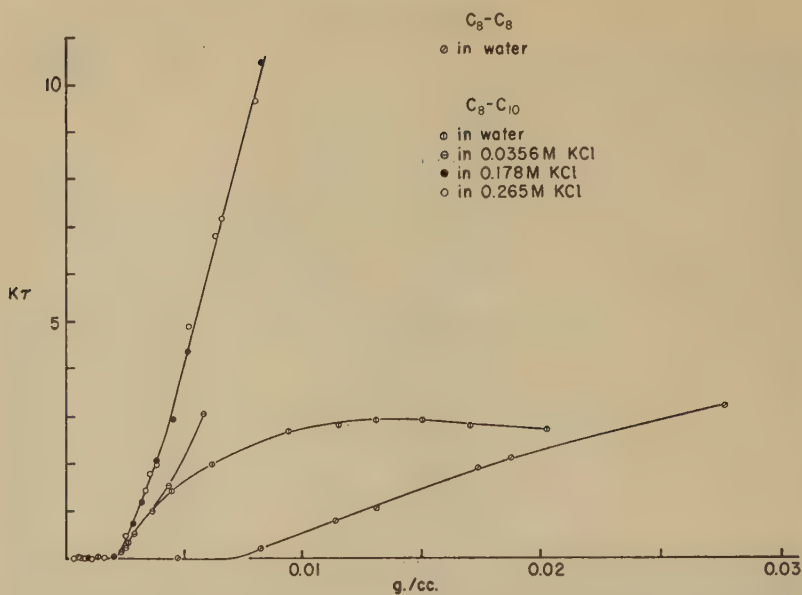


FIG. 3. τ vs. C plots for C_8-C_8 in water and C_8-C_{10} in water and aqueous KCl solutions.

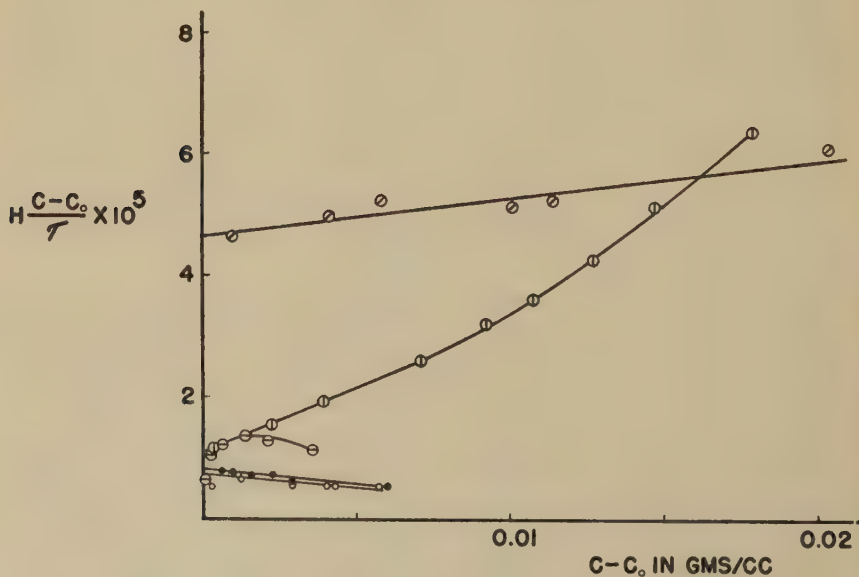


FIG. 4. $H(C - C_0/\tau)$ vs. $C - C_0$ plots for C_3-C_8 in water and C_8-C_{10} in water and in aqueous KCl solutions.

⊙ C_3-C_8 in water

○ C_8-C_{10} in water

⊖ C_8-C_{10} in 0.0356 M KCl

● C_8-C_{10} in 0.178 M KCl

○ C_8-C_{10} in 0.265 M KCl

Molecular weights and critical concentrations for C_8-C_8 and C_8-C_{10} in water were determined by the least squares method described under the section *Experimental Methods*. In the case of C_8-C_{10} in aqueous salt solutions the assumption was made that turbidities just above the critical concentration increased linearly with the concentration. Molecular weights were computed from the slopes of the least squares straight lines. A common straight line for C_8-C_{10} in the two highest salt concentrations was determined from the experimental data. Results are given in Table II. For comparison, values determined in an earlier investigation with a typical cationic detergent are included.

The turbidity curve for C_8-C_8 is similar in appearance to those obtained with cationic detergents, such as *n*-dodecylammonium chloride and *n*-dodec-

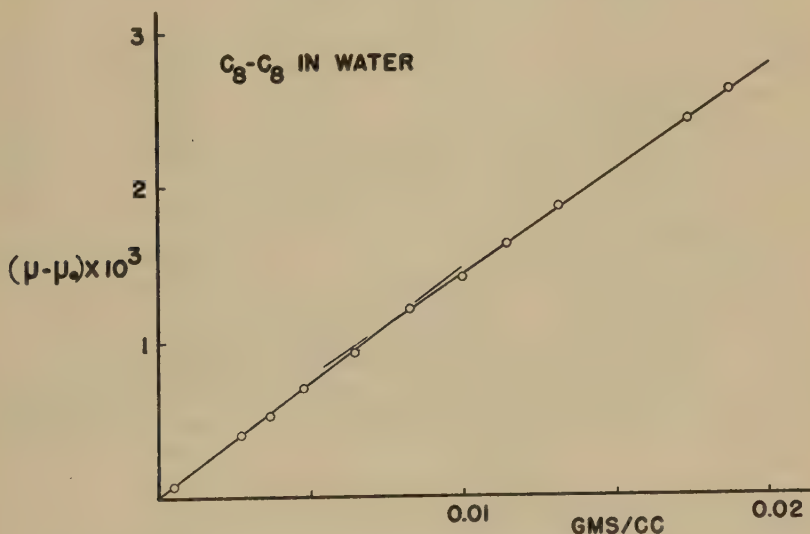


FIG. 5. $\mu - \mu_0$ vs. C plot for C_8-C_8 in water.

yltrimethylammonium bromide (1). The maximum in the C_8-C_{10} -water scattering curve is the first noted for a surface-active agent. Ordering in solution is one possible explanation for this maximum; a decrease in micelle size as the concentration increases is another.

The scattering curves for C_8-C_{10} in aqueous KCl solutions are not easily explained. When small amounts of inorganic salts are added to aqueous solutions of cationic detergents, turbidities and micellar weights usually increase markedly and critical concentrations decrease significantly. The great sensitivity of cationic detergents has been explained elsewhere (8). With C_8-C_{10} relatively large amounts of KCl have little or no influence on the critical concentration. At the same time turbidities and micellar weights are increased up to a point and then become insensitive to ad-

ditional KCl. As insufficient data have been accumulated to completely characterize the role of KCl in its influence on the C_8 - C_{10} micelles, speculation on the salt effect would be unwise.

The ratio of the intensity of the light scattered at 50 degrees to that at 130 degrees was determined for the majority of solutions and found to be 1.08 ± 0.03 . The dissymmetry was not considered to be significant, and consequently specific micelle shapes could not be obtained. That the aggregates are not spherical can be shown, however. Unless permitted to acquire large vacua or the inclusion of polar ends in the interior portion,

TABLE II

System	$\frac{d\mu}{dC} \times 10$	$H \times 10^4$	C_0	M
C_8 - C_8 in H_2O	1.352	5.005	0.0199 M^a	21,600
C_8 - C_{10} in H_2O	1.359	5.052	0.00575 M	89,700
C_8 - C_{10} in 0.0356 M KCl.....		5.008 ^b	0.00573 M^b	92,800
C_8 - C_{10} in 0.178 M KCl.....		4.830 ^b	0.00567 M	138,000
C_8 - C_{10} in 0.265 M KCl.....	1.312	4.722	0.00567 M	141,000
Dodecylammonium chloride in H_2O (1).....			0.0131 M	12,300
Dodecylammonium chloride in 0.04598 M NaCl (1).....			0.00722 M	31,400

^a C_0 (4) = 0.0202 M .

^b Obtained by interpolation.

$$\% \text{ increase in weight of } C_8\text{-}C_{10} \text{ micelles per mole KCl added} = \frac{(141 - 89.7) \times 100}{89.7 \times 0.265} = 216.$$

$$\% \text{ increase in weight of dodecylammonium chloride micelles per mole NaCl added} = \frac{(314 - 123) \times 100}{123 \times 0.04598} = 3,377.$$

$$\% \text{ decrease in } C_0 \text{ for } C_8\text{-}C_{10} \text{ per mole KCl added} = \frac{(575 - 567) \times 100}{575 \times 0.265} = 5.25.$$

$$\% \text{ decrease in } C_0 \text{ for dodecylammonium chloride per mole NaCl added} = \frac{(131 - 72.2) \times 100}{131 \times 0.04598} = 976.$$

spherical micelles are limited geometrically in size. Scott *et al.* (4) calculate that spherical micelles of C_8 - C_8 of the Hartley (14) type—interior of micelle paraffinic in nature and radius equal to length of a hydrocarbon chain—would contain about 13 cations and 13 anions. This corresponds to a molecular weight of less than 5000. The molecular weight obtained by light scattering for micelles of C_8 - C_8 was 21,600. A similar comparison of calculated and observed molecular weights for micelles of C_8 - C_{10} likewise rules out the spherical micelle.

SUMMARY

1. Molecular weights of micelles of C_8 - C_8 in water and C_8 - C_{10} in water and aqueous KCl solutions have been determined.

2. Micelles of C_8-C_8 and C_8-C_{10} are not Hartley spheres.
3. A least squares method for obtaining critical concentrations and particle weights of association colloids has been presented.

ACKNOWLEDGMENTS

The author takes this opportunity to express his sincere gratitude to the Research Corporation for the grant which made this work possible. He also acknowledges his indebtedness to Mr. Harry Bush and to Dr. A. M. Bueche for their part in the construction of the scattering instrument.

REFERENCES

1. ANACKER, E. W., Technical Report CR 2026, Office of Rubber Reserve, Reconstruction Finance Corporation, Washington, D. C. (1949).
2. DEBYE, P. J., AND ANACKER, E. W., *J. Phys. & Colloid Chem.* **55**, 644 (1951).
3. HUTCHINSON, E., Office of Naval Research Technical Report #1, Project #NR 054244 (1951).
4. SCOTT, A. B., TARTAR, H. V., AND LINGAFELTER, E. C., *J. Am. Chem. Soc.* **65**, 698 (1943).
5. REED, R. M., AND TARTAR, H. V., *J. Am. Chem. Soc.* **57**, 570 (1935).
6. SCOTT, A. B., AND TARTAR, H. V., *J. Am. Chem. Soc.* **65**, 692 (1943).
7. DEBYE, P. P., *J. Appl. Phys.* **17**, 392 (1946).
8. DEBYE, P. J., *Ann. N. Y. Acad. Sci.* **51**, 575 (1949).
9. WALL, F. T., DRENAN, J. W., HATFIELD, M. R., AND PAINTER, C. L., *J. Chem. Phys.* **19**, 585 (1951).
10. FUOSS, R. M., AND EDELSON, D., *J. Polymer Sci.* **6**, 767 (1951).
11. HERMANS, J. J., *Rec. trav. chim.* **68**, 859 (1948).
12. DOTY, P., AND STEINER, R. F., *J. Chem. Phys.* **17**, 743 (1949).
13. DOSCHER, T. M., AND MYSELS, K. J., *J. Chem. Phys.* **19**, 254 (1951).
14. HARTLEY, G. S., Aqueous Solutions of Paraffin Chain Salts. Hermann et Cie., Paris, 1936.

THE SPECIFIC AND PARTIAL SPECIFIC VOLUMES OF POTASSIUM LAURATE AND LAURYL SULFONIC ACID IN AQUEOUS SOLUTIONS

Hira Lal

Division of Physical Chemistry, The National Chemical Laboratory of India, Poona

Received January 15, 1953; revised April 6, 1953

NOTATION

v_0	= Specific volume of solvent.
v	= Specific volume of solution.
\bar{v}_2	= Partial specific volume of the solute.
m	= Molal concentration.
x	= Concentration in grams of soap per gram of solution.
$c.m.c.$	= Critical concentration of micelle formation.
g	= Osmotic coefficient.
t	= Temperature in $^{\circ}\text{C}$.
a, b	= Constants.

ABSTRACT

The specific and partial specific volume data for potassium laurate and lauryl sulfonic acid at 25° and 0.2°C . are presented. An empirical equation has been formulated which relates the specific volumes with the osmotic coefficients of colloidal electrolytes.

INTRODUCTION

In our studies on the moving boundary electrophoresis of colloidal electrolytes using concentration boundaries (1), it became desirable to correct the position of the boundaries for solvent displacement. This required a knowledge of the partial molal volumes of the electrolytes, especially at 0°C . A survey of the literature showed that these data for colloidal electrolytes were meager. Kirkby (2) determined the specific volumes of lauryl sulfonic acid solutions at 25°C . Bury and Parry (3) showed that the specific volume of potassium laurate at 25°C . changed rapidly in a narrow concentration region in the neighborhood of the $c.m.c$. We have investigated potassium laurate and lauryl sulfonic acid in aqueous solutions at 25° and 0.2°C .; the results are reported in the present communication.

EXPERIMENTAL

Lauryl sulfonic acid used was the same as prepared by M. E. Synerholm and used by McBain and co-workers in other investigations (4). Lauric acid (equivalent weight = 200.8) obtained from trilaurin was converted into

potassium laurate by neutralizing an acetone solution of lauric acid with its equivalent of alcoholic potassium hydroxide. The final product crystallized from alcohol-acetone mixture as white flakes. The trilaurin (5) was extracted from *pisa* seeds (*Actinodaphne Hookeri*) and thrice crystallized from absolute alcohol.

The solutions were made with CO_2 -free distilled water by weighing, corrections being made for buoyancy. To suppress hydrolysis, potassium laurate solutions contained 4 eq. % excess of potassium hydroxide on the basis of soap. A concentrated lauryl sulfonic acid solution was estimated by titration, and solutions were prepared by successive dilutions.

TABLE I
The Specific Volume of Aqueous Potassium Laurate

<i>m</i>	$25 \pm 0.02^\circ\text{C.}$		$0.2 \pm 0.1^\circ\text{C.}$		<i>x</i>
	<i>v</i>	$10^3\Delta v^a$	<i>v</i>	$10^3\Delta v^a$	
0.4324	0.99402	-2	0.98888	+28	0.09337
0.3835	0.99510	+16	0.98999	+23	0.08376
0.3339	0.99596	+8	0.99107	+8	0.07367
0.2919	0.99664	-6	0.99200	-4	0.06501
0.2285	0.99792	-4	0.99365	-1	0.05163
0.1692	0.99904	-6	0.99506	-6	0.03875
0.1192	1.00007	-2	0.99636	-1	0.02762
0.0835	1.00080	-4	0.99730	+4	0.01951
0.0625	1.00124	-3	0.99785	+9	0.01468
0.0455	1.00167	+10	0.99835	+9	0.01072
0.0322	1.00191	+4	0.99878	+7	0.00785
0.0168	1.00237	0	0.99942	+1	0.00398
0.00744	1.00268	-1	0.99982	+1	0.00177
0.00288	1.00287	+1	1.00003	+1	0.000686
0.00000	1.00296	—	1.00015	—	0.000000

^a *v* observed minus the value computed from Eq. [2].

The pycnometer consisted of a 12-cm. capillary stem (internal diameter ~ 1.5 mm.) fused into a 25-ml. Pyrex bulb. The capillary stem carried a mark to which all volumes were referred. The pycnometer was calibrated at $25 \pm 0.02^\circ\text{C.}$ and $0.2 \pm 0.1^\circ\text{C.}$ with CO_2 -free distilled water. An electronically controlled thermostat was used for maintaining the former temperature and an ice bath, for the latter. The procedure consisted in filling the pycnometer with a known weight of the solution; bringing it to the required temperature; and measuring the level of the meniscus with respect to the reference mark. From this, the volume of a given weight of the solution and, hence, its specific volume could be evaluated. The results, corrected for the small additions of potassium hydroxide in case of potassium laurate solutions, are given in Tables I and II and plotted in Fig. 1.

Excellent agreement is indicated between our results and those of Bury

TABLE II
The Specific Volume of Aqueous Lauryl Sulfonic Acid

w	25 ± 0.02°C.		0.2 ± 0.1°C.		s
	v	10 ⁴ Δs ^o	v	10 ⁴ Δs ^o	
0.5182	0.99767	+13	0.99248	+29	0.11473
0.3499	0.99912	-3	0.99480	+21	0.08046
0.2545	1.00012	-1	0.99605	+5	0.05984
0.1840	1.00080	-8	0.99717	+8	0.04400
0.1309	1.00138	-7	0.99790	-5	0.03170
0.0946	1.00189	+4	0.99849	-4	0.02310
0.0607	1.00223	+3	0.99906	+1	0.01494
0.0404	1.00247	+6	0.99936	-1	0.01002
0.0234	1.00264	+4	0.99967	+6	0.00582
0.0135	1.00273	+3	0.99979	+3	0.00338
0.00787	1.00280	+1	0.99987	-1	0.00196
0.00347	1.00288	0	1.00004	+1	0.000866
0.00137	1.00293	0	1.00011	0	0.000343
0.00000	1.00296	—	1.00015	—	0.000000

^ov observed minus the value computed from Eq. [3].

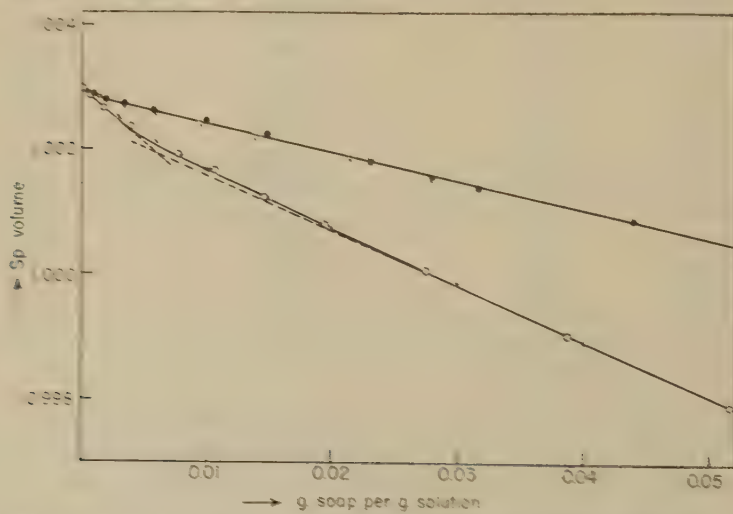


FIG. 1. The specific volume vs. concentration, for potassium laurate and lauryl sulfonic acid at 25°C.

- potassium laurate (this work)
- ×— potassium laurate (Bury and Parry)
- lauryl sulfonic acid (this work)
- △— lauryl sulfonic acid (Kirkby)

and Parry [3] for potassium laurate solutions at 25°C. Our results for lauryl sulfonic acid solutions at 25°C., however, differ somewhat from those

of Kirkby (2), especially for the more concentrated solutions. This difference, which may be as much as 0.00010 for 10 % lauryl sulfonic acid, is probably due to uncertainty in the determination of concentration of lauryl sulfonic acid solutions.

DISCUSSION

The specific volume-composition graphs (Fig. 1) consist largely of two straight lines intersecting in the region of the critical concentration for micelle formation. These points of intersection correspond to x values of 0.008 and 0.002 for potassium laurate and lauryl sulfonic acid solutions, respectively¹. The results are similar to those reported by Davies and Bury for potassium *n*-octoate (6).

TABLE III

The Partial Specific Volume of Potassium Laurate in Aqueous Solutions

x	\bar{v}_2 at 25°C.	\bar{v}_2 at 0.2°C.
0.001	0.849	0.809
0.002	0.849	0.809
0.003	0.862	0.809
0.004	0.870	0.821
0.005	0.879	0.830
0.006	0.886	0.841
0.007	0.893	0.845
0.008	0.896	0.851
0.009	0.899	0.858
0.010	0.901	0.863
0.012	0.904	0.873
0.015	0.906	0.879
0.020	0.910	0.884
0.030	0.913	0.887
0.050	0.913	0.887
0.070	0.913	0.887
0.090	0.913	0.887

The relatively sharp change of slope in the v - x graphs near the *c.m.c.* corresponds to an equally sharp change in the partial specific volume of the colloidal electrolytes. The partial specific volume data for potassium laurate are given in Table III and plotted in Fig. 2 as a function of concentration. The partial specific volumes were calculated from the equation,

$$\bar{v}_2 = v + (1 - x) \frac{dv}{dx}, \quad [1]$$

dv/dx being evaluated graphically from the v - x curves. It is clear that the partial specific volume of potassium laurate increases sharply near the

¹ The *c.m.c.* for potassium laurate is 0.035 *m* and 0.024 *m* at 0° and 25°C., respectively. The *c.m.c.* for lauryl sulfonic acid is 0.010 *m* and 0.0085 *m* at 0° and 25°C., respectively (7).

c.m.c. and becomes constant at $x \sim 0.03$, the region of complete micelle formation (8).

The evaluation of the partial specific volume of lauryl sulfonic acid near the *c.m.c.* presents difficulties in that the *c.m.c.* has a low value and dv/dx changes even more rapidly than is the case with potassium laurate solutions. As a result, it can only be stated that the partial specific volume of

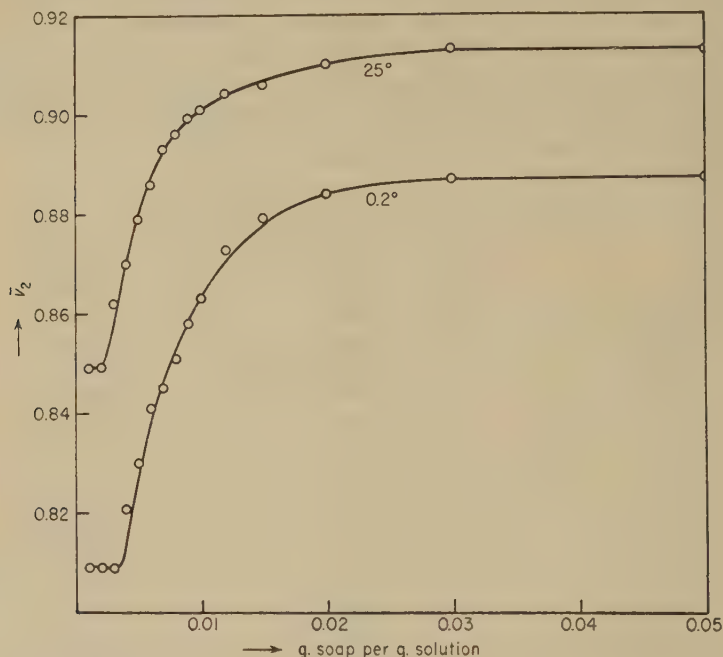


FIG. 2. Partial specific volume of potassium laurate in aqueous solutions.

TABLE IV

	<i>t</i>	10 ³ <i>a</i>	10 ³ <i>b</i>
Potassium laurate	25	154	73
Potassium laurate	0.2	191	84
Lauryl sulfonic acid	25	91.4	51.5
Lauryl sulfonic acid	0.2	135.0	77.0

lauryl sulfonic acid at 25°C. increases from 0.912 to 0.956 as the *c.m.c.* is exceeded, the corresponding values at 0.2°C. being 0.865 and 0.935. This agrees well with the values of 0.910 and 0.960 calculated from the data of Kirkby for lauryl sulfonic acid at 25°C.

It may, therefore, be concluded that the partial specific volume of colloidal electrolytes increases sharply with the aggregation of ions to form micelles. It should, therefore, be possible to correlate the specific and,

hence, the partial specific volume of a colloidal electrolyte with any of its colligative properties. Thus, for colloidal electrolytes with a low *c.m.c.*, the specific volume may be related to the osmotic coefficient by the following empirical equation.

$$v = v_0 (1 - ax) \{ 1 + b (1 - g)x \} \quad [2]$$

The constants *a* and *b* are given in Table IV for potassium laurate and lauryl sulfonic acid solutions.

The specific volumes computed² from Eq. [2] are represented in Tables I and II as the differences between the observed and the computed values. The agreement is good in view of the fact that osmotic coefficients cannot be determined with the same degree of accuracy as the specific volumes. The rather large deviations at higher concentrations are probably due to a slight minimum observed at such concentrations in the *g*-*x* curves.

The computation of partial specific volumes requires the differentiation of Eq. [2] to give *dv/dx*. The impracticability of such a procedure is obvious since, to our knowledge, no simple relation representing the variation of the osmotic coefficient with the concentration of a colloidal electrolyte exists. The problem is being investigated and will form the subject matter for a separate communication.

ACKNOWLEDGMENTS

The author is grateful to (the late) Professor J. W. McBain and to Dr. S. S. Marsden for their interest in this work.

REFERENCES

1. LAL, H., *Nature* **171**, 175 (1953).
2. KIRKBY, H. E., M.A. Thesis (Stanford University).
3. BURY, C. R., AND PARRY, G. A., *J. Chem. Soc.* **1935**, 626.
4. See, for example, MCBAIN, M. E. L., DYE, W. B., AND JOHNSTON, S. A., *J. Am. Chem. Soc.* **61**, 3210 (1939).
5. PUNTAMBEKAR, S. V., AND KRISHNA, S., *J. Indian Chem. Soc.* **10**, 395 (1933).
6. DAVIES, G. D., AND BURY, C. R., *J. Chem. Soc.* **1930**, 2263.
7. BRADY, A. P., AND HUFF, H., *J. Colloid Sci.* **3**, 511 (1948).
8. GREEN, A. A., AND MCBAIN, J. W., *J. Phys. & Colloid Chem.* **51**, 286 (1947).
9. BRADY, A. P., HUFF, H., AND MCBAIN, J. W., *J. Phys. & Colloid Chem.* **55**, 304 (1951).

² For potassium laurate solutions at 25° and 0.2°C., the osmotic data of Brady, Huff, and McBain (9) at 30°C. and 0°C. were used. For lauryl sulfonic acid solutions at 25°C. and 0.2°C., the osmotic data of McBain, Dye, and Johnston (4) at 0°C. were used.

THERMODYNAMICS OF ELECTROKINETIC PHENOMENA

J. Th. G. Overbeek*

*Metallurgy Department, Massachusetts Institute of Technology,
Cambridge, Massachusetts*

Received April 6, 1953

ABSTRACT

The thermodynamics of irreversible processes are applied to electrokinetic experiments. By investigating the correlation between fluctuations in volume and charge in an electroosmosis cell, the Onsager relation for this case is derived. From this and the empirical equation relating flow of liquid and electricity to pressure and potential difference, general relations between electrokinetic effects are derived, showing that for a given system the total electrokinetic behavior is described only by one coefficient. From an application of the same method to the case of suspended particles, relations between electrophoresis and sedimentation are derived.

Attention is drawn to electrokinetic corrections to be applied to the coefficients of permeation or of sedimentation in the form in which they are usually determined.

I. INTRODUCTION

Experiments on electrokinetics usually are interpreted in terms of the ζ -potential. Recently it has become clear that this is an oversimplification. Except when the thickness of the electrical double layer is small compared to the size of particles or pores under investigation, corrections have to be applied to the simple Helmholtz-Smoluchowski equations. Although several attempts have been made, it has not yet been possible to calculate these corrections accurately. A general survey of these attempts has been made by the present author (1), electrophoresis has been investigated by Henry (2), Overbeek (3) and Booth (4), and electroosmosis and streaming potential by Rutgers and DeSmet (5) and by Overbeek and van Est (6).

The question arises as to whether in these more complicated situations some electrokinetic techniques may have advantages over others or whether they all give essentially the same information.

Since all electrokinetic processes are irreversible, this is the type of problem to which the thermodynamics of irreversible processes can be applied. With the aid of this relatively recently developed doctrine, it has been found possible to derive a number of general relations between different electrokinetic processes and to show that for a given system there exists only one electrokinetic coefficient that can be determined by any one of the electrokinetic experiments.

* Visiting Professor in the Massachusetts Institute of Technology.

II. THE METHOD OF FLUCTUATIONS

This is not the place to treat the fundamentals of the thermodynamics of irreversible processes (7, 8, 9, 10) extensively; however, a brief discussion of the method, as applied to the present case, seems pertinent.

Electrokinetic experiments can be performed on two different types of systems: one, where a liquid moves through a capillary or through the pores of a plug or diaphragm, and the other, where particles (usually solid) move through a liquid that is kept stationary by a surrounding vessel. We shall treat the first system, that is, the one for electroosmosis and streaming potential, completely, and after that the second one, on electrophoresis and sedimentation, only in passing.

The system (see Fig. 1) consists of two reservoirs, I and II, connected by a capillary or diaphragm. The reservoirs are partially filled with an electrolyte solution. The electrical potential and the pressure in the left-hand reservoir are designated E and P , respectively. Potential and pressure in

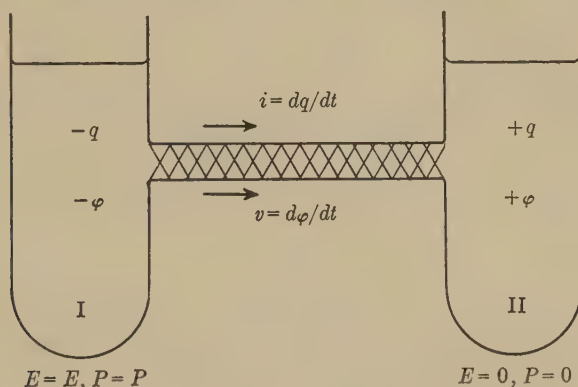


FIG. 1. Cell for electroosmosis and streaming potential.

the right-hand reservoir are assumed to be zero. The right-hand reservoir contains a charge q and a volume of liquid φ in excess of the volume at equilibrium. Charge and excess volume of the left-hand reservoir are $-q$ and $-\varphi$ respectively.

The electric current i through the diaphragm is equal to dq/dt . The hydrodynamic current (volume passing through the diaphragm) is $v = d\varphi/dt$.

If the treatment is limited to the linear region, the most general relations (11) between the "currents" i and v and the "forces" E and P are:

$$\begin{aligned} i &= L_{11}E + L_{12}P \\ v &= L_{21}E + L_{22}P \end{aligned} \quad [1]$$

where L_{ij} are constants.

Considering now small (thermal) fluctuations q and φ , we may ask for the relation between a fluctuation q at time t and a fluctuation φ at $t + \tau$, τ being a time that is short as compared to the time necessary for the decay of a fluctuation.

As a result of the insensitivity of all equations of motion to a change in the sign of the time, a completely equivalent system is obtained by changing the sign but not the value of all velocities of ions, molecules, electrons, etc. Consequently, the average relationship between $q(t)$ and $\varphi(t + \tau)$ must be the same as that between $q(t)$ and $\varphi(t - \tau)$. Thus,

$$\overline{q(t)\varphi(t + \tau)} = \overline{q(t)\varphi(t - \tau)} \quad [2]$$

or, shifting all the times at the right-hand side by τ , we get

$$\overline{q(t)\varphi(t + \tau)} = \overline{q(t + \tau)\varphi(t)} \quad [3]$$

in which the bar denotes that the average has to be taken over the time, t . Subtracting the average value of $q(t)\varphi(t)$ from both sides, we get

$$\overline{q(t)[\varphi(t + \tau) - \varphi(t)]} = \overline{\varphi(t)[\varphi(t + \tau) - q(t)]}. \quad [4]$$

If we assume that on the average fluctuations die out in agreement with the macroscopic laws as given in Eq. [1], Eq. [4] can be replaced by

$$\overline{q(t) \left(\frac{d\varphi}{dt} \right) \tau} = \overline{\varphi(t) \left(\frac{dq}{dt} \right) \tau} \quad [5]$$

or

$$\overline{qv} = \overline{\varphi i}. \quad [6]$$

If we substitute v and i from Eq. [1], this becomes

$$L_{21} \overline{qE} + L_{22} \overline{qP} = L_{11} \overline{\varphi E} + L_{12} \overline{\varphi P}. \quad [7]$$

Now the fluctuations in charge and pressure (at the same moment) or in volume and electric potential are independent of each other. Consequently,

$$\overline{qP} = \overline{\varphi E} = 0. \quad [8]$$

But there is an obvious correlation between the fluctuation in charge and potential or between volume and pressure. Considering¹ the combinations charge and potential or volume and pressure as degrees of freedom of the system, the average potential energy in such a degree of freedom, according to the law of equipartition, is equal to $\frac{1}{2} kT$, and thus,

$$\overline{qE} = \overline{\varphi P} = -kT. \quad [9]$$

¹ It is realized that this is not a completely rigorous proof, but it comes as close to it as is possible without actually performing the necessary calculations of statistical mechanics. See, e.g., De Groot (9) p. 13 ff.

From [7], [8], and [9] *Onsager's* relation

$$L_{12} = L_{21}$$

immediately follows.

III. CONCLUSIONS FROM COMBINATION OF THE PHENOMENOLOGICAL EQUATIONS WITH THE ONSAGER RELATION

With the system as described, four different experiments in electrokinetics can be performed (plus an infinite number of combinations), namely, rate of electroosmosis at zero pressure, electroosmotic pressure at zero rate of flow, streaming potential (at zero current), and streaming current (at zero potential difference). These phenomena can be expressed as functions of current, potential difference, flow of liquid, or pressure difference, leading to eight electrokinetic coefficients. Because of the existence of the Onsager relation these coefficients are pairwise equal.

The coefficient for streaming potential is found by putting $i = 0$ in Eq. [1], and thus

$$(E/P)_{i=0} = -L_{12}/L_{11}, \quad [10]$$

$$(E/v)_{i=0} = \frac{-L_{12}}{L_{11} L_{22} - L_{12} L_{21}}. \quad [11]$$

For the rate of electroosmosis when $P = 0$,

$$(v/i)_{P=0} = L_{21}/L_{11}, \quad [12]$$

$$(v/E)_{P=0} = L_{21}. \quad [13]$$

Similarly it is found that for the streaming current when $E = 0$,

$$(i/P)_{E=0} = L_{12}, \quad [14]$$

$$(i/v)_{E=0} = L_{12}/L_{22}, \quad [15]$$

and for the electroosmotic pressure when $v = 0$,

$$(P/E)_{v=0} = -L_{21}/L_{22}, \quad [16]$$

$$(P/i)_{v=0} = \frac{-L_{21}}{L_{11} L_{22} - L_{12} L_{21}}. \quad [17]$$

It appears that the absolute values of these coefficients are pairwise equal; e.g.,

$$(E/P)_{i=0} = -(v/i)_{P=0}, \quad [18]$$

$$(i/P)_{E=0} = (v/E)_{P=0}. \quad [19]$$

But regardless of what experiment is done or what combination is chosen, the system is described completely by the three constants L_{11} , L_{22} , and $L_{12} =$

L_{21} . Of these constants, L_{11} represents the electric conductance, L_{22} the hydrodynamic conductance, and the cross coefficient $L_{12} = L_{21}$ the electrokinetic effect.

Incidentally, the coefficient L_{12} , when interpreted in the usual way in terms of the ζ -potential, is given by

$$L_{12} = \epsilon \zeta A / 4\pi\eta,$$

where ϵ represents the dielectric constant, ζ the ζ -potential, η the viscosity, and A the effective cross section through the diaphragm.

Consequently there is no reason to do more than one electrokinetic experiment with a given system, and the choice is determined by convenience or by reasons of accuracy rather than by principle. At high conductivity of the liquid (L_{11} large), for instance, the streaming potential will be extremely low and difficult to determine, whereas the streaming current will have a normal value; thus, although both experiments lead to the same quantity L_{12} , the second may be preferred.

Incidentally, it is easy to see that it makes a difference whether electrical conductance is measured at zero flow or at zero pressure difference, for

$$\left(\frac{i}{E}\right)_{P=0} = L_{11}, \quad [20]$$

but

$$\left(\frac{i}{E}\right)_{v=0} = L_{11} - \frac{L_{12} L_{21}}{L_{22}}. \quad [21]$$

The correction may be considerable when the pores are narrow and the major transport of electricity takes place in the form of electroosmosis, included in L_{11} but eliminated in $(i/E)_{v=0}$.

For the hydrodynamic resistance a similar conclusion can be drawn; this resistance is smaller when short-circuited electrodes connect the two reservoirs than when no electric current is allowed to flow in an outside circuit.

$$\left(\frac{v}{P}\right)_{E=0} = L_{22}; \quad [22]$$

$$\left(\frac{v}{P}\right)_{i=0} = L_{22} - \frac{L_{12} L_{21}}{L_{11}}. \quad [23]$$

There need be no fear that the correction terms may become larger than the main term because if $L_{12}L_{21} > L_{11}L_{22}$, a combination of values of P and E could be found which would make the energy dissipation $iE + Pv$ negative, and this would be in disagreement with the second law of thermodynamics.

IV. SUSPENDED PARTICLES

In the case of suspended particles the "currents" and "forces" that are most easy to handle are the electric current density, i , and the electric field strength, E , on the one hand, and the velocity, v , of the center of

gravity of the system (with respect to the vessel in which it is contained) and the centrifugal or gravitational acceleration, g , multiplied by the density, d , on the other hand.

The phenomenological or empirical equations are now:

$$\begin{aligned} i &= L_{11}E + L_{12}dg; \\ v &= L_{21}E + L_{22}dg. \end{aligned} \quad [24]$$

It can again be proved² that

$$L_{12} = L_{21} \quad [25]$$

In order to apply these equations successfully, the velocity of the center of gravity, which is not measured directly, has to be converted into other quantities. For colloidal systems the velocity of the particles, neglecting the motions of all other ions, is a suitable choice. In systems containing only electrolytes the motion of all charged particles expressed by the transport numbers, and the volume changes near the electrodes have to be introduced.

In the colloid case, designating the velocity of the particles U , we find with good approximation.

$$vd = U C_p(1 - V_p d_{sol}) \quad [26]$$

where C_p is the concentration of particles in grams per milliliter; V_p , the specific volume of the particles; and d_{sol} , the density of the particle-free solution.

If we combine Eq. [26] with [24] and use the Onsager relation [25], the following relations between electrophoresis and sedimentation (or centrifugation) potential or current are easily derived:

$$\left(\frac{U}{E}\right)_{g=0} = \left[\frac{i}{C_p(1 - V_p d_{sol})g}\right]_{E=0} \quad [27]$$

electrophoretic velocity sedimentation current

$$\left(\frac{U}{i}\right)_{g=0} = \left[\frac{-E}{C_p(1 - V_p d_{sol})g}\right]_{i=0} \quad [28]$$

electrophoretic velocity sedimentation potential

² It will be clear that a judicious choice of currents and forces is necessary to obtain the relationship again in this simple form. The criterion for the choice is that the sum of the products of currents and forces have to be equal to the absolute temperature times the entropy production. In this case

$$T \frac{dS}{dt} = iE + vd g.$$

See Onsager (7), Casimir (8), De Groot (9), and Prigogine (10); and for this particular case, De Groot, Mazur, and Overbeek (12).

These relations show that the measurement of sedimentation potential or current gives the same information as that of electrophoretic velocity and that the choice between the methods should be governed by convenience and not by principle. The derivation given shows that the validity of the relations [27] and [28] is independent of the possibility to express the electrokinetic coefficients by an explicit formula, as for instance $(U/E)_{g=0} = \epsilon \zeta / 4\pi\eta$.

Again, as in the case of the liquid moving through a plug, we may remark here that the sedimentation constant U/g will depend on whether the cell contains two short-circuited electrodes or not.

In fact,

$$\left(\frac{U}{g}\right)_{g=0} = \frac{d^2}{C_p(1 - V_p d_{sol})} \left(L_{22} - \frac{L_{12}L_{21}}{L_{11}}\right); \quad [29]$$

$$\left(\frac{U}{g}\right)_{g=0} = \frac{d^2}{C_p(1 - V_p d_{sol})} L_{22} \quad [30]$$

In the usual sedimentation or centrifugal experiments the first rather than the second coefficient is determined, and it is easily seen that the correction term becomes small when (1) the experiment is carried out near the isoelectric point (L_{12} is small), (2) at low colloid concentration ($L_{12}::C_p$), or (3) at high conductivity (L_{11} is large).

In a consideration of solutions of electrolytes not containing colloid particles, Eq. [26], which only takes account of the motion of one kind of particles, is not valid any more. The velocity of the center of gravity has now to be connected with the mobilities of all species present. Moreover, the volume changes at the electrodes give rise to displacements comparable to those caused by the sedimentation. If all this is taken into account, a relation between the sedimentation potential and the transport numbers can be derived, which was already known from Des Coudres' (13) work and which has been used again recently by MacInnes and Ray (14).

REFERENCES

1. KRUYT, H. R., *Colloid Science*, Vol. I, p. 194 ff. Elsevier Publishing Co., Amsterdam, New York, 1952.
2. HENRY, D. C., *Proc. Roy. Soc. (London)* **133**, 106 (1931); *Trans. Faraday Soc.* **44**, 1021 (1948).
3. OVERBEEK, J. TH. G., *Kolloid-Beih.* **54**, 287 (1943); *Advances in Colloid Science* **3**, 97-135 (1950).
4. BOOTH, F., *Nature* **161**, 83 (1948); *Proc. Roy. Soc. (London)* **A203**, 514 (1950); *Trans. Faraday Soc.* **44**, 955 (1948).
5. RUTGERS, A. J., AND DE SMET, M., *Trans. Faraday Soc.* **41**, 758 (1945); *ibid.* **43**, 102 (1947).
6. OVERBEEK, J. TH. G., AND VAN EST, W. T., *Proc. Koninkl. Ned. Akad. Wetenschap.* **A55**, 347 (1952).

7. ONSAGER, L., *Phys. Rev.* **37**, 405 (1931); *ibid.* **38**, 2265 (1931).
8. CASIMIR, H. B. G., *Rev. Modern Phys.* **17**, 343 (1945).
9. DE GROOT, S. R., *Thermodynamics of Irreversible Processes*. North-Holland Publishing Company, Amsterdam, and Interscience Publishers Inc., New York, 1951.
10. PRIGOGINE, I., *Étude thermodynamique des phénomènes irréversibles*. Liège, 1947.
11. MAZUR, P., AND OVERBEEK, J. TH. G., *Rec. trav. chim.* **70**, 83 (1951).
12. DE GROOT, S. R., MAZUR, P., AND OVERBEEK, J. TH. G., *J. Chem. Phys.* **20**, 1825 (1952).
13. DESCOUTDRES, TH., *Ann. Physik u. Chem.* **49**, 284 (1892); *ibid.* **57**, 232 (1896).
14. MACINNES, D. A., AND RAY, B. R., *J. Am. Chem. Soc.* **71**, 2987 (1949).

ELECTRICAL CONDUCTANCE OF SOME PARAFFIN-CHAIN SALTS IN PROPANOL-WATER AND PROPIONIC ACID-WATER MIXTURES

B. D. Flockhart and A. R. Ubbelohde

Chemistry Department, Queen's University, Belfast, Northern Ireland

Received October 8, 1952; revised March 6, 1953

ABSTRACT

Measurements have been carried out with aqueous solutions of 1- and 2-propanol and propionic acid, respectively, with the object of studying the effect of changes in polar third components of related structure on the soap-water systems.

The addition of propionic acid does not alter the form of the conductance function; the $\Lambda - \sqrt{C}$ curve exhibits a normal break point. Replacement of the carboxyl group by the hydroxyl, however, produces a maximum in the plot. When present in small amounts the three additives lower the critical concentration and thus favor micelle formation. Larger additions of the acid raise the critical concentration for micelle formation. With increasing alcohol concentration the effects are complex.

As the temperature is raised the critical concentration of sodium dodecyl sulfate in water passes through a minimum. In the alcohol-water mixtures this minimum occurs at lower temperatures than for pure water. Values for the heats of aggregation have been calculated from these observations.

INTRODUCTION

In solutions of paraffin-chain salts the critical concentration for micelle formation (CMC) is determined by a number of factors. It is markedly dependent upon the size and shape of the paraffin chain and on the nature of the polar group. A rise of temperature usually increases the value. Polar organic additives have been shown to alter it appreciably.

The main objects of the present investigation were (a) to extend information on the influence of the solvent on micelle formation, especially when a third component was added, and (b) to calculate the change in heat content for the process: soap molecule in solution \rightarrow soap molecule in the micelle, using different solvents.

A study has been made of the conductance of sodium dodecyl sulfate in aqueous solutions of 1-propanol, since this is the highest member of the monohydric saturated alcohol series completely miscible with water. The results have been compared with measurements in 2-propanol-water mixtures to examine the effect of branching in the hydrocarbon chain. In investigating the influence of the polar group, propionic acid-water mix-

tures have been employed for comparison. Measurements have been made with sodium tetradecyl sulfate to test how sensitive the results are to the length of the hydrocarbon chain of the soap molecule. New experimental facts presented include the observance of maxima in the equivalent conductance- $\sqrt{\text{concentration}}$ plots in certain solvent mixtures and a minimum in the CMC of sodium dodecyl sulfate as the temperature is raised. These results are discussed in relation to theories of micellar structure.

EXPERIMENTAL

Imperial Chemical Industries (I.C.I.) kindly supplied the sodium dodecyl and tetradecyl sulfates. Purities were 100 % and 99.7 % respectively, calculated from the SO_3 liberated on acid hydrolysis. The water employed had a specific conductance ranging between 1.0 and 1.5×10^{-6} mho. 1-Propanol and 2-propanol were middle fractions from redistillation in an atmosphere of nitrogen. Propionic acid was similarly fractionated under reduced pressure.

The electrical conductances were determined in the manner and with the equipment described in a previous communication (1). The (gray) platinum electrodes caused no catalytic oxidation of the alcohol, since the resistance remained constant. Adsorption of salt was insignificant. Measurements were made at various temperatures over the range 0.5° to 55°C . Around 0.5° the temperature was controlled to $\pm 0.1^\circ$, around 25° to $\pm 0.02^\circ$, and around 50° to $\pm 0.04^\circ$.

Solvent mixtures were recorded in terms of weight per cent of organic additive. At the highest dilutions in the alcohol-water mixtures the solvent correction ranged between 4 and 9 %. In the case of the acid-water mixtures the results give the conductance by difference.

Viscosities of the 2-propanol-water mixtures were measured using an Ostwald viscometer. Other viscosity values (2) and the density (2) and dielectric constant (3) of the various mixtures were interpolated from the literature data.

RESULTS

Equivalent Conductance- $\sqrt{\text{Concentration}}$ Curves

Figures 1 to 3 show the equivalent conductance (Λ) of sodium dodecyl sulfate plotted against the square root of the concentration (in moles per liter of solution) in water and in mixtures containing varying amounts of 1-propanol, 2-propanol, and propionic acid, respectively, at 25.2°C . The results of measurements with sodium tetradecyl sulfate in pure water and in the presence of 1-propanol are shown in Fig. 4. Most of the curves represent at least two series of measurements.

Previous investigations (4, 5) have shown that in water sodium dodecyl

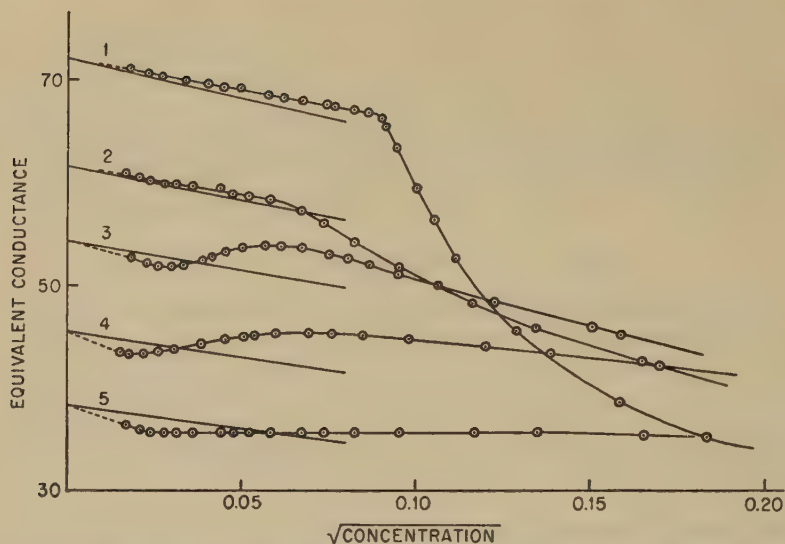


FIG. 1. Conductance curves for sodium dodecyl sulfate in 1-propanol-water mixtures at 25.2°C.: 1-propanol for curve (1) 0%, (2) 5.03%, (3) 9.21%, (4) 13.39%, (5) 19.14%.

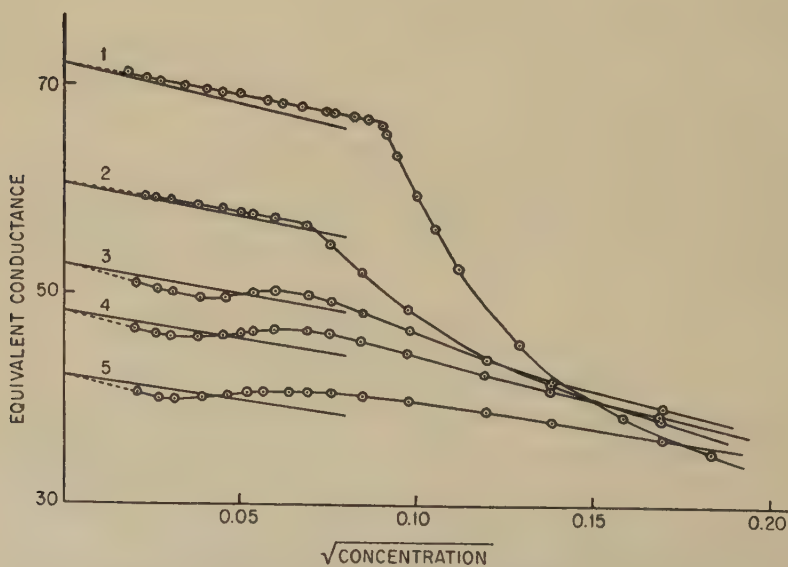


FIG. 2. Conductance curves for sodium dodecyl sulfate in 2-propanol-water mixtures at 25.2°C.: 2-propanol for curve (1) 0%, (2) 5.71%, (3) 10.40%, (4) 13.48%, (5) 17.41%.

and tetradecyl sulfates exhibit the conductance behavior of typical paraffin-chain salts. Present findings show, however, that in many propanol-water mixtures, the conductance, after decreasing initially with an increase in concentration, begins to rise and passes through a maximum at concentrations dependent upon the alcohol content of the solvent.

Conductance measurements were also made with sodium oleate, but the plots have been omitted from this paper. In these studies about 6 mole % of sodium hydroxide (based on the soap) was added to suppress hydrolysis.

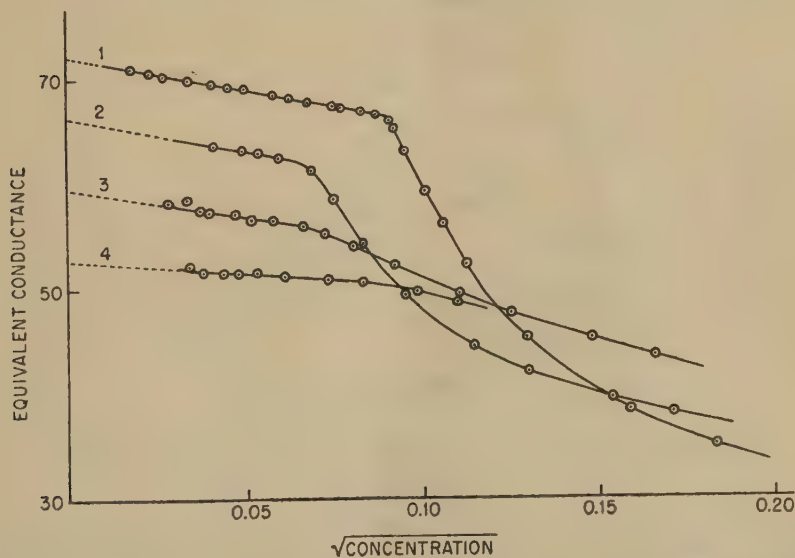


FIG. 3. Conductance curves for sodium dodecyl sulfate in propionic acid-water mixtures at 25.2°C.: propionic acid for curve (1) 0%, (2) 5.06%, (3) 10.42%, (4) 15.19%.

A pronounced maximum was again evident in a 5% 1-propanol mixture. The curve for a 5% 2-propanol solvent only exhibits a slight arrest; however, at 9% 2-propanol it has a well-defined maximum.

The maximum effect is very sensitive to relatively small changes in temperature (Fig. 4).

From Fig. 3 it will be noted that no maximum is evident in the $\Lambda\text{-}\sqrt{C}$ curves of sodium dodecyl sulfate in propionic acid-water mixtures containing up to 15% propionic acid.

CMC Values

A plot of specific conductance against concentration normally gives two nearly straight lines which intersect at the CMC (6). Systems with a maximum in Λ show two break points. These are somewhat on the high

concentration side of the minimum and maximum respectively on the $\Lambda\text{-}\sqrt{C}$ curves.

Slightly different break points are sometimes obtained from the specific conductance-concentration curves and the $\Lambda\text{-}\sqrt{C}$ curves. The mean values from the two procedures for sodium dodecyl sulfate are plotted as a function of additive concentration in Fig. 5.

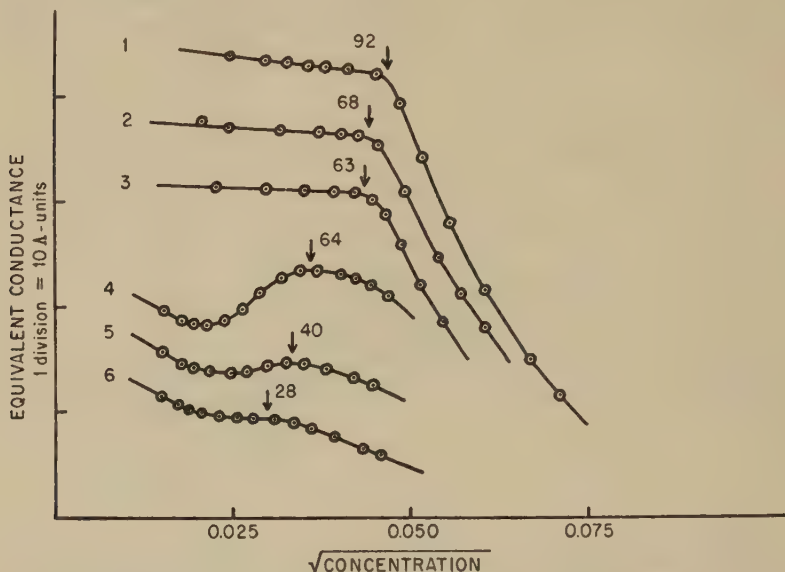


FIG. 4. Conductance curves for sodium tetradecyl sulfate in water at (1) 40.1°, (2) 25.2°, and (3) 21.5°C.; and in 5.04% 1-propanol at (4) 25.2°, (5) 10.5°, and (6) 0.7°C. The zeros of the ordinate axes of the curves have been adjusted to bring all in the same figure. Ordinates of the break points or maxima are as indicated.

The present value of $8.0 \times 10^{-3} M$ for the CMC of sodium dodecyl sulfate in water at 25.2°C. is in good agreement with the values recorded in the literature (7, 8).

In addition to the results plotted in the figures, the conductance results for sodium dodecyl sulfate in water, 5.0% 1-propanol and 5.7% 2-propanol, respectively, were obtained up to 55°C. In water and 5.7% 2-propanol, measurements were also carried down to the lowest temperatures at which CMC values could be obtained (8.0° and 0.5°C., respectively). At these temperatures the salt crystallized from solutions only slightly more concentrated than the CMC. Until this occurred, however, the resistance showed only a slow drift to higher values. Two readings were quickly made after the time interval for the temperature equilibrium to be established, and the mean value was taken. Values for the CMC are plotted as a function of temperature in Fig. 6.

The CMC of sodium tetradecyl sulfate does not pass through a minimum. From the lowest temperature possible in water (21.5°C.) a steady increase in the value is recorded (not plotted).

Limiting Slopes

The Onsager theoretical slopes for sodium dodecyl sulfate in water and mixtures containing varying amounts of 1- and 2-propanol, respectively, are indicated by solid lines in Figs. 1 and 2. To compute the theoretical slope, values of Λ_0 were obtained from the experimental data by graphical

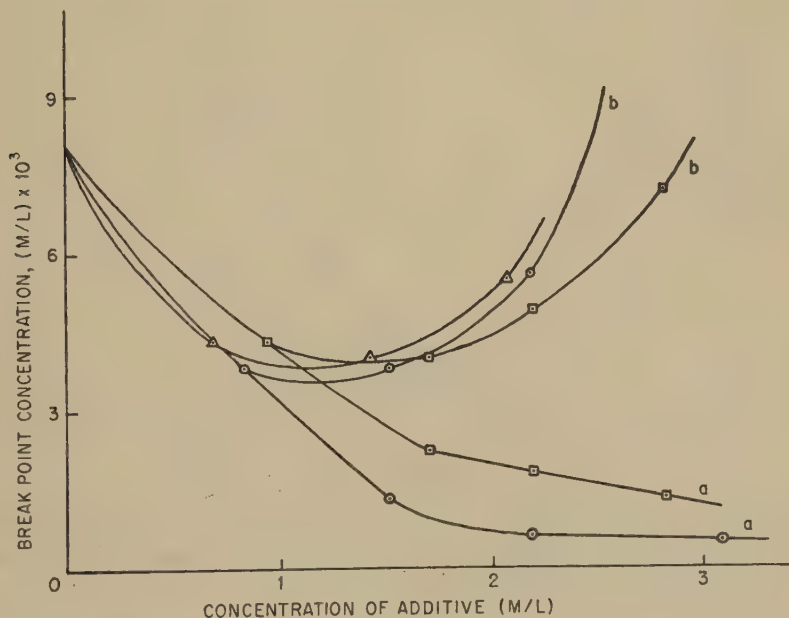


FIG. 5. Effect of 1-propanol (\odot), 2-propanol (\square), and propionic acid (\triangle), at 25.2°C. on the break point concentration of sodium dodecyl sulfate; the curve for the lower concentration break point observed in the presence of alcohol is marked *a* and for the second break point *b*.

ical extrapolation. The values can only be regarded as very approximate owing to the high conductance of the solvent mixtures and to the fact that the measurements have not been carried to sufficiently low concentrations.

In water, 5% 1-propanol, and 6% 2-propanol the observed slope is smaller than the theoretical, whereas for mixtures having a higher alcohol content the observed slope is the greater.

Conductance Viscosity Product

The value of $\Lambda_0\eta$ for sodium dodecyl sulfate in water at 25.2°C. is 0.644; at 20°C. it is stated to be 0.661 (9). The $\Lambda_0\eta$ curves for sodium dodecyl sul-

fate have maxima at about 1.5 moles/l. of 1-propanol, 2.7 moles/l. of 2-propanol, and 1.5 moles/l. of propionic acid. Over the range studied the viscosities of the mixtures rise steadily with increasing additive concentration.

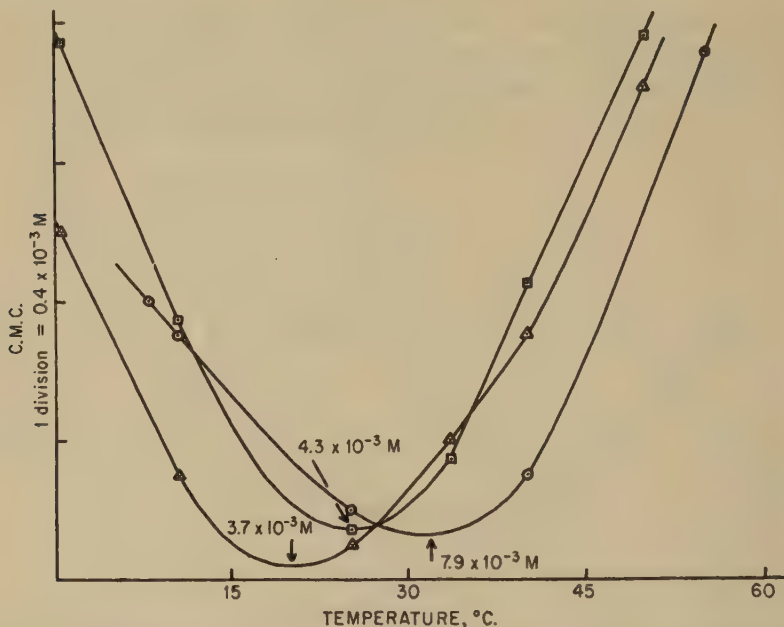


Fig. 6. Effect of temperature on the critical micelle concentration of sodium dodecyl sulfate in water (○), 5.03% 1-propanol (△), and 5.71% 2-propanol (□). The zeros of the ordinate axes of the curves have been adjusted to bring all in the same figure. Ordinates of the minima are as indicated.

DISCUSSION

Effect of Maximum in the Λ - \sqrt{C} Curve on the Interpretation of the CMC

The occurrence of a maximum effect in dilute solutions of simple paraffin-chain salts of the anionic type has not apparently been previously observed. In ethanol-water mixtures of sodium dodecyl sulfate there is no evidence of such an effect (10). A maximum conductance in dilute solution was first observed for cetylpyridinium chloride in water at very high field strengths (11) and later for methylene blue in water at ordinary field strengths (12). More recently, maxima have been found at normal field strengths for a number of cationic paraffin-chain salts in solvent mixtures containing 10 to 35% methanol (13) as well as for certain cationic salts in pure water (14).

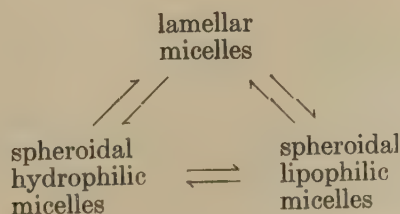
From the application of Stokes's law one would expect a rise in the equivalent conductance above the CMC. According to Hartley (15) the

observed fall is due to the much increased "braking" effect of the ionic atmospheres and the partial neutralization of the micellar charge by the inclusion of gegenions. The initial rise of total equivalent conductance above the straight line given by the most dilute solutions may be realized if the paraffin-chain ions commence to aggregate in very dilute solution and the gegenions have a relatively low mobility, owing to the predominant Stokes's law effect of aggregation. Present measurements support this explanation. The tendency to exhibit a maximum increases with a decrease in the CMC (Figs. 1 and 4 and sodium oleate data). Sodium is a relatively slow counterion. In the present investigation, however, the phenomenon has only been observed in alcohol-water *mixtures*. It is suggested that another factor must also be taken into account. A micelle formed in the presence of an alcohol is likely to contain alcohol molecules in its oriented structure [cf. Schulman and Hughes (16), Harkins, Mattoon, and Mittelman (17)]. These alcohol molecules, introduced between the soap ions in the micelle, will produce a further charge separation. Owing to the lowered charge density the conditions are thus more favorable to abnormally small atmospheric and inclusion effects.

This *partition* of additive between the solution and the micelles may be sensitive both to the structure of the polar third component and to temperature. Thus no maximum is observed in the Λ - \sqrt{C} curves of sodium dodecyl sulfate in ethanol-water mixtures. The partition of ethanol between micelles and water is likely to be more in favor of water than is the case with the propanols. According to Schulman and McRoberts (18), penetration of the micelle lattice by alcohol molecules is first noticeable at C3 carbons in the penetrating molecule.

In an aqueous solution containing up to 15 % propionic acid there is also no evidence of a maximum conductance. Measurements of pH on propionic acid-water solutions of sodium dodecyl sulfate indicated that where the acid molecules are removed from the water by inclusion in the micelle, the carboxyl groups are still in contact with the water at the micelle surface. Thus while the partition is probably little different from that of 1-propanol, the presence of a much stronger polar group does not allow an appreciable lowering of the charge density.

An alternative explanation of the maximum phenomenon can be given in terms of an intermicellar equilibrium such as that suggested by Winsor (19):



From phase studies, addition of a water-soluble alcohol is considered to increase the interaction between the amphiphilic substance and water so that the equilibrium shifts to the left. The rise of equivalent conductance may then be attributed to association into ionic aggregates. Increasing concentration will displace the equilibrium to the right thus accounting for the decreasing conductance beyond the maximum [cf. Ralston, Eggenberger, and Du Brow (14)].

On the basis of an intermicellar equilibrium hypothesis the effect of temperature on the maximum also finds a possible explanation. Increase of temperature most frequently tends to shift the equilibrium to the left (20). The maximum may therefore be expected to become more pronounced with an increase of temperature, as in Fig. 4. Shift of the maximum to higher salt concentrations is also to be expected. With the equilibrium being shifted toward ionic micelles upon a rise of temperature, a higher salt concentration will be required to counter the displacement.

Study of the effect of alcohols not completely soluble in water on the electrical conductance of paraffin-chain salt solutions has revealed no evidence of the maximum effect (21, 22). This agrees with either of the above hypotheses. Reduction in mobility of the micelle through the incorporation of a high molecular weight alcohol is possibly greater than the increase expected on the basis of decreased atmospheric and inclusion effects. On Winsor's view, addition of a water-insoluble alcohol facilitates the formation of lamellar micelles, and again no conductance rise is to be expected.

Effect of Organic Additives upon the CMC

Very material additions of formic or acetic acid are stated to be without influence upon the CMC of dodecylammonium chloride (23, 24). Figure 5 shows that propionic acid has a marked influence upon the CMC of sodium dodecyl sulfate, closely paralleling the effect of ethanol (10). A similar minimum has been obtained for dodecylammonium chloride on the addition of ethanol (25, 26) or 2-propanol (22). The CMC of a number of cationic salts, however, increases on the addition of methanol (13, 22, 27), though sometimes a slight initial decrease is noted (25). The addition of alcohols partially miscible with water is known to depress the CMC [cf. Klevens (28) and Herzfeld, Corrin, and Harkins (29)].

With systems exhibiting two break points it is not immediately clear which corresponds with the CMC when there is only one break point. Starting with very dilute solutions, the rising conductance at concentrations above the first break point would appear to necessitate the presence of small micelles, as discussed in the preceding section. Taking the second break point as the normal CMC, however, brings the results into line with the effect of ethanol and propionic acid on the CMC of sodium dodecyl sulfate. Two distinct types of aggregation may in fact be involved.

It is of interest to note that at low concentrations of additive 2-propanol is less effective than 1-propanol in decreasing the CMC. This result may indicate some difficulty in fitting the branched-chain alcohol into the micelle [cf. Herzfeld, Corrin, and Harkins (29)].

Effect of Temperature on the CMC

A rise of temperature has usually been shown to increase the CMC (6, 28, 30, 31), but a minimum has been observed (32). The slight minimum for lauryl sulfonic acid in water at about 35°C. (32) corresponds to the present result obtained for sodium dodecyl sulfate in water at approximately 32°C. and a pronounced minimum for potassium laurate in water at about 50°C.

Experimental values for the heats of aggregation ΔH for the process:

soap molecule in solution \rightarrow soap molecule in the micelle,

of a number of soaps in aqueous solution have been calculated from a plot of $\log \text{CMC}$ vs. $1/T$ (33). Corresponding values of ΔH for sodium dodecyl sulfate in water, 5% 1-propanol, and 6% 2-propanol at 5°, 25°, and 45°C. have been calculated from the present data as in Table I. The present experiments were deliberately extended to lower temperatures and confirm a change in sign of ΔH indicated by the earlier work.

This change of sign is seen to be the outcome of the balance of terms at low temperatures. According to Stainsby and Alexander the change in heat content per molecule on aggregation ($H_f - H_i$) is given by the equation

$$H_f - H_i = \gamma(A_f - A_i) + (L_f - L_i) + E - (5/2)kT$$

where $A_i\gamma$ is the interfacial energy for the curled molecule in solution, A_i being the surface area of the tail and γ the total surface energy; $A_f\gamma$ is the interfacial energy per molecule in the micelle, nA_f being the total surface area of the micelle for which a hydrocarbon-water interface still exists, assuming n long-chain ions per micelle;

L_i is the total energy of the chain ion in solution arising from various forms of internal rotation, libration, and vibration;

L_f is the total energy per molecule in the micelle arising from internal motions, the interior of the micelle being considered to resemble a liquid hydrocarbon;

E is the electrical energy per ion in the micelle;

$(5/2)kT$ is the difference between $6 kT$ which arises from the translational energy and rotational energy of both the long-chain ion and the gegenion $[(4 \times 3/2)kT]$ and $7/2 kT$ which arises from the rotation of the long-chain ion in the micelle about an axis along the length of the tail $[(1/2)kT]$, from the translational energy of the

hydrocarbon tail $[(3/2)kT]$ and from the rotational energy of the geignon $[(3/2)kT]$.

A decrease in temperature will decrease A_i because of increased crumpling. It will also increase the $(L_f - L_i)$ term (33). By way of illustration, a 25 % decrease in A_i and a 25 % increase in the theoretical $(L_f - L_i)$ term gives a positive value for the heat of aggregation of sodium dodecyl sulfate in water at 5°C. But since the theoretical value of ΔH is very much larger than the experimental value, only slight alterations in the above quantities with a decrease in temperature are actually required to change the sign of ΔH .

Addition of polar molecules will decrease nA_f , the total surface area of the micelle for which a hydrocarbon-water interface still exists. This is a possible explanation for the change in sign occurring at a lower temperature in the alcohol-water mixtures and for the numerically higher values being obtained at 45°C.

TABLE I
Heats of Aggregation^a of Sodium Dodecyl Sulfate

Temp. °C.	Water kcal./mole	1-Propanol, 5.03%	2-Propanol, 5.71%
5	0.8	2.5	2.3
25	0.6	-0.5	0
45	-1.9	-2.8	-2.8

^a Negative sign indicates liberation of heat.

Whichever break point is considered as the CMC, with sodium tetradecyl sulfate no positive ΔH values are obtained. Crystallization prevented measurements being carried to a sufficiently low temperature in a 5 % 1-propanol solvent. It seems probable, however, that by using a solvent having a higher alcohol content a change of sign should be realized.

REFERENCES

1. FLOCKHART, B. D., AND GRAHAM, H., *J. Colloid Sci.* **8**, 105 (1953).
2. WASHBURN, E. W., ed., International Critical Tables of Numerical Data, Vol. 3, p. 112, 119, 120 (1928); vol. 5, pp. 20, 23 (1929).
3. AKERLOF, G., *J. Am. Chem. Soc.* **54**, 4125 (1932).
4. LOTTERMOSER, A., AND PUSCHEL, F., *Kolloid-Z.* **63**, 175 (1933).
5. HOWELL, O. R., AND ROBINSON, H. G. B., *Proc. Roy. Soc. (London)* **A155**, 386 (1936).
6. WRIGHT, K. A., ABBOTT, A. D., SIVERTZ, V., AND TARTAR, H. V., *J. Am. Chem. Soc.* **61**, 549 (1939).
7. SCHMID, G., AND LARSEN, E. C., *Z. Electrochem.* **44**, 651 (1938).
8. HAFFNER, F. D., PICCIONE, G. A., AND ROSENBLUM, C., *J. Phys. Chem.* **46**, 662 (1942).
9. WARD, A. F. H., *J. Chem. Soc.* **1939**, 522.

10. WARD, A. F. H., *Proc. Roy. Soc. (London)* **A176**, 412 (1940).
11. MALSCH, J., AND HARTLEY, G. S., *Z. physik. Chem.* **A170**, 321 (1934).
12. MOILLIET, J. L., COLLIE, B., ROBINSON, C., AND HARTLEY, G. S., *Trans. Faraday Soc.* **31**, 120 (1935).
13. GRIEGER, P. F., AND KRAUS, C. A., *J. Am. Chem. Soc.* **70**, 3803 (1948).
14. RALSTON, A. W., EGGENBERGER, D. N., AND DU BROW, P. L., *J. Am. Chem. Soc.* **70**, 977 (1948).
15. HARTLEY, G. S., *Ann. Repts. Progr. Chem. (Chem. Soc. London)* **45**, 33 (1949).
16. SCHULMAN, J. H., AND HUGHES, A. H., *Biochem. J. (London)*, **29**, 1242 (1935).
17. HARKINS, W. D., MATTOON, R. W., AND MITTELMANN, R., *J. Chem. Phys.* **15**, 763 (1947).
18. SCHULMAN, J. H., AND McROBERTS, T. S., *Trans. Faraday Soc.* **42B**, 165 (1946).
19. WINSOR, P. A., *J. Phys. & Colloid Chem.* **56**, 391 (1952).
20. WINSOR, P. A., *Trans. Faraday Soc.* **44**, 455 (1948).
21. RALSTON, A. W., AND EGGENBERGER, D. N., *J. Am. Chem. Soc.* **70**, 983 (1948).
22. BROWN, G. L., GRIEGER, P. F., AND KRAUS, C. A., *J. Am. Chem. Soc.* **71**, 95 (1949).
23. RALSTON, A. W., EGGENBERGER, D. N., AND BROOME, F. K., *J. Am. Chem. Soc.* **71**, 2145 (1949).
24. RALSTON, A. W., AND EGGENBERGER, D. N., *J. Am. Chem. Soc.* **70**, 980 (1948).
25. CORRIN, M. L., AND HARKINS, W. D., *J. Chem. Phys.* **14**, 640 (1946).
26. RALSTON, A. W., AND EGGENBERGER, D. N., *J. Phys. & Colloid Chem.* **52**, 1494 (1948).
27. EVERS, E. C., AND KRAUS, C. A., *J. Am. Chem. Soc.* **70**, 3049 (1948).
28. KLEVENS, H. B., *J. Phys. & Colloid Chem.* **52**, 130 (1948).
29. HERZFELD, S. H., CORRIN, M. L., AND HARKINS, W. D., *J. Phys. & Colloid Chem.* **54**, 271 (1950).
30. POWNEY, J., AND ADDISON, C. C., *Trans. Faraday Soc.* **33**, 1243 (1937).
31. RALSTON, A. W., AND HOERR, C. W., *J. Am. Chem. Soc.* **64**, 772 (1942).
32. BRADY, A. P., AND HUFF, H., *J. Colloid Sci.* **3**, 511 (1948).
33. STAINSBY, G., AND ALEXANDER, A. E., *Trans. Faraday Soc.* **46**, 587 (1950).

THE STABILITY OF ELEMENTARY EMULSION DROPS AND EMULSIONS

E. G. Cockbain and T. S. McRoberts

Received June 30, 1952; revised March 17, 1953

British Rubber Producers' Research Association, Herts, England

ABSTRACT

The rates of coalescence of oil and water drops at the oil-water interface have been measured in the presence of soaps, cholesterol, saponin, serum albumin, and polyvinyl alcohol. Interfacial viscosity and tension data have been obtained for some of the systems.

With potassium laurate, cetyltrimethylammonium bromide, or sodium desoxycholate as stabilizer, benzene and paraffin drops possess maximum stabilities at concentrations slightly greater than the critical micellar concentration (c.m.c.). Drops of the aqueous soap solutions in a continuous oil medium coalesce very rapidly, in accordance with the preferential oil-in-water emulsifying power of the above soaps. Mixed adsorbed films of cholesterol and potassium laurate at the paraffin-water interface have a greater stabilizing effect than either cholesterol or potassium laurate films alone. The stability of oil drops in aqueous solutions of saponin or serum albumin is very high, but drops of aqueous saponin or serum albumin in a continuous oil phase are stable for only a few seconds, despite the high viscosity of the adsorbed films.

It is concluded that the main factor determining stability in all the systems examined is the resistance to wetting of segments of the adsorbed film by the discontinuous phase. An explanation is given for certain empirical rules relating emulsion type to preferential wettability or solubility of the stabilizing agent in oil and water.

INTRODUCTION

Following Hardy's experiments (1) on the stabilization of air bubbles by insoluble monolayers spread on water, the stability of bubbles at the surface of aqueous solutions of capillary active solutes has been studied by several workers (2, 3, 4). The stability is defined by the time required for the bubbles to burst. Corresponding data for elementary emulsion drops are very meager, although the method provides a ready means of studying drops of uniform and known size under conditions where the aging of an adsorbed film can be controlled.

The distinction between the ease of formation of an emulsion and its subsequent stability is widely recognized. Surface-active compounds which are not particularly effective stabilizers are sometimes very efficient in assisting the formation of emulsions, in which rapid adsorption of the

surface-active compound at the oil-water interface may be an important factor. If, in addition, the interfacial tension of the system is low, the work involved in increasing the total interfacial area by a given amount is correspondingly small, and emulsions of small particle size can be made without the use of homogenizing machinery. The subsequent rate of coalescence of the particles depends on a number of properties of the newly formed emulsion, of which temperature, viscosity of the continuous phase, particle-size distribution and the nature of the adsorbed film may each assume differing degrees of importance in different systems. The main object of the present work was to study the influence of the nature of the adsorbed film on the stability of elementary emulsion drops (at least several seconds old) while maintaining constant the other variables referred to above.

It was shown by Reh binder and Wenström (2) that the lifetimes of toluene drops at the aqueous sodium oleate-toluene interface were much higher than those of drops of sodium oleate solution at the same interface, in agreement with the fact that sodium oleate stabilizes oil-in-water (O/W) emulsions rather than emulsions of the opposite type (W/O). In both systems the stability of the drops increased continuously with increasing soap concentration. With isoamyl alcohol as stabilizer, a maximum in the lifetime of mercury drops was found at moderately small concentrations of the alcohol. It is well known (4, 5) that a similar maximum often occurs in the stability of individual gas bubbles and bulk foams. According to Reh binder and Wenström, the occurrence of a stability maximum in both foam and elementary emulsion systems depends on the mechanical properties of the adsorbed film; other authors (4, 6) attribute the maximum in foam systems to differences between the equilibrium and dynamic surface tensions.

In the present investigation, a study has been made of the stability of water and oil drops at the oil-water interface in the presence of different types of surface-active agents. Interfacial tension and viscosity measurements on adsorbed films of some of the agents are reported, and the factors determining emulsion type and stability are discussed.

EXPERIMENTAL

Interfacial tensions were obtained by the drop-volume method, using an apparatus similar to that described by Cockbain and McMullen (7). Interfacial viscosities were determined by measuring the damping of an oscillating pyrex glass cylinder suspended in the interface. This method and the approximations involved in the calculation of the coefficient of interfacial viscosity (μ_s) have been fully discussed by Joly (8) and others (9). All viscosity measurements were carried out at $25 \pm 0.1^\circ\text{C}$.

To measure the stability of oil drops at the oil-water interface, the

apparatus shown in Fig. 1 was used. The aqueous phase was filtered directly into the pyrex glass vessel A, surrounded by the thermostat jacket B, and the surface of the solution cleaned by suction, using a drawn-out glass tube. The oil was then filtered into the vessel, forming a layer about 1 cm. thick, and the interface was again cleaned by suction. The bottom of the vessel was closed by a rubber bung which held the barrel of an Agla micrometer syringe filled with the same oil as that in vessel A. Inserted into the top of the barrel was a hollow ground-glass tip of suitable internal diameter, enabling oil drops of the required size to be obtained. A drop whose volume was just too small to cause detachment from the tip was formed and allowed to age for the required time (if a slow decrease in

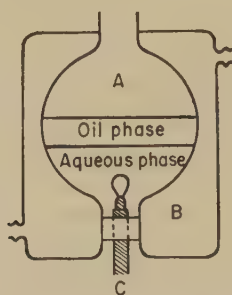


FIG. 1. Apparatus for determining the lifetimes of oil drops.

interfacial tension with time occurs, allowance must be made for the decrease). A slight turn of the micrometer head of the syringe was then sufficient to detach the drop, and the time required for it to coalesce with the layer of oil in A was measured. It is necessary to have available a series of tips of different diameters so that the volume of the detached drop can be controlled and varied. Unless stated otherwise, a loose-fitting cover was placed over the top of vessel A to prevent access of dust; in a few experiments a vessel was used which was closed at the top with a ground-glass cap.

The stability of drops of the aqueous phase was determined by closing the bottom end of the vessel and inserting the micrometer syringe, containing the aqueous phase, into a layer of the oil through the opening at the top. Drops of the aqueous solution were formed as before and allowed to fall to the interface between the two bulk phases, where their lifetimes were measured.

With a given system the stabilities of individual drops were not constant, but if thirty or more were examined separately, a distribution curve was obtained (Fig. 2) sufficiently reproducible for analysis. N is the number of drops which do not coalesce within time t . The distribution curve usually consisted of two fairly well-defined regions, one in which N decreased very

slowly with time, followed by a region in which the decrease in N was much more rapid and approximately exponential. Such a distribution curve indicates that the lifetimes of the drops are determined by two distinct processes, viz., drainage of the continuous phase from between the drop and the plane interface, followed by rupture of the adsorbed film. In the present work, a rate constant k for the film rupture process was obtained from that part (BC) of the distribution curve where the relation

$$\ln N = -kt + \text{constant} \quad [1]$$

was obeyed, while the over-all stability of the drops was characterized by their half-life time $\tau_{1/2}$. It is assumed that the difference $\tau_{1/2} - \frac{1}{k} \ln 2 = t_D$ (see Fig. 2) is determined mainly by the rate of film drainage.

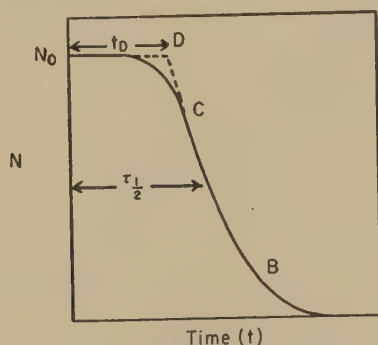


FIG. 2. Typical distribution curve for the lifetimes of oil drops.

When the drops were sufficiently stable, it was possible to follow the rate of coalescence with the plane interface of groups of drops (5–30) formed at suitable intervals, e.g., 5–10 seconds. The rate constants k did not differ significantly, when this method was used, from those obtained by studying the drops singly. This was due, presumably, to the fact that the drops nearly always coalesced with the plane interface rather than with themselves, and that disturbance of the interface caused by the rupture of one drop did not markedly affect the rate of coalescence of its neighbors. In determining $\tau_{1/2}$, zero time on the distribution curve was taken as the time at which half the drops of the group had been formed. This “multiple-drop” method is unsuitable for systems in which adsorption of solute occurs slowly, e.g., dilute protein solutions in contact with air or oil. All measurements of drop stability were carried out at 20–25°C.

MATERIALS

The paraffin hydrocarbon used was a colorless light petroleum fraction (from Manchester Oil Refineries Ltd.) consisting of paraffin and cyclo-

paraffin hydrocarbons. The benzene was of A.R. quality. Saponin, *n*-decane, and cholesterol were supplied by B.D.H. Ltd., the cholesterol being recrystallized from ethanol before use. The cetyltrimethylammonium bromide (CTAB), kindly provided by I.C.I. Ltd., was also recrystallized twice from acetone. Desoxycholic acid (from L. Light and Co. Ltd.) and pure lauric acid were dissolved directly in alkali to give solutions of pH 11.0. The polyvinyl alcohol was provided by Messrs. Revertex Ltd., and the bovine serum albumin by the Armour Laboratories.

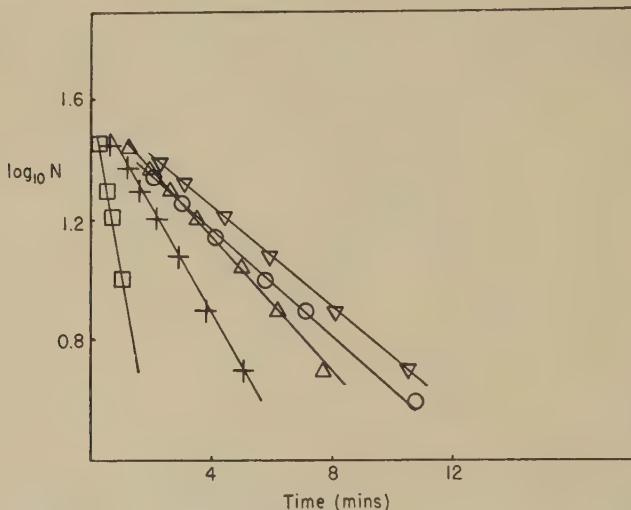


FIG. 3. Rate of coalescence of paraffin drops in aqueous CTAB.

Drop volume = 0.004 ml.

□ 0.00007 M CTAB

+ 0.0005 M CTAB

▽ 0.001 M CTAB

○ 0.002 M CTAB

△ 0.010 M CTAB

RESULTS

Potassium Laurate and Cetyltrimethylammonium Bromide

Preliminary experiments on the stability of benzene and paraffin drops in aqueous solutions of potassium laurate or sodium dodecyl sulfate showed that the half-life times of the drops were not markedly affected by volume in the range 0.0005–0.01 ml., whereas below 0.0005 ml. the stability increased rapidly with decreasing volume. All subsequent experiments were therefore carried out with drops of volume not less than 0.002 ml., where small errors in the measurement of volume would be unimportant.

In the absence of soap the half-life times of benzene and paraffin drops of volume 0.01 ml., in distilled water, were 6 and 12 seconds, respectively.

In 0.001 *N* KOH solution the stabilities were only slightly higher (*ca.* 8 seconds for benzene). The drops did not coalesce completely with the bulk oil phase in a single stage; partial coalescence occurred leaving a drop of about one-third the original volume, which in turn partially coalesced after several seconds, leaving a still smaller drop. In the presence of low concentrations of soaps the same phenomenon was usually observed, but at higher concentrations where the interfacial tensions of the soap solutions were small, coalescence appeared to occur in a single stage in most cases. Although the coalescence process takes place very rapidly, it is not rapid enough in the former systems to prevent the high interfacial tension forces from restoring part of the coalescing drop to a discrete spherical form.

TABLE I

Stability of Paraffin and Benzene Drops in Aqueous Solutions of CTAB

Oil phase	CTAB concn., <i>M</i>	Rate constant <i>k</i> , <i>min.</i> ⁻¹	$\tau_{\frac{1}{2}}$, <i>min.</i>	<i>t_D</i> , <i>min.</i>
Paraffin (drop volume 0.004 ml.)	0.00007	1.3	0.7	0.15
	0.0005	0.4	2.4	0.7
	0.001	0.19	4.9	1.2
	0.002	0.21	3.9	0.6
	0.01	0.25	3.7	0.9
Benzene (drop volume 0.005 ml.)	0.00007	1.6	0.55	0.12
	0.00014	0.53	1.9	0.6
	0.0007	0.39	5.0	3.2
	0.0014	0.32	6.1	3.9
	0.0054	0.38	3.1	1.3

The rate of coalescence of paraffin drops in aqueous solutions of CTAB is shown in Fig. 3. The corresponding values of *k*, $\tau_{\frac{1}{2}}$, and *t_D* are summarized in Table I, with similar data for benzene.

The stabilities of paraffin and benzene drops in aqueous potassium laurate at pH 11.0 are given in Fig. 4. It can be seen that the stability is a maximum at concentrations close to (usually a little higher than) the c.m.c. of the soap, which is 0.0008 *M* for CTAB (10) and 0.023 *M* for potassium laurate (11). This maximum stability is due to a minimum in both the rate of film drainage (maximum *t_D*) and the rate constant *k* for film rupture.

If the loose-fitting cover on vessel A is replaced by a gas-tight cap, the stability of the paraffin drops is unaffected, but a large increase in the stability of benzene drops occurs, which can amount to several hundred per cent. This may be due to the elimination of convection currents at the interface, caused by the volatility of benzene. The same effect could be

produced when the benzene vapor in a completely closed system was removed by a slow stream of nitrogen. It is apparent that only the relative values of the drop stabilities can be considered significant in systems containing benzene as the oil phase. Similar large differences have been observed (12) in the stability of foam bubbles in closed and open vessels.

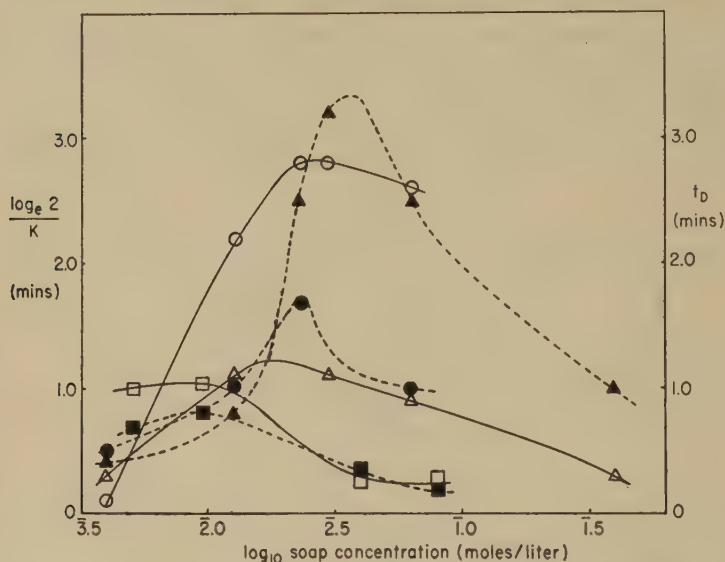


FIG. 4. Rates of film rupture and film drainage for oil drops in aqueous soap solutions.

- $\ln 2/k$ } for paraffin in aqueous potassium laurate, pH 11.0; volume = 0.007 ml.
 ● t_D }
 △ $\ln 2/k$ } for benzene in aqueous potassium laurate, pH 11.0; volume = 0.005 ml.
 ▲ t_D }
 □ $\ln 2/k$ } for paraffin in aqueous sodium desoxycholate, pH 11.0; volume =
 ■ t_D } 0.010 ml.

$$\text{Half-life time of drops } \tau_{\frac{1}{2}} = t_D + \ln 2/k$$

When drops of an aqueous solution of potassium laurate at pH 11.0 or CTAB were allowed to fall through benzene or paraffin to the hydrocarbon-soap solution interface, values of $\tau_{\frac{1}{2}}$ ranging from 10 seconds at low soap concentrations to approximately 30 seconds at concentrations five to ten times the c.m.c. were obtained. No maximum in stability could be detected in the region of the c.m.c. These half-life times are small compared with those in Table I and Fig. 4, corresponding to the fact that potassium laurate and CTAB are oil-in-water emulsifying agents.

Cholesterol, Sodium Desoxycholate, and Mixed Films of Potassium Laurate and Cholesterol

For water drops at the interface between water and solutions of cholesterol in paraffin, $\tau_{1/2}$ increases from 1.4 to 6.0 minutes over the concentration range 0.0025 *M* to 0.013 *M* cholesterol, without showing any maximum. The stability is due mainly to a slow rate of film rupture, t_D being small in comparison with $\tau_{1/2}$. The half-life times, in water, of paraffin drops containing cholesterol are small at all concentrations, e.g., $\tau_{1/2} = 0.3$ minute for a 0.005 *M* cholesterol solution, as compared with $\tau_{1/2} = 4.3$ minutes for water drops in a continuous phase of paraffin + cholesterol at the same concentration. These results are in accordance with the action of cholesterol in stabilizing preferentially emulsions of the W/O type.

The effect of introducing an ionic group into the sterol side chain can be seen in experiments with sodium desoxycholate at pH 11.0; $\tau_{1/2}$ for drops of an aqueous solution of this soap (0.005 *M* to 0.08 *M*) in a continuous phase of paraffin was only 0.15 to 0.3 minute. Inversion of the system to the oil-in-water type gave significantly higher stabilities, shown in Fig. 4, in which a maximum occurred at a concentration of approximately 0.01 *M*. This is close to the critical concentration (13) for commencement of micelle formation, viz., 0.005 *M*.

It was shown by Schulman and Cockbain (14) that the stability of nujol emulsions stabilized by soaps such as sodium cetyl sulfate was increased by adding cholesterol or suitable long-chain aliphatic polar compounds to the oil phase. However, the increased stability of the emulsions in the above experiments may have been due in part to their small particle size, since the interfacial tension of such systems is often extremely low. It was of interest therefore to measure the stability of drops of paraffin containing cholesterol in an aqueous soap solution (potassium laurate) by the present technique. The results showed that $\tau_{1/2}$ was considerably higher than the values obtained in the absence of cholesterol, the increase being due almost entirely to a decreased rate of film rupture. A maximum in stability, corresponding to $\tau_{1/2} = 10$ minutes, again occurs close to the c.m.c. of the soap. By contrast, benzene drops containing up to 1.0% cholesterol by volume possess stabilities little different from those of pure benzene, with aqueous potassium laurate as the continuous phase. This result is to be expected, since interfacial tension measurements indicate that very little cholesterol is adsorbed at the interface benzene + cholesterol-aqueous potassium laurate (7).

Saponin, Polyvinyl Alcohol, and Serum Albumin

Whereas the aqueous soap solutions described above possess interfacial viscosities too small to measure with our apparatus, i.e., less than 0.01 c.g.s. unit, bovine serum albumin and saponin form highly viscous or

elastic adsorbed films at both air and oil interfaces. In this respect serum albumin resembles many other proteins, and the permanence of both foams and emulsions, stabilized by proteins or saponin, has been attributed (15, 16) to the viscosity or elasticity of their films. In the present work, the lifetimes of benzene or paraffin drops at the aqueous saponin-oil interface were so high ($\tau_{1/2} \gg 20$ minutes) in the concentration range 0.01 % to 2.0 %

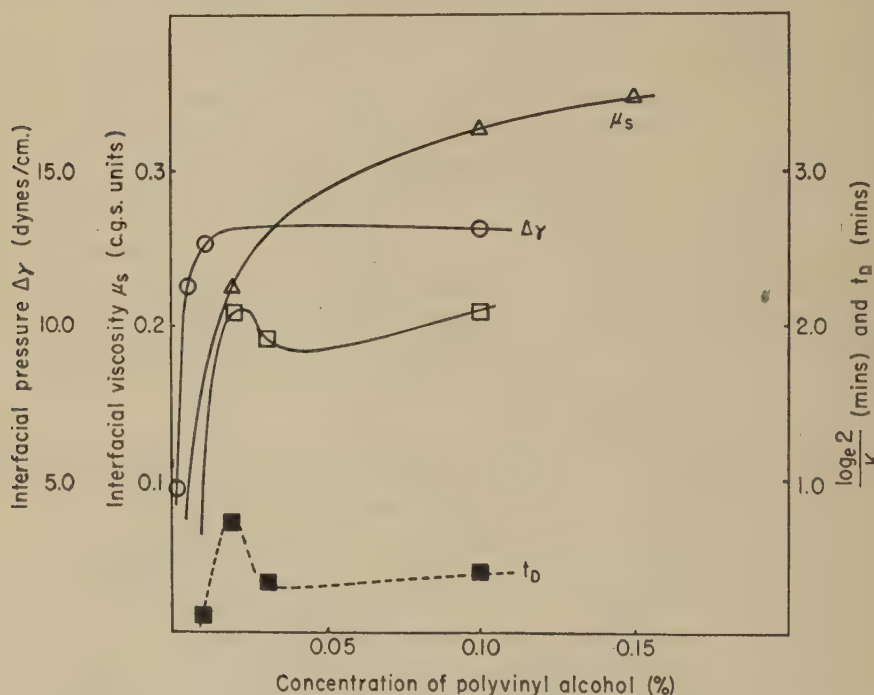


FIG. 5. Drop stability ($\tau_{1/2}$), interfacial pressure ($\Delta\gamma$), and interfacial viscosity (μ_s) for the system *n*-decane/aqueous polyvinyl alcohol.

□ $\ln 2/k$ } drop volume = 0.005 ml.
 ■ t_D

saponin that their stabilities were not determined quantitatively. The interfaces were aged for 3 minutes, by which time the adsorbed films of saponin already possessed rigidity. Inversion of the system disclosed an interesting effect. With the same period of aging, drops of aqueous saponin solution in benzene or paraffin possessed half-life times of only 2 to 10 seconds at concentrations between 0.01 % and 2.0 %. The drops did not burst suddenly, however, as in soap-stabilized systems but slowly deflated and merged with the bulk aqueous phase over a period of a few seconds. It is apparent, therefore, that a rigid adsorbed film will not of itself impart a

high stability to the disperse phase. The same is true of viscous films such as those formed by polyvinyl alcohol. The interfacial viscosity (μ_s) and interfacial tension lowering ($\Delta\gamma$) for polyvinyl alcohol solutions in contact with *n*-decane are given in Fig. 5. The viscosity of the adsorbed film was almost independent of the amplitude of oscillation and reached a value of 0.33 c.g.s. unit at a concentration of 0.1 %. Even so, drops of the aqueous solution at this concentration had a half-life time of less than 5 seconds, using *n*-decane as the continuous phase. Although inversion of the system gave considerably higher stabilities (Fig. 5), $\tau_{1/2}$ remained below the values obtained for potassium laurate or CTAB at the c.m.c. A small maximum in $\tau_{1/2}$ appears to exist at a polyvinyl alcohol concentration slightly greater than that at which the interfacial tension becomes approximately constant.

The stability of paraffin or benzene drops in aqueous solutions of serum albumin depended markedly on the age of the adsorbed film. For 0.1 % albumin solutions at pH 5.6 or 9.2, in buffer solutions of ionic strength 0.1, the interfacial tension against benzene changed very little after 30 minutes; both the plane interface and the oil drop was therefore aged for this period in order to determine the potential stabilizing efficiency of the protein. Under these conditions the half-life times of both benzene and paraffin drops in 0.1 % albumin solutions at pH 5.6 and 9.2 were very high ($\tau_{1/2} > 20$ minutes) compared with the soap-stabilized oil drops described above. When only the plane interface was aged, a large reduction in stability occurred, $\tau_{1/2}$ being approximately 5 minutes for benzene and varying little with pH over the range 3.7–9.2. Acetate buffers were used except at pH 9.2 (borate buffer). Inversion of the system again resulted in a large decrease in stability. For example, drops of a 0.1 % albumin solution at pH 9.2 possessed a half-life time of only 10 seconds with benzene as the continuous phase, even after the plane interface and the drop had both been aged for 30 minutes. Under these conditions, the viscosity of the albumin film was very high, viz., 2.6 and 3.1 c.g.s. units at pH 5.6 and 9.2, respectively.

DISCUSSION

For coalescence of drops to occur, it is presumably necessary that localized displacement of the stabilizer molecules at the interface should take place. If this displacement occurred in the plane of the interface, as envisaged by Gibbs (17), the process would be resisted by the viscosity or elasticity of the adsorbed film and by the local inequalities produced in the boundary tension. The alternative of localized displacement into one of the bulk phases involves a different process, viz., complete wetting of a segment of the film by oil or water. It is difficult to attribute the much greater lifetimes of oil drops, as compared with water drops, in the presence of albumin, saponin, or soaps, to either the viscosity or boundary tension of

the films, since these quantities should be the same whichever phase is the continuous one. Electric repulsion between the particles has often been suggested as a factor contributing to the stability of O/W emulsions, but our results with serum albumin at different pH values indicate that with this stabilizer, at least, charge effects are of minor importance. The same is presumably true of the alkyl polyglycol ethers, which are being used increasingly in industry as emulsifying agents.

When drainage of liquid between two drops is approaching completion, displacement of a film segment into the continuous phase is likely to be hindered by the close juxtaposition of the interfaces (in some systems indeed, the two films probably constitute a solvated bimolecular leaflet of the surface-active agent). No such steric hindrance to displacement of film molecules into the discontinuous phase is to be expected, and if small segments of the film can be readily wetted by the latter phase, drops of low stability should result and vice versa. All the water-soluble stabilizers examined in the present work, including the unionized polyvinyl alcohol, stabilized oil drops much more effectively than water drops, whereas the reverse was true for the oil-soluble cholesterol. It is probable, therefore, that the main factor determining stability in all these systems is the resistance to wetting of segments of the film by the discontinuous phase. In emulsions stabilized by solid powders, displacement of the stabilizer from the interface is already recognized (18) as the major cause of instability.

With solid powders as emulsifying agents, *emulsion type* usually depends on the relative wettability of the powder by the two liquid phases. A similar rule often holds also for soluble emulsifiers, water-soluble agents tending to form O/W emulsions, and oil-soluble agents tending to form emulsions of the opposite type (19). These empirical rules are readily explicable, of course, if the emulsion type obtained is a direct consequence of the different stabilities of the oil and water drops, both of which will commence to form when the two bulk phases are mixed.

The occurrence of a maximum lifetime for oil drops stabilized with potassium laurate, CTAB, and sodium desoxycholate, at concentrations slightly higher than the c.m.c. of these soaps, may also be due to displacement of segments of the adsorbed films into the oil phase. It has been shown previously (20) that aggregation of benzene or paraffin particles in aqueous soap solutions increases greatly at concentrations which are usually a little greater than the c.m.c. Aggregation was attributed to the adsorption of soap molecules as an incomplete second layer with their hydrocarbon chains oriented towards the water phase. If the resulting dimers at the interface are more readily wetted by the oil phase than are the single soap molecules, as appears likely, a stability maximum would be expected at concentrations a little higher than the c.m.c. of the soap, in accordance with experiment.

This work forms part of a program of fundamental research undertaken

by the Board of the British Rubber Producers' Research Association. Our thanks are due to Messrs. Unilever Ltd. for the gift of pure samples of lauric acid and to Mr. P. E. Turner for assistance in the experimental work.

REFERENCES

1. HARDY, W. B., *J. Chem. Soc.* **127**, 1225 (1925).
2. REHBINDER, P. A., AND WENSTRÖM, E., *Kolloid-Z.* **53**, 145 (1930).
3. TALMUD, D., AND SUCHOWOLSKAJA, S., *Z. physik. Chem.* **154A**, 277 (1931).
4. BURCIK, E. J., *J. Colloid Sci.* **5**, 421 (1950).
5. BARTSCH, O., *Kolloid-Z.* **38**, 177 (1926).
6. WARK, I. W., Australian and New Zealand Association for the Advancement of Science, Section B, Presidential Address, Adelaide, 1946.
7. COCKBAIN, E. G., AND McMULLEN, A. I., *Trans. Faraday Soc.* **47**, 322 (1951).
8. JOLY, M., *Kolloid-Z.* **89**, 26 (1939).
9. LANGMUIR, I., AND SCHAEFER, V. J., *J. Am. Chem. Soc.* **59**, 2400 (1937).
10. SCOTT, A. B., AND TARTAR, H. V., *J. Am. Chem. Soc.* **65**, 692 (1943).
11. MERRILL, R. C., AND GETTY, R., *J. Phys. & Colloid Chem.* **52**, 774 (1948).
12. SCHUTZ, F., *Trans. Faraday Soc.* **38**, 85 (1942).
13. MCBAIN, J. W., MERRILL, R. C., AND VINOGRAD, J. R., *J. Am. Chem. Soc.* **63**, 670 (1941).
14. SCHULMAN, J. H., AND COCKBAIN, E. G., *Trans. Faraday Soc.* **36**, 651 (1940).
15. REHBINDER, P. A., AND TRAPEZNIKOV, A. A., *Acta Physicochim. U.R.S.S.* **9**, 257 (1938).
16. CUMPER, C. W. N., AND ALEXANDER, A. E., *Trans. Faraday Soc.* **46**, 253 (1950).
17. GIBBS, J. W., *Collected Works*, Vol. 1, pp. 300-314. London, 1928.
18. ADAM, N. K., *Physics and Chemistry of Surfaces*, p. 206. Oxford University Press, 1938.
19. ADAM, N. K., *Physics and Chemistry of Surfaces*, p. 151. Oxford University Press, 1938.
20. COCKBAIN, E. G., *Trans. Faraday Soc.* **48**, 185 (1952).

CRITICAL SEDIMENTATION AND VISCOSITY STUDIES ON CALF THYMUS SODIUM DESOXYRIBONUCLEATE¹

Virgil L. Koenig and J. D. Perrings

*From the Los Alamos Scientific Laboratory, University of California, Los Alamos,
New Mexico*

Received February 9, 1953; revised April 28, 1953

ABSTRACT

Sedimentation data for sodium desoxyribonucleate collected on the Spinco ultracentrifuge at 15°, 20°, 25°, and 30°C. at 50,773 r.p.m. using 0.2 *M* NaCl as solvent have been corrected to 20°C. with water as solvent. When the S_{20} value was extrapolated mathematically to zero concentration, significant differences were obtained in the values calculated from data collected at 20°, 25°, and 30°C. There were no significant differences in the values of S_{20} at zero concentration for data collected at 20°C. but at different speeds of rotation, 59,733, 50,773, and 39,466 r.p.m. Intrinsic viscosities were obtained by means of the Ostwald capillary viscometer and the Brookfield rotational viscometer. No significant difference was detected in the partial specific volume determined at 15°, 20°, 25°, and 30°C. on two concentrations of the nucleate. Molecular weights for the nucleate were calculated using the average value of S_{20} , 14.79 *S*; average value of partial specific volume, 0.514; and the volume intrinsic viscosities determined on the capillary and rotational viscometers, 2887 and 3906.6, respectively. The molecular weight was found to be $1.4\text{--}1.6 \times 10^6$. If we assume a cylindrical model, the diameter is 1.85–1.87 μ , and the length is 445–523 μ .

INTRODUCTION

In the light of the recent findings regarding the influence of temperature on the sedimentation behavior of bovine fibrinogen and bovine crystalline plasma albumin (1, 2, 3), a similar investigation on thymus sodium desoxyribonucleate seemed valuable. Although recent sedimentation studies have been carried out on sodium desoxyribonucleate by Tennent and Vilbrandt (4), Kahler (5), Cecil and Ogston (6), and Krejci, Sweeny, and Hambleton (7), no emphasis has been placed on the influence of temperature on sedimentation. It was found (1, 2, 3) that the formula developed by Svedberg for correcting sedimentation values determined at an experimental temperature using an experimental solvent to 20°C. and water as solvent did not in all cases adequately correct the data in the cases of plasma albumin and

¹ Work done under the auspices of the U. S. Atomic Energy Commission. Presented in preliminary form before Colloid Division of 122nd meeting of American Chemical Society, Atlantic City, September, 1952.

fibrinogen. The purpose of this investigation is to test again the correction formula of Svedberg in the case of thymus sodium desoxyribonucleate.

The viscosity of desoxyribonucleic acid solutions has been investigated by various workers, Vallet and Schwander (8), Schwander (9), Basu (10), and Pouyet (11, 12). It was decided that an investigation of the viscosity of thymus sodium desoxyribonucleate at various temperatures would be desirable. Vallet and Schwander (8) have pointed out that viscosity determinations for desoxyribonucleic acid by means of a capillary viscometer give abnormally low values inasmuch as the material exhibits non-Newtonian behavior. The value of the viscosity coefficient is strongly dependent on the flow gradient. They have suggested the use of the Couette viscometer, which employs the principle of the rotating cylinder at different speeds. In the work reported here, viscosity studies have been carried out at various temperatures using a capillary viscometer and using a rotating cylinder viscometer at four different speeds.

Signer and Schwander (13, 14) have described a method of preparing highly polymerized thymus sodium desoxyribonucleate. A quantity of this material was prepared by the same procedure for the physicochemical studies described here.

The molecular weight of the sodium desoxyribonucleate was determined by means of the method of Lauffer (23) and described recently for plasma albumin (3). The sodium desoxyribonucleate was assumed to be a prolate ellipsoid of revolution, and the molecular dimensions were calculated for a cylindrical rod.

Molecular weights have been determined for sodium desoxyribonucleate by various methods. The method of light scattering has been used by Smith and Sheffer (15), Katz (16), and Reichmann, Varin, and Doty (17). Schwander and co-workers (18, 19) have determined the molecular weight by the method of streaming birefringence. Jungner and co-workers (20) have determined the molecular weight by dielectric measurements.

METHODS

For the preparation of the sodium desoxyribonucleate, 2.3 kg. freshly frozen calf thymus were treated according to the Signer and Schwander procedure (13). Instead of removal of the protein entirely by high-speed centrifugation, filtration with a Sperry filter press was employed. Around 13 g. of a white, highly fibrous preparation of sodium desoxyribonucleate was obtained.

For sedimentation studies, the sodium desoxyribonucleate was dissolved in 0.2 *M* NaCl. Sedimentation determinations were made using the Spinco ultracentrifuge on at least nine different concentrations of the nucleate in the solvent. As in (1), the temperature could be controlled usually within less than 1° of the desired value. These determinations were made at 15°,

20°, 25°, and 30°C. The temperature of the rotor was measured at the beginning and at the end of the centrifugal run by means of the thermocouple. Care was taken to see that the temperature indicated by the stationary thermocouple mounted near the rotor suspension did not vary excessively. This control of temperature was accomplished by turning on and off the refrigeration during the run. Temperature differences at 5° intervals were used to minimize the possibility of small admissible errors in measuring the temperature. All of these determinations were made with the centrifuge running at 50,773 r.p.m. In addition, sedimentation studies were made at 20°C. and at speeds of 59,733 and 39,466 r.p.m.

When S_{20} for the nucleate was plotted against concentration, it was found that the correlation was a nonlinear relation and not a straight line as in the case of fibrinogen and plasma albumin (1, 2, 3). For this reason, the extrapolation of S_{20} to zero concentration became difficult using the S_{20} versus concentration curves. For low concentrations, $1/S_{20}$ versus concentration forms a straight line, but at higher concentrations, the curve bends away from the $1/S_{20}$ axis. It was decided to find an equation that would fit the S_{20} versus concentration plot and thus determine the intercept mathematically. It was found that the equation

$$S_{20} = \frac{A + Bc}{1 + Dc}$$

fitted the data very well. To fit the data to this equation by the method of least squares became a difficult task because upon partial differentiation of this equation with respect to the constants, difficulties were encountered in the solution of the expressions obtained. It was found, however, that by solving the following three simultaneous equations, values could be found for the constant terms resulting in an equation that fitted the experimental data rather well:

$$\begin{aligned} nA + B\sum c - D\sum cS &= \sum S; \\ A\sum c + B\sum c^2 - D\sum c^2S &= \sum cS; \\ A\sum S + B\sum cS - D\sum cS^2 &= \sum S^2. \end{aligned}$$

By substituting the concentrations in the final equation, the theoretical values of S_{20} could be found. From the difference between the theoretical and experimental values of S_{20} , the standard error of estimate, S_y , could be calculated by standard methods. The correlation coefficient could be obtained by the method outlined in Kenney (22) for nonlinear regressions.

The value of A in the main equation is the most interesting quantity to be determined, because it represents the value of S_{20} at zero concentration. In order to compare the values of A from the different sets of data, the expression in Table I for the critical ratio has been used. The critical ratio represents the ratio of the difference of the intercepts to the total standard error of estimate of the two curves. From the degrees of freedom ($n - 3$

pieces of data for each curve) and this ratio, one can from Fisher and Yates' tables (26) determine the probability of this difference happening by chance alone.

The viscosity studies were carried out on six different concentrations of the nucleate in 0.2 *M* NaCl at 20°, 25°, and 30°C. In all cases the nucleate solutions were dialyzed against the solvent for 72 hours at 5°C. before the above determinations were made. The solutions were filtered through a sintered-glass filter before viscosity determinations were made in order to remove any large particles. The ordinary Ostwald viscometer with 80–100 sec. flow time for water was used. The determinations were made in a bath

TABLE I

Summary of Sedimentation Regression Curves for Various Temperatures

0.2 *M* NaCl as solvent at 50,773 r.p.m.

Temp. °C.	Equation of curve	Correlation coefficient, <i>r</i>	Standard error of estimate for curve, <i>S_y</i>
30	$S_{20} = \frac{17.42 + 42.15c}{1 + 15.16c}$	0.994	0.33
25	$S_{20} = \frac{18.14 + 37.79c}{1 + 14.00c}$	0.996	0.31
20	$S_{20} = \frac{15.02 + 26.91c}{1 + 10.45c}$	0.994	0.33
15	$S_{20} = \frac{15.12 + 30.07c}{1 + 11.39c}$	0.991	0.38

C.R. for intercepts 30° and 25°C. = 1.600 for 12 degrees of freedom.

C.R. for intercepts 25° and 20°C. = 6.887 for 13 degrees of freedom.

C.R. for intercepts 20° and 15°C. = 0.196 for 14 degrees of freedom.

C.R. for intercepts 20° and 30°C. = 5.139 for 13 degrees of freedom.

C.R. = $(A_1 - A_2) / \sqrt{S_{y1}^2 + S_{y2}^2}$, where *A* = intercept and C.R. = critical ratio

thermostated to within $\pm 0.1^\circ\text{C}$. of the desired temperature. The concentration of the original nucleate solution and the density of the nucleate solutions and solvent were determined as previously described (21). The original nucleate solution was serially diluted by weight producing the remaining five concentrations. The viscosity, η , of the solutions were referred to water as standard. The data were then plotted as $\log \eta$ against concentration in grams nucleate/100 ml. solvent. The method of least squares was used to determine the equations of the lines of regression. The relative viscosities, η_r , of the nucleate solutions to the solvent were also calculated. The equations for the lines of regression of $\log \eta_r$ on concentration were determined by the method of least squares. The slopes of these lines after the common logarithms were converted to natural logarithms became the weight intrinsic viscosities.

For the determination of viscosity by use of the rotating cylinder method,

the Brookfield viscometer, Model LVF with UL Adapter, was employed. The Brookfield viscometer, Model LVF with UL Adapter, approaches the Couette viscometer in that the center cylinder can rotate at various speeds within the outer cylinder of the adapter. In that the inner cylinder rotates rather than the outer, the viscometer resembles more closely the Searles viscometer than that of Couette. With this viscometer, it is possible to determine viscosities at 60, 30, 12, and 6 r.p.m. Most commercially available viscometers are designed for the determination of high viscosities such as pitch and tars. With the UL Adapter it is possible to determine materials having viscosities of the magnitude of water and greater. The general difficulty with rotational viscometers is in the measurement of small amounts of torque with sufficient accuracy. In the case of this work, the determinations were made at 20°C. first on 0.2 *M* NaCl, then on six concentrations of the nucleate at each speed, namely, 60, 30, 12, and 6 r.p.m. At the highest concentration, it was impossible to read the viscometer at 60 and 30 r.p.m., because the readings were off scale. Inasmuch as the value for the viscosity of 0.2 *M* NaCl could not be obtained accurately at speeds of 30, 12, and 6 r.p.m., all values of the viscosity of the nucleate at each speed of rotation and at each concentration were divided by the viscosity of 0.2 *M* NaCl at 60 r.p.m. This gave the relative viscosity, η_r . The equations for the lines of regression of $\log \eta_r$ on concentration were determined by the method of least squares, assuming that the lines were through the origin in all cases. The slopes of these lines after conversion from common logarithms to natural logarithms became the weight intrinsic viscosities. In all cases the weight intrinsic viscosities were converted to volume intrinsic viscosities by multiplying the weight intrinsic viscosity by 100 and dividing by the partial specific volume.

The partial specific volume of the sodium desoxyribonucleate was determined by the method (21) previously described. Determinations were made at 15°, 20°, 25°, and 30°C.

RESULTS

A typical boundary of sodium desoxyribonucleate is given in Fig. 1. This boundary represents a 0.75% solution in 0.2 *M* NaCl after 142 minutes running at 50,773 r.p.m. The direction of migration is toward the right from the axis of rotation. The angle of the Schlieren bar was 70°. The material appears homogeneous and can be considered to be a very good preparation of thymus sodium desoxyribonucleate. Although no claim is made that this single sedimenting boundary represents only one desoxyribonucleate, it is nevertheless felt that a nucleate of narrow molecular weight distribution is being considered, inasmuch as no visible contaminating boundaries are present. There was a minimum of spreading of the centrifuging boundary with decrease in concentration. The boundary for a con-

centration of 0.025% was still hypersharp. The possibility of polydispersity is not denied in this preparation of nucleate, yet ultracentrifugal determinations can be made at much lower concentrations of the nucleate than can be made for plasma albumin or fibrinogen. Table I gives a summary of the equations for the curves of S_{20} versus concentration, the correlation co-

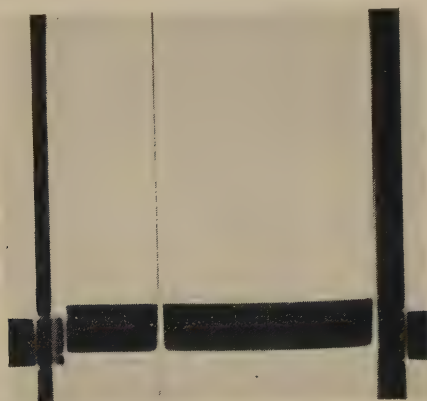


FIG. 1. Sedimentation boundary for 0.75% thymus sodium desoxyribonucleate solution in 0.2 *M* NaCl after 142 min. at 50,733 r.p.m., 20°C.

TABLE II

Summary of Sedimentation Regression Curves for Various Speeds

0.2 *M* NaCl as solvent at 20°C.

Speed, r.p.m.	Equation of curve	Correlation coefficient, r	Standard error of estimate for curve, S_y
59,733	$S_{20} = \frac{14.81 + 28.74c}{1 + 10.64c}$	0.993	0.33
50,773	$S_{20} = \frac{15.02 + 26.91c}{1 + 10.45c}$	0.994	0.33
39,466	$S_{20} = \frac{14.55 + 26.21c}{1 + 10.17c}$	0.996	0.26

efficients, and the standard errors of estimate of the curves when the sodium nucleate was dissolved in 0.2 *M* NaCl and the sedimentation experiments were performed at various temperatures. Table II gives a summary of the equations for the curves of S_{20} versus concentration, the correlation coefficient, and the standard errors of estimate for the curves at the various speeds of rotation when sodium desoxyribonucleate was dissolved in 0.2 *M* NaCl at 20°C. Table III gives a complete summary of the ultracentrifugal data. S_{20} is in Svedberg units.

The log η vs. c curves for sodium desoxyribonucleate at 20°, 25°, and

TABLE III

Summary of Sedimentation Data

0.2 M NaCl as solvent

Concentration g./100 ml.	S_{20} at 30°C.	At 50,773 r.p.m.			At 20°C.	
		S_{20} at 25°C.	S_{20} at 20°C.	S_{20} at 15°C.	S_{20} at 59,733 r.p.m.	S_{20} at 39,466 r.p.m.
1.000	3.66	3.63	3.56	3.63	3.61	3.55
0.800			4.00	3.76	3.99	3.85
0.600	4.23	4.57	4.27	4.30	4.63	4.54
0.500			4.64	4.69	4.70	4.65
0.400	5.00	5.26	5.03	5.05	5.08	5.03
0.300	5.53	5.69	5.99	5.53	5.60	5.54
0.200	6.38	6.52	6.25	6.30	6.43	6.16
0.150	7.06	7.35				
0.100	8.47	8.70	8.16	7.91	8.10, 8.12	8.17, 8.29
0.050	10.59	12.09	10.50	10.16	10.62	10.64
0.025	13.95	14.33	12.81	12.99	12.81	12.44

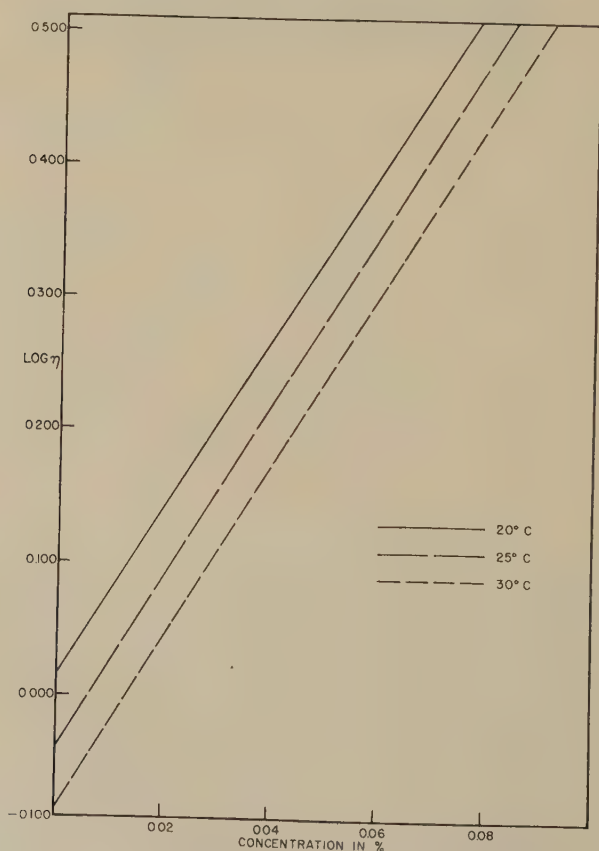


Fig. 2. Log η versus concentration curves for thymus sodium desoxyribonucleate in 0.2 M NaCl.

30°C. and determined by the Ostwald viscometer are given in Fig. 2. The viscosity here is referred to the viscosity of water at the various temperatures and therefore represents absolute units. Table IV gives a summary of the viscosity data as well as the equations for the lines of regression of $\log \eta$ on concentration and the respective correlation coefficients. η is given in centipoises. In the table the equations for the lines of regression for $\log \eta_r$ on concentration, respective correlation coefficients, r , and standard errors of the slope, σ , are given. The equations for the lines of regression of $\ln \eta_r$ on concentration are also given. There are no significant differences in the slopes of the equations of $\log \eta_r$ vs. c ; therefore, the slopes, i.e., in-

TABLE IV
Capillary Viscometer Data

20°C.		25°C.		30°C.	
Concentration g./100 ml.	Log η	Concentration g./100 ml.	Log η	Concentration g./100 ml.	Log η
0.0766	0.501	0.0770	0.461	0.0769	0.413
0.0577	0.384	0.0576	0.337	0.0575	0.288
0.0462	0.309	0.0461	0.262	0.0461	0.215
0.0384	0.258	0.0383	0.210	0.0383	0.164
0.0308	0.211	0.0308	0.162	0.0307	0.116
0.0257	0.177	0.0256	0.127	0.0256	0.080
Log $\eta = 0.0141 + 6.37c$		Log $\eta = -0.0385 + 6.50c$		Log $\eta = -0.0838 + 6.47c$	
$r = 0.99994$		$r = 0.99994$		$r = 0.99997$	
Log $\eta_r = 0.0038 + 6.38c$		Log $\eta_r = 0.0007 + 6.50c$		Log $\eta_r = 0.0028 + 6.45c$	
Ln $\eta_r = 0.0088 + 14.69c$		Ln $\eta_r = 0.0016 + 14.97c$		Ln $\eta_r = 0.0064 + 14.86c$	
$r = 0.99996$		$r = 0.99995$		$r = 0.99997$	
$\sigma = 0.04$		$\sigma = 0.03$		$\sigma = 0.02$	

Average weight intrinsic viscosity = 14.84.

Average volume intrinsic viscosity = $(14.84 \times 100/0.514) = 2887.0$.

trinsic viscosities, can be considered the same. The average value for weight intrinsic viscosity is listed in the table, and the volume intrinsic viscosity is also listed.

In Table V is found a summary of the viscosity data obtained on the Brookfield rotational viscometer at speeds of 60, 30, 12, and 6 r.p.m. In this table, the relative viscosity of the nucleate solution to 0.2 *M* NaCl as solvent is used. The equations for the lines of regression of $\log \eta_r$ on concentration are listed together with the correlation coefficients, r , and the standard errors of the slopes, σ . The equations for the lines of regression of $\ln \eta_r$ on concentration are also given. Since there are no significant differences in the slopes of the lines of regression for the various speeds of rotation, the average value of the slope is listed and represents the weight intrinsic viscosity of thymus desoxyribonucleate. The volume intrinsic viscosity also is listed.

Table VI gives the values of the partial specific volume of thymus sodium

desoxyribonucleate at various temperatures. Since no significant difference in the partial specific volumes at various temperatures was apparent, the average partial specific volume was considered to be 0.514 for this preparation of thymus sodium desoxyribonucleate.

TABLE V
Brookfield Viscometer Data

Concentration g./100 ml.	Log η_r 60 r.p.m.	Log η_r 30 r.p.m.	Log η_r 12 r.p.m.	Log η_r 6 r.p.m.
0.180			1.444	1.515
0.108	0.851	0.922	0.979	0.980
0.072	0.619	0.660	0.688	0.692
0.060	0.530	0.565	0.556	0.604
0.036	0.339	0.373	0.401	0.455
0.030	0.277	0.318	0.326	0.358
	Log $\eta_r = 8.34c$	Log $\eta_r = 9.01c$	Log $\eta_r = 8.59c$	Log $\eta_r = 8.93c$
	Ln $\eta_r = 19.21c$	Ln $\eta_r = 20.75c$	Ln $\eta_r = 19.78c$	Ln $\eta_r = 20.57c$
	$r = 0.982$	$r = 0.978$	$r = 0.977$	$r = 0.972$
	$\sigma = 0.26$	$\sigma = 0.30$	$\sigma = 0.34$	$\sigma = 0.39$

No significant difference in slopes.

Average weight intrinsic viscosity = 20.08.

Volume intrinsic viscosity = $(20.08/0.514) \times 100 = 3906.6$.

TABLE VI
Partial Specific Volume at Various Temperatures

T°C.	ϕ	Concentration g./100 ml.
15°C.	0.519	0.2814
15°C.	0.514	0.1625
20°C.	0.516	0.2812
20°C.	0.506	0.1624
25°C.	0.517	0.2808
25°C.	0.517	0.1622
30°C.	0.517	0.2804
30°C.	0.506	0.1620

Average value of $\phi = 0.514$.

DISCUSSION

By observing the equations and the critical ratios of Table I it can be seen that the values of S_{20} at zero concentration, A , at 30° and 25°C. are not significantly different. The difference between the S_{20} values at 25° and 20°C. is highly significant, and the difference in the S_{20} values at 20° and 15°C. is not at all significant. The difference in S_{20} values at 30° and 20°C. is highly significant. Differences are taken to be significant when the critical ratios indicate, according to Fisher and Yates's tables (26), that

the difference is less than two in one-hundred due to chance alone. In Table I, the critical ratios indicating significance show less than one in a thousand that the difference is due to chance. This difference in the values of S_{20} at zero concentration for the data obtained at different temperatures, although corrected to standard conditions at 20°C., indicates that this method of correcting the data is not entirely adequate. There is also a possibility that this difference is real and due to changes of the shape of the molecule or to changes in their interaction as a function of temperature. The differences in values of S_{20} at zero concentration from data collected at different temperatures and corrected to standard conditions at 20°C. is much greater than that for albumin (3). This difference may be due in part to the high viscosities of the solutions.

The data collected at different speeds of rotation of the centrifuge show no significant differences in the values of S_{20} at zero concentration, as shown in Table II. This observation would indicate that there is no measurable orientation of the molecule in the ultracentrifugal field, such as was noticed at the same speeds of rotation for fibrinogen (2). This observation does not preclude that differences in orientation might have been observed had lower speeds been used. In addition the centrifugal field might not be sufficient to orient the molecules. That the molecule is asymmetric is evident by the large amount of concentration dependence that S_{20} exhibits in Tables I and II. The lack of evidence for orientation in the centrifugal field may indicate a tremendous amount of tangling and interaction among the molecules or a lack of rigid asymmetry.

The viscosity data of Fig. 2 and Table IV indicate a great change in viscosity of the nucleate solution with temperature. The slopes of the equations in Table IV indicate a high intrinsic viscosity. This high intrinsic viscosity indicates high asymmetry of the molecule. By a comparison of the values of the slopes of the equations for log relative viscosity vs. concentration in Table IV and V, it can be seen that the data on the rotational viscometer give a significantly higher intrinsic viscosity than is obtained using the Ostwald viscometer. There is no significant difference in the values of the slopes for different speeds, which indicates that all speeds are sufficiently low to maintain approximately the same random distribution of the molecules in solution. Extrapolation to viscosity at zero gradient is thus impossible. The data on the rotational viscometer are not as precise as those taken on the Ostwald viscometer. This difference in precision is due largely to the difficulty on the part of rotational viscometers to measure small amounts of torque. The higher value of intrinsic viscosity with the rotational viscometer is as it should be. Non-Newtonian solutions always give abnormally low values on the Ostwald viscometers. Vallet and Schwander (8) have indicated the inadequacy of the capillary viscometer for the measurement of the viscosity of nucleic acid solutions. By the use of ex-

tremely dilute solutions of nucleate, values of viscosity obtained on capillary viscometers are more nearly normal, especially if the molecule is not rigidly asymmetric.

The equations Lauffer (23) used for the determination of molecular weight from sedimentation constant, intrinsic viscosity, and partial specific volume have been discussed recently (3) in the case of crystalline bovine plasma albumin. This same method has been employed in the determination of the molecular weight of thymus sodium desoxyribonucleate from the data presented in the present investigation.

First utilizing the viscosity data obtained from the capillary viscometer and assuming the nucleate to be a prolate ellipsoid of revolution, one obtains from Simha's equation for a volume intrinsic viscosity of 2887.0 an axial ratio of 237.5. By introducing the value of axial ratio into the corresponding Perrin equation, one finds the frictional ratio (f/f_0) to be 6.22. By introducing this frictional ratio, the average sedimentation constant, 14.79×10^{-13} cm./sec., partial specific volume at 20°C., 0.514 cm³/g., into the Svedberg equation (3), one obtains a value of 1,436,000 for the molecular weight of thymus sodium desoxyribonucleate. This molecular weight together with the partial specific volume and Avogadro's number substituted in the formula for the volume of a cylinder gives the following dimensions for the nucleate molecule; diameter, 1.87 m μ and length, 444.9 m μ . When the value of volume intrinsic viscosity obtained on the rotational viscometer, 3906.6, is substituted in the Simha equation, one obtains 283.32 for the axial ratio. This value introduced into the appropriate Perrin equation gives 6.80 for the frictional ratio. This value substituted into the Svedberg equation instead of the value obtained from the capillary viscometer gives a molecular weight of 1,643,000. The molecular dimensions are: diameter, 1.85 m μ and length, 523.3 m μ . In view of all factors, the two values of molecular weight agree rather well. These values of molecular weight fall well within the values reported in Davidson (24). Of course, the molecular weight of nucleates can vary because they exist in varying degrees of polymerization. Recent values of molecular weight by light scattering have been exceptionally high: 24×10^6 by Smith and Sheffer (15), 8×10^6 by Katz (16), and $6.7\text{--}7.7 \times 10^6$ by Reichmann, Varin, and Doty (17). Schwander and Cerf (18) found a value of 8×10^5 from flow birefringence measurements compared to an earlier value by means of the ultracentrifuge of 2×10^6 (27). They suggest that the high values found by light scattering may be due to small amounts of protein impurity. Jungner *et al.* (20), using dielectric measurements, got much lower values, 200,000–600,000, depending upon the preparation and salt concentration. Kahler (5) from sedimentation and diffusion data reports a value of 1.5×10^6 for the molecular weight, and Cecil and Ogston (6), using a similar method, report 8.2×10^5 . Part of the differences in the above values for molecular weight can be attributed to differences in the degree of polymerization of

the preparation studied. In the case of the values obtained by light scattering, something fundamentally different seems to cause the high values of molecular weight. Perhaps protein impurity can account for part of it, inasmuch as complete removal of all protein from a nucleic acid preparation is extremely difficult. Inasmuch as the light scattering technique can be considered a static method for determining molecular weight, a structure may exist in the nucleate solution consisting of molecular aggregates. If the suggestion of Butler and James (25) is true that the nucleate may form a gel structure even in dilute solutions, the role of thixotropy could explain some of the discrepancies. In the dynamic methods for determining molecular weight such as viscosity, sedimentation, and flow birefringence, this gel structure can be in a state of break-down or disturbance depending upon the amount of stress the method exerts upon the system. In measuring molecular weight by the static method one may be measuring aggregates, whereas by the dynamic methods smaller units are being measured. The assumption of a prolate ellipsoid of revolution as the molecular model may be inadequate. In the cases of viruses and some nucleic acids, electron microscopical studies have supported the rod and the unbranched filamentous shapes, respectively (28).

Acknowledgment is made to Mr. Bengt Carlson for material assistance in fitting the data to a suitable equation. The authors appreciate the support of Dr. W. H. Langham.

SUMMARY

Sedimentation studies have been carried out on calf thymus sodium desoxyribonucleate at various temperatures at 50,773 r.p.m. using 0.2 *M* NaCl as solvent for the nucleate. Sedimentation studies on the nucleate were also carried out at three different speeds at 20°C.

Significant differences in the value of S_{20} at zero concentration were observed when the determinations were carried out at various temperatures and corrected by the conventional formula to 20°C. and water as solvent. The greatest differences were noticed between 25° and 20°C. and between 30° and 20°C. No significant differences were noticed in the values of S_{20} at zero concentration when the experiments were made at different speeds of rotation. The average value of S_{20} at 20°C. and zero concentration was 14.79 *S*.

The viscosities of the nucleate solutions were found, as could be expected, to vary with temperature; the relative viscosity did not vary significantly with temperature. The average volume intrinsic viscosity obtained by use of the Ostwald viscometer was 2887 and with the Brookfield rotational viscometer, 3906.6.

No significant variation of partial specific volume with temperature was noticed. The average value was found to be 0.514.

Molecular weight using sedimentation constant, intrinsic viscosity, and

partial specific volume was found to be approximately $1.4\text{--}1.6 \times 10^6$. The molecular dimensions were found to be: diameter, $1.85\text{--}1.87 \text{ m}\mu$; length, $445\text{--}523 \text{ m}\mu$.

The prolate ellipsoid model of the nucleate molecule was discussed. Possible reasons for the disagreement in values for the molecular weight of sodium desoxyribonucleate determined by various methods was discussed.

REFERENCES

1. KOENIG, V. L., AND PERRINGS, J. D., *Arch. Biochem. and Biophys.* **36**, 147 (1952).
2. KOENIG, V. L., AND PERRINGS, J. D., *Arch. Biochem. and Biophys.* **40**, 218 (1952).
3. KOENIG, V. L., AND PERRINGS, J. D., *Arch. Biochem. and Biophys.* **41**, 367 (1952).
4. TENNENT, H. G., AND VILBRANDT, C. F., *J. Am. Chem. Soc.* **65**, 424 (1943).
5. KAHLER, HERBERT, *J. Phys. & Colloid Chem.* **52**, 676 (1948).
6. CECIL, R., AND OGSTON, A. G., *J. Chem. Soc.* **1948**, 1382.
7. KREJCI, LAURA E., SWEENEY, LUCILE, AND HAMBLETON, JOHN, *J. Franklin Inst.* **248**, 177 (1949).
8. VALLET, G., AND SCHWANDER, H., *Helv. Chim. Acta* **32**, 2508 (1949).
9. SCHWANDER, H., *Helv. Chim. Acta* **32**, 2510 (1949).
10. BASU, SADHAN, *Nature* **168**, 341 (1951).
11. POUYET, JEAN, *Compt. rend.* **234**, 152 (1952).
12. POUYET, JEAN, *J. Chem. Phys.* **48**, 16 (1951).
13. SIGNER, R., AND SCHWANDER, H., *Helv. Chim. Acta* **32**, 853 (1949).
14. SCHWANDER, H., AND SIGNER, R., *Helv. Chim. Acta* **33**, 1521 (1950).
15. SMITH, D. B., AND SHEFFER, H., *Can. J. Research* **28B**, 96 (1950).
16. KATZ, SIDNEY, *J. Am. Chem. Soc.* **74**, 2238 (1952).
17. REICHMANN, M. E., VARIN, ROGER, AND DOTY, PAUL, *J. Am. Chem. Soc.* **74**, 3203 (1952).
18. SCHWANDER, H., AND CERF, R., *Helv. Chim. Acta* **34**, 436 (1951).
19. SCHWANDER, H., AND SIGNER, R., *Helv. Chim. Acta* **34**, 1344 (1951).
20. JUNGNER, G., JUNGNER, I., AND ALLGEN, L. G., *Nature* **163**, 849 (1949); and *Trans. Faraday Soc.* **46**, 792 (1950).
21. KOENIG, V. L., *Arch. Biochem.* **25**, 241 (1950).
22. KENNEY, JOHN F., *Mathematics of Statistics*. D. Van Nostrand Company, Inc., New York. 1945.
23. LAUFFER, M. A., *J. Am. Chem. Soc.* **66**, 1188-1201 (1944).
24. DAVIDSON, J. N., *The Biochemistry of the Nucleic Acids*. Methuen & Co., Ltd., London, 1950.
25. BUTLER, J. A. V., AND JAMES, D. W. F., *Nature* **167**, 844 (1951).
26. FISHER, R. A., AND YATES, F., *Statistical Tables*. Hafner Publishing Co., New York. 1948.
27. CARTER, R. O., *J. Am. Chem. Soc.* **63**, 1960 (1941).
28. SCOTT, J. F., *Biachim. et Biophys. Acta* **2**, 1 (1948).

STATISTICAL THERMODYNAMICS OF A ONE-DIMENSIONAL POLYMER CHAIN INCORPORATING ENERGY AND ENTROPY EFFECTS

K. W. Scott* and A. V. Tobolsky

Frick Chemical Laboratory, Princeton University, Princeton, New Jersey

Received April 6, 1953

INTRODUCTION

A one-dimensional model is presented which incorporates both intramolecular energy and entropy effects analogous to those occurring in actual polymer chains. The complete statistical thermodynamics of this model can be worked out, and the equation of state, specific heat, and mean square end to end dimensions of the chain can be obtained.

The model is a one-dimensional chain whose segments (of equal length) point either in the positive or negative direction. When successive segments are pointed in opposite directions, this is said to constitute an interaction, measured by an interaction energy ϵ . The zero point of energy is assigned to the configuration consisting of successive segments pointed in the same direction, i.e., the straight or extended form. When ϵ is negative, the interaction is favored, and hence the folded form of the chain is favored. When ϵ is positive, the interaction (or fold) is not favored, and hence the extended form of the chain is preferred. To simplify the mathematics we shall constrain the end segments of this model to point in opposite directions.

To what extent can physical reality be associated with this one-dimensional model? This model can be related to a certain extent to a polymer chain with hindered internal rotation. Let us consider four successive inner carbon atoms (1, 2, 3, 4) of an unbranched hydrocarbon chain. The restricted rotation of the carbon-carbon bond 3-4 can be described in terms of a potential barrier with three minima corresponding to the so-called staggered configurations. One of these potential minima corresponds to a configuration in which the carbon atoms 1, 2, 3, 4 lie in the same plane (the planar zigzag configuration). The other two minima correspond to equivalent nonplanar configurations. In general an energy difference be-

* Present Address: Kodak Research Laboratories, Eastman Kodak Co., Rochester, N. Y. This paper represents a portion of a thesis submitted by K. W. Scott to the Faculty of Princeton University in partial fulfillment of the requirements of the degree of Doctor of Philosophy, June, 1949. Firestone Tire and Rubber Company Fellow, Princeton University, 1948-1949.

tween the planar and the nonplanar configurations may exist. The planar zigzag form of four carbon atoms may be related conceptually to two successive segments in our one-dimensional model which point in the same direction. The two nonplanar configurations may be associated conceptually with two successive segments of our one-dimensional model pointing in opposite directions. The exact geometric treatment of the configurations of an actual three-dimensional polymer chain is one of great mathematical complexity.

Our model may perhaps be useful in connection with the so-called α and β forms of protein molecules—one form being a folded form and the other an extended form.

In any condensed phase the interaction of a polymer chain with the surrounding medium also plays a very important role in determining the configuration and the statistical thermodynamic properties of the individual chain. The model in question here accounts only for short-range intramolecular interactions.

THE EQUATION OF STATE

Let us first obtain the equation of state for a chain of N segments, for which P segments are pointing in the positive direction and Q segments are pointing in the negative direction. For mathematical convenience we assume that the two end segments are pointing in opposite directions and that $P \geq Q$. The extension of the chain L , which defines its external condition of restraint, is given by

$$L = (P - Q)a \quad [1]$$

where a is the length of each segment.

To maintain the chain at extension L (i.e., at a fixed value of P and Q), a tension f is required. The value of f can be obtained from the equation

$$f = \left(\frac{\partial A}{\partial L} \right)_T \quad [2]$$

where A is the Helmholtz free energy.

We can classify the macrostates corresponding to a fixed value of P , Q with respect to a parameter I . This parameter is defined as the number of sequences of positive segments in a particular chain configuration. Since each sequence of positive segments is followed by a sequence of negative segments, I is also the number of sequences of negative segments. For example, in the configuration written below the values of I , P , and Q are 6, 19, and 14, respectively.

++++++ - +++ - - + - - - - + - ++++++ - - ++ - - - -

The total number of interactions (changes from positive to negative

sequences) is clearly $2I - 1$. In the above example the number of interactions is 11. The energy of any given chain configuration is $\epsilon(2I - 1)$.

The number of configurations $W(I)$ of a macrostate corresponding to I sequences of each type is given by

$$W(I) = \binom{P-1}{I-1} \binom{Q-1}{I-1}. \quad [3]$$

Equation [3] follows, since $W(I)$ is the number of ways of arranging P segments into I groups, such that each group has at least one segment in it, times the number of ways of arranging Q segments into I groups, such that each group has at least one segment in it.

The free energy for the macrostate is

$$A = \epsilon(2I - 1) - kT \ln W(I). \quad [4]$$

The macrostate of minimum free energy is defined by $I = I_0$ obtained from the relation:

$$\frac{(P - I_0)(Q - I_0)}{(I_0 - 1)^2} = \exp[2\epsilon/kT]. \quad [5]$$

Employing equations [2]–[5], one obtains for the equation of state

$$\sinh \frac{fa}{kt} = \frac{t}{(1 - t^2)^{1/2}} \exp[-\epsilon/kT]; \quad [6]$$

$$t = (P - Q)/N.$$

Equation [6] for the one-dimensional polymer chain was announced simultaneously by Guth and James (1) and by Scott and Tobolsky (1). Guth and James pointed out that the model used here is similar to the Ising model (2) used in attacking the problems of ferromagnetism and order disorder transformations. They showed that Eq. [6] can be obtained from the ferromagnetic results of Montroll (3) and Kramers and Wannier (4) by considering the analogy between the magnetic force field and the stress force field. We have thought that it would be valuable to record the elementary and explicit derivation given here. Details of the mathematics are given in the appendix.

Using Eq. [6] a plot has been made in Fig. 1 of the relation of force to temperature at a constant value of $t = 0.1$. The equation is plotted for both positive and negative values of the energy of interaction ϵ . A negative energy of interaction means that the chain has a tendency to fold up as the temperature is lowered. In order to maintain a given end to end separation for this model a high force will be required at low temperatures. For a positive interaction energy the chain tends to straighten out at lower temperatures, and hence the force required to maintain a given end to end

separation is less than the kinetic theory force. The kinetic theory force ($\epsilon = 0$) required to maintain the chain at constant extension is proportional to the absolute temperature.

Fig. 2 shows the same effect for various values of t in the case of a negative energy of interaction.

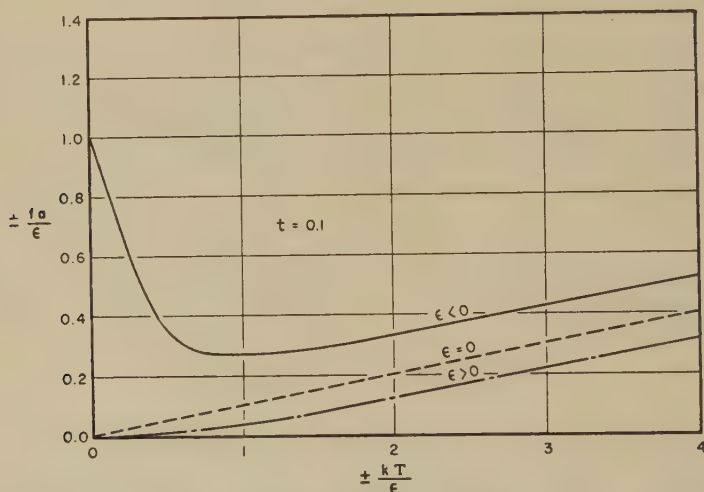


FIG. 1. Dependence of force on temperature for $t = 0.1$ and for various interaction energies ϵ according to Eq. [6].

The heat capacity at constant length for this model is given by

$$C_L = \frac{4k\mu^2 I_0^2 \exp(2\mu)}{N - 2I_0[1 - \exp(2\mu)]} \quad [7]$$

$$\mu = \epsilon/kT$$

For $t^2 \ll 1$ Eq. [7] reduces to

$$C_L = kN \frac{\mu^2}{4} \operatorname{sech}^2 \frac{\mu}{2} \quad [8]$$

Equation [8] is the same expression obtained by Montroll (3) and by Hartmann (5).

A plot of Eq. [8] is shown in Fig. 3.

CONFIGURATIONAL CHANGES IN POLYMER CHAINS INCORPORATING ENERGY AND ENTROPY EFFECTS

In a previous publication (6) it was shown that for a one-dimensional chain containing N segments each of length a , it was possible to obtain the mean square end to end separation under conditions where the *a priori* probabilities of positive and negative segments were conditional (6). If

the probability that a segment is pointed in the same direction as the previous segment is p , and the probability that the segment is pointed in the opposite direction from the previous segment is q ($p = 1 - q$), then the mean square end to end separation is (6).

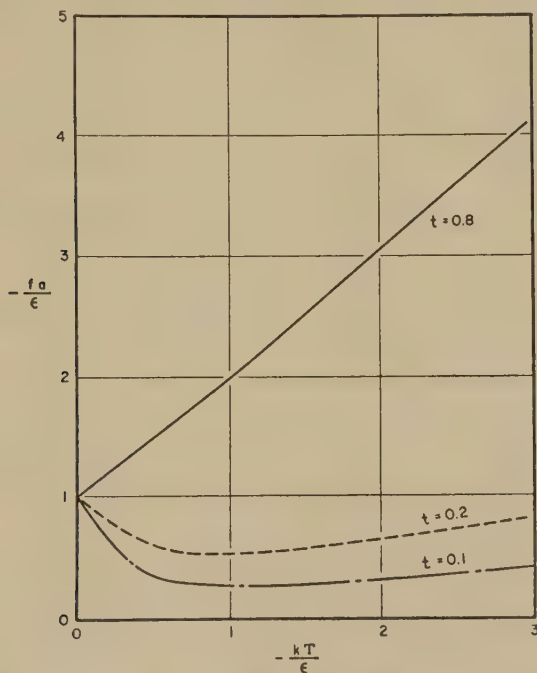


FIG. 2. Dependence of force on temperature for negative interaction energies and certain values of t according to Eq. [6].

$$\bar{x}^2 = \frac{p}{q} N a^2. \quad [9]$$

It is clear that q is related to the most probable number of positive and negative sequences I_0 as follows:

$$q = \frac{2I_0}{N} \quad [10]$$

In this case I_0 is obtained from Eq. [15] when $P = Q = N/2$, since we are here interested in the stress free case. From Eqs. [9], [10], and [15] one obtains:

$$\bar{x}^2 = \frac{1 - \frac{2I_0}{N}}{\frac{2I_0}{N}} N a^2 = e^\mu N a^2. \quad [11]$$

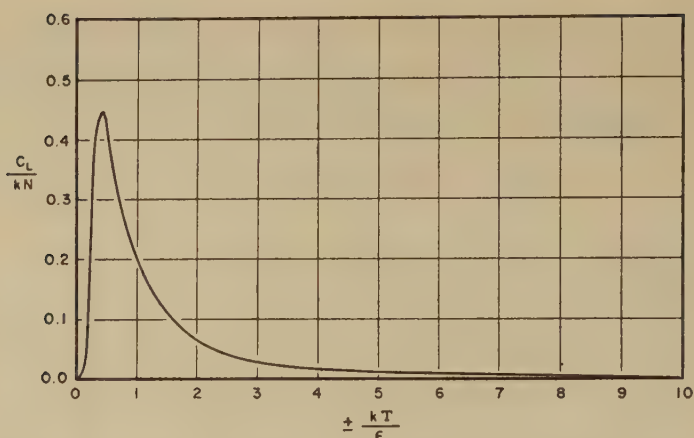


FIG. 3. Dependence of heat capacity at constant length on temperature for small extensions according to Eq. [8].

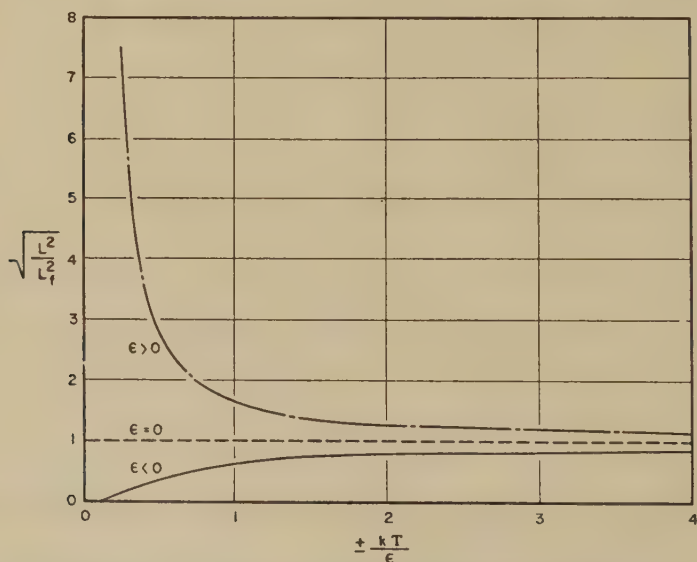


FIG. 4. Dependence of the end to end separation L on temperature for various interaction energies according to Eq. [13].

Equation [11] can be generalized to three dimensions if we consider that $a = l_0 \sqrt{3}$, where l_0 is the length of the polymer segment. The mean square end to end separation for the three-dimensional case is

$$\bar{L}^2 = 3x^2 = e^\mu N l_0^2. \quad [12]$$

The mean square free rotation length \bar{L}_f^2 is $N l_0^2$; thus,

$$\frac{\bar{L}^2}{\bar{L}_f^2} = e^\mu. \quad [13]$$

Fig. 4 presents a plot of Eq. [13].

Equation [13] can be compared with the numerical results of Taylor (7) obtained by a more refined method. According to Eq. [13] the logarithm of \bar{L}^2/\bar{L}_f^2 plotted against reciprocal absolute temperature should yield a straight line with a slope of ϵ/k . Fig. 5 shows the extent to which Eq. [13] can represent Taylor's results for the internal rotation potential function

$$V(\varphi) = 2050[0.26(1 - \cos \varphi) + 0.74(1 - \cos 3\varphi)]. \quad [14]$$

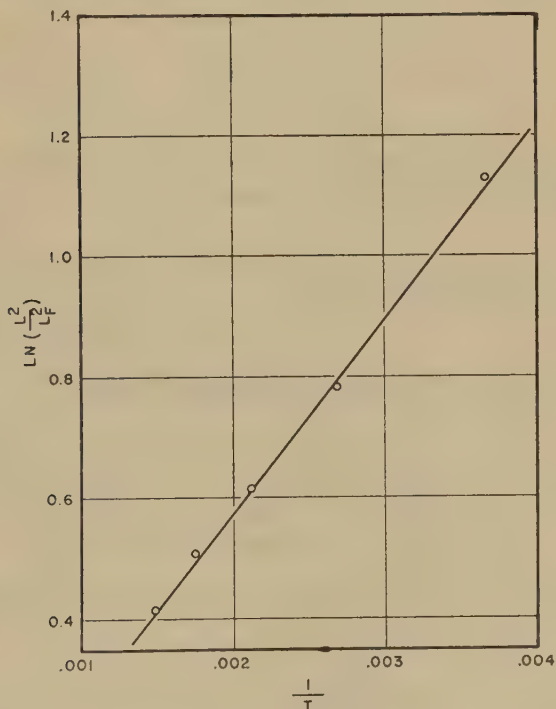


FIG. 5. A comparison of Eq. [13] with the numerical results of Taylor (circles).

The slope of the straight line in Fig. 5 corresponds to a value of 650 cal./mole. This compares with the value of 800 cal./mole given by Eq. [14] for the energy difference between the potential minima.

APPENDIX

The macrostate of minimum free energy for a given P and Q is determined by $(\partial A/\partial I)_{P,Q} = 0$. From Eq. [4], with the use of the Stirling approximation, one obtains

$$\left(\frac{\partial A}{\partial I}\right)_{P,Q} = 2\epsilon - kT \ln \frac{(P - I_0)(Q - I_0)}{(I_0 - 1)^2} = 0. \quad [5a]$$

For $I_0 \gg 1$, as required by the use of the Stirling approximation, Eq. [5a] becomes

$$(P - I_0)(Q - I_0) = I_0^2 \exp\left(\frac{2\epsilon}{kT}\right) \equiv I^2 \exp(2\mu) \quad [15]$$

or
$$\frac{2I_0}{N} = \frac{1 - [1 - (1 - t^2)(1 - e^{2\mu})]^{1/2}}{1 - e^{2\mu}} \equiv \gamma.$$

Using the definitions $P = (1/2)(N + R)$ and $Q = (1/2)(N - R)$ one obtains

$$L = Ra; \quad [1a]$$

$$fa = (\partial A / \partial R)_T. \quad [2a]$$

Using Eq. [4] for the macrostate of minimum free energy in Eq. [2a] yields through the use of the Stirling approximation

$$\frac{fa}{kT} = \frac{1}{2} \ln \frac{(Q - 1)(P - I_0)}{(P - 1)(Q - I_0)} = \frac{1}{2} \ln \frac{\left(1 - \frac{R}{N - 2}\right)\left(1 + \frac{R}{N - 2I_0}\right)}{\left(1 + \frac{R}{N - 2}\right)\left(1 - \frac{R}{N - 2I_0}\right)}. \quad [16]$$

From the definition of the inverse hyperbolic tangent

$$\frac{fa}{kT} = \tanh^{-1} \frac{R}{N - 2I_0} - \tanh^{-1} \frac{R}{N - 2}, \quad [17]$$

or
$$\tanh^{-1} \frac{fa}{kT} = \frac{R2(I_0 - 1)}{(N - 2)(N - 2I_0) - R^2}.$$

For $t \equiv R/N$, $N \gg 2$, $I_0 \gg 1$, and $\gamma \equiv 2I_0/N$ as given by [15], Eq. [17] becomes

$$\tanh \frac{fa}{kT} = \gamma t / 1 - \gamma - t^2. \quad [18]$$

Using Eq. [15] and the hyperbolic identity $\sinh x = (1 - \tanh^2 x)^{-1/2} \tanh x$, one obtains Eq. [6].

The heat capacity at constant length for this model is given by

$$C_L = (\partial E / \partial T)_R = (\partial \epsilon [2I_0 - 1] / \partial T)_R. \quad [19]$$

Using I_0 as given by Eq. [15] for the case $I_0 \gg 1$ one obtains Eq. [7]

The energy contribution to the force for this model is given by

$$f_E = (\partial E / \partial L)_T = \frac{2\epsilon}{a} (\partial I_0 / \partial R)_T = - \frac{\epsilon t}{a} [1 - (1 - t^2)(1 - e^{2\mu})]^{-1/2}$$

Although the derivation given above is not applicable for the limiting

cases $\mu \rightarrow \infty$, i.e., $I_0 = 1$ and $\mu \rightarrow -\infty$, i.e., $I_0 = Q$, Eq. [6] and [8] are nevertheless correct for these limits. In these limiting cases Eq. [4] becomes

$$A = \epsilon - kT \ln \binom{P-1}{0} \binom{Q-1}{0} = \epsilon, \quad \text{for } I_0 = 1; \quad [4a]$$

$$\begin{aligned} A &= \epsilon(2Q-1) - kT \ln \binom{P-1}{Q-1} \binom{Q-1}{Q-1}; \\ &= \epsilon(2Q-1) - kT \ln \binom{P-1}{Q-1}, \quad \text{for } I_0 = Q. \quad [4b] \end{aligned}$$

Equation [4a] in [2] and [19] yields $fa = 0$ and $C_L = 0$ for $\mu \rightarrow \infty$. For the case of large negative values of μ Eq. [4b] yields $C_L = 0$ and

$$\frac{-fa}{\epsilon} = 1 - \frac{1}{\mu} \ln 2t(1-t^2)^{-1/2}. \quad [21]$$

Equation [21] is the limit of [6] for large negative values of μ .

REFERENCES

1. GUTH, E., AND JAMES, H. M., Am. Phys. Soc. Meeting, New York, January, 1948; SCOTT, K. W., AND TOBOLSKY, A. V., *ibid.*.
2. ISING, E., *Z. Physik* **31**, 253 (1925).
3. MONTROLL, E. W., *J. Chem. Phys.* **9**, 706 (1941).
4. KRAMERS, H. A., AND WANNIER, G. H., *Phys. Rev.* **60**, 252 (1941).
5. HARTMANN, H., *Z. Naturforsch.* **3**, 617 (1948).
6. TOBOLSKY, A. V., POWELL, R. E., AND EYRING, H., *The Chemistry of Large Molecules*. R. E. BURK and O. GRUMMITT, editors. Interscience Publishers Inc., New York 1943, p. 182.
7. TAYLOR, W. J., *J. Chem. Phys.* **16**, 257 (1948).

SOLUBILIZATION OF BENZENE IN CERTAIN DETERGENT SOLUTIONS THAT APPEAR TO GIVE TWO DIFFERENT VALUES

J. W. McBain¹ and S. Gulvady Das Gupta

National Chemical Laboratory of India, Poona, India

Received February 9, 1953; revised May 6, 1953

ABSTRACT

Far below saturation of a soap solution with solubilized benzene or toluene there is a zone of maximum turbidity caused by the formation of acid soap which is largely resorbed in the micelle before true saturation is reached. The phenomenon has been observed with potassium laurate, dodecylamine hydrochloride, and cetyl pyridinium chloride, all of which are hydrolyzable, but not with sodium lauryl sulfate, where hydrolysis is absent.

The material causing the turbidity has been centrifuged out in the case of potassium laurate and has been found to be pure acid soap, HL·KL, containing no benzene. The maximum in turbidity in this intermediate zone is accompanied by a maximum in pH.

This intermediate turbid region tends to be suppressed by all factors that reduce hydrolysis or solubilize the products of hydrolysis. These are high alkalinity in the case of ordinary soaps, high concentration of soap or detergent, and high temperature, where the amount of solubilization is greatly increased.

A mechanism is suggested which might cover the known facts.

INTRODUCTION

Measurements of solubilization in soap and detergent solutions are usually as reproducible as those of true solubility. However, McBain and Richards (1) in papers published in different years were embarrassed by finding two quite different values for the solubilization of benzene and toluene by cetyl pyridinium chloride. Thus the solubility of benzene was found to be either 0.74 or 2.03 moles of benzene to 1 mole of detergent in the solution. Normally, saturation with hydrocarbon becomes immediately evident because any excess appears as a turbid emulsion.

Brady and Huff, as reported in the paper by Kaminski and McBain (2), verified, with solutions of dodecylamine hydrochloride, that there are actually two zones of clear solution separated by an intermediate cloudy zone: When benzene is added to solutions of these detergents, the solutions remain clear up to a certain point. Further addition renders them turbid, as if excess had been added; but still further addition clarifies them once

¹ Dr. McBain returned to his home at Stanford University in August, 1952, where he remained until his death in March, 1953.

more until enough has been added to produce emulsified droplets. This latter then indicates the true value for solubilization, but makes it necessary to explain the surprising intermediate cloudy zone. Incidentally, Brady and Huff showed that at elevated temperatures this intermediate cloudiness did not occur.

The present paper shows that this intermediate cloudy zone occurs when benzene is added to solutions of potassium laurate, sodium laurate, dodecylamine hydrochloride, and cetyl pyridinium chloride. It is due to hydrolysis, each of these detergents being derived from a weak base or weak acid. This finding is supported by the fact that it does not occur with solutions of sodium lauryl sulfate. Its absence at higher temperatures is explained by the well-known greatly increased solubilizing power at higher temperatures which would solubilize any products of hydrolysis and leave the solutions clear.

POTASSIUM LAURATE

The lauric acid was prepared from Pissa seeds (*Actinodaphne Hookeri*) whose oil consists of 96% trilaurin and 4% triolein. The trilaurin was purified by recrystallization from ethyl alcohol to a melting point of 45.0°C. and saponified with alcoholic potassium hydroxide; and the lauric acid (m.p. 47.0°C.) was recovered by treatment with hydrochloric acid. The latter was reconverted to potassium laurate using carbonate-free alcoholic potassium hydroxide. The potassium laurate was analyzed by a simple method suggested by C. G. McGee, using two indicators. About 0.5 g. of potassium laurate was dissolved in water and titrated against standard hydrochloric acid, with methyl red or methyl orange used as the indicator. Next, sufficient ethyl alcohol was added to dissolve the lauric acid, which was back-titrated with standard sodium hydroxide, using thymol blue as the indicator. Thus, total base and total lauric acid could be analyzed separately.

The benzene used was prepared from British Drug House's benzene, analytical reagent grade, by shaking it with concentrated sulfuric acid until there was no discoloration of the acid layer and then distilling it over phosphorus pentoxide.

In a typical experiment, an aqueous decinormal solution of potassium laurate was prepared, and the pH brought to 9.6 by adding carbonate-free potassium hydroxide. To a series of tubes having tapering necks and capacities of about 8 ml. was given 5 ml. each of the soap solution. Varying amounts of benzene, i.e., 0.002, 0.004, ... 0.080 ml., were then added to the soap solutions, chilled to suppress evaporation of benzene by means of a previously calibrated Agla micrometer syringe. The tubes were further cooled in an ice-salt mixture and sealed. They were then shaken at 25°C. for ten days to ensure equilibrium. The optical densities were measured on

a Lumetron colorimeter, with distilled water used as standard; and they were plotted against the amount of added benzene, as in Fig. 1.

The reality of the phenomenon of the double zone of clear solutions was also tested in two further qualitative experiments which altogether avoided contact of liquid benzene with the solution by approaching equilibrium solely through the vapor phase.

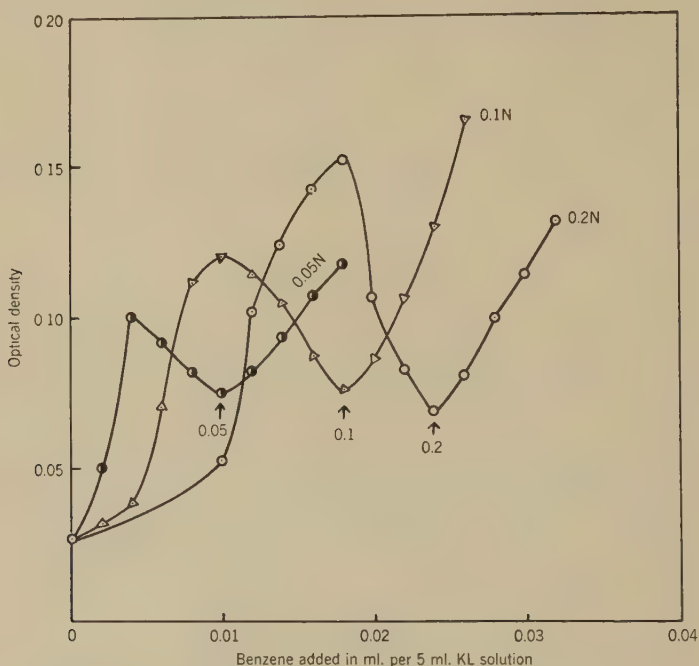


FIG. 1. Turbidity of solutions of potassium laurate of three different concentrations, all at initial pH 9.6 and 25°C., to which progressive amounts of benzene are added, showing an intermediate turbid zone before saturation and the beginning of an emulsified excess of benzene. The true solubilization for each concentration is shown by the arrows.

1. In volumetric flasks, containing various concentrations of potassium laurate, were placed open graduated tubes containing benzene. The soap solutions were observed visually while kept at 25°C. for ten days. The visible increase of turbidity with time was followed by an evident decrease and finally by a distinct increase again.

2. A Faraday tube having a calibrated capillary tube as one arm was used. Benzene was added to the capillary and potassium laurate to the other arm. The whole was cooled, evacuated, and sealed. The soap solution was kept at 22°C. and the benzene at 25°C. The rate of loss of benzene from

one arm and the change of turbidity with time was measured on a Klett-Summerson colorimeter, and the same sequence was confirmed.

The values found were not corrected for solubility of benzene nor expressed in moles per mole of soap, as this investigation was not intended to establish solubility data but to demonstrate a solubility phenomenon.

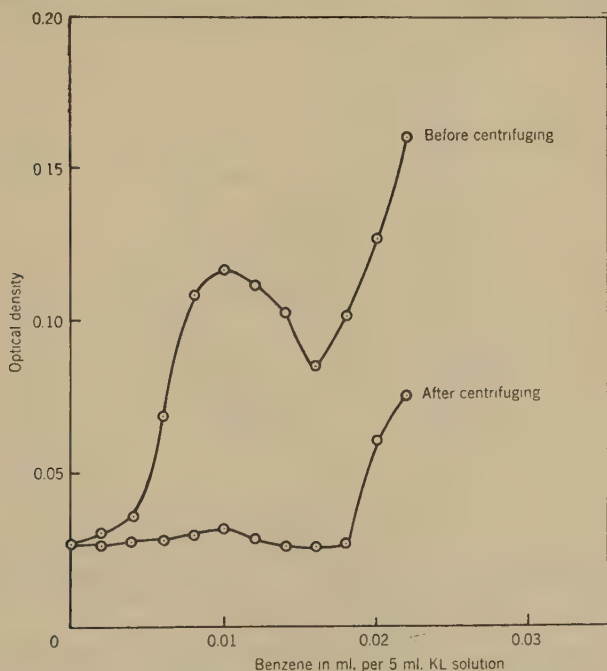


FIG. 2. Turbidity of 0.1 *N* potassium laurate solutions at 25°C. to which varying amounts of benzene have been added, showing that the intermediate turbid zone is removed by centrifuging out the acid soap, $KL \cdot HL$, in that region.

Separation of an Acid Soap by Centrifugation

It was found possible to centrifuge out the material causing the intermediate turbidity as a separate phase. This clarified the solution, as is shown in Fig. 2. It was possible to carry out an approximate analysis of the minute amount of the second phase. The ratio of laurate radical to potassium was approximately 2:1, corresponding to the well-known insoluble acid soap, $KL \cdot HL$. A microanalysis using butanone and alcoholic sodium hydroxide indicated that the acid soap contained no benzene. Analysis of the major phase also corresponded to the loss of acid soap in the intermediate turbid region. The amount of acid soap formed is very small—never more than a few per cent of the total soap in solution.

Correlation of pH with Turbidity

Several experiments were carried out in order to follow the change in pH corresponding to the development of turbidity. The tubes were shaken at 15°C. for ten days to ensure equilibrium before measurements were made. Figure 3 illustrates the results of a typical experiment, showing optical density and pH, both with respect to amount of benzene added.

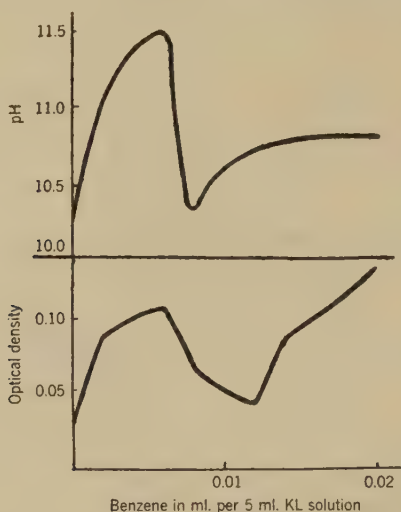


FIG. 3. Optical density and pH in relation to the amount of benzene added to a 0.1 *N* potassium laurate solution at 15°C.

The maximum pH coincides with the intermediate turbidity maximum and with the separation of insoluble acid soap from the major phase. An immediate drop in pH occurs, closely approaching the original value, as the turbidity lessens. As further benzene is added, the pH again rises, this time more slowly and to a lower value.

Summary of Results

The intermediate zone of turbidity is most pronounced at 15°C. and nearly disappears at 35°C., as illustrated in Fig. 4. This turbidity completely disappears for 0.5 *N* potassium laurate at 35°C. (not shown in figure).

As temperature increases, both the amount of solubilization and the amount of benzene required to produce the intermediate zone of turbidity increases (Fig. 5).

The turbidity is most pronounced in dilute solutions, and there occurs with the smallest amount of benzene. The solubilization of benzene increases with increase of concentration of laurate. The maximum pH value attained coincides with the maximum turbidity.

Increase in alkalinity or pH progressively suppresses the turbidity and requires more benzene for its production. At pH 13 it has practically disappeared, and the solubilization by 0.1 *N* potassium laurate is double the value observed at pH 9.6. This agrees with the usual experience that electro-

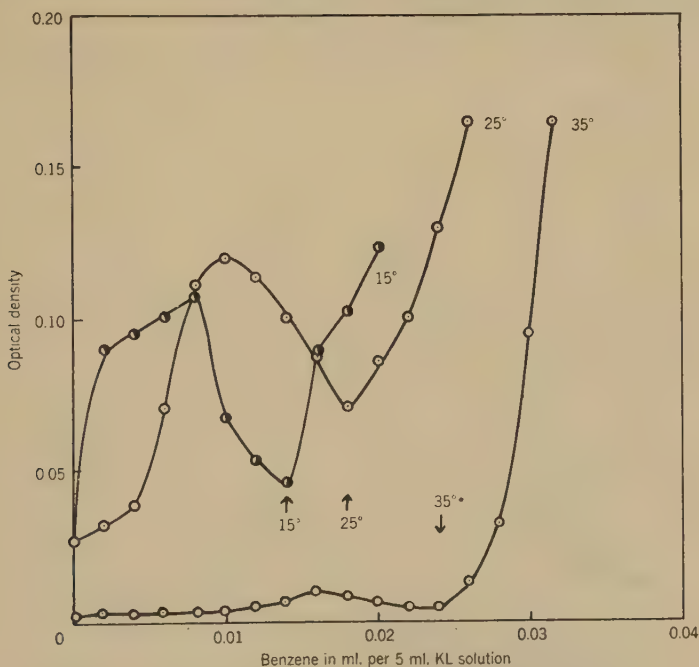


FIG. 4. Effect of temperature in increasing solubilization of benzene by 0.1 *N* potassium laurate and the suppression of the intermediate turbid zone above 35°C.

lytes (such as potassium hydroxide here) promote solubilization of hydrocarbon. Fryling and Harrington (3) also found that excess alkalinity suppressed their observed pH effect, apparently by suppressing hydrolysis.

Parallel Experiments with Toluene

These experiments showed that for a given soap concentration at the same temperature, about three-quarters as much toluene was solubilized as benzene. The intermediate turbid zone was also prominent. There was the usual increased solubilization with increased concentration of potassium laurate, and the effect of temperature was again pronounced.

Sodium Laurate

Results with sodium laurate were in general similar to those with potassium laurate and therefore need not be further recorded.

DODECYLAMINE HYDROCHLORIDE

The dodecylamine was purified by recrystallization from a specimen provided by Armour Co. Its molecular weight by titration was high, namely, 228. The chloride was made by mixing equivalent quantities of amine and hydrochloric acid as determined by titration.

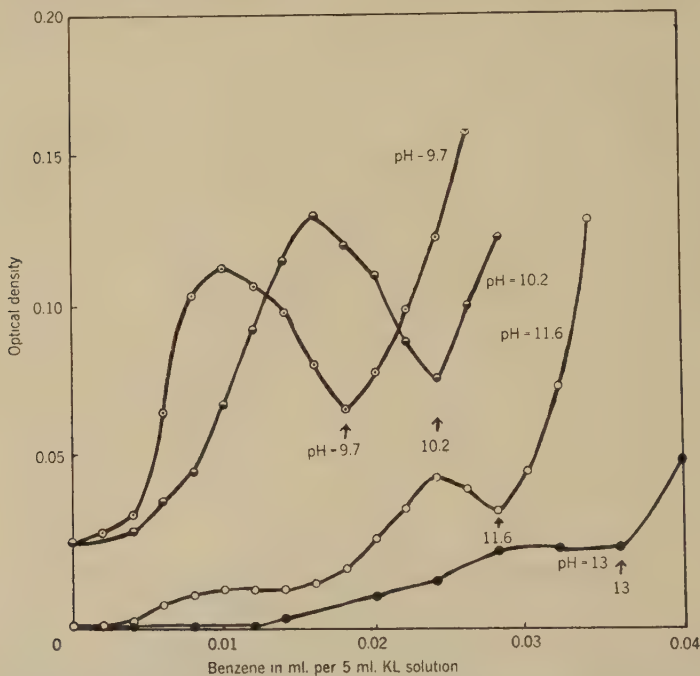


FIG. 5. Effect of increasing initial pH upon the suppression of the intermediate turbid zone in 0.1 *N* potassium laurate at 25°C. to which different amounts of benzene are added. The amount solubilized by each pH is indicated by the arrow.

The results with benzene and decinormal solution were substantially independent of pH between 4 and 9 at 25°C. The maximum turbidity at pH 4 was less than at pH 9, as would be expected from suppression of hydrolysis.

Finally experiments were conducted with decinormal solutions of pH 4.9 at 15°, 25°, and 35°C., observations being made with a Klett-Summerson colorimeter. The results are shown graphically in Fig. 6.

POLYELECTROLYTES

It was of interest to determine whether or not polyelectrolytes would solubilize substances in the same way as other colloidal electrolytes. Dr. M. K. Gharpurey undertook the preparation of several polyelectrolytes

and determined that some of them do solubilize dye but only in relatively concentrated solutions. Polyethylene oxide has only very slight solubilizing power. It is probable that the number of polar groups distributed along the macromolecule hinder the association which is so prominent a feature when the polar and nonpolar parts of the molecule are as definitely segregated as in most soaps and detergents, including some of the nonionic detergents which have large hydrophobic groups at one end.

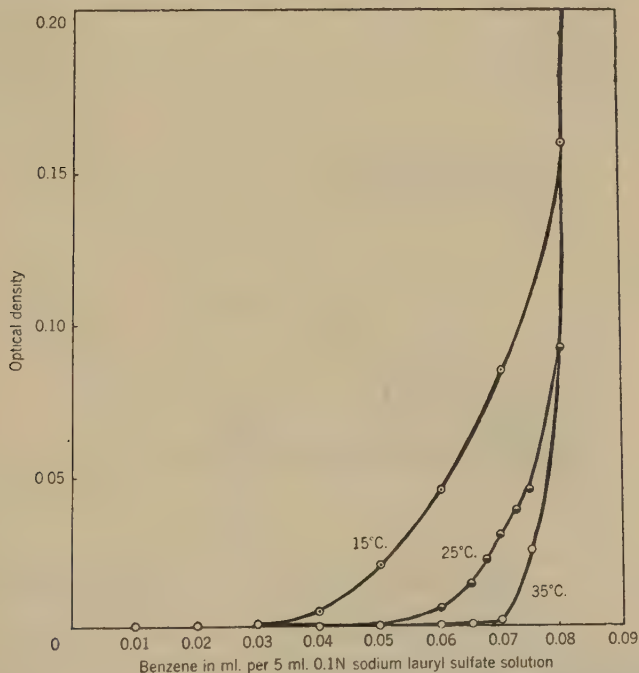


FIG. 6. The addition of increasing amounts of benzene to 5 ml. of a 0.1 *N* solution of dodecylamine hydrochloride at initial pH 4.9 at several temperatures.

SODIUM LAURYL SULFATE

Sodium lauryl sulfate, obtained from the Amend Drug Co., New York, was purified by several thermal crystallizations from anhydrous ethyl alcohol. It is a much better solubilizer for benzene than is potassium laurate with the same number of carbon atoms, 5 ml. of decinormal solution taking up 0.060 ml. of benzene, as compared with 0.022 ml. with potassium laurate and 0.050 ml. with dodecylamine hydrochloride.

At 15°C., decinormal sodium lauryl sulfate solidifies, but on addition of 0.02 ml. of benzene, it redissolves to form a clear solution.

As is seen from Fig. 7, the phenomena of the maxima and minima of optical density, observed for the potassium laurate solutions solubilizing

benzene, are not observed for the sodium lauryl sulfate solutions. Rather, the optical density of the latter solutions was practically constant up to the limit of solubilization, at which point it rose sharply. The usual large positive temperature coefficient for solubilization is also noted for this detergent.

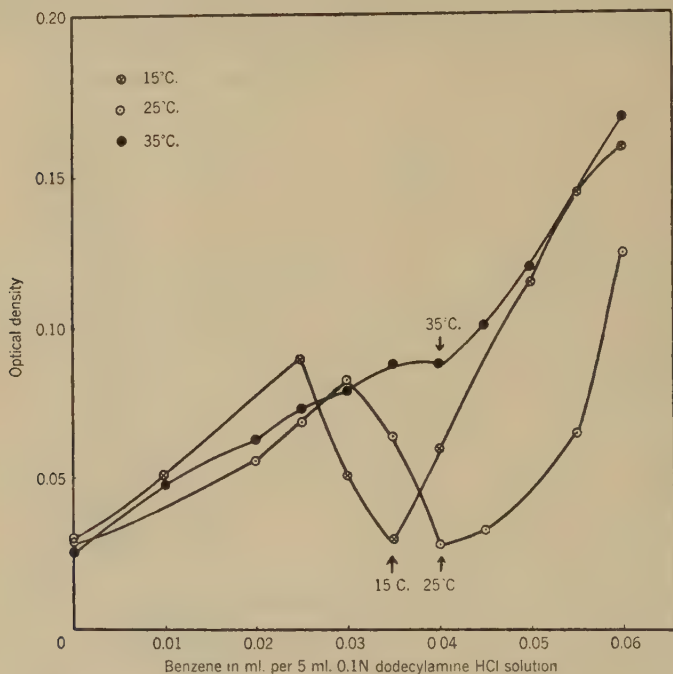


Fig. 7. Clarity of solutions of decinormal sodium lauryl sulfate to which benzene is added at different temperatures, showing no intermediate turbid zone but showing the usual high coefficient of temperature solubilization.

GENERAL DISCUSSION

It has been shown in the foregoing, in the case of the hydrolyzable detergents, that small additions of benzene can be made without marked change in the transparency of the detergent solution but that somewhat more benzene or toluene produces strong turbidity which might easily be mistaken for the formation of an emulsion. It has been proved to be precipitation of finely divided acid soap, which is highly insoluble in water though freely soluble in benzene. Still further additions of the hydrocarbon clarify the solution until the true value for the limit of solubilization is reached, and any excess appears as emulsified droplets of benzene. The material causing turbidity in the intermediate zone was centrifuged out in the case of potassium laurate, analyzed, and found to be pure acid soap, HL·KL, containing no benzene.

This series of phenomena was unexpected, but might be due to the initial benzene partially disrupting the soap micelle and rendering the micelle less stable and less able to keep the insoluble acid soap solubilized. The process is reversed when the benzene layer becomes thick enough itself to dissolve the acid soap. Some of the soap molecules in the original soap micelle may now be replaced by molecules of acid soap, $HL \cdot KL$, the whole acid end of which can reside in the benzene layer, as illustrated in Fig. 8. This will increase the stability of the micelle.

Fryling and Harrington (3) have reported on the pH of mixtures of aqueous soap solutions and monomers in a study of emulsion polymerization. Solutions of myristate and oleate were used, ranging from 85 %

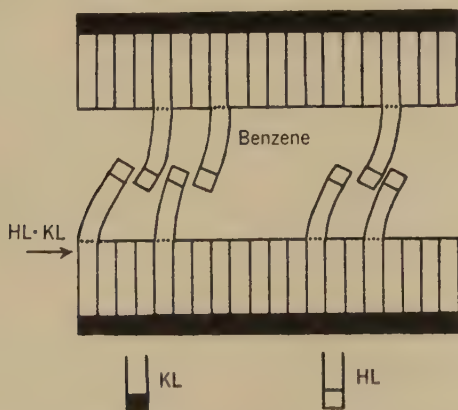


FIG. 8. Diagrammatic cross-section of a lamellar micelle, showing solubilization of acid soap in the thick lamellar layer of benzene.

neutralized (i.e., containing free fatty acid) to 185% neutralized (excess alkali). They find, generally, a decrease in pH on the initial solution of monomer (acrylonitrile, methyl methacrylate, styrene, isoprene, benzene, and methyl ethyl ketone) and an increase after the formation of a second phase. In one case, the addition of acrylonitrile to 100 % neutralized soap—comparable to the soap solutions used in the present investigation—a slight increase in pH was noted previous to the decrease generally found. Thus, if the results using neutralized soap are compared, they appear to agree with the present findings.

A similar explanation may be given for these results. If an organic micelle is formed from the solubilization of the fatty ions by the organic solvent, the hydrolysis would be lessened and the pH must decrease. However, when the product of hydrolysis is itself solubilized the solution clears and with its removal hydrolysis is favored and the pH again rises.

If we assume that the initial addition of organic solvent disrupts the soap micelle, throwing the acid soap out of solution, an explanation for

the initial rise of pH follows. As the benzene begins to be solubilized by the ionized soap, a decrease in pH results and the organic micelle resorbs the acid soap. Formation of the second phase—the benzene layer—and incorporation of acid soap combined with any slight further hydrolysis would tend to cause an increase in pH. This earlier work is thus extended by the present findings.

REFERENCES

1. MCBAIN, J. W., AND RICHARDS, P. H., *Ind. Eng. Chem.* **38**, 642 (1946); *J. Am. Chem. Soc.* **70**, 1338 (1948).
2. KAMINSKI, A., AND MCBAIN, J. W., *Proc. Roy. Soc. (London)* **198A**, 447 (1949).
3. FRYLING, C. F., AND HARRINGTON, E. W., *Ind. Eng. Chem.* **36**, 114 (1944).

RETARDATION OF FLOW IN NARROW CAPILLARIES

Recent articles by John C. Henniker (1, 2) have revived interest in the question of increased viscosity of liquid layers adjacent to a solid wall. In the second reference cited, Henniker has misquoted a paper of mine published twenty-two years ago (3), and has stated exactly the opposite conclusion from that indicated by the experiments.

From viscosity tests in platinum tubes as small as $9.35\ \mu$ in radius (as calculated from the bulk viscosity of the liquids), it was shown in my paper that for benzene, white mineral oil, *p*-cymene, and two fatty acids no rigid adsorbed layer could exist on the walls for any of the liquids thicker than about $0.03\ \mu$ (unless it had the same thickness for all). This was believed to be within experimental error. No increase in viscosity greater than 1.4% above bulk viscosity could have been produced in any of these liquids (unless it was produced in all). Again, this is believed to be within experimental error.

In glass tubes, more definite information was obtainable. Here the radius calculated from flow tests was checked by microscopic measurements. The radius measured optically was found to be $0.115\ \mu$ smaller than the radius calculated from flow tests. My paper states: "The discrepancy . . . is in the wrong direction to be accounted for on the assumption either of an adsorbed layer on the walls or of an increase in viscosity. . . ." Referring to the tests in glass tubes, Henniker says: "The capillary radius calculated from the bulk viscosity of the oil and rate of flow was less than the radius measured optically by 200 or 300A. . . . This would permit that thickness to be completely solidified oil, or a greater thickness to be partially solidified." As indicated above, this is just the reverse of the actual findings.

By reporting Wilson and Barnard's work (4) without critical comment in a paragraph by itself, Henniker seems to subscribe to their conclusions that the plugging of their tubes (up to about $350\ \mu$ in diameter) was produced by adsorption on the walls. It was shown in my paper that this plugging was due to foreign particles. Henniker also frequently quotes the Hardy school to show long-range orientation of liquid molecules under the influence of solids. But Bastow and Bowden (5), working in Hardy's own laboratory, discredited much of Hardy's work and stated: "These experiments argue against an oriented layer of liquid molecules extending to great distances

from the surface, and support the recent work of Bulkley on the viscosity of oils through fine capillaries."

I am indebted to Mr. Charles C. Templeton of Shell Development Company for calling Henniker's articles to my attention.

REFERENCES

1. HENNIKER, J. C., *J. Colloid Sci.* **7**, 443 (1952).
2. HENNIKER, J. C., *Revs. Modern Physics* **21**, 322 (1949).
3. BULKLEY, R., *Bur. Standards J. Research* **6**, 89 (1931).
4. WILSON, R. E., AND BARNARD, D. P., *J. Ind. Eng. Chem.* **14**, 683 (1922).
5. BASTOW, S. H., AND BOWDEN, F. P., *Proc. Roy. Soc. (London)* **134A**, 404 (1931).

*Socony Vacuum Laboratories,
Paulsboro, New Jersey*

RONALD BULKLEY

Received April 6, 1953

BOOK REVIEW

Colloid Science. Vol. I. Irreversible Systems, Edited by H. KRUYT. Elsevier Publishing Co., Amsterdam, 1952. 389 pages. Price \$11.00.

Volume I of *Colloid Science*, edited by Kruyt, has at last appeared. Like the preceding Volume II it is presented as a co-operative effort, but since Volume I deals with irreversible colloidal phenomena, to the understanding of which Professor Overbeek has so prominently contributed, it is only natural that he should be the main author. In fact, with 78 per cent of the pages to his credit, his name should appropriately appear on the title page.

The book presents a unified treatment of a wide and involved field. The unifying concept, that of large, delicately stabilized, kinetic units, has been given a sound theoretical foundation and is advantageously employed throughout. Of particular value is the repeated emphasis on the fundamental instability of colloidal systems and the cross reference to aging. Equally welcome is the chapter on flocculation, the first comprehensive treatment of this crucial phenomenon. Valuable contributions are also made by the chapters on electrokinetic phenomena, interaction between colloid particles, and on stability; a matured and well-integrated version of the earlier book by Verveij and Overbeek is presented, although a general acceptance of the part played by Van der Waal's forces is somewhat too readily assumed.

The reviewer is thus most favorably impressed with the book as far as it goes but cannot help being disappointed by an arbitrariness in dealing with the literature. The discussion of Dutch work and of that section of the foreign literature which is pertinent to it, is carried to the point of serious exclusion of a substantial volume of information and of different points of view. Although it is to be hoped that the touch of our Dutch Masters will be applied more uniformly in future, the penetrating quantitative analysis and the stimulating approach presented to so many obscure problems of colloid chemistry will make this book an indispensable companion to earlier texts in the field.

FREDERICK R. EIRICH, New York, New York

General College Chemistry. FRANK BRESCIA. The Blakiston Company, Inc., New York, 1953. 581 pp. Price \$6.00.

This excellent text is designed for use by students majoring in science and engineering. Although there is less descriptive inorganic chemistry than is usual, the text includes a thorough discussion of the principles of theoretical chemistry as well as unusually interesting chapters on the colloidal state and the chemistry of large molecules. A large number of excellent problems are included.

The arrangement of material and the sequence of chapters are somewhat unconventional and might create a problem in integrating lecture and laboratory work. A considerable amount of additional advanced and explanatory material is given in appendices.

B. P. DAILEY, New York, New York

FOURTH SYMPOSIUM ON PLASTICITY

The Fourth Symposium on Plasticity will be held at Brown University, Providence, Rhode Island, on September 1, 2, and 3, 1953. The three principal topics of this symposium will be:

1. Stress-strain relations (perfectly plastic, work-hardening, viscoelastic, and viscoplastic materials).

2. Distribution of stress and strain in bodies exhibiting inelastic properties (static and dynamic problems, infinitesimal and finite deformations).

3. Structural analysis and design in the inelastic range (limit analysis, static and dynamic loading, shakedown, inelastic buckling). Both foreign and American experts in the field will present papers covering their most recent experimental and analytical research, and everyone is invited to participate in the discussion.

Certain sessions of the symposium, containing papers of particular interest to civil engineers, are being sponsored, jointly with Brown University, by the Engineering Mechanics Division of the American Society of Civil Engineers. The remaining sessions are under the joint sponsorship of the Office of Naval Research and Brown University.

All persons interested in receiving further information concerning the symposium should write to Professor H. J. Weiss at the Graduate Division of Applied Mechanics, Brown University, Providence 12, Rhode Island. Copies of the program and reservation cards will be sent out approximately six weeks before the date of the symposium.

ERRATA

Volume 7, No. 6, "Electrophoresis Measurements in Benzene-Correlation with Stability. Part I. Development of Method," by J. L. van der Minne and P. H. J. Hermanie:

Page 612, $1 - e^{t/RC}$ should read: $1 - e^{-(t/RC)}$

Volume 8, No. 1, "Electrophoresis Measurements in Benzene-Correlation with Stability. Part II. Results on Electrophoresis, Stability and Absorption," by J. L. van der Minne and P. H. J. Hermanie:

Page 52, line 6, 20-100 μ moles/l should read: 20-100 m moles/l

THE SURFACE VISCOSITY OF DETERGENT SOLUTIONS AS A FACTOR IN FOAM STABILITY¹

A. G. Brown, William C. Thuman, and J. W. McBain²

Stanford Research Institute, Stanford, California

Received January 14, 1953; revised April 28, 1953

ABSTRACT

A rotational viscometer, capable of providing rheological data for surface films on solutions of surface active agents, has been developed and is described in detail.

Surface viscosity data have been obtained with a group of detergents and detergent mixtures specially selected to illustrate the role of surface viscosity in the stability of the foams obtained from the solutions by beating.

Foams of highest stability appear to be produced from solutions showing appreciable surface viscosity; solutions yielding foams of very poor stability show very low surface viscosity.

Some foams of intermediate stability which rapidly become thin and tenuous, although relatively persistent in total volume, appear as exceptions to the rule. It is suggested that the change in specific surface, in addition to the change in foam volume, with time is necessary to characterize properly the processes taking place.

Finally, it is suggested that detergents yielding foams of high foam stability consist of two or more compounds, one of which has high solubility and provides a reservoir of surface active material of poorly developed coherence; and the other of which, though much lesser in amount and also less soluble, provides the necessary coherence in the mixed surface film.

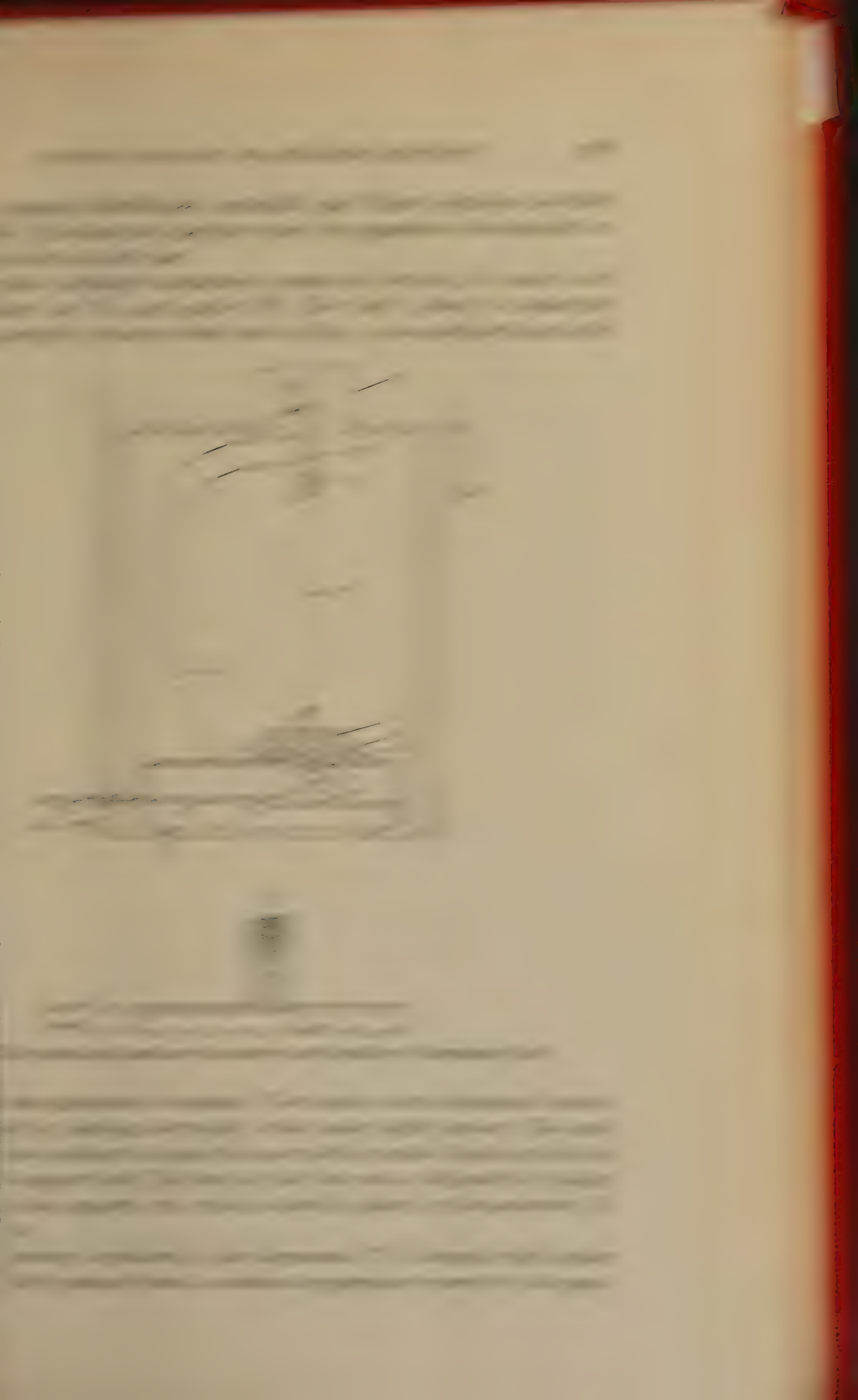
INTRODUCTION

The concept that the surface layer of a detergent solution may have mechanical properties different from those of the bulk solution is a relatively old one, apparently having been first proposed by Plateau (1), and supported by the early measurements of Wilson and Ries (2) and of Freundlich and Kores (3) on soap solutions. From these early measurements, it was concluded that the most important factor for the formation of stable bubbles or films from such solutions was the existence of a plastic, or semi-rigid, adsorbed film. In spite of the generally acknowledged importance of this factor to the development of an adequate theory of foaming behavior, practically no quantitative data have yet been published for the surface viscosity of detergent solutions.

¹ This investigation was conducted under a contract between Stanford Research Institute and the Office of Naval Research, supervised by Professor J. W. McBain.

Presented at 118th Meeting of the American Chemical Society at Chicago, September, 1950.

² Deceased.



ing in the top allows manipulation of the suspension support rod and is closed during a run by the cover (P). An opening in the front allows removal and replacement of the viscometer cup, addition of solution, sweeping, and reading of speed of rotation of cup and deflection of bob. This window is closed by a block of 1 inch thick Plexiglas during a run. Rotation speed and bob deflection are observed through a short-focal-length telescope fitted with a cross hair.

Cup and bob are protected and made somewhat hydrophobic by a coat of silicone lacquer. The lacquer was General Electric Silicone Resin Solution 9982. A baking cycle of 5 hours to 150°C., followed by 16 hours at 250–270°C., was used.

Instrumental Constants

The radius of the bob was 3.79 cm. Various cups were tried. The one used for most of this work was 1 cm. deep and 4.44 cm. in radius. The torsion wire was 0.0043 inch in diameter and 28.3 cm. long.

The "wire constant" was determined by adding a small known moment of inertia (concentric cylinder) to the bob and observing the change in period of the system. The constant K for the wire used mostly in this work was 44.3 dyne-cm. The moment of inertia of the system without added mass was 240 g.-cm.²

Materials

The "pure" sodium lauryl sulfate used in this work was specially prepared by the Organic Section of these laboratories. A large sample of 95% methyl laurate (El Dorado Oil Works, San Francisco) was carefully refractionated under reduced pressure. The middle cuts, of constant refractive index, were first reduced to the alcohol and then refractionated, and the alcohol was converted to the sulfate by the method of Dreger *et al.* (16) and was finally recrystallized several times from pure methyl alcohol. Solutions of this material still showed a slight minimum in the surface tension-concentration curve. However, it was considered sufficiently pure for our purposes without further fractionation.

The octadecyl sodium sulfate used in some experiments was a special, relatively pure sample from E. I. du Pont de Nemours & Company.

The lauryl alcohol used was Eastman Kodak white label, without further purification.

The potassium laurate used was a relatively pure material prepared by titrating Eastman Kodak white label lauric acid (dissolved in pure methanol) until the phenolphthalein end point was reached. Salts were removed by filtering hot. The solution was then cooled to precipitate the potassium laurate, which was collected on a sintered glass funnel and dried *in vacuo*. The pH of the 0.1% (wt./vol.) solution was 9.8. The product may have contained a slight excess of alkali.

The commercial materials used were as follows: sodium lauryl sulfate (City Chemical Co.), Santomerse 3 (Monsanto Chemical Co.), Quaternary O (Alrose Chemical Co.), and E 607L (The Emulsol Corp.). They were employed "as received."

Preparation of Solutions

Solutions were made up in conductivity water and are referred to on the basis of grams of surface active agent per 100 ml. of solution.

The preparation of the lauryl alcohol-(pure) sodium lauryl sulfate solutions requires special mention. The pure sodium lauryl sulfate required to give a 0.1 % or a 0.5 % solution was weighed into the respective flasks. The lauryl alcohol required to give the desired lauryl alcohol:sodium lauryl sulfate ratios was then added in a few milliliters of highly purified, Florisil-treated (17) methanol. The whole was brought into solution by gentle warming, the flasks were chilled, and the methanol removed completely (as indicated by the flasks attaining constant weight) in a vacuum desiccator. The mixture was then brought into solution and made to volume with conductivity water.

This procedure was adopted in order rapidly to obtain uniform mixtures in which solubilization effects had reached equilibrium. Solutions prepared in this way appeared to be very reproducible.

Procedure for Measuring Surface Viscosity

The shearing stress-rate of shear relations for the adsorbed films was determined as follows.

Bob and cup were cleaned by several immersions in distilled water and, finally, in conductivity water.

The cup was placed in position under the bob, the instrument carefully levelled, and the bob made as nearly concentric with the cup as possible. This is an important requirement in the design of the viscometer, since preliminary runs suggested that appreciable "off-centering" led to serious oscillation of the bob and erratic results.

The thermostat was now positioned over the viscometer and brought to temperature (25°C.). The atmosphere around the viscometer was kept at high humidity by means of wet cloths around the base of the instrument.

The "water effect" alone was first obtained. The cup was filled with conductivity water at 25°C., swept off to give a flat meniscus, and the bob lowered so as just to touch the surface of the water in the cup (giving a flat meniscus). Top cover and front window were replaced, the bob was allowed to come to rest, and its zero position was read in the telescope. Rotation of the cup was now started and speed gradually increased stepwise. For each step an initial deflection of the bob was noted, the rate of rotation of the cup determined by timing a suitable interval (degrees) on

the graduated periphery of the viscometer turntable, and a final deflection of the bob noted.

The procedure was nearly identical when a solution of surface active agent was being examined. Chief differences were that the surface of the solution was always aged for a half-hour before starting rotation, and that a flat meniscus between the bob and the edge of the cup could not always be achieved because of the low surface tension of some of the solutions. This would lead to a small change in the effective immersion depth of the bob and in the dimensions of the free surface. However, since the "water effect" is small in any case, these additional corrections were neglected. A slight oscillation of the bob (about 1% to 3% of observed deflection) was noted in most experiments but seemed to arise from slight changes in motor speed.

In calculating the constants for the viscosity curves, we have considered the adsorbed film as a mathematical plane (i.e., of unit thickness) and have employed the following easily derived modification of the Reiner equation:

$$\Omega = \frac{T}{4\pi\eta_s} \left(\frac{1}{R_b^2} - \frac{1}{R_c^2} \right) - \frac{f_s}{\eta_s} \ln \frac{R_c}{R_b} \quad [1]$$

where η_s is the coefficient of *surface* viscosity, f_s is the *surface* yield value, T is the torque produced by the *film* for an angular velocity Ω of the cup, and R_b and R_c are the radii of bob and cup, respectively. T is given by:

$$T = K(\theta - \theta_w) \quad [2]$$

where θ is the experimentally observed deflection of the bob for a given angular velocity of the cup, θ_w is the corresponding deflection of the bob in pure water, and K is the torsion constant of the suspension. Substituting and solving for η_s and f_s , one obtains:

$$\eta_s = \frac{(\theta - \theta_w - \theta_0)}{\Omega} \frac{K}{4\pi} \left(\frac{1}{R_b^2} - \frac{1}{R_c^2} \right); \quad [3]$$

$$f_s = \theta_0 \frac{K}{4\pi} \left(\frac{1}{R_b^2} - \frac{1}{R_c^2} \right) \frac{1}{\ln \frac{R_c}{R_b}} \quad [4]$$

where θ_0 is the intercept of the curve (in practice the extrapolated intercept of the linear, rising part of the curve) on the θ axis (i.e., when $\Omega = 0$). When expressed in absolute units, η_s has the dimensions (mt^{-1}), rather than ($ml^{-1}t^{-1}$) as for the three dimensional or bulk coefficient, and the unit is usually called the "surface poise." Similarly, the *surface* yield value appears as dynes per centimeter.

Equation [3] assumes that the true deflection for the film alone can be obtained simply by subtracting the deflection due to the water alone from

that due to the solution. This is a well-established convention and has been used throughout this work. It should be noted that the bulk viscosity of none of these solutions differed from that of water by more than one or two per cent.

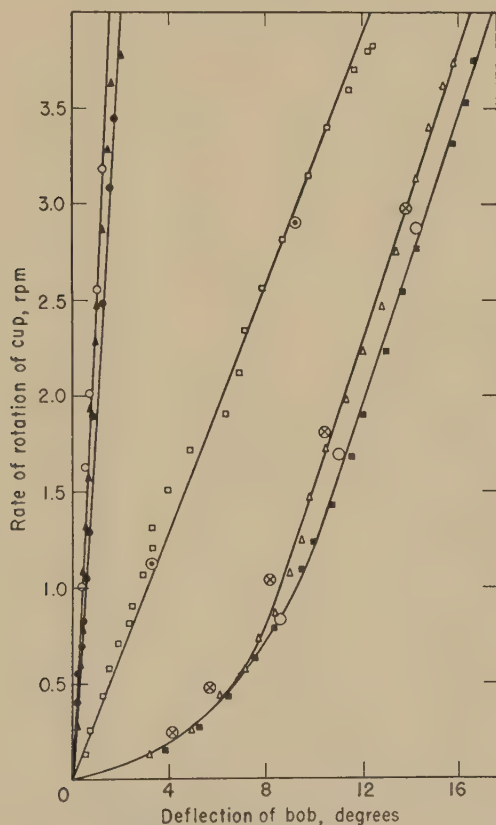


FIG. 2. Surface viscosity curves for solutions of mixtures of pure sodium lauryl sulfate and lauryl alcohol. Small circles indicate curve for water alone. The remaining curves are for solutions 0.1% in pure sodium lauryl sulfate. Lauryl alcohol concentrations are: \blacktriangle none; \bullet 0.001%; \square 0.003%; \triangle 0.005%; \blacksquare 0.008%. Large circles show points obtained on decreasing speed.

Procedure for Measuring Foam Stability

Foams were prepared from the various solutions by a beating method which produced bubbles of very small size, initially approximately 0.2 mm. in diameter.

A disc of stainless steel gauze (20-mesh, wire diameter 0.0125 inch) was welded to the bottom of a $\frac{1}{4}$ -inch brass rod which ran through a set of vertical guides and was connected through a pivot arm to a circular metal

plate. This plate was mounted on the end of a shaft rotating at a closely controlled speed of 180 r.p.m. so that a vertical reciprocating motion (180 strokes per minute; stroke length 10 inches) was given to the rod carrying the gauze. Rod and gauze were chrome-plated, and the lower half of the rod could be detached for ease of cleaning.

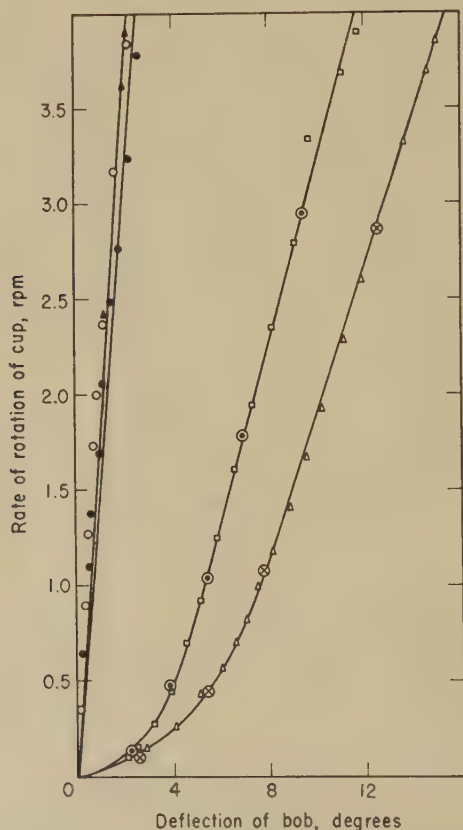


FIG. 3. Surface viscosity curves for solutions of mixtures of pure sodium lauryl sulfate and lauryl alcohol. All solutions 0.5% in sodium lauryl sulfate. Lauryl alcohol concentrations are: \circ none; \blacktriangle 0.005%; \bullet 0.015%; \square 0.025%; \triangle 0.040%. Points in large circles obtained on decreasing speed.

A 500-ml., graduated Pyrex cylinder containing 50 ml. of the solution under test was clamped in a position such that the clearance between the wire gauze and the graduate wall was about 1 mm. The beater was run exactly 5 minutes, the rod removed from the foam, and the foam volume read immediately. The graduate was then stoppered and immersed nearly to the top in a water bath at $25^\circ \pm 0.1^\circ\text{C}$. Foam volumes V_f were recorded over the lifetime of the foam and average lifetime values L_f obtained

graphically by the method of Brady and Ross (18), by dividing the area (in ml.-minutes) under the foam volume vs. time curve by the initial volume V_0 of the foam, according to the definition

$$L_f = \frac{\int V_t dt}{V_0}.$$

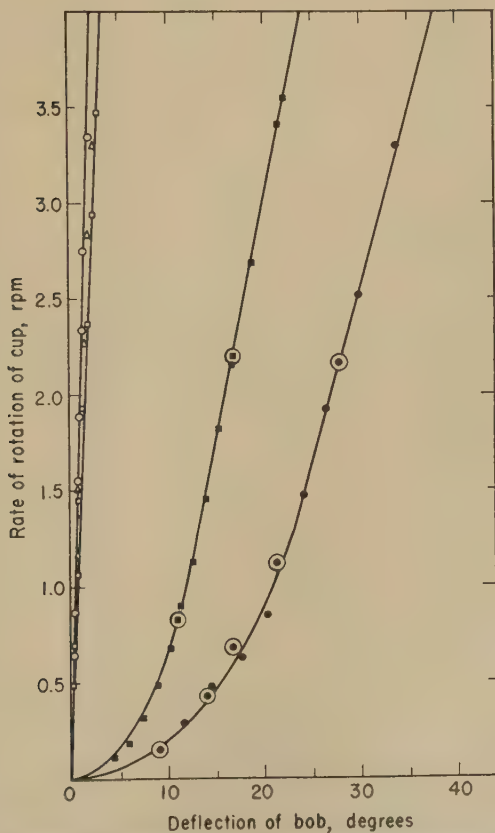


FIG. 4. Surface viscosity curves of some commercial detergents. Δ Santomerse 3; \bigcirc Quaternary O; \square E 607 L; \blacksquare potassium laurate; \bullet commercial sodium lauryl sulfate. Circled points obtained on decreasing speed.

RESULTS

The experimentally determined force-flow curves are shown in Figs. 2, 3, 4, and 5 plotted as rate of rotation (revolutions per minute) of the cup vs. deflection (degrees) of the bob. Circled points refer to data obtained by stepwise decrease in speed after maximum speed had been attained.

Figure 2 provides the data for the system pure sodium lauryl sulfate-

lauryl alcohol in which the sodium lauryl sulfate concentration (0.1% wt./vol.) is below the critical micelle concentration of the pure sulfate (0.0075 M ; 0.216%), whereas Fig. 3 provides corresponding data with the sodium lauryl sulfate concentration (0.5%) well above the critical. Corre-

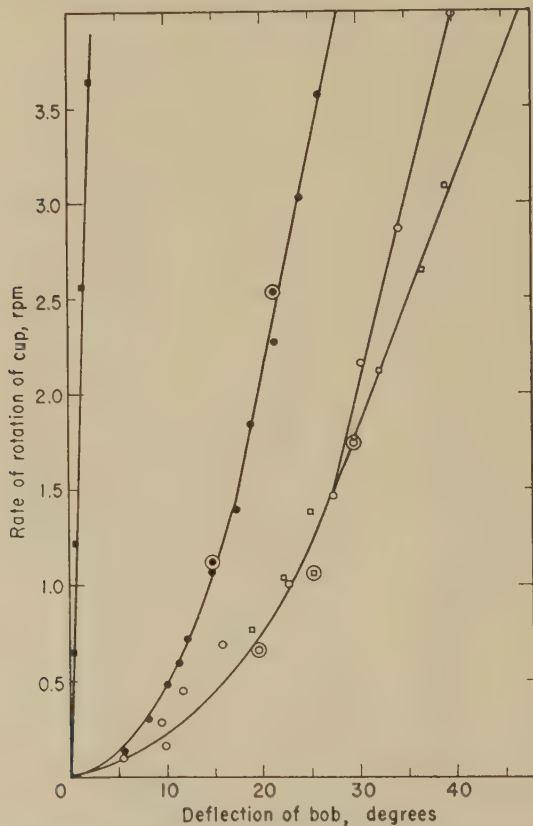


FIG. 5. Surface viscosity curves for solutions of mixtures of pure sodium lauryl sulfate (NaLS), lauryl alcohol (LOH), and sodium octadecyl sulfate (NaSS). ■ NaLS 0.1% solution saturated with NaSS; ● LOH, saturated solution; ○ NaLS 0.1%, LOH 0.008% solution saturated with NaSS; □ LOH and NaSS, solution saturated with both. Points in large circles obtained on decreasing speed.

sponding foam stability curves are shown in Figs. 6 and 7. It should be noted that the same series of *ratios* of lauryl alcohol to sodium lauryl sulfate are used in the two groups of experiments.

Figure 4 presents the "viscosity" curves for 0.1% (wt./vol.) solutions of Quaternary O, E 607 L, potassium laurate, Santomerse 3, and commercial sodium lauryl sulfate. Corresponding foam stability curves are shown in Fig. 8.

Figure 5 provides the viscosity curves for saturated solutions of lauryl

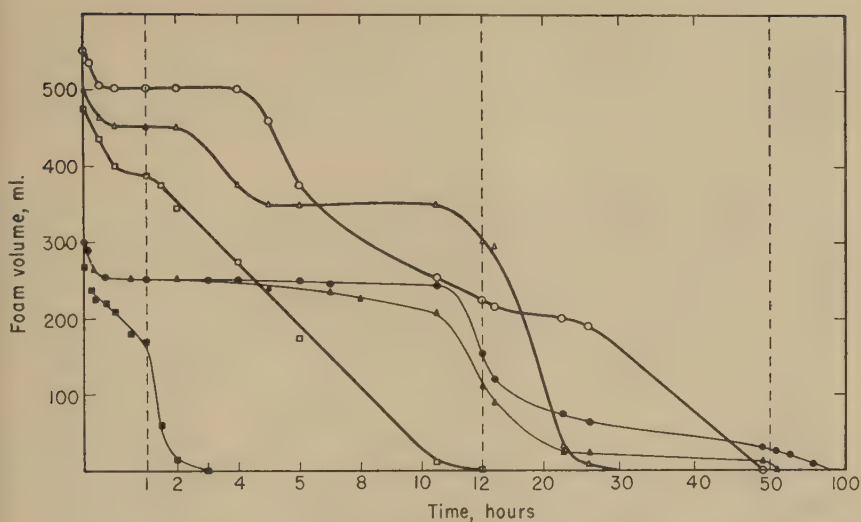


FIG. 6. Foam life curves for solutions of mixtures of pure sodium lauryl sulfate (NaLS) and lauryl alcohol. Solid points are for solutions 0.1%, open points for solutions 0.5% in NaLS. Lauryl alcohol concentrations are: \blacksquare , \square none; \blacktriangle 0.001%; \bullet 0.003%; \triangle 0.005%; \circ 0.015%. Vertical dotted lines indicate changes in time scale.

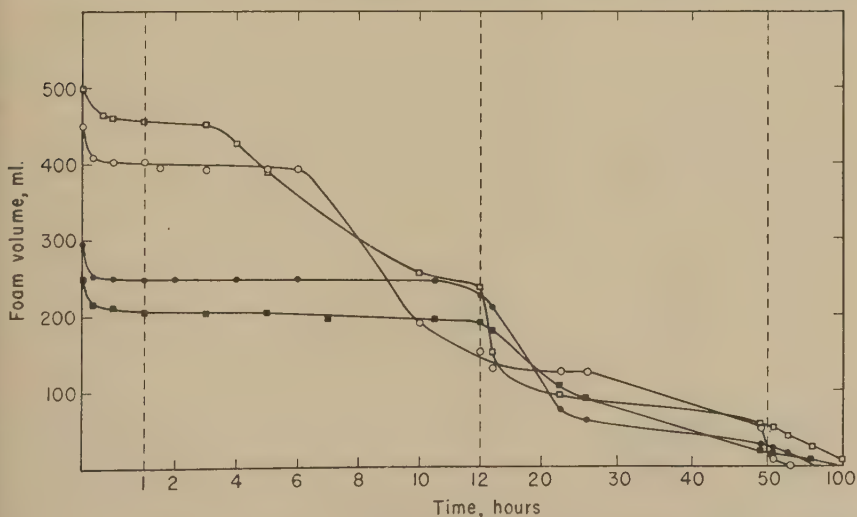


FIG. 7. Foam life curves for solutions of mixtures of pure sodium lauryl sulfate (NaLS) and lauryl alcohol. Solid points are for solutions 0.1%; open points are for solutions 0.5% in NaLS. Lauryl alcohol concentrations are: \bullet 0.005%; \circ 0.025%; \blacksquare 0.008%; \square 0.040%. Dotted lines indicate changes in time scale.

alcohol and of sodium octadecyl sulfate, alone and in various combinations with 0.1% solutions of pure sodium lauryl sulfate. While a 0.1% solution of pure sodium lauryl sulfate will dissolve up to 8% lauryl alcohol (cal-

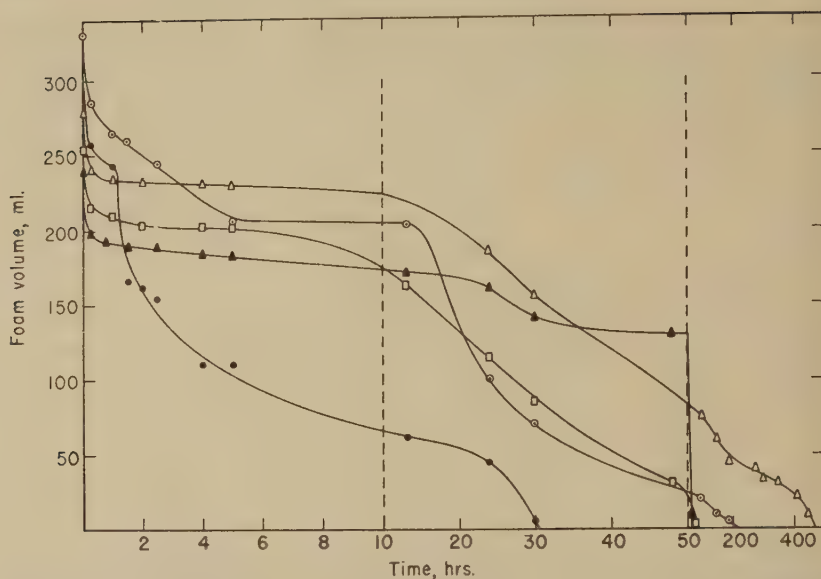


FIG. 8. Foam life curves for 0.1% solutions of some commercial detergents. ● Santomerse 3; ▲ potassium laurate; □ Quaternary O; ○ E 607 L; △ commercial sodium lauryl sulfate. Dotted lines indicate changes in time scale.

TABLE I

Surface Viscosity, Surface Yield Value, and Foam Stability Values for Solutions of Pure Sodium Lauryl Sulfate Containing Added Lauryl Alcohol

Concentration (g./100 ml.)		η_s surface poises $\times 10^3$	f_s (dynes/cm.) $\times 10^3$	L_f min.
lauryl sulfate	lauryl alcohol			
0.1	—	2.	0	70
0.1	0.001	2.	0	825
0.1	0.003	37.	0	1260
0.1	0.005	32.	54.	1380
0.1	0.008	32.	62.	1590
0.5	—	4.	0	295
0.5	0.005	3.	0	960
0.5	0.015	3.	0	1100
0.5	0.025	24.	29.	1220
0.5	0.040	31.	47.	1400

culated on the weight of sodium lauryl sulfate), a saturated solution of lauryl alcohol alone contains less than half this amount. A saturated solution of the octadecyl sulfate contains less than 1 mg. of the latter per 100 ml. of either water or 0.1% sodium lauryl sulfate solution. Lauryl alcohol or sodium octadecyl sulfate produces negligible foam by itself in the absence of sodium lauryl sulfate.

The constants calculated for the various "viscosity" curves are summarized in Tables I-III along with foam stability values derived from the corresponding curves in Figures 6, 7, and 8. The surface viscosity η_s ("plastic surface viscosity" for curves showing a yield point) is given in

TABLE II

Surface Viscosity, Surface Yield Value, and Foam Stability Values for 0.1% Solutions of Some Common Detergents

Detergent	η_s surface poises $\times 10^3$	f_s (dynes/cm.) $\times 10^3$	L_f min.
Santomerse No. 3	3.	0	440
Quaternary O	1.	0	1750
E 607 L	4.	0	1650
Potassium laurate	39.	59.	2200
Sodium lauryl sulfate (commercial)	55.	118.	6100

TABLE III

Surface Viscosity Data for Solutions Containing Mixtures of Pure Sodium Lauryl Sulfate, Lauryl Alcohol, and Sodium Octadecyl Sulfate

Solution	Material	Concentration	η_s surface poises $\times 10^3$	f_s (dynes/cm.) $\times 10^3$
1	Sodium lauryl sulfate	0.1%	2.	0
2	Sodium lauryl sulfate	0.1%		
	Sodium octadecyl sulfate	saturated	1.5	0
3	Lauryl alcohol	soln. satd.	41.	82.
4	Lauryl alcohol	soln. satd.	80.	118.
	Sodium octadecyl sulfate	soln. satd.		
5	Sodium lauryl sulfate	0.1%		
	Lauryl alcohol	0.008%	32.	62.
6	Sodium lauryl sulfate	0.1%		
	Sodium octadecyl sulfate	soln. satd.		
	Lauryl alcohol	0.008%	50.	147.

surface poises, the surface yield values in dynes per centimeter, and the values for the average lifetime of the foam, L_f , in minutes.

DISCUSSION

It is readily apparent from the figures that the viscometer as designed is capable of providing "surface viscosity" data for detergent solutions, especially when the strength of the surface film is well developed. Some improvement in the apparatus could be achieved by extending the maximum speed of rotation to at least 8 r.p.m., since the rising linear portion of some of the curves is not too well defined. The limit on the maximum

speed permissible is the onset of turbulence which, in the rotational viscometer, has been indicated by Taylor (19) as occurring when:

$$\Omega \frac{\rho}{\eta} R_c^2 \left(1 - \frac{R_b}{R_c}\right) \geq 1900$$

where Ω is the angular velocity (radians/sec.), ρ is the density (g./ml.) of the liquid of viscosity η (poises), and R_c and R_b are radii, in centimeters, of cup and bob, respectively. This would lead to a critical angular velocity of 31 r.p.m. for the present instrument with water alone in the cup; thus, it would appear that the maximum rate of rotation could be safely increased with advantage. Some additional sensitivity could be obtained by use of a finer suspension wire. However, it was found in preliminary experiments that this led to an increase in oscillations induced by small changes in motor speed and was of doubtful advantage.

In general, examples of both Newtonian and plastic viscosity are found among the systems studied, and the coincidence of "up" and "down" points on the curves indicates thixotropy to be absent. The question as to whether those systems showing an apparent yield value are truly plastic or simply pseudoplastic is of some interest. A method for distinguishing such systems in the case of bulk viscosity has been suggested by Krakauer (20) and may readily be applied to surface viscometric measurements. In the rotational surface viscometer complete "laminar" flow should start at a deflection D_2 given by

$$D_2 = 2\pi R_c^2 C D_1$$

where D_1 is the intercept on the deflection axis of the extrapolated "linear" part of the curve corrected for "water effect," the instrumental constant C is given by

$$C = \frac{1}{4\pi} \left(\frac{1}{R_b^2} - \frac{1}{R_c^2} \right) \frac{1}{\ln \frac{R_c}{R_b}}$$

and R_c and R_b are the radii of cup and bob, respectively. For true surface plasticity, D_2 so calculated should be close to the deflection corresponding to the start of the linear part of the curve (start of the extrapolation). For pseudoplastic surface films, on the other hand, if similar to bulk systems, the start of the linear part of the curve should be three or more times that calculated. In most of our curves showing non-Newtonian behavior, calculated and observed values for the onset of laminar flow agree within a few per cent, and truly plastic behavior would appear to be demonstrated. A possible exception is shown by the curve (Fig. 5) for the saturated solution of lauryl alcohol and sodium octadecyl sulfate, for which the observed onset of linearity occurs at about twice that calculated.

If one considers now the actual results obtained and examines first the viscosity data alone, the striking effect (Table I) of small amounts of lauryl alcohol in increasing the surface viscosity of the pure sodium lauryl sulfate is at once apparent. It is of interest that a greater lauryl alcohol ratio is required to produce appreciable viscosity, when the sodium lauryl sulfate concentration is above that for micelle formation than when this concentration is below the critical. The activity of the lauryl alcohol appears to be appreciably reduced by solubilization in the micelles.

That the lauryl alcohol is responsible for these viscosity effects is evident from the data (Table III) for the saturated lauryl alcohol solution alone. These data also provide a check on the method, since the plastic viscosity of the lauryl alcohol is of at least the order of magnitude to be expected from the work of Fourt and Harkins (12) on the surface viscosity of the fatty alcohols. It is instructive also to calculate the bulk viscosity corresponding to the monolayer data for the lauryl alcohol. This value should be obtainable simply by dividing the surface viscosity by the thickness of the monolayer, and corresponds to a plastic material with a "plastic viscosity" of 2.5×10^5 poises, as compared to an experimentally determined (Newtonian) bulk viscosity of 0.2 poise at 25°C. The effect of surface orientation in producing coherence in the monolayer is evident.

It has been shown by Brady (21) that pure sodium lauryl sulfate yields an expanded type of adsorbed surface film in which coherence would be very poorly developed. The present data are entirely in agreement with this. The lauryl alcohol, however, appears to act as a "condensing agent" for the sodium lauryl sulfate when both are present in the film. Small quantities increase the (Newtonian) viscosity, whereas further quantities produce a plastic structure with true yield value, and still further amounts increase mainly the yield value. Alternatively, of course, the sodium lauryl sulfate in the film may be considered to "plasticize" the lauryl alcohol in the film.

The high surface viscosity and also yield value of the commercial sodium lauryl sulfate (Table II and Fig. 5) appear to be owing to the presence of both lauryl alcohol and higher homologous sulfates, as shown by the curves of Fig. 5 and the corresponding data of Table III. The low surface viscosity of the Quaternary O, Santomerse 3, and E 607 L solutions suggests that these materials are essentially "pure" compounds. The plastic surface film on the potassium laurate solution may again indicate a two-solute component system (neutral soap + fatty acid), since Brady (21) has indicated that unhydrolyzed potassium laurate essentially gives an expanded adsorbed film.

These results for potassium laurate are in contrast to those recently reported (22) for sodium laurate solutions. The method of the oscillating disc was employed, and no surface viscosity could be detected. However,

the sensitivity of this apparatus was only one thirty-fifth that of ours, and would have provided little indication of viscosities of the magnitude found for potassium laurate. Small effects would have been masked by the large end effects (10) characteristic of the solid disc. End effects are largely eliminated by the use of the sharp-edged cylinder.

Considering now the nature of the correlations between surface viscosity and foam stability, as represented by the figures for the average lifetime of the foam, one observes that, in a general way, the solutions yielding highly coherent surface films also give the most stable foams; solutions yielding foams of very poor stability show very little surface viscosity.

Detailed correlation is, however, very much less satisfactory, especially in regard to the quaternary ammonium compounds, Quaternary O and E 607 L, and in regard to some of the sodium lauryl sulfate-lauryl alcohol systems of intermediate lauryl alcohol concentrations. It is observed that, under our carefully controlled conditions, these solutions yield foams which rapidly become thin and tenuous, with large air cells of a diameter of a centimeter or more. Although they are relatively persistent with respect to total volume, these foams should probably not be considered stable in spite of the relatively large L_f values. Volume alone does not appear to be a sufficient measure of the changes taking place in a foam. A transfer of air between the bubbles occurs owing to differences in internal pressure, and results in small bubbles becoming smaller and large bubbles larger. This thinning of the foam suggests that a measure of foam stability is required which also includes a factor for the specific surface of the foam and for its variation with time.

Finally, it appears that high foam stability is generally the result of special solute pairs present in the detergent. The major constituent has relatively high solubility, but its solution yields surface films of low viscosity. The second constituent, though lesser in amount and also less soluble, is highly surface active and gives surface films of high "viscosity." The solubility of the main constituent provides a reservoir of surface active material for the foam; the stability of the foam depends on the ability of the second member of the pair to develop the necessary coherence in the mixed adsorbed surface film.

ACKNOWLEDGMENT

The authors acknowledge with pleasure the many helpful discussions with Dr. A. P. Brady of these laboratories during the course of the work.

REFERENCES

1. PLATEAU, J., *Pogg. Ann.* **141**, 44 (1870).
2. WILSON, R. E., AND RIES, E. D., *Colloid Symposium Monograph* **1**, 145 (1923).
3. FREUNDLICH, H., AND KORES, H. J., *Z. physik. Chem.* **104**, 233 (1923).

4. BRESSLER, S. E., TALMUD, B. A., AND TALMUD, D. L., *Physik Z. Sowjetunion*, **4**, 864 (1933).
5. DERVICHIAN, D. G., AND JOLY, M., *Compt. rend.* **204**, 1318 (1937); *J. phys. radium* **8**, 471 (1937).
6. MYERS, R. J., AND HARKINS, W. D., *Nature* **140**, 465 (1937); *J. Chem. Phys.* **5**, 601 (1937).
7. WASHBURN, E. R., AND WAKEHAM, H. R. R., *J. Am. Chem. Soc.* **60**, 1294 (1938).
8. HARKINS, W. D., MEYERS, R. J., AND KIRKWOOD, J. G., *J. Chem. Phys.* **6**, 53 (1938).
9. NUTTING, G. C., AND HARKINS, W. D., *J. Am. Chem. Soc.* **62**, 3155 (1940).
10. LANGMUIR, I., AND SCHAEFER, V. J., *J. Am. Chem. Soc.* **59**, 2400 (1937).
11. TRAPEZNIKOV, A. A., *Acta Physicochim. U.R.S.S.* **9**, 273 (1938).
12. FOURT, L., AND HARKINS, W. D., *J. Phys. Chem.* **42**, 897 (1938).
13. BROWN, A. G., National Research Council of Canada, unpublished work.
14. VAN WAZER, J. R., *J. Colloid Sci.* **2**, 223 (1947).
15. CLARK, N. O., "A Study of Mechanically Produced Foam for Combatting Petrol Fires," pp. 41, 52, Chemistry Research Special Report No. 6, Department of Scientific and Industrial Research, His Majesty's Stationery Office, London.
16. DREGER, E., KEIM, G. J., MILES, G. D., SHEDLOVSKY, L., AND ROSS, J., *Ind. Eng. Chem.* **36**, 610 (1944).
17. Florisil is an activated mineral adsorbent, The Floridin Co., Warren, Pa.
18. BRADY, A. P., AND ROSS, S., *J. Am. Chem. Soc.* **66**, 1348 (1944).
19. TAYLOR, G. I., *Proc. Roy. Soc. (London)* **A157**, 546, 565 (1936).
20. KRAKAUER, V. O., *J. Appl. Phys.* **21**, 850-852 (1950).
21. BRADY, A. P., *J. Phys. & Colloid Chem.* **53**, 56 (1949).
22. BURCIK, E. J., *J. Colloid Sci.* **5**, 421 (1950).

TRANSFER OF AIR THROUGH ADSORBED SURFACE FILMS AS A FACTOR IN FOAM STABILITY¹

A. G. Brown, William C. Thuman, and J. W. McBain²

Stanford Research Institute, Stanford, California

Received January 14, 1953; revised April 28, 1953

ABSTRACT

A simple floating bubble method for determining the permeability of adsorbed surface films to air is described. Data are presented for a selected group of pure detergents and detergent mixtures, and factors affecting the interpretation of the data in terms of foam stability are discussed.

High foam stability depends on the adsorbed surface film having low permeability to air and high surface viscosity, and both of these effects may be the result of special solute pairs. Measurements of permeability and of surface viscosity provide valuable information regarding interreactions in adsorbed monolayers and in turn indicate the possibility of relating foam stability in a fundamental way to the chemical structure and composition of the detergent.

INTRODUCTION

In a previous study (1) of foam stability, it was suggested that the thinning of a stable foam may be almost entirely due to a transfer of air between the bubbles. A similar observation has recently been made by Clark and Blackman (2). Since the excess pressure within a bubble is inversely proportional to the radius, this air transfer results in small bubbles becoming smaller and large bubbles becoming larger. The object of the present study is to determine to what extent the permeability of the films between the bubbles is dependent on detergent composition, and to compare these results with data for the stability of the foams from these solutions.

Rideal (3), Langmuir (4), and more recently Sebba and Briscoe (5), have shown that insoluble monolayers spread on water may retard its evaporation, especially if the film is highly compressed. Although suggestive, this type of experiment was not directly adaptable to our purpose. A method was therefore adopted for the direct determination of the rate with which small single bubbles, floating at the surface of detergent solutions, change in size with time. The dependence of this rate on the nature of the deter-

¹ This work was carried out under a contract between Stanford Research Institute and the Office of Naval Research, supervised by Prof. J. W. McBain.

Presented at the 118th meeting of the American Chemical Society in Chicago, Sept. 1950.

² Deceased.

gent solution and on that of the adsorbed surface film has been demonstrated, and the results compared with stability data for the foams derived from these solutions.

EXPERIMENTAL

The all-glass permeability apparatus used in these experiments is shown in Fig. 1. An outer Pyrex cup (A), 5 cm. in diameter, is fitted with an inner cup (B), 2 cm. in diameter, and closed on top with a thin glass plate cemented in place with pure paraffin wax. A glass tube (D) serves to maintain the inside of the cup at atmospheric pressure. The inner cell can be filled with detergent solution through a tube (F). Air bubbles are released to

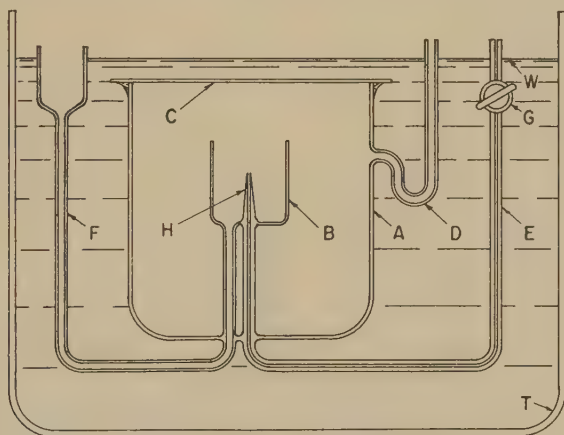


FIG. 1. Permeability apparatus.

the surface of the solution in B by forcing a small amount of air through the capillary (E) by means of a micro syringe (not shown). Stopcock (G) is left open only until the bubble has been released from the fine tip H. This stopcock is placed just below the surface (W) of the water in the glass-walled thermostat (T) to prevent changes in temperature in the capillary (E), which might cause release of further bubbles or suck-back of solution from B.

In practice, cell and thermostat were mounted on a vibration-free pier. The detergent solution in cup (B) had a slightly raised meniscus so that the bubble remained centered and still. The bubble was illuminated from two opposite sides, and its diameter determined by a travelling microscope mounted above the cell. Thermostat stirrers were stopped while diameter readings were being taken.

In the standard procedure, the inner cup of the cell was filled with solution (by its manner of preparation, essentially saturated with air),

and extraneous bubbles were removed by a sharp shake of the cell. The whole was brought to temperature (25°C. in these experiments), and the inner cup overflowed again to present a fresh surface. Approximately a half-hour later a bubble was released to the surface, and its diameter determined immediately and at regular intervals of time after initial release. With the tip used in these experiments, initial bubble diameters were in the range 1.9–3.2 mm., depending mostly on the surface tension of the solution but to some extent on the speed with which the bubble was released.

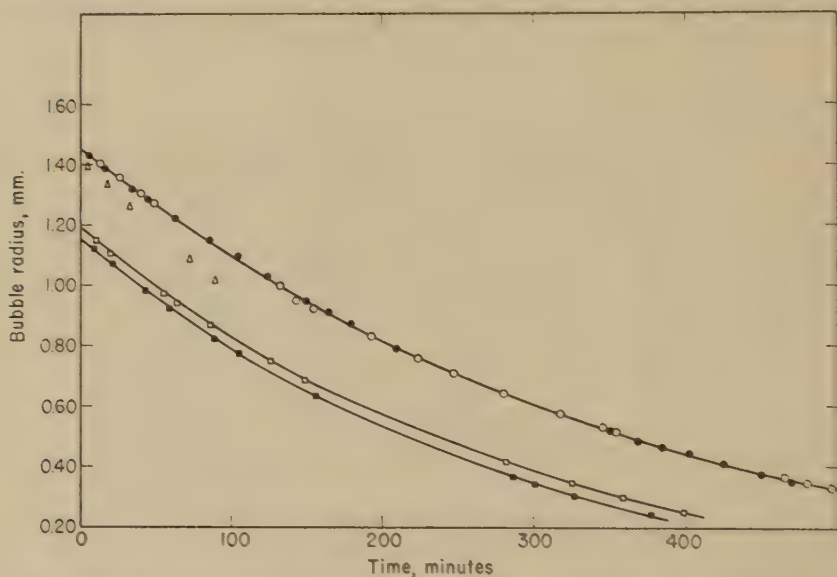


FIG. 2. Change of bubble radius with time for solutions of mixtures of pure sodium lauryl sulfate (NaLS) and lauryl alcohol (LOH). ○ ● NaLS 0.1% alone (2 runs); □ NaLS 0.5% alone; ■ NaLS 0.5%, LOH 0.01%; Δ NaLS 0.5%, LOH 0.02%.

Surface tension was determined with a Becker chainomatic interfacial tension balance, employing a calibrated 4-cm. platinum ring, and results were corrected by the method of Harkins and Jordan (6). The solution being investigated was held in a porcelain crucible cover, 5 cm. in diameter. This "dish" was thoroughly rinsed and then flamed before being used for a new solution. The atmosphere in the balance was kept saturated with moisture by damp blotters.

It was found that for many of the solutions, particularly those containing more than one solute component, the surface tension changed considerably with time. Values used here were those obtained three-fourths of an hour after a fresh surface had been exposed by sweeping, and are practically equilibrium values.

The preparation of the "pure" sodium lauryl sulfate and the potassium laurate used in these experiments has been previously described (1). Also provided in this reference is the special procedure used to prepare the lauryl alcohol (Eastman white label)-sodium lauryl sulfate solutions. Concentrations are expressed throughout as grams solute per 100 ml. of solution.

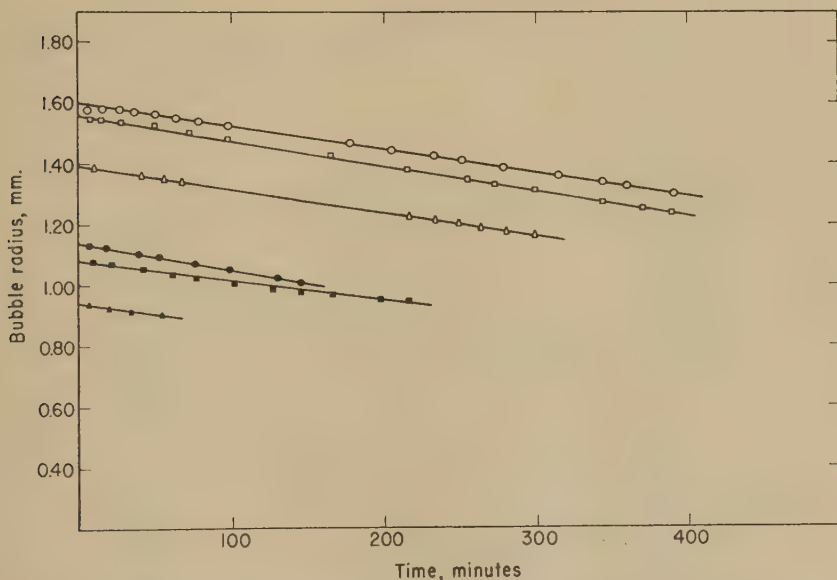


Fig. 3. Change of bubble radius with time for solutions of mixtures of pure sodium lauryl sulfate and lauryl alcohol. Sodium lauryl sulfate concentrations are 0.1% for open points and 0.5% for solid points. Lauryl alcohol concentrations are: Δ 0.0005%; \circ 0.002%; \square 0.008%; \bullet 0.025%; \blacktriangle 0.030%; \blacksquare 0.040%.

The commercial materials used were as follows: sodium lauryl sulfate (City Chemical Co.), Santomerse 3 (Monsanto Chemical Co.), Quaternary O (Alrose Chemical Co.), E 607 L (The Emulsol Corp.), and Triton X-100 (Rohm and Haas Co.). They were employed as received.

RESULTS

Curves showing the change of bubble radius with time are plotted in Figs. 2 and 3 for solutions of mixtures of pure sodium lauryl sulfate and lauryl alcohol. Both 0.1% and 0.5% concentrations of sodium lauryl sulfate, respectively below and above the critical concentration for micelle formation (0.0075 M ; 0.21%), were used. Data for the lower lauryl alcohol:sodium lauryl sulfate ratios are shown in Fig. 2, data for the higher ratios, in Fig. 3. In Fig. 4 additional curves, selected to illustrate the

effects of initial bubble size and age of the surface, are shown for these mixtures.

Data for representative commercial materials are shown in Fig. 5, plotted as change in bubble radius with time.

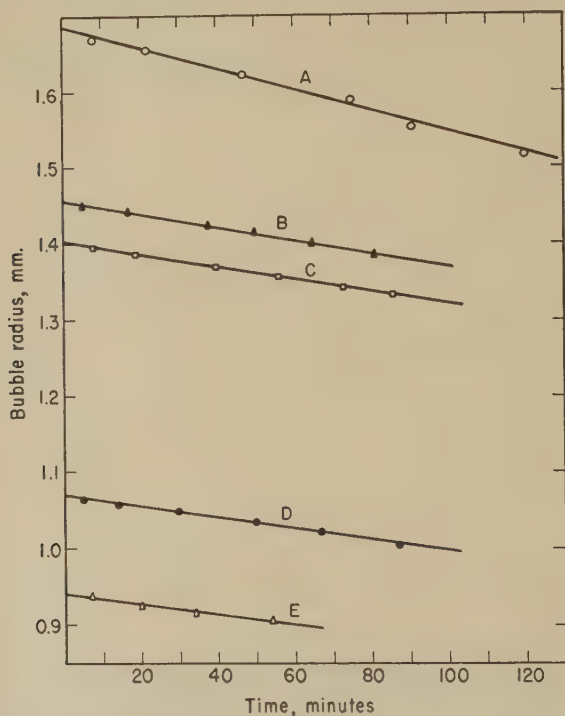


FIG. 4. Effect of initial bubble size and of age of surface on change of bubble radius with time.

A, B, C, sodium lauryl sulfate 0.10%, lauryl alcohol 0.00025%. Age of surfaces respectively 20, 30, 120 minutes.

D, E, sodium lauryl sulfate 0.5%, lauryl alcohol 0.03%. Age of surfaces both 30 minutes.

Two methods have been used to summarize the data so that results from the various solutions may be readily compared. In the first method the average rate of decrease of bubble radius with time is calculated for the first hour. In the second method an attempt is made to evaluate a permeability constant for the film between the air in the bubble and in the atmosphere. The permeability constant, k , of this film, may be defined by the equation

$$-\frac{dM}{dt} = kA\Delta C \quad [1]$$

where $-\frac{dM}{dt}$ is the number of moles of gas passing through the film per second and A is the area of this film in square centimeters. ΔC is the difference in concentration (moles/cm.³) between the gas inside the bubble

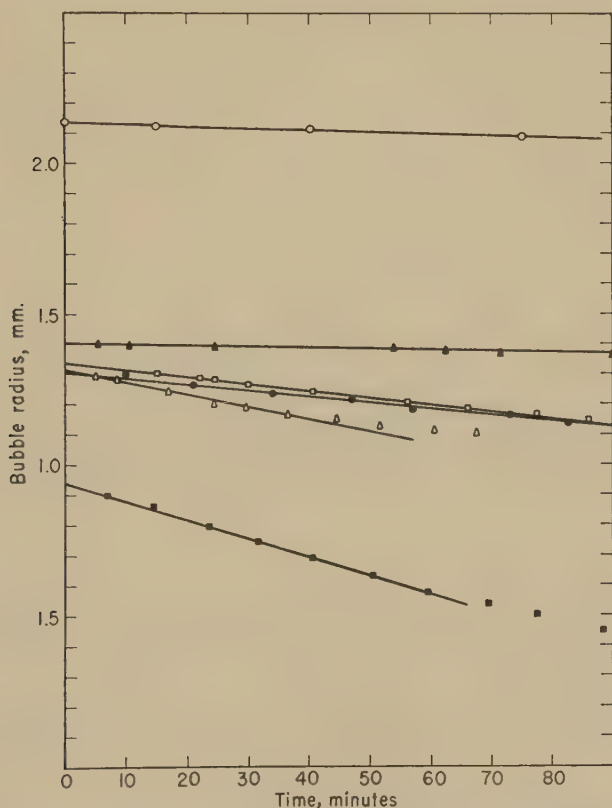


FIG. 5. Change of bubble radius with time for 0.1% solutions of some common detergents. ○ commercial sodium lauryl sulfate; ▲ potassium laurate (pH 9.8); □ E 607 L; ● Quaternary O; △ Santomerse 3; ■ Triton X-100.

and the atmosphere above the bubble. It may be expressed in terms of the excess pressure, ΔP (dynes/cm.²), which for a floating bubble is related to the surface tension of the solution by $\Delta P = \frac{4\gamma}{r}$. If the bubble is assumed to be a sphere of radius r , and the effective escape area to be a hemisphere, Eq. [1] leads to the relation

$$r^2 = r_0^2 - \frac{4\gamma}{P} kt \quad [2]$$

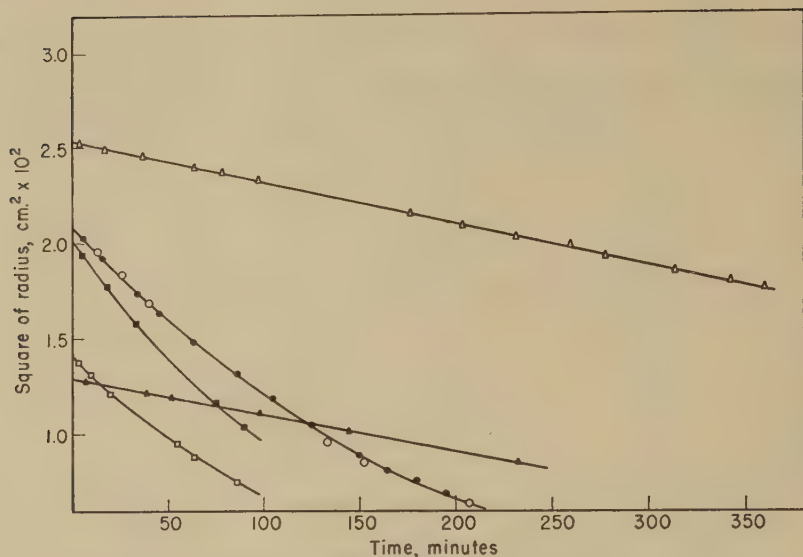


FIG. 6. Plot of square of bubble radius against time for representative solutions of mixtures of sodium lauryl sulfate and lauryl alcohol. ● ○ NaLS 0.1%; △ NaLS 0.1%, LOH 0.00 2%; □ NaLS 0.5%; ■ NaLS 0.5%; LOH 0.02%; ▲ NaLS 0.5%, LOH 0.04%.

TABLE I

Foam Life, Surface Viscosity, and Permeability Data for 0.1% Solutions of Pure Sodium Lauryl Sulfate Containing Added Lauryl Alcohol

No.	Lauryl alcohol conc. (g./100 ml.)	Permeability		Surface viscosity		Foam life L_f minutes
		$-\frac{dr}{dt}$ (cm./hr.) $\times 10^3$	k (cm./sec) $\times 10^3$	η_s surface poises $\times 10^3$	f_s (dynes/cm.) $\times 10^3$	
1	0	2.84	0.99	2	0	69
2a	0.00025	0.85	0.51	—	—	—
2b	0.00025	0.56	0.30	—	—	—
2c	0.00025	0.48	0.24	—	—	—
3	0.0005	0.47	0.27	—	—	—
4	0.001	—	—	2	0	825
5	0.002	0.43	0.39	—	—	—
6	0.003	—	—	31	0	1260
7	0.005	—	—	32	54	1380
8	0.008	0.43	0.47	32	64	1590

where r is the radius of the bubble at time t , r_0 is the radius at $t = 0$, γ is the surface tension, and P is the pressure of the atmosphere (dynes/cm.²). The constant k should give a measure of the permeability of the bubble film which is independent of the size of bubble used and also of the surface

tension of the detergent solution being investigated. Expressed in absolute units, k appears as cm./sec. Some representative plots of r^2 against time are shown in Fig. 6.

TABLE II

Foam Life, Surface Viscosity, and Permeability Data for 0.5% Solutions of Pure Sodium Lauryl Sulfate Containing Added Lauryl Alcohol

No.	Lauryl alcohol conc. (g./100 ml.)	Permeability		Surface viscosity		Foam life L_f minutes
		$-dr/dt$ (cm./hr.) $\times 10^2$	k (cm./sec.) $\times 10^2$	η_s surface poises $\times 10^3$	f_s (dynes/cm.) $\times 10^3$	
1	0	2.37	0.92	4.0	0	295
2	0.005	—	—	2.5	0	960
3	0.010	2.40	1.12	—	—	—
4	0.015	—	—	2.5	0	1100
5	0.020	2.50	1.30	—	—	—
6	0.025	0.51	0.32	24.5	29	1220
7	0.030	0.41	0.22	—	—	—

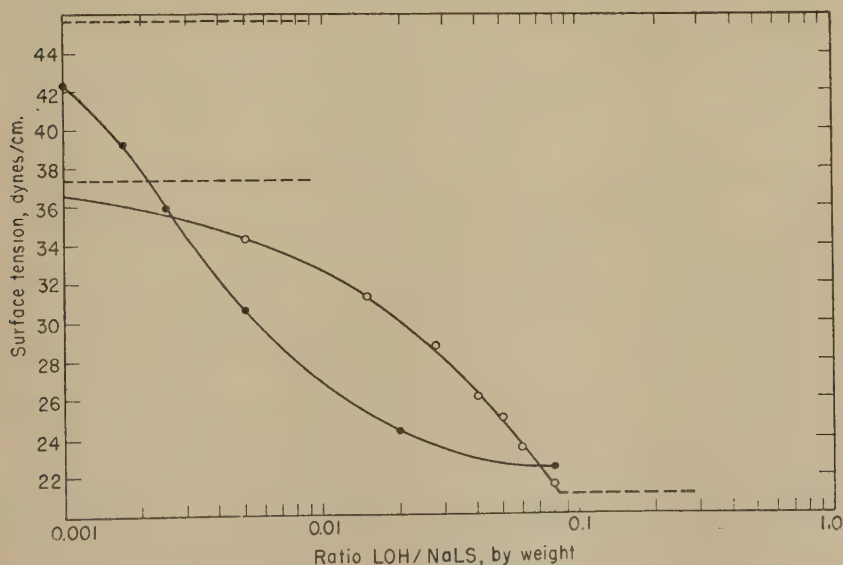


FIG. 7. Effect of lauryl alcohol on surface tension of 0.1% (dots) and 0.5% (circles) sodium lauryl sulfate. Surface tension values for the solutions without lauryl alcohol, and also with excess lauryl alcohol, indicated by dashed lines.

Permeability data for 0.1% and 0.5% solutions of pure sodium lauryl sulfate containing various amounts of added lauryl alcohol are summarized respectively in Tables I and II. Also shown are surface viscosity and foam

stability values previously obtained (1). Corresponding surface tensions for these solutions are plotted in Fig. 7 against the logarithm of the lauryl alcohol:sodium lauryl sulfate ratios (by weight).

Corresponding permeability, surface tension, surface viscosity, and foam stability data are summarized in Table III for a series of commercial detergents.

TABLE III
Foam Life, Surface Tension, Surface Viscosity, and Permeability Data for 0.1% Solutions of Some Commercial Detergents

No.	Material	Surface tension dynes/cm.	Permeability		Surface viscosity		Foam life L_f minutes
			$-\frac{dr}{dt}$ (cm./hr.) $\times 10^2$	k (cm./sec.) $\times 10^2$	η_s surface poises $\times 10^3$	f_s (dynes/cm.) $\times 10^3$	
1	Triton X-100	30.5	3.7	1.5	—	—	60
2	Santomerse 3	32.5	2.0	1.3	3	0	440
3	Quaternary O	37.0	1.4	0.65	1	0	1750
4	E 607 L	25.6	1.5	0.91	4	0	1650
5	Potassium laurate	35.0	0.28	0.14	39	59	2200
6	Sodium lauryl sulfate (comm.)	23.5	0.30	0.37	55	118	6100

DISCUSSION

Considering first the permeability curves alone one observes that for a given solution $-\frac{dr}{dt}$ is to a first approximation a constant, at least for the first hour after release of the bubble, and is largely independent of initial bubble size (Fig. 4). Actually the data appear to fit an r^2 vs. time plot (Fig. 6) somewhat better, but it is evident that either $-\frac{dr}{dt}$ or k_{perm} may be used to compare permeabilities of surface films on detergent solutions, particularly if initial (first-hour) values are employed. At longer periods of time both r vs. t and r^2 vs. t curves slope off (decreasing permeability). Solutions giving low permeability values show r^2 vs. t linear to at least 6 hours. The subsequent decrease in permeability seems to be related mostly to the amount of gas which has escaped from the bubble.

The data on the system (pure) sodium lauryl sulfate-lauryl alcohol (Tables I and II) illustrate the remarkable effect of lauryl alcohol on adsorbed surface films of sodium lauryl sulfate and provide some insight into the factors involved in permeability differences. In either the 0.1% or the 0.5% solutions, it is observed that there is a narrow range of lauryl alcohol concentration through which the permeability of the solution changes sharply from a relatively high to a relatively low value. A higher

lauryl alcohol ratio is required to produce this effect above the critical micelle concentration of the sodium lauryl sulfate than is required below this concentration, probably because of solubilization effects.

That the sharp change in permeability closely parallels the lauryl alcohol concentration in the surface film may be further deduced from the surface tension curves of Fig. 7. Here, if the activity of the lauryl alcohol can be assumed proportional to some reasonably constant power of the concentration, the slopes of the curves give a relative measure of the surface concentration of lauryl alcohol up to the solubility limit. It is observed that the sharp decrease in permeability as the lauryl alcohol ratio is raised agrees closely with the point at which maximum slope, that is, maximum surface adsorption, first occurs (at a lauryl alcohol concentration of 0.0002 % for 0.1 % sodium lauryl sulfate solutions and 0.025 % for 0.5 % solutions). It is of some further interest in this connection that at a lauryl alcohol concentration of 0.00025 % in a 0.1 % sodium lauryl sulfate solution the permeability is rather sensitive to the age of the surface (Fig. 4). Subsequent studies (7) have shown that equilibrium surface tension, that is, lauryl alcohol adsorption, is reached slowly at this concentration.

It has been suggested previously (1), from "surface viscosity" data, that the effect of lauryl alcohol in the surface film adsorbed on sodium lauryl sulfate solutions is to condense or give coherence to the film. Such an effect might also be expected to decrease the (gas) permeability of the surface film. A further example of this "condensation" effect in a two-solute component system is probably to be found in the very low permeability shown by surface films on potassium laurate solution.

The fact that the increase in surface viscosity and the decrease in permeability first occur at different lauryl alcohol concentrations (especially for the 0.1 % sodium lauryl sulfate solutions) is not unreasonable in view of the fact that surface viscosity effects involve only one adsorbed film, whereas permeability involves two such films, with a layer of solution between them. Permeability might be expected to depend both on the extent of condensation of the surface film and on the thickness of the liquid layer, whereas surface viscosity should be dependent only on the condensation or coherence of the adsorbed film. The thickness of the liquid layer is a complex function of many variables and may well be more sensitive to the condensation of the adsorbed film than is surface viscosity.

Film drainage experiments recently reported by Miles, Ross, and Shedlovsky (8) suggest that at any given time the liquid layer would be thicker the higher the surface viscosity of the solution. However, the fact that low permeability and high surface viscosity first occur at different lauryl alcohol concentrations, and also the fact that permeability *decreases* with time, would seem to preclude drainage as the chief factor involved in these permeability effects, although the thickness of the liquid layer is of course

an important factor. Much of the resistance to air transfer must be due to the surface film itself.

The apparent existence of a minimum in the calculated permeability constant as the lauryl alcohol content of the solution is increased is difficult to explain. Possibly adsorbed films of high lauryl alcohol content do not maintain as thick a solution layer in the bubble film "sandwich." In this connection it is interesting that another nonionic, Triton X-100, gives the highest permeability constant of all the materials studied.

The decrease of permeability with time, as suggested by the r^2 vs. t curves, may be due to a number of factors. The first, of course, may lie in the assumptions employed in the derivation of k with respect to the change in radius. It is possible, for example, that the true "escape area" for air in the bubble is actually a complex function of the radius. This factor may also be involved in the apparent minimum in value for k noted above.

Another factor in the decrease of permeability with time may be a change taking place in the film itself, that is, a gradual perfection of film structure as suggested by the change of surface tension with time and the variation of permeability with initial age of the surface.

A final, obvious factor in this effect is the fact that the gas in the bubble consists of two main components, oxygen and nitrogen, with different solubilities in water. The concentration gradients across the sandwich structure between air in the bubble and in the atmosphere would thus differ for the two gases. On this basis, the initial permeability would be determined by the oxygen, the final permeability by the nitrogen. It has been shown by Clark and Blackman (2) that the rate of decrease of specific surface in a foam is greater, the greater the solubility of the gas used to make the foam.

Considering now the nature of the correlations, if any, between permeability and foam stability, one sees that, in general, solutions giving low permeability values give foams of high stability. Low permeability appears to be related to the coherence developed in the monolayer and also to the thickness of the solution film between the bubbles, that is, to the hydration of the monolayers. Both of these factors are highly dependent on detergent concentration and composition.

Detailed correlation is much less satisfactory, in that solutions giving intermediate permeability values have a tendency to yield foams of too high a stability (L_f value). An explanation may lie in the fact that the process of air transfer results in a thinning of the foam (decrease in specific surface), since by this process foam-stabilizing constituents may accumulate in the remaining foam and lead to relatively high L_f values. For example, in sodium lauryl sulfate solutions of low lauryl alcohol content, lauryl alcohol may be expected to remain largely in the foam (9) during the

thinning process, thus resulting in an increased lauryl alcohol content of the remaining surface. It is suggested that a more useful measure of foam stability than that based on volume changes alone would also include a factor for the change of specific surface of the foam with time.

Finally, it appears that low permeability to air for surface films adsorbed on detergent solutions may be the result of special solute pairs, one of which has relatively high solubility and provides an adequate reservoir of surface active material (of high permeability when pure) and the other of which, though lesser in amount, produces the necessary coherence in the mixed surface film. Entrance of this second component into the adsorbed film appears to be related to its lesser solubility (greater surface activity) and to a nonionic structure. Its condensing action is probably due to hydrogen bonding. High foam stability depends on both low permeability and high surface viscosity, and measurements of these properties provide the possibility of relating foam stability in a fundamental way to the chemical structure and composition of the detergent.

ACKNOWLEDGEMENT

The authors acknowledge with pleasure the many helpful discussions, during the course of this work, with Dr. A. P. Brady of these laboratories.

REFERENCES

1. BROWN, A. G., THUMAN, W. C., AND MCBAIN, J. W. *J. Colloid Sci.* **8**, 491 (1953).
2. CLARK, N. O., AND BLACKMAN, M., *Trans. Faraday Soc.* **44**, 1 (1948).
3. RIDEAL, E. K., *J. Phys. Chem.* **29**, 1585 (1925).
4. LANGMUIR, I., *J. Phys. Chem.* **31**, 1719 (1927).
5. SEBBA, F., AND BRISCOE, H. V. A., *J. Chem. Soc.* **1940**, 106, 128.
6. HARKINS, W. D., AND JORDAN, H. F., *J. Am. Chem. Soc.* **52**, 1751 (1930).
7. BROWN, A. G., AND THUMAN, W. C., unpublished data.
8. MILES, G. D., ROSS, J., AND SHEDLOVSKY, L., *J. Am. Oil Chemists' Soc.* **27**, 268 (1950).
9. MILES, G. D., ROSS, J., AND SHEDLOVSKY, L., *J. Phys. Chem.* **49**, 93 (1945).

EFFECT OF ELECTROLYTES ON THE RATE OF SURFACE TENSION LOWERING; THE RATE OF SURFACE EQUILIBRIUM ATTAINMENT AS A FACTOR IN DETERGENCY¹

Emil J. Burcik

School of Mineral Industries, The Pennsylvania State College, State College, Pennsylvania

Received February 9, 1953; revised May 18, 1953

INTRODUCTION

Results have been reported (2) which show that electrolytes affect the initial time rate of surface tension lowering of ionic surface-active agents. The addition of sodium chloride causes a marked increase in this rate for sodium laurate. On the other hand, electrolytes have little or no effect on nonionic agents. These effects can be explained if one allows that the surface-active components of sodium laurate in solution are electrically charged. As these components diffuse into the interface a charge will build up which tends to repel other incoming ions (4). The addition of electrolyte decreases the potential at the interface and allows a more rapid rate of equilibrium attainment. Nonionic agents, being uncharged, will not show this effect. One purpose of this research was to investigate the electrolyte effect more fully. Ions of charge opposite to that of the surface-active component should be more effective in reducing the potential than ions of like charge. Furthermore, the higher the valence of the oppositely charged ion, the more effective it should be in reducing the potential.

It will be shown that, in general, a correlation exists between rate of surface equilibrium attainment and detergency. In the past numerous attempts have been made to correlate detergency with various properties of the detergent solution but with only moderate success. In particular, since preferential wetting is undoubtedly an important factor in detergency, attempts have been made to correlate with the static solution/oil interfacial tension (11, 12). It is suggested, since detergency generally takes place under nonequilibrium conditions, that the rate of surface equilibrium attainment is an important factor in determining the surface energies that are manifested in the detergent bath. If one takes this factor into account some of the broader aspects of detergent action can be explained.

¹ This investigation is a joint undertaking of The Pennsylvania State College Mineral Industries Experiment Station and the Office of Naval Research.

EXPERIMENTAL

Techniques and Materials

The rate of surface tension lowering was determined by the vibrating jet technique previously described (2). Rates of flow of 91.3 cc./min. and 100.0 cc./min. were employed. To determine the effect of temperature on rate the entire apparatus was enclosed in a thermostated glass-fronted box. No detergency tests were made in this laboratory. All data of this type were taken from the literature.

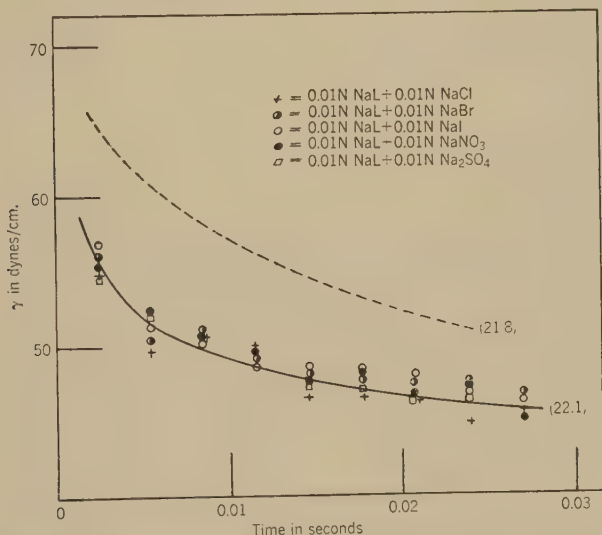


FIG. 1. Effect of valence of added anion on rate of surface tension lowering of 0.01 *N* sodium laurate at 20.0°C.

The inorganic compounds employed were reagent grade chemicals. All solutions were freshly prepared with distilled water. The preparation and physical properties of the sodium laurate and sodium dodecyl sulfate employed have been described previously (2). The dodecylpyridinium chloride was prepared by refluxing lauryl chloride and an excess of pyridine for eight hours at 150°C. The product was recrystallized several times from mixtures of acetone and ether and ethyl alcohol and ether. Chlorine content by analysis was 12.3% (theory 12.48%).

RESULTS

The effect of the added electrolyte anion on the rate of surface tension lowering of 0.01 *N* sodium laurate at 20°C. is shown in Fig. 1. Results with added sodium chloride, bromide, iodide, nitrate, and sulfate all at a concentration of 0.01 *N* are shown. Within experimental error all solutions

have the same rate of surface tension lowering. The dotted curve represents previous results (2) for 0.01 *N* sodium laurate without addition of electrolyte. The increase in rate resulting from the presence of salts is readily apparent but appears to be independent of the nature of the added anion. The figures at the end of each curve represent the corrected static equilibrium tensions determined with a du Noüy tensiometer. The added salts had but little effect on the static tension. One can conclude from these

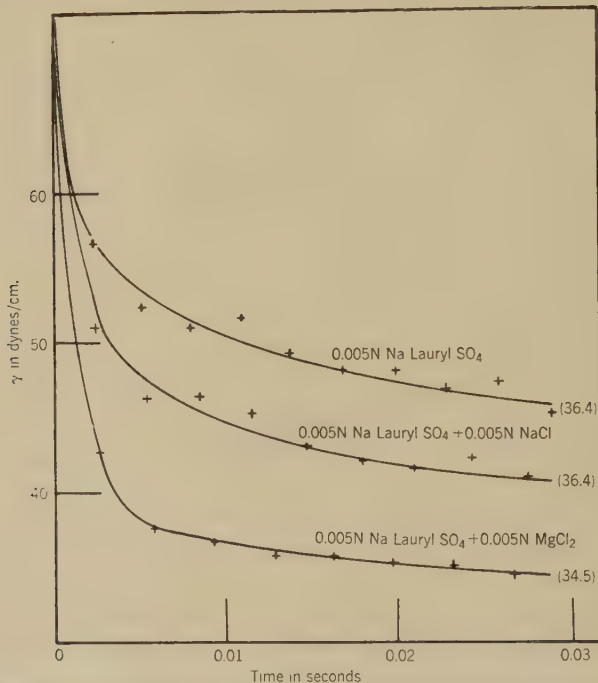


FIG. 2. Effect of valence of added cation on rate of surface tension lowering of 0.005 *N* sodium dodecyl sulfate. Temperature 20.0°C.

results that the nature of the added anion is of little consequence in determining the rate of surface tension lowering of an anionic surface-active agent.

The effect of increasing the positive charge of the added cation on the rate of surface tension lowering of 0.005 *N* sodium dodecyl sulfate, an anionic surface-active agent, is shown in Fig. 2. The added sodium chloride and magnesium chloride were both at a concentration of 0.005 *N*. Even though the concentrations are on a normality basis, the increase in rate with increasing cationic charge is readily apparent.

The effect of added electrolytes on 0.005 *N* dodecylpyridinium chloride, a cationic surface-active agent, is shown in Figs. 3 and 4. These experiments,

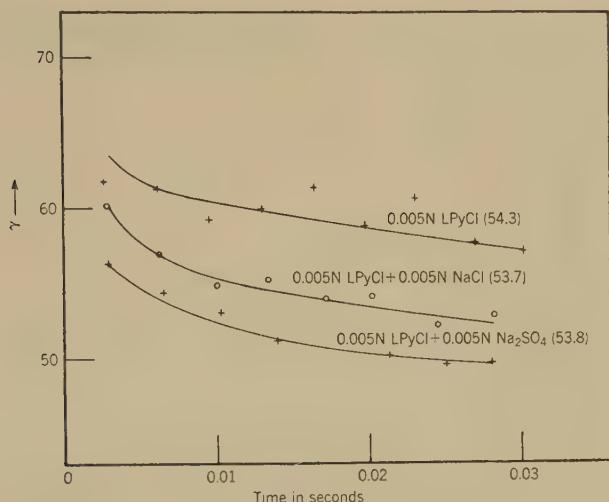


FIG. 3. Effect of valence of added anion on rate of surface tension lowering of 0.005 *N* dodecylpyridinium chloride. Temperature 20.0°C.

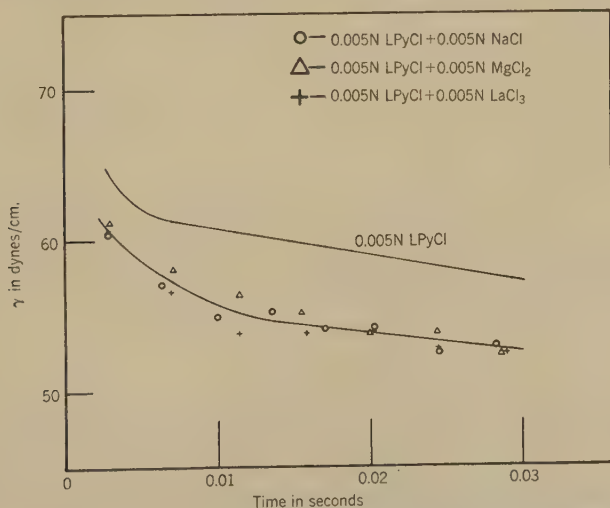


FIG. 4. Effect of valence of added cation on rate of surface tension lowering of 0.005 *N* dodecylpyridinium chloride. Temperature 20.0°C.

conducted at 20°C., show that the nature of the added cation is of little consequence in determining the rate of surface tension lowering. However, as the charge of the added anion is increased an increase in rate of surface equilibrium attainment is apparent.

The effect of increased temperature on the rate of surface tension lowering was determined to supply data for a detergency correlation. The results at

9.2°, 20.0°, and 29.4°C. are shown in Fig. 5, the results at 20°C. having been previously reported (2). As might be anticipated, the rate increases with increasing temperature.

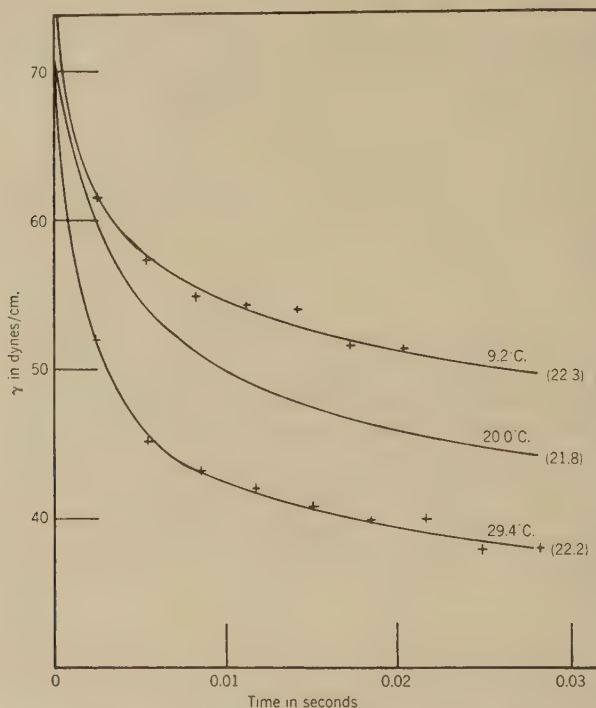


FIG. 5. Surface tension vs. time for 0.015 *N* sodium laurate as a function of temperature.

DISCUSSION

The results obtained suggest the following generalizations:

1. Surfactants whose surface-active components are negatively charged show an increase in rate of surface tension lowering on addition of electrolyte; the effectiveness increases with the charge of the added cation, but the nature of the added anion is of little consequence.
2. Surfactants whose surface-active components are positively charged show an increase in rate of surface tension lowering on addition of an electrolyte; the effectiveness increases with the charge of the added anion, but the nature of the added cation is of little consequence.
3. Surfactants whose surface-active components are uncharged have rates of surface tension lowering which are uninfluenced by the addition of electrolytes (2).

These results are in accord with double layer theory. The potential of

the charged interface, which hinders diffusion, is decreased, since the charge will be effectively reduced by the presence of ions of opposite charge. Moreover, the higher the charge of opposite sign, the more effective the reduction in potential will be. However, this does not imply that all ions of a given valence are equally effective in increasing the rate of surface tension lowering. Other factors such as ion size and activity would influence, to some extent, the effectiveness of a particular ion.

Data have been presented in the literature showing the influence of various factors on detergency. Although these data are not extensive, the effects of concentration, temperature, pH, and added electrolytes have been investigated. Preston (8) showed that, in general, detergency increases with increasing concentration of the detergent and approaches a maximum. He also presented data which indicate that with but few anomalies an increase in temperature increases detergency for a given concentration of the detergent. Experiments conducted by Palmer (7) show the effect of added salts on detergency. For a given detergent at a given concentration, the detergent power is raised as the concentration of the added salt is increased and then decreases again at high salt concentrations. He found further that in dilute salt solution the increase in detergent power depends only on the valence of the added cation for an anionic detergent. Rhodes and Wynn (10) agree that added salts increase detergent power but found that the anion of the added salt exerted some influence on detergency. Palmer (7) also investigated the effect of pH on detergency and found that an increase in pH had little effect on the detergent power of sulfonated alcohols but increased detergency of sodium oleate. Rhodes and Bascom (9) also report a beneficial effect with increased pH with a commercial soap. However, at very high values of pH the detergent power is decreased. If one allows that these results and those obtained in this laboratory on rate of surface tension lowering can be generalized, the following table can be constructed.

Except for the disagreement in case 7 there is a correlation between the effect on the rate of surface equilibrium attainment and the effect on detergency. A possible explanation of this correlation is presented below.

Detergency is a complex phenomenon involving numerous separate and distinct mechanisms (5, 6, 13). The soil or "dirt," which is usually oily in character, must be removed from the fiber and then dispersed in the detergent medium in such a way as to prevent redeposition on the fiber. This process would involve the preferential wetting of the fiber with subsequent emulsification of the oily constituents of the soil and peptization of the solid. Undoubtedly solubilization of the oil in the detergent micelle plays a part in detergency (5), but its relative importance has not yet been fully determined. This discussion will be limited to the effects of non-equilibrium conditions on preferential wetting. Singling out one factor in

this manner does not imply that the others are unimportant. On the other hand, it must be conceded that before emulsification and peptization can occur the soil must be removed from the fiber; thus, in this respect at least, they are of secondary importance.

Since most soils are oily in nature the manner of attachment of the solid particles to the fiber is largely by adhesion or wetting of the fiber by the oil. Consequently, the problem of removing soil becomes one of oil removal.

TABLE I

	Effect on detergency	Effect on rate of surface equilibrium attainment
1. Increasing temperature	<i>Increases</i> (8)	<i>Increases</i> (This research)
2. Increasing concentration of surface-active agent	<i>Increases</i> (8)	<i>Increases</i> (2)
3. Increasing pH of nonhydrolyzable surface-active agent	<i>No effect</i> (7)	<i>No effect</i> (3)
4. Increasing pH of a surface-active agent which is a salt of strong base and a weak acid	<i>Increases</i> for moderate increase in pH (7, 9)	<i>Increases</i> (3)
5. Addition of an electrolyte to an ionic surface-active agent	<i>Increases</i> for low concentrations of added electrolyte (7, 10)	<i>Increases</i> (2)
6. Increasing cationic valence of added electrolyte on anionic surface-active agents	<i>Increases</i> (7)	<i>Increases</i> (This research)
7. Increasing anionic valence of added electrolyte on anionic surface-active agents	<i>No effect</i> (7) <i>Increases</i> (10)	<i>No effect</i> (This research)

For an oily fiber immersed in a detergent solution the following relation must exist between the interfacial tensions and the contact angle.

$$\cos \theta = \frac{\gamma_{FO} - \gamma_{FS}}{\gamma_{SO}} \quad [1]$$

where γ_{FO} , γ_{FS} , and γ_{SO} are the fiber/oil, fiber/solution, and the solution/oil interfacial tensions, respectively. The interfacial tensions involving the solid fiber are not measurable. For complete removal of oil the contact angle θ must be zero, so the right-hand side of Eq. [1] must be equal to or greater than unity. As pointed out by Adam (1), this equation clearly shows the importance of the various surface energies in determining the value of the contact angle.

However, in most cases, detergency is a nonequilibrium process. If conditions are such that the oil is not spontaneously removed, it is desirable to reduce θ to as small a value as possible and then to remove the oil from

the fiber by mechanical work. Consequently, for the effective removal of a given oil from a given fiber, it is necessary that the detergent have the power to reduce the fiber/solution and the solution/oil interfacial tensions to a low value under the nonequilibrium conditions that exist in a strongly agitated detergent bath. This implies that an effective detergent must fulfill the following requirements:

1. It must have the power to produce a large lowering of the equilibrium values of γ_{FS} and γ_{SO} .

2. The rates of surface equilibrium attainment must be rapid so that the surface energies involved approach the static values under the nonequilibrium conditions which exist in a strongly agitated detergent bath.

In this research the time rate of change of surface energy at the solution/air interface has been measured. However, it is probable that a variable that will affect the rate of surface tension lowering in a given manner will have the same effect on the rate of lowering of the interfacial tensions involved in preferential wetting. This is reasonable, since this rate is a function of the rate of adsorption of the surface-active agent contained in the solution at the interface.

Attempts to correlate the static solution/oil interfacial tension with detergency have been made, but in general they have not been successful (11, 12). This is understandable, since only one of the surface energies which determine preferential wetting is being considered. It should be pointed out that since solid interfacial tensions are not measurable it is possible that Eq. [1] alone could explain the detergent process, provided a change in temperature, pH, etc., altered the solid interfacial tensions involved in the proper manner. However, the correlation between rate and detergency presented here suggests that the rate of surface equilibrium attainment is an important factor in detergency. Only further experiments can substantiate the generality of this correlating principle.

SUMMARY

1. The effect of electrolytes on the initial time rate of surface tension lowering of anionic surface-active agents has been investigated. The increase in rate observed is largely determined by the charge of the added positive ion. In the case of cationic surface-active agents the increase in rate is largely determined by the charge of the added negative ion.

2. An increase in temperature results in an increase in rate of surface tension lowering for sodium laurate.

3. Detergent power and initial time rate of surface equilibrium attainment can, in most cases, be correlated where data are available, if it is assumed that any variable which affects the rate of surface tension lowering at the solution-air interface will have the same effect at the interface between the solution and any second phase.

4. This correlation is reasonable if one assumes that most soils are oily in nature and that the first step in detergency is the removal of oil from the fiber by preferential wetting under nonequilibrium conditions.

REFERENCES

1. ADAM, N. K., *J. Soc. Dyers Colourists* **53**, 121 (1937).
2. BURCIK, E. J., *J. Colloid Sci.* **5**, 421 (1950).
3. BURCIK, E. J., *J. Colloid Sci.* **6**, 522 (1951).
4. DOSS, K. S. G., *Kolloid-Z.* **86**, 205 (1939).
5. MCBAIN, J. W., *Advances in Colloid Science* **1**, 99 (1942).
6. NIVEN, W. W., *Fundamentals of Detergency*. Reinhold Publishing Corporation, 1950.
7. PALMER, R. C., *J. Soc. Chem. Ind. (London)* **60**, 56, 60 (1941).
8. PRESTON, W. C., *J. Phys. & Colloid Chem.* **52**, 84 (1948).
9. RHODES, F. H., AND BASCOM, C. H., *Ind. Eng. Chem.* **23**, 778 (1931).
10. RHODES, F. H., AND WYNN, C. S., *Ind. Eng. Chem.* **29**, 55 (1937).
11. ROBINSON, C., *Conf. of Wetting and Detergency*, p. 137. Harvey, London, 1937.
12. SPEAKMAN, J. B., AND CHAMBERLAIN, N. H., *Trans. Faraday Soc.* **29**, 358 (1933).
13. SCHWARTZ, A. M., AND PERRY, J. W., *Surface Active Agents*, p. 349ff. Interscience Publishers Inc., New York, 1949.

VISCOSITIES OF CONCENTRATED POLYMER SOLUTIONS.

III. POLYSTYRENE AND STYRENE-MALEIC ACID COPOLYMER

John D. Ferry, Lester D. Grandine, Jr.,¹ and Doyle C. Udy²

Department of Chemistry, University of Wisconsin, Madison, Wisconsin

Received July 15, 1953

INTRODUCTION

Viscosities of concentrated solutions of polyvinyl acetate (1) and polyisobutylene (2) have been reported in previous papers of this series. The present communication describes some similar measurements on solutions of polystyrene in Decalin and in xylene, and of a copolymer of styrene and maleic acid in 50 % aqueous dioxane; and gives a comparison of the behavior of the four polymers.

MATERIALS AND METHODS

The polystyrene was a specially prepared sample (19F) kindly given us by Mr. R. F. Boyer, Dow Chemical Company; its number-average and weight-average molecular weights were 0.19 and 0.37 million, respectively. The styrene-maleic acid copolymer was the fraction SY-MA-B2 described in an earlier paper (3), prepared by fractionation of the anhydride copolymer with subsequent hydrolysis in water at 60°C. Its number-average molecular weight was 0.19 million, and it was believed to be a fairly sharp fraction. Decalin, xylene, and dioxane were purified as previously described (2, 4). The solvent for the copolymer was a mixture of equal parts by weight of water and dioxane.

Viscosities were measured by the capillary and falling ball methods as before (1, 2). It was necessary to use stainless steel balls in the copolymer solutions, since ordinary steel underwent slight corrosion and there was some evidence of cross-linking of the polymer by the dissolved iron. Under the conditions of these experiments, the flow is essentially Newtonian (1). In addition, one very concentrated solution of polystyrene in Decalin was studied by the falling cylinder viscosimeter described by Fox and Flory

¹ Union Carbide and Carbon Fellow in Physical Chemistry, 1950-1952. Present address: Fiber Department, E. I. du Pont de Nemours and Company, Wilmington, Delaware.

² Present address: Agricultural Experiment Station, Pullman, Washington.

(5). This instrument, made available through the kindness of Professor J. W. Williams, to whom it had been transferred under an Office of Naval Research contract, was modified by milling slots in the bottom section of the block to take overflow of excess sample during molding. End plates were attached during molding to hold the rod properly centered; a ruled Lucite scale and a knife edge were attached to the block and the cylinder, respectively, to facilitate following the descent of the cylinder with a cathetometer telescope. The position of the cylinder could be determined

TABLE I
Viscosities of Solutions of Polystyrene in Decalin, Falling Ball Method

w_2	Log η in poises at				Q_η at 25°C. (kcal.)
	15.0°C.	25.2°C.	35.2°C.	45.1°C.	
0.159	1.42	1.16	0.98	0.84	8.8
0.200	1.92	1.63	1.42	1.26	10.0
0.250	2.65	2.30	2.05 ^a	1.86	11.8
0.300	3.34	2.96	2.68	2.46	13.2
0.350	4.03	3.55	3.23	3.01 ^b	15.2
0.400	4.72	4.20	3.84	3.54 ^b	17.0
0.457	5.38 ^c	5.01	4.53	4.19 ^b	19.8

^a At 35.0°C.

^b At 45.3°C.

^c At 17.2°C.

TABLE II
Viscosities of Solutions of Polystyrene in Decalin, Falling Cylinder Method; $w_2 = 0.620$

$Q_\eta = 27.9$ kcal. at 25°C.

Temp., °C.....	0.2	5.1	10.2	15.4	19.6	25.4
Log η in poises.....	9.80	9.08	8.50	8.01	7.59	7.19

to within 0.002 mm. The entire apparatus was placed in an air thermostat, and its temperature was read by a mercury thermometer placed in an oil-filled well.

RESULTS

Viscosities of solutions of polystyrene in Decalin are given in Tables I and II, those of polystyrene in xylene in Table III, and those of solutions of the styrene-maleic acid copolymer in 50 % aqueous dioxane in Table IV. The weight fraction of polymer is denoted by w_2 . The logarithm of viscosity is plotted against the reciprocal absolute temperature in Figs. 1 to 3. For the copolymer, where the temperature range is rather narrow, these plots are nearly linear, but for the polystyrene there is definite upward curvature, as in the case of polyisobutylene solutions (2). The apparent

heats of activation, Q_η , were calculated from the slopes measured at 25°C., and are given in the Tables.

The logarithm of the relative viscosity, η_r , at 25°C. is plotted against the square root of the concentration, c_2 , in g./cc. in Figs. 4 and 5 for the

TABLE III

Viscosities of Solutions of Polystyrene in Xylene, Falling Ball Method

w_2	Log η in poises at				Q_η at 25°C. (kcal.)
	15.0°C.	25.0°C.	35.0°C.	45.3°C.	
0.201	1.27	1.21	1.11	1.01	3.98
0.255	1.80	1.69	1.58	1.47	4.67
0.302	2.12	1.98	1.87	1.76 ^a	5.04
0.372	2.75	2.57	2.43	2.32 ^a	6.18
0.412	3.12	2.94	2.78	2.66	6.82
0.478	3.66	3.44	3.26	3.14 ^a	8.24

^a At 45.0°C.

TABLE IV

Viscosities of Solutions of Styrene-Maleic Acid Copolymer in 50% Aqueous Dioxane

Method ^a	w_2	Log η in poises at			Q_η at 25°C. (kcal.)
		15.0°C.	25.0°C.	35.0°C.	
C	0.084	-0.15	-0.29	-0.41	5.4
C	0.100		-0.06	-0.19	—
C	0.122	0.44	0.24	0.11	6.6
C	0.140		0.51	0.34	—
C	0.163	1.04	0.82	0.64	8.3
F	0.197	1.49	1.24	1.04	9.2
F	0.208	1.63	1.38	1.17	9.5
F	0.220	1.79	1.54	1.32	9.7
F	0.233	2.00	1.70	1.47	10.1
F	0.248	2.09 ^b	1.87	1.64	10.1
F	0.285	2.54 ^b	2.31	2.06	11.2
F	0.335	3.23	2.90	2.61	12.6

^a C = capillary; F = falling ball.

^b At 17.0°C.

polystyrene and copolymer, respectively. For this purpose, the viscosities of Decalin, xylene, and 50% aqueous dioxane were taken to be 0.0239, 0.00582, and 0.0190 poise, respectively, and the volumes of polymer and solvent were assumed to be additive. Data obtained by Streeter and Boyer on the same polystyrene 19-F in Decalin over a range of lower concentrations (6) are included in Fig. 4, as well as a few values for solutions in tolu-

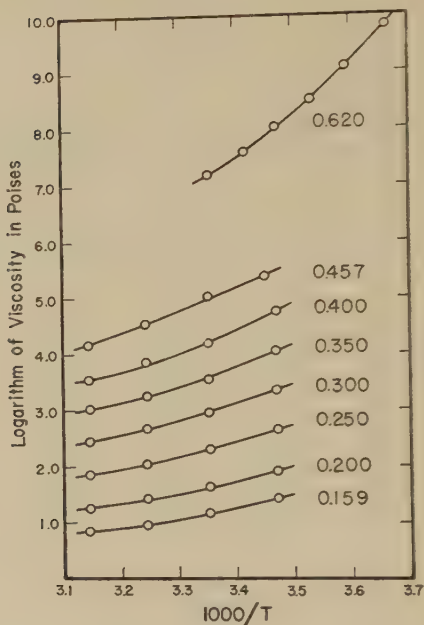


FIG. 1. Logarithm of viscosity plotted against reciprocal of absolute temperature for solutions of polystyrene in Decalin. Figures denote weight fraction of polymer.

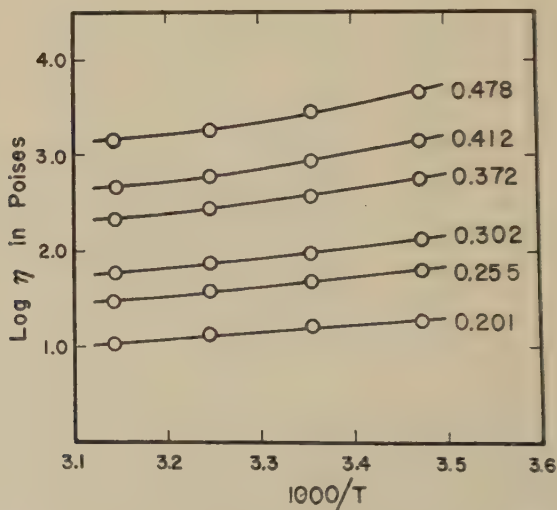


FIG. 2. Logarithm of viscosity plotted against reciprocal of absolute temperature for solutions of polystyrene in xylene. Figures denote weight fraction of polymer.

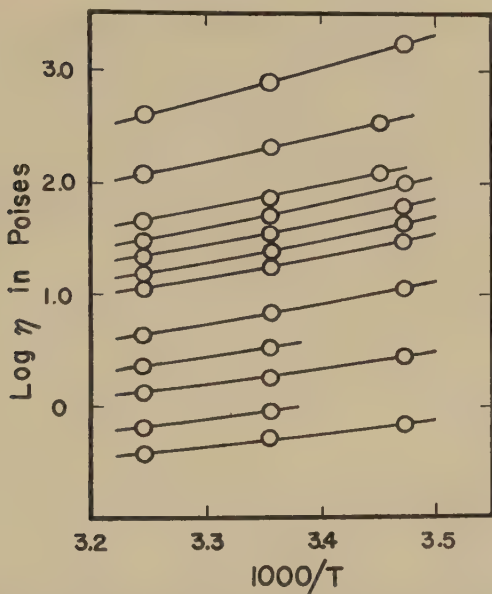


FIG. 3. Logarithm of viscosity plotted against reciprocal of absolute temperature for solutions of styrene-maleic acid copolymer in 50% aqueous dioxane, at various weight fractions of polymer, as given in Table III (ascending order of curves).

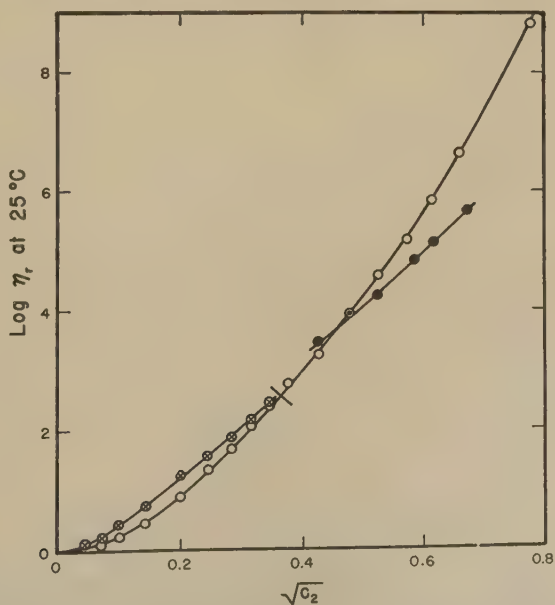


FIG. 4. Logarithm of viscosity of solutions of polystyrene 19F at 25°C. plotted against square root of concentration in g./cc. Open circles: in Decalin, above cross line from Table I, below cross line from Reference 6; solid circles, in xylene, from Table II; crossed circles, in toluene, from Reference 6.

ene from the same authors. All the plots show upward curvature over the entire concentration range, and in this respect resemble the corresponding curves for polyvinyl acetate (1) but not those for polyisobutylene (2).

The apparent heat of activation for viscous flow at 25°C. is plotted against c_2 in Fig. 6. In each system there is a progressive increase of Q_7 with concentration, roughly linear over a moderate range, as previously observed (1, 2, 7). The values for polystyrene in xylene are in reasonable agreement

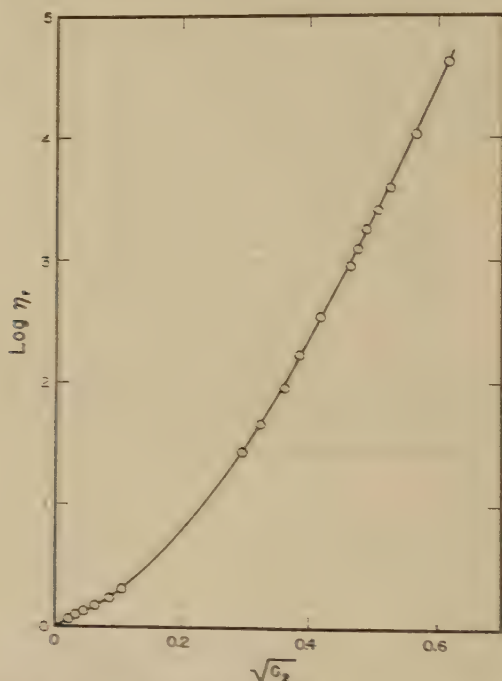


Fig. 5. Logarithm of viscosity of solutions of styrene-maleic acid copolymer at 25°C., plotted against square root of concentration in g. cc. The lower points are derived from intrinsic viscosity measurements reported in Reference 3.

with those determined a number of years previously for a sample of different molecular weight (7).

DISCUSSION

Temperature Dependence of Viscosity

The apparent activation energy serves as an index of temperature dependence of viscosity, even though it has no straightforward interpretation because of the importance of free volume considerations (8, 9). Subtraction of the apparent flow activation energy of the solvent, Q_7 , permits compari-

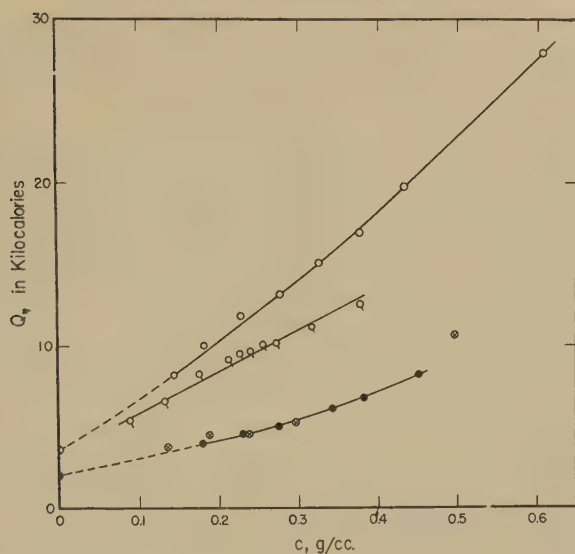


FIG. 6. Apparent heat of activation for viscous flow plotted against concentration in g./cc. Open circles, polystyrene 19F in Decalin; closed circles, in xylene; crossed circles, polystyrene A200 in xylene, from Reference 7; tagged circles, styrene-maleic acid copolymer in 50% aqueous dioxane.

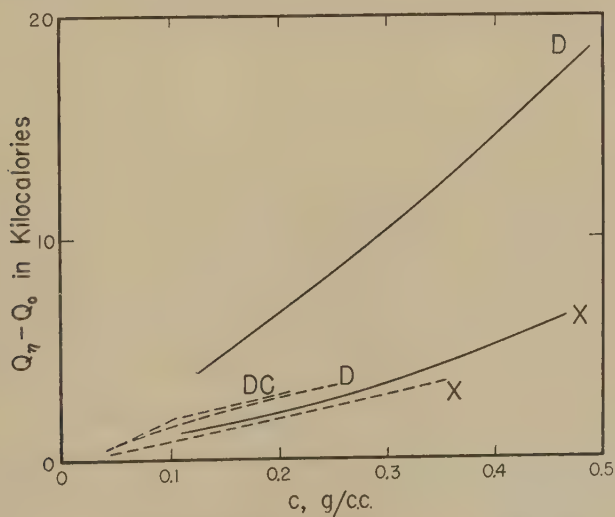


FIG. 7. Apparent heat of activation for viscous flow of polymer solution minus that of solvent, plotted against concentration. Solid lines, polystyrene; dashed lines, polyisobutylene, from Reference 2. Solvents: X, xylene; D, Decalin; DC, mixture of 69.9% Decalin and 30.1% cyclohexanol.

son of different polymers in different solvents. Figure 7 shows $Q_\eta - Q_0$ plotted against concentration for polystyrene in two solvents (data of Fig. 6) and polyisobutylene in three solvents (data of Reference 2). The selection includes both good and very poor solvents, as judged by values of intrinsic viscosity and the thermodynamic constant μ , as well as phase separation, discussed elsewhere (2, 6, 10). For polyisobutylene, the character of the solvent is of minor importance, since the curves for Decalin (a good solvent) and a mixture of Decalin and cyclohexanol (a very poor one) lie close together, and that for xylene is not far removed. For polystyrene, on the other hand, the curve for xylene (a good solvent) is close to the polyisobutylene curves, but that for Decalin (a very poor solvent) lies far higher.

This distinction is no doubt related to the fact that the glass transition of polystyrene, unlike that of polyisobutylene, is above room temperature, so that at 25°C. Q_η must attain a very high value as the concentration approaches that of pure polymer. A rapid increase of Q_η at high concentrations of polystyrene (above 60%) has been observed by Fox in dibenzyl ether (11) and by Bueche (12) in diethyl benzene, both of which would be expected to be quite good solvents. For a poor solvent, this rise apparently begins at much lower concentrations. Similarly, for polyvinyl acetate, whose glass transition is also above room temperature, limited data (1) indicate that Q_η at 25°C. rises faster with concentration in methyl isobutyl ketone (a moderately poor solvent) than in 1,2,3-trichloropropane (a good one).

Concentration Dependence of Viscosity

The upward curvature of plots of $\log \eta_r$ at 25°C. against $c_2^{\frac{1}{2}}$ in polystyrene (Fig. 4), styrene-maleic acid copolymer (Fig. 5), and polyvinyl acetate (1), as contrasted to the inflection point followed by downward curvature for such plots in polyisobutylene (2), is no doubt also related to the fact that polyisobutylene is the only one of these polymers whose glass transition lies below room temperature. Its viscosity approaches a finite value as the concentration approaches that of pure polymer, whereas the others increase essentially without limit.

For polyisobutylene, values of η_r were found to be closely similar in different solvents when compared at equal volume concentrations (2). For polyvinyl acetate, the values of η_r were rather close, though at high concentrations somewhat lower in a good solvent than in a poor one (1). For polystyrene, the latter divergence appears in more marked form in Fig. 4. At a concentration of 0.4 g./cc., the relative viscosity in the poor solvent Decalin is higher than that in xylene by a factor of ten. At rather low concentrations, however, the relative viscosity in Decalin is lower than

that in the good solvent toluene (data of Streeter and Boyer, Reference 6; also shown in Fig. 4).

Comparisons of Different Polymers

In the preceding paper (2), it was shown that viscosity data for polyisobutylenes of different molecular weights at different concentrations and in different solvents (at 25°C.) could be made to coincide in a single composite curve by plotting $\log \eta_r$ against $(c_2 M^{0.68})^{\frac{1}{2}}$, or against an equivalent reduced abscissa (ten times its logarithm), $5 \log c_2 + 3.4 \log M$. The relative viscosity was, approximately, simply equal to this logarithmic reduced abscissa plus a constant. The effect of molecular weight cannot be examined in this way in the present study, since there are data for only one sample of each polymer. However, it is of interest to compare different polymer types by a similar reduced plot. Here, the number of bonds in the chain, rather than the molecular weight, is probably the best measure of chain length or coil volume, upon which the viscosity of the solution presumably depends. Accordingly, we may choose as a reduced variable c_2 times some power of jZ , where, in the notation of Kuhn and Kuhn (13), Z is the degree of polymerization and j the number of bonds per monomer unit (here two).

It is not obvious whether the exponent 0.68, corresponding to the factor 3.4 in the logarithmic abscissa, which was chosen empirically for polyisobutylene (2), should be applicable to other polymers. However, it has been tentatively adopted, and in Fig. 8 the relative viscosity is plotted logarithmically against $5 \log c_2 + 3.4 jZ$ for four polymers. The data include all those on various polyisobutylenes (2), Fraction II of polyvinyl acetate (1), and the two polymers of the present paper. In calculating jZ , the weight or viscosity average degree of polymerization was chosen in each case except for the polyvinyl acetate Fraction II and the styrene-maleic acid copolymer, for which only the number-average values were available. The latter polymers are both fractions and their number and weight averages are probably nearly equal.

Figure 8 shows order of magnitude coincidence for all these systems in the relative viscosity range from 10 to 10^5 poises, despite the wide differences in chemical structures of the side chains. At higher concentrations, the curves diverge; the extremes are polyisobutylene, which gives a straight line with a slope of unity in accordance with the empirical equation previously given (2), and polystyrene in Decalin, which rises very steeply. This comparison has only qualitative significance, since at any other temperature than 25°C. the relationships among the polymer-solvent systems would be somewhat different. The steep rise for polystyrene-Decalin at high concentrations is undoubtedly related to the steep rise in Q_η shown in

Fig. 7. It might be expected that the better the solvent and the higher the temperature (the lower Q_1), the more nearly the dependence on concentration and molecular weight would approach that exhibited by polyisobutylene in Fig. 8. Subject to these reservations, the generalization expressed by Fig. 8 may be of some practical value for rough estimates of viscosity in other polymer-solvent systems.

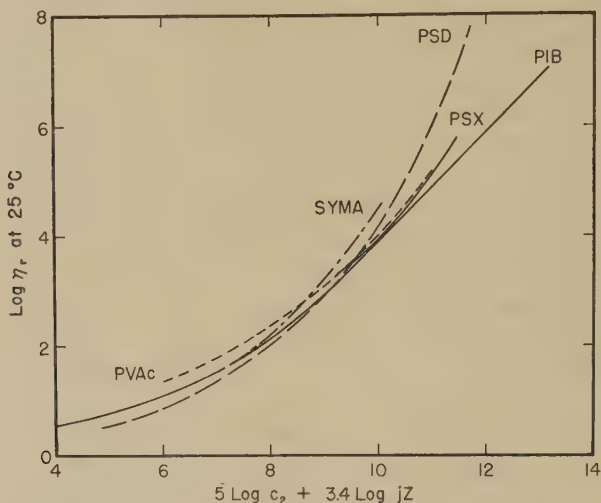


FIG. 8. Logarithm of relative viscosity at 25°C. plotted against $5 \log c_2 + 3.4 \log jZ$, for four polymers. PIB, polyisobutylene, eight samples in three solvents, from Reference 2; PVAc, polyvinyl acetate, Fraction II in 1,2,3-trichloropropane, from Reference 1; PSX, polystyrene in xylene, PSD, polystyrene in Decalin, from Fig. 4; SYMA, styrene maleic acid copolymer, from Fig. 5.

ACKNOWLEDGMENTS

This work was supported in part by the Research Committee of the Graduate School of the University of Wisconsin from funds supplied by the Wisconsin Alumni Research Foundation, and in part by a grant from Research Corporation. We are indebted to Union Carbide and Carbon Corporation for support through its Fellowship in Physical Chemistry.

SUMMARY

Viscosities of solutions of a sample of polystyrene (weight-average molecular weight 370,000) in Decalin and xylene, and of a sample of styrene-maleic acid copolymer (number-average molecular weight 190,000) in 50 % aqueous dioxane, have been measured over a wide range of concentrations at several different temperatures. The apparent activation energy for viscous flow at 25°C. increases far more rapidly with concentration for polystyrene in the poor solvent Decalin than in the good solvent xylene. Plots

of the logarithm of the relative viscosity at 25°C. against the square root of the volume concentration (c_2) curve upward, more steeply for polystyrene in Decalin than in xylene. When the logarithm of the relative viscosity is plotted against $[c_2(jZ)^{0.68}]^{\frac{1}{2}}$, or against $5 \log c_2 + 3.4 \log jZ$, where jZ is the number of bonds in the polymer chain, data for these systems as well as previously reported data for solutions of polyvinyl acetate and polyisobutylene fall fairly close together, except for the system polystyrene-Decalin at high concentrations.

REFERENCES

1. FERRY, J. D., FOSTER, E. L., BROWNING, G. V., AND SAWYER, W. M., *J. Colloid Sci.* **6**, 377 (1951).
2. JOHNSON, M. F., EVANS, W. W., JORDAN, I., AND FERRY, J. D., *J. Colloid Sci.* **7**, 498 (1952).
3. FERRY, J. D., UDY, D. C., WU, F. C., HECKLER, G. E., AND FORDYCE, D. B., *J. Colloid Sci.* **6**, 429 (1951).
4. FORDYCE, D. B., AND FERRY, J. D., *J. Am. Chem. Soc.* **73**, 62 (1951).
5. FOX, T. G., JR., AND FLORY, P. J., *J. Am. Chem. Soc.* **70**, 2384 (1948).
6. STREETER, D. J., AND BOYER, R. F., *Ind. Eng. Chem.* **43**, 1790 (1951).
7. FERRY, J. D., *J. Am. Chem. Soc.* **64**, 1330 (1942).
8. FOX, T. G., JR., AND FLORY, P. J., *J. Appl. Phys.* **21**, 581 (1950).
9. DOOLITTLE, A. K., *J. Appl. Phys.* **22**, 1471 (1951).
10. GRANDINE, L. D., JR., AND FERRY, J. D., *J. Appl. Phys.* **24**, 679 (1953).
11. FOX, T. G., JR., *Phys. Rev.* **86**, 652 (1952).
12. BUECHE, F., *J. Appl. Phys.* **24**, 423 (1953).
13. KUHN, W., AND KUHN, H., *Helv. Chim. Acta* **29**, 609 (1946).

EFFECT OF CONCENTRATION ON FLOW BEHAVIOR OF GLASS SPHERE SUSPENSIONS

Samuel H. Maron and Shiu-Ming Fok

*Physical Chemistry Laboratory, Department of Chemistry and Chemical Engineering,
Case Institute of Technology, Cleveland, Ohio*

Received May 13, 1953

INTRODUCTION

In a recent paper Williams (1) presented data on the flow behavior of suspensions of glass spheres in glycerol-water solutions of viscosity 0.59 poise. No temperature was given. Three samples of spheres of different average size were used, designated nominally as 12, 8, and 4 μ . The concentration range covered was 0.10–0.50 volume fraction for the first two sizes, and 0.10–0.44 for the last. For all suspensions the flow was found to be Newtonian.

Williams attempted to represent the dependence of the relative viscosity η_r on volume fraction ϕ by means of the Mooney (2) equation,

$$\ln \eta_r = \frac{2.5\phi}{1 - \lambda_1 \phi}, \quad [1]$$

and by means of the Roscoe (3) equation,

$$\eta_r = (1 - k\phi)^{-2.5}, \quad [2]$$

where λ_1 and k are constants. Neither equation reproduced the data satisfactorily. Since the equation proposed by Maron, Madow, and Krieger (4), namely,

$$\log_{10} \eta_r = bZ = \frac{b\alpha\phi}{1 - \alpha\phi} \quad [3]$$

where b and α are constants, reproduced satisfactorily flow data on latices and latex mixtures (4, 5, 6) as a function of ϕ , it was decided to see whether this equation would apply as well to the data of Williams. The results obtained are described below.

APPLICABILITY OF EQUATION [3]

Preliminary plots of $\phi/\log \eta_r$ vs. ϕ indicated a fairly satisfactory linear relationship between the two, as demanded by Eq. [3]. Consequently the

data were treated by least squares to obtain the constants b and α shown in Table I. These constants reproduce quite well Williams' data, as may be seen from the plots of $\log \eta_r$ vs. Z shown in Fig. 1. The lines have been drawn with b as the slope in each instance.

It was shown before (4) that $1/\alpha$ is the volume fraction at which the viscosity becomes infinite, whereas $2.033\alpha b$ is the slope for the dependence

TABLE I
Flow Parameters for Glass Sphere Suspensions

Nominal Sphere Size	b	α	$\frac{1}{\alpha}$	$2.303\alpha b$
4 μ	1.29	1.13	0.88	3.35
8 μ	1.11	1.26	0.79	3.22
12 μ	0.930	1.47	0.68	3.15

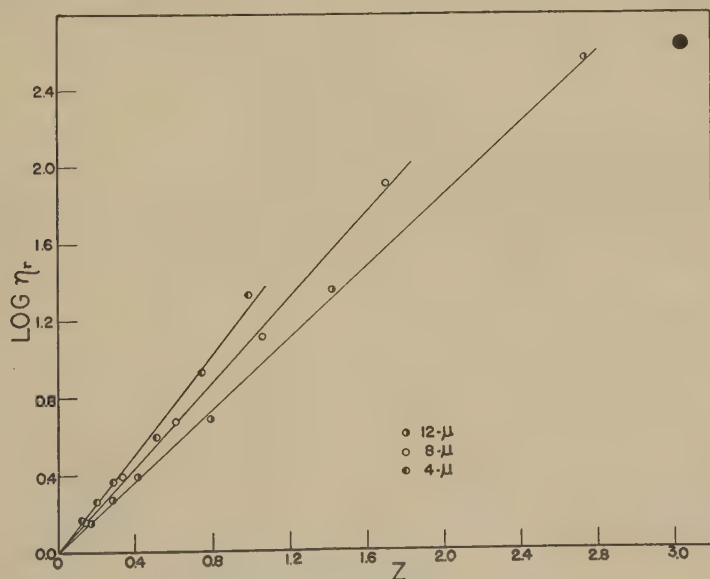


FIG. 1. Plot of $\log \eta_r$ vs. Z for glass sphere suspensions.

of η_r on ϕ as ϕ approaches zero. Values of $1/\alpha$ and $2.303\alpha b$ are shown in the last two columns of Table I. For monodisperse spheres in rhombohedral close packing, $1/\alpha$ should be 0.74, and for polydisperse spheres, above this figure. The polydisperse character of the sphere distributions suggested by the two lower size samples is borne out by the data given by Williams in his Table III. Again, the fact that $2.303\alpha b$ is here 3.15–3.35 rather than the Einstein 2.5 shows why the Mooney and Roscoe equations do not apply

to Williams' data. Both of these equations assume 2.5 for this slope, whereas here the slopes are larger, possibly owing to interaction of the glass spheres with the water-glycerol dispersion medium.

SUMMARY

The flow data obtained by Williams (1) on dispersions of glass spheres in water-glycerol as a medium do not obey the Mooney (2) and Roscoe (3) equations connecting relative viscosity η_r to volume fraction ϕ . However, it has been found possible to represent the data by means of the equation proposed by Maron, Madow, and Krieger (4), namely,

$$\log \eta_r = \frac{b\alpha\phi}{1 - \alpha\phi}$$

where b and α are constants. The results obtained show that the limiting slope relating η_r to ϕ is 3.15–3.35 rather than 2.5 called for by the Einstein relation. Since both the Mooney and Roscoe equations assume 2.5 for this slope, the equations break down when applied to this system.

REFERENCES

1. WILLIAMS, P. S., *J. Applied Chemistry* **3**, 120 (1953).
2. MOONEY, M., *J. Colloid Sci.* **6**, 162 (1951).
3. ROSCOE, R., *Brit. J. Appl. Phys.* **3**, 267 (1952).
4. MARON, S. H., MADOW, B. P., AND KRIEGER, I. M., *J. Colloid Sci.* **6**, 584 (1951).
5. MARON, S. H., AND MADOW, B. P., *J. Colloid Sci.* **8**, 130 (1953).
6. MARON, S. H., AND MADOW, B. P., *J. Colloid Sci.* **8**, 300 (1953).

LETTERS TO THE EDITORS

EFFECT OF MAGNETIC FIELDS ON THE RHEOLOGY OF FERROMAGNETIC DISPERSIONS

Several recent references in the literature to the effect of applied magnetic forces on the consistency of ferromagnetic colloidal dispersions (1, 2) prompt me to summarize a brief investigation of this topic undertaken in 1945 in association with Agnes S. Dyer (Mrs. A. D. Livingood) and the late Earl K. Fischer, with the assistance of Mrs. E. Engel and J. Wyart.

It was noted that dispersions of carbonyl iron powder and magnetic iron oxide ("Mapico black") in nonaqueous media would "freeze" on a plastic spatula upon the approach of a magnet. Green's rotational viscometer (3) proved suitable for exploring the magnetic effects semiquantitatively. Its brass cup permitted, after draining the constant-temperature bath, a magnet to be brought close enough to affect the material being measured in the cup. Spherical SF carbonyl iron powder (General Aniline and Film Co.) was dispersed in glycerol and in a #00 bodied linseed oil of 4.9 poises at several concentrations. The iron powder was stirred into the dispersion medium. The magnetic iron oxide was ground in on a three-roll mill.

A laboratory horseshoe magnet of 7600 gauss was the usual source of magnetic force, although weaker heavy bar magnets were used in a few experiments. The magnet was held perpendicular to the cup, its poles horizontal. It acted through the brass wall 2.5 mm. thick on the 2.0 mm. thickness of the annulus of dispersion surrounding the stainless steel bob. The bob was 26 mm. in diameter and 51 mm. high. To minimize temperature effects, since the viscometer was not thermostated, the original consistency measurement without the magnet was usually repeated immediately after a measurement with the magnet.

Typical flow curves are shown in Figs. 1 and 2. It is readily seen that in all cases the magnetic effect was primarily on the yield value of the plastic dispersions and that similar results were obtained with either ferromagnetic powder and with either dispersion medium. Plastic viscosity was little affected by magnetization, particularly in the case of the iron oxide.

Comparison of Fig. 1 with Fig. 2 shows that the iron powder dispersion, with an initial low yield value (little flocculation), was affected by magnetization much more, both absolutely and relatively, than the iron-oxide dispersion, which was initially more highly flocculated (had a substantial

yield value). Figure 2 shows that the iron oxide was less flocculated in the linseed oil than in the glycerol, as judged by the respective yield values, but that the two dispersions were affected in nearly equal proportions by magnetization. Differences between the iron and iron-oxide powders in magnetic permeability and particle size are probably responsible for these observations. The d_3 diameter of the iron was approximately 1.5μ (vapor

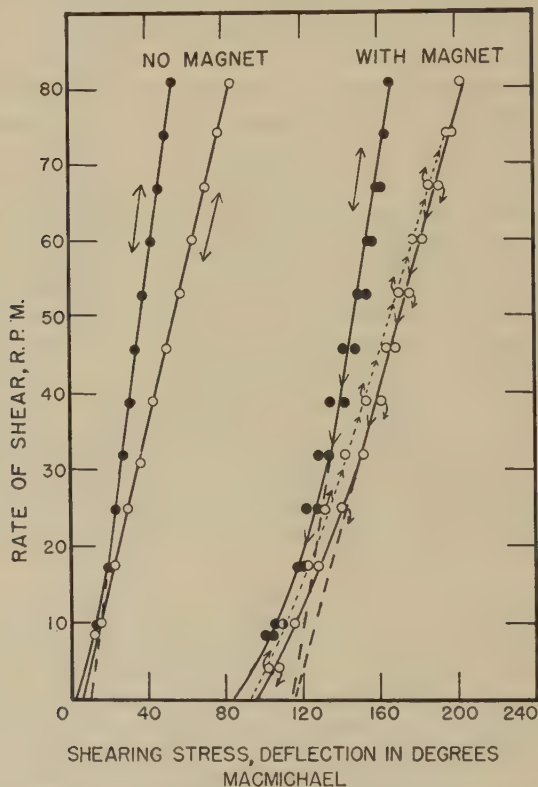


FIG. 1. Flow curves of iron powder (27.9 vol. %) in glycerol (solid circles) and in linseed oil (hollow circles) with and without horseshoe magnet present. Arrows indicate observations at increasing or decreasing r.p.m. Plastic viscosities (left to right) were 9.1, 16.4, 11.7, and 17.3 poises; yield values were 120, 85, 1465, and 1465 dynes/sq. cm., respectively.

adsorption, microscopy, air permeability), whereas that of the oxide was 0.2μ (nitrogen adsorption).

Table I summarizes the experimental work done on this topic and adds emphasis to the remarks already made. The rheological behavior of the magnetized iron dispersions is dominated by their high yield values, which are considered to depend largely on interactions between dispersed particles. The dispersion medium plays a larger role in the iron-oxide disper-

sions. With linseed oil as dispersion medium the yield values of the magnetized dispersions diminish regularly with decreasing solids content, and the percentage increases in yield values on magnetization rise regularly. With glycerol as dispersion medium there is a less orderly progression;

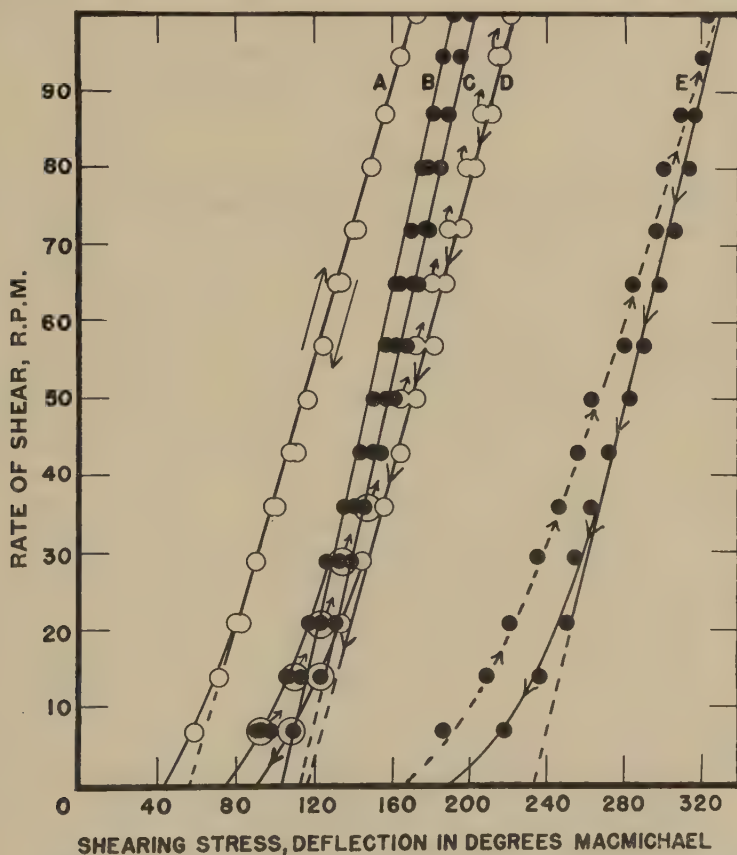


FIG. 2. Flow curves of magnetic iron oxide (21.2 vol. %) in glycerol (solid circles) and in linseed oil (hollow circles) with and without horseshoe magnet present. Arrows indicate observations at increasing or decreasing r.p.m. Curve A: No magnet, duplicate set of runs made before and after curve D; plastic viscosity, 6.8 poises; yield value, 240 dynes/sq. cm. Curve B: No magnet, initial curve; plastic viscosity, 5.1 poises; yield value, 445 dynes/sq. cm. Curve C: No magnet, duplicate of B but run after curve E; 5.1 poises, 480 dynes/sq. cm. Curve D: With magnet; 6.3 poises, 505 dynes/sq. cm. Curve E: With magnet; 5.7 poises, 990 dynes/sq. cm.

in fact there appears to be a maximum in the yield value of the magnetized dispersion at 25.2% solids. Perhaps the hygroscopic nature of glycerol may account for some irregularity. Failure to obtain exactly reproducible flow data from pairs of supposedly identical dispersions at different times may

have resulted from slight differences in grinding or from ambient temperature changes. In comparing the same dispersion magnetized and unmagnetized, however, no temperature effect is evident, since the duplicate unmagnetized determinations were usually almost undistinguishable from the original ones. This result also indicates that the dispersions reverted to their original state of flocculation on removal of the magnet—a process that would be accelerated by the shearing action of the viscometer.

TABLE I

Effects of Bar (B) and Horseshoe (H) Magnets on Plastic Viscosity (in poises) and Yield Value (Y.V. in dynes/sq. cm.) of Ferromagnetic Dispersions

Dispersoid	Medium	Solids (Vol. %)	Without magnet		With magnet		
			Visc.	Y.V.	Visc.	Y.V.	Magnet
Carbonyl iron powder	Linseed oil	27.9	16.4	85	17.3	1465	H
		39.0	42.2	145	51.7	2130	H
	Glycerol	27.9	9.1	120	11.7	1465	H
		39.0	18.4	200	25.6	2610	H
Magnetic iron oxide pigment	Linseed oil	21.2	6.82 ^a	240 ^a	6.29	505	H
		25.2	27.6 ^a	1055 ^a	27.6	1980	H
		27.9	33.8	1400	35.8	2500	B
			33.8 ^b	1505 ^b			
			45.0 ^c	2060 ^c	44.6	2820	H
	Glycerol	33.6	67.7 ^a	3160 ^a	72.2	3980	H
		21.2	5.09	445	5.70	900	H
			5.09 ^b	480 ^b			
		25.2	30.4 ^a	3640 ^a	28.8	5340	H
		27.9	19.7	3385	26.8	3560	B
			21.2 ^b	3280 ^b			
			30.6 ^c	3640 ^c	30.6	5010	H
		33.6	No readings possible because too thick				

^a Duplicate determinations after removal of magnet gave same values.

^b Result of duplicate determinations after removal of magnet.

^c Determined 7 weeks earlier than corresponding values listed just above.

These experiments were undertaken as part of a study to correlate the strengths of attractive forces between flocculant particles in nonaqueous media with the outward manifestation of those forces, the quantity measurable as yield value of a flocculated dispersion. It is not unreasonable to conclude from the results presented that this approach has been shown to be feasible. An extension of the work with better defined magnetic fields more readily expressed in terms of the forces between individual particles would serve to clarify the fundamental nature of forces of flocculation.

I am indebted to the individuals mentioned above for their cooperation in the work and to Interchemical Corporation for permission to publish these data.

The following paragraphs, quoted from J. Pryce-Jones (2) *Kolloid-Zeitschrift* **129**, pp. 118-119 (1952), are included here as pertinent to the preceding letter to the Journal of Colloid Science.

"The twin Couette apparatus is well adapted to the study of the effect of a magnetic field upon the viscosity of colloidal systems, for example. For these experiments the lower rotating cylinder is made of "Perspex" and is surrounded by a coil of wire which produces a field of 118 gaussess when an E.M.F. of 12 volts is applied. The liquid in the upper cylinder is selected so that it affords a convenient viscosity. The lower cylinder is filled with a dispersion of black magnetic oxide of iron, 25% by volume, in boiled oil of viscosity 2 poises. This dispersion shows anomalous viscosity in the absence of the field, on application of the current the viscosity is increased at all rates of shear. On the other hand the viscosity is reduced when an alternating current passes through the coil.

"A system prepared from 25% by volume of magnetic oxide in stand oil of 10 poises viscosity is Newtonian, but it becomes an anomalous fluid on the application of a field of 118 gaussess, it increases in viscosity when left at rest and behaves as a typical false-body system. As far as is known this behaviour has not been observed before."

REFERENCES

1. VOET, A., AND SURIANI, L. R., *J. Colloid Sci.* **6**, 155-161 (1951).
2. PRYCE-JONES, J., *Kolloid-Z.* **129**, 96-122, esp. 118-119 (1952).
3. GREEN, H., *Ind. Eng. Chem., Anal. Ed.* **14**, 576-585 (1942).

The Research Laboratories of Interchemical Corporation EDMUND N. HARVEY, JR.
Received June 3, 1953.

MOLECULAR CROSS SECTIONS IN FILMS OF FATTY ACIDS ON WATER

In a recent letter to this journal, Vold (1) has pointed out that the paraffin hydrocarbon chain lacks cylindrical symmetry, and that this should be taken into account in considering the packing of long-chain fatty acids in monolayers on aqueous substrates. We had also considered this possibility and would now support the arrangement which she suggests for stearic acid molecules occupying an area of 20.5 sq. Å. per molecule. Her drawings imply that the —OH groups are directed into the substrate ("closed" configuration, Fig. 1), where they presumably form hydrogen bonds with the water. This seems preferable to Alexander's (2) suggestion of hydrogen bonding to adjacent molecules, which involved a long and therefore weak bond. The alternative suggestion (3) that free rotation is possible in such compressed films seems to be based on incorrect calculations.

We would make two further points which seem relevant to this consideration:

1. Early workers were concerned by the discrepancy between the molecular area of 20.5 sq. A. found in monolayers of fatty acids and the area of 18.5 sq. A. in crystals of the same materials and of long-chain paraffins.

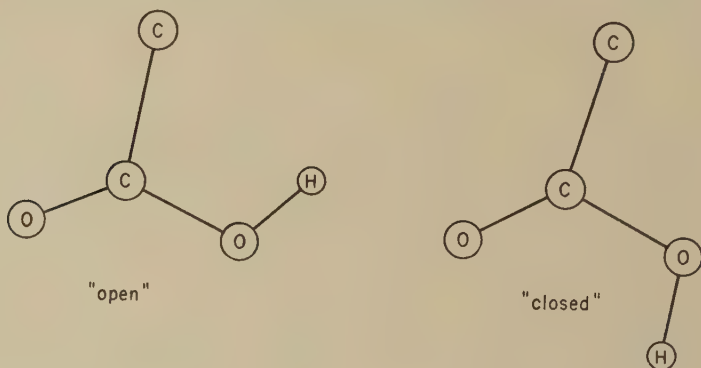


FIG. 1.

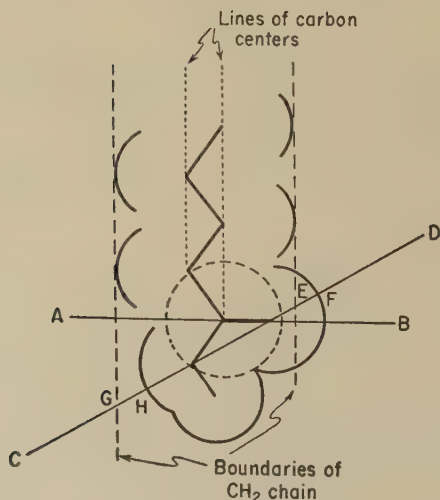


FIG. 2.

Reference to models shows that if the hydrocarbon chain is vertical, the carboxyl group in the position described by Vold (in which the O—C—O plane lies along the longer horizontal axis of the hydrocarbon chain) has the line joining the centers of the two oxygen atoms inclined at an angle of about $26\frac{1}{2}^\circ$ to the horizontal (Fig. 2*). This is also the configuration in

* Vold's use of 1.00 A. as the van der Waals radius of the carbon atom involves the anomaly of the overlapping of the hydrogen atoms in the CH_2 group. In Fig. 2

the crystal, in which there is hydrogen bonding between carboxyl groups in adjacent layers.

In the crystal, the molecules are arranged so that the carboxyl groups in a given layer lie along the plane through CD . From the scale drawing of Fig. 2, it is seen that the distance EF is less than GH , and therefore that

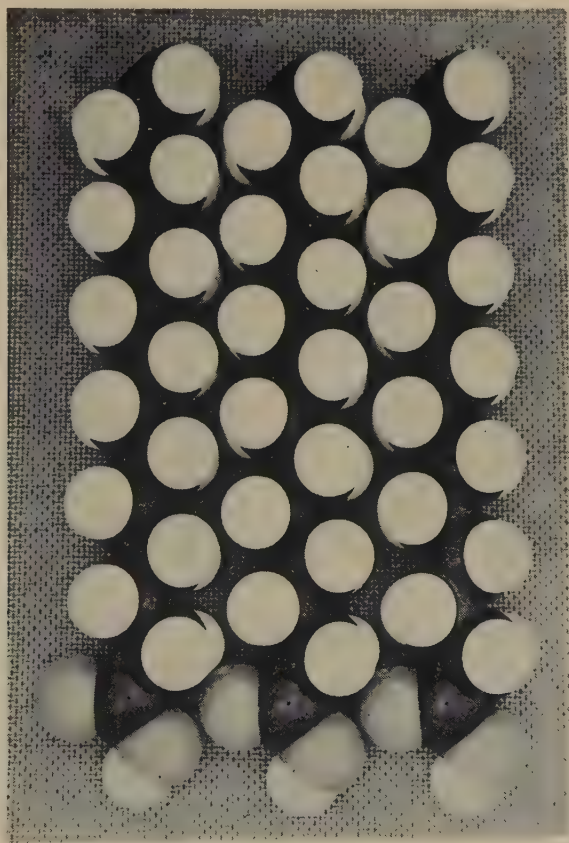


PLATE I

the packing is determined by the size of the hydrocarbon chains, not by that of the carboxyl groups. The spacing is consequently the same as that in crystals of the long-chain paraffins (4).

On the water surface, however, with the carbon atoms of the carboxyl groups all lying in the plane through AB , the projecting part of the carbonyl oxygen atom cannot wholly be accommodated within a recess of the adjacent molecule. This leads to the wider spacing, with a molecular

we have used the value of 1.6 Å., which seems more likely to be correct and which involves no such overlapping. The significant conclusions are, however, unaffected by this change.

area of 20.5 sq. A., described by Vold, in which adjacent hydrocarbon chains are not quite in contact (see Plate I).

It is worth recalling that the early suggestion of Lyons and Rideal (5), that on aqueous substrates the hydrocarbon chains may be tilted, involves the same packing of the molecules as in a single layer of the crystal. The

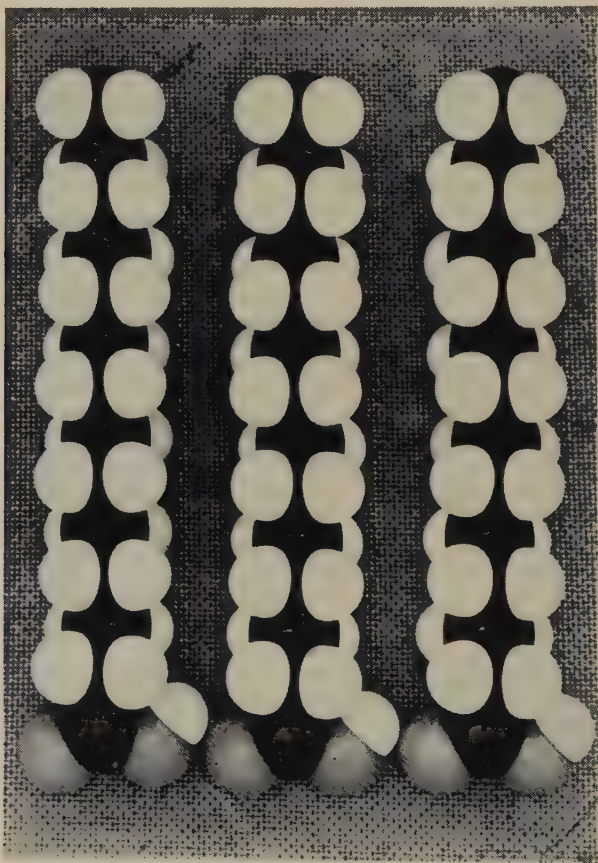


PLATE II

molecular area, measured along the surface, instead of perpendicular to the chain, becomes $18.5 \cos 26\frac{1}{2}^\circ = 20.5$ sq. A. It seems to us to be fortuitous that the two arrangements should give almost identical molecular areas. In view of later work, and especially that of Blodgett and Langmuir (6), however, the vertical orientation of the chains seems generally to be preferred.

2. Alexander (2) has suggested that, in the monolayer on an acid substrate at a molecular area of 25 sq. A., there is intra-layer hydrogen bonding. This implies the "open" configuration of the carboxyl group (Fig. 1),

and inclined chains. As against this, Vold has suggested an arrangement with vertical chains. We would suggest another possible arrangement with vertical chains. This involves the "open" carboxyl group lying along the *shorter* horizontal axis of the chain. In this arrangement the line through the centers of the oxygen atoms is effectively horizontal (Plate II), and there is no accommodation of any part of the carboxyl group in a recess of the adjacent molecule. The length of the group is then 5.53 Å.; with the relevant dimension of the hydrocarbon chain (4.55 Å.), this gives a molecular area of 25.2 sq. Å. This arrangement, like that suggested by Vold but unlike that of Alexander, requires that the height of the monolayer should be the full height of the molecule. It is possible that such measurements as those suggested by Vold will lead to a more definite conclusion.

REFERENCES

1. VOLD, M. J., *J. Colloid Sci.* **7**, 196 (1952).
2. ALEXANDER, A. E., *Proc. Roy. Soc. (London)* **179A**, 470 (1942).
3. WEITZEL, G., FRETZDORFF, A-M., HELLER, S., AND GRAESER, E., *Kolloid-Z.* **127**, 110 (1952).
4. MÜLLER, A., *Proc. Roy. Soc. (London)*, **114A**, 542 (1927); *ibid.* **120A**, 437 (1928).
5. LYONS, C. G., AND RIDEAL, E. K., *Proc. Roy. Soc. (London)* **124A**, 333 (1929).
6. BLODGETT, K. B., AND LANGMUIR, I., *Phys. Rev.* **51**, 964 (1937).

University College
Hull, England
Received June 18, 1953

J. J. KIPLING
A. D. NORRIS

SUPPLEMENT TO "PRODUCTION OF MONODISPERSE LIQUID PARTICLES BY ELECTRICAL ATOMIZATION"

In the article, "Production of Monodisperse Liquid Particles by Electrical Atomization," (1) a phenomenon was described by which liquids are atomized from a positively charged capillary tube to give a monodisperse aerosol having a particle radius of a micron or less. Further experiments have been made to determine how this phenomenon is related to the electrical conductivity of the liquid being atomized.

To reduce the number of variables in these experiments, a single horizontally clamped capillary, as shown in Fig. 1, was used throughout. The liquids were not under pressure and the temperature was maintained at 25°C. Conductivities were measured at 1 kc., or, for standard solutions, were taken from the tables (2).

When the liquid has a very low conductivity, the smoke comes off the capillary tip through a wide angle and shows the colors of higher-order Tyndall spectra. As the conductance increases, the angle of smoke generation and the number of particles produced, decreases, and the required voltage increases. A further increase in conductivity requires that an ex-

ternal ground or negative potential electrode be placed close to the capillary tip to produce smoke. The production of smoke is quite erratic and the rate of particle production is small. A still higher conductance gives very unstable production, and droplets of larger diameter are present in the smoke. This conductivity is listed under "not possible" in Table I,

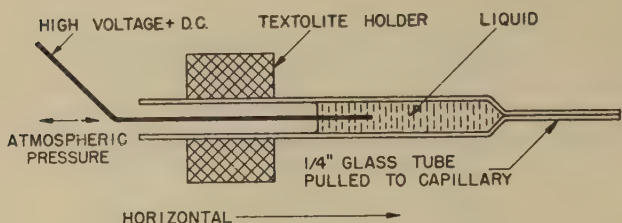


FIG. 1.

TABLE I

Production of Monodisperse Liquid Particles by Electrical Atomization

Specific conductivity MHO/CM

Production of 1 micron particle size	Good	Poor	Possible	Not possible
Solution				
Water.....	1×10^{-5}	2×10^{-5}	4×10^{-5}	8×10^{-5}
NaCl.....	2×10^{-5}	6×10^{-5}	2×10^{-4}	5×10^{-4}
HCl.....	4×10^{-5}	4×10^{-4}	4×10^{-3}	4×10^{-2}

since the aerosol is no longer monodisperse. The values of conductivity for the three liquids in the table will vary with different capillaries and with the pressure on the liquid.

It is possible to produce uniform particles of liquids of high conductivity, but as we have previously reported, these particles are quite large, 25μ in radius or larger. This appears to be a somewhat different phenomenon, for it works with either polarity and the particles leave the capillary tip in a fine stream rather than as a smoke, as is the case with liquids of low conductivity.

REFERENCES

1. VONNEGUT, B., AND NEUBAUER, R., "Production of Monodisperse Liquid Particles by Electrical Atomization," *J. Colloid Sci.* **7**, 616 (1952).
2. International Critical Tables, Vol. VI. McGraw-Hill Book Co., New York, 1929.

General Electric Research Laboratory
Received December 11, 1952

RAYMOND L. NEUBAUER
BERNARD VONNEGUT¹

¹ Present address: Arthur D. Little, Inc., Cambridge 42, Massachusetts.

BOOK REVIEW

Ion Exchangers in Analytical Chemistry. By OLAF SAMUELSON. John Wiley & Sons, Inc., New York, 1953. 291 pp. Price \$6.50.

Although from the title of this book one might expect it to be limited to information on analytical chemical applications, it contains what is probably the most comprehensive review of the general principles of ion exchange yet to appear. The field is one which is developing rapidly and which had not been the subject of enough satisfactory books. Thus those interested in ion exchange should welcome this new addition to the literature.

The author divides his work into two sections. The first, which is nearly half of the book, is devoted to general ion exchange theory and practice. This is presented logically and in a particularly understandable fashion. He starts with discussions of the properties of the resins and with the principles of ion exchange equilibrium, centering attention on the Donnan approach. This interpretation is one which probably will be challenged by specialists but which seems adequate for the explanation of the phenomena involved in the applications considered. The author then discusses ion exchange kinetics. In contrast to earlier authors, he gives emphasis to the important diffusional rate mechanisms rather than to the chemical kinetics mechanisms which had been postulated. However, his interpretation of liquid film mass transfer resistances is surprisingly weak, in view of the fact that he is listed as a professor of engineering chemistry. In applying the principles of equilibrium and kinetics to column operation, the author presents interesting results of some of his own researches which have not been well known to readers of English-language technical journals. In his treatment of column operation, he suffers from unfamiliarity with recent work in which nonequilibrium cases were interpreted by diffusional mechanisms. It is also surprising that the author gives only brief mention to the *theoretical plate* concept of ion exchange separations. Despite the inherent theoretical weakness of this model as applied to packed beds, its use is accepted by many in ion exchange chromatography, and it would be a basis for better visualization of elution chromatographic separations. The separate treatment of breakthrough and regeneration curves by the author indicates a leaning towards the art, rather than the science, of ion exchange. However, despite its specific weaknesses, the treatment of the general principles is a valuable review of the field and is more than adequate as an introduction to the major subject of the book.

The latter portion of this book deals with specific analytical problems including determinations of sugars and polyhydric alcohols, alkaloids, amino acids, and vitamins. This is not limited to elution chromatography; rather it covers more cases of simple ion removal or exchange. For example, a chapter deals with the removal by ion exchange of ions which would interfere with conventional analytical procedures. He describes in detail the techniques of applying ion exchange to the analysis of such varied materials as sulfite waste liquor, blood, and dyes. On a more fundamental level, he discusses the special problems of solutions in which complex ions are formed. In all cases ample references are given. At the end he covers miscellaneous uses of ion exchange in the preparation of laboratory reagents.

Ion Exchangers in Analytical Chemistry should be a useful book for anyone wishing to employ the techniques described. More than that, it is recommended for its general picture of ion exchange to anyone commencing research in that field.

W. A. SELKE, New York, New York

NUMERICAL EVALUATION OF THE MIE SCATTERING FUNCTIONS; TABLE OF THE ANGULAR FUNCTIONS π_n AND τ_n OF ORDERS 1 TO 32, AT 2.5° INTERVALS¹

Frank T. Gucker, Jr., and Stanley H. Cohn²

*Contribution No. 584 from the Chemical Laboratory of Indiana University,
Bloomington, Indiana*

Received August 25, 1952

ABSTRACT

In connection with a program of calculating the light-scattering properties of isotropic spherical particles over a wide range of the parameter α and refractive index m , we have tabulated the angular functions π_n and τ_n for values of the angle 0° (2.5°) 180° , and orders 1 to 32.

From our experience in this work, the following suggestions are made toward standardizing and simplifying the form of the Mie scattering coefficients: (1) Use of van de Hulst's scattering coefficients a_n and b_n . (2) Use of the scattering angle θ measured from the *forward* direction of the propagation of the incident light, as suggested by Stratton and van de Hulst. (3) Incorporation of the factor $F(n) = (2n + 1)/n(n + 1)$ into the augmented angular functions, $\Pi_n(x) = F(n)\pi_n(x)$ and $T_n(x) = F(n)\tau_n(x)$, which are independent of particle size and refractive index, instead of the coefficients A_n and P_n , which are functions of these variables. (4) Use of a suitable transformation to express the scattering functions for real arguments in terms of real-valued functions only, eliminating all derivatives and separating the terms which are functions of α alone from those which are functions of β , m . The functions of β , m , may be calculated by means of a simple recurrence formula which is particularly useful when the refractive index is complex. Equations are given for calculating the Stokes parameters, which completely characterize the scattered light, when a spherical particle is illuminated with light plane-polarized in an arbitrary direction.

INTRODUCTION

The problem of wave scattering from spheres occurs in a surprising number of different fields. Light scattering from colloidal solutions and aerosols interests the physicist and physical chemist, that from interstellar particles interests the astronomer, and microwave scattering from rain and clouds concerns the meteorologist and communications engineer. All of these prob-

¹ The calculations herein described are part of a program of research on aerosols carried out under Contract No. AF19(122)-375 with the Geophysics Research Division, Air Force Cambridge Research Center, Cambridge, Massachusetts.

² Present address: Department of Mathematics, Fournier Institute of Technology, Lemont, Illinois.

lems use the same mathematical theory developed in 1908 by Gustav Mie (1-6), and current trends in research indicate that increasing practical use will be made of it (7, 8). The closely allied problems of sound scattering and wave-mechanical collision require analogous mathematical techniques, and many of the same functions (9, 10). Certainly contact among workers in all of these fields would help to avoid duplication of mathematical derivations and extensive computations, and would give wider use to existing theoretical techniques and tabulations. We are engaged in the calculation of the scattering coefficients and angular scattering from isotropic spherical particles over the range $\alpha = 0.1(0.1)25.0$, for values of the refractive index $m = 1.20, 1.25, 1.33, 1.40(0.02)1.50, 1.75, 2.00$. Most of the points treated below arose during these computations, and during many fruitful discussions with workers in some of the other fields mentioned earlier. Doubtless many further aids can be offered by others working in these fields.

The classical form (4, 11) of the Mie theory gives the intensity functions for the two plane-polarized components of the light scattered at any angle γ as:

$$\begin{aligned} i_1 &= \left| \sum_{n=1}^{\infty} [A_n \pi_n(\cos \gamma) + P_n \tau_n(\cos \gamma)] \right|^2 \equiv |J_1|^2, \\ i_2 &= \left| \sum_{n=1}^{\infty} [A_n \tau_n(\cos \gamma) + P_n \pi_n(\cos \gamma)] \right|^2 \equiv |J_2|^2. \end{aligned} \quad [1]$$

Here A_n and P_n , the scattering coefficients, are complex numbers. $\pi_n(x) = P_n'(x)$ and $\tau_n(x) = [xP_n'(x) - (1 - x^2)P_n''(x)]$ are angular functions, whereas $P_n'(x)$ and $P_n''(x)$ are, respectively, the first and second x -derivatives of the Legendre polynomial of argument $x = \cos \gamma$ and order n . The symbol τ was introduced by van de Hulst. The scattering angle γ is measured from the *reversed* direction of propagation of the incident light. J_1 , J_2 are the so-called complex amplitudes.

ANGULAR FUNCTIONS

Since we wished to determine the intensity functions at closer intervals than had been tabulated, we calculated the angular functions π_n and τ_n for values of the angle $0^\circ(2.5^\circ)180^\circ$ and for values of $n = 1$ to 32, which are given on pp. 563-574. These orders, corresponding to the available tabulated Legendre polynomials, may be used in combination with published values of A_n and P_n (4, 11) to calculate the angular scattering up to values of $\alpha = 25$, where $\alpha = 2\pi r/\lambda$, r is the radius of the scattering sphere, and λ is the wavelength of the incident light.

The π_n and τ_n functions were computed on a desk calculator by E. Eugenia Schmidt, whose assistance we gratefully acknowledge. The values of $P_n'(\cos \gamma)$, $P_n''(\cos \gamma)$, for $n = 1$ to 8 were taken from an unpublished book by Harold T. Davis (12) of Northwestern University, which he

kindly made available to us. Most values of π_n and τ_n for higher n were calculated by one of the following recurrence formulas:

$$\pi_n = \frac{n+1}{\sin^2 \gamma} (P_n \cdot \cos \gamma - P_{n+1}) = \frac{n}{\sin^2 \gamma} (P_{n-1} - P_n \cdot \cos \gamma); \quad [2]$$

$$\tau_n = n(n+1)P_n - \pi_n \cdot \cos \gamma = n \left(n + \frac{1}{\sin^2 \gamma} \right) P_n - \frac{\cos \gamma}{\sin^2 \gamma} P_{n-1}. \quad [3]$$

The values of $P_n(\cos \gamma)$ used in these computations were taken from the six-place tables of Tallqvist (13). Values of π_1 to π_{31} were checked by an independent recurrence relation. Values of π_{32} and of τ_n were checked by recalculation.

When the recurrence relations failed to yield five significant figures, the series expansion given by Tallqvist for $P_n(\cos \gamma)$ was used to calculate the necessary Legendre polynomials, or differentiated to yield a series for $P'_n(\cos \gamma)$ or $P''_n(\cos \gamma)$, which was then evaluated. The tabulated figures were checked to a maximum uncertainty of ± 2 in the fifth significant figure.

SIMPLIFIED NOTATION, AUGMENTED ANGULAR FUNCTIONS

An important consideration in discussing and calculating the Mie intensity functions is a unified and simple notation. Here advances have been made by Stratton (2) and particularly by van de Hulst (3, 5), whose notation in general we prefer. He used scattering coefficients a_n , b_n , equal respectively to Stratton's $-b_n^s$, $-a_n^s$, which are complex quantities related to the classical scattering coefficients as follows:

$$A_n = (-1)^n i F(n) a_n, \quad P_n = (-1)^{n+1} i F(n) b_n; \quad [4]$$

where $F(n) = (2n+1)/n(n+1)$ and $i^2 = -1$.

Stratton and van de Hulst used the scattering angle $\theta = 180^\circ - \gamma$ measured from the *forward* direction of propagation of the incident light, thus eliminating the factors $(-1)^n$, $(-1)^{n+1}$ from Eqs. [4], because of the following simple relationships connecting the π and τ functions of an angle and its supplement:

$$\begin{aligned} \pi_n(\cos(180^\circ - \gamma)) &= (-1)^{n+1} \pi_n(\cos \gamma), \\ \tau_n(\cos(180^\circ - \gamma)) &= (-1)^n \tau_n(\cos \gamma). \end{aligned} \quad [5]$$

We find that it simplifies calculations to absorb the factor $F(n)$ in the angular functions, which are independent of particle size and refractive index, rather than in the coefficients A_n and P_n , which are functions of these variables. We suggest the use of these augmented functions:

$$\Pi_n(x) = F(n)\pi_n(x), \quad \mathbf{T}_n(x) = F(n)\tau_n(x). \quad [6]$$

We are tabulating these functions over the same values of angles and order, and expect to publish them in connection with our other calculations. We can then calculate the intensity functions from the amplitudes given by:

$$J_1 = -i \sum_{n=1}^{\infty} [a_n \Pi_n(\cos \theta) + b_n T_n(\cos \theta)] = \text{Re}_1 + i\text{Im}_1, \quad [7]$$

$$J_2 = i \sum_{n=1}^{\infty} [a_n T_n(\cos \theta) + b_n \Pi_n(\cos \theta)] = \text{Re}_2 + i\text{Im}_2.$$

The factors i and $-i$ do not affect the *intensities* but are important in determining the *complex amplitudes*, which are necessary to calculate the Stokes parameters of the scattered light. These parameters are particularly important since they characterize completely the intensity and polarization characteristics of any beam of light, and are additive for any number of superposed incoherent beams. Hans Mueller (14) has shown that if a spherical particle is illuminated by plane-polarized light with the electric vector making an angle Ψ with the plane of observation, the Stokes parameters of the scattered light are:

$$\begin{aligned} I &= (\text{Re}_1^2 + \text{Im}_1^2) \cos^2 \Psi + (\text{Re}_2^2 + \text{Im}_2^2) \sin^2 \Psi, \\ Q &= (\text{Re}_1^2 + \text{Im}_1^2) \cos^2 \Psi - (\text{Re}_2^2 + \text{Im}_2^2) \sin^2 \Psi, \\ U &= (\text{Re}_1 \text{Re}_2 + \text{Im}_1 \text{Im}_2) \sin 2\Psi, \\ V &= (\text{Re}_1 \text{Im}_2 - \text{Re}_2 \text{Im}_1) \sin 2\Psi. \end{aligned} \quad [8]$$

EVALUATION OF SCATTERING COEFFICIENTS

In evaluating a_n and b_n we prefer the Riccati-Bessel functions and their derivatives which occur explicitly in the Mie coefficients, rather than the spherical Bessel functions, j_n and $h_n^{(2)}$, used by Stratton. Lowan's notation S_n , C_n , Φ_n for the Riccati-Bessel functions, used also in *An Index of Mathematical Tables* (15) and in *A Guide to Tables of Bessel Functions* (16) seems preferable to van de Hulst's ψ_n , χ_n , ζ_n for these same functions. The various functions are related to each other and to the ordinary Bessel function, J , thus:

$$\begin{aligned} S_n(\alpha) &= \alpha j_n(\alpha) = \sqrt{(\pi\alpha/2)} J_{n+1/2}(\alpha); \\ C_n(\alpha) &= -\alpha n_n(\alpha) = (-1)^n \sqrt{(\pi\alpha/2)} J_{-(n+1/2)}(\alpha); \\ \Phi_n(\alpha) &= \alpha h_n^{(2)}(\alpha) = S_n(\alpha) + iC_n(\alpha); \\ h_n^{(2)}(\alpha) &= j_n(\alpha) - in_n(\alpha). \end{aligned} \quad [9]$$

Even though the spherical Bessel functions have been more extensively tabulated (17), these tables may be used unaltered in the computation, which actually involves *ratios* of the functions (see Eqs. [16] and [18] be-

low). Thus we obtain initially the following forms for the scattering coefficients:

$$\begin{aligned} a_n &= \frac{S_n'(\beta)S_n(\alpha) - mS_n'(\alpha)S_n(\beta)}{S_n'(\beta)\Phi_n(\alpha) - m\Phi_n'(\alpha)S_n(\beta)}, \\ b_n &= \frac{mS_n'(\beta)S_n(\alpha) - S_n'(\alpha)S_n(\beta)}{mS_n'(\beta)\Phi_n(\alpha) - \Phi_n'(\alpha)S_n(\beta)}, \end{aligned} \quad [10]$$

where α , r , and λ have their previous significance, $\beta = m\alpha$, m is the refractive index of the sphere relative to the surrounding medium, and a prime denotes a partial derivative with respect to the argument in parentheses. As a mnemonic, we observe that each denominator is obtained from the corresponding numerator by replacing $S_n(\alpha)$, $S_n'(\alpha)$ by $\Phi_n(\alpha)$, $\Phi_n'(\alpha)$, whereas the factor m in a_n is simply replaced by $1/m$ in b_n . Since $\Phi_n(\alpha) = S_n(\alpha) + iC_n(\alpha)$ is complex-valued, it must always be separated into its real and imaginary parts for numerical computation; hence, we make this substitution initially and rewrite the coefficients as:

$$\begin{aligned} a_n &= \left[1 + i \frac{S_n'(\beta)C_n(\alpha) - mC_n'(\alpha)S_n(\beta)}{S_n'(\beta)S_n(\alpha) - mS_n'(\alpha)S_n(\beta)} \right]^{-1} = [1 + iG_n(\alpha, \beta)]^{-1}; \\ b_n &= \left[1 + i \frac{mS_n'(\beta)C_n(\alpha) - C_n'(\alpha)S_n(\beta)}{mS_n'(\beta)S_n(\alpha) - S_n'(\alpha)S_n(\beta)} \right]^{-1} = [1 + iH_n(\alpha, \beta)]^{-1}. \end{aligned} \quad [11]$$

For nonabsorbing spheres m is real, as are G_n and H_n ; hence, it is readily seen that $\text{Re}(a_n) = |a_n|^2$, and $\text{Re}(b_n) = |b_n|^2$. This is required physically by the fact that E , the total energy scattered and absorbed by the sphere, must equal S , the total energy scattered. These energies are given (2, 3) by:

$$\begin{aligned} E &= (2/\alpha^2) \sum_{n=1}^{\infty} (2n+1) \text{Re}(a_n + b_n), \\ S &= (2/\alpha^2) \sum_{n=1}^{\infty} (2n+1)(|a_n|^2 + |b_n|^2). \end{aligned} \quad [12]$$

The form of Eqs. [11] has led van de Hulst to introduce auxiliary phase angles α_n , β_n by writing [11] as

$$\begin{aligned} a_n &= [1 - \cot \alpha_n]^{-1} = \frac{1}{2}(1 - e^{-2i\alpha_n}), \\ b_n &= [1 - \cot \beta_n]^{-1} = \frac{1}{2}(1 - e^{-2i\beta_n}), \end{aligned} \quad [13]$$

where α_n , β_n are continuous functions of α and m . These angles, analogous to the phase shift in wave mechanics, are real for real m , and considerably more regular in behavior than the scattering coefficients themselves. Further, they completely characterize the coefficients:

$$\begin{aligned} \text{Re}(a_n) &= |a_n|^2 = \frac{1}{2}(1 - \cos 2\alpha_n) = \sin^2 \alpha_n, \\ \text{Im}(a_n) &= \frac{1}{2} \sin 2\alpha_n = \sin \alpha_n \cos \alpha_n, \end{aligned} \quad [14]$$

and similarly for b_n . Clearly the auxiliary angles are most useful in the case of real refractive index, but the form of Eqs. [11] is useful in the complex case, which will be discussed later.

In computation it is desirable to eliminate the derivatives of the Bessel functions, which are not usually tabulated, by means of the standard relation between the derivatives and the functions themselves, in the form:

$$\frac{S_n'(\alpha)}{S_n(\alpha)} = \frac{S_{n-1}(\alpha)}{S_n(\alpha)} - \frac{n}{\alpha}, \quad \frac{C_n'(\alpha)}{C_n(\alpha)} = \frac{C_{n-1}(\alpha)}{C_n(\alpha)} - \frac{n}{\alpha}. \quad [15]$$

At the same time, we find it advisable to separate the functions G_n and H_n each into two parts: one depending on m , the other independent of m , and therefore applicable in subsequent calculations for other refractive indices. Rearranging $H_n(\alpha, \beta)$ in the second of Eqs. [11], making the substitution indicated above and remembering that $\beta/m = \alpha$, we find

$$H_n(\alpha, \beta) = \frac{mR_n(\beta)C_n(\alpha) - C_{n-1}(\alpha)}{mR_n(\beta)S_n(\alpha) - S_{n-1}(\alpha)}; \quad R_n(\beta) \equiv \frac{S_{n-1}(\beta)}{S_n(\beta)}. \quad [16]$$

If m is complex, so also is β , and the corresponding Riccati-Bessel functions are not extensively tabulated; hence, the simplest way to evaluate the function $R_n(\beta)$ is by the following recurrence relation, based on the usual one for Bessel functions of three successive orders:

$$R_n(\beta) = \left[\frac{2n-1}{\beta} - R_{n-1}(\beta) \right]^{-1}. \quad [17]$$

Here $R_0(\beta) = \cot \beta$ may be had from standard tables. Aden (7) has successfully used a modified but more complicated form of this procedure, since he does not take advantage of the cancellation of terms $(mn/\beta) - (n/\alpha)$ and also, employing Stratton's notation, he retains the complex-valued function $\alpha h_n^{(2)}(\alpha)$ equivalent to the $\Phi_n(\alpha)$, which we have eliminated.

The corresponding expression in the case of a_n is obtained by replacing m by $1/m$:

$$G_n(\alpha, \beta) = \frac{W_n(\beta)C_n(\alpha) - C_{n-1}(\alpha)}{W_n(\beta)S_n(\alpha) - S_{n-1}(\alpha)}; \quad [18]$$

$$W_n(\beta) = \frac{1}{m} R_n(\beta) + \frac{n}{\alpha} \left(1 - \frac{1}{m^2} \right).$$

Finally, in checking numerical results, it is useful to know the following relation connecting the four functions of α which occur in Eqs. [16] and [18]:

$$S_{n-1}(\alpha)C_n(\alpha) - C_{n-1}(\alpha)S_n(\alpha) = 1. \quad [19]$$

Using this and [17], we may eliminate $R_n(\beta)$ entirely and obtain relations between any two of $\cot \alpha_n$, $\cot \beta_n$, $\cot \alpha_{n-1}$, and $\cot \beta_{n-1}$. These relations

would involve only $S_n(\alpha)$, $C_n(\alpha)$, $S_{n-1}(\alpha)$, n , m , and α , but there is probably little computational advantage in using them.

REFERENCES

1. MIE, G., *Ann. Physik* **25**, 377 (1908).
2. STRATTON, J. A., *Electromagnetic Theory*, Chap. IX. McGraw-Hill Book Company, Inc., New York, 1941.
3. VAN DE HULST, H. C., *Optics of Spherical Particles, Recherches Astronomiques de L'Observatoire d'Utrecht XI*, part I (1946).
4. LOWAN, A. N., *Tables of Scattering Functions for Spherical Particles*. National Bureau of Standards, Appl. Math. Series No. 4, U. S. Government Printing Office, Washington, 1948.
5. VAN DE HULST, H. C., *J. Colloid Sci.* **4**, 79 (1949).
6. SINCLAIR, D., AND LA MER, V. K., *Chem. Revs.* **44**, 245 (1949).
7. ADEN, A. L., *J. Appl. Phys.* **22**, 601 (1951).
8. GUMPRECHT, R. O., SUNG, N. L., CHIN, J. H., AND SLIEPCEVICH, C. M., *J. Opt. Soc. Amer.* **42**, 226 (1952).
9. LOWAN, A. N., MORSE, P. M., FESHBACH, H., AND LAX, M., *Scattering and Radiation from Circular Cylinders and Spheres*. U. S. Navy Department, Office of Research and Inventions, Washington, 1946.
10. LAX, M., AND FESHBACH, H., *J. Acoust. Soc. Amer.* **20**, 108 (1948).
11. GUMPRECHT, R. O., AND SLIEPCEVICH, C. M., *Tables of Light Scattering Functions for Spherical Particles*. Engineering Research Institute, University of Michigan, 1951.
12. DAVIS, H. T., *Legendre Polynomials* (unpublished).
13. TALLQVIST, H. J., *Sechsstellige Tafeln der 32 ersten Kugelfunktionen $P_n(\cos \theta)$* . *Acta Soc. Sci. Fennicae*, Nova Series A, Vol. II, No. 11, Helsingfors, 1938.
14. MUELLER, H., unpublished report.
15. FLETCHER, A., MILLER, J. C. P., AND ROSENHEAD, L., *An Index of Mathematical Tables*. McGraw-Hill Book Company, New York, 1946.
16. BATEMAN, H., AND ARCHIBALD, R. C., *Mathematical Tables and Other Aids to Computation* **1**, 207 (1944).
17. LOWAN, A. N., *Tables of Spherical Bessel Functions*, Vols. I and II. Prepared by the Mathematical Tables Project, National Bureau of Standards. Columbia University Press, New York, 1947.

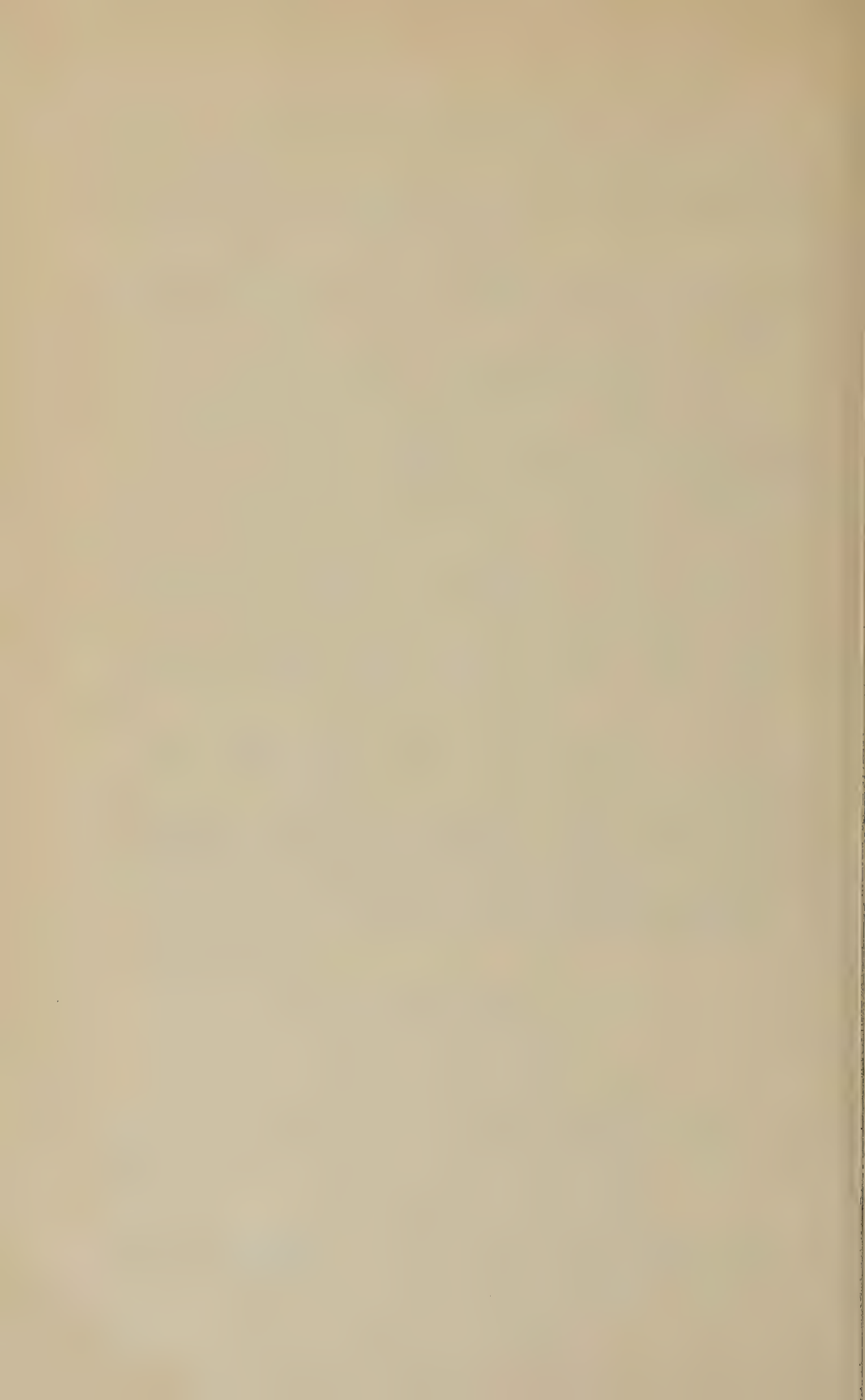


TABLE OF MIE ANGULAR SCATTERING FUNCTIONS*

0°			2.5°		5°		7.5°		
n	π_n	τ_n	π_n	τ_n	π_n	τ_n	π_n	τ_n	n
1	1	±1	1.0000	±0.99905	1.0000	±0.99619	1.0000	±0.99144	1
2	±3	3	±2.9973	2.9885	±2.9886	2.9544	±2.9743	2.8978	2
3	6	±6	5.9856	±5.9517	5.9430	±5.8070	5.8722	±5.5686	3
4	±10	10	±9.9571	9.8625	±9.8293	9.4535	±9.6187	8.7853	4
5	15	±15	14.900	±14.687	14.603	±13.762	14.117	±12.268	5
6	±21	21	±20.801	20.384	±20.210	18.574	±19.249	15.688	6
7	28	±28	27.643	±26.900	26.584	±23.702	24.880	±18.675	7
8	±36	36	±35.407	34.180	±33.653	28.936	±30.858	20.840	8
9	45	±45	44.065	±42.162	41.334	±34.046	37.024	±21.778	9
10	±55	55	±53.599	50.768	±49.534	38.788	±43.205	21.096	10
11	66	±66	63.978	±59.920	58.160	±42.906	49.228	±18.420	11
12	±78	78	±75.176	69.525	±67.106	46.132	±54.920	13.419	12
13	91	±91	87.158	±79.496	76.268	±48.198	60.105	±5.8122	13
14	±105	105	±99.887	89.736	±85.528	48.842	±64.622	-4.6096	14
15	120	±120	113.33	±100.14	94.779	±47.798	68.316	±17.975	15
16	±136	136	±127.44	110.58	±103.90	44.827	±71.049	-34.319	16
17	153	±153	142.19	±120.98	112.78	±39.688	72.698	±53.576	17
18	±171	171	±157.53	131.17	±121.29	32.164	±73.164	-75.570	18
19	190	±190	173.42	±141.06	129.33	±22.088	72.370	±100.02	19
20	±210	210	±189.79	150.53	±136.78	9.2862	±70.263	-126.54	20
21	231	±231	206.61	±159.44	143.53	±6.3566	66.819	±154.61	21
22	±253	253	±223.84	167.64	±149.50	-24.924	±62.040	-183.64	22
23	276	±276	241.41	±175.03	154.56	±46.472	55.958	±212.94	23
24	±300	300	±259.28	181.46	±158.65	-70.987	±48.634	-241.74	24
25	325	±325	277.38	±186.80	161.68	±98.433	40.154	±269.21	25
26	±351	351	±295.68	190.90	±163.56	-128.73	±30.634	-294.47	26
27	378	±378	314.10	±193.66	164.26	±161.72	20.214	±316.64	27
28	±406	406	±332.59	194.93	±163.70	-197.21	±9.0562	-334.81	28
29	435	±435	351.10	±194.58	161.86	±234.98	-2.6583	±348.10	29
30	±465	465	±369.58	192.46	±158.70	-274.73	±14.730	-355.72	30
31	496	±496	387.95	±188.48	154.21	±316.14	-26.948	±356.88	31
32	±528	528	±406.16	182.51	±148.38	-358.81	±39.092	-350.94	32
n	π_n	τ_n	π_n	τ_n	π_n	τ_n	π_n	τ_n	n
180°			177.5°		175°		172.5°		

*Where two signs appear before an entry, the upper sign is for angles listed at top of page, the lower sign for angles at bottom.

TABLE OF MIE ANGULAR SCATTERING FUNCTIONS*

n	10°		12.5°		15°		n
	π_0	τ_0	π_0	τ_0	π_0	τ_0	
1	1.0000	± 0.98481	1.0000	± 0.97630	1.0000	± 0.96593	1
2	± 2.9544	2.8190	± 2.9288	2.7190	± 2.8978	2.5981	2
3	5.7738	± 5.2407	5.6486	± 4.8288	5.4976	± 4.3397	3
4	± 9.3283	7.8776	± 8.9624	6.7574	± 8.5270	5.4574	4
5	13.453	± 10.272	12.627	± 7.8626	11.660	± 5.1512	5
6	± 17.952	11.908	± 16.366	7.4780	± 14.545	2.6793	6
7	22.610	± 12.254	19.888	± 4.9840	16.838	∓ 2.5140	7
8	± 27.200	10.787	± 22.902	-0.11555	± 18.228	-10.683	8
9	31.482	± 7.0473	25.138	∓ 8.1266	18.472	∓ 21.692	9
10	± 35.232	0.66146	± 26.367	-19.108	± 17.416	-34.979	10
11	38.232	∓ 8.6149	26.406	∓ 32.830	15.007	∓ 49.540	11
12	± 40.292	-20.872	± 25.138	-48.758	± 11.310	-63.998	12
13	41.245	∓ 36.018	22.525	∓ 66.059	6.5014	∓ 76.696	13
14	± 40.974	-53.781	± 18.601	-83.631	± 0.86327	-85.847	14
15	39.392	∓ 73.676	13.484	∓ 100.16	-5.2384	∓ 89.712	15
16	± 36.468	-95.040	± 7.3648	-114.18	∓ 11.378	-86.793	16
17	32.218	∓ 117.03	0.50303	∓ 124.22	-17.102	∓ 76.020	17
18	± 26.712	-138.65	∓ 6.7870	-128.82	∓ 21.962	-56.921	18
19	20.065	∓ 158.80	-14.151	∓ 126.76	-25.555	∓ 29.750	19
20	± 12.442	-176.30	∓ 21.214	-117.06	∓ 27.549	4.4463	20
21	4.0502	∓ 189.95	-27.600	∓ 99.142	-27.718	± 43.824	21
22	∓ 4.8667	-198.60	∓ 32.949	-72.917	∓ 25.962	85.821	22
23	-14.038	∓ 201.16	-36.945	∓ 38.807	-22.317	± 127.30	23
24	∓ 23.172	-196.73	∓ 39.324	2.2058	∓ 16.958	164.78	24
25	-31.968	∓ 184.58	-39.900	± 48.576	-10.198	± 194.67	25
26	∓ 40.125	-164.26	∓ 38.570	98.269	∓ 2.4569	213.62	26
27	-47.353	∓ 135.61	-35.324	± 148.81	5.7520	± 218.80	27
28	∓ 53.383	-98.788	∓ 30.253	197.40	± 13.866	208.20	28
29	-57.978	∓ 54.321	-23.540	± 241.10	21.307	± 180.89	29
30	∓ 60.940	-3.0822	∓ 15.462	276.91	± 27.528	137.19	30
31	-62.118	± 53.694	-6.3678	± 302.04	32.050	± 78.776	31
32	∓ 61.413	114.45	± 3.3259	314.04	± 34.497	8.6623	32
n	π_0	τ_0	π_0	τ_0	π_0	τ_0	n
170°			167.5°		165°		

* Note: Use lower sign for angles listed at the bottom.

TABLE OF MIE ANGULAR SCATTERING FUNCTIONS*

n	17.5°		20°		22.5°		n
	π_n	τ_n	π_n	τ_n	π_n	τ_n	
1	1.0000	± 0.95372	1.0000	± 0.93969	1.0000	± 0.92388	1
2	± 2.8612	2.4574	± 2.8191	2.2982	± 2.7716	2.1214	2
3	5.3218	± 3.7818	5.1227	± 3.1649	4.9016	± 2.4990	3
4	± 8.0280	4.0166	± 7.4732	2.4770	± 6.8711	0.88389	4
5	10.575	± 2.2584	9.3975	∓ 0.68598	8.1560	∓ 3.5506	5
6	± 12.554	-2.1852	± 10.460	-6.8090	± 8.3322	-10.905	6
7	13.604	∓ 9.6097	10.332	∓ 15.714	7.1633	∓ 20.330	7
8	± 13.455	-19.777	± 8.8512	-26.451	± 4.6592	-30.034	8
9	11.964	∓ 31.857	6.0510	∓ 37.339	1.0883	∓ 37.543	9
10	± 9.1388	-44.450	± 2.1690	-46.178	∓ 3.0542	-40.188	10
11	5.1425	∓ 55.718	-2.3757	∓ 50.586	-7.1227	∓ 35.736	11
12	± 0.28509	-63.589	∓ 7.0340	-48.434	∓ 10.427	-23.010	12
13	-5.0047	∓ 66.039	-11.197	∓ 38.304	-12.354	∓ 2.3923	13
14	∓ 10.220	-61.389	∓ 14.277	-19.877	∓ 12.476	23.947	14
15	-14.828	∓ 48.608	-15.795	± 5.8097	-10.638	± 52.176	15
16	∓ 18.325	-27.554	∓ 15.444	36.303	∓ 7.0056	77.298	16
17	-20.291	± 0.86353	-13.151	± 67.913	-2.0458	± 93.971	17
18	∓ 20.440	34.648	∓ 9.0900	96.116	± 3.5264	97.515	18
19	-18.652	∓ 70.813	-3.6763	± 116.16	8.8565	± 84.936	19
20	∓ 14.998	105.62	± 2.4771	123.76	± 13.084	55.762	20
21	-9.7383	± 134.92	8.6320	± 115.84	15.480	± 12.499	21
22	∓ 3.3052	154.63	± 14.014	91.179	± 15.578	-39.414	22
23	3.7333	± 161.21	17.912	± 50.794	13.254	∓ 92.214	23
24	± 10.725	152.14	± 19.772	-1.8890	± 8.7686	-136.93	24
25	16.994	± 126.34	19.275	∓ 61.257	2.7332	∓ 164.86	25
26	± 21.909	84.444	± 16.387	-120.06	∓ 3.9683	-169.11	26
27	24.946	± 28.928	11.373	∓ 170.28	-10.312	∓ 146.11	27
28	± 25.744	-35.966	± 4.7764	-204.14	∓ 15.291	-96.521	28
29	24.146	∓ 104.53	-2.6422	∓ 215.30	-18.078	∓ 25.644	29
30	± 20.218	-170.05	∓ 9.9924	-199.79	∓ 18.163	57.033	30
31	14.256	∓ 225.48	-16.362	∓ 156.89	-15.438	± 139.04	31
32	± 6.7614	-264.10	∓ 20.933	-89.482	∓ 10.238	206.79	32
π	π_n	τ_n	π_n	τ_n	π_n	τ_n	n
	162.5°		160°		157.5°		

* Note: Use lower sign for angles listed at the bottom.

TABLE OF MIE ANGULAR SCATTERING FUNCTIONS*

n	25°		27.5°		30°		n
	π_n	τ_n	π_n	τ_n	π_n	τ_n	
1	1.0000	± 0.90631	1.0000	± 0.88701	1.0000	± 0.86603	1
2	± 2.7189	1.9284	± 2.6610	1.7208	± 2.5981	1.5000	2
3	4.6604	± 1.7958	4.4010	± 1.0668	4.1250	± 0.32476	3
4	± 6.2303	-0.71594	± 5.5606	-2.2758	± 4.8714	-3.7500	4
5	6.8792	∓ 6.2084	5.5964	∓ 8.5430	4.3359	∓ 10.453	5
6	± 6.2400	-14.223	± 4.2482	-16.565	± 2.4154	-17.801	6
7	4.2274	∓ 23.101	1.6354	∓ 23.832	-0.52637	∓ 22.514	7
8	± 1.0788	-30.226	∓ 1.7466	-27.113	∓ 3.7373	-21.156	8
9	-2.6784	∓ 32.634	-5.1320	∓ 23.504	-6.2856	∓ 11.618	9
10	∓ 6.3233	-27.845	∓ 7.6694	-11.577	∓ 7.3392	5.5818	10
11	-9.0884	∓ 14.727	-8.6408	± 7.7236	-6.4334	± 26.785	11
12	∓ 10.324	5.8630	∓ 7.6591	30.806	∓ 3.6430	45.775	12
13	-9.6484	± 30.866	-4.7927	± 51.962	0.39677	± 55.468	13
14	∓ 7.0428	55.365	∓ 0.58111	64.674	± 4.6368	50.267	14
15	-2.8842	± 73.475	4.0674	± 63.414	7.8930	± 28.344	15
16	± 2.1102	79.630	± 8.0760	45.470	± 9.1807	-6.9677	16
17	7.0088	± 70.004	10.453	± 12.256	8.0122	∓ 47.294	17
18	± 10.844	43.732	± 10.538	-30.350	± 4.5649	-81.072	18
19	∓ 12.804	± 3.5956	8.1808	∓ 72.894	-0.33102	∓ 96.744	19
20	± 12.404	-44.038	± 3.8019	-104.35	∓ 5.3936	-86.469	20
21	9.6017	∓ 90.136	-1.6767	∓ 114.87	-9.2278	∓ 49.166	21
22	± 4.8244	-124.65	∓ 7.0279	-98.585	∓ 10.713	8.1255	22
23	-1.0948	∓ 138.60	-10.998	∓ 55.709	-9.3305	± 71.272	23
24	∓ 7.0615	-126.23	∓ 12.602	6.6865	∓ 5.3330	122.42	24
25	-11.926	∓ 86.620	-11.365	± 75.625	0.28980	± 144.93	25
26	∓ 14.706	-24.524	∓ 7.4592	134.84	± 6.0583	128.58	26
27	-14.784	± 49.999	-1.6852	± 168.50	10.394	± 73.411	27
28	∓ 12.043	123.12	± 4.6906	165.37	± 12.054	-9.1392	28
29	-6.9076	± 179.74	10.216	± 122.06	10.485	∓ 98.278	29
30	∓ 0.27823	206.57	± 13.582	44.754	± 6.0048	-169.04	30
31	6.6253	± 195.04	13.942	∓ 51.295	-0.26088	∓ 199.16	31
32	± 12.490	143.60	± 11.110	-144.71	∓ 6.6577	-175.89	32
n	π_n	τ_n	π_n	τ_n	π_n	τ_n	n
	155°		152.5°		150°		

* Note: Use lower sign for angles listed at the bottom.

TABLE OF MIE ANGULAR SCATTERING FUNCTIONS*

n	32.5°		35°		37.5°		n
	π_n	τ_n	π_n	τ_n	π_n	τ_n	
1	1.0000	± 0.84339	1.0000	± 0.81915	1.0000	± 0.79335	1
2	± 2.5302	1.2679	± 2.4575	1.0260	± 2.3801	0.77645	2
3	3.8348	∓ 0.41792	3.5326	∓ 1.1486	3.2206	∓ 1.8552	3
4	± 4.1730	-5.0962	± 3.4754	-6.2754	± 2.7884	-7.2542	4
5	3.1254	∓ 11.859	1.9898	∓ 12.703	0.95164	∓ 12.955	5
6	± 0.79130	-17.873	∓ 0.58468	-16.802	∓ 1.6850	-14.682	6
7	-2.2002	∓ 19.320	-3.3590	∓ 14.584	-4.0068	∓ 8.7710	7
8	∓ 4.8808	-13.129	∓ 5.2281	-4.0290	∓ 4.8860	5.0510	8
9	-6.2720	± 1.1993	-5.3216	± 13.048	-3.7294	± 22.231	9
10	∓ 5.7443	20.546	∓ 3.3936	30.738	∓ 0.81743	34.539	10
11	-3.2746	± 38.552	0.015816	± 40.867	2.7404	± 33.725	11
12	± 0.49191	47.548	± 3.7292	36.452	± 5.4376	16.142	12
13	4.4118	± 41.485	6.3472	± 15.381	6.0188	∓ 14.053	13
14	∓ 7.1982	18.816	± 6.7823	-17.426	± 4.0612	-45.172	14
15	7.8486	∓ 15.881	4.7079	∓ 50.671	0.22563	∓ 62.296	15
16	± 6.0020	-52.433	± 0.73550	-70.394	∓ 3.9622	-54.129	16
17	2.1014	∓ 77.907	-3.7594	∓ 65.592	-6.7230	∓ 19.353	17
18	∓ 2.7063	-81.010	∓ 7.1192	-33.539	∓ 6.7858	30.833	18
19	-6.9098	∓ 56.600	-8.0190	± 17.577	-3.9698	± 75.878	19
20	∓ 9.1133	-8.6163	∓ 5.9893	70.273	± 0.67836	94.129	20
21	-8.5012	± 49.926	-1.6378	± 103.59	5.2716	± 72.902	21
22	∓ 5.1338	100.27	± 3.5274	101.24	± 7.8528	15.816	22
23	0.031155	± 123.81	7.6225	± 58.954	7.2322	∓ 56.502	23
24	± 5.4108	108.75	± 9.0786	-12.078	± 3.5306	-113.58	24
25	9.2844	± 55.082	7.2434	∓ 87.710	-1.8148	∓ 127.79	25
26	± 10.347	-23.792	± 2.6624	-138.87	∓ 6.6090	-87.325	26
27	8.1470	∓ 104.19	-3.0763	∓ 142.59	-8.8036	∓ 3.5249	27
28	± 3.2666	-159.13	∓ 7.8942	-91.852	∓ 7.3736	91.508	28
29	-2.8294	∓ 167.20	-9.9778	∓ 0.20375	-2.7907	± 157.00	29
30	∓ 8.2344	-120.63	∓ 8.4624	101.36	± 3.1236	160.85	30
31	-11.197	∓ 29.255	-3.7844	± 174.70	7.9224	± 94.891	31
32	∓ 10.692	80.947	± 2.4354	188.72	± 9.5491	-19.017	32
n	π_n	τ_n	π_n	τ_n	π_n	τ_n	n
147.5°			145°		142.5°		

* Note: Use lower sign for angles listed at the bottom.

TABLE OF MIE ANGULAR SCATTERING FUNCTIONS*

n	40°		42.5°		45°		n
	π_n	τ_n	π_n	τ_n	π_n	τ_n	
1	1.0000	*0.76604	1.0000	*0.73728	1.0000	*0.70711	1
2	*2.2981	0.52094	*2.2118	0.26147	*2.1213	0	2
3	2.9012	*2.5254	2.5768	*3.1478	2.2500	*3.7124	3
4	*2.1215	-8.0052	*1.4839	-8.5081	*0.88388	-8.7500	4
5	0.030142	*12.614	-0.75954	*11.703	-1.4063	*10.275	5
6	*2.4950	-11.679	*3.0126	-8.0100	*3.2483	-3.9376	6
7	-4.1763	*2.4344	-3.9264	*3.8373	-3.3359	*9.4742	7
8	*4.0040	13.048	*2.7602	19.057	*1.3424	22.430	8
9	-1.8196	*27.495	0.092755	*28.217	1.7358	*24.471	9
10	*1.5062	31.554	*3.2112	22.655	*4.0828	9.7753	10
11	4.4247	*19.209	4.8697	*0.96001	4.1532	*16.689	11
12	*5.4438	-7.4768	*4.0042	-27.882	*1.6866	-39.681	12
13	3.8949	*37.429	0.87459	*47.674	-2.0148	*42.132	13
14	*0.33390	-54.840	*2.9727	-43.803	*4.7751	-17.050	14
15	-3.6431	*47.204	-5.4771	*13.008	-4.8356	*25.114	15
16	*6.1237	-13.124	*5.1746	32.070	*1.9730	59.884	16
17	-5.8046	*34.637	-2.0492	*67.459	2.2604	*62.686	17
18	*2.6706	73.461	*2.3684	70.367	*5.3798	25.526	18
19	1.9217	*81.383	5.7525	*33.213	5.4336	*34.596	19
20	*5.8328	49.010	*6.2124	-29.196	*2.2234	-82.659	20
21	7.1422	*13.428	3.3495	*84.815	-2.4822	*85.774	21
22	*5.0923	-78.449	*1.4516	-100.58	*5.9232	-35.054	22
23	0.51238	*113.19	-5.6910	*61.664	-5.9722	*45.030	23
24	*4.5116	-95.756	*7.0593	17.362	*2.4487	107.75	24
25	-7.5898	*28.054	-4.6981	*96.946	2.6859	*111.14	25
26	*7.1691	62.143	*0.27551	132.13	*6.4210	45.530	26
27	-3.3129	*132.21	5.2929	*97.648	6.4662	*56.336	27
28	*2.2650	144.65	*7.6634	4.7088	*2.6550	-134.95	28
29	6.9632	*86.741	6.0200	*101.19	-2.8752	*138.61	29
30	*8.5090	-20.307	*1.1023	-162.24	*6.8826	-56.875	30
31	6.0587	*128.41	-4.5684	*139.68	-6.9248	*68.453	31
32	*0.64860	-184.04	*7.9828	-37.580	*2.8465	164.11	32
n	π_n	τ_n	π_n	τ_n	π_n	τ_n	n
	140°		137.5°		135°		

* Note: Use lower sign for angles listed at the bottom.

TABLE OF MIE ANGULAR SCATTERING FUNCTIONS*

47.5°			50°		52.5°		
n	π_n	τ_n	π_n	τ_n	π_n	τ_n	n
1	1.0000	± 0.67559	1.0000	± 0.64279	1.0000	± 0.60876	1
2	± 2.0268	-0.26147	± 1.9284	-0.52094	± 1.8263	-0.77645	2
3	1.9232	∓ 4.2093	1.5988	∓ 4.6303	1.2794	∓ 4.9686	3
4	± 0.32927	-8.7261	∓ 0.17318	-8.4394	∓ 0.61769	-7.9013	4
5	-1.9034	∓ 8.4054	-2.2490	∓ 6.1890	-2.4454	∓ 3.7370	5
6	∓ 3.2242	0.25461	∓ 2.9726	4.2785	∓ 2.5338	7.8626	6
7	-2.4988	± 13.976	-1.5161	± 16.959	-0.48908	± 18.186	7
8	± 0.067243	22.853	± 1.3090	20.376	± 2.2577	15.397	8
9	2.9078	± 17.008	3.4936	∓ 7.1207	3.4708	∓ 3.5609	9
10	± 4.0724	-4.4721	± 3.2864	-17.305	± 1.9520	-26.296	10
11	2.5792	∓ 29.702	0.59315	∓ 35.242	-1.3224	∓ 32.280	11
12	∓ 0.79928	-40.009	∓ 2.7878	-29.215	∓ 3.8128	-10.661	12
13	-3.9191	∓ 23.230	-4.3759	± 2.4639	-3.4029	± 26.449	13
14	∓ 4.6383	14.916	∓ 2.8396	40.085	∓ 0.19640	49.370	14
15	-2.2920	± 50.987	0.90755	± 54.184	3.3984	± 34.174	15
16	± 1.7474	57.853	± 4.2345	28.122	± 4.4850	-14.087	16
17	4.8700	± 24.480	4.6498	∓ 25.413	2.0204	∓ 59.820	17
18	± 4.9238	-32.656	± 1.6697	-69.025	∓ 2.2165	-62.676	18
19	1.6970	∓ 76.692	-2.7019	∓ 66.391	-4.9063	∓ 12.419	19
20	∓ 2.8296	-73.869	∓ 5.3224	-11.684	∓ 3.7976	56.796	20
21	-5.7008	∓ 18.628	-4.1766	± 60.717	0.41237	± 88.819	21
22	∓ 4.9218	57.964	± 0.078874	97.174	± 4.4924	50.681	22
23	-0.84148	± 105.05	4.4701	± 64.192	5.1628	∓ 35.531	23
24	± 3.9740	85.472	± 5.7892	-22.441	± 1.7348	-103.73	24
25	6.3581	± 4.0610	2.9412	∓ 103.25	-3.2218	∓ 94.138	25
26	± 4.6297	-90.345	∓ 2.1640	-115.58	∓ 5.8052	-4.8949	26
27	-0.22674	∓ 133.77	-5.8898	∓ 41.627	-3.8582	± 99.132	27
28	∓ 5.1132	-90.149	∓ 5.4676	72.393	± 1.2358	132.96	28
29	-6.7974	± 20.220	-1.0547	± 144.37	5.5275	± 60.509	29
30	∓ 4.0534	128.57	± 4.2771	115.17	± 5.5676	-69.675	30
31	1.4559	± 160.20	6.6800	∓ 3.7582	1.1798	∓ 155.90	31
32	± 6.1830	85.625	± 4.3111	-131.76	∓ 4.2875	-122.45	32
n	π_n	τ_n	π_n	τ_n	π_n	τ_n	n
132.5°		130°		127.5°			

* Note: Use lower sign for angles listed at the bottom.

TABLE OF MIE ANGULAR SCATTERING FUNCTIONS*

n	55°		57.5°		60°		n
	π_n	τ_n	π_n	τ_n	π_n	τ_n	
1	1.0000	± 0.57358	1.0000	± 0.53730	1.0000	± 0.50000	1
2	± 1.7207	-1.0260	± 1.6119	-1.2679	± 1.5000	-1.5000	2
3	0.96742	∓ 5.2182	0.66518	∓ 5.3754	0.37500	∓ 5.4375	3
4	∓ 0.99956	-7.1304	∓ 1.3153	-6.1527	∓ 1.5626	-5.0000	4
5	-2.4993	∓ 1.1702	-2.4215	± 1.3862	-2.2266	± 3.8086	5
6	∓ 1.9543	10.770	∓ 1.2841	12.811	∓ 0.57422	13.863	6
7	0.48714	± 17.590	1.3303	± 15.276	1.9756	± 11.508	7
8	± 2.8322	8.6116	± 2.9992	0.91912	± 2.7730	-6.6887	8
9	2.9040	∓ 13.331	1.9278	∓ 20.670	0.72373	∓ 24.473	9
10	± 0.36950	-29.824	∓ 1.1457	-27.361	∓ 2.3170	-19.547	10
11	-2.7492	∓ 21.780	-3.4132	∓ 6.4248	-3.2291	± 10.046	11
12	∓ 3.7003	10.272	∓ 2.5847	27.707	∓ 0.84808	36.889	12
13	-1.4433	± 41.043	0.80441	± 41.805	2.6148	± 28.869	13
14	± 2.2656	39.842	± 3.6812	15.625	∓ 3.6286	-13.821	14
15	4.2382	± 0.21429	3.2353	∓ 32.825	0.95670	∓ 50.883	15
16	± 2.6072	-48.122	∓ 0.33417	-57.872	∓ 2.8819	-39.320	16
17	-1.4187	∓ 60.764	-3.8078	∓ 28.765	-3.9885	± 17.972	17
18	∓ 4.4360	-18.844	∓ 3.8583	35.032	∓ 1.0543	66.292	18
19	-3.7326	± 48.042	-0.24204	± 74.696	3.1263	± 50.788	19
20	± 0.27490	81.538	± 3.7944	45.858	± 4.3186	-22.470	20
21	4.2426	± 45.053	4.4336	∓ 33.452	1.1438	∓ 82.999	21
22	± 4.6946	-38.336	± 0.90264	-91.304	∓ 3.3530	-63.192	22
23	1.0726	∓ 98.521	-3.6432	∓ 66.685	-4.6252	± 27.288	23
24	∓ 3.6417	-76.943	∓ 4.9418	27.351	∓ 1.2267	100.91	24
25	-5.3818	± 17.510	-1.6262	± 106.64	3.5655	± 76.465	25
26	∓ 2.5099	107.88	± 3.3570	90.806	± 4.9128	-32.406	26
27	2.6541	± 111.45	5.3656	∓ 16.157	1.3044	∓ 119.94	27
28	± 5.7039	14.636	± 2.3914	-119.62	∓ 3.7662	-90.553	28
29	3.9112	∓ 106.06	-2.9417	∓ 117.58	-5.1844	± 37.810	29
30	∓ 1.3365	-144.25	∓ 5.6894	-0.51592	∓ 1.3778	140.05	30
31	-5.6002	∓ 56.810	-3.1760	± 129.16	3.9564	± 105.41	31
32	∓ 5.1485	90.314	± 2.4049	146.16	± 5.4425	-43.483	32
n	π_n	τ_n	π_n	τ_n	π_n	τ_n	n
	125°		122.5°		120°		

* Note: Use lower sign for angles listed at the bottom.

TABLE OF MIE ANGULAR SCATTERING FUNCTIONS*

n	62.5°		65°		67.5°		n
	π_n	τ_n	π_n	τ_n	π_n	τ_n	
1	1.0000	± 0.46175	1.0000	± 0.42262	1.0000	± 0.38268	1
2	± 1.3853	-1.7208	± 1.2679	-1.9284	± 1.1480	-2.1213	2
3	0.099090	∓ 5.4038	-0.16045	∓ 5.2748	-0.40165	∓ 5.0533	3
4	∓ 1.7402	-3.7097	∓ 1.8487	-2.3229	∓ 1.8894	-0.88388	4
5	-1.9318	± 5.9812	-1.5573	± 7.8014	-1.1248	± 9.1841	5
6	± 0.12582	13.872	± 0.77048	12.855	± 1.3203	10.905	6
7	2.3797	± 6.6853	2.5224	± 1.2983	2.4070	∓ 4.1147	7
8	± 2.2109	-13.251	± 1.4038	-17.956	± 0.46486	-20.240	8
9	-0.50787	∓ 24.218	-1.5770	∓ 20.077	-2.3298	∓ 12.672	9
10	∓ 2.9516	-8.0422	∓ 2.9666	4.8093	∓ 2.3988	16.448	10
11	-2.3034	± 23.720	-0.89826	± 31.426	0.63507	± 31.458	11
12	± 0.99602	35.463	± 2.4426	24.065	± 3.1250	6.0944	12
13	3.4534	± 6.7861	3.1238	∓ 17.036	1.8034	∓ 34.778	13
14	± 2.2393	-37.326	± 0.11130	-46.199	∓ 1.9320	-37.402	14
15	-1.5583	∓ 46.622	-3.2494	∓ 22.380	-3.4638	± 11.029	15
16	∓ 3.8757	-2.1422	∓ 2.9568	35.248	∓ 0.67858	54.728	16
17	-2.0353	± 53.785	0.87522	± 59.512	3.1446	± 32.672	17
18	± 2.1688	56.697	± 3.8923	-12.980	± 3.1960	-37.732	18
19	4.2069	∓ 6.4672	2.4574	∓ 58.114	-0.80518	∓ 69.776	19
20	± 1.7044	-72.604	∓ 1.9654	-68.220	∓ 3.9968	-13.680	20
21	-2.8039	∓ 64.684	-4.2831	± 5.2262	-2.2900	± 69.525	21
22	∓ 4.4366	19.421	∓ 1.6474	83.194	± 2.3926	72.813	22
23	-1.2590	± 93.106	3.0536	± 69.221	4.2670	∓ 19.867	23
24	± 3.4415	69.612	± 4.3562	-32.157	± 0.84010	-98.957	24
25	4.5559	∓ 36.889	0.57787	∓ 107.16	-3.7884	∓ 58.086	25
26	± 0.71226	-114.46	∓ 4.0322	-59.910	∓ 3.8312	64.167	26
27	-4.0607	∓ 70.568	-4.0738	± 66.419	0.94542	± 117.04	27
28	∓ 4.5581	58.828	± 0.67446	126.12	± 4.7101	23.053	28
29	-0.078870	± 135.69	4.7994	± 38.590	2.6902	∓ 111.45	29
30	± 4.6412	66.737	± 3.4290	-105.31	∓ 2.7780	-115.29	30
31	4.4391	∓ 84.976	-2.0130	∓ 136.10	-4.9414	± 30.276	31
32	∓ 0.62533	-155.73	∓ 5.2687	-4.8226	∓ 0.97538	151.12	32
n	π_n	τ_n	π_n	τ_n	π_n	τ_n	n
	117.5°		115°		112.5°		

* Note: Use lower sign for angles listed at the bottom.

TABLE OF MIE ANGULAR SCATTERING FUNCTIONS*

n	70°		72.5°		75°		n
	π_n	τ_n	π_n	τ_n	π_n	τ_n	
1	1.0000	± 0.34202	1.0000	± 0.30071	1.0000	± 0.25882	1
2	± 1.0261	-2.2982	± 0.90211	-2.4575	± 0.77646	-2.5981	2
3	-0.62267	∓ 4.7432	-0.82182	∓ 4.3499	-0.99760	∓ 3.8804	3
4	∓ 1.8650	0.56187	∓ 1.7795	1.9687	∓ 1.6377	3.2925	4
5	-0.65686	± 10.067	-0.17668	± 10.411	0.29327	± 10.206	5
6	± 1.7437	8.1764	± 2.0185	4.8785	± 2.1323	1.2584	6
7	2.0585	∓ 9.0215	1.5212	∓ 12.945	0.85357	∓ 15.512	7
8	∓ 0.48415	-19.852	∓ 1.3266	-16.882	∓ 1.9635	-11.748	8
9	-2.6678	∓ 3.3702	-2.5590	± 6.3401	-2.0402	± 14.883	9
10	∓ 1.3883	24.597	∓ 0.15056	27.697	± 1.0669	25.203	10
11	1.9374	± 23.948	2.7200	± 10.803	2.8241	∓ 4.7628	11
12	± 2.9000	-13.284	± 1.8744	-28.595	± 0.36440	-35.581	12
13	-0.032487	∓ 40.744	-1.7723	∓ 33.169	-2.8629	∓ 14.734	13
14	∓ 3.1462	-14.577	∓ 3.1254	13.427	∓ 1.9314	35.946	14
15	-2.1941	± 39.081	-0.047906	± 49.790	2.0320	± 38.791	15
16	± 1.8050	47.177	± 3.3041	16.710	± 3.1471	-21.511	16
17	3.6046	∓ 11.532	2.1000	∓ 48.736	-0.47903	∓ 58.754	17
18	± 0.62700	-64.625	∓ 2.1982	-51.800	∓ 3.5874	-7.6113	18
19	-3.3640	∓ 34.400	-3.5754	± 23.536	-1.4029	± 64.849	19
20	∓ 3.0217	49.974	± 0.10698	75.729	± 3.0308	45.150	20
21	1.4136	± 76.628	3.8202	± 21.770	3.0811	∓ 49.933	21
22	± 4.1555	-1.2442	± 2.2402	-73.046	∓ 1.5423	-79.649	22
23	1.4293	∓ 88.488	-2.6160	∓ 71.856	-4.0377	± 12.979	23
24	∓ 3.3371	-63.126	∓ 3.9450	36.929	∓ 0.52616	97.675	24
25	-3.8193	± 54.110	0.30297	± 104.85	3.9278	± 39.096	25
26	± 0.80592	110.29	± 4.2887	25.350	± 2.6212	-88.416	26
27	4.5282	± 19.247	2.3143	∓ 101.30	-2.6962	∓ 92.233	27
28	± 2.3188	-109.10	∓ 3.0300	-92.625	∓ 4.1397	48.188	28
29	-3.0752	∓ 100.07	-4.2516	± 53.822	0.61130	± 128.78	29
30	∓ 4.5386	48.760	± 0.53332	136.61	± 4.6044	16.800	30
31	0.021278	± 145.46	4.7195	± 26.928	1.7914	∓ 132.97	31
32	± 4.6998	50.735	± 2.3336	-133.29	∓ 3.8105	-90.677	32
n	π_n	τ_n	π_n	τ_n	π_n	τ_n	n
110°			107.5°		105°		

* Note: Use lower sign for angles listed at the bottom.

TABLE OF MIE ANGULAR SCATTERING FUNCTIONS*

n	77.5°		80°		82.5°		n
	π_n	τ_n	π_n	τ_n	π_n	τ_n	
1	1.0000	± 0.21644	1.0000	± 0.17365	1.0000	± 0.13053	1
2	± 0.64932	-2.7189	± 0.52094	-2.8190	± 0.39158	-2.8978	2
3	-1.1486	∓ 3.3431	-1.2738	∓ 2.7474	-1.3722	∓ 2.1037	3
4	∓ 1.4458	4.4916	∓ 1.2107	5.5283	∓ 0.94003	6.3703	4
5	0.73170	± 9.4670	1.1193	± 8.2362	1.4392	± 6.5794	5
6	± 2.0834	-2.4162	± 1.8805	-5.8756	± 1.5413	-8.8674	6
7	0.12338	∓ 16.481	-0.59831	∓ 15.771	-1.2432	∓ 13.467	7
8	∓ 2.3238	-5.1342	∓ 2.3717	2.0900	∓ 2.1092	8.9861	8
9	-1.2076	± 20.886	-0.20208	± 23.402	0.81354	± 22.048	9
10	± 2.0302	17.679	± 2.5612	6.6702	± 2.5678	-5.5975	10
11	2.2512	∓ 19.003	1.1562	∓ 28.526	-0.19108	∓ 31.087	11
12	∓ 1.1960	-32.372	∓ 2.3742	-19.978	∓ 2.8533	-1.9854	12
13	-2.9781	± 8.3650	-2.1115	± 28.472	-0.56892	± 38.981	13
14	∓ 0.050699	44.518	± 1.7954	36.037	± 2.9186	13.867	14
15	3.1680	± 11.096	2.9082	∓ 21.150	1.3987	∓ 43.959	15
16	± 1.4712	-48.762	∓ 0.87136	-51.859	∓ 2.7358	-29.491	16
17	-2.7094	∓ 36.451	-3.4020	± 5.6419	-2.2226	± 44.314	17
18	∓ 2.7650	40.705	∓ 0.29362	63.718	± 2.2995	47.632	18
19	1.6297	± 62.003	3.4862	± 17.374	2.9630	∓ 38.642	19
20	± 3.6346	-18.490	± 1.5517	-67.820	∓ 1.6267	-66.471	20
21	-0.098495	∓ 80.409	-3.1082	∓ 45.470	-3.5464	± 26.066	21
22	∓ 3.8513	-16.073	∓ 2.7306	61.054	± 0.75626	83.740	22
23	-1.6021	± 84.457	2.2796	± 74.640	3.9096	∓ 6.4134	23
24	± 3.3102	57.248	± 3.6582	-41.740	± 0.25366	-96.945	24
25	3.1316	∓ 69.120	-1.0775	∓ 99.792	-4.0049	∓ 19.663	25
26	∓ 2.0599	-96.145	∓ 4.1863	10.192	∓ 1.3302	103.62	26
27	-4.1608	± 33.361	-0.36292	± 115.51	3.8050	± 50.654	27
28	± 0.30166	122.49	± 4.2130	31.008	± 2.3912	-101.60	28
29	4.4423	± 18.834	1.8652	∓ 117.00	-3.3056	∓ 84.247	29
30	± 1.6441	-127.04	∓ 3.6992	-77.091	∓ 3.3514	89.348	30
31	-3.8670	∓ 78.557	-3.2335	± 100.97	2.5262	± 117.47	31
32	∓ 3.3981	104.07	± 2.6775	121.59	± 4.1297	-66.118	32
n	π_n	τ_n	π_n	τ_n	π_n	τ_n	n
	102.5°		100°		97.5°		

* Note: Use lower sign for angles listed at the bottom.

TABLE OF MIE ANGULAR SCATTERING FUNCTIONS*

n	85°		87.5°		90°		n
	π_n	τ_n	π_n	τ_n	π_n	τ_n	
1	1.0000	± 0.087156	1.0000	± 0.043619	1.0000	0	1
2	± 0.26147	-2.9544	± 0.13086	-2.9886	0	-3.0000	2
3	-1.4430	∓ 1.4232	-1.4857	∓ 0.71786	-1.5000	0	3
4	∓ 0.64208	6.9912	∓ 0.32569	7.3718	0	7.5000	4
5	1.6779	± 4.5836	1.8252	± 2.3522	1.8750	0	5
6	± 1.0922	-11.174	± 0.56598	-12.629	0	-13.125	6
7	-1.7513	∓ 9.8062	-2.0759	∓ 5.1616	-2.1875	0	7
8	∓ 1.5753	14.664	∓ 0.84087	18.390	0	19.688	8
9	1.6784	± 17.070	2.2575	± 9.2949	2.4609	0	9
10	± 2.0592	-16.668	± 1.1422	-24.333	0	-27.070	10
11	-1.4694	∓ 26.119	-2.3786	∓ 14.847	-2.7070	0	11
12	∓ 2.5142	16.472	∓ 1.4630	30.156	0	35.176	12
13	1.1354	± 36.484	2.4438	± 21.867	2.9326	0	13
14	± 2.9131	-13.475	± 1.7969	-35.560	0	-43.989	14
15	-0.69052	∓ 47.512	-2.4560	∓ 30.357	-3.1421	0	15
16	∓ 3.2316	7.2320	∓ 2.1380	40.260	0	53.416	16
17	0.15274	± 58.396	2.4171	± 40.278	3.3385	0	17
18	± 3.4492	2.5090	± 2.4809	-43.979	0	-63.431	18
19	0.45672	∓ 68.226	-2.3290	∓ 51.548	-3.5239	0	19
20	∓ 3.5490	-15.777	∓ 2.8200	46.450	0	74.003	20
21	-1.1136	± 76.039	2.1933	± 64.049	3.7001	0	21
22	± 3.5193	32.361	± 3.1502	-47.423	0	-85.103	22
23	1.7916	∓ 80.870	-2.0120	∓ 77.624	-3.8683	0	23
24	∓ 3.3532	-51.805	∓ 3.4666	46.670	0	96.708	24
25	-2.4630	± 81.815	1.7871	± 92.078	4.0295	0	25
26	± 3.0494	73.410	± 3.7642	-43.982	0	-108.80	26
27	3.0994	∓ 78.088	-1.5211	∓ 107.19	-4.1845	0	27
28	∓ 2.6122	-96.258	∓ 4.0388	39.180	0	121.35	28
29	-3.6736	± 69.076	1.2168	± 122.70	4.3339	0	29
30	± 2.0508	119.24	± 4.2860	-32.112	0	-134.35	30
31	4.1595	∓ 54.385	-0.87727	∓ 138.34	-4.4784	0	31
32	∓ 1.3802	-141.11	∓ 4.5020	22.665	0	147.79	32
n	π_n	τ_n	π_n	τ_n	π_n	τ_n	n
	95°		92.5°		90°		

* Note: Use lower sign for angles listed at the bottom.

THE KINETICS OF ADSORPTION FROM SOLUTION TO THE AIR/WATER INTERFACE.

PART I. NORMAL ALIPHATIC ALCOHOLS

A. M. Posner¹ and A. E. Alexander

*Department of Colloid Science, Cambridge, England, and New South Wales University
of Technology, Sydney, Australia*

Received April 24, 1953

ABSTRACT

The surface potential technique has been used to study the kinetics of adsorption of a series of *n*-aliphatic alcohols (butyl, hexyl, heptyl, octyl) at the air/water interface, mostly over the time interval 1–15 milliseconds. The effect of concentration and of temperature was determined, and the results are discussed in the light of current theories of the adsorption process.

INTRODUCTION

An earlier paper by the authors (1) described a method for determining the kinetics of adsorption of surface-active substances at an air/water interface for time intervals down to *ca.* 1 millisecond after the formation of a fresh surface. The present papers present the results obtained by this technique. A series of normal aliphatic alcohols was first studied because their solutions are free from such complicating factors as ionization and micelle formation; subsequently the work was extended to soap solutions, including the effects of salts.

EXPERIMENTAL

Surface potential (ΔV) vs. surface age (t) curves were determined by the method described earlier (1). From studies of static systems (2) it was found that, in the case of alcohol solutions, ΔV is proportional to the surface concentration (n), so that the experimental ΔV - t curves are equivalent to n - t curves.

Temperature control to $\pm 0.2^\circ\text{C}$. in the jet was obtained by surrounding the supply tubes with a circulating water system from a thermostat. When necessary the air temperature in the box was raised to the required level by electrical heating pads. The air was also kept saturated with the vapor

¹ Present address: Department of Physical Chemistry, King's College, London, W.C. 2., England.

of the solution under test by having, in the box, vessels containing the solution at a temperature of *ca.* 2°C. above the jet temperature.

The alcohols were pure materials from Messrs. Theodore St. Just; they were distilled twice before use and had boiling points within 1°C. of those given in the literature. Solutions in distilled water were normally made 0.001 *N* with respect to pure HCl. Alcohol concentrations are expressed as % (w/v.)

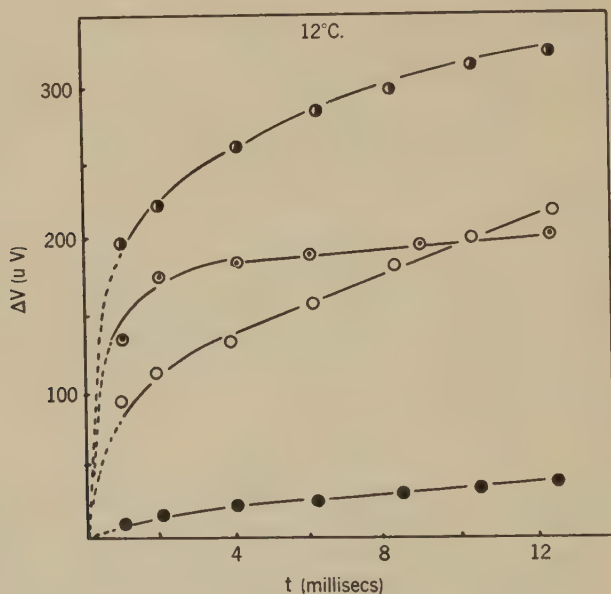


FIG. 1. Surface potential (ΔV) plotted against surface age (t) at 12°C. ●, 0.005% *n*-octyl alcohol solution $\Delta V_E = 186$ mv. ○, 0.03% *n*-octyl alcohol solution $\Delta V_E = 300$ mv. ○, 0.4% *n*-butyl alcohol solution $\Delta V_E = 230$ mv. ●, 2.4% *n*-butyl alcohol solution $\Delta V_E = 326$ mv.

RESULTS

The general shape of the ΔV - t curve is shown in Fig. 1. The time taken to reach equilibrium depends on the chain length and molar concentration of the alcohol: the greater these quantities, the shorter the time. Thus for two equimolar solutions of alcohols of different chain length the one with the longer chain will attain its equilibrium more rapidly despite its slower rate of bulk diffusion (see *Discussion* below).

Under almost all conditions the experimental results fitted the equation:

$$\ln (\Delta V_E - \Delta V) = -Kt + \text{constant} \quad [1]$$

where ΔV_E = equilibrium surface potential, ΔV = surface potential at time t , and K is a constant (of dimensions sec^{-1}) at each concentration. (See Fig. 2.)

K was measured as a function of alcohol concentration for *n*-butyl, *n*-hexyl, *n*-heptyl, and *n*-octyl alcohols at 12°, 25°, and 39°C. Fig. 3 shows some of the results. There is an approximately linear relationship between K and concentration (c), and as the chain length is increased the intercept on the K axis decreases, while the slope (on a molecular basis) increases. At any given concentration the system reached equilibrium more rapidly the higher the temperature, though the over-all effect was not very large.

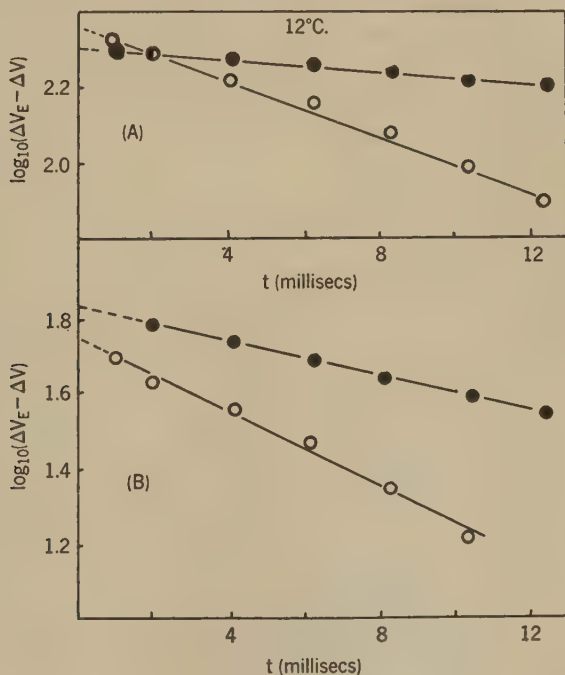


FIG. 2. $\log_{10} (\Delta V_E - \Delta V)$ plotted against surface age (t) at 12°C. A. ●, 0.005% *n*-octyl alcohol solution. $\log_{10} \Delta V_E = 2.27$. ○, 0.03% *n*-octyl alcohol solution. $\log_{10} \Delta V_E = 2.46$. B. ●, 0.4% *n*-butyl alcohol solution. $\log_{10} \Delta V_E = 2.36$. ○, 1.6% *n*-butyl alcohol solution. $\log_{10} \Delta V_E = 2.46$.

DISCUSSION

Many theories have been advanced to account for the time required for the surface tension of a solution to fall to its equilibrium value. Ward and Tordai (3) applied classical diffusion theory to the kinetics of adsorption, taking into account both forward and backward diffusion. However, comparison with experiment showed certain anomalies—e.g., the apparent rate of diffusion increased with molecular weight. Rideal and Sutherland (4) modified Ward and Tordai's treatment to give a more readily applicable

form, and from their own results (obtained with the oscillating technique) and other published work, they came to the following conclusions:

1. The rate of attainment of equilibrium is dependent upon the orifice and jet velocity.

2. Solutions of 3-methyl-1-butanol accumulate molecules slower in their surfaces than can be predicted by diffusion alone so that there is hindrance (energy barrier) to molecules entering the surface.

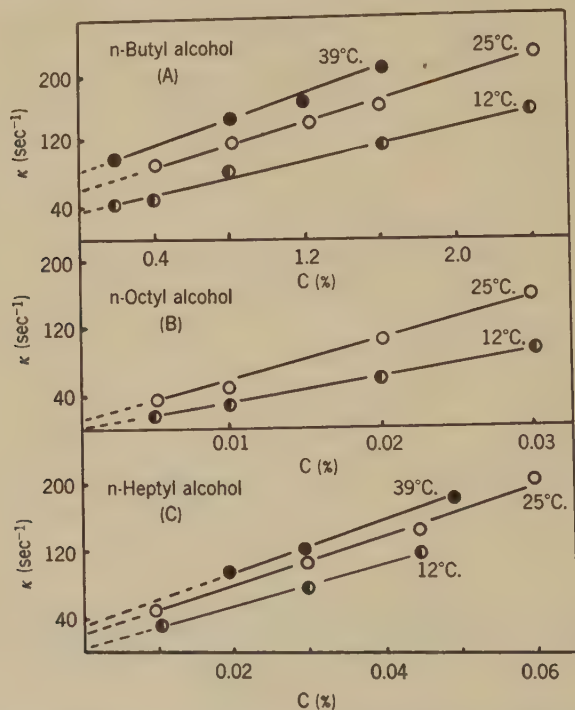


FIG. 3. K plotted against bulk concentration ($C\%$) at 12°, 25°, and 39°C. A. *n*-butyl alcohol solution. B. *n*-octyl alcohol solution. C. *n*-heptyl alcohol solution.

3. Heptanol and octanol molecules enter faster than is possible by diffusion, the solute being moved by liquid motion.

4. Molecules of all alcohols are hindered in entering the surface, and liquid motions are more important for heptanol and octanol than for solutions of the lower alcohols.

5. Liquid motions do not dominate the adsorption processes.

6. It is not yet possible to evaluate the worth of published data on dynamic surface tension.

Since adsorption of solute due to flow processes will be of lesser importance near the jet orifice, it is convenient to consider the initial stages separately from the remainder.

(a) *Adsorption in the Initial Stages (< ca. 1 Millisecond)*

Although Eq. [1] is obeyed for times greater than *ca.* 1 millisecond, this is not the case over the very initial stages of the jet's life. This can readily be seen by extrapolating the curves of $\ln (\Delta V_E - \Delta V) - t$ to zero time, when the intercept is found to be less than the value of $\ln \Delta V_E$ predicted by Eq. [1]. This is so with all systems examined, including the soaps (Part II).

For such short times it would be anticipated that transfer of solute by bulk movement of liquid would be of lesser importance, so that in the limit

TABLE I
P (Ratio of Observed to Calculated Rates)

Alcohol	Concn. (%)	12°C.	25°C.	39°C.
<i>n</i> -butyl	1.2	—	0.016	0.019
	0.8	0.023	0.024	0.023
	0.4	0.036	0.035	0.034
	0.2	—	0.038	0.043
<i>n</i> -hexyl	0.06	—	0.41	0.33
	0.04	—	0.52	0.30
	0.02	—	0.32	0.13
<i>n</i> -heptyl	0.045	1.0	1.0	0.95
	0.030	1.1	1.1	1.2
	0.015	1.0	1.3	1.2
<i>n</i> -octyl	0.03	0.8	—	1.4
	0.02	0.8	—	1.2
	0.01	0.7	—	1.0

the classical laws of diffusion would apply. If we neglect back diffusion, the relation between n and t would then be given by the well-known expression

$$n = 2c \sqrt{\frac{Dt}{\pi}} \quad [2]$$

where D is the classical diffusion coefficient. Since $\Delta V = \alpha n$ (2),

$$\Delta V = \frac{2c}{\alpha} \sqrt{\frac{Dt}{\pi}} \quad [3]$$

From the known values of α (2) and calculating D from the molecular volumes and the Stokes-Einstein equation, the theoretical slopes of the $\Delta V - \sqrt{t}$ curves can be found for comparison with the experimental values. The experimental values are necessarily only approximate, since they were obtained from the $\Delta V - t$ curves extrapolated to zero time. The ratio of observed to calculated slopes (P) for the homologous series of alcohols at 25°C. is shown in Table I.

P is seen to be little affected by temperature over the range studied and to increase from *ca.* 0.03 with butyl alcohol to about unity with heptyl and octyl alcohols. The effect of temperature is in keeping with classical diffusion theory ($D \propto T$); the variation in P with chain length is probably to be explained by the neglect of back diffusion which would become progressively less important at the longer chain lengths.

(b) *Adsorption after the Initial Stages (ca. 2–15 Milliseconds)*

This can be treated from two points of view, namely, diffusion through an unstirred layer (with an energy barrier at the surface in some cases) or hindered film penetration alone.

TABLE II

Alcohol	Concn. (%)	$2l$ (cm.)
<i>n</i> -butyl	0.2–2.5	No fit even with $2l =$ jet diam. (see below)
<i>n</i> -hexyl	0.02–0.12	
<i>n</i> -heptyl	0.015	<i>ca.</i> 2.0×10^{-3}
	0.030	<i>ca.</i> 6.0×10^{-5}
	0.060	<i>ca.</i> 6.4×10^{-5}
<i>n</i> -octyl	0.005	1.8×10^{-3}
	0.010	1.2×10^{-4}
	0.020	7.6×10^{-5}
	0.030	5.8×10^{-5}

(i) *Diffusion through an Unstirred Layer.* Following the treatment of Sutherland (5), the results calculated for the thickness of the unstirred layer ($2l$) are set out in Table II.

In the case of *n*-butyl alcohol, even with $2l =$ jet diameter (i.e., the maximum possible thickness of the unstirred layer) the diffusion theory predicts a rate that is faster than that found experimentally. Accordingly there must be some type of barrier hindering penetration into the surface—a conclusion in accord with that of Rideal and Sutherland (4). With the higher alcohols this same type of barrier would become increasingly important, since the difficulty of the hydrocarbon part of the molecule in penetrating the comparatively close-packed film structure increases with chain length. (It is seldom appreciated that the areas per adsorbed molecule in this region lie in the range 30–50 Å., i.e., only 50%–150% greater than the smallest area to which the longest homologs can be compressed.) Introduction of an energy barrier into this treatment has the effect of reducing the requisite thickness of the unstirred layer, but in the absence

of any means of separating the two factors, it is useless to pursue the matter further.

(ii) *The Theory of Hindered Film Penetration.* In this treatment the sole resistance to adsorption is ascribed to the difficulty of penetrating the existing adsorbed film—i.e., it corresponds to the previous case with an unstirred layer of effectively zero thickness.

As pointed out earlier (p. 576), the present experimental results obey the equation

$$\ln (\Delta V_E - \Delta V) = -Kt + \text{constant}$$

under almost all experimental conditions. This equation can be interpreted on the basis of a Langmuir type of hindered adsorption as follows:

Let θ = fraction of surface covered at time t ,

k_1 = velocity coefficient of adsorption (dimensions cc. molecule⁻¹ sec.⁻¹),

c = concentration in the bulk solution (molecules/cc.),

k_2 = velocity coefficient of desorption (dimensions cc. molecule⁻¹ sec.⁻¹.)

\therefore Rate of adsorption = $k_1 c(1 - \theta)$,

and rate of desorption = $k_2 n_F \theta / \delta$,

where n_F = number of molecules/cm.² when the molecules are close-packed on the surface, and δ = thickness of surface layer (in cm.). The net rate of adsorption is therefore:

$$\frac{d\theta}{dt} = k_1 c(1 - \theta) - k_2 \frac{n_F \theta}{\delta}. \quad [4]$$

At equilibrium $d\theta/dt = 0$;

$$\therefore \theta_E = \frac{k_1 c}{k_1 c + k_2 \frac{n_F}{\delta}}.$$

Now $\theta = n/n_F$;

$$\therefore \theta_E = \frac{n_E}{n_F} = \frac{k_1 c}{k_1 c + k_2 \frac{n_F}{\delta}}. \quad [5]$$

Eq. [4] can therefore be rewritten as

$$\frac{1}{n_F} \frac{dn}{dt} = k_1 c - \frac{n}{n_F} \left(k_1 c + k_2 \frac{n_F}{\delta} \right).$$

Substituting in the value of n_F from [5]

$$\begin{aligned} \frac{dn}{dt} &= n_E \left(k_1 c + k_2 \frac{n_F}{\delta} \right) - \left(k_1 c + k_2 \frac{n_F}{\delta} \right) n \\ &= \left(k_1 c + k_2 \frac{n_F}{\delta} \right) (n_E - n). \end{aligned}$$

Integrating, we obtain

$$\ln (n_E - n) = - \left(k_1 c + k_2 \frac{n_F}{\delta} \right) t + \text{constant.}$$

At zero time the number of adsorbed molecules/cm.² would be negligibly small for the solutions used, i.e., at $t = 0$, $n = 0$, and $\text{constant} = \ln n_E$. Thus

$$\ln (n_E - n) = - \left(k_1 c + k_2 \frac{n_F}{\delta} \right) t + \ln n_E \quad [6]$$

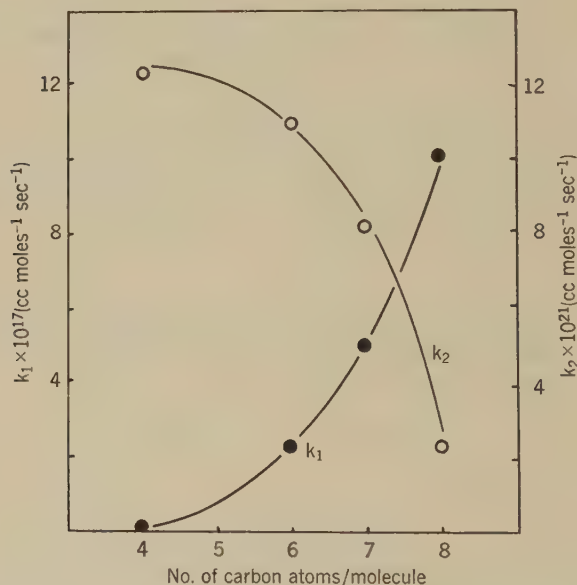


FIG. 4. ●, k_1 at 25°C. plotted against number of carbon atoms/molecule. ○, k_2 at 25°C. plotted against number of carbon atoms/molecule.

Since $n \propto \Delta V$,

$$\ln^e (\Delta V_E - \Delta V) = - \left(k_1 c + k_2 \frac{n_F}{\delta} \right) t + \ln \Delta V_E \quad [7]$$

and

$$K = k_1 c + k_2 \frac{n_F}{\delta},$$

which is identical with the form of the experimentally determined kinetic equation.

The slope of the K - c curve gives k_1 and the intercept k_2 ; these velocity coefficients form a useful basis on which to compare the adsorption and desorption processes for the homologous series of alcohols. From Fig. 4 it is seen that, with increasing chain length, k_1 increases and k_2 decreases, at a progressively greater rate.

TABLE III

No. of C atoms	Temp. °C.	$k_1 \times 10^{17}$ cc. molecule ⁻¹ sec. ⁻¹	$k_2 \times 10^{21}$ cc. molecule ⁻¹ sec. ⁻¹	E_1 kcal./mole	E_2 kcal./mole
4	12	6.2×10^{-2}	7.4	2.0	5.5
	25	8.4×10^{-2}	12.4		
	39	9.6×10^{-2}	17.0		
6	25	1.9	9.2	2.1	—
	39	2.2	11.0		
7	12	4.4	1.2	1.9	11.5
	25	5.1	5.5		
	39	5.9	7.3		
8	12	6.6	~0	2.3	>11.5
	25	10.1	2.3		
	39	8.4	—		

TABLE IV

<i>n</i> -Butyl alcohol 25°C.		<i>n</i> -Heptyl alcohol 25°C.		<i>n</i> -Octyl alcohol 12°C.	
Concn. (%)	\bar{K}	Concn. (%)	$\bar{K} \times 10^{-3}$	Concn. (%)	$\bar{K} \times 10^{-4}$
3.0	55	0.08	3.74	0.04	1.00
2.0	64	0.06	3.90	0.03	1.10
1.5	70	0.04	4.35	0.02	1.38
1.0	80	0.03	4.26	0.015	1.48
0.75	87	0.02	5.25	0.01	1.77
0.50	118	0.015	5.93	0.0075	1.90
0.375	108	0.01	4.62	0.005	1.97
0.25	130	0.0075	5.25	0.00375	2.86
0.188	134	0.005	3.27	0.0025	2.29
0.125	88	0.00375	3.22	0.00188	1.66
				0.00125	1.04
Average \bar{K}	93		4.38		1.77

TABLE V

	<i>n</i> -Butyl (25°C.)	<i>n</i> -Octyl (12°C.)	<i>n</i> -Heptyl (25°C.)
Langmuir (kinetic).....	68	4.4×10^4	9.2×10^3
Langmuir (static).....	93	1.77×10^4	4.4×10^3
Law of Mass Action.....	88	1.45×10^4	3.0×10^3

The effect of temperature upon k_1 and k_2 is shown in Table III. Both increasing temperature, but k_2 is much more temperature-dependent than k_1 . From the temperature variations the activation energies for the forward

(E_1) and backward (E_2) processes were calculated from the Arrhenius equation. It appears (see Table III) that E_1 is relatively small and independent of chain length, whereas E_2 is larger and increases with chain length.

On the Langmuir theory of hindered adsorption E_1 would presumably represent the energy necessary to make a "hole" of appropriate size to enable the penetrating molecule to enter the surface film. In view of the coiling up which hydrocarbon chains undergo when dissolved in water, an approximate constancy for E_1 is not unexpected, although its absolute magnitude is rather greater than simple calculation would predict (ca. 0.5–1 kcal.). On the same picture E_2 would be the sum of E_1 and ΔH , where ΔH is the energy liberated when the hydrocarbon chain goes from an aqueous to its essentially hydrocarbon environment in the film. Since ΔH will increase with increasing chain length, E_2 will also, as was found experimentally.

(c) *The Equilibrium Constant* ($\bar{K} = k_1/k_2$)

This may be determined by the following methods:

1. From the kinetic measurements above, from which k_1 and k_2 are determined separately.
2. From the equilibrium condition of Eq. [5] which gives

$$\bar{K} = \frac{n_E n_F}{\delta c(n_F - n_E)}.$$

Taking $\delta = 10 \text{ \AA.}$ and $n_F = 5 \times 10^{14} \text{ molecules/cm.}^2$ (from the data on insoluble monolayers), values of \bar{K} were evaluated with the aid of equations of state determined previously (2). Results are shown in Table IV.

3. From the application of the Law of Mass Action to the equilibrium between the surface and bulk which leads to the result (6)

$$\bar{K} = \frac{\beta kT}{\delta}$$

where β is the slope of the initial linear portion of the surface pressure (π)- c curve.

Table V compares the values obtained for n -butyl, n -octyl, and n -heptyl alcohols by these three methods. The agreement is reasonable in view of the assumptions made and of experimental errors in the kinetic results.

REFERENCES

1. POSNER, A. M., AND ALEXANDER, A. E., *Trans. Faraday Soc.* **45**, 651 (1949).
2. POSNER, A. M., ANDERSON, J. R., AND ALEXANDER, A. E., *J. Colloid Sci.* (in the press).
3. WARD, A. F. H., AND TORDAI, L., *J. Chem. Physics* **14**, 453 (1946).
4. RIDEAL, E. K., AND SUTHERLAND, K. L., *Trans. Faraday Soc.* **48**, 1109 (1952).
5. SUTHERLAND, K. L., Private communication in the course of publication.
6. WARD, A. F. H., AND TORDAI, L., *Trans. Faraday Soc.* **42**, 413 (1946).

THE KINETICS OF ADSORPTION FROM SOLUTION TO THE AIR/WATER INTERFACE.

PART II. ANIONIC AND CATIONIC SOAPS

A. M. Posner¹ and A. E. Alexander

Department of Colloid Science, Cambridge, England, and New South Wales University of Technology, Sydney, Australia

Received April 24, 1953

ABSTRACT

The same technique as in Part I has been used to measure the kinetics of adsorption of a typical cationic and a typical anionic soap. The effect of soap concentration in both the molecular and micellar ranges was first studied, followed by the effect of added salts, both as regards concentration and type.

INTRODUCTION

Measurement of the kinetics of adsorption of soaps from solution to the air/water interface should be of value in connection with such dynamic problems as the formation of soap-stabilized foams and emulsions, the adsorption of soaps in detergency, and the uptake of surface-active drugs by biological systems (1).

EXPERIMENTAL

The soaps used were cetyl trimethyl ammonium bromide (C.T.A.B.) and Aerosol OT, di-octyl sodium sulfosuccinate (A.O.T.). The C.T.A.B. was titrated against a very pure sample of sodium hexadecyl sulfate (taken as 100 %) using a dye adsorption method (2) and was found to have a purity of 100 %; the A.O.T. by titration against C.T.A.B. had a purity of 95 %.

The dynamic surface tensions were determined as in Part I, save that in certain cases it was found impossible to use an Ag/AgCl half-cell directly, e.g., when studying the effect of acetate and sulfate ions on the rate of adsorption of C.T.A.B. In such cases an agar gel bridge was used to connect the flowing solution with the Ag/AgCl electrode.

The interfacial tension of the various solutions against purified medicinal paraffin (Nujol) was measured by the drop-volume method using a micrometer syringe with a stainless steel tip of appropriate diameter.

¹ Present address: Department of Physical Chemistry, King's College, London, W.C.2., England.

The saturation solubilities of soaps in salt solutions were determined by a light absorptiometric method using a Hilger "Spekker." Various amounts of soap were dissolved in the salt solutions by warming, and the system allowed to come to equilibrium in a thermostat at 25°C. The resulting turbidity was measured as a function of soap concentration. A plot of scale reading against soap concentration gave two intersecting straight lines, the intersection being the saturation solubility.

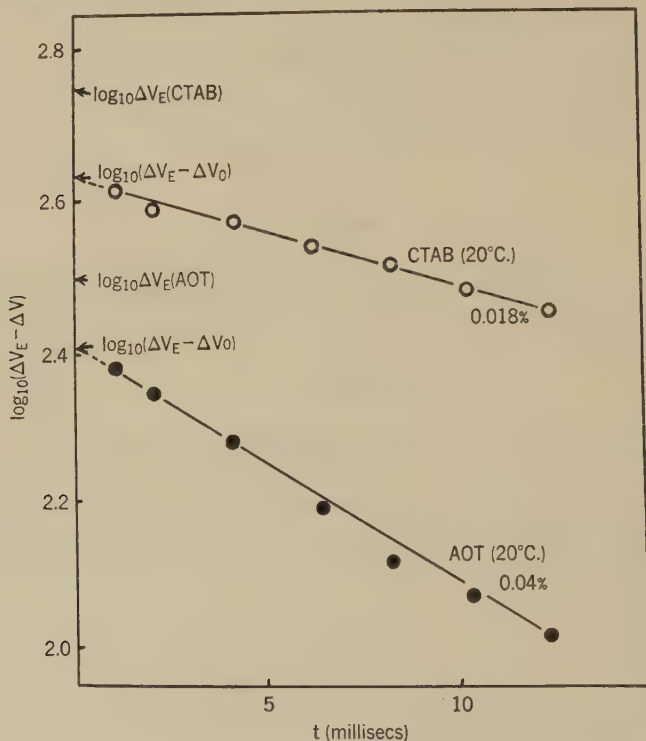


FIG. 1. $\log (\Delta_E - \Delta V)$ plotted against surface age (t). \circ , 0.018% C.T.A.B. at 20°C. \bullet , 0.04% A.O.T. at 20°C.

The saturation solubility of *trans*-azobenzene in the various soap solutions was measured by means of the Hilger "Spekker," since it was thought that changes in micellar size might be reflected in the solvent power of the micelle.

Electrophoretic mobilities of Nujol particles in the various soap solutions were found using a microcataphoretic method (3).

RESULTS

The experimental results again fitted the equation

$$\ln (\Delta V_E - \Delta V) = -Kt + \text{constant} \quad [1]$$

both above and below the micelle point, as shown in Fig. 1. K was measured as a function of:

1. Soap concentration at a fixed HCl concentration, 0.001 N for A.O.T. and 0.01 N for C.T.A.B. (see Fig. 2).

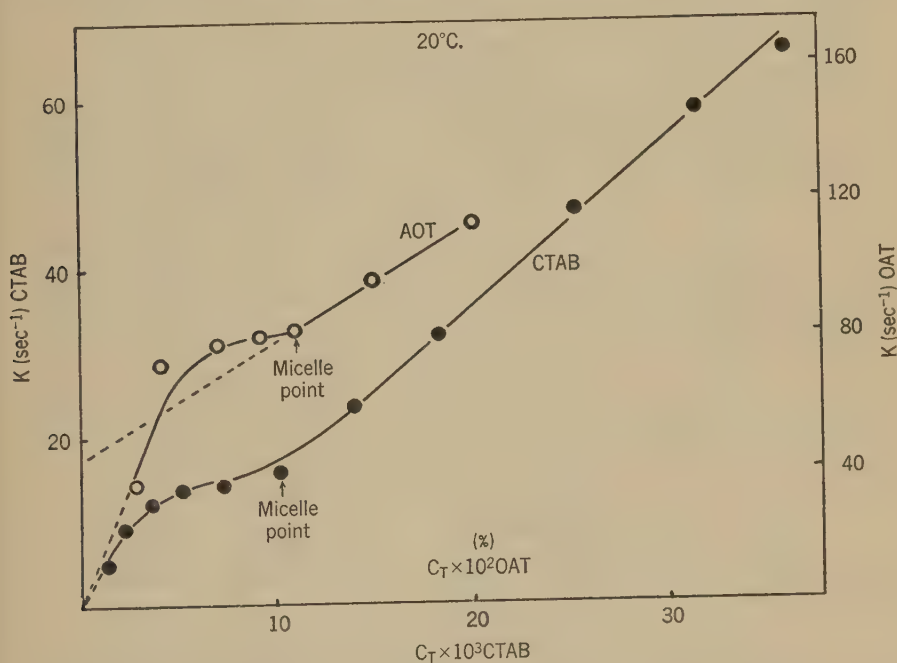


FIG. 2. K plotted against bulk concentration ($C_T\%$). \circ , A.O.T. at 20°C . in 0.001 N HCl. \bullet , C.T.A.B. at 20°C . in 0.01 N HCl.

TABLE I

Salt concn. (N)	$K (\text{sec}^{-1})$	
	KCl	HCl
0.1	6.3	—
0.01	9.0	15.4
0.001	20.0	18.5

2. Salt concentration, using HCl or KCl and a fixed C.T.A.B. concentration of 0.01 % (see Table I).

3. Nature of added salt, at a fixed ionic strength of 0.01 and at various soap concentrations.

Results for C.T.A.B. are shown in Table II and those for A.O.T. (including saturation solubilities in the corresponding salt solutions), in Fig. 3.

(a) *The Initial Stages of the Adsorption Process (< ca. 1 Millisecond)*

P (the ratio of observed to calculated rates in the initial stages) was calculated as for the alcohols in Part I, and values are shown in Table III. Above the micelle point allowance for transport to the surface via micelles has to be made.

TABLE II
Ionic strength of added salt = 0.01

Concn. C.T.A.B. (%)	K (sec. ⁻¹)				
	HCl	KCl	K Br	Potassium acetate	K ₂ SO ₄
0.003 ^a	10.6	6.9	5.3	1.4	10.6
0.010	14.7	8.5	11.6	26.0 ^a	27.6
0.020	35.4	—	—	51.0	—
0.036	65.0	—	—	—	—
0.040	—	40.2	32.3	87.5	77.0
0.060	—	—	—	127—	—

^a Below micelle point.

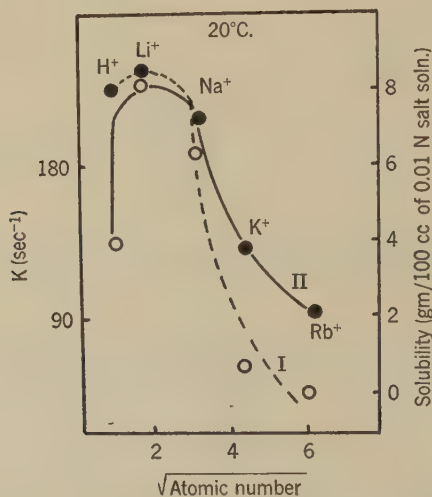


FIG. 3. ○, I. Solubility of A.O.T. plotted against $\sqrt{\text{Atomic Number}}$ of added cation (0.01 N cation chloride present). ●, II. K (0.12% A.O.T.) plotted against $\sqrt{\text{Atomic Number}}$ of added cation (0.01 N cation chloride present).

Since P is considerably larger than unity (cf. the alcohols, Part I), some process must be present in the initial stages of adsorption which considerably accelerates simple diffusion. Since it is absent with the alcohols, it would appear to be related in some way to the ionic nature of the soaps.

One possible explanation is that it arises indirectly from the diffuse electrical double layer present at the glass/solution interface. Glass in contact with water or in the presence of anionic soaps such as A.O.T. carries a negative charge with a corresponding excess of cations in the diffuse double layer. It is conceivable that part of this diffuse double layer is swept off by the rapidly flowing liquid when it leaves the glass orifice, thus producing an excess of positive charge very close to the freshly created interface and a rapid diffusion of soap *anions* under the influence of electrical forces. The same basic mechanism could apply to cationic soaps such as C.T.A.B., since glass in their presence carries a positive charge with an excess of *anions* in the diffuse double layer.

(b) *Adsorption after the Initial Stages 2-15 Milliseconds*

(i) *Effect of Soap Concentration.* Above a certain critical concentration the molecules in a soap solution aggregate to form micelles, and this must

TABLE III

C.T.A.B. in 0.01 N HCl		A.O.T. in 0.001 N HCl	
C(%)	P	C(%)	P
0.001 ^a	5.5	0.03 ^a	3.5
0.002 ^a	7.0	0.05 ^a	4.6
0.0035 ^a	4.0	0.11	4.0
0.025	3.3	0.20	3.5
0.036	2.4		

^a Below micelle point.

be taken into account in any interpretation of the kinetic results. Because of its hydrophilic nature the micelle is unstable in the surface and on being adsorbed will dissociate into its constituent single molecules.

Using the Langmuir theory of hindered adsorption as in Part I and assuming that the single molecules and the micelles can be treated independently, the differential equation giving the rate of adsorption is:

$$\frac{d\theta}{dt} = k_1^s C_s (1 - \theta) + x k_1^m C_m (1 - \theta) - k_2 \frac{n_F}{\delta} \theta \quad [2]$$

where the superscripts *s* and *m* denote single molecules and micelles, respectively, and *x* is the number of single molecules in a micelle. It can be integrated as before, giving:

$$\ln (n_\infty - n) = - \left(k_1^s C_s + x k_1^m C_m + k_2 \frac{n_F}{\delta} \right) t + \text{constant.}$$

(In the absence of micelles the above equation becomes identical with that derived in Part I.) Assuming $n \propto \Delta V$, an equation identical with that found experimentally is obtained:

$$\ln (\Delta V_E - \Delta V) = -Kt + \text{constant} \quad [1]$$

Hence

$$K = k_1^s C_s + x k_1^m C_m + k_2 \frac{n_F}{\delta}$$

when micelles are present, and

$$K = k_1^s C_s + k_2 \frac{n_F}{\delta}$$

when micelles are absent. Since

$$C_m = \frac{C_T - C_s}{x}$$

where C_T is the stoichiometric concentration in terms of single molecules,

$$K = k_1^s C_s - k_1^m C_s + k_2 \frac{n_F}{\delta} + k_1^m C_T.$$

Accordingly, the plot of $K-C_T$ should be a straight line of slope k_1^s and intercept $k_2 n_F / \delta$ below the micelle point, and of slope k_1^m and intercept $(k_1^s C_s - k_1^m C_s + k_2 n_F / \delta)$ above the micelle point. Thus the plot of $K-C_T$ over a concentration range to include the micelle point should be two straight lines with an intersection at the micelle point. The experimental data (see Fig. 2) show a linear plot above the micelle point but considerable curvature below the micelle point. The precise reason for this is not clear.

(ii) *Effect of Salt Concentration (HCl or KCl).* As shown in Table I, addition of salt decreases K , i.e., decreases the rate of equilibration. This probably arises at least in part from the increased aggregation tendency, since a micelle diffuses less rapidly than its equivalent number of single molecules (see below).

(iii) *Effect of Nature of Added Salts. C.T.A.B. Solutions.*

From the data of Table II, which gives the values for K for C.T.A.B. solutions in the presence of different salts at a constant ionic strength ($\mu = 0.01$), k_1^s and k_1^m were calculated. The results are shown in Table IV.

The observed variations in k_1^s and k_1^m could be explained in terms of the differences in surface activity of C.T.A.B. in the presence of the various salts. It will be recalled from Part I that the more surface-active a molecule the larger is k_1 . Thus from the above variations in k_1^m for C.T.A.B. it might

be expected that the surface activity in the presence of the salts would vary in the order:



It actually varies in the order:



as shown in Table IV, the micellar concentration running inversely to the surface activity. Although the order is correct for the first three salts, potassium acetate presents a definite anomaly.

The variations in k_1^m for C.T.A.B. in the presence of various electrolytes (Table IV) could conceivably be accounted for in terms of variations in micellar size. However, the bulk-diffusion experiments of Hartley and Runnicles (4), and the present findings on the solubility of *trans*-azobenzene,

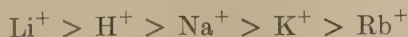
TABLE IV
Effect of Salts on k_1^s , k_1^m , and Micelle Point (C.T.A.B.)
Ionic strength 0.01

	HCl	KCl	KBr	Potassium acetate	K ₂ SO ₄
$k_1^s \times 10^{16}$ cc. molecule ⁻¹ sec. ⁻¹	0.94	1.15	1.25	1.93	2.07
$k_1^m \times 10^{16}$ cc. micelle ⁻¹ sec. ⁻¹	1.01	0.60	0.41	1.16	0.98
Micelle point (%).....	0.01	0.005	0.007	0.016	0.004

would indicate only minor changes in micellar size—certainly insufficient to account for the observed differences between the various salt solutions.

Finally the effect of the different salts on the zeta potential has to be considered, for the zeta potential will give some indication of the magnitude of the electrical forces which oppose adsorption. A direct determination of ζ at the air/water interface is difficult. Measurements made on the Nujol/water interface showed that SO₄²⁻ is least (75 mv.), with the others having the same order of magnitude (150 mv.). Thus it would seem that the zeta potential is not a major factor in the over-all rate of adsorption.

A.O.T. Solutions. A study was made of the value of K in the presence of differing cations, but at the same soap and added salt concentration. It was found to increase in the order



when the A.O.T. is dissolved in a 0.01 *N* solution of the chloride of these cations. (See Fig. 3.)

The solubility of A.O.T. in these salt solutions varies in this order as well, as shown in Fig. 3, but the reason for such a parallelism is not at all obvious.

ACKNOWLEDGEMENTS

The authors would like to thank the Wm. S. Merrell Company, U. S. A., for a supply of pure cetyl trimethyl ammonium bromide, and the American Cyanamid Company for a supply of Aerosol O.T. Our thanks are also due to Dr. C. Kemball and Messrs. Theodore St. Just for the gifts of alcohols. One of us (A. M. Posner) is indebted to the D. S. I. R. for a grant during the tenure of which the present work was carried out.

REFERENCES

1. See, for example, ALEXANDER, A. E., AND JOHNSON, P., *Colloid Science*. Oxford University Press, 1949.
2. SALTON, M., AND ALEXANDER, A. E., *Research (London)* **2**, 247 (1949).
3. ALEXANDER, A. E., AND SAGGERS, L., *J. Sci. Instr.* **25**, 374 (1948).
4. HARTLEY, G. S., AND RUNNICES, V., *Proc. Roy. Soc. (London)* **168 A**, 42 (1938).

DONNAN-E.M.F. AND SUSPENSION EFFECT

J. Th. G. Overbeek*

Department of Metallurgy, Massachusetts Institute of Technology,

Cambridge, Massachusetts

Received June 10, 1953

ABSTRACT

The Donnan-e.m.f. may be defined as the e.m.f. of the cell obtained by connecting two identical electrodes by means of saturated KCl bridges to a suspension and its equilibrium liquid. The suspension effect is the difference in e.m.f. obtained in the conventional determination of the pH in a suspension and in its equilibrium solution. It is shown that the Donnan-e.m.f. and the suspension effect are identical. The Donnan-e.m.f. can be calculated from the chemical potentials and the transference numbers in the two liquid junctions. It is pointed out that the measured potential can not be separated into a "true" Donnan- or membrane-potential and two liquid junction potentials without arbitrariness. Explicit equations for the Donnan-e.m.f. are given for a number of typical cases. It appears that the classical equation for the Donnan-potential is in error if the mobilities of the gegenions are modified by the presence of the particles, which presumably is the case, unless the particle charge is extremely small.

1. INTRODUCTION

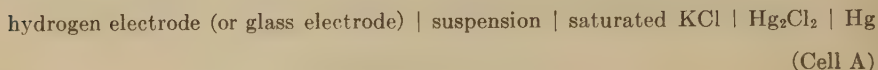
Recently (1-8) there has been a great deal of discussion of the suspension effect, that is, the difference in pH between a suspension and its equilibrium liquid, and of the relation between the suspension effect and the Donnan-potential. Although some of the contributions to this discussion have helped to clarify the situation, a completely satisfactory understanding has not been reached.

It is proposed to show in this paper that the suspension effect and the Donnan-potential are identical, and that attempts to separate the measured potential difference in the sum of a membrane-potential and a liquid junction (diffusion) potential are based on arbitrary assumptions. Moreover, it will be shown how the suspension effect can be calculated approximately from the composition of the system.

*Visiting Professor in the Massachusetts Institute of Technology. Present address: Van't Hoff Laboratory, University of Utrecht, Netherlands.

2. THE RELATION BETWEEN THE SUSPENSION EFFECT AND THE DONNAN-POTENTIAL

The pH of a suspension is calculated from the e.m.f. of the following cell.

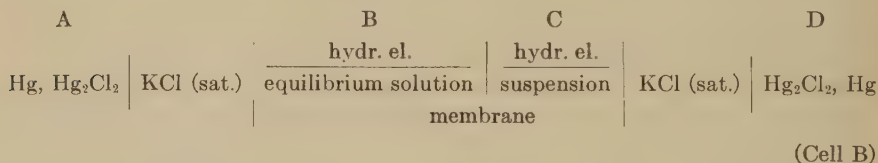


We shall call this e.m.f. E_1 , considering the calomel electrode as the positive pole. When the suspension is replaced by its equilibrium liquid, a different e.m.f. is found (E_2). The suspension effect may be defined as the difference between these two e.m.f.'s.

$$E_{\text{susp}} = E_1 - E_2. \quad [1]$$

As a rule it has the same sign as the electric charge of the particles.

The Donnan-potential is measured with the aid of cell B, where the suspension and its equilibrium liquid are separated by a membrane, which is impermeable to the suspended particles but not to any other component of the system.



Hydrogen electrodes B and C are inserted in the equilibrium solution and in the suspension of the Donnan cell. The potentials of the four electrodes will be indicated as ψ_A , ψ_B , ψ_C , and ψ_D .

It has long been recognized (9-11) that the two hydrogen electrodes are at the same potential, because the circuit

hydrogen electrode B \mid equilibrium liquid \mid suspension \mid hydrogen electrode C

is in equilibrium and thus cannot perform work. Therefore

$$\psi_B = \psi_C. \quad [2]$$

The suspension effect is defined as

$$E_1 - E_2 = (\psi_D - \psi_C) - (\psi_A - \psi_B) = \psi_D - \psi_A, \quad [3]$$

which is just the e.m.f. of the Donnan cell.

In this paper we shall therefore mainly consider the e.m.f. of cell B.

$$E_{\text{cell B}} = \psi_D - \psi_A = \text{Donnan-e.m.f.} = \text{suspension-effect.}$$

In the past a clear distinction has not always been made between the potential difference between the suspension and the equilibrium liquid, "which thermodynamically is not completely determined," (12, 13) and the e.m.f. of cell B, which is a well-defined quantity. Many authors take the point of view that the potential difference between the suspension and the equilibrium liquid is the "true Donnan-potential" and that the e.m.f. of cell B is an approximate value for it—approximate because of the presence of two liquid junctions. However, we avoid ambiguity in considering the potential of the complete cell rather than the potential difference between phases of unequal composition.

The situation with respect to the Donnan potential is closely similar to that in the determination of the pH. Likewise, the current definition of the pH is based not upon an alleged knowledge of the "activity of the hydrogen ions" but upon the total e.m.f. of the measuring cell, with inclusion of the liquid junction involved (14).

3. EXPRESSION FOR THE E.M.F. OF CELL B.

Because the two calomel electrodes of cell B have the same composition and are in contact with identical solutions, the reactions at the electrodes do not influence the e.m.f. of the cell, which can therefore be described as the sum of three liquid junction potentials. If we number the four liquid sections of the cell I, II, III, and IV and the liquid junctions 1, 2, and 3 as follows:

I	II	III	IV
KCl (sat.)	equilibrium liquid	suspension	KCl (sat.)
1	2	3	

the e.m.f., E , of the cell is given by (see, for example, reference 14, p. 220):

$$-EF = \int_I^{IV} \sum_i \frac{t_i}{z_i} d\mu_i, \quad [4]$$

where F is the Faraday, 96500 Coulombs, t_i the Hittorf transference number, z_i the valency with sign included, and μ_i the chemical potential of the ion i .

This equation, although correct, does not lend itself easily to calculations because it includes single-ion activities. To remedy this defect we add therefore to the right-hand side of Eq. [4]:

$$-\int_I^{IV} \sum_i t_i \frac{d\mu_R}{z_R} + \frac{\mu_R^{IV}}{z_R} - \frac{\mu_R^I}{z_R} = 0,$$

where R is a reference ion of valency z_R . (This method has been described in references 15 and 16.) As solutions I and IV are identical, this leads to:

$$-EF = \int_I^{IV} \sum_i t_i \left(\frac{d\mu_i}{z_i} - \frac{d\mu_R}{z_R} \right). \quad [5]$$

All the chemical potentials are now combined in such a way as to refer to neutral substances. If for instance $i = \text{Cl}^-$ and $R = \text{K}^+$, $\frac{\mu_i}{z_i} - \frac{\mu_R}{z_R}$ just means $-\mu_{\text{KCl}}$.

The integral of Eq. [5] gives only contributions to the cell potential at places where the chemical potentials change, i.e., at the liquid junctions 1 and 3. *At the membrane 2, the chemical potentials of all the salts that can pass through the membrane do not change, because equilibrium is assumed to exist, and for i = suspended particles, t_i is zero, because the particles cannot pass through the membrane.*

Consequently we arrive at the equation:

$$E = \frac{1}{F} \left[\int_{IV}^{III} \sum_i t_i \left(\frac{d\mu_i}{z_i} - \frac{d\mu_R}{z_R} \right) - \int_I^{II} \sum_i t_i \left(\frac{d\mu_i}{z_i} - \frac{d\mu_R}{z_R} \right) \right]. \quad [6]$$

The Donnan-e.m.f. and the suspension effect can be completely derived from the conditions at the two liquid junctions with saturated KCl, whereas the situation at the membrane does not enter into the final equation. This does not prove, however, whether there is or is not a potential difference between the suspension and its equilibrium liquid. Information on this potential difference simply can not be derived from the measurements with cell B nor, as far as we know, from any other measurement.

In order to treat the e.m.f. of the Donnan cell as the sum of two liquid junction potentials and a membrane potential, one adds the following expression to Eq. [4]:

$$-\int_{II}^{III} \sum_i t_i \frac{d\mu_R}{z_R} + \frac{\mu_R^{III}}{z_R} - \frac{\mu_R^{II}}{z_R} = 0,$$

and obtains:

$$E = \frac{1}{F} \left[\underbrace{\int_{IV}^{III} \sum_i t_i \frac{d\mu_i}{z_i}}_A + \underbrace{\frac{\mu_R^{III}}{z_R} - \frac{\mu_R^{II}}{z_R}}_B - \underbrace{\int_I^{II} \sum_i t_i \frac{d\mu_i}{z_i}}_C \right]. \quad [7]$$

The three terms of this expression can, however, be evaluated only when single-ion activities are known, and therefore an additional assumption has to be made. Some of the assumptions used in the past are:

1. The two liquid junction potentials A and C cancel.

2. The ion R (usually the gegenion is chosen) has identical activity coefficients in solution and suspension.

3. The ion R has identical activities on both sides of the membrane.

4. The membrane potential (part B) can be calculated from a model as the difference of the average potential of solution and suspension.

5. The membrane potential can be calculated from the osmotic pressure. None of these methods is at variance with thermodynamics. Provided we choose only *one* of these assumptions, we cannot run into conflict with experimental evidence, but we cannot learn anything from it either.

We may learn something from the examination of the complete cell potential by determining, experimentally or by calculation, relations among the transference numbers and the chemical potentials which will enable us to integrate Eq. [6]. Since the chemical potentials have the same values at the limits of integration of the two integrals, a finite value of the e.m.f. can be obtained only when the transference numbers are different in the suspension and in the equilibrium solution. This difference is due to the presence of the charged particles and the excess of ions in the double layers surrounding them.

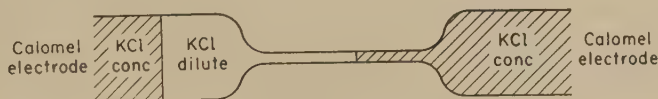


FIG. 1. Capillary effect, cell C.

In contradistinction to the usual theories, in which the Donnan potential is considered as an equilibrium quantity, related to ion activities in solution and suspension, we see here that the Donnan-e.m.f. is dependent upon mobilities also and that it can only be measured on a system that is *not* in equilibrium. The unequal distribution of ions between suspension and solution and the osmotic pressure, however, are independent of the presence of salt bridges and are characteristic of the Donnan equilibrium in the strict sense of the word.

In order to illustrate this point of view, we shall now give a few examples in which the integrals of Eq. [6] can be evaluated by assuming suitable relationships between transference numbers and chemical potentials. Since the major contributions to the integrals are made by the more dilute parts of the liquid junctions, the assumption of ideal behavior of the solutions as far as activity is concerned would be a good starting point. The cases to be treated will be of increasing order of complexity.

4. CAPILLARY EFFECT IN KCl

Loosjes (17) discovered that something analogous to the suspension effect can be measured in cell C, in which the suspension of cell B is re-

placed by a capillary. The capillary wall carries an electrical double layer and shows a certain amount of surface conductance. As this surface conductance presumably is carried by the gegenions (in this example cations), the transference number of the cations in the capillary will be increased above the value for the bulk of the solution.

The e.m.f. of cell C can be derived from Eq. [6], taking K^+ ions as the reference ions R .

$$E_{\text{capillary effect}} = \frac{1}{F} \left[\int_{KCl \text{ conc.}}^{KCl \text{ dil.}} (-t_{Cl} d\mu_{KCl})_{\text{cap.}} + \int_{KCl \text{ conc.}}^{KCl \text{ dil.}} (t_{Cl} d\mu_{KCl})_{\text{wide tube}} \right] \quad [8]$$

$$= \frac{1}{F} \int_{KCl \text{ dil.}}^{KCl \text{ conc.}} \left[t_{Cl(\text{cap.})} - t_{Cl(\text{wide tube})} \right] d\mu_{KCl}.$$

If $t_{Cl} = t$ in the wide tube and we assume that the surface conductance in the capillary is completely carried by an excess of K^+ ions, we find:

$$t_{Cl(\text{cap.})} = \frac{t\pi r^2 \lambda c}{\pi r^2 \lambda c + 2\pi r \sigma} = \frac{t}{1 + \frac{2\sigma}{\lambda cr}}, \quad [9]$$

where λ is the equivalent conductance of KCl , c the concentration of the solution, r the radius of the capillary, and σ the specific surface conductance along the glass wall.

Considering KCl as an ideal solute we have:

$$\mu_{KCl} = \mu_0 + 2RT \ln c \quad [10]$$

and considering the surface conductance constant,¹ the e.m.f. of the capillary effect becomes:

$$E_{\text{cap. eff.}} = \frac{2RT}{F} t \int_{c_{\text{dil.}}}^{c_{\text{conc.}}} \left(\frac{1}{1 + \frac{2\sigma}{\lambda rc}} - 1 \right) \frac{dc}{c} = -\frac{2RT}{F} t \int_{c_{\text{dil.}}}^{c_{\text{conc.}}} \left(\frac{1}{c} - \frac{1}{c + \frac{2\sigma}{\lambda r}} \right) dc;$$

$$= -\frac{2RT}{F} t \ln \frac{c_{\text{conc.}} \left(c_{\text{dil.}} + \frac{2\sigma}{\lambda r} \right)}{c_{\text{dil.}} \left(c_{\text{conc.}} + \frac{2\sigma}{\lambda r} \right)}. \quad [11]$$

When the surface conductance is small even in the dilute solution and negligible in the concentrated one, Eq. [11] can be approximated by

$$E_{\text{cap. eff.}} = -\frac{2RTt}{F} \frac{2\sigma}{r\lambda c_{\text{dil.}}}. \quad [12]$$

¹ Although this is rather a crude approximation, it is permissible because what little reliable data we have on surface conductance indicate that there is only a slight variation of surface conductance with concentration.

The right-hand terminal of cell C is negative; the e.m.f., inversely proportional to the radius of the capillary and the conductance of the dilute solution, and virtually independent of the concentration of the concentrated one—all in agreement with Loosjes' results. From the e.m.f.'s as measured, a specific surface conductance of the order of 2×10^{-7} mho is derived—not an improbable value for the soft glass used (Corning 015). Unfortunately Loosjes did not measure the surface conductance, so that a direct check is not possible.

For comparison with later examples we point out that the capillary effect does not depend on the surface charge but on the surface conductance, that is, on the number of ions in the surface multiplied by their mobility.

5. SUSPENSION EFFECT AND DONNAN-E.M.F.

Considering now a suspension of negatively charged particles, and taking again K^+ as the reference ion, the equation [6] for the Donnan-e.m.f. can be written as follows:

$$E_{\text{Donnan}} = \frac{1}{F} \int_{\text{susp.}}^{\text{KCl sat.}} \left[t_{\text{Cl}} d\mu_{\text{KCl}} - \sum_{i \neq \text{K, Cl}} t_i \left(\frac{d\mu_i}{z_i} - d\mu_{\text{K}} \right) \right] - \frac{1}{F} \int_{\text{solut.}}^{\text{KCl sat.}} \left[t_{\text{Cl}} d\mu_{\text{KCl}} - \sum_{\substack{i \neq \text{K, Cl} \\ \text{part.}}} t_i \left(\frac{d\mu_i}{z_i} - d\mu_{\text{K}} \right) \right]. \quad [13]$$

In order to proceed, an assumption has to be made about the liquid junction between the suspension and the saturated potassium chloride. We will suppose that the concentrations of particles and all other ions of the suspension are constant and that the only variation in the liquid junctions is a gradient of the KCl concentration. This assumption makes calculations very easy, and results are only slightly different from the ones obtained with a Henderson-type boundary.

a. Ideal Behavior

The simplest possible assumption about the relation between transference numbers and chemical potentials is that of ideal behavior of all components with respect both to activity and mobility. In that case the following relations can be used to transform Eq. [13]:

$$t_{\text{Cl}} + \sum_{i \neq \text{K, Cl}} t_i = 1 - t_{\text{K}}$$

$$d\mu_{\text{KCl}} = RT \frac{dc_{\text{K}}}{c_{\text{K}}} + RT \frac{dc_{\text{Cl}}}{c_{\text{Cl}}} \quad [14]$$

$$d\mu_i (i \neq \text{K, Cl}) = 0; \quad d\mu_{\text{K}} = RT \frac{dc_{\text{K}}}{c_{\text{K}}}$$

$$dc_{\text{K}} = dc_{\text{Cl}}.$$

With the aid of the relations [14], Eq. [13] is transformed into

$$E_{\text{Donnan}} = \frac{RT}{F} \int_{\text{susp.}}^{\text{KCl sat.}} \left[\left(\frac{t_{\text{Cl}}}{c_{\text{Cl}}} - \frac{t_{\text{K}}}{c_{\text{K}}} \right) dc_{\text{K}} + \frac{dc_{\text{K}}}{c_{\text{K}}} \right] - \frac{RT}{F} \int_{\text{solut.}}^{\text{KCl sat.}} \left[\left(\frac{t_{\text{Cl}}}{c_{\text{Cl}}} - \frac{t_{\text{K}}}{c_{\text{K}}} \right) dc_{\text{K}} + \frac{dc_{\text{K}}}{c_{\text{K}}} \right].$$

The first terms of the two integrals give a very small contribution, which is proportional to the difference in mobility of the Cl^- and the K^+ ions and which will be neglected.

Then we obtain the simple result:

$$E_{\text{Donnan}} = \frac{RT}{F} \ln \frac{c_{\text{K, equil. sol.}}}{c_{\text{K, suspension}}} \quad [15]$$

When the only ions in the system are K^+ and Cl^- and when the concentration of particles is small, the distribution of ions is given by the relation:

$$c_{\text{K, suspension}} = c_0 + \frac{c_p}{2},$$

where c_p is the equivalent concentration of suspended particles, and c_0 is the concentration of KCl in the equilibrium solution, both expressed in equivalents per unit volume.

With this relation Eq. [15] simplifies to:

$$E_{\text{Donnan}} = - \frac{RT}{2F} \frac{c_p}{c_0} \quad [16]$$

So, although our approach has been different, we obtain in this ideal case the classical equations for the Donnan potential.

The assumption of ideal behavior in a suspension or in a polyelectrolyte is, however, often quite unrealistic. Not only will the distribution of ions deviate from the ideal one, forcing us to introduce activity coefficients, but the mobility of the ions in the neighborhood of the suspended particles will also be modified by electric and hydrodynamic interaction.

We shall now show that even for the limiting case of small particle concentrations, especially the modified mobilities affect the Donnan-e.m.f. seriously.

b. Nonideal Distribution: Nonideal Mobilities

A very important reason for departure from ideal behavior is the high concentration of ions around the suspended particles. When the charge density on the particles is very low, half of this charge is compensated by an excess of gegenions, and the other half by a deficiency of ions of the same sign of charge as the particles. When the particle charge is high, the

gegenions compensate more than $\frac{1}{2}$, say a fraction x of the particle charge, and the deficiency of ions of the same sign compensates less than $\frac{1}{2}$, say a fraction y , even when the concentration of particles is very low. This asymmetry is the more pronounced the smaller the concentration of electrolyte (18; cf. 19, p. 191 ff.)

Considering a suspension of negatively charged particles in KCl, in equilibrium with a KCl solution of concentration c_0 , the concentrations of K^+ and Cl^- ions will be:

$$\begin{aligned}c_K &= c_0 + xc_P \\c_{Cl} &= c_0 - yc_P; \\x + y &= 1.\end{aligned}\tag{17}$$

This amounts to taking the activity coefficient of KCl for small values of c_P equal to:

$$f_{\pm} = 1 - \frac{x - y}{2} \frac{c_P}{c_0}\tag{18}$$

if we assume the activity coefficient in the solution to be equal to one.

The mobilities of the ions will be affected as well. We expect some of the Cl^- ions close to the particles to have an increased mobility, and the K^+ gegenions will certainly have a lower mobility than normal.

That this is by no means a small effect may be illustrated by the case of the AgI sol., where the mobility of the counterions is only 20% to 25% of the normal value (20; cf. 19, p. 239). Investigations on ion exchange (21; cf. 19, p. 176 ff.) in the double layer of AgI have shown that this cannot be ascribed to incomplete dissociation between particle and counterions. Another example of a large change in mobility is given by the negative transference-number of the counterions of some paraffin-chain salts (22).

These facts can be taken into account by placing the contribution of the K^+ and Cl^- ions to the conductance equal to

$$\begin{aligned}c_K \lambda_K &= \lambda_0(c_0 + uc_P) \\c_{Cl} \lambda_{Cl} &= \lambda_0(c_0 - vc_P)\end{aligned}\tag{19}$$

where λ_0 is the limiting equivalent conductance of Cl^- or K^+ , and u and v are constants. This means that from now on we neglect the small difference in limiting equivalent conductance of K^+ and Cl^- .

The following values for the mobility coefficients in the case of small c_P can be calculated from Eq. [19]:

$$\begin{aligned}\lambda_K/\lambda_0 &= 1 - (x - u) \frac{c_P}{c_0} \\ \lambda_{Cl}/\lambda_0 &= 1 + (y - v) \frac{c_P}{c_0}.\end{aligned}$$

There are no simple relations between u , v , and x , y although v should not be very different from y but u should be considerably smaller than x , so that

$$u + v < 1. \quad [20]$$

Applying now Eq. [13] for the case considered here we find:

$$E_{\text{Donnan}} = \frac{1}{F} \int_{\text{susp.}}^{\text{KCl sat.}} \left(t_{\text{Cl}} d\mu_{\text{KCl}} + \frac{t_P}{z_P} d\mu_{PK_z} \right) - \frac{1}{F} \int_{\text{sol.}}^{\text{KCl sat.}} t_{\text{Cl}} d\mu_{\text{KCl}} \quad [21]$$

where t_P is the transference number and z_P the valency of the particles and μ_{PK_z} the chemical potential of a particle with its z gegenions.

In order to eliminate μ_{PK_z} we apply the Gibbs-Duhem relation to a suspension and to the liquid with which it is in equilibrium. We find

$$\text{for the solution} \quad 55 d\mu_{\text{H}_2\text{O}} + c d\mu_{\text{KCl}} = 0,$$

$$\text{for the suspension} \quad 55 d\mu_{\text{H}_2\text{O}} + (c - y c_P) d\mu_{\text{KCl}} + \frac{c_P}{z_P} d\mu_{PK_z} = 0,$$

where 55 represents the number of moles of water in a liter.

From these relations we derive

$$\frac{1}{z_P} d\mu_{PK_z} = y d\mu_{\text{KCl}} \quad [22]$$

and consequently the equation for the e.m.f. becomes

$$E_{\text{Donnan}} = \frac{1}{F} \int_{\mu_0}^{\text{KCl sat.}} (t_{\text{Cl, susp.}} - t_{\text{Cl, sol.}} + y t_P) d\mu_{\text{KCl}} \quad [23]$$

where μ_0 is the chemical potential of KCl in the suspension or the solution.

The transference numbers and the chemical potentials to be substituted in Eq. [23] are:

$$\begin{aligned} t_{\text{Cl, susp.}} &= \frac{c - v c_P}{2c + (u - v + r) c_P} \\ t_{\text{Cl, sol.}} &= \frac{1}{2} \\ t_P &= \frac{r c_P}{2c + (u - v + r) c_P} \\ d\mu_{\text{KCl}} &= 2RT \frac{dc}{c} \end{aligned} \quad [24]$$

where r is the ratio of the mobility of a particle to that of a free K^+ or Cl^- ion. Assuming that y , u , v , and r are independent of the KCl concentration (or taking suitable averages for them) we find:

$$E_{\text{Donnan}} = -\frac{RT}{F} \int_{c_0}^{c^{\text{sat.}}} \frac{(u + v + (1 - 2y)r) c_P}{2c + (u - v + r) c_P} \frac{dc}{c}. \quad [25]$$

On integration this leads to

$$E_{\text{Donnan}} = -\frac{RT}{F} \frac{u + v + (1 - 2y)r}{u - v + r} \ln \frac{c_{\text{sat.}}}{c_0} \frac{c_0 + \frac{u - v + r}{2} c_P}{c_{\text{sat.}} + \frac{u - v + r}{2} c_P}, \quad [26]$$

which usually can be simplified to

$$E_{\text{Donnan}} = -\frac{RT}{F} \frac{u + v + (1 - 2y)r}{u - v + r} \ln \left(1 + \frac{u - v + r}{2} \frac{c_P}{c_0} \right), \quad [27]$$

and which, in the case of small concentrations of particles, can be further simplified to

$$E_{\text{Donnan}} = -\frac{RT}{2F} \frac{c_P}{c_0} \left[u + v + (1 - 2y)r \right]. \quad [28]$$

We see that even in the case of small particle concentrations the Donnan-e.m.f. is not determined in a simple way by the charge of the particles but mainly by the contribution to the conductance of the ions in the double layer. The fact that the mobility of the counterions is much lower than normal (it may even be negative) and that $u + v$ is always smaller than one (see Eq. [20]), explains why the Donnan-e.m.f. is often found to be lower than the value calculated from the ideal equation. This lower value need therefore not necessarily reflect incomplete dissociation, nor can it give much information on the activity coefficients of the system.

When the charge density on the particles is high, v and y will be quite low and may be neglected. In that case the Donnan-e.m.f. and the contribution of the particles plus gegenions to the conductance (micellar conductance) are both determined by $u + r$, and Eq. [27] can be written

$$E_{\text{Donnan}} = \frac{RT}{F} \ln \frac{\text{conductance of suspension}}{\text{conductance of equil. solution}},$$

showing clearly the close analogy to the capillary effect (Eqs. [11] and [12]).

Not a single Donnan system has been investigated in sufficient detail to test the Eqs. [26]–[28] quantitatively. Information on the mobilities of all components of the system would be particularly desirable.

Incidentally Eq. [26] is rather similar to an equation obtained by Jenny *c.s.* (1) for the suspension effect. They applied it to compressed plugs of clay and other ion exchange materials. It should be remarked that in such cases, although the particles are fixed with respect to the apparatus, their Hittorf transference number is not zero, because electro-osmosis drives the solvent through the plug. An approach using “reduced” transference numbers (23, 24) instead of Hittorf ones appears more natural, although both methods are correct and finally lead to the same result.

6. SEPARATION OF THE CELL POTENTIAL INTO THREE CONTRIBUTIONS

If an attempt is made to separate the cell potential into three contributions by using Eq. [7], one encounters the following difficulty. The total cell potential contains mobilities according to Eqs. [26]–[28], but the true membrane-potential $\frac{1}{Fz_R} (\mu_R^{\text{II}} - \mu_R^{\text{III}})$ should depend only upon activities. Consequently the assumption that the two liquid junction potentials cancel would imply that the activity of the R ion is connected in a very special way with the mobilities of the ions of the system, even in the limit of a very small concentration of particles. On the other hand, any other plausible assumption on the single-ion activities would lead to a value for the liquid junction potentials which is significantly different from zero, even if the particle concentration is small. Since it is at any rate impossible to test assumptions of this nature experimentally, the discussion on the Donnan potential in the sense of a potential difference between suspension and solution loses much of its attraction, and it appears more satisfactory to concentrate on the Donnan-e.m.f., that is, on the e.m.f. of the total cell.

7. FINAL REMARKS

The Donnan potential has often been used to determine particle charges (25, 26). It is now evident that this is only justified when the charge density on the particles is small, so that all electrostatic and hydrodynamic interaction may be neglected. A small value of the Donnan-e.m.f. in itself, which can also be obtained by a small concentration of particles, or a high concentration of electrolyte, is not a sufficient condition.

Finally it should be remarked that Loosjes in his thesis (17) suggested an explanation for the capillary effect and for the suspension effect based upon the different contributions of the surface of the capillary or the particles and the bulk of the liquid to the conductivity of the system. Quantitatively his explanation comes therefore rather close to the one offered in this paper.

ACKNOWLEDGEMENTS

The author acknowledges gratefully discussions with Dr. G. Scatchard and Dr. P. L. De Bruyn, and correspondence with Dr. A. J. Staverman and Dr. M. Peech, who have all been very helpful in giving this paper its final form.

REFERENCES

1. JENNY, H., NIELSEN, T. R., COLEMAN, N. T., AND WILLIAMS, D. E., *Science* **112**, 164 (1950).
2. MARSHALL, C. E., *Science* **113**, 43 (1951).
3. ERIKSSON, E., *Science* **113**, 418 (1951).
4. MYSELS, K. J., *Science* **114**, 424 (1951).

5. MARSHALL, C. E., *Science* **115**, 361 (1952).
6. COLEMAN, N. T., WILLIAMS, D. E., NIELSEN, T. R., AND JENNY, H., *Soil Sci. Soc. Amer. Proc.* **15**, 106 (1951).
7. PEECH, M., AND SCOTT, A. D., *Soil Sci. Soc. Amer. Proc.* **15**, 115 (1951).
8. SOLLNER, K., *J. Colloid Sci.* **8**, 179 (1953).
9. DONNAN, F. G., *Chem. Revs.* **1**, 80 (1924).
10. RABINOVICH, A. J., AND KARGIN, V. A., *Trans. Faraday Soc.* **31**, 55 (1935).
11. DU RIETZ, C., Ueber das Ionenbindungsvermögen fester Stoffe, Diss., Stockholm, 1938.
12. DONNAN, F. G., *Z. physik. Chem.* **168A**, 369 (1934).
13. GUGGENHEIM, E. A., *J. Phys. Chem.* **33**, 842 (1929).
14. MACINNES, D. A., *The Principles of Electrochemistry*, p. 258. New York, 1939.
15. SCATCHARD, G., In E. J. COHN and J. T. EDSALL, eds., *Proteins, Amino Acids and Peptides*, p. 44. New York, 1943.
16. WIEBENGA, E. H., 2e Symposium over sterke electrolyten en de elektrische dubbellaag, p. 72. Utrecht, Holland, 1944.
17. LOOSJES, R., pH meting in suspensies, Thesis, Utrecht, Holland, 1942; *Chem. Weekblad* **46**, 902 (1950).
18. KLAARENBEEK, F. W., Over DONNAN evenwichten bij solen van arabische gom, Thesis, Utrecht, Holland, 1946.
19. KRUYT, H. R., *Colloid Science*, Vol. I, p. 191 ff. Amsterdam, New York, 1952; *ibid.*, p. 239; *ibid.*, p. 176 ff.
20. DE BRUYN, H., AND OVERBEEK, J. TH. G., *Kolloid-Z.* **84**, 186 (1938).
21. VAN OS, G. A. J., Thesis, Utrecht, Holland, 1943.
22. HARTLEY, G. S., *Aqueous Solutions of Paraffin-Chain Salts*. Coll. Hermann, Paris, 1936.
23. STAVERMAN, A. J., *Trans. Faraday Soc.* **48**, 176 (1952).
24. SCATCHARD, G., *J. Am. Chem. Soc.* **75**, 2883 (1953).
25. ADAIR, G. S., AND ADAIR, M. E., *Trans. Faraday Soc.* **36**, 23 (1940); *ibid.* **31**, 130 (1935).
26. ADAIR, G. S., *Trans. Faraday Soc.* **33**, 1106 (1937).

**DETERGENT SOLUBILITY AS A LIMITING FACTOR IN
SOLUBILIZATION BY AQUEOUS SOLUTIONS OF TWO
NONIONIC DETERGENTS**

In studies of the solubilization of organic liquids by ionic detergents, the solubilization end point can be determined turbidimetrically because excess solubilize forms an emulsion (1, 2, 3). This method has also been applied to nonionic detergents (4, 5, 6, 7); however, an examination of the temperature-phase relations of dilute (5% wt./vol. or less) aqueous mixtures of either of two nonionic detergents with several aromatic liquid compounds, taken one at a time (8), leads one to the conclusion that turbidity may result not only from the presence of excess solubilize but also from the separation of a detergent-rich phase.

At room temperatures, the nonionic detergents Triton X-100 and Thio-solve 8139 (a polyethylene glycol ether) are completely miscible in water, but as the temperature is increased above 60°C., a cloud point is soon reached after which a detergent-rich phase appears and readily settles out. As a solubilize such as benzene, benzaldehyde, dibenzyl ether, Parathion (O, O-diethyl O-*p*-nitrophenyl thiophosphate), dibutyl phthalate, or Santicizer E-15 (ethyl phthalyl ethyl glycolate) is added in small increments to such detergent solutions, the temperatures at which this second phase forms drop, as illustrated by phase Diagrams 1 and 2. The data for these diagrams were obtained by visual observation, after attainment of equilibrium at the specified temperature in capped or sealed test-tubes, of aqueous solutions of detergent into which the solubilize had been weighed (8).

The separation of the detergent-rich phase occurs when phenol is the solubilize despite the fact that it is quite soluble in pure water (Diagram 3). Thus, by using turbidity as the only criterion for the appearance of excess solubilize, an apparent decrease in the solubility of the latter in the presence of solubilizer takes place. This may explain the observation of McBain and Lissant (7), who found that with "benzene in very dilute Triton X-100—the solubility was less in the solution than in pure water; that is, the dilute Triton X-100 "salts out" benzene." An examination of the second phase formed on the addition of benzene to aqueous Triton X-100 reveals that the volume of this phase is greater than the total volume of benzene and detergent added, and that its density is greater than water. It is concluded, therefore, that the benzene is not "salted out" but that

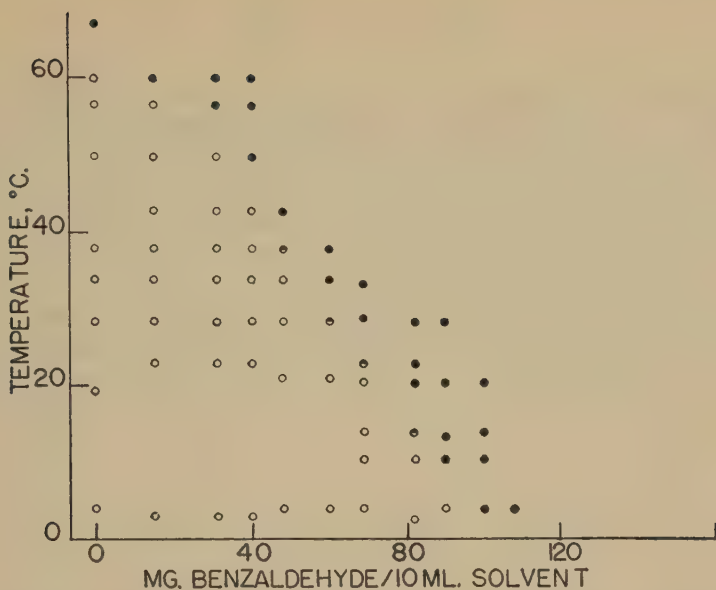


DIAGRAM 1. Temperature-phase diagram of small amounts of benzaldehyde in 10 ml. of 2% (wt./vol.) aqueous Triton X-100. ○—one-phase system (solubilization + solubility); ●—two-phase system (one phase detergent-rich); ◐—system borderline. Taken from unpublished data of Hilchey, Norton, and Weiden (8).

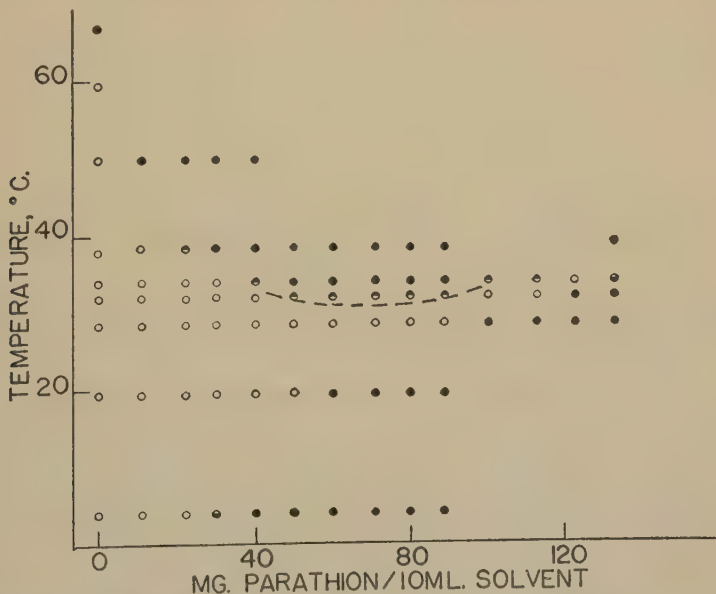


DIAGRAM 2. Temperature-phase diagram of small amounts of Parathion in 10 ml. of 2% (wt./vol.) aqueous Triton X-100. ○—as in diagram 1; ●—two- (or more) phase system (phase composition dependent on temperature); ◐—system borderline; ---- indicates minimum in upper boundary of solubilization. Taken from unpublished data of Hilchey, Norton, and Weiden (8).

solubilization of the benzene by the Triton X-100 lowers the temperature at which the Triton-rich phase separates out, possibly by a decrease in the hydrophilic character of the detergent micelles through the incorporation of benzene molecules into these micelles. The fact that, for the same amount of solubilize, the detergent-rich phase appears at a lower temperature when the concentration of detergent is decreased supports this idea as opposed to the salting out effect (Diagram 4).

As shown in Diagram 2, the separation of a solubilizer-rich phase is not necessarily the only limit to the existence of the one phase system water-solubilizer-solubilizant, at least for the concentrations studied. With the

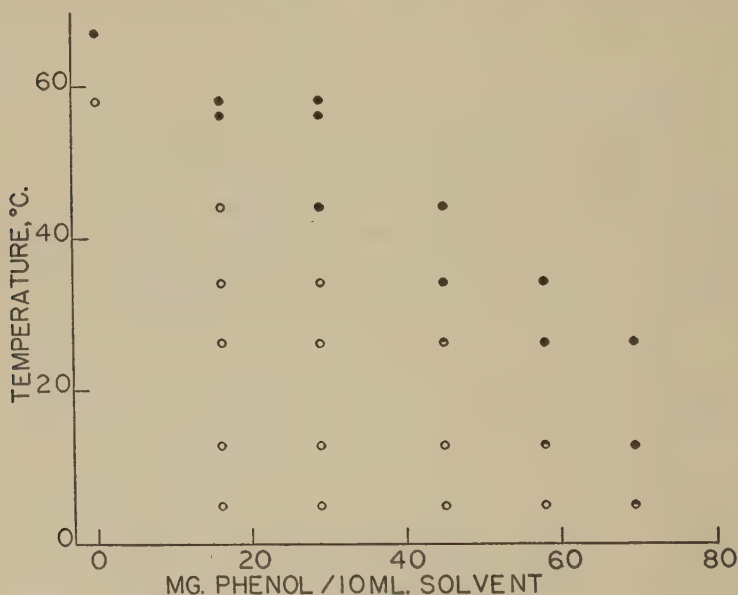


DIAGRAM 3. Temperature-phase diagram of small amounts of phenol in 10 ml. of 2% (wt./vol.) aqueous Triton X-100. O, ●, and ◐—as in diagram 1.

larger molecules as dibenzyl ether, Parathion, dibutyl phthalate, or Santizer E-15 but not with the smaller ones as benzene or benzaldehyde, it was found that a three-component system, which is transparent at room temperature owing to solubilization, becomes turbid not only when the temperature is raised but also when it is lowered, provided that sufficient solubilize is present. The phase that separates out at the lower temperatures differs from the type obtained at the higher temperatures and appears to consist mainly of excess solubilize. With Parathion in Triton X-100 solutions, the excess solubilize can be cosolubilized by benzene or benzaldehyde; in contrast, the cloud points of these solutions drop still more in the presence of such additives (8). Thus in the lower range of the temperatures

studied, solubilization by the two nonionic detergents, as with ionic detergents, is limited by saturation of the solubilizer micelles.

With dibenzyl ether, Parathion and dibutyl phthalate, a definite transition region was observed between the two tendencies, namely, the separation of a solubilizer-rich phase and the separation of excess solubilize. This transition area leads to the formation of a definite minimum in the upper boundary of solubilization as depicted by the broken line in Diagram 2. As a result, there is a limited temperature range over which the addition of excess solubilize clears the initial turbidity first formed. The effect of

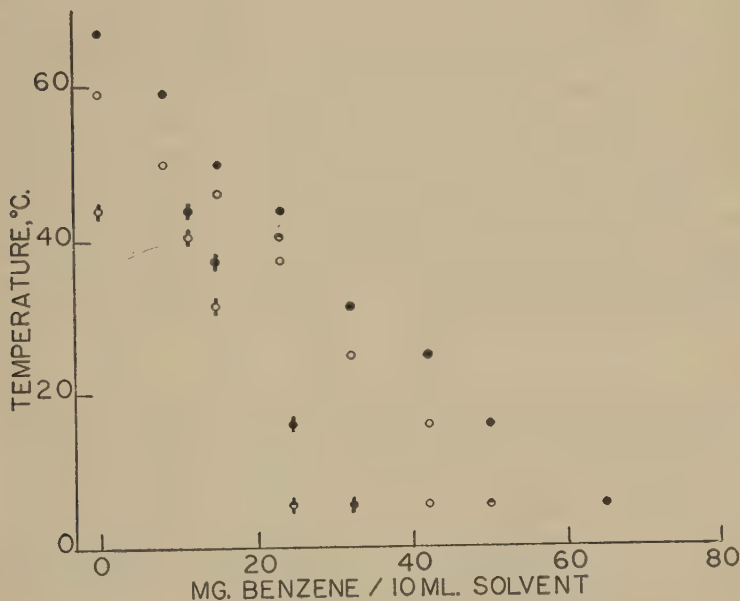


DIAGRAM 4. The effect of reducing solubilizer concentration on temperature-phase diagrams of small amounts of benzene in 10 ml. of aqueous Triton X-100 solutions. ○, ●, and ●—2% (wt./vol.) Triton X-100; ○, ●, and ●—0.5% (wt./vol.) Triton X-100; ○ and ○—one-phase system (solubility + solubilization); ● and ●—turbidity, indicating more than one phase; ● and ●—system borderline.

this transition region cannot be disregarded in an evaluation of the positive temperature coefficient of solubilization at the lower temperatures.

In conclusion, it is evident that the extent of solubilization by a nonionic detergent can be limited not only by the saturation of the solubilizer micelles but also by a decrease in the miscibility of the solubilizer with water, possibly owing to the incorporation of solubilize molecules into the solubilizer micelles; and that a knowledge of the temperature-phase relations is necessary for the interpretation of a solubilization study involving a nonionic detergent. Furthermore, a comparative study of the more hydro-

philic nonionic detergents, which have higher or no cloud points in proportion to the number of ethylene oxide units contained (9), is strongly indicated.

The writers wish to thank the Geary Chemical Corp. of New York for a sample of Thiosolve 8139 and the Monsanto Chemical Co. of St. Louis for a sample of Santicizer E-15.

SUMMARY

An examination of the temperature-phase diagrams, and of the phases themselves, obtained in solubilization studies with two polyethyleneoxide side-chain type nonionic detergents and several liquid aromatic compounds indicates that the presence of the latter decreases the cloud points of the detergents, thus limiting solubilization. With certain of the solubilizates studied, excess solubilizate will form the second phase at below room temperatures, indicating that the solubilizer micelles are saturated, the behavior of the system now corresponding to that found with solubilization by ionic detergents. A marked transition region may separate the manifestations of these two phenomena. The results obtained thus limit the validity of the turbidity criterion for solubilization end point when studying solubilization in aqueous solutions of nonionic detergents.

REFERENCES

1. HELLER, W., AND KLEVENS, H. B., *J. Chem. Phys.* **14**, 567 (1946).
2. MCBAIN, J. W., AND RICHARDS, P. H., *Ind. Eng. Chem.* **38**, 642 (1946).
3. KLEVENS, H. B., *J. Am. Chem. Soc.* **72**, 3581 (1950).
4. MCBAIN, J. W., AND MCHAN, H., *J. Am. Chem. Soc.* **70**, 3838 (1948).
5. RICHARDS, P. H., AND MCBAIN, J. W., *J. Am. Chem. Soc.* **70**, 1338 (1948).
6. COHEN, M., *Compt. rend.* **229**, 1074 (1949).
7. MCBAIN, J. W., AND LISSANT, K. L., *J. Phys. & Colloid Chem.* **55**, 655 (1951).
8. HILCHEY, J. D., NORTON, L. B., AND WEIDEN, M. H. J., Unpublished data, Department of Entomology, Cornell University (1951-1953).
9. FINEMAN, M. N., BROWN, G. L., AND MYERS, R. J., *J. Phys. Chem.* **56**, 963 (1952).

Department of Entomology
Cornell University
Ithaca, New York

MATHIAS H. J. WEIDEN
LELAND B. NORTON

Received June 25, 1953

Book Review

Review of Textile Progress. Vol. III (1951). Edited by W. J. HALL AND C. J. W. HOOPER. Published jointly by The Textile Institute, Manchester, England, and The Society of Dyers and Colourists, Bradford, England, 1952. 590 pp. Price 35/-.

This volume covers very completely the literature and patents for 1951 in the textile field. It is similar to Volume I (1949) and Volume II (1950) but is not a duplication or enlargement of the earlier volumes.

The various parts of this review were contributed by thirty-two eminent British textile scientists. The topics covered are: (a) "Physics and Chemistry of Fibrous Materials," (b) "Fibre Production," (c) "The Conversion of Fibres into Finished Yarns," (d) "Fabric Production," (e) "Colouring Matters," (f) "Colouring of Textiles," (g) "Finishing," (h) "Analysis, Testing, Grading and Defects," (j) "Laundering and Dry Cleaning," (k) "Building and Engineering," and (l) "Industrial Applications of Textiles." Each topic is subdivided into sections on cotton, rayon, silk, synthetic, and other fibers.

A new section, not present in the previous volumes, on the physics and chemistry of synthetic fibers will be of special interest to the colloid chemist. A large number of papers dealing with the effects of crystalline and amorphous regions on fibers properties are discussed. The production of synthetic fibers is also treated in some detail.

The last chapter on "Industrial Applications of Textiles" is also new. This deals primarily with the use of fibers in the rubber industry.

This book is a collection of abstracts of the various papers. Since each paper is dealt with very briefly, one misses the lack of detail on subjects of particular interest. Tables and graphs are completely absent. However, as a source book to see what work has been done it serves an excellent purpose, and it is to be hoped that it will be continued as a regular annual survey.

R. H. EWART, Passaic, New Jersey

AUTHOR INDEX

A

- ALEXANDER, A. E. See Posner, 575, 585
 ANACKER, E. W. Light scattering by solutions of octyltrimethylammonium octanesulfonate and octyltrimethylammonium decanesulfonate, 402

B

- BAILEY, JOHN HAYS. See Ross, 385
 BANKS, W. H., AND MILL, C. C. Tacky adhesion—A preliminary study, 137
 BARTELL, F. E. See Ray, 214
 BASU, SADHAN. See Das Gupta, 355
 BRADY, A. P., BROWN, A. G., AND HUFF, HARRIETTE. The polymerization of aqueous potassium silicate solutions, 252
 BROWN, A. G. See Brady, 252
 And THUMAN, WILLIAM C., AND McBAIN, J. W. The surface viscosity of detergent solutions as a factor in foam stability, 491
 And THUMAN, WILLIAM C., AND McBAIN, J. W. Transfer of air through adsorbed surface films as a factor in foam stability, 508
 BULKLEY, RONALD. Retardation of flow in narrow capillaries, 485
 BURCIK, EMIL J. Effect of electrolytes on the rate of surface tension lowering; the rate of surface equilibrium attainment as a factor in detergency, 520
 BURGOYNE, J. H., AND COHEN, L. The production of monodisperse aerosols of large drop size, 364

C

- COCKBAIN, E. G., AND McROBERTS, T. S. The stability of elementary emulsion drops and emulsions, 440
 COHEN, L. See BURGOYNE, 364
 COHN, STANLEY H. See Gucker, 555
 CRIDDLE, DEAN W. See Meader, 170

D

- DAS GUPTA, PARES CH., AND BASU, SADHAN. Studies on polyelectrolytes. III. Polyglucosamine, 355

DAS GUPTA, S. GULVADY. See McBain, 474

- DEAN, ROBERT B., HAYES, KENNETH E., AND NEVILLE, ROY G. The sorption of vapors by monolayers. VII. The effect of anesthetic vapors on some monolayers of biological interest, 377
 DUNNING, H. N. The interfacial activity of mesoporphyrin IX and some derivatives, 279

E

- EWING, WARREN W., AND LIU, FRED W. J. Adsorption of dyes from aqueous solutions on pigments, 204

F

- FERRY, JOHN D. See Fitzgerald, 1
 And FITZGERALD, EDWIN R. Mechanical and electrical relaxation distribution functions of two compositions of polyvinyl chloride and dimethyl thianthrene, 224
 GRANDINE, LESTER D., JR., AND UDY, DOYLE C. Viscosities of concentrated polymer solutions. III. Polystyrene and styrene-maleic acid copolymer, 529
 FINEMAN, MANUEL N., AND KLINE, PHYLLIS J. The role of the substrate in the detergency process, 288
 FITZGERALD, EDWIN R., AND FERRY, JOHN D. Method for determining the dynamic mechanical behavior of gel and solids at audiofrequencies; comparison of mechanical and electrical properties, 1
 And MILLER, ROBERT F. Dielectric properties of the system polyvinyl chloride-dimethylthianthrene, 148
 See Ferry, 224
 FLOCKHART, B. D., AND GRAHAM, H. Study of dilute aqueous solutions of sodium oleate, 105
 And UBBELOHDE, A. R. Electrical conductance of some paraffin-chain salts in propanol-water and propionic acid-water mixtures, 428

- FOK, SHIU-MING. See Maron, 540
- FOX, H. W., HARE, E. F., AND ZISMAN, A.
The spreading of liquids on low-energy surfaces. VI. Branched-chain monolayers, aromatic surfaces, and thin liquid films, 194
- FRIEDMAN, HENRY L., AND KERKER, MILTON. Ultraviolet absorption of aqueous sulfur solutions, 80
- G
- GODDARD, E. D., AND SCHULMAN, J. H.
Molecular interaction in monolayers.
I. Complex formation, 309
II. Steric effects in the nonpolar portion of the molecules, 329
- GRAHAM, H. See Flockhart, 105
- GRANDINE, LESTER D., JR. See Ferry, 529
- GUCKER, FRANK T., JR., AND COHN, STANLEY H. Numerical evaluation of the Mie scattering functions; table of the angular functions π_n and τ_n of orders 1 to 32 and 2.5° intervals, 555
- H
- HARE, E. F. See Fox, 194
- HARMSSEN, G. J., VAN SCHOOTEN, J., AND OVERBEEK, J. TH. G. Viscosity and electroviscous effect of the AgI sol. I. Influence of the velocity gradient and of aging of the sol, 64
II. Influence of the concentration of AgI and of electrolyte on the viscosity, 72
- HARVEY, EDMUND N., JR. Effect of magnetic fields on the rheology of ferromagnetic dispersions, 543
- HAYES, KENNETH E. See Dean, 377
- HERMANIE, P. H. J. See van der Minne, 38
- HIRSCHHORN, ERNESTINE. See Mathews, 86
- HUFF, HARRIETTE. See Brady, 252
- I
- INOKUCHI, KIYOSHI. See Tachibana, 341
- K
- KERKER, MILTON. See Friedman, 80
- KIPLING, J. J., AND NORRIS, A. D.
Molecular cross sections in films of fatty acids on water, 547
- KLINE, PHYLLIS J. See Fineman, 288
- KOENIG, VIRGIL L., AND PERRINGS, J. D.
Critical sedimentation and viscosity studies on calf thymus sodium deoxyribonucleate, 452
- KWARTLER, C. E. See Ross, 385
- L
- LAL, HIRA. The specific and partial specific volumes of potassium laurate and lauryl sulfonic acid in aqueous solutions, 414
- LIU, FRED W. J. See Ewing, 204
- LOWER, GEORGE W., WALKER, WILLIAM C., AND ZETTMEOYER, ALBERT C.
The rheology of printing inks. II. Temperature control studies in the rotational viscometer, 116
- M
- MCBAIN, J. W., AND DAS GUPTA, S. GULVADY. Solubilization of benzene in certain detergent solutions that appear to give two different values, 474
See Brown, 491, 508
- MCRROBERTS, T. S. See Cockbain, 440
- MADONNA, L. A. See Pound, 187
- MADOW, BENJAMIN P. See Maron, 130, 300
- MARON, SAMUEL H., AND MADOW, BENJAMIN P. Rheology of synthetic latex.
III. Concentration dependence of flow in type III GR-S latex, 130
IV. Effect of polydispersity on flow behavior, 300
And FOK, SHIU-MING. Effect of concentration on flow behavior of glass sphere suspensions, 540
- MATALON, R. On monolayer penetration, 53
- MATHEWS, MARTIN B., AND HIRSCHHORN, ERNESTINE. Solubilization and micelle formation in a hydrocarbon medium, 86
- MEADER, ARTHUR L., JR., AND CRIDDLE, DEAN W. Force-area curves of surface films of soluble surface-active agents, 170
- MILL, C. C. See Banks, 137
- MILLER, ROBERT F. See Fitzgerald, 148
- MOORE, W. R., AND RUSSELL, J. Viscosity and initial phase separation

- studies on solutions of cellulose acetate, 243
- N**
- NEUBAUER, RAYMOND L., AND VONNEGUT, BERNARD. Supplement to "Production of monodisperse liquid particles by electrical atomization," 551
- NEVILLE, ROY G. See Dean, 377
- NORRIS, A. D. See Kipling, 547
- O**
- OVERBEEK, J. TH. G. See Harmsen, 64, 72
- Thermodynamics of electrokinetic phenomena, 420
- Donnan-E.M.F. and suspension effect, 593
- OWENS, H. S. See Phippen, 97
- P**
- PEAKE, S. L. See Pound, 187
- PERRINGS, J. D. See Koenig, 452
- PIPPEN, E. L., SCHULTZ, T. H., AND OWENS, H. S. Effect of degree of esterification on viscosity and gelation behavior of pectin, 97
- POSNER, A. M., AND ALEXANDER, A. E. The kinetics of adsorption from solution to the air/water interface. Part I. Normal aliphatic alcohols, 575
- Part II. Anionic and cationic soaps, 585
- POUND, G. M., MADONNA, L. A., AND PEAKE, S. L. Critical supercooling of pure water droplets by a new microscopic technique, 187
- R**
- RAY, ROGER B., AND BARTELL, F. E. Hysteresis of contact angle of water on paraffin. Effect of surface roughness and of purity of paraffin, 214
- RICHARDSON, E. G. The flow of emulsions. II, 367
- ROSS, SYDNEY, KWARTLER, C. E., AND BAILEY, JOHN HAYS. Colloidal association and biological activity of some related quaternary ammonium salts, 385
- RUSSELL, J. See Moore, 243
- S**
- SCHULMAN, J. H. See Goddard, 309, 329
- SCHULTZ, T. H. See Phippen, 97
- SCOTT, K. W., AND TOBOLSKY, A. V. Statistical thermodynamics of a one-dimensional polymer chain incorporating energy and entropy effects, 465
- SHERMAN, P. Studies in water-in-oil emulsions. III. The properties of interfacial films of sorbitan sesquioleate, 35
- SOLLNER, KARL. Some remarks concerning the measurement of ion activities in colloidal systems and the suspension effect, 179
- T**
- TACHIBANA, TARO AND INOKUCHI, KIYOSHI. Rheological approach for the study of protein monolayers, 341
- THUMAN, WILLIAM C. See Brown, 491, 508
- TOBOLSKY, A. V. See Scott, 465
- U**
- UBBELOHDE, A. R. See Flockhart, 428
- UDY, DOYLE C. See Ferry, 529
- V**
- VAN DER MINNE, J. L., AND HERMANIE, P. H. J. Electrophoresis measurements in benzene-correlation with stability. II. Results of electrophoresis, stability, and adsorption, 38
- VAN SCHOOTEN, J. See Harmsen, 64, 72
- VONNEGUT, BERNARD. See Neubauer, 551
- W**
- WALKER, WILLIAM C. See Lower, 116
- WEIDEN, MATHIAS H. J., AND NORTON, LELAND B. Detergent solubility as a limiting factor in solubilization by aqueous solutions of two nonionic detergents, 606
- Z**
- ZETTMEOYER, ALBERT C. See Lower, 116
- ZISMAN, A. See Fox, 194

SUBJECT INDEX

A

- Adhesion, see *Tacky*
 Adsorption (see also *Dyes*, *Electrophoresis*, — from solution to air/water interface, POSNER AND ALEXANDER, 575, 585
 Aerosols, production of monodisperse —, BURGOYNE AND COHEN, 364
 Ammonium salts, see *Colloidal, Light*
 Atomization, see *Monodisperse*

B

- Benzene, see *Detergent, Electrophoresis*

C

- Capillaries, flow in narrow —, BULKLEY, 485
 Cellulose acetate, viscosity and initial phase separation studies on solutions of — —, MOORE AND RUSSELL, 243
 Colloidal, — systems and the suspension effect, SOLLNER, 179; — association and biological activity of quaternary ammonium salts, ROSS *et al.*, 385
 Concentration, — and flow of glass sphere suspensions, MARON AND FOK, 540
 Conductance, see *Paraffin*
 Contact angle, hysteresis of — — of water on paraffin; effect of surface roughness and of purity of paraffin, RAY AND BARTELL, 214

D

- Desoxyribonucleate, sedimentation and viscosity, KOENIG AND PERRINGS, 452
 Detergency (see also *Surface*); — and substrate, FINEMAN AND KLINE, 288; — and solubilization, WEIDEN AND NORTON, 606
 Detergent, benzene in — solutions, Mc-BAIN AND DAS GUPTA, 474; surface

- viscosity of — solutions and foam stability, BROWN *et al.*, 491
 Dimethylthianthrene, see *Polyvinyl chloride*
 Dispersion, see *Magnetism, Monodisperse*
 Distribution, see *Polyvinyl chloride*
 Donnan, see *Suspension*
 Dyes, adsorption from aqueous solutions on pigments, EWING AND LIU, 204

E

- Electrical atomization, see *Monodisperse*
 Electrical conductance, see *Paraffin*
 Electrokinetics, thermodynamics and —, OVERBEEK, 420
 Electrophoresis, — measurements in benzene, and stability; —, stability, adsorption, VAN DER MINNE AND HERMANIE, 38
 Electroviscous effect, viscosity and — — of the AgI sol, HARMSSEN *et al.*, 64, 72
 E.m.f., see *Suspension*
 Emulsions, water-in-oil —, films of sorbitan sesquioleate, SHERMAN, 35; flow of —, RICHARDSON, 367; stability of —, COCKBAIN AND McROBERTS, 440
 Errata, 185, 489
 Esterification, see *Pectin*

F

- Fatty acids, films of — —, KIPLING AND NORRIS, 547
 Foam, see *Detergent, Surface*

G

- Gel, dynamic mechanical behavior of gels and solids, FITZGERALD AND FERRY, 1
 Gelation, see *Pectin*
 Glass, see *Concentration*

H

- Hydrocarbon, see *Solubilization*
 Hysteresis, see *Contact angle*

I

- Ink, rheology of printing inks in the rotational viscometer, LOWER *et al.*, 116

L

- Latex, rheology of synthetic —, MARON AND MADOW, 130, 300
 Laurate, see *Volumes*
 Light, — scattering by solutions of octyltrimethylammonium salts, ANACKER, 402; Mie scattering functions, GUCKER AND COHN, 555

M

- McBAIN, J. W., Obituary, 375
 Magnetism, — and ferromagnetic dispersions, HARVEY, 543
 Mechanical behavior, see *Gel*
 Mesoporphyrin IX, interfacial activity, DUNNING, 279
 Micelle, see *Solubilization*
 Mie, see *Light* (see also *Aerosols*);
 Monodisperse, — liquid particles by electrical atomization, NEUBAUER AND VONNEGUT, 551
 Monolayer(s), — penetration, MATALON, 53; molecular interaction in —, GODDARD AND SCHULMAN, 309, 329; rheology of protein —, TACHIBANA AND INOKUCHI, 341; sorption of vapors by —, DEAN *et al.*, 377

O

- Obituary, McBAIN, J. W., 375
 Octyltrimethylammonium, see *Light*
 Oil, see *Emulsions*
 Oleic acid, dilute aqueous solutions of sodium oleate, FLOCKHART AND GRAHAM, 105

P

- Paraffin (see also *Contact angle*); electrical conductance of — -chain salts, FLOCKHART AND UBBELOHDE, 428
 Pectin, effect of esterification on viscosity and gelation of —, PIPPEN *et al.*, 97

Phase separation, see *Cellulose acetate*
 Pigments, see *Dyes*

- Plasticity, fourth symposium, 488
 Polyelectrolytes, polyglucosamine, BASU AND DAS GUPTA, 355
 Polyglucosamine, see *Polyelectrolytes*
 Polymers, polystyrene and styrene-maleic acid —, FERRY *et al.*, 529
 Polyvinyl chloride, dielectric properties of the system — — -dimethylthianthrene, FITZGERALD AND MILLER, 148; relaxation distribution functions of — — and dimethylthianthrene, FERRY AND FITZGERALD, 224
 Potassium silicate, polymerization of aqueous — — solutions, BRADY *et al.*, 252

Protein, see *Monolayers*

R

- Relaxation, see *Polyvinyl chloride*
 Rubber, see *Latex*

S

- Silicate, see *Potassium*
 Silver iodide, see *Electroviscous effect*
 Solids, see *Gel*
 Solubilization (see also *Detergency*); — and micelle formation in a hydrocarbon medium, MATHEWS AND HIRSCHHORN, 86
 Sorbitan sesquileate, see *Emulsions*
 Spreading, — of liquids on low-energy surfaces, FOX *et al.*, 194
 Stability, see *Electrophoresis*
 Styrene, see *Polymers*
 Sulfur, ultraviolet absorption of — solutions, FRIEDMAN AND KERKER, 80
 Supercooling, critical — of pure water droplets, POUND *et al.*, 187
 Surface (see also *Contact angle*, *Detergent*, *Spreading*); force-area curves of — films of soluble — -active agents, MEADER AND CRIDDLE, 170; — films and foam, BROWN *et al.*, 508; — and detergency, BURCIK, 520
 Suspension (see also *Colloidal*, *Concen-*

tration); Donnan-e.m.f. and —, OVER-
BEEK, 593

T

Tacky adhesion, BANKS AND MILL, 137

Thermodynamics (see also *Electro-*
kinetics); statistical — in a model,
SCOTT AND TOBOLSKY, 465

U

Ultraviolet absorption, see *Sulfur*

V

Vapors, see *Monolayer*

Viscometer, see *Ink*

Viscosity, see *Cellulose acetate*, *Deter-*
gent, *Electroviscous effect*, *Pectin*

Volumes, specific — of potassium laurate
and lauryl sulfonic acid, LAL, 414

W

Water, see *Contact angle*, *Emulsions*,
Supercooling

INDEX OF BOOK REVIEWS

- | | |
|--|---|
| <p>BRESCIA, F., General College Chemistry (DAILEY, B. P.), 487</p> <p>COMITÉ INTERNATIONAL DE THERMODYNAMIQUE ET DE CINÉTIQUE ÉLECTROCHIMIQUES, Comptes rendus de la III^e réunion. Berne, 1951 (BIKERMAN, J. J.), 277</p> <p>FRANKENBURG, W. G., KOMEREWSKY, V. I., AND RIDEAL, E. K. (ed.), Advances in Catalysis, Vols. I, II, and III (POTTER, C.), 183</p> <p>FROST, A. A., AND PEARSON, R. G., Kinetics and Mechanism (LA MER, V. K.), 374</p> | <p>HALL, W. J., AND HOOPER, C. J. W. (ed.), Review of Textile Progress. Vol. III (EWART, R. H.), 611</p> <p>KRUYT, H. (ed.), Colloid Science. Vol. I (EIRICH, F. R.), 487</p> <p>RICCI, J. E., Hydrogen Ion Concentration. New concepts in a systematic treatment (CLARK, W. M.), 184</p> <p>SAMUELSON, O., Ion Exchangers in Analytical chemistry (SELKE, W. A.), 553</p> <p>SHAW, B. T. (ed.), Soil Physical Conditions and Plant Growth (JENNY, H.), 374</p> |
|--|---|

